EXTRACELLULAR MATRIX DYNAMICS IN BIOLOGY, BIOENGINEERING, AND PATHOLOGY

EDITED BY: Rajprasad Loganathan, Charles D. Little and Brenda J. Rongish
PUBLISHED IN: Frontiers in Cell and Developmental Biology and
Frontiers in Physiology

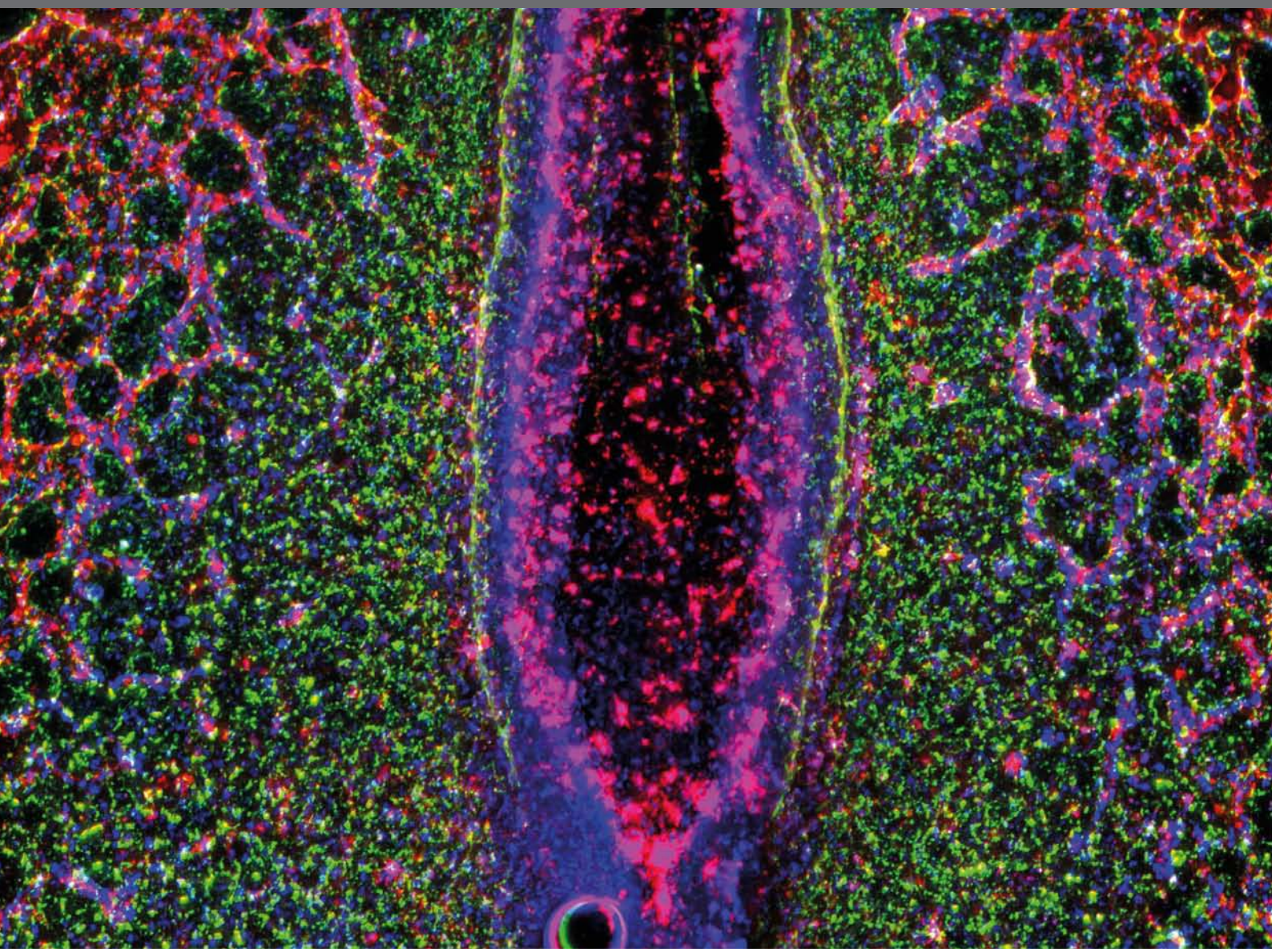

frontiers Research Topics

ISSN 1664-8714
ISBN 978-2-88966-119-0
DOI 10.3389/978-2-88966-119-0

About Frontiers

Frontiers is more than just an open-access publisher of scholarly articles: it is a pioneering approach to the world of academia, radically improving the way scholarly research is managed. The grand vision of Frontiers is a world where all people have an equal opportunity to seek, share and generate knowledge. Frontiers provides immediate and permanent online open access to all its publications, but this alone is not enough to realize our grand goals.

Frontiers Journal Series

The Frontiers Journal Series is a multi-tier and interdisciplinary set of open-access, online journals, promising a paradigm shift from the current review, selection and dissemination processes in academic publishing. All Frontiers journals are driven by researchers for researchers; therefore, they constitute a service to the scholarly community. At the same time, the Frontiers Journal Series operates on a revolutionary invention, the tiered publishing system, initially addressing specific communities of scholars, and gradually climbing up to broader public understanding, thus serving the interests of the lay society, too.

Dedication to Quality

Each Frontiers article is a landmark of the highest quality, thanks to genuinely collaborative interactions between authors and review editors, who include some of the world's best academicians. Research must be certified by peers before entering a stream of knowledge that may eventually reach the public - and shape society; therefore, Frontiers only applies the most rigorous and unbiased reviews.
Frontiers revolutionizes research publishing by freely delivering the most outstanding research, evaluated with no bias from both the academic and social point of view. By applying the most advanced information technologies, Frontiers is catapulting scholarly publishing into a new generation.

What are Frontiers Research Topics?

Frontiers Research Topics are very popular trademarks of the Frontiers Journals Series: they are collections of at least ten articles, all centered on a particular subject. With their unique mix of varied contributions from Original Research to Review Articles, Frontiers Research Topics unify the most influential researchers, the latest key findings and historical advances in a hot research area! Find out more on how to host your own Frontiers Research Topic or contribute to one as an author by contacting the Frontiers Editorial Office: researchtopics@frontiersin.org

EXTRACELLULAR MATRIX DYNAMICS IN BIOLOGY, BIOENGINEERING, AND PATHOLOGY

Topic Editors:
Rajprasad Loganathan, Johns Hopkins University, United States
Charles D. Little, University of Kansas Medical Center, United States
Brenda J. Rongish, University of Kansas Medical Center, United States

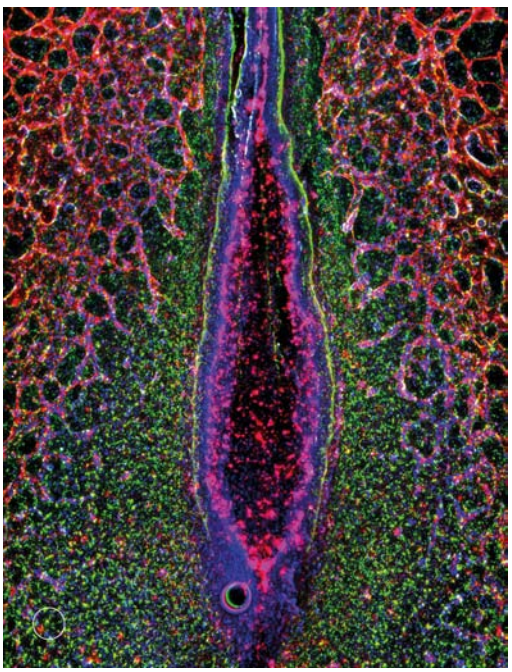

On the Cover: Tail-bud region of a whole-mounted quail embryo at the 12-13 somite stage showing the extracellular matrix component fibronectin (green), vascular endothelial cells (red) and cell nuclei (blue).
Image courtesy of Charles D. Little.

Citation: Loganathan, R., Little, C. D., Rongish, B. J., eds. (2020). Extracellular Matrix Dynamics in Biology, Bioengineering, and Pathology. Lausanne: Frontiers Media SA. doi: 10.3389/978-2-88966-119-0

Table of Contents

frontiers in Cell and Developmental Biology

EDITORIAL
published: 21 August 2020
doi: 10.3389/fcell.2020.00759

Editorial: Extracellular Matrix Dynamics in Biology, Bioengineering, and Pathology

Rajprasad Loganathan[1]*, *Charles D. Little*[2] and *Brenda J. Rongish*[2]

[1] Department of Cell Biology, Johns Hopkins University, Baltimore, MD, United States, [2] Department of Anatomy and Cell Biology, University of Kansas Medical Center, Kansas City, KS, United States

Keywords: ECM, matrisome, EMT, stem cell, angiogenesis, rheometry, bioscaffold

Editorial on the Research Topic

Extracellular Matrix Dynamics in Biology, Bioengineering, and Pathology

INTRODUCTION

Research aimed at understanding the nature of extracellular matrix (ECM) dynamics has been, in recent years, a shared endeavor that is spread across many disciplines including biology, bioengineering, and pathology. Novel findings have illuminated our current understanding that the ECM is a dynamic composite; this emerging concept challenges the conventional school of thought that the ECM is a passive/static substrate for cellular functions. These advances have come from the students of ECM adopting an interdisciplinary approach to investigate its role in multiple model systems. The collection of articles published under the Research Topic, "Extracellular matrix dynamics in biology, bioengineering, and pathology," is an exemplar of the collective effort advanced by investigators bridging the interdisciplinary divides.

BIOLOGY

Bres and Faissner, in their comprehensive review, discuss Low Density Receptor-Related Protein 1 (Lrp1)—a functionally versatile member of the low density lipoprotein receptor family. Its role extends beyond ligand uptake, receptor mediated endocytosis, and endocytosis transport. Indeed, Lrp1 interacts with the ECM with consequential effects for integrin-mediated cell adhesion and tissue plasminogen activator-mediated ECM dynamics in the nervous system.

Huss et al. present their compilation of the quail matrisome genes, which we expect will serve as a standard reference guide for the ECM research community. It will be of significant utility for investigating the roles of ECM dynamics in avian embryogenesis, for which quail embryos have served as a critical model system. Using a multidisciplinary approach, Huss et al., also report that the avian primordial germ cell motion occurs in the backdrop of a dynamic (motile) ECM fibril meshwork—its architecture dependent on integrin β1 receptors and germ cell-secreted fibronectin. The cellular motion itself is, unexpectedly, independent of these integrin receptors.

Bone development, as a physiological process, has no parallels in its enmeshment with ECM dynamics. With dual live-cell imaging of collagen and osteocyte dynamics in the murine model, Shiflett et al. gain new insights into the dynamic ECM assembly processes and osteocyte entrapment in the collagen matrix that characterize bone development and remodeling. Their results suggest multiple mechanisms for osteocyte entrapment in the collagen matrix that are largely directed by ECM dynamics.

OPEN ACCESS

Edited and reviewed by:
Akihiko Ito,
Kindai University, Japan

***Correspondence:**
Rajprasad Loganathan
rlogana2@jhmi.edu

Specialty section:
This article was submitted to Cell Adhesion and Migration, a section of the journal Frontiers in Cell and Developmental Biology

Received: *15 July 2020*
Accepted: *20 July 2020*
Published: *21 August 2020*

Citation:
Loganathan R, Little CD and Rongish BJ (2020) Editorial: Extracellular Matrix Dynamics in Biology, Bioengineering, and Pathology. Front. Cell Dev. Biol. 8:759. doi: 10.3389/fcell.2020.00759

Epithelial-Mesenchymal Transition (EMT) is a fundamental characteristic that defines diverse developmental and pathological processes. Although the intracellular signaling and regulatory processes involved in EMT have received wide attention, an understanding of how tissue mechanics, and ECM mechanics in particular, affect this cell morphological transformation is lacking. The review by Scott et al. contributes to this poorly understood aspect of EMT by discussing evidence for the involvement of mechanochemical signaling of the ECM in EMT. Their work emphasizes the importance of bidirectional influences in which ECM mechanosignaling impinges on EMT and vice versa while highlighting the prominent roles played by non-structural matricellular proteins.

BIOENGINEERING

The importance of utilizing tissue engineering applications in the clinical setting with a clear understanding of the potential for ECM dynamics to shape/influence therapeutic outcomes is demonstrated by Wu et al.. Using human salivary stem/progenitor cells encapsulated in biocompatible hyaluronate-based hydrogels, they examine microstructure formation, growth, and reorganization with time-lapse imaging. Their results support an active role for the ECM components and integrin-mediated signaling in directing tissue assembly.

Advances in time-lapse imaging methods have proved critical for gaining a better understanding of ECM dynamics. These advances have been instrumental for the study of blood vessel formation and growth. Rauff et al. provide a thorough overview of the time-lapse imaging techniques that have helped reveal the multiple facets of ECM dynamics—a critical factor in shaping the interactions between a blood vessel and its microenvironment during sprouting angiogenesis.

Although great strides have been made in the development of methods for measuring and evaluating the biomechanics of ECM assembly/maintenance in various tissues and cell assemblies, studies investigating the local material and mechanical properties of matrix in an *in vivo* 3D tissue are scarce. Akos et al. attempt to alleviate this deficiency by taking the initial steps in measuring the local viscoelastic properties of ECM during avian embryogenesis. The authors devise a magnetic force-based rheometry method to measure the local rheological properties of the mesoderm-endoderm interface within quail embryos. By tracing the rotational displacement of injected ferromagnetic nanorod probes, they measure the local elasticity of the embryonic tissue at a given region of interest. More investigations along these lines are expected in future studies to help render a "viscoelasticity map" for the whole embryo. Extending this line of investigation further, it is now possible to imagine the construction of maps depicting the fluctuating material properties as cells and ECM determine/direct the forces that shape the embryo.

PATHOLOGY

Tucker and Degen's review of tenascin-W—a member of the family of chordate ECM—describes its discovery, architecture, evolution, and expression patterns while highlighting its role in osteogenesis and adult stem cell niches. The authors also discuss the translational research merits of considering tenascin-W as a potential target for anti-cancer therapies due to its prominence in many solid tumors and its absence in the ECM of most adult tissues.

Pattar et al. review the clinical potential of ECM bioscaffolds to attenuate cardiac remodeling, and to restore ECM homeostasis by their ability to steer endogenous mechanisms of tissue repair following post-myocardial infarction ischemic injury. The array of ECM bioscaffolding options discussed in this review reveals a window of opportunity available for use as an adjunct therapy to surgical revascularization. An ideal ECM bioscaffold could positively alter the course of fibrotic remodeling, which often complicates the recovery of cardiac pump function.

Cleft lip/palate is among the frequently occurring congenital anomalies. ECM dynamics is a critical, yet poorly understood, component of palatogenesis. The review by Paiva et al. offers the current perspectives on both palatogenesis and on the occurrence of cleft lip/palate in terms of ECM dynamics and its dysregulation.

In their presentation of epithelial ECM dynamics under pathological contexts, Bhattacharjee et al. discuss the myriad dimensions of ECM-immune cell signaling exemplified during skin diseases. The effects on the immunomodulatory roles of cells and on ECM dynamics by atopic dermatitis, psoriasis, epidermolysis bullosa, and skin cancers are their primary focus.

SUMMARY

Each article included in this collection is a vignette that captures the intricacies and idiosyncrasies of ECM dynamics in diverse contexts within the realms of biology, bioengineering, and pathology. We hope that this collection will both inform and inspire the students of ECM dynamics working across various disciplines.

AUTHOR CONTRIBUTIONS

All authors listed have made a substantial, direct and intellectual contribution to the work, and approved it for publication.

Conflict of Interest: The authors declare that the research was conducted in the absence of any commercial or financial relationships that could be construed as a potential conflict of interest.

frontiers in Cell and Developmental Biology

REVIEW
published: 15 March 2019
doi: 10.3389/fcell.2019.00031

Low Density Receptor-Related Protein 1 Interactions With the Extracellular Matrix: More Than Meets the Eye

*Ewa E. Bres and Andreas Faissner**

Department of Cell Morphology and Molecular Neurobiology, Ruhr University Bochum, Bochum, Germany

The extracellular matrix (ECM) is a biological substrate composed of collagens, proteoglycans and glycoproteins that ensures proper cell migration and adhesion and keeps the cell architecture intact. The regulation of the ECM composition is a vital process strictly controlled by, among others, proteases, growth factors and adhesion receptors. As it appears, ECM remodeling is also essential for proper neuronal and glial development and the establishment of adequate synaptic signaling. Hence, disturbances in ECM functioning are often present in neurodegenerative diseases like Alzheimer's disease. Moreover, mutations in ECM molecules are found in some forms of epilepsy and malfunctioning of ECM-related genes and pathways can be seen in, for example, cancer or ischemic injury. Low density lipoprotein receptor-related protein 1 (Lrp1) is a member of the low density lipoprotein receptor family. Lrp1 is involved not only in ligand uptake, receptor mediated endocytosis and lipoprotein transport—functions shared by low density lipoprotein receptor family members—but also regulates cell surface protease activity, controls cellular entry and binding of toxins and viruses, protects against atherosclerosis and acts on many cell signaling pathways. Given the plethora of functions, it is not surprising that Lrp1 also impacts the ECM and is involved in its remodeling. This review focuses on the role of Lrp1 and some of its major ligands on ECM function. Specifically, interactions with two Lrp1 ligands, integrins and tissue plasminogen activator are described in more detail.

Keywords: low density receptor-related protein 1, tissue plasminogen activator, integrins, extracellular matrix, migration, matrix remodeling

OPEN ACCESS

Edited by:
Charles D. Little,
University of Kansas Medical Center,
United States

Reviewed by:
Nagaraj Balasubramanian,
Indian Institute of Science Education and Research Pune, India
David Lutz,
Ruhr-Universität Bochum, Germany
Ralf Kleene,
University Medical Center Hamburg-Eppendorf, Germany

***Correspondence:**
Andreas Faissner
andreas.faissner@rub.de

Specialty section:
This article was submitted to Cell Adhesion and Migration, a section of the journal Frontiers in Cell and Developmental Biology

Received: *13 November 2018*
Accepted: *25 February 2019*
Published: *15 March 2019*

Citation:
Bres EE and Faissner A (2019) Low Density Receptor-Related Protein 1 Interactions With the Extracellular Matrix: More Than Meets the Eye. Front. Cell Dev. Biol. 7:31. doi: 10.3389/fcell.2019.00031

INTRODUCTION

Lrp1: A Hidden Multitasker

Low density lipoprotein receptor-related protein-1 (Lrp1), also known as CD91 or α-2-macroglobulin (α-2-M) receptor, is a member of the low density lipoprotein receptor family and is expressed in various tissues including liver, adipose tissue, lungs and brain. The receptor, with a mass of 600 kDa, during its biosynthesis, undergoes a furin-mediated proteolytical cleavage in the Golgi apparatus. This cleavage results in two, non-covalently bound polypeptide subunits—an 85 kDa membrane-bound C-terminal fragment (the light β chain) and a 515 kDa

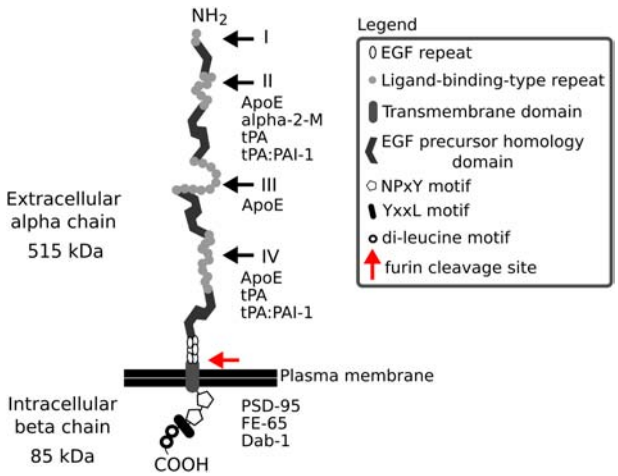

FIGURE 1 | The structure of Lrp1. Lrp1 is cleaved by furin (red arrow) in the Golgi complex and afterwards is transported to the cell membrane. The resulting mature Lrp1 receptor consists of a 515 kDa alpha chain and an 85 kDa beta chain bound to each other non-covalently. The alpha chain consists of ligand-binding-type repeats forming four clusters (I–IV) that are rich in cysteine. The clusters contain 2, 8, 10, and 11 repeats, respectively. The clusters II and IV are responsible for the majority of ligand binding to Lrp1. The ligand-binding clusters are separated by 1–4 EGF homology domains, with cysteine-rich EGF repeats. The intracellular beta chain consists of two NPxY motifs, one YxxL motif and two di-leucine motifs that have been associated with the endocytotic functions of Lrp1. The beta chain also interacts with scaffolding proteins like PSD-95, Dab-1, and FE-65. Both the extra- and intracellular chain can act independently of each other, when the alpha chain is shed as a soluble Lrp1 and the beta chain translocates to the nucleus and activates gene transcription and signaling cascades. α-2-M, α-2-macroglobulin; ApoE, apolipoprotein E; COOH, carboxy terminal; Dab-1, disabled 1; EGF, epidermal growth factor; NH_2, amino terminal; PAI-1, plasminogen activator inhibitor 1; PSD-95, postsynaptic density protein 95; tPA, tissue plasminogen activator.

N-terminal fragment located extracellularly (the heavy α chain)—that form the mature Lrp1 (**Figure 1**). The Lrp1 α chain contains 4 ligand binding complement-like repeat clusters separated by epidermal growth factor (EGF) repeats. Clusters II and IV are considered to be responsible for the majority of ligand binding (Herz, 2001; Herz and Strickland, 2001; Croy et al., 2003; Meijer et al., 2007) and have previously been shown to display minor differences regarding the kinetics of the interactions but to be also highly similar in their ligand binding properties (duplication of the domains) (Neels et al., 1999). As suggested by Huang et al. (1999), each ligand-binding domain of Lrp1 presents very different charge densities and hydrophobic patches. These differences in turn lead to varying receptor-ligand interactions and are responsible for a distinct ligand specificity of each cluster, despite similar backbone folds. Because Lrp1 interacts with a wide variety of protein ligands (**Table 1**), it is necessary to study each domain individually to elucidate its exact ligand-binding capacities. Interestingly, receptor-associated protein (RAP) binds to the ligand-binding clusters and completely blocks interactions with all known Lrp1 ligands (Bu et al., 1994).

As shown by Li et al. (2000, 2001), the Lrp1 β chain C-terminus contains motifs, proposed later by Deane et al. (2008) to be involved in generating the rapid endocytotic rate of Lrp1: two NPxY motifs, one YxxL motif and two di-leucine motifs. The C-terminus of Lrp1 interacts with many intracellular ligands (Betts et al., 2008; Guttman et al., 2009) and binds to endocytic and scaffold adaptors like disabled-1, FE-65 and postsynaptic density protein 95 (PSD-95) that link the Lrp1 receptor to membrane-bound proteins such as amyloid precursor protein (APP) (Herz and Chen, 2006; Waldron et al., 2008) and are involved in many cell signaling pathways (Trommsdorff et al., 1998; Gotthardt et al., 2000; May et al., 2004; Pietrzik et al., 2004; Herz et al., 2009; Klug et al., 2011). Lrp1 can additionally undergo an intramembrane proteolysis that results in a shed extracellular Lrp1 fragment and a γ-secretase cleaved intracellular Lrp1 domain. Upon cleavage, the intracellular Lrp1 domain translocates to the cell nucleus and modulates gene expression (May et al., 2002; Zurhove et al., 2008).

Lrp1 is nowadays considered to be a multifunctional receptor: it is involved not only in ligand uptake, receptor-mediated endocytosis, cellular signaling and lipoprotein transport (Herz and Bock, 2002) but also regulates cell surface protease activity (Makarova et al., 2003), controls cellular entry and binding of toxins and viruses (Kounnas et al., 1992b; Hofer et al., 1994; Liu et al., 2000), participates in dendritic cell efferocytosis (Subramanian et al., 2014), protects against atherosclerosis (Boucher and Herz, 2011), is critical for angiogenesis and the maintenance of the blood–brain barrier (BBB) (Polavarapu et al., 2007; Pi et al., 2012; Strickland et al., 2014) and acts on many signaling cascades including the Wnt and Notch pathways (Zilberberg et al., 2004; Lillis et al., 2008; Meng et al., 2010).

In the central nervous system (CNS), Lrp1 is highly expressed not only in neurons, astrocytes and microglia (Bu et al., 1994; Ishiguro et al., 1995; Rebeck et al., 1995; Marzolo et al., 2000; Makarova et al., 2003; Andersen and Willnow, 2006; Kanekiyo et al., 2011; Auderset et al., 2016) but also in brain endothelial cells, vascular smooth muscle cells, pericytes and the choroid plexus (Herz and Bock, 2002).

In the mouse, the complete knock-out of Lrp1 is lethal for the embryos (Herz et al., 1992, 1993), making it challenging to study the role and function of Lrp1 in embryonic as well as adult brain *in vivo*. However, various mutant mouse models generated in the last decades shed more light onto the possible function of Lrp1 in the CNS.

With their studies, May et al. (2004); Liu et al. (2010) and Nakajima et al. (2013), highlight and support earlier findings showing that Lrp1 regulates postsynaptic signaling via interactions with PSD-95 and *N*-methyl-D-aspartate receptor (NMDAR) and is crucial for synaptic transmission (Bacskai et al., 2000; Qiu et al., 2002). The studies of Liu et al. (2010) and Liu et al. (2011) additionally provide evidence for the importance of Lrp1 in maintaining proper brain lipid metabolism and leptin signaling and define Lrp1 as a major apolipoprotein E (ApoE) transport receptor, strengthening the role of Lrp1 in Alzheimer's disease pathogenesis.

Knock-in mutations in the NPxY2 region lead to a reduced Lrp1 internalization rate (Roebroek et al., 2006; Reekmans et al., 2010; Gordts et al., 2012) and interfere with NMDAR recycling and NMDAR-mediated activation of the ERK1/2

TABLE 1 | Representative molecules interacting with the Lrp1 receptor.

Molecule and function		Reference
α1-antitrypsin (A1AT or A1PI)	Member of the serpin superfamily, inhibits various proteases, regulates enzymes produced by inflammatory cells like neutrophil elastase	Poller et al., 1995
α1-antitrypsin:trypsin complexes	Serpin-enzyme complex	Kounnas et al., 1996
α-2 macroglobulin (α-2-M)	Member of the α-2 globulin family. Protease inhibitor, inhibits a wide range of proteinases	Ashcom et al., 1990; Strickland et al., 1990
Amidoglycosides: gentamicin, polymixcin B	Antibiotics used to treat various bacterial infections	Moestrup et al., 1995
Amyloid β peptide	Peptide derived from amyloid precursor protein processing. Main component of amyloid plaques found in Alzheimer's patients	Kang et al., 2000; Shibata et al., 2000
Amyloid precursor protein (APP)	Integral membrane protein, during its proteolysis the amyloid β peptide is generated	Kounnas et al., 1995a; Ulery et al., 2000
Annexin VI	Member of the calcium-dependent membrane and phospholipid binding proteins; co-receptor of Lrp1, involved in endocytosis processes, interacts with α-2-M	Ling et al., 2004
Apolipoprotein E (ApoE)/ApoE-containing lipoproteins	Fat-binding protein produced by astrocytes, essential for the catabolism of lipoproteins and their transport; main cholesterol carrier in the brain	Herz et al., 1988; Beisiegel et al., 1989; Hayashi et al., 2007
Aprotinin	Single-chain globular polypeptide derived from bovine lungs; inhibits serine proteases	Hussain et al., 1999
Bone morphogenic factor 4 (BMP4) BMP-binding endothelial cell precursor-derived regulator	Growth and differentiation factor; important for neurogenesis, bone and cartilage metabolism	Pi et al., 2012
C1s/C1q	Form the complement component C1 complex that initiates the classical pathway of component activation	Storm et al., 1997
C4b-binding protein (C4BP)	Inhibitor in the complement system	Spijkers et al., 2008
Calreticulin	Calcium-binding chaperone protein, regulates many cellular processes	Gardai et al., 2005
Cathepsin D	Lysosomal aspartic protease, member of the peptidase A1 family, involved in protein degradation	Derocq et al., 2012
CCN1, cysteine-rich angiogenic inducer 61 (CYR61)	Secreted, matrix-associated signaling protein involved in apoptosis, adhesion, migration and vascular integrity	Juric et al., 2012
Chylomicron remnants	Lipoprotein particles comprising triglycerides, phospholipids, cholesterol, and proteins involved in lipid transport	Rohlmann et al., 1998; Kowal et al., 1989
Coagulation factor VIII	Blood-clotting protein, participates in blood coagulation	Lenting et al., 1999; Saenko et al., 1999
Coagulation factor Xa: tissue factor pathway inhibitor (TFPI) complexes	Coagulation factor X is a serine protease that in its active form (Xa) converts prothrombin into thrombin and plays a role in blood coagulation; TFPI reversibly inhibits factor Xa	Ho et al., 1996
Coagulation factor XIa:nexin complexes	Coagulation factor XI is a serine protease that in its active form (XIa) initiates the intrinsic pathway of blood coagulation by activating factor IX; complexes with nexin-1 inhibit its function	Knauer et al., 2000
Complement component 3	Plays a role in the activation of the classical and alternative complement activation pathways	Meilinger et al., 1999
Connective tissue growth factor (CTGF; CCN2)	Matricellular protein of the extracellular matrix-associated heparin-binding protein family, involved in cell adhesion, migration, and angiogenesis	Segarini et al., 2001; Gao and Brigstock, 2003
Decorin (Dcn)	Member of the small leucine-rich proteoglycan family that impacts the activities of growth factors, regulates extracellular matrix assembly and cell adhesion	Brandan et al., 2006
Disabled 1 (Dab1)	Adaptor protein known to activate Src	Trommsdorff et al., 1998; Gotthardt et al., 2000
FE-65	Adaptor protein involved in APP processing	Trommsdorff et al., 1998; Gotthardt et al., 2000
Fibronectin	Glycoprotein of the extracellular matrix vital for cell differentiation, migration and adhesion	Salicioni et al., 2002
Frizzled-1	G-coupled receptor protein involved in the Wnt pathway	Zilberberg et al., 2004
Glypican-3:Hedgehog complexes	Glypican-3 is a heparan sulfate proteoglycan that impacts embryonic growth by inhibiting the hedgehog signaling pathway	Capurro et al., 2012
Heat shock protein 90, 96, 70	Intracellular chaperon proteins assisting in protein folding	Basu et al., 2001; Tsen et al., 2013
Heparan sulfate proteoglycans (HSPGs)	Glycoproteins containing one or more covalently attached heparan sulfate chains; present at the cell surface and in the extracellular matrix; endocytic and adhesion receptors, regulate cell migration	Wilsie and Orlando, 2003

(Continued)

TABLE 1 | Continued

	Molecule and function	Reference
Hepatic lipase	Lipase involved in lipoprotein metabolism and transport	Kounnas et al., 1995b
HIV-Tat protein	Transactivator of viral genes in cells infected with HIV	Liu et al., 2000
Insulin	Peptide hormone produced by the pancreas that regulates the metabolism of carbohydrates, fats and proteins	Bilodeau et al., 2010
Insulin-like growth factor-binding protein 3 (IGFBP-3)	Protein produced and secreted by the liver, carrier of insulin-like growth factors	Huang et al., 2003
Lactoferrin	Multifunctional protein of the transferrin family with an antibacterial function	Willnow et al., 1992; Meilinger et al., 1995
Leptin	Hormone produced by adipose cells involved in energy balance and neuronal functioning	Liu et al., 2011
Lipoprotein lipase (LPL)	Lipase involved in lipoprotein metabolism and transport	Beisiegel et al., 1991; Chappell et al., 1992
Malaria circumsporozoite protein (CSP)	Secreted protein of the sporozoite stage of the malaria parasite	Shakibaei and Frevert, 1996
Matrix metalloproteinase 2 (MMP-2)	Proteinase involved in the degradation of the extracellular matrix, metastasis	Yang et al., 2001
Matrix metalloproteinase 9 (MMP-9)	Proteinase involved in the degradation of the extracellular matrix, angiogenesis, metastasis	Hahn-Dantona et al., 2001
Matrix metalloproteinase 13 (collagenase-3) (MMP-13)	Proteinase involved in the degradation of the extracellular matrix, angiogenesis, metastasis	Barmina et al., 1999
Metallothionein II	Cysteine-rich low molecular weight metallothionein family member involved in protection against oxidative stress and chemotactic signal transduction	Landowski et al., 2016
Midkine (MDK)	Heparin-binding growth factor induced during mid-gestation involved in cell migration, survival and angiogenesis	Muramatsu et al., 2000; Lee et al., 2012
Minor-group human rhinovirus (HRV2)	Minor group rhinovirus	Hofer et al., 1994
Myelin-associated glycoprotein (MAG)	Cell membrane glycoprotein involved in myelination	Stiles et al., 2013
Myelin basic protein (MBP)	Major protein forming the myelin sheath of oligodendrocytes and Schwann cells	Gaultier et al., 2009
Nexin-1	Member of the serine protease inhibitor (Serpin) superfamily	Crisp et al., 2000; Vaillant et al., 2007
Plasminogen activator inhibitor (PAI-1)	Serpin, Regulator of tPA/uPA activity	Stefansson et al., 1998
Platelet-derived growth factor (PDGF)-BB PDGF receptor (PDGFR) β	PDGF-BB is a dimeric glycoprotein composed of two B subunits and a major growth factor that binds with high affinity to the cell surface receptor PDGFR β	Boucher et al., 2002; Loukinova et al., 2002; Takayama et al., 2005; Zhou et al., 2009
Postsynaptic density protein 95 (PSD-95)	Adaptor protein crucial for synapse stability and coupling to NMDA receptors	Gotthardt et al., 2000; May et al., 2004
Prion protein (PrP)	Cell-surface glycoprotein that upon conversion can cause prion diseases	Sunyach et al., 2003; Taylor and Hooper, 2007
Pregnancy zone protein (PZP):protease complexes	PZP is a member of the α-2 globulin family; protease inhibitor and extracellular chaperone; role in immune regulation during pregnancy	Moestrup et al., 1987; Sanchez et al., 2001
Pro-urokinase	Serine protease, urokinase-type plasminogen activator single-chain zymogen with little intrinsic enzymatic activity	Kounnas et al., 1993
Pseudomonas exotoxin A	Toxin from *Pseudomonas aeruginosa*	Kounnas et al., 1992b
Receptor-associated protein (RAP)	Endoplasmic reticulum resident chaperone glycoprotein, inhibits binding of ligands to low density lipoprotein receptor family members	Herz et al., 1991; Kounnas et al., 1992a
Ricin A	Ribosome-inactivating protein found in the seeds of *Ricinus communis*; potent toxin	Cavallaro et al., 1995
Saporin	Ribosome-inactivating protein found in the seeds of *Saponaria officinalis*; potent toxin	Cavallaro et al., 1993a,b, 1995
Saposin (SAP) precursor	Glycoprotein precursor of saposins (sphingolipid activator proteins) involved in glycosphingolipid catabolism	Hiesberger et al., 1998
Shc	Adaptor protein that becomes phosphorylated on tyrosine residues in response to extracellular stimuli	Barnes et al., 2001
Trigliceride-rich lipoproteins (TLRs)	Main carriers of triglycerides in the blood; involved in lipoprotein metabolism and transport	Mahley and Huang, 2007; Foley et al., 2013
Tissue inhibitors of matrix metalloproteases (TIMPs)	Protease inhibitors of matrix metalloproteinases	Scilabra et al., 2013; Thevenard et al., 2014
Tissue factor pathway inhibitor (TFPI)	Single-chain polypeptide that reversibly inhibits coagulation factor Xa, thereby regulating blood clotting	Warshawsky et al., 1994
TpeL	*Clostridium perfringens* toxin	Schorch et al., 2014

(Continued)

TABLE 1 | Continued

	Molecule and function	Reference
Transforming growth factor-β 1 (TGF-β 1)	Multifunctional growth factor, involved in interactions with extracellular proteins, cell growth, differentiation and vascular remodeling	Huang et al., 2003
Transforming growth factor-β 2 (TGF-β 2)	Multifunctional growth factor, involved in interactions with extracellular proteins, cell growth, differentiation and vascular remodeling	Muratoglu et al., 2011
Thrombospondin 1	Extracellular matrix glycoprotein, member of the thrombospondin family, vital for cell-cell and cell-matrix interactions	Godyna et al., 1995; Mikhailenko et al., 1995
Thrombospondin 2	Extracellular matrix glycoprotein, member of the thrombospondin family, vital for cell-cell and cell-matrix interactions	Meng et al., 2010
Tissue-type plasminogen activator (tPA)	Serine protease mediating the conversion of plasminogen to plasmin and cell signaling	Bu et al., 1992; Zhuo et al., 2000
tPA:PAI-1 complexes	Serine protease–protease inhibitor complex	Orth et al., 1992
tPA:neuroserpin complexes	Serine protease–protease inhibitor complex	Makarova et al., 2003
Thrombin:protein inhibitor C complexes	Serine protease–protease inhibitor complex	Kasza et al., 1997
Thrombin:nexin-1 complexes	Serine protease–protease inhibitor complex	Knauer et al., 1997
Thrombin:antithrombin III complexes	Serine protease–protease inhibitor complex	Kounnas et al., 1996
Thrombin:heparin cofactor II complexes	Serine protease–protease inhibitor complex	Kounnas et al., 1996
Thrombin:PAI-1 complexes	Serine protease–protease inhibitor complex	Stefansson et al., 1996
Trichosanthin	Ribosome-inactivating protein derived from *Trichosanthes kirilowii*	Chan et al., 2000
Urokinase-type plasminogen activator (uPA)	Serine protease, involved in tissue remodeling, wound healing, cell migration	Kounnas et al., 1993
uPA:PAI-1 complexes	Serine protease–protease inhibitor complex	Herz et al., 1992; Nykjaer et al., 1992
uPA:PAI-2 complexes	Serine protease–protease inhibitor complex	Croucher et al., 2006
uPA:C inhibitor complexes	Serine protease–protease inhibitor complex	Kasza et al., 1997
uPA:Nexin-1 complexes	Serine protease–protease inhibitor complex	Conese et al., 1994
Von Willebrand factor (vWF)	Adhesive, glycoprotein involved in blood coagulation and wound healing	Rastegarlari et al., 2012

pathway (Martin et al., 2008; Reekmans et al., 2010). Alterations in NMDAR subunits on the cell surface can lead to alterations and deficits in memory processes. Animals harboring the knock-in mutation in the NPxY2 motif display hyperactivity, impaired learning as well as deficits in spatial and reversal learning, similarly to animals with impaired NMDAR signaling (Bannerman et al., 1995; Sakimura et al., 1995).

A recent study from our laboratory discovered that Lrp1 is a novel carrier protein for Lewis X glycans expressed by mouse radial glial cells [neural stem precursor cells (NSPCs)] in the developing and adult CNS (Hennen et al., 2013). With this and a follow-up study we showed that Lrp1 plays a role in the differentiation of NSPCs (Hennen et al., 2013; Safina et al., 2016). The impaired differentiation of Lrp1-lacking NSPCs toward oligodendrocytes is supported by the work of Lin et al. (2017) where deficits in myelination and oligodendrocyte precursor differentiation were observed upon Lrp1 deletion specifically from the oligodendrocyte lineage. According to this study, these impairments are a combined result of altered AKT, sterol regulatory element-binding protein 2 and peroxisome proliferation-associated receptor γ pathways in oligodendrocytes.

The Extracellular Matrix

The extracellular matrix (ECM) is a biological substrate that is composed of collagens, proteoglycans and glycoproteins. The highly organized honeycomb-like structures of the ECM were first described by Camillo Golgi over a century ago and, since then, the ECM has been found to be essential not only for cell migration, adhesion and structural support but also for proper neuronal and glial development, BBB maturation and function, synaptogenesis and synaptic signaling in the CNS (Faissner et al., 2010; Menezes et al., 2014; Song and Dityatev, 2018). The composition of the ECM is heterogeneous and tissue-specific. In the CNS, the ECM is formed by proteoglycans like heparan sulfate proteoglycans (HSPGs), chondroitin sulfate proteoglycans and glycoproteins including tenascins, laminins, and thrombospondins. During embryonic and early postnatal development, the ECM provides an environment supporting cell migration, differentiation and synapse formation. Here, the ECM forms a loose structure consisting of neuronal neurocan and matures simultaneously with synapses (Pyka et al., 2011). In adult mice, neurocan expression becomes decreased while brevican, aggrecan, and tenascin R become upregulated.

Both ECM components released by neurons and astrocytes are essential for ECM generation (Geissler et al., 2013). Such molecules tend to accumulate especially in ECM structures termed perineuronal nets (PNNs). These consist of chondroitin sulfate proteoglycans, tenascin-R, hyaluronic acid and link proteins. PNNs are found predominantly on the soma and dendrites of parvalbumin-expressing GABAergic neurons (Hartig et al., 1992), however, excitatory pyramidal neurons have also been shown to bear PNNs (Carstens et al., 2016; Lensjø et al., 2017; Morikawa et al., 2017). Both PNN and ECM formation impairments are associated with neurodegenerative and psychiatric disorders including epilepsy, Alzheimer's disease and schizophrenia (Heck et al., 2004; Pitkänen et al., 2014;

Dzyubenko et al., 2016; Song and Dityatev, 2018). Hence, it is of importance to study not only how factors released by cells impact the ECM, but also how molecules and receptors located at the plasma membrane, Lrp1 included, interact with the ECM and modify its composition.

Lrp1 AND LIPID RAFTS

Lipid rafts are regions of the plasma membrane enriched in cholesterol and sphingolipids that are involved in assembling protein complexes for cell signaling events (Brown and London, 1998, 2000; Simons and Toomre, 2000). In the CNS, lipid rafts are essential for synaptic integrity and they are implicated in the pathogenesis of neurodegenerative diseases (Hicks et al., 2012; Rushworth et al., 2013). Although Lrp1 has been firstly found to localize nearly exclusively to coated pits in, for example, vascular smooth muscle cells (Weaver et al., 1996), Lrp1 localization to caveolae, a specialized type of lipid rafts, was later shown by Boucher et al. (2002) on the example of human fibroblasts. In neurons and neuronal-like PC12 and N2a cells, Lrp1 localizes, at least partially, to lipid rafts (Laudati et al., 2016). Upon the disruption of lipid rafts by methyl-β-cyclodextrin, Lrp1-mediated signaling is impaired, while ligand binding and endocytosis capacities remain intact (Laudati et al., 2016). The authors suggest that the presence of Lrp1 in lipid rafts in neuronal cells is due to the scaffolding activity of PSD-95. PSD-95 is a constituent protein of the post-synaptic complex in excitatory synapses (El-Husseini et al., 2000) and functions in stabilization of dendritic spines (Ehrlich et al., 2007). Lrp1, similarly, is present at the synapse and is known to interact with PSD-95 and to affect NMDAR functioning, long-term potentiation (LTP) and synaptic signaling (May et al., 2004; Liu et al., 2010; Nakajima et al., 2013). A decrease in PSD-95 levels upon Lrp1 deletion has been previously reported for the hippocampi of the α CAMKII-Cre-Lrp1 KO mice (Liu et al., 2010). Simultaneous application of methyl-β-cyclodextrin with either enzymatically inactive tissue plasminogen activator (tPA) or active α-2-M to both PC12 cells and cultured cerebellar granule neurons, blocks neurite outgrowth, as does RAP application (Laudati et al., 2016). The mechanism behind this effect has been traced to the fact that, in PC12 and N2a cells, upon treatment with these ligands, Lrp1 forms a complex with PSD-95 and NMDARs that activates tyrosine receptor kinase receptors, stimulates ERK1/2 activity and leads to various cellular responses, including neurite outgrowth (Bacskai et al., 2000; Mantuano et al., 2013). Interestingly, upon Lrp1 loss or blockage, a reduction in the formation, length, branching and outgrowth of neurites is found (Qiu et al., 2004; Nakajima et al., 2013; Safina et al., 2016). Lrp1 is found essential also for neurite growth inhibition mediated by myelin associated-glycoprotein and CNS myelin (Stiles et al., 2013) and has been found to mediate myelin phagocytosis itself (Gaultier et al., 2009).

By a comparison of various cell types, Wu and Gonias (2005) proposed that the presence of Lrp1 in different plasma membrane compartments depends on the cell type analyzed, as does Lrp1-mediated signaling. For example, although in neuronal and neuronal-like cells Lrp1 is found both in lipid rafts and lipid raft-free membrane compartments, in vascular smooth muscle cells and CHO-K1 cells Lrp1 is present mostly in lipid raft-free membrane compartments (Wu and Gonias, 2005). Lrp1 distribution in the cell membrane remains nevertheless dynamic, as the receptor can translocate from lipid-rafts to clathrin-coated pits where it undergoes endocytosis (Boucher et al., 2002; Wu and Gonias, 2005) (**Figure 2**). The capacity of Lrp1 to shift between membrane compartments is influenced by plasma membrane microdomains and depends on available extracellular ligands. For example, insulin promotes Lrp1 localization to caveolae in mouse fibroblasts and adipocytes while platelet-derived growth factor (PDGF)-BB decreases it (Zhang et al., 2004). As shown in the example of cultured hepatic cells and mouse embryonic fibroblasts (MEFs), endocytosis of Lrp1 can also occur in lipid rafts. In this case, the kinesin-3 family motor protein, KIF3B, promotes caveolin-dependent endocytosis of Lrp1 by forming a complex with Lrp1 and utrophin, a cytoskeleton protein vital for adequate muscle functioning (Zhang et al., 2004; Kanai et al., 2014).

In the CNS, the localization of Lrp1 to both lipid rafts and clathrin-coated pits has been proposed to be one of the mechanisms enabling a separation of Lrp1 endocytic and signaling activities and their independent regulation (Laudati et al., 2016). For example, PDGF-BB via the PDGF receptor

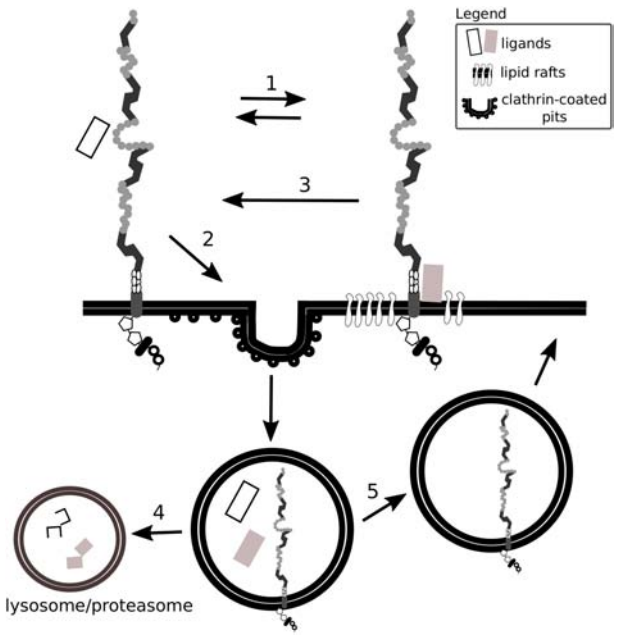

FIGURE 2 | Lrp1 interacts with ligands located in lipid rafts and clathrin-coated pits. Lrp1 distribution in the cell membrane is dynamic: Lrp1 can be found in both lipid raft-containing and lipid raft-free membrane compartments (1). Lrp1-mediated endocytosis requires clathrin and is restricted to lipid raft-free regions (2). Lrp1 can interact with lipid raft-associated receptors and proteins, translocate back to lipid raft-free compartments and mediate the endocytosis of the bound ligand (3). The ligand undergoes either lysosomal or proteasomal degradation (4) while Lrp1 is recycled back to the membrane (5).

(PDGFR) β and the Src is required for mediating the phosphorylation of tyrosine residues in the cytoplasmic tail of Lrp1 (Boucher et al., 2002; Loukinova et al., 2002). This interaction occurs only when Lrp1 is located to lipid rafts and therefore modulates Lrp1-dependent cell signaling in specific cell compartments (Boucher et al., 2002).

Taken together, interactions between Lrp1, the plasma membrane and ECM molecules highlight the presence of a heterogeneous modulation of Lrp1-dependent cell signaling in specific cell compartments and cell types.

Lrp1 INTERACTIONS WITH ECM MOLECULES

Given the multitude of Lrp1 ligands, it is not surprising that ECM molecules also interact with Lrp1. Lrp1 is primarily responsible for the endocytosis and subsequent transport of extracellular proteins to lysosomes (Herz and Strickland, 2001). Although Lrp1-mediated endocytosis occurs in non-lipid raft areas via clathrin-coated pits, due to the receptors' mobility, GPI proteins like the prion protein and other proteins associated with lipid rafts can also undergo Lrp1-clathrin-dependent endocytosis (Czekay et al., 2001; Wu and Gonias, 2005; Taylor and Hooper, 2007; Jen et al., 2010). Protein complexes and membrane-associated receptors are also Lrp1 ligands. With their endocytosis, Lrp1 further impacts on the protein composition of the plasma membrane and the ECM (Strickland et al., 2002; Gonias et al., 2004).

Although Lrp1's main function remains the endocytosis of extracellular ligands, it regulates the composition of the ECM also by controlling messenger ribonucleic acid (mRNA) expression and stability (Gaultier et al., 2006). In this way Lrp1 balances the protein levels of, for example, type III collagen, pigment epithelium-derived factor and urokinase-type plasminogen activator (uPA) receptor (uPAR)/Endo-180 in MEFs (Gaultier et al., 2006).

Lrp1 and HSPGs

Heparan sulfate proteoglycans are core constituents of the ECM implemented in ECM integrity and in facilitating the entry of molecules including morphogens, growth factors and viruses. Some protein ligands of Lrp1 are shown to bind with low affinity to glycosaminoglycan chains of surface HSPGs that in turn facilitate binding to and Lrp1-mediated endocytosis of these proteins (Wilsie and Orlando, 2003; Kanekiyo et al., 2011). Consistent with such a mechanism, the endocytosis of such proteins is blocked by heparin and heparitinase and does not occur in cells lacking HSPGs (Kanekiyo et al., 2011). HSPGs can be cleaved by heparanase-1, an enzyme that requires a proteolytic cleavage to become active. This process is partly dependent on Lrp1-mediated internalization of the inactive pro-enzyme (Vreys et al., 2005). Interestingly, both Lrp1 and HSPGs are required for the endocytosis of mature heparanase-1 (Vreys and David, 2007).

A summary of Lrp1 interactions with the HSPGs described in this section is presented in **Figures 3**, **4**.

In the liver, Lrp1 was previously shown to clear triglyceride-rich lipoproteins either independently or as a coreceptor with HSPGs (Mahley and Huang, 2007). A recent study questioned this idea and suggested instead that Lrp1 and HSPGs are rather responsible for independent clearing of distinct triglyceride-rich lipoproteins (Foley et al., 2013).

Lrp1 has been proposed to regulate the availability of lipoprotein binding sites by associating with HSPGs. Upon Lrp1 dissociation from HSPGs, more lipoprotein binding sites are revealed, and lipoprotein particle clearance becomes enhanced (Wilsie and Orlando, 2003). These findings were among the first to imply a role for Lrp1 firstly as a mediator of various signaling pathways, independent of its endocytic function and secondly as a regulator of HSPG function. HSPGs were also proposed by the same study to play an active role in lipoprotein uptake (Wilsie and Orlando, 2003). So far, Lrp1 and HSPGs have been shown to mediate the uptake of a complement inhibitor, the C4b-binding protein (Spijkers et al., 2008), the coagulation factor VIII (Sarafanov et al., 2001), cellular prion protein (Sunyach et al., 2003; Taylor and Hooper, 2007), connective tissue growth factor (CTGF) (Gao and Brigstock, 2003) and thrombospondin (Mikhailenko et al., 1995). HSPGs are furthermore found essential for the binding of protease Nexin-1 to Lrp1 (Li X. et al., 2006). Although the internalization of complexed (e.g., with tPA and uPA) and free Nexin-1 is mediated by Lrp1 (Knauer et al., 1997; Crisp et al., 2000), it can be partially substituted by an Lrp1-independent pathway. In Lrp1 deficient cells, the HSPG syndecan-1 takes over the internalization of free Nexin-1 and results in the activation of the Ras-ERK pathway instead of the PKA pathway that becomes active upon Lrp1-mediated internalization (Li X. et al., 2006). Given that Nexin-1 is involved in the regulation of extracellular proteolytic activity, the efficiency of its uptake and cellular responses triggered upon its internalization are crucial, especially for tumor cell invasiveness studies (Li X. et al., 2006).

Another HSPG member involved in Lrp1-mediated endocytosis is glypican-3. Glypican-3 has been shown to regulate embryonic growth by inhibiting the Hedgehog signaling pathway (Capurro et al., 2008). The binding of Hedgehog to glypican-3 triggers Hedgehog:glypican-3 complex endocytosis and degradation, impacting Hedgehog availability for binding with Patched (Capurro et al., 2008). Mechanistically, although glypican-3 and Sonic Hedgehog can directly bind to Lrp1, endocytosis is suggested to occur only upon simultaneous glypican-3 and Sonic Hedgehog interaction with Lrp1 (Capurro et al., 2012). This mechanism is found in MEFs and breast cancer cells, indicating a general role for Lrp1 and HSPGs in Hedgehog signaling (Capurro et al., 2012).

Lrp1 and Amyloid β

In neuronal cells, APP processing pathways are heterogeneous. In the non-amyloidogenic pathway, APP undergoes an α-and γ-secretase-mediated cleavage that leads to the generation of the soluble α APP fragment and APP C-terminal fragments. When APP is processed in this way, no amyloid β is generated. In contrast, in the amyloidogenic pathway, upon APP cleavage by the β-secretase BACE1 and γ-secretases, amyloid β is produced

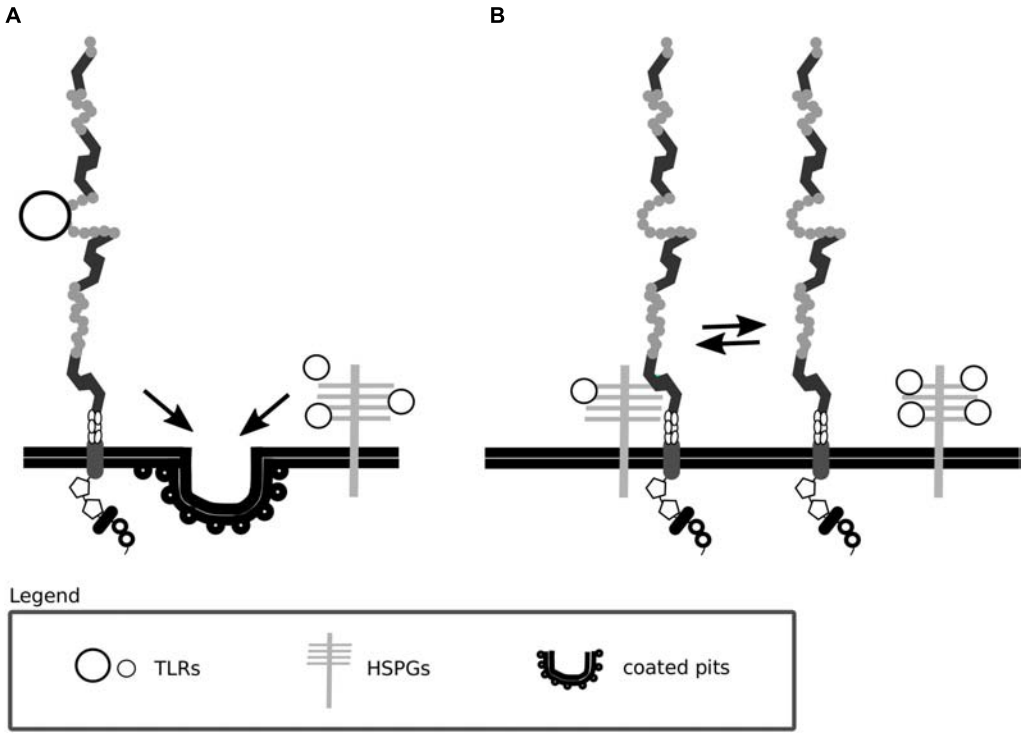

FIGURE 3 | Lrp1 interacts with heparan sulfate proteoglycans. **(A)** Lrp1 and heparan sulfate proteoglycans (HSPGs) are responsible for the independent endocytosis of distinct trigliceride-rich lipoproteins (TRLs) in the liver. **(B)** Lrp1 association with HSPGs determines the availability of lipoprotein binding sites, such that upon the dissociation of Lrp1 from HSPGs, more binding sites appear.

together with the soluble β APP and APP C-terminal fragments (Chow et al., 2010). Depending on the position of the cleavage, two principal forms of amyloid β can be generated: amyloid β with 40 amino acid residues and amyloid β with 42 amino acid residues. Both forms of amyloid β are released outside the cell in response to normal synaptic signaling and are incorporated into the ECM (Kamenetz et al., 2003; Cirrito et al., 2005). The majority of produced amyloid β is the shorter form. If the longer amyloid β form is produced, it exhibits a higher tendency to form fibrils and later on amyloid plaques that fail to be cleared and therefore accumulate in the brain parenchyma. Amyloid β overproduction, increased processing, aggregation and deposition in the form of plaques leads to neurotoxicity and neurodegeneration and is considered central for Alzheimer's disease development. It should be noted that, together with amyloid β, various ECM proteins are found in plaques and neurofibrillary tangles, for example ECM-located and cell-surface HSPGs (van Horssen et al., 2003). In this respect, ECM molecules have been analyzed and grouped with regard to the amyloid β form they interact with by Salza et al. (2017). The proteins investigated in this study included reelin, integrins, laminins and collagens. These authors and others showed that fibrillar and oligomeric forms of amyloid β can diversely interact with ECM and membrane proteins, influencing cell homeostasis (Genedani et al., 2010; de Jager et al., 2013; Salza et al., 2017).

For the CNS, the importance of amyloid β generation and its multiplex interactions with the ECM are highlighted by studies showing that the ECM regulates APP levels in fibroblasts and neuronal cells (Bronfman et al., 1996), amyloid β induces ECM degradation in rat astrocytes (Deb et al., 2003) and that both fibrillar and oligomeric forms of amyloid β associate with proteins present at synapses, a characteristic closely related to synapse loss and neurodegeneration observed in Alzheimer's disease (Selkoe, 2000; Spires-Jones and Hyman, 2014).

In the CNS, Lrp1 interacts with soluble and transmembrane forms of APP and impacts their internalization, processing and transactivation (Kounnas et al., 1995a; Knauer et al., 1996; Pietrzik et al., 2002) (**Figure 5**). Upon Lrp1 loss in fibroblasts and CHO cells, APP degradation and trafficking is impaired (Pietrzik et al., 2002). An introduction of a truncated, intracellular domain of Lrp1 to these cells is sufficient to restore APP processing and amyloid β production (Pietrzik et al., 2002). Furthermore, the presence of a functional Lrp1 on the cell surface was shown to reduce the amount of soluble α APP produced and to favor amyloidogenic processing of APP (Ulery et al., 2000).

As Lrp1 and APP are both substrates for γ- and β-secretases, Lrp1 not only stimulates but also interferes with the processing of APP (May et al., 2002; Lleo et al., 2005; von Arnim et al., 2005). APP cleavage is favored when both Lrp1 and APP are present; however, upon Lrp1 overexpression, the cleavage of APP becomes impaired because Lrp1 competes with APP for binding to BACE1 (Lleo et al., 2005; von Arnim et al., 2005; von Einem et al., 2010). Upon γ-secretase-mediated cleavage of Lrp1 (May et al., 2002), the intracellular domain translocates to the nucleus

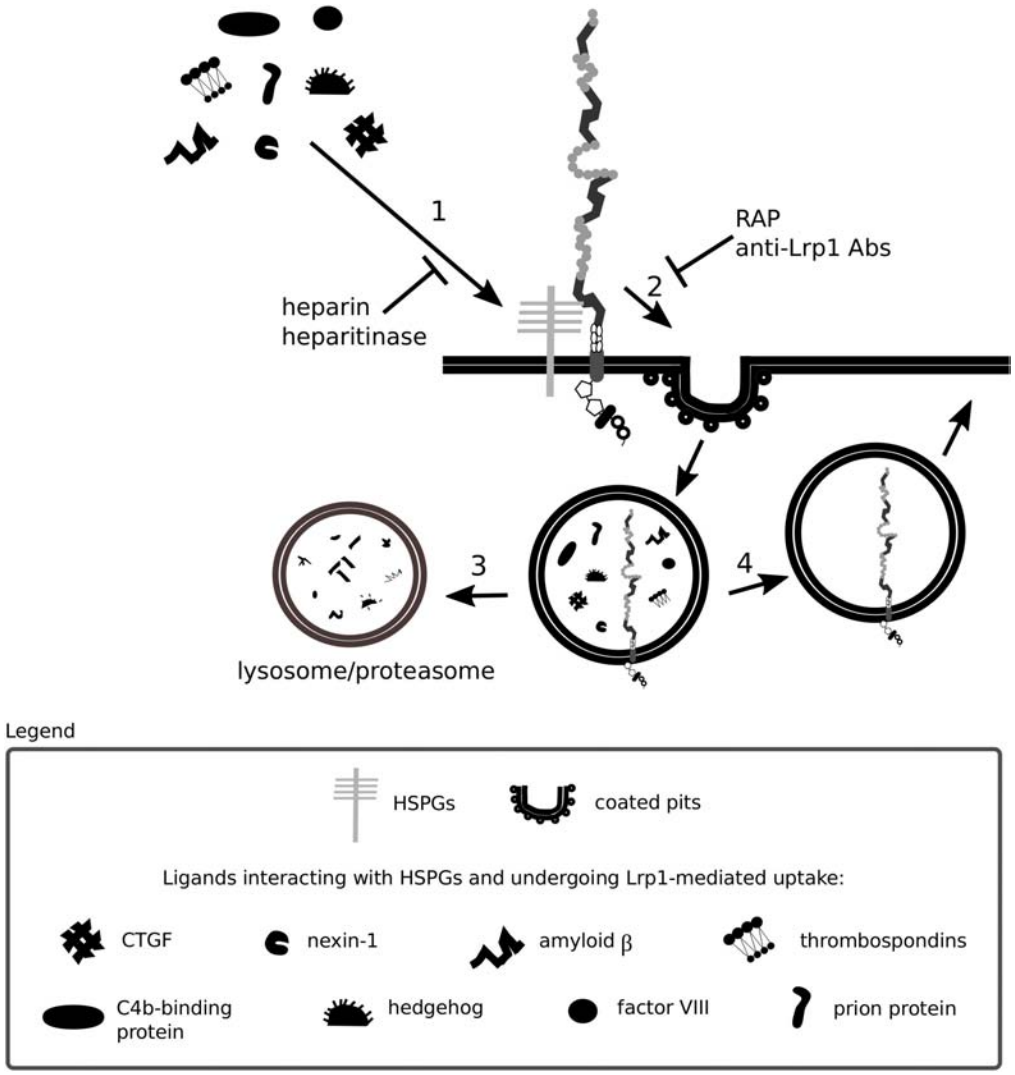

FIGURE 4 | Heparan sulfate proteoglycans act as bridging molecules. Various ligands, including connective tissue growth factor (CTGF) and the prion protein, have been shown to bind to heparan sulfate proteoglycans (HSPGs) (1). After association with HSPGs, the binding of the ligand to Lrp1 is facilitated and Lrp1-mediated endocytosis is triggered (2). Upon endocytosis, the molecules are transported to lysosomes/proteasomes for degradation (3) and Lrp1 is recycled back to the membrane (4). The depicted processes are inhibited both by blockage of Lrp1 and HSPGs.

and impacts APP-mediated signaling by interacting with the transcriptional modulator, Tip60 (May et al., 2002; Kinoshita et al., 2003). Lrp1 expression is regulated by APP itself as the APP:FE-65:Tip60 complex is able to suppress the transcription of the Lrp1 promoter (Liu et al., 2007). As a consequence, in fibroblasts of APP knock-out mice Lrp1 expression is increased (Liu et al., 2007). Interestingly, increased levels of APP can lead to a decreased production of shed Lrp1, impairing amyloid β clearance (von Einem et al., 2010).

Fibrils of amyloid β do not accumulate in excessive amounts in healthy individuals due to several efficient clearance mechanisms: extracellular proteolysis, BBB transport, efflux of soluble amyloid β to the peripheral circulation and receptor-mediated endocytosis (Deane et al., 2009; Ramanathan et al., 2015). Lrp1 is vital for the production, internalization and catabolism of amyloid β (Kounnas et al., 1995a; Knauer et al., 1996; Pietrzik et al., 2002; Deane et al., 2004, 2008; Lillis et al., 2008) (**Figures 5**, **6**), and in the brains of Alzheimer's disease patients, according to some studies, Lrp1 levels are significantly reduced (Kang et al., 1997, 2000; Jaeger and Pietrzik, 2008; Shinohara et al., 2017).

Amyloid β has so far been shown to form complexes with ApoE, lactoferrin, prion protein and activated α-2-M that undergo Lrp1-mediated endocytosis (Qiu et al., 1999; Yang et al., 1999; Kang et al., 2000; Laurén et al., 2009; Rushworth et al., 2013). Monomeric forms of amyloid β can also bind directly to the extracellular ligand-binding domains of Lrp1 and undergo endocytosis (Deane et al., 2004). Microglia were shown to migrate to plaques and engulf amyloid β predominantly via micropinocytosis (Frackowiak et al., 1992; Mandrekar et al., 2009; Lee and Landreth, 2010). Lrp1-mediated amyloid β

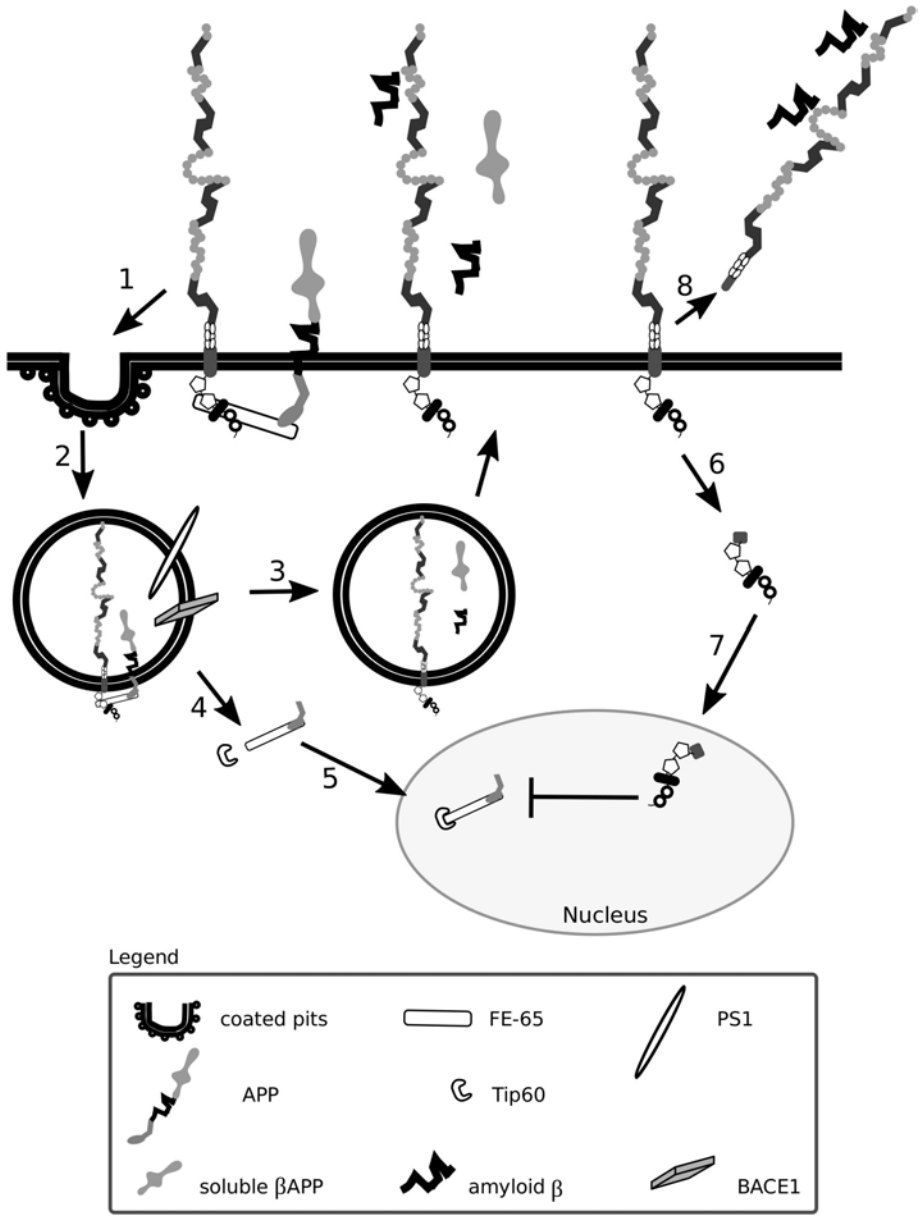

FIGURE 5 | Lrp1 is crucial for the uptake and processing of amyloid precursor protein. The cytoplasmic tail of Lrp1 interacts with the cytoplasmic tail of amyloid precursor protein (APP) via the bridging molecule FE-65. This results in the endocytosis of the Lrp1:APP:FE-65 complex (1) and subsequent proteolysis of APP by the enzyme BACE1 and proteinase presenilin-1 (PS1), which is part of the γ-secretase complex (2). The proteolysis results in the generation of soluble β APP and amyloid β peptides that are released outside the cell in recycling vesicles, like Lrp1 (3). The cytoplasmic tail of APP, after γ-secretase cleavage, forms a complex with FE-65 that interacts with the transcriptional modulator Tip60 (4). This complex translocates to the nucleus where it suppresses the transcription of the Lrp1 promoter, influencing Lrp1-mediated processes (5). Upon γ-secretase-mediated cleavage of Lrp1 (6), its cytoplasmic tail can influence APP processing by competing with the intracellular domain of APP complexed with FE-65 for binding with Tip60 in the nucleus (7). After β-secretase cleavage, the shed extracellular domain of Lrp1 can bind to amyloid β peptides and enhance their clearance (8).

clearance in pericytes helps prevent amyloid β deposition in the cerebrovasculature (Sagare et al., 2013). Lrp1 expressed on the surface of endothelial cells at the BBB mediates rapid clearance of amyloid β from the brain parenchyma via transcytosis and degradation (Nazer et al., 2008; Yamada et al., 2008; Pflanzner et al., 2011). In the periphery, β-secretase cleaved, shed, soluble Lrp1 can bind amyloid β, further enhancing its clearance from the brain (Sagare et al., 2007). Supporting amyloid β removal via Lrp1 from the system are the liver, spleen, and kidney (Ramanathan et al., 2015). Lrp1 impacts amyloid β metabolism also by activating signaling pathways. By modulating RhoA signaling in Schwann cells, Lrp1 influences cell adhesion and migration (Mantuano et al., 2010). RhoA has been shown to facilitate dynamin-dependent amyloid β endocytosis in neuronal

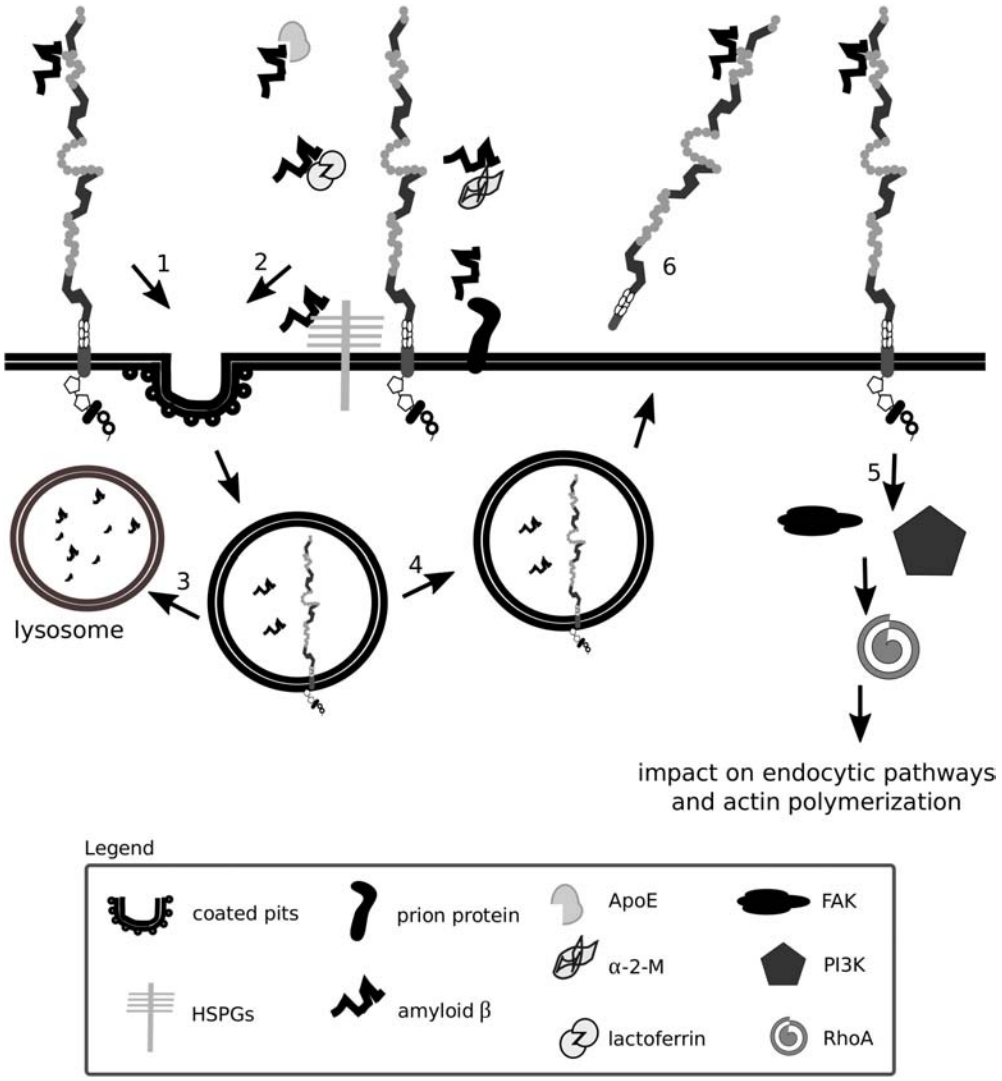

FIGURE 6 | Lrp1 is a receptor mediating amyloid β uptake. Lrp1 can regulate the internalization of amyloid β in several ways. Amyloid β can directly interact with ligand-binding domains of Lrp1 (1). Amyloid β can interact with several molecules including α-2-macroglobulin (α-2-M), apolipoprotein E (ApoE) and heparan sulfate proteoglycans (HSPGs), which bridge it to Lrp1 and facilitate its endocytosis (2). Upon endocytosis, amyloid β can either undergo degradation (3) or, to a smaller extent, be recycled back to the extracellular space (4). Lrp1 can also influence signaling pathways, especially the RhoA pathway that can facilitate amyloid β clearance by stimulating actin polymerization (5). The shed extracellular domain of Lrp1 additionally sequesters soluble amyloid β present at the blood-brain barrier and in the circulation (6).

cells (Yu et al., 2010). It is thereby proposed that Lrp1 could activate RhoA and facilitate RhoA-dependent endocytosis of amyloid β (Kanekiyo and Bu, 2014). HSPGs have been identified to be required for the binding of amyloid β and act as a coreceptor for Lrp1 in the process of neuronal amyloid β uptake (Kanekiyo et al., 2011, 2013; Kanekiyo and Bu, 2014). Astrocytic Lrp1 has also been shown to be essential for the uptake and degradation of amyloid β (Kanekiyo and Bu, 2014; Liu et al., 2017). Whether Lrp1 requires HSPGs for amyloid β uptake also in this cell type remains to be elucidated, however, it is suggested that astrocytic Lrp1 affects the degradation of amyloid β in the ECM by modulating the levels of matrix metalloprotease (MMP)-2 and MMP-9 (Yin et al., 2006; Liu et al., 2017).

In summary, although the involvement of Lrp1 in APP and amyloid β processing and Alzheimer's disease pathogenesis is undeniable, given the complexity of interactions, their true nature may be hidden by the variability in cell lines and the systems used, and is still yet to be fully unraveled.

Impact of Lrp1 on Cell Adhesion, Migration and Cell Signaling

The ECM is vital for many cellular processes including cell proliferation, survival, differentiation and migration. In order for the cell to migrate, the ECM surrounding it needs to be degraded. This is performed by a variety of proteases including MMPs and

serine proteases and tightly controlled by their inhibitors. Both uPA and tPA proteases mediate for example the activation of plasminogen to plasmin that leads to the digestion of the ECM and MMP activation (Werb et al., 1977; Mignatti and Rifkin, 1993; Sappino et al., 1993). One of the first reports showing Lrp1 involvement in ECM turnover and cell migration was published by Okada et al. (1996). Here, by using a Transwell filter migration assay, the authors discovered that the presence of Lrp1 facilitates the migration of smooth muscle cells on fibronectin-coated filters. These observations were reproduced by Wijnberg et al. (1997). The stimulating effect of Lrp1 was not apparent when smooth muscle cells were tested on a collagen gel invasion assay, indicating that the effects of Lrp1 depend on the composition of the matrix (Okada et al., 1996). The addition of uPA, tPA or α -2-M—potent Lrp1 ligands—to the cells is found to be stimulatory for cell migration, neurite outgrowth and axon elongation (Friedman and Seeds, 1995; Holtzman et al., 1995; Okada et al., 1996; Seeds et al., 1996, 1999; Qiu et al., 2004; Lillis et al., 2005).

Lrp1 directly interacts with uPA and the plasminogen activator inhibitor-1 (PAI-1). As the binding affinity of PAI-1 and uPA alone is lower than when in a complex with the uPAR, Lrp1-mediated endocytosis occurs only after PAI-1 binds to the uPA:uPAR complex (Herz et al., 1992; Nykjaer et al., 1994; Nykjaer et al., 1997; Czekay et al., 2001). By the binding and subsequent endocytosis of such complexes, Lrp1 reduces uPAR levels on the cell surface. In this manner, Lrp1 regulates uPAR-mediated proteolysis of the ECM (Conese et al., 1995; Weaver et al., 1996; Nykjaer et al., 1997; Degryse et al., 2001) and impacts plasminogen conversion to plasmin (Weaver et al., 1997). By regulating uPAR levels on the cell surface and decreasing uPA-mediated plasminogen activation, Lrp1 inhibits fibronectin remodeling (Gaultier et al., 2010). By regulating uPAR levels, Lrp1 also influences plasmin-mediated cleavage of ECM glycoproteins lacking collagen in their composition, as well as plasmin-dependent activation of MMP-2 and MMP-9 that degrade the ECM by cleaving collagens (Mignatti and Rifkin, 1993; Brinckerhoff and Matrisian, 2002).

Upon Lrp1 silencing from MEFs, collagen remodeling is increased (Gaultier et al., 2010). This occurs independently of the membrane type-1 matrix metalloprotease (MT1-MMP), a metalloprotease previously shown to impact collagen remodeling and Lrp1 cleavage in malignant cells (Rozanov et al., 2004; Sabeh et al., 2004; Lehti et al., 2009; Sabeh et al., 2009). As upon treatment of MT1-MMP-deficient and wild type skin fibroblasts with RAP collagen remodeling becomes enhanced in both cell types, it hints at the presence of an MT1-MMP-independent pathway that becomes active upon Lrp1 signal blockade.

PAI-1 facilitated migration in rat smooth muscle cells is Lrp1-dependent (Degryse et al., 2004). Interaction of the extracellular heat shock protein 90 with Lrp1 activates Akt 1/2 kinases that facilitate the migration of skin cells to the wound and promote its closure (Tsen et al., 2013). Lrp1 was shown to interact with PDGFR β and regulate PDGFR β cell surface levels and PDGFR β signaling which is of importance, among others, for the integrity of vascular walls and cell chemotaxis (Boucher et al., 2002, 2003; May et al., 2005; Craig et al., 2013; Strickland et al., 2014).

Actin organization and cell migration in smooth muscle cells are, for example, controlled by PDGFR β phosphatidylinositol 3-kinase (PI3K) activation that is Lrp1-dependent (Zhou et al., 2009). The interaction of PDGF β with Lrp1 can also result in the activation of the mitogen-activated protein kinase (MAPK) signaling cascade—a major player in cell survival and proliferation (Takayama et al., 2005).

Mouse embryonic fibroblasts respond with migratory behavior on fibronectin and vitronectin matrixes upon interaction of thrombospondin 1 and the calreticulin:Lrp1 complex (Orr et al., 2003a). The impaired cell migration observed upon Lrp1 loss in MEFs was suggested by Orr et al. (2003a) to be a result of improper lamellipodia generation in Lrp1-deficient cells.

Cell migration is also regulated by Lrp1 via blockage of the effect of stimulatory ligands. This is the case for ApoE, which has been shown to inhibit PDGF-B-dependent smooth muscle cell migration by binding to Lrp1 (Swertfeger et al., 2002). This interaction results in the activation of protein kinase A and increase in intracellular cAMP levels (Swertfeger et al., 2002; Zhu and Hui, 2003) and is of particular importance for protection against vascular disease. ApoE-deficient mice exhibit atherosclerosis (Plump et al., 1992; Zhang et al., 1994), while Lrp1 loss from smooth muscle cells enhances vascular cell activation and also leads to atherosclerosis (Boucher et al., 2003).

Weaver et al. (1997) detected moreover that MEFs that lacked Lrp1 and were plated on serum-, vitronectin-, and fibronectin-coated plates migrated faster than wild type MEFs upon subjection to a scratch assay in the presence of PDGF-BB. This effect was not detectable on Matrigel- and type I collagen-plated cells, highlighting the varying effects of Lrp1 in different matrices. The increased migration capacities of MEFs lacking Lrp1 were suggested by the study to be a result of increased surface levels of the uPAR in these cells (Weaver et al., 1997). As mentioned earlier, Lrp1 can bind PAI-1:uPA:uPAR complexes and facilitate their endocytosis (Nykjaer et al., 1997). This in turn leads to altered levels of the uPAR on the cell surface (Weaver et al., 1997). When cultured under high serum conditions, fibroblasts lacking Lrp1 show increased levels of Rac, a GTPase vital for lamellipodia formation and cell spreading (Ma et al., 2002). In the Lrp1-deficient MEFs, analyzed in the study of Weaver et al. (1997), elevated migration is proposed to be a result of persistent Rac activity and/or increased proteolysis. This reasoning is in agreement with studies showing that, by interacting with proteases, Lrp1 protects ECM proteins from degradation (Herz and Strickland, 2001; Strickland et al., 2002).

A requirement enabling the cell to migrate is the restructuring or disassembly of integrin-linked focal adhesion complexes. Focal adhesion disassembly is mediated by ECM proteins including thrombospondin 1 and 2. Thrombospondins are large oligomeric ECM proteins that participate in cell-cell and cell-matrix interactions by binding to other ECM molecules, cytokines and cell surface receptors. Thrombospondins are considered vital for the development of the CNS, as a lack of thrombospondins 1/2 impairs astrocyte-mediated synaptogenesis and a lack of thrombospondin 1 impairs neural progenitor proliferation and neuronal differentiation *in vivo* and *in vitro*

(Christopherson et al., 2005; Lu and Kipnis, 2010). Thrombospondin 1 has been shown to interact with Lrp1, HSPGs, calreticulin and integrins in various cell types (McKeown-Longo et al., 1984; Mikhailenko et al., 1995, 1997; Merle et al., 1997; Li S. S. et al., 2006; Staniszewska et al., 2007).

Thrombospondins favor cell migration by disassembling and detaching focal adhesions from the ECM—processes dependent on calreticulin and Lrp1 and requiring intact lipid rafts (Orr et al., 2003a,b; Barker et al., 2004; Talme et al., 2013). Both the intact thrombospondin 1 and its cleaved N-terminal domain mediate focal adhesion disassembly (Murphy-Ullrich et al., 1993). The sequence responsible for this effect and binding to calreticulin is located in the N-terminal domain of thrombospondin 1, and a peptide mimetic termed hep I was developed to specifically study interactions of this thrombospondin 1 domain (Murphy-Ullrich et al., 1993). The signaling mediated by thrombospondin 1 via the calreticulin-Lrp1 complex is a process independent of Lrp1-mediated thrombospondin 1 endocytosis (Mikhailenko et al., 1995, 1997) (**Figure 7A**). Although the sequence responsible for the binding of thrombospondin 1 to Lrp1 and subsequent endocytosis is also located to the N-terminal domain, it does not include the sequence mimicked by hep I, as hep I lacks Lrp1 binding capacity (Orr et al., 2003b; Wang et al., 2004). Interactions of the calreticulin:Lrp1 complex with thrombospondin 1 have been evidenced to result in a temporary association of the G protein α i-2 subunit with Lrp1. This interaction results in FAK and Src phosphorylation (Thy-1-dependent) and activation of ERK, PI3K, and RhoA inactivation and favors cell migration. These events do not occur upon either loss of calreticulin or Lrp1 (Orr et al., 2002, 2003a,b, 2004; Barker et al., 2004).

Thrombospondins also function as bridging molecules between Lrp1 and its extracellular ligands that facilitate their clearance (**Figure 7B**). Thrombospondin 1 was found to participate in the clearance of vascular endothelial growth factor via Lrp1 in the ovary (Greenaway et al., 2007).

Notch signaling is crucial for proper development, hair pigmentation and homeostasis, and mediates short-range, direct communications between neighboring cells (Schouwey et al., 2007). Lrp1 facilitates Notch 3 *trans*-endocytosis and thrombospondin 2-mediated potentiation of Notch 3 signaling (Meng et al., 2009, 2010), highlighting that the ECM is involved in the modulation of Notch function, and Lrp1 and thrombospondins support non-cell autonomous short-range signaling (Meng et al., 2010).

The activity of MMPs, adamalysin-like metalloproteinases with thrombospondin domains and membrane-anchored adamalysins, is tightly regulated by four members of the tissue inhibitors of the MMPs (TIMPs) family. In the TIMP family, TIMP3 is unique as it controls the activity of all three metalloproteinase classes. The lack of TIMP3 leads to excessive ECM turnover caused by uncontrolled proteinase activity. TIMP3 extracellular levels are regulated by Lrp1-mediated endocytosis (Scilabra et al., 2013; Thevenard et al., 2014). The shed, soluble Lrp1 competes with cell-surface Lrp1 for TIMP binding and results in increased extracellular levels of TIMP, promoting its inhibitory action (Scilabra et al., 2013, 2017).

In addition, Lrp1 mediates the endocytosis of MMP-2, MMP-9, and MMP-13 and adamalysin-like metalloproteinases with thrombospondin domains 4 and 5, preventing their proteolytic and signaling functions (Emonard et al., 2005; Yamamoto et al., 2014). Thrombospondin 1/2 was also evidenced to interact with MMP-2 and MMP-9 (Bein and Simons, 2000). Upon binding of pro-MMP-2 to thrombospondin 2, the complex associates with Lrp1 and undergoes endocytosis, which can be blocked by an anti-thrombospondin 1 antibody (Yang et al., 2001; Emonard et al., 2004).

MMP-2 activity favors angiogenesis and endothelial cell invasion in malignant gliomas. In thrombospondin 2 knock-out mice, microvessel density is enhanced and MMP-2 levels are significantly upregulated (Fears et al., 2005). MMP-2 levels and invasion capabilities of microvessel endothelial cells in these mice are reduced upon addition of thrombospondin 2. This effect is blocked by downregulating Lrp1. Curiously, the endocytosis of pro-MMP-2 can also take place by formation of complexes with TIMP-2 and is Lrp1-dependent. This interaction, however, does not require thrombospondin (Emonard et al., 2004).

Vital for the normal function of elastic arteries are collagens and elastins, prominent members of the ECM. It is appreciated that excess protease activity can contribute to the elastic fiber degradation in these vessels. Smooth muscle cells are essential for establishment of proper vessel diameter, correct deposition of the ECM and assembly of elastic fibers. The deletion of Lrp1 from the embryo proper results in severe impairments in investment of vessels with pericytes and vascular smooth muscle cells. The deletion of Lrp1 from vascular smooth muscle cells leads to increased proliferation and aneurysms (Boucher et al., 2003; Nakajima et al., 2014). The deletion of Lrp1 from smooth muscle cells also impacts the integrity of the vasculature by altering PDGFR β signaling and levels of various ECM molecules pivotal for proper vessel development, contributing to the development of hypertension, atherosclerosis and other cardiovascular diseases (Zhou et al., 2009; Strickland et al., 2014). Alongside a lack of Lrp1 in smooth muscle cells, matrix decomposition becomes dysregulated due to CTGF protein level upregulation (Muratoglu et al., 2013). CTGF accumulation is traced to the missing Lrp1-mediated clearance of CTGF (Segarini et al., 2001). Lrp1-mediated endocytosis of CTGF occurs tissue-independently as it has also been shown to take place in the liver (Gao and Brigstock, 2003; Gerritsen et al., 2016). The disrupted elastin fiber architecture and ECM disorganization upon Lrp1 deletion from smooth muscle cells was found by Muratoglu et al. (2013) to increase protein levels of MMP-2, MMP-9, MT1-MMP, and serine protease high-temperature requirement factor A1 (HtrA1). HtrA1 is abundant in smooth muscle cells, degrades many ECM proteins including aggrecan, fibulin-5 and collagens and has been previously associated with disorganized elastic fibers (Hadfield et al., 2008; Vierkotten et al., 2011). Lrp1 was found by Muratoglu et al. (2013) to regulate the levels of HtrA1 in the vessel wall by rapid endocytosis of this protease, thereby impacting vessel wall integrity.

In conclusion, the presence of different tissue-dependent Lrp1-mediated mechanisms for serine protease and MMP

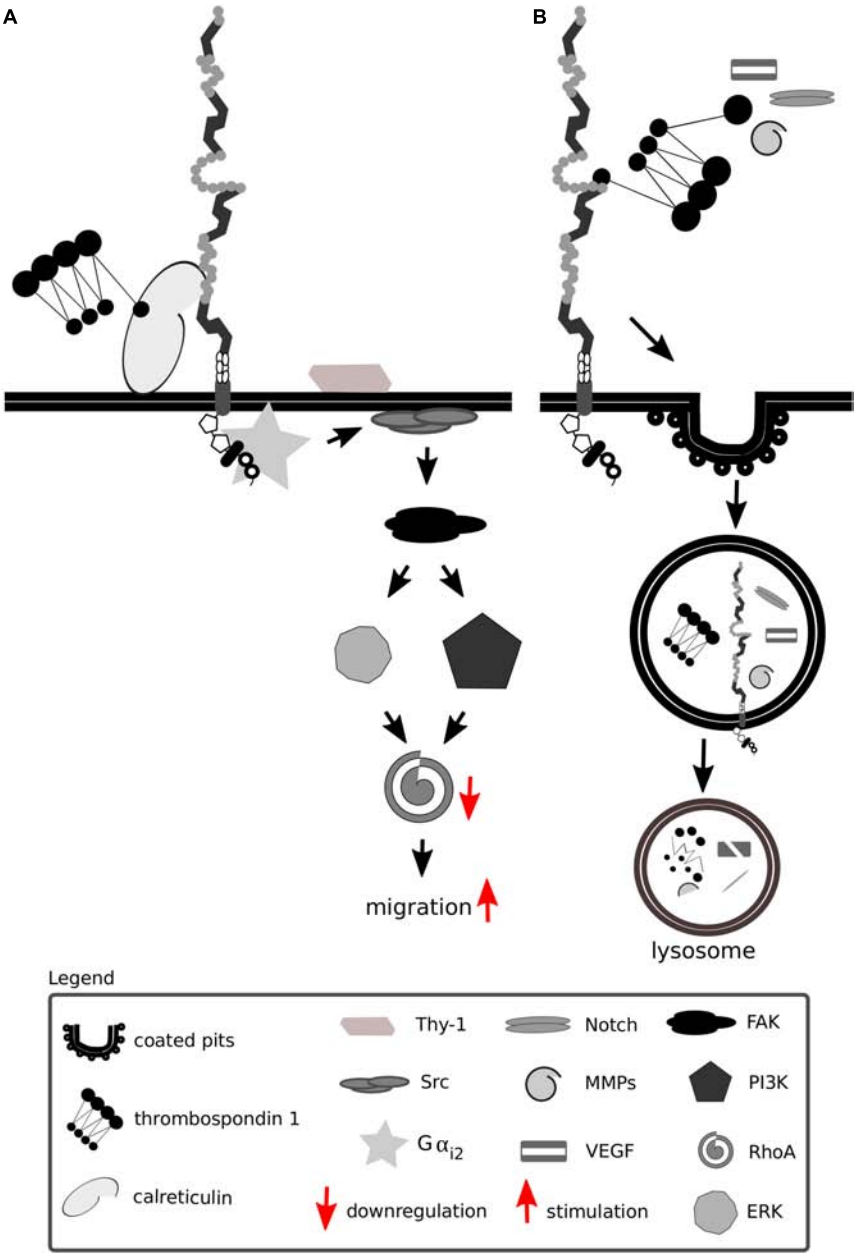

FIGURE 7 | Lrp1 interacts with thrombospondins. **(A)** Upon binding of thrombospondin 1 to calreticulin, its binding to Lrp1 is facilitated. The Lrp1:calreticulin complex leads to the association of the G protein α_{i2} that in turn phosphorylates FAK and Src. Required for the effect of thrombospondin on Src activation is additionally the GPI-linked protein Thy-1. The activation of Src and FAK further activates the ERK and phosphatidylinositol 3-kinase (PI3K) pathways and leads to the downregulation of RhoA, focal adhesion disassembly and cell migration. **(B)** Thrombospondins can function as bridging molecules, enabling Lrp1-mediated endocytosis of various molecules, including Notch, vascular endothelial growth factor (VEGF) and matrix metalloproteinases (MMPs).

clearance highlights that Lrp1-mediated uptake and degradation provides a vital mechanism for limiting excessive extracellular proteolytic activity (Yang et al., 2001). By eliciting control over MMP extracellular levels, Lrp1 additionally modifies cell adhesion and migration capabilities that are crucial not only for processes like wound healing and angiogenesis but also for tumor growth (Fears et al., 2005; Van Gool et al., 2015). For example, EGF-mediated downregulation of Lrp1 activity in astrocytic tumors impacts ECM composition and may contribute to tumor invasiveness (Hussaini et al., 1999).

Lrp1 Binding to and Regulation of Integrins

Integrins are transmembrane glycoprotein receptors consisting of α and β heterodimers. Integrins have been implemented in molecular adhesion, cell survival and migration (Pan et al., 2016).

The process of binding of integrins to the ECM provokes a change in conformation of integrins that connects the ECM with the cell and leads to adhesion. An integrin that is especially crucial for triggering the cell-matrix interactions is β1 integrin. β1 integrin outside-in signaling leads to integrin recruitment and clustering, phosphorylation of focal adhesion kinase and the assembly of focal adhesions, promoting cell spreading and adhesion.

Fibronectin is a ubiquitous and multifunctional ECM protein vital for cell adhesion, migration and differentiation. Lrp1 participates in the catabolism of fibronectin by mediating fibronectin endocytosis (Salicioni et al., 2002). In particular, Lrp1 prevents fibronectin upregulation on the cell surface and in the cell-secreted medium, as shown for MEFs and Chinese Hamster ovary cells (Salicioni et al., 2002).

Tissue transglutaminase is a ubiquitously expressed Ca^{2+}-dependent protein crosslinking enzyme present in the cytoplasm, at the cell surface and in the ECM. Fibronectin and β integrins are major interaction partners of tissue transglutaminase that impact on cell adhesion and migration (Turner and Lorand, 1989; Akimov et al., 2000) (**Figure 8**). Fibronectin, aside from being internalized in an Lrp1-dependent manner, also acts as a bridging molecule and enhances Lrp1-mediated surface tissue transglutaminase endocytosis (Zemskov et al., 2007).

Interaction of tissue transglutaminase with β integrins results in the formation of fibronectin-tissue transglutaminase-integrin complexes that stabilize the interactions of fibronectin with integrins (Akimov et al., 2000). The interaction of tissue transglutaminase with integrins facilitates their clustering and activates RhoA (Janiak et al., 2006).

Surface tissue transglutaminase has been recently shown to associate with Lrp1 and promote the formation of β1 integrin-Lrp1 complexes (Zemskov et al., 2007). As tissue transglutaminase associates with integrins, they are internalized by Lrp1 as a complex, resulting in a modification of cell-matrix interactions. Upon Lrp1 loss, transglutaminase activity of surface tissue transglutaminase is upregulated and cell adhesion enhanced (Zemskov et al., 2007).

Fibulin-5 is an ECM integrin-binding protein that is involved in elastic fiber formation (Yanagisawa et al., 2002). The binding of fibulin-5 to uPA stimulates plasminogen activation. This leads to the proteolysis of fibulin-5, its dissociation from integrins and stimulation of β1 integrin-mediated migration of MEFs, independently of the uPAR (Kapustin et al., 2012). Czekay et al. (2003) found, however, that if uPARs are associated with integrins and the uPA:PAI-1 complex binds to such an uPAR, integrins are internalized by Lrp1 together with the uPA:PAI-1:uPAR complex, influencing integrin functioning.

Lrp1 promotes β1 integrin activation via kindlin 2 and is considered to be a driver for the trafficking and proteasomal and lysosomal degradation of endocytosed activated β1 integrin via the protein kinase C (Wujak et al., 2017) (**Figure 9A**). Knock-in mutations in the intracellular NPxY2 motif of Lrp1, similarly to the knock-out of Lrp1, lead to elevated levels of immature β1 integrin on the cell surface, disrupting β1 integrin functionality (Salicioni et al., 2004; Rabiej et al., 2015; Wujak et al., 2017). Immature β1 integrin lacks the full glycosylation pattern that is acquired in the endoplasmic apparatus and the Golgi complex. Changes in glycosylation patterns are known to disturb transit through the Golgi apparatus, formation of complexes with α integrin subunits and ligand-binding affinities (Bellis, 2004). Knock-in mutations in the intracellular NPxY2 motif of Lrp1 lead moreover to reduced β1 integrin recycling and cause increased cell adhesion to collagen and fibronectin matrices and reduced cell migration of MEFs (Rabiej et al., 2015). This effect is due to the fact that the impaired Lrp1 endocytosis of β1 integrin leads to increased numbers of focal adhesions, increased focal adhesion kinase phosphorylation status and decreased MMP-2 and MMP-9 activity in MEFs and neurons (Rabiej et al., 2015) (**Figure 9B**).

Interactions of Lrp1 with β1 integrin are proposed to be similar to Lrp1 interactions with APP. The knock-in mutation in the intracellular NPxY2 motif of Lrp1 leads to surface accumulation of not only β1 integrin but also APP (Pietrzik et al., 2002; Rabiej et al., 2015). β1 integrin and APP are also endocytosed together by Lrp1 upon complex formation with the scaffolding protein Ran-binding protein 9, an interaction of importance for Alzheimer's disease pathogenesis and synaptic plasticity (Woo et al., 2012a,b).

In the CNS, β1 integrin is known for participating in neuronal migration and neurite outgrowth (Belvindrah et al., 2007b; Ribeiro et al., 2013; Rabiej et al., 2015), however, its function is not limited to cell adhesion and migration. β1 integrin is expressed by NSPCs and is vital for the formation of cell layers in the cerebral cortex (Belvindrah et al., 2007a). An *in vivo* conditional deletion of β1 integrin in radial glia cells leads to spontaneous seizures and reactive astrogliosis (Robel et al., 2009, 2015). β1 integrin presence is put forward as being inhibitory for astrocyte differentiation in adult hippocampal neural stem cells as well as in embryonic neural stem cells (Pan et al., 2014; Brooker et al., 2016). This inhibitory effect is mediated via the integrin-linked kinase (Pan et al., 2014; Brooker et al., 2016) and appears to be more prominent in female mice, as shown by Brooker et al. (2016). Interestingly, integrin-linked kinase, as a major downstream effector kinase of β1 integrin signaling, is vital for ECM deposition and controls its expression.

In a different β1 integrin mutant, β1 integrin loss restricted to astrocytes has been found to impact endothelial cell number at the neurovascular unit, blood vessel branching and aquaporin 4 levels (Venkatesan et al., 2015). Given that Lrp1 is found on astrocytes and contributes to vessel development as well as BBB integrity (Boucher et al., 2003; Nakajima et al., 2014; Fredriksson et al., 2015; Auderset et al., 2016) it is of interest for future studies to elucidate to what extent Lrp1 participates in β1 integrin-mediated effects in the developing CNS.

As Lrp1 was recently identified as a receptor for β1 integrins also in thyroid cancer cells (Theret et al., 2017), Lrp1 and integrins emerge as potential candidate genes for preventing cancer invasiveness.

Lrp1 has also been shown to bind β2 integrins located on leukocytes and monocytes (Spijkers et al., 2005; Cao et al., 2006). The interactions of Lrp1 with β2 integrins are suggested to modulate cell adhesion and migration by regulating integrin recycling, as shown in the example of macrophages (Cao et al., 2006). Hypercholesterolemia is proposed to induce

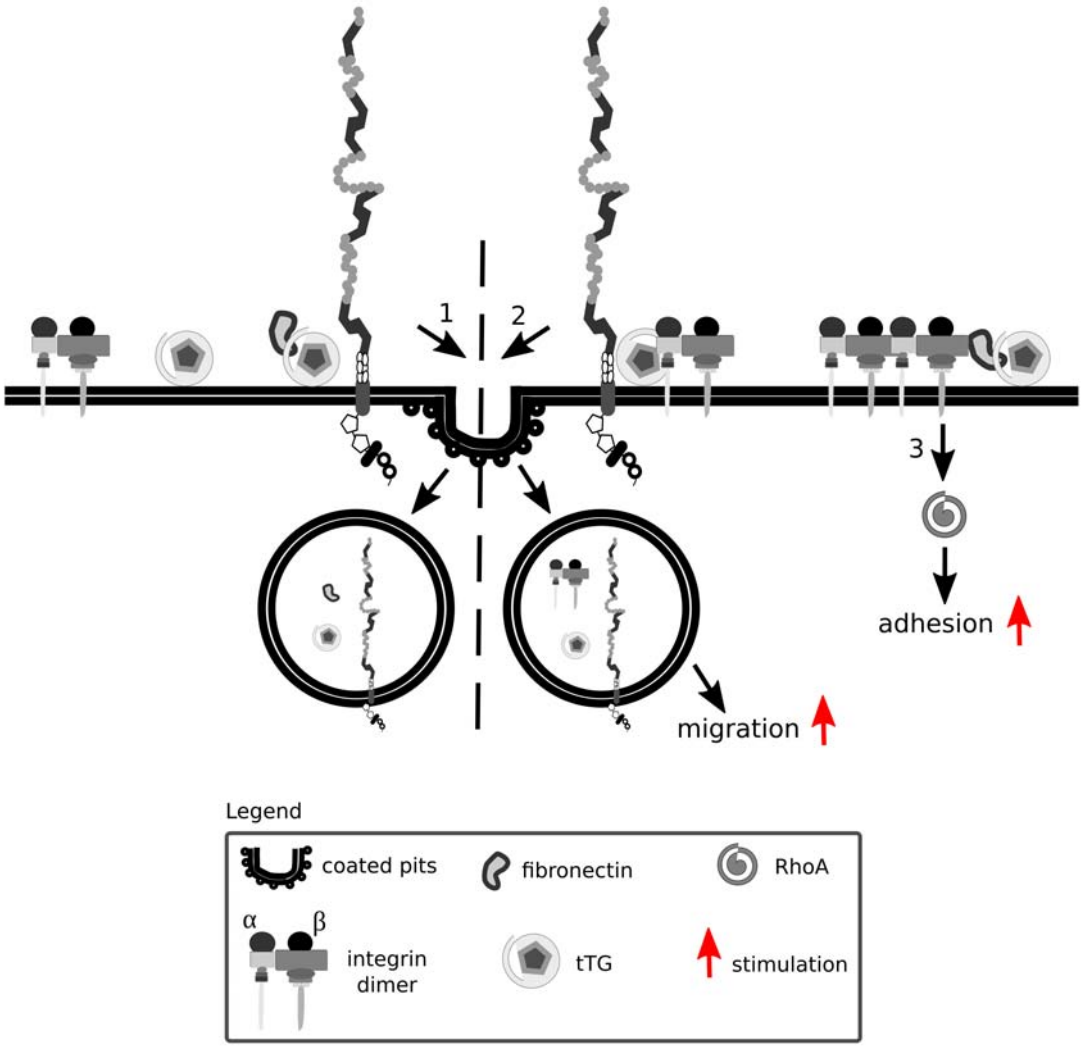

FIGURE 8 | Lrp1 is vital for integrin signaling and function. Integrins are formed by α and β heterodimers. Fibronectin and integrins can interact with tissue transglutaminase (tTG) and impact on cell migration and adhesion. Upon fibronectin binding, surface tTG is endocytosed by Lrp1 (1). tTG mediates the formation of Lrp1:integrin complexes that facilitate integrin endocytosis and cell migration (2). Interaction of tTG with integrins stabilizes fibronectin:integrin complexes and stimulates RhoA activation and cell adhesion (3).

hematopoietic stem/progenitor cell (HSPC) proliferation and their migration into lesioned sites, where they are suggested to undergo differentiation into leukocytes and form plaques found in arteriosclerosis patients (Wang et al., 2014). Vital for HSPC adhesion, migration and homing is β2 integrin (Wang et al., 2014). Loss of Lrp1 does not influence expression levels of β2 integrin, but leads to inhibition of HSPC adhesion, suggesting Lrp1 in this context impacts β2 integrin functioning (Wang et al., 2014).

Lrp1 Interactions With tPA

Tissue plasminogen activator is a serine protease that belongs to the chymotrypsin family, mostly known for its role in degrading the extracellular matrix components via activating plasmin. This glycoprotein is built up from the heavy A-chain and the light B-chain (**Figure 10**). The heavy A-chain is composed of the finger domain, EGF-like domain and Kringle 1 and 2 domains. The finger domain is responsible for binding to fibrin and the membrane receptors Annexin II and Lrp1 (Kagitani et al., 1985; Bu et al., 1992; Hajjar et al., 1994). The EGF-like domain is crucial for binding to the EGF receptor (Correa et al., 2011). The Kringle 1 domain is involved in the uptake of tPA in the liver and the Kringle 2 domain is vital for interactions with NMDARs and PDGFs (Kuiper et al., 1988; Fredriksson et al., 2004; Lesept et al., 2016). The light B-chain comprises the serine protease domain with the catalytic triad (His^{322}, Asp^{371}, and Ser^{478}), responsible for the proteolytic activity of tPA.

Unlike other members of the chymotrypsin family, tPA is secreted as a proteolytically active single chain form that can be subsequently processed into the equally proteolytically active

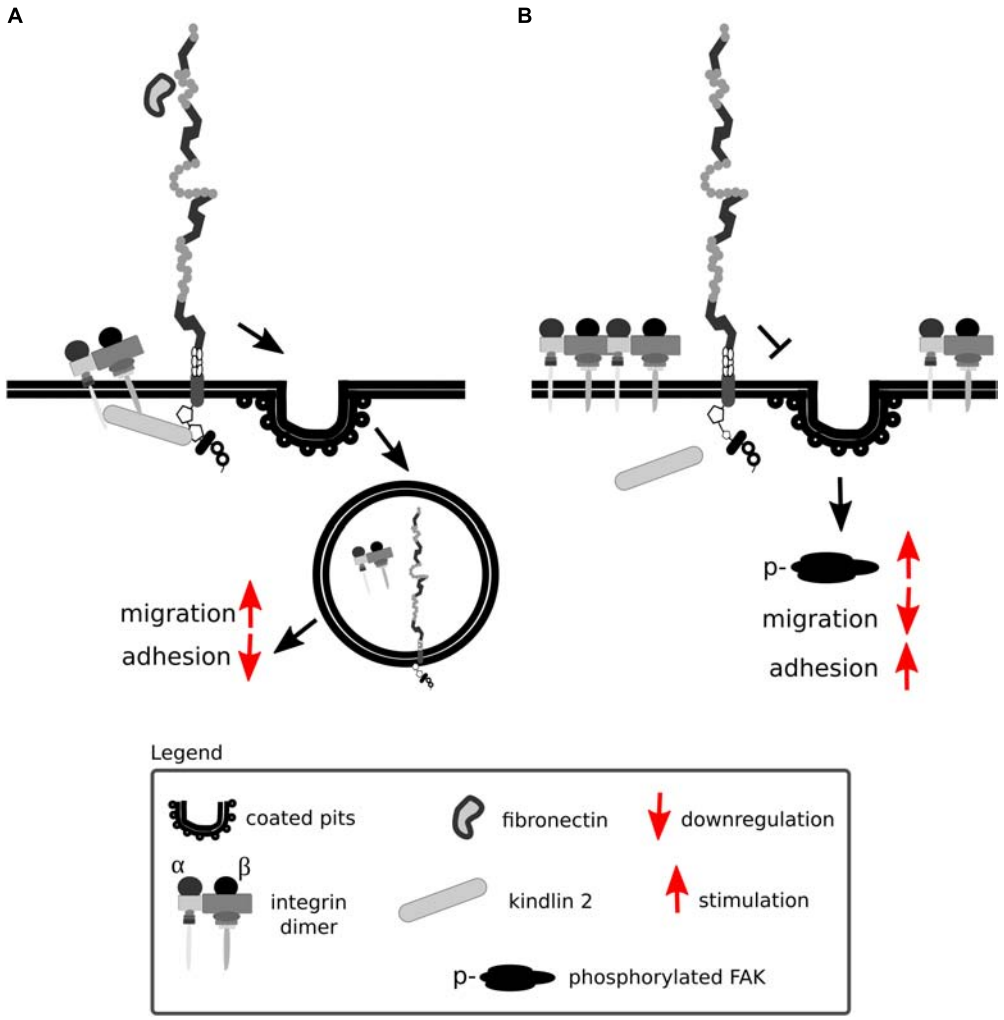

FIGURE 9 | Lrp1 mediates β1 integrin endocytosis. **(A)** The NPxY2 motif located in the cytoplasmic domain of Lrp1 is responsible for the endocytosis of β1 integrins via kindlin 2 that enhances cell migration. **(B)** Upon mutations in the NPxY2 motif of Lrp1, interactions with kindlin 2 do not occur, resulting in reduced β1 integrin recycling and facilitation of cell adhesion.

two-chain tPA by plasmin or kallikrein. Given its prominent matrix degradation capacities, tPA levels and activity must be strictly regulated. In the CNS, Lrp1 together with protease inhibitors PAI-1 and neuroserpin is especially crucial for controlling the effect of tPA on ECM remodeling (Orth et al., 1992; Makarova et al., 2003; Yepes and Lawrence, 2004; Czekay et al., 2011; Hébert et al., 2015).

For many years, tPA has been mostly appreciated for its fibrinolytic activity, however, it possesses a plethora of other functions vital for CNS homeostasis, some of which are summarized in **Figure 11** (Sappino et al., 1993; Briens et al., 2017; Hébert et al., 2015).

TPA, alike Lrp1, is implicated in the pathology of neurodegenerative diseases, including Alzheimer's disease, psychotic disorders like schizophrenia (Fabbro and Seeds, 2009; Hoirisch-Clapauch and Nardi, 2015) and is recognized for supporting BBB integrity (Polavarapu et al., 2007; Fredriksson et al., 2015; Stefanitsch et al., 2015).

The tPA has been found to facilitate neurite outgrowth by promoting local proteolysis (Seeds et al., 1996) and to favor neuronal (synaptic) maturation after differentiation from cortical neural progenitor cells (Lee et al., 2014). TPA is highly expressed in brain regions undergoing cellular migration. TPA gene expression is found most prominently in the cerebellum in the period of neuronal migration and is induced in granule neurons leaving the external granule layer of the cerebellum (Friedman and Seeds, 1995). Mice that lack tPA show an increased amount of granule neurons migrating in the molecular layer of the cerebellum (Seeds et al., 1999). The mechanism behind enhanced tPA expression in granule cells is suggested to be related to NMDAR signaling as these receptors are crucial for granule cell migration (Komuro and Rakic, 1992, 1993; Friedman and Seeds, 1995). TPA-mediated signaling is also supportive for Schwann cell migration via direct interaction with NMDARs and is present even upon blockage of Lrp1 (Mantuano et al., 2015). Recently, tPA has been implicated in the control of proper

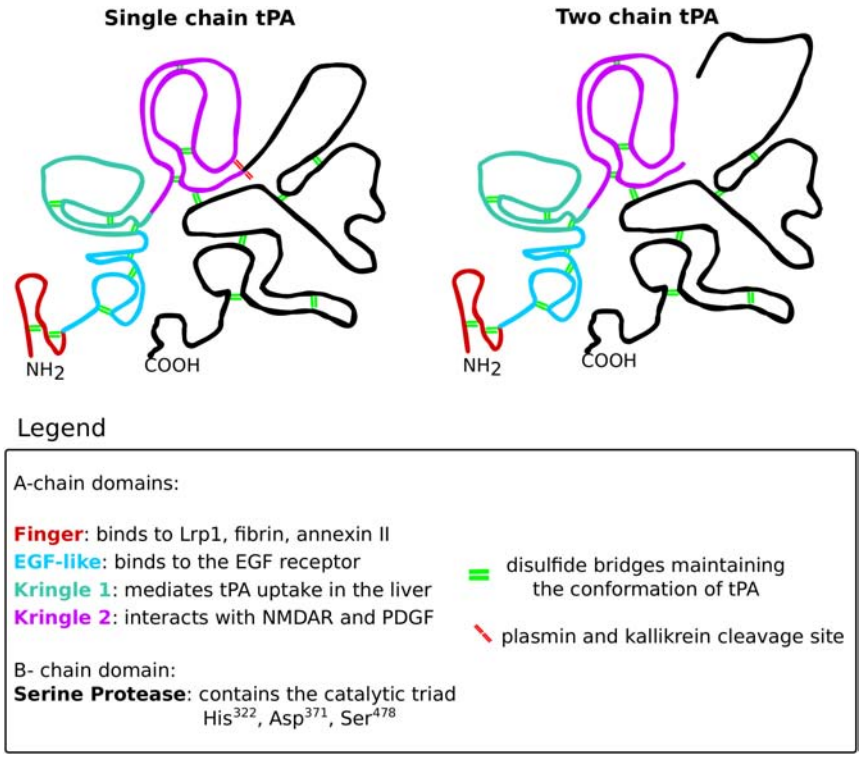

FIGURE 10 | The structure of tissue plasminogen activator. Tissue plasminogen activator (tPA), like all serine proteases, exists in two forms: the single-chain and the two-chain form. The conformation of tPA is maintained by 17 disulfide bridges (green double lines). The structure of both tPA forms consists of two chains: the A-chain and the B-chain. The A-chain consists of four domains that are color-coded on the scheme. The finger domain (red) is responsible for interacting with Lrp1, fibrin and annexin II. The EGF-like domain (blue) binds the EGF receptor. The kringle 1 domain (green) mediates tPA uptake in the liver. The kringle 2 domain (violet) is vital for interactions with NMDARs and PDGFs. The B-chain (black) consists of the catalytic triad that mediates the proteolytic activity of tPA. The single-chain form of tPA is catalytically active and can be further cleaved by kallikrein and plasmin (red double lines), resulting in the two-chain form of tPA. The two-chain tPA is also catalytically active.

radial glial cell organization and differentiation. The interaction between neuronal tPA and NMDAR on radial glia cells was found to be crucial for proper cortical migration and maturation (Pasquet et al., 2018). In a mouse model of Fragile X syndrome, a stimulating effect of tPA on Fmr1-deficient cells migrating out of neurospheres was also apparent (Achuta et al., 2014).

TPA and plasmin have been shown to regulate mossy fiber outgrowth in the hippocampus via the proteolysis of the proteoglycan DSD-1/phosphacan (Wu et al., 2000).

In murine renal and non-renal myofibroblasts, tPA promotes transforming growth factor (TGF)-β1-mediated activation and ECM production which is independent of its proteolytic activity. TPA exerts this action by directly activating Lrp1 by a phosphorylation of tyrosine residues located in the C-terminus of Lrp1. This process results in Lrp1-mediated β1 integrin recruitment and integrin-linked kinase signaling (Hu et al., 2007). Upon Lrp1 loss, tPA fails to induce myofibroblast activation and ECM overproduction as evidenced by type I collagen expression (Hu et al., 2007). TGF-β1 fibrogenic activity is not disturbed in Lrp1-deficient cells, suggesting Lrp1 loss affects only tPA-mediated signaling (Hu et al., 2007). In other cell types, however, Lrp1 was shown to impact TGF-β expression and signaling, for example during vessel wall remodeling (Muratoglu et al., 2011).

TPA is not only supportive of cell migration, but, under certain conditions, it also favors cell adhesion. This effect is reversed upon binding of tPA to PAI-1, which induces an Lrp1-mediated internalization of the adhesion complex and cell detachment (Cao et al., 2006; Kozlova et al., 2015).

Extracellular matrix remodeling by tPA and other proteases is not only involved in axonal growth and cell migration but also activates cellular signaling cascades. For example, degraded fibronectin particles interact with integrin receptors and trigger cell signaling that further remodels the ECM by regulating mRNA levels of metalloproteases and other factors (Werb et al., 1989). TPA also acts as a cytokine by upregulating MMP-9 gene expression in an Lrp1-dependent manner (Wang et al., 2003; Yepes et al., 2003; Hu et al., 2006). Lrp1 expression is increased upon ischemic stroke, and treatment with RAP or antibodies against Lrp1 decreases the degree of tissue edema after middle cerebral artery occlusion (Polavarapu et al., 2007). Vasocontraction of smooth muscle cells is facilitated by tPA and requires a functional interaction between Lrp1 and α and β integrins (Akkawi et al., 2006). Astrocytic Lrp1 and tPA have been directly shown to regulate BBB permeability (Polavarapu et al., 2007; Su et al., 2008; Niego et al., 2012). Improper tPA-Lrp1 and tPA-Mac-1-Lrp1-PDGFR α interactions at the BBB are

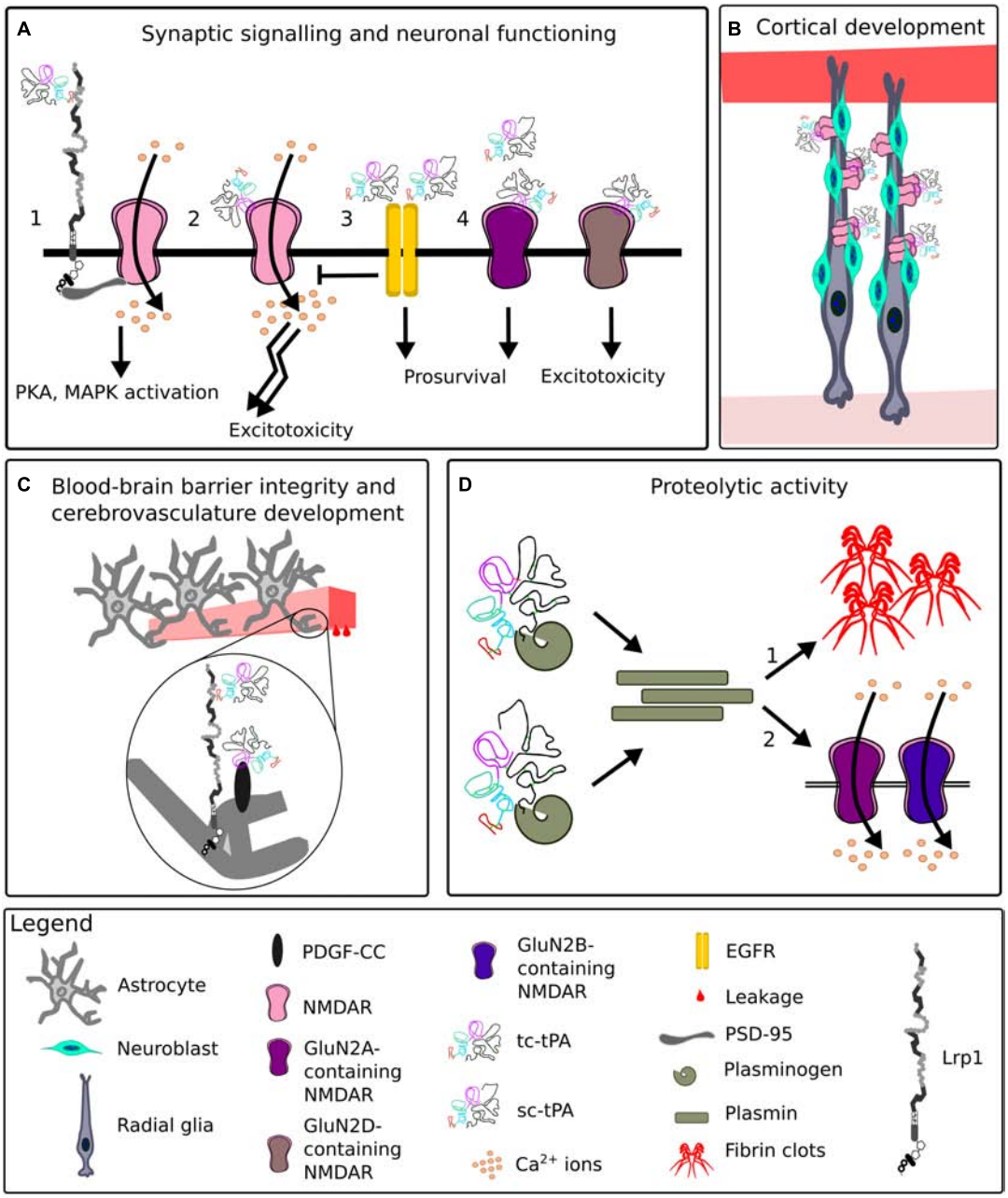

FIGURE 11 | Representative functions of tissue plasminogen activator in the CNS. **(A)** At the synapse, upon binding of tissue plasminogen activator (tPA), Lrp1 recruits postsynaptic density protein 95 (PSD-95). PSD-95 bridges the NPxY2 motif of Lrp1 and *N*-methyl-D-aspartate receptor (NMDAR). NMDAR allows Ca^{2+} influx, leading to an activation of signaling cascades (1). TPA can directly interact with the NMDAR, enhancing its extrasynaptic surface diffusion and resulting in excitotoxicity (2). Interactions of low levels of single-chain tPA (sc-tPA) and two-chain tPA (tc-tPA) with epidermal growth factor receptor (EGFR) result in neuroprotection and inhibition of NMDAR neurotoxicity (3). Interactions of tPA with synaptic GluN2A-NMDARs are neuroprotective, while with extrasynaptic GluN2D-NMDARs, neurotoxic (4). **(B)** During corticogenesis, tPA released by migrating neuroblasts clusters NMDARs on radial glia cells and ensures proper cortical migration and maturation of neurons. **(C)** TPA enhances blood-brain barrier permeability by interacting with astrocytic Lrp1 and platelet-derived growth factor (PDGF)-CC. **(D)** Both sc-tPA and tc-tPA are proteolytically active and convert plasminogen to plasmin. Plasmin digests fibrin, a process especially vital for renewing blood flow after ischemia (1). Plasmin cleaves GluN2A and GluN2B-containing NMDARs, impacting NMDAR functionality (2).

known to influence the permeability of the neurovascular unit in relation to seizures and ischemia (Polavarapu et al., 2007; Zhang et al., 2007, 2009; Su et al., 2008; Nakajima et al., 2014; Fredriksson et al., 2015).

In the CNS, tPA is synthesized and released by various cell types including neurons and astrocytes (Hébert et al., 2015). The majority of neuronal tPA is present in dendrites and axons and is released following depolarization of presynaptic terminals.

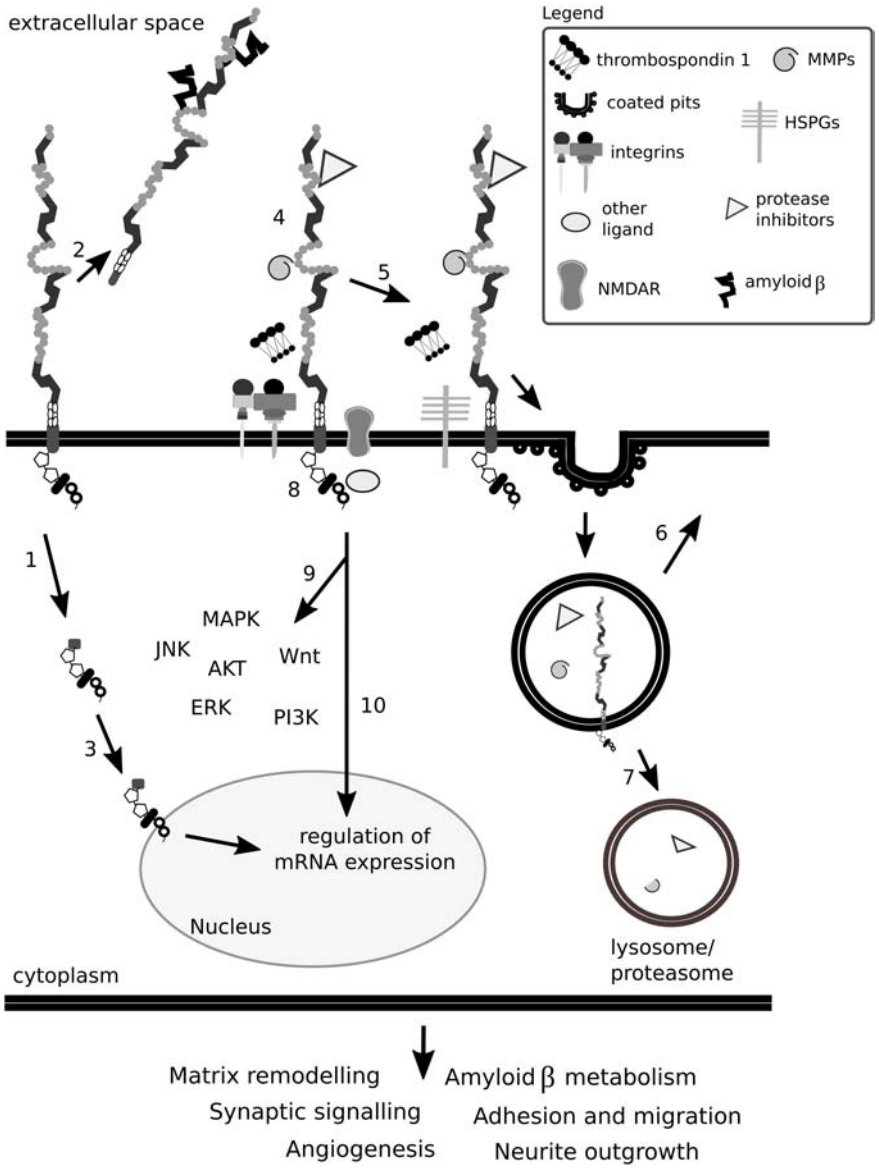

FIGURE 12 | Lrp1 impact on the ECM is complex. Lrp1 can undergo β- and γ-secretase-mediated cleavages that result in two functional receptor domains that exhibit different properties (1). The shed extracellular domain of Lrp1 can interact with ligands located in the matrix and in the circulation (2). The intracellular Lrp1 domain can translocate to the nucleus and regulate the expression of many genes (3). Lrp1 has been reported to interact with more than 40 different molecules, among them matrix metalloproteinases (MMPs) and protease inhibitors, thrombospondins, *N*-methyl-D-aspartate receptors (NMDAR) and integrins (4). Mirroring this multitude, the binding of ligands to Lrp1 can lead to various effects. Ligands can directly bind to the extracellular domain of Lrp1, undergo endocytosis (5) and be transported to lysosomes/proteasomes for degradation (7) while Lrp1 is recycled back to the membrane (6). Some ligands require bridging molecules like thrombospondins or heparan sulfate proteoglycans (HSPGs) to undergo efficient uptake (5). Upon ligand binding to the extracellular and/or cytoplasmic domains of Lrp1, the receptor can become phosphorylated (8), result in the activation of signaling cascades (9) and/or regulate gene transcription (10). Given the above, Lrp1 impacts the ECM either directly or indirectly and influences its remodeling. Lrp1 signaling alters not only the composition of the ECM but also other homeostatic processes like synaptic signaling and angiogenesis, which impact brain functioning.

tPA liberation impacts the release of glutamate, thereby exerting a modulatory function on synaptic activity (Wu et al., 2015; Yepes et al., 2016). Simultaneously, tPA release is proposed to exhibit an independent, homeostatic effect on the cortical glutamatergic postsynapse, which is dependent on the degree of neuronal activation and extracellular Ca^{2+} concentrations (Jeanneret et al., 2016).

The tPA interacts with proteins and receptors located at the synapse, among them Lrp1 and NMDAR (Nicole et al., 2001; Pawlak et al., 2005; Benchenane et al., 2007; Macrez et al., 2010; Jullienne et al., 2011; Ng et al., 2012; Obiang et al., 2012; Parcq et al., 2012; Mantuano et al., 2013; Lesept et al., 2016). Both single- and two-chain tPA at low concentrations can activate neuronal EGF receptors, which decrease NMDAR

signaling and result in neurotrophic effects. High concentrations of single-chain tPA lead to neurotoxic effects by activating NMDAR signaling (Bertrand et al., 2015; Chevilley et al., 2015). Neuronal survival is enhanced via astrocytic TGF-α induction of PAI-1. PAI-1 inhibits tPA and thereby prevents NMDAR-mediated neurotoxicity (Gabriel et al., 2002). Additionally, tPA exerts neuroprotective effects by activating the annexin II and mTOR pathways (Chevilley et al., 2015; Grummisch et al., 2016; Lemarchand et al., 2016).

The interaction of tPA with Lrp1 is vital for the generation of hippocampal late LTP and enhancement of PKA activity (Zhuo et al., 2000; Makarova et al., 2003).

The tPA is tightly connected with LTP induction and synaptic signaling also by its ability to degrade the ECM (Qian et al., 1993; Huang et al., 1996; Baranes et al., 1998; Madani et al., 1999; Trotter et al., 2014). TPA-mediated proteolytic cleavage of plasminogen results in the generation of plasmin that enhances the NMDAR-mediated increase in Ca^{2+} influx upon glutamate application to cultured hippocampal neurons (Inoue et al., 1994). TPA and plasmin have also been shown to convert pro brain-derived neurotrophic factor to mature brain-derived neurotrophic factor, a protein critical for LTP generation (Pang and Lu, 2004; Pang et al., 2004).

Healthy astrocytes possess the ability to uptake tPA, via Lrp1, from the synaptic cleft and modulate the efficacy of synaptic responses (Makarova et al., 2003; Fernández-Monreal et al., 2004; Cassé et al., 2012). Meanwhile, *in vitro* cultured astrocytes with reduced Lrp1 levels do not uptake neuron-derived tPA efficiently and as a result cause elevated levels of tPA in the synaptic cleft (Cassé et al., 2012). Astrocytic Lrp1 uptake of tPA is thereby crucial in preventing surplus tPA-mediated activation of NMDARs and neuronal cell death (Cassé et al., 2012) and is a promising target for epilepsy research.

The tPA is an immediate early gene expressed not only upon LTP but also early after seizures (Qian et al., 1993; Carroll et al., 1994). The exact impact of tPA on seizure generation and epilepsy progression is, however, complex (Tan et al., 2012). TPA-deficient mice are resistant to excitotoxin-induced neuronal death, but mice overexpressing tPA in adult neurons do not show neurodegeneration, only a selective enhancement of hippocampal LTP and memory (Tsirka et al., 1997; Madani et al., 1999). Involvement of tPA in activity-dependent synaptic plasticity has also been hypothesized to occur in the cerebellum upon motor learning. Here, tPA secreted at either Purkinje cell dendrites or granule neurons and parallel fibers, could eliminate synapses by degrading cell surface receptors and adhesion molecules, or facilitate new synapse formation by degrading the ECM (Seeds et al., 1995, 1996).

Lrp1 and the extracellular protease tPA impact cell migration, adhesion and NMDAR-mediated signaling. TPA exerts its effects not only via its proteolytic activity but also via activating signaling cascades (Nicole et al., 2001; Yuan et al., 2009; Parcq et al., 2012; Chevilley et al., 2015). Interactions of Lrp1 with tPA have been shown so far to depend on the animal age, the cell type, the exact co-factors available, the extracellular/intracellular tPA ratio and the form of tPA. These myriad parameters need consideration when studying the intriguing relationship between Lrp1 and tPA and partially explains contradictory findings in the literature regarding the function of this ECM protein (Nicole et al., 2001; Fernández-Monreal et al., 2004; Benchenane et al., 2007; Jullienne et al., 2011; Robinson et al., 2015).

CONCLUSION

Lrp1 is a potent modulator of ECM function in the CNS and beyond. Lrp1 can impact on the composition of the cell plasma membrane, and thereby the ECM, by the endocytosis of a wide range of ECM proteins and protein complexes. ECM molecules themselves can facilitate Lrp1-mediated endocytosis by acting as bridging and docking molecules, as do surface-bound HSPGs. By mediating the endocytosis of a wide range of proteases and protease inhibitors, Lrp1 directly impacts ECM composition. By associating with scaffolding and adaptor proteins and forming co-receptor complexes, Lrp1 appears vital for cell signaling events and activation of many downstream signaling cascades that lead to, among others, ECM remodeling. In this context, the interactions of Lrp1 with its ligands, especially tPA and integrins, have proven critical for normal development, synaptic signaling, cell adhesion and migration. Therefore, it is not surprising that changes in Lrp1 expression and phosphorylation status are associated with neurodegenerative and cardiovascular diseases and cancer.

A general overview of how Lrp1 can interact with the ECM is depicted in **Figure 12**.

In summary, as the impact of Lrp1 on the ECM is complex and both cell type- and cofactor-dependent, an integrative approach for deciphering Lrp1 function should be implemented for each studied interaction and system.

AUTHOR'S NOTE

Parts of the review content (especially **Figures 1**, **10**, **11** and the integrin and tPA sections) first appeared in the dissertation thesis (Bres, 2018). This is the only form in which this content has appeared, is in line with the author's university policy and will be soon available online.

AUTHOR CONTRIBUTIONS

EB and AF discussed the concept and content of the review. EB drafted and wrote the manuscript and designed the figures, AF read and revised the manuscript. Both authors agreed to the submitted version.

FUNDING

This work was supported by a graduate training grant of the International Graduate School for Neuroscience (IGSN) to EB. Grant support by the German Research Foundation (DFG, SPP 1757, Fa 159-20-1 & 2) to AF is gratefully acknowledged. We acknowledge support by the DFG Open Access Publication Funds of the Ruhr-Universität Bochum.

REFERENCES

Achuta, S., Rezov, V., Uutela, M., Louhivuori, V., Louhivuori, L., and Castrén, M. (2014). Tissue plasminogen activator contributes to alterations of neuronal migration and activity-dependent responses in fragile X mice. *J. Neurosci.* 34, 1916–1923. doi: 10.1523/JNEUROSCI.3753-13.2014

Akimov, S. S., Krylov, D., Fleischman, L. F., and Belkin, A. M. (2000). Tissue transglutaminase is an integrin-binding adhesion coreceptor for fibronectin. *J. Cell Biol.* 148, 825–838. doi: 10.1083/jcb.148.4.825

Akkawi, S., Nassar, T., Tarshis, M., Cines, D. B., and Higazi, A. A. (2006). LRP and alphavbeta3 mediate tPA activation of smooth muscle cells. *Am. J. Physiol. Heart Circ. Physiol.* 291, H1351–H1359. doi: 10.1152/ajpheart.01042.2005

Andersen, O. M., and Willnow, T. E. (2006). Lipoprotein receptors in Alzheimer's disease. *Trends Neurosci.* 29, 687–694. doi: 10.1016/j.tins.2006.09.002

Ashcom, J. D., Tiller, S. E., Dickerson, K., Cravens, J. L., Argaves, W. S., and Strickland, D. K. (1990). The human alpha 2-macroglobulin receptor: identification of a 420-kD cell surface glycoprotein specific for the activated conformation of alpha 2-macroglobulin. *J. Cell Biol.* 110, 1041–1048. doi: 10.1083/jcb.110.4.1041

Auderset, L., Cullen, C., and Young, K. (2016). Low density lipoprotein-receptor related protein 1 is differentially expressed by neuronal and glial populations in the developing and mature mouse central nervous system. *PLoS One* 11:e0155878. doi: 10.1371/journal.pone.0155878

Bacskai, B., Xia, M., Strickland, D., Rebeck, G., and Hyman, B. (2000). The endocytic receptor protein LRP also mediates neuronal calcium signalling via N -methyl-D-aspartate receptors. *Proc. Natl. Acad. Sci. U.S.A.* 97, 11551–11556. doi: 10.1073/pnas.200238297

Bannerman, D., Good, M., Butcher, S., Ramsay, M., and Morris, R. (1995). Distinct components of spatial learning revealed by prior training and NMDA receptor blockade. *Nature* 378, 182–186. doi: 10.1038/378182a0

Baranes, D., Lederfein, D., Huang, Y.-Y., Chen, M., Bailey, C., and Kandel, E. (1998). Tissue plasminogen activator contributes to the late phase of LTP and to synaptic growth in the hippocampal mossy fiber pathway. *Neuron* 21, 813–825. doi: 10.1016/S0896-6273(00)80597-8

Barker, T. H., Pallero, M. A., MacEwen, M. W., Tilden, S. G., Woods, A., Murphy-Ullrich, J. E., et al. (2004). Thrombospondin-1-induced focal adhesion disassembly in fibroblasts requires Thy-1 surface expression, lipid raft integrity, and Src activation. *J. Biol. Chem.* 279, 23510–23516. doi: 10.1074/jbc.M402169200

Barmina, O. Y., Walling, H. W., Fiacco, G. J., Freije, J. M., López-Otín, C., Jeffrey, J. J., et al. (1999). Collagenase-3 binds to a specific receptor and requires the low density lipoprotein receptor-related protein for internalization. *J. Biol. Chem.* 274, 30087–30093. doi: 10.1074/jbc.274.42.30087

Barnes, H., Larsen, B., Tyers, M., and van der Geer, P. (2001). Tyrosine-phosphorylated low density lipoprotein receptor-related protein 1 (LRP1) associates with the adaptor protein SHC in SRC-transformed cells. *J. Biol. Chem.* 276, 19119–19125. doi: 10.1074/jbc.M011437200

Basu, S., Binder, R. J., Ramalingam, T., and Srivastava, P. K. (2001). CD91 is a common receptor for heat shock proteins gp96, hsp90, hsp70, and calreticulin. *Immunity* 14, 303–313. doi: 10.1016/S1074-7613(01)00111-X

Bein, K., and Simons, M. (2000). Thrombospondin type 1 repeats interact with matrix metalloproteinase 2. Regulation of metalloproteinase activity. *J. Biol. Chem.* 275, 32167–32173. doi: 10.1074/jbc.M003834200

Beisiegel, U., Weber, W., and Bengtsson-Olivecrona, G. (1991). Lipoprotein lipase enhances the binding of chylomicrons to low density lipoprotein receptor-related protein. *Proc. Natl. Acad. Sci. U.S.A.* 88, 8342–8346. doi: 10.1073/pnas.88.19.8342

Beisiegel, U., Weber, W., Ihrke, G., Herz, J., and Stanley, K. K. (1989). The LDL-receptor-related protein, LRP, is an apolipoprotein E-binding protein. *Nature* 341, 162–164. doi: 10.1038/341162a0

Bellis, S. L. (2004). Variant glycosylation: an underappreciated regulatory mechanism for beta1 integrins. *Biochim. Biophys. Acta* 1663, 52–60. doi: 10.1016/j.bbamem.2004.03.012

Belvindrah, R., Graus-Porta, D., Goebbels, S., Nave, K.-A., and Müller, U. (2007a). Beta1 integrins in radial glia but not in migrating neurons are essential for the formation of cell layers in the cerebral cortex. *J. Neurosci.* 27, 13854–13865.

Belvindrah, R., Hankel, S., Walker, J., Patton, B. L., and Müller, U. (2007b). Beta1 integrins control the formation of cell chains in the adult rostral migratory stream. *J. Neurosci.* 27, 2704–2717.

Benchenane, K., Castel, H., Boulouard, M., Bluthé, R., Fernández-Monreal, M., Roussel, B., et al. (2007). Anti-NR1 N-terminal-domain vaccination unmasks the crucial action of tPA on NMDA- receptor-mediated toxicity and spatial memory. *J. Cell Sci.* 120, 578–585. doi: 10.1242/jcs.03354

Bertrand, T., Lesept, F., Chevilley, A., Lenoir, S., Aimable, M., Briens, A., et al. (2015). Conformations of tissue plasminogen activator (tPA) orchestrate neuronal survival by a crosstalk between EGFR and NMDAR. *Cell Death Dis.* 6:e1924. doi: 10.1038/cddis.2015.296

Betts, G., van der Geer, P., and Komives, E. (2008). Structural and functional consequences of tyrosine phosphorylation in the LRP1 cytoplasmic domain. *J. Biol. Chem.* 283, 15656–15664. doi: 10.1074/jbc.M709514200

Bilodeau, N., Fiset, A., Boulanger, M. C., Bhardwaj, S., Winstall, E., Lavoie, J. N., et al. (2010). Proteomic analysis of src family kinases signaling complexes in golgi/endosomal fractions using a site-selective anti-phosphotyrosine antibody:identification of lrp1-insulin receptor complexes. *J. Proteome Res.* 9, 708–717. doi: 10.1021/pr900481b

Boucher, P., Gotthardt, M., Li, W., Anderson, R., and Herz, J. (2003). LRP: role in vascular wall integrity and protection from atherosclerosis. *Science* 300, 329–332. doi: 10.1126/science.1082095

Boucher, P., and Herz, J. (2011). Signaling through LRP1, protection from atherosclerosis and beyond. *Biochem. Pharmacol.* 81, 1–5. doi: 10.1016/j.bcp.2010.09.018

Boucher, P., Liu, P., Gotthardt, M., Hiesberger, T., Anderson, R., and Herz, J. (2002). Platelet-derived growth factor mediates tyrosine phosphorylation of the cytoplasmic domain of the low density lipoprotein receptor-related protein in caveolae. *J. Biol. Chem.* 277, 15507–15513. doi: 10.1074/jbc.M200428200

Brandan, E., Retamal, C., Cabello-Verrugio, C., and Marzolo, M. P. (2006). The low density lipoprotein receptor-related protein functions as an endocytic receptor for decorin. *J. Biol. Chem.* 281, 31562–31571. doi: 10.1074/jbc.M602919200

Bres, E. E. (2018). *Unravelling the Role of Low-Density Lipoprotein Receptor-Related Protein-1 in Radial Glia and Neuronal and Glial Progeny in the Developing Mouse Brain*. Ph.D. thesis, Ruhr University Bochum, Bochum.

Briens, A., Bardou, I., Lebas, H., Miles, L., Parmer, R., and Vivien, D. (2017). Astrocytes regulate the balance between plasminogen activation and plasmin clearance via cell-surface actin. *Cell Discov.* 3, 17001–17018. doi: 10.1038/celldisc.2017.1

Brinckerhoff, C. E., and Matrisian, L. M. (2002). Matrix metalloproteinases: a tail of a frog that became a prince. *Nat. Rev. Mol. Cell Biol.* 3, 207–214. doi: 10.1038/nrm763

Bronfman, F. C., Soto, C., Tapia, L., Tapia, V., and Inestrosa, N. C. (1996). Extracellular matrix regulates the amount of the β-amyloid precursor protein and its amyloidogenic fragments. *J. Cell. Physiol.* 166, 360–369. doi: 10.1002/(SICI)1097-4652(199602)166:2<360::AID-JCP14>3.0.CO;2-F

Brooker, S. M., Bond, A. M., Peng, C.-Y., and Kessler, J. A. (2016). β1-integrin restricts astrocytic differentiation of adult hippocampal neural stem cells. *Glia* 64, 1235–1251. doi: 10.1002/glia.22996

Brown, D. A., and London, E. (1998). Functions of lipid rafts in biological membranes. *Annu. Rev. Cell Dev. Biol.* 14, 111–136. doi: 10.1146/annurev.cellbio.14.1.111

Brown, D. A., and London, E. (2000). Structure and function of sphingolipid-and-cholesterol-rich membrane rafts. *J. Biol. Chem.* 275, 17221–17224. doi: 10.1074/jbc.R000005200

Bu, G., Maksymovitch, E., Nerbonne, J., and Schwartz, A. (1994). Expression and function of the low density lipoprotein receptor-related protein (LRP) in mammalian central neurons. *J. Biol. Chem.* 269, 18521–18528.

Bu, G., Williams, S., Strickland, D., and Schwartz, A. (1992). Low density lipoprotein receptor-related protein/alpha 2-macroglobulin receptor is an hepatic receptor for tissue-type plasminogen activator. *Proc. Natl. Acad. Sci. U.S.A.* 89, 7427–7431. doi: 10.1073/pnas.89.16.7427

Cao, C., Lawrence, D. A., Li, Y., Von Arnim, C. A., Herz, J., Su, E. J., et al. (2006). Endocytic receptor LRP together with tPA and PAI-1 coordinates Mac-1-dependent macrophage migration. *EMBO J.* 25, 1860–1870. doi: 10.1038/sj.emboj.7601082

Capurro, M. I., Shi, W., and Filmus, J. (2012). LRP1 mediates Hedgehog-induced endocytosis of the GPC3-Hedgehog complex. *J. Cell Sci.* 125, 3380–3389. doi: 10.1242/jcs.098889

Capurro, M. I., Xu, P., Shi, W., Li, F., Jia, A., and Filmus, J. (2008). Glypican-3 inhibits Hedgehog signaling during development by competing with patched for Hedgehog binding. *Dev. Cell* 14, 700–711. doi: 10.1016/j.devcel.2008.03.006

Carroll, P., Tsirka, S., Richards, W., Frohman, M., and Strickland, S. (1994). The mouse tissue plasminogen activator gene 5' flanking region directs appropriate expression in development and a seizure-enhanced response in the CNS. *Development* 120, 3173–3183.

Carstens, K. E., Phillips, M. L., Pozzo-Miller, L., Weinberg, R. J., and Dudek, S. M. (2016). Perineuronal nets suppress plasticity of excitatory synapses on ca2 pyramidal neurons. *J. Neurosci.* 36, 6312–6320. doi: 10.1523/JNEUROSCI.0245-16.2016

Cassé, F., Bardou, I., Danglot, L., Briens, A., Montagne, A., Parcq, J., et al. (2012). Glutamate controls tPA recycling by astrocytes, which in turn influences glutamatergic signals. *J. Neurosci.* 32, 5186–5199. doi: 10.1523/JNEUROSCI.5296-11.2012

Cavallaro, U., del Vecchio, A., Lappi, D. A., and Soria, M. R. (1993a). A conjugate between human urokinase and saporin, a type 1 ribosome-inactivating protein, is selectively cytotoxic in urokinase receptor-expressing cells. *J. Biol. Chem.* 268, 23186–23190.

Cavallaro, U., del Vecchio, A., Tazzari, P. L., Massazza, G., and Soria, M. R. (1993b). Targeting of cytotoxic conjugates to Kaposi's sarcoma-derived cells. *Drug Deliv.* 1, 119–124. doi: 10.3109/10717549309022765

Cavallaro, U., Nykjaer, A., Nielsen, M., and Soria, M. R. (1995). Alpha 2-macroglobulin receptor mediates binding and cytotoxicity of plant ribosome-inactivating proteins. *Eur. J. Biochem.* 232, 165–171. doi: 10.1111/j.1432-1033.1995.tb20795.x

Chan, W. L., Shaw, P. C., Tam, S. C., Jacobsen, C., Gliemann, J., and Nielsen, M. S. (2000). Trichosanthin interacts with and enters cells via LDL receptor family members. *Biochem. Biophys. Res. Commun.* 270, 453–457. doi: 10.1006/bbrc.2000.2441

Chappell, D. A., Fry, G. L., Waknitz, M. A., Iverius, P. H., Williams, S. E., and Strickland, D. K. (1992). The low density lipoprotein receptor-related protein/alpha 2-macroglobulin receptor binds and mediates catabolism of bovine milk lipoprotein lipase. *J. Biol. Chem.* 267, 25764–25767.

Chevilley, A., Lesept, F., Lenoir, S., Ali, C., Parcq, J., and Vivien, D. (2015). Impacts of tissue-type plasminogen activator (tPA) on neuronal survival. *Front. Cell. Neurosci.* 9:415. doi: 10.3389/fncel.2015.00415

Chow, V. W., Mattson, M. P., Wong, P. C., and Gleichmann, M. (2010). An overview of APP processing enzymes and products. *Neuromolecular Med.* 12, 1–12. doi: 10.1007/s12017-009-8104-z

Christopherson, K. S., Ullian, E. M., Stokes, C. C., Mullowney, C. E., Hell, J. W., Agah, A., et al. (2005). Thrombospondins are astrocyte-secreted proteins that promote CNS synaptogenesis. *Cell* 120, 421–433. doi: 10.1016/j.cell.2004.12.020

Cirrito, J. R., Yamada, K. A., Finn, M. B., Sloviter, R. S., Bales, K. R., May, P. C., et al. (2005). Synaptic activity regulates interstitial fluid amyloid-beta levels in vivo. *Neuron* 48, 913–922. doi: 10.1016/j.neuron.2005.10.028

Conese, M., Nykjaer, A., Petersen, C. M., Cremona, O., Pardi, R., Andreasen, P. A., et al. (1995). Alpha-2 macroglobulin receptor/Ldl receptor-related protein (Lrp)-dependent internalisation of the urokinase receptor. *J. Cell Biol.* 131, 1609–1622. doi: 10.1083/jcb.131.6.1609

Conese, M., Olson, D., and Blasi, F. (1994). Protease nexin-1-urokinase complexes are internalized and degraded through a mechanism that requires both urokinase receptor and alpha 2-macroglobulin receptor. *J. Biol. Chem.* 269, 17886–17892.

Correa, F., Gauberti, M., Parcq, J., Macrez, R., Hommet, Y., Obiang, P., et al. (2011). Tissue plasminogen activator prevents white matter damage following stroke. *J. Exp. Med.* 208, 1229–1242. doi: 10.1084/jem.20101880

Craig, J., Mikhailenko, I., Noyes, N., Migliorini, M., and Strickland, D. K. (2013). The LDL receptor-related protein 1 (LRP1) regulates the PDGF signaling pathway by binding the protein phosphatase SHP-2 and modulating SHP-2-mediated PDGF signaling events. *PLoS One* 8:e70432. doi: 10.1371/journal.pone.0070432

Crisp, R. J., Knauer, D. J., and Knauer, M. F. (2000). Roles of the heparin and low density lipid receptor-related protein-binding sites of protease nexin 1 (PN1) in urokinase-PN1 complex catabolism. The PN1 heparin-binding site mediates complex retention and degradation but not cell surface binding or internalization. *J. Biol. Chem.* 275, 19628–19637. doi: 10.1074/jbc.M909172199

Croucher, D., Saunders, D. N., and Ranson, M. (2006). The urokinase/PAI-2 complex: a new high affinity ligand for the endocytosis receptor low density lipoprotein receptor-related protein. *J. Biol. Chem.* 281, 10206–10213. doi: 10.1074/jbc.M513645200

Croy, J., Shin, W., Knauer, M., Knauer, D., and Komives, E. (2003). All three LDL receptors homology regions of the LDL receptor-related protein bind multiple ligands. *Biochemistry* 42, 13049–13057. doi: 10.1021/bi034752s

Czekay, R. P., Aertgeerts, K., Curriden, S. A., and Loskutoff, D. J. (2003). Plasminogen activator inhibitor-1 detaches cells from extracellular matrices by inactivating integrins. *J. Cell Biol.* 160, 781–791. doi: 10.1083/jcb.200208117

Czekay, R. P., Kuemmel, T. A., Orlando, R. A., and Farquhar, M. G. (2001). Direct binding of occupied urokinase receptor (uPAR) to LDL receptor-related protein is required for endocytosis of uPAR and regulation of cell surface urokinase activity. *Mol. Biol. Cell* 12, 1467–1479. doi: 10.1091/mbc.12.5.1467

Czekay, R. P., Wilkins-Port, C. E., Higgins, S. P., Freytag, J., Overstreet, J. M., Klein, R. M., et al. (2011). PAI-1: an integrator of cell signalling and migration. *Int. J. Cell Biol.* 2011:562481. doi: 10.1155/2011/562481

de Jager, M., van der Wildt, B., Schul, E., Bol, J. G., van Duinen, S. G., Drukarch, B., et al. (2013). Tissue transglutaminase colocalizes with extracellular matrix proteins in cerebral amyloid angiopathy. *Neurobiol. Aging* 34, 1159–1169. doi: 10.1016/j.neurobiolaging.2012.10.005

Deane, R., Bell, R. D., Sagare, A., and Zlokovic, B. V. (2009). Clearance of amyloid-beta peptide across the blood-brain barrier: implication for therapies in Alzheimer's disease. *CNS Neurol. Disord. Drug Targets* 8, 16–30. doi: 10.2174/187152709787601867

Deane, R., Sagare, A., Hamm, K., Parisi, M., Lane, S., Finn, M., et al. (2008). apoE isoform-specific disruption of amyloid beta peptide clearance from mouse brain. *J. Clin. Invest.* 118, 4002–4133. doi: 10.1172/JCI36663

Deane, R., Wu, Z., Sagare, A., Davis, J., Du, Y., Hamm, K., et al. (2004). LRP/amyloid beta-peptide interaction mediates differential brain efflux of Abeta isoforms. *Neuron* 43, 333–344. doi: 10.1016/j.neuron.2004.07.017

Deb, S., Wenjun Zhang, J., and Gottschall, P. E. (2003). Beta-amyloid induces the production of active, matrix-degrading proteases in cultured rat astrocytes. *Brain Res.* 970, 205–213. doi: 10.1016/S0006-8993(03)02344-8

Degryse, B., Neels, J. G., Czekay, R. P., Aertgeerts, K., Kamikubo, Y., and Loskutoff, D. J. (2004). The low density lipoprotein receptor-related protein is a motogenic receptor for plasminogen activator inhibitor-1. *J. Biol. Chem.* 279, 22595–22604. doi: 10.1074/jbc.M313004200

Degryse, B., Sier, C. F., Resnati, M., Conese, M., and Blasi, F. (2001). PAI-1 inhibits urokinase-induced chemotaxis by internalizing the urokinase receptor. *FEBS Lett.* 505, 249–254. doi: 10.1016/S0014-5793(01)02797-1

Derocq, D., Prébois, C., Beaujouin, M., Laurent-Matha, V., Pattingre, S., and Smith, G. K. (2012). Cathepsin D is partly endocytosed by the LRP1 receptor and inhibits LRP1-regulated intramembrane proteolysis. *Oncogene* 31, 3202–3212. doi: 10.1038/onc.2011.501

Dzyubenko, E., Gottschling, C., and Faissner, A. (2016). Neuron-Glia interactions in neural plasticity: contributions of neural extracellular matrix and perineuronal nets. *Neural Plast.* 2016:5214961. doi: 10.1155/2016/5214961

Ehrlich, I., Klein, M., Rumpel, S., and Malinow, R. (2007). PSD-95 is required for activity-driven synapse stabilisation. *Proc. Natl. Acad. Sci. U.S.A.* 104, 4176–4181. doi: 10.1073/pnas.0609307104

El-Husseini, A., Schnell, E., Chetkovich, D., Nicoll, R., and Bredt, D. (2000). PSD-95 involvement in the maturation of excitatory synapses. *Science* 290, 1364–1368.

Emonard, H., Bellon, G., de Diesbach, P., Mettlen, M., Hornebeck, W., and Courtoy, P. J. (2005). Regulation of matrix metalloproteinase (MMP) activity by the low-density lipoprotein receptor-related protein (LRP). A new function for an "old friend". *Biochimie* 87, 369–376. doi: 10.1016/j.biochi.2004.11.013

Emonard, H., Bellon, G., Troeberg, L., Berton, A., Robinet, A., Henriet, P., et al. (2004). Low density lipoprotein receptor-related protein mediates endocytic clearance of pro-MMP-2. *TIMP*-2 complex through a thrombospondin-independent mechanism. . *J. Biol. Chem.* 279, 54944–54951. doi: 10.1074/jbc.M406792200

Fabbro, S., and Seeds, N. (2009). Plasminogen activator activity is inhibited while neuroserpin is up-regulated in the Alzheimer disease brain. *J. Neurochem.* 109, 303–315. doi: 10.1111/j.1471-4159.2009.05894.x

Faissner, A., Pyka, M., Geissler, M., Sobik, T., Frischknecht, R., Gundelfinger, E. D., et al. (2010). Contributions of astrocytes to synapse formation and maturation-potential functions of the perisynaptic extracellular matrix. *Brain Res. Rev.* 63, 26–38. doi: 10.1016/j.brainresrev.2010.01.001

Fears, C. Y., Grammer, J. R., Stewart, JE Jr, Annis, D. S., Mosher, D. F., Bornstein, P., et al. (2005). Low-density lipoprotein receptor-related protein contributes to the antiangiogenic activity of thrombospondin-2 in a murine glioma model. *Cancer Res.* 65, 9338–9346. doi: 10.1158/0008-5472.CAN-05-1560

Fernández-Monreal, M., López-Atalaya, J. P., Benchenane, K., Léveillé, F., Cacquevel, M., Plawinski, L., et al. (2004). Is tissue-type plasminogen activator a neuromodulator? *Mol. Cell. Neurosci.* 25, 594–601. doi: 10.1016/j.mcn.2003.11.002

Foley, E. M., Gordts, P. L. S. M., Stanford, K. I., Gonzales, J. C., Lawrence, R., Stoddard, N., et al. (2013). Hepatic remnants lipoprotein clearance by heparan sulfate proteoglycans and low-density lipoprotein receptors depend on dietary conditions in mice. *Arterioscler. Thromb. Vasc. Biol.* 33, 2065–2074. doi: 10.1161/ATVBAHA.113.301637

Frackowiak, J., Wisniewski, H. M., Wegiel, J., Merz, G. S., Iqbal, K., and Wang, K. C. (1992). Ultrastructure of the microglia that phagocytose amyloid and the microglia that produce beta-amyloid fibrils. *Acta Neuropathol.* 84, 225–233. doi: 10.1007/BF00227813

Fredriksson, L., Li, H., Fieber, C., Li, X., and Eriksson, U. (2004). Tissue plasminogen activator is a potent activator of PDGF-CC. *EMBO J.* 23, 3793–3802. doi: 10.1038/sj.emboj.7600397

Fredriksson, L., Stevenson, T. K., Su, E. J., Ragsdale, M., Moore, S., Craciun, S., et al. (2015). Identification of a neurovascular signaling pathway regulating seizures in mice. *Ann. Clin. Transl. Neurol.* 2, 722–738. doi: 10.1002/acn3.209

Friedman, G. C., and Seeds, N. W. (1995). Tissue plasminogen activator mRNA expression in granule neurons coincides with their migration in the developing cerebellum. *J. Comp. Neurol.* 360, 658–670. doi: 10.1002/cne.903600410

Gabriel, C., Ali, C., Lesné, S., Fernández-Monreal, M., Docagne, F., Plawinski, L., et al. (2002). Transforming growth factor alpha-induced expression of type 1 plasminogen activator inhibitor in astrocytes rescues neurons from excitotoxicity. *FASEB J.* 17, 277–279. doi: 10.1096/fj.02-0403fje

Gao, R., and Brigstock, D. R. (2003). Low density lipoprotein receptor-related protein (LRP) is a heparin-dependent adhesion receptor for connective tissue growth factor (CTGF) in rat activated hepatic stellate cells. *Hepatol. Res.* 27, 214–220. doi: 10.1016/S1386-6346(03)00241-9

Gardai, S. J., McPhillips, K. A., Frasch, S. C., Janssen, W. J., Starefeldt, A., Murphy-Ullrich, J. E., et al. (2005). Cell-surface calreticulin initiates clearance of viable or apoptotic cells through trans-activation of LRP on the phagocyte. *Cell* 123, 321–334. doi: 10.1016/j.cell.2005.08.032

Gaultier, A., Hollister, M., Reynolds, I., Hsieh, E., and Gonias, S. L. (2010). LRP1 regulates remodelling of the extracellular matrix by fibroblasts. *Matrix Biol.* 29, 22–30. doi: 10.1016/j.matbio.2009.08.003

Gaultier, A., Salicioni, A. M., Arandjelovic, S., and Gonias, S. L. (2006). Regulation of the composition of the extracellular matrix by low density lipoprotein receptor-related protein-1: activities based on regulation of mRNA expression. *J. Biol. Chem.* 281, 7332–7340. doi: 10.1074/jbc.M511857200

Gaultier, A., Wu, X., Le Moan, N., Takimoto, S., Mukandala, G., Akassoglou, K., et al. (2009). Low-density lipoprotein receptor-related protein 1 is an essential receptor for myelin phagocytosis. *J. Cell Sci.* 122, 1155–1162. doi: 10.1242/jcs.040717

Geissler, M., Gottschling, C., Aguado, A., Rauch, U., Wetzel, C. H., Hatt, H., et al. (2013). Primary hippocampal neurons, which lack four crucial extracellular matrix molecules, display abnormalities of synaptic structure and function and severe deficits in perineuronal net formation. *J. Neurosci.* 33, 7742–7755. doi: 10.1523/JNEUROSCI.3275-12.2013

Genedani, S., Agnati, L. F., Leo, G., Buzzega, D., Maccari, F., Carone, C., et al. (2010). β-Amyloid fibrillation and/or hyperhomocysteinemia modify striatal patterns of hyaluronic acid and dermatan sulfate: possible role in the pathogenesis of Alzheimers disease. *Curr. Alzheimers Res.* 7, 150–157. doi: 10.2174/156720510790691074

Gerritsen, K. G. F., Bovenschen, N., Nguyen, T. Q., Sprengers, D., Koeners, M. P., van Koppen, A. N., et al. (2016). Rapid hepatic clearance of full length CCN-2/CTGF: a putative role for LRP1-mediated endocytosis. *J. Cell Commun. Signal.* 10, 295–303. doi: 10.1007/s12079-016-0354-6

Godyna, S., Liau, G., Popa, I., Stefansson, S., and Argraves, W. S. (1995). Identification of the low density lipoprotein receptor-related protein (LRP) as an endocytic receptor for thrombospondin-1. *J. Cell Biol.* 129, 1403–1410. doi: 10.1083/jcb.129.5.1403

Gonias, S. L., Wu, L., and Salicioni, A. M. (2004). Low density lipoprotein receptor-related protein: regulation of the plasma membrane proteome. *Thromb. Haemost.* 91, 1056–1064. doi: 10.1160/TH04-01-0023

Gordts, P. L., Bartelt, A., Nilsson, S. K., Annaert, W., Christoffersen, C., Nielsen, L. B., et al. (2012). Impaired LDL receptor-related protein 1 translocation correlates with improved dyslipidemia and atherosclerosis in apoE-deficient mice. *PLoS One* 7:e38330. doi: 10.1371/journal.pone.0038330

Gotthardt, M., Trommsdorff, M., Nevitt, M., Shelton, J., Richardson, J., Stockinger, W., et al. (2000). Interactions of the low density lipoprotein receptor gene family with cytosolic adaptor and scaffold proteins suggest diverse biological functions in cellular communication and signal transduction. *J. Biol. Chem.* 275, 25616–25624. doi: 10.1074/jbc.M000955200

Greenaway, J., Lawler, J., Moorehead, R., Bornstein, P., LaMarre, J., and Petrik, J. (2007). Thrombospondin-1 inhibits VEGF levels in the ovary directly by binding and internalization via the low density lipoprotein receptor-related protein-1 (LRP-1). *J. Cell. Physiol.* 210, 807–818. doi: 10.1002/jcp.20904

Grummisch, J. A., Jadavji, N. M., and Smith, P. D. (2016). TPA promotes cortical neuron survival via mTOR-dependent mechanisms. *Mol. Cell. Neurosci.* 74, 25–33. doi: 10.1016/j.mcn.2016.03.005

Guttman, M., Betts, G., Barnes, H., Ghassemian, M., van der Geer, P., and Komives, E. (2009). Interactions of the NPXY microdomains of the low density lipoprotein receptor-related protein 1. *Proteomics* 9, 5016–5028. doi: 10.1002/pmic.200900457

Hadfield, K. D., Rock, C. F., Inkson, C. A., Dallas, S. L., Sudre, L., Wallis, G. A., et al. (2008). HtrA1 inhibits mineral deposition by osteoblasts: requirement for the protease and PDZ domains. *J. Biol. Chem.* 283, 5928–5938. doi: 10.1074/jbc.M709299200

Hahn-Dantona, E., Ruiz, J. F., Bornstein, P., and Strickland, D. K. (2001). The low density lipoprotein receptor-related protein modulates levels of matrix metalloproteinase 9 (MMP-9) by mediating its cellular catabolism. *J. Biol. Chem.* 276, 15498–15503. doi: 10.1074/jbc.M100121200

Hajjar, K., Jacovina, A., and Chacko, J. (1994). An endothelial cell receptor for plasminogen/tissue plasminogen activator. I. identity with annexin II. *J. Biol. Chem.* 269, 21191–21197.

Hartig, W., Brauer, K., and Bruckner, G. (1992). Wisteria floribunda agglutinin-labelled nets surround parvalbumin-containing neurons. *Neuroreport* 3, 869–872. doi: 10.1097/00001756-199210000-00012

Hayashi, H., Campenot, R. B., Vance, D. E., and Vance, J. E. (2007). Apolipoprotein E-containing lipoproteins protect neurons from apoptosis via a signaling pathway involving low-density lipoprotein receptor-related protein-1. *J. Neurosci.* 27, 1933–1941. doi: 10.1523/JNEUROSCI.5471-06.2007

Hébert, M., Lesept, F., Vivien, D., and Macrez, R. (2015). The story of an exceptional serine protease, tissue-type plasminogen activator (tPA). *Rev. Neurol.* 172, 186–197. doi: 10.1016/j.neurol.2015.10.002

Heck, N., Garwood, J., Loeffler, J.-P., Larmet, Y., and Faissner, A. (2004). Differential upregulation of extracellular matrix molecules associated with the appearance of granule cell dispersion and mossy fiber sprouting during epileptogenesis in a murine model of temporal lobe epilepsy. *Neuroscience* 129, 309–324. doi: 10.1016/j.neuroscience.2004.06.078

Hennen, E., Safina, D., Haussmann, U., Wörsdörfer, P., Edenhofer, F., Poetsch, A., et al. (2013). A LewisX glycoprotein screen identifies the low density lipoprotein receptor-related protein 1 (LRP1) as a modulator of oligodendrogenesis in mice. *J. Biol. Chem.* 288, 16538–16545. doi: 10.1074/jbc.M112.419812

Herz, J. (2001). The LDL receptor gene family: (un)expected signal transducers in the brain. *Neuron* 29, 571–581. doi: 10.1016/S0896-6273(01)00234-3

Herz, J., and Bock, H. (2002). Lipoprotein receptors in the nervous system. *Annu. Rev. Biochem.* 71, 405–434. doi: 10.1146/annurev.biochem.71.110601.135342

Herz, J., and Chen, Y. (2006). Reelin, lipoprotein receptors and synaptic plasticity. *Nat. Rev. Neurosci.* 7, 850–859. doi: 10.1038/nrn2009

Herz, J., Chen, Y., Masiulis, I., and Zhou, L. (2009). Expanding functions of lipoprotein receptors. *J. Lipid Res.* 50, S287–S292. doi: 10.1194/jlr.R800077-JLR200

Herz, J., Clouthier, D., and Hammer, R. (1992). LDL receptor-related protein internalizes and degrades uPA-PAI-1 complexes and is essential for embryo implantation. *Cell* 71, 411–421. doi: 10.1016/0092-8674(92)90511-A

Herz, J., Clouthier, D., and Hammer, R. (1993). Correction: LDL receptor-related protein internalizes and degrades uPA-PAI-1 complexes and is essential for embryo implantation. *Cell* 73:428. doi: 10.1016/0092-8674(93)90130-I

Herz, J., Goldstein, J. L., Strickland, D. K., Ho, Y. K., and Brown, M. S. (1991). 39-kDa protein modulates binding of ligands to low density lipoprotein receptor-related protein/alpha 2-macroglobulin receptor. *J. Biol. Chem.* 266, 21232–21238.

Herz, J., Hamann, U., Rogne, S., Myklebost, O., Gausepohl, H., and Stanley, K. K. (1988). Surface location and high affinity for calcium of a 500-kd liver membrane protein closely related to the LDL-receptor suggest a physiological role as lipoprotein receptor. *EMBO J.* 7, 4119–4127. doi: 10.1002/j.1460-2075.1988.tb03306.x

Herz, J., and Strickland, D. K. (2001). LRP: a multifunctional scavenger and signaling receptor. *J. Clin. Invest.* 108, 779–784. doi: 10.1172/JCI200113992

Hicks, D. A., Nalivaeva, N. N., and Turner, A. J. (2012). Lipid rafts and Alzheimer's disease: protein-lipid interactions and perturbation of signaling. *Front. Physiol.* 3:189. doi: 10.3389/fphys.2012.00189

Hiesberger, T., Hüttler, S., Rohlmann, A., Schneider, W., Sandhoff, K., and Herz, J. (1998). Cellular uptake of saposin (SAP) precursor and lysosomal delivery by the low density lipoprotein receptor-related protein (LRP). *EMBO J.* 17, 4617–4625. doi: 10.1093/emboj/17.16.4617

Ho, G., Toomey, J. R., Broze, G. J. Jr., and Schwartz, A. L. (1996). Receptor-mediated endocytosis of coagulation factor Xa requires cell surface-bound tissue factor pathway inhibitor. *J. Biol. Chem.* 271, 9497–9502. doi: 10.1074/jbc.271.16.9497

Hofer, F., Gruenberger, M., Kowalski, H., Machat, H., Huettinger, M., Kuechler, E., et al. (1994). Members of the low density lipoprotein receptor family mediate cell entry of a minor- group common cold virus. *Proc. Natl. Acad. Sci. U.S.A.* 91, 1839–1842. doi: 10.1073/pnas.91.5.1839

Hoirisch-Clapauch, S., and Nardi, A. (2015). Improvement of psychotic symptoms and the role of tissue plasminogen activator. *Int. J. Mol. Sci.* 16, 27550–27560. doi: 10.3390/ijms161126053

Holtzman, D. M., Pitas, R. E., Kilbridge, J., Nathan, B., Mahley, R. W., Bu, G., et al. (1995). Low density lipoprotein receptor-related protein mediates apolipoprotein E-dependent neurite outgrowth in a central nervous system-derived neuronal cell line. *Proc. Natl. Acad. Sci. U.S.A.* 92, 9480–9484. doi: 10.1073/pnas.92.21.9480

Hu, K., Wu, C., Mars, W. M., and Liu, Y. (2007). Tissue-type plasminogen activator promotes murine myofibroblast activation through LDL receptor-related protein 1-mediated integrin signaling. *J. Clin. Invest.* 117, 3821–3832. doi: 10.1172/JCI32301

Hu, K., Yang, J., Tanaka, S., Gonias, S. L., Mars, W. M., and Liu, Y. (2006). Tissue-type plasminogen activator acts as a cytokine that triggers intracellular signal transduction and induces matrix metalloproteinase-9 gene expression. *J. Biol. Chem.* 281, 2120–2127. doi: 10.1074/jbc.M504988200

Huang, S. S., Ling, T. Y., Tseng, W. F., Huang, Y. H., Tang, F. M., Leal, S. M., et al. (2003). Cellular growth inhibition of IGFBP-3 and TGF-(beta)1 requires LRP-1. *FASEB J.* 17, 2068–2081. doi: 10.1096/fj.03-0256com

Huang, W., Dolmer, K., and Gettins, P. (1999). NMR solution structure of complement-like repeat CR8 from the low density lipoprotein receptor-related protein. *J. Biol. Chem.* 274, 14130–14136. doi: 10.1074/jbc.274.20.14130

Huang, Y.-Y., Bach, M., Lipp, H.-P., Zhuo, M., Wolfer, D., Hawkins, R., et al. (1996). Mice lacking the gene encoding tissue-type plasminogen activator show a selective interference with late-phase long-term potentiation in both Schaffer collateral and mossy fiber pathways. *Proc. Natl. Acad. Sci. U.S.A.* 93, 8699–8704. doi: 10.1073/pnas.93.16.8699

Hussain, M. M., Strickland, D. K., and Bakillah, A. (1999). The mammalian low-density lipoprotein receptor family. *Annu. Rev. Nutr.* 19, 141–172. doi: 10.1146/annurev.nutr.19.1.141

Hussaini, I. M., Brown, M. D., Karns, L. R., Carpenter, J., Redpath, G. T., Gonias, S. L., et al. (1999). Epidermal growth factor differentially regulates low density lipoprotein receptor-related protein gene expression in neoplastic and fetal human astrocytes. *Glia* 25, 71–84. doi: 10.1002/(SICI)1098-1136(19990101)25:1<71::AID-GLIA7>3.0.CO;2-0

Inoue, K., Koizumi, S., Nakajima, K., Hamanoue, M., and Kohsaka, S. (1994). Modulatory effect of plasminogen on NMDA-induced increase in intracellular free calcium concentration in rat cultured hippocampal neurons. *Neurosci. Lett.* 179, 87–90. doi: 10.1016/0304-3940(94)90941-5

Ishiguro, M., Imai, Y., and Kohsaka, S. (1995). Expression and distribution of low density lipoprotein receptor-related protein mRNA in the rat central nervous system. *Brain Res. Mol. Brain Res.* 33, 37–46. doi: 10.1016/0169-328X(95)00104-Z

Jaeger, S., and Pietrzik, C. U. (2008). Functional role of lipoprotein receptors in Alzheimer's disease. *Curr. Alzheimer Res.* 5, 15–25. doi: 10.2174/156720508783884675

Janiak, A., Zemskov, E. A., and Belkin, A. M. (2006). Cell surface transglutaminase promotes RhoA activation via integrin clustering and suppression of the Src-p190RhoGAP signaling pathway. *Mol. Biol. Cell* 17, 1605–1619. doi: 10.1091/mbc.e05-06-0549

Jeanneret, V., Wu, F., Merino, P., Torre, E., Diaz, A., Cheng, L., et al. (2016). Tissue-type plasminogen activator (tPA) modulates the postsynaptic response of cerebral cortical neurons to the presynaptic release of glutamate. *Front. Mol. Neurosci.* 9:121. doi: 10.3389/fnmol.2016.00121

Jen, A., Parkyn, C. J., Mootoosamy, R. C., Ford, M. J., Warley, A., Liu, Q., et al. (2010). Neuronal low-density lipoprotein receptor-related protein 1 binds and endocytoses prion fibrils via receptor cluster 4. *J. Cell Sci.* 123, 246–255. doi: 10.1242/jcs.058099

Jullienne, A., Montagne, A., Orset, C., Lesept, F., Jane, D., Monaghan, D., et al. (2011). Selective inhibition of GluN2D-containing n-methyl-d-aspartate receptors prevents tissue plasminogen activator-promoted neurotoxicity both in vitro and in vivo. *Mol. Neurodegener.* 6, 68–78. doi: 10.1186/1750-1326-6-68

Juric, V., Chen, C.-C., and Lau, L. F. (2012). TNF α-induced apoptosis enabled by CCN1/CYR61: pathways of reactive oxygen species generation and Cytochrome C release. *PLoS One* 7:e31303. doi: 10.1371/journal.pone.0031303

Kagitani, H., Tagawa, M., Hatanaka, K., Ikari, T., Saito, A., Bando, H., et al. (1985). Expression of e. coli of finger-domain lacking tissue-type plasminogen activator with high fibrin activity. *FEBS Lett.* 189, 145–149. doi: 10.1016/0014-5793(85)80860-7

Kamenetz, F., Tomita, T., Hsieh, H., Seabrook, G., Borchelt, D., Iwatsubo, T., et al. (2003). APP processing and synaptic function. *Neuron* 37, 925–937. doi: 10.1016/S0896-6273(03)00124-7

Kanai, Y., Wang, D., and Hirokawa, N. (2014). KIF13B enhances the endocytosis of LRP1 by recruiting LRP1 to caveolae. *J. Cell Biol.* 204, 395–408. doi: 10.1083/jcb.201309066

Kanekiyo, T., and Bu, G. (2014). The low-density lipoprotein receptor-related protein 1 and amyloid-β clearance in Alzheimer's disease. *Front. Aging Neurosci.* 6:93. doi: 10.3389/fnagi.2014.00093

Kanekiyo, T., Cirrito, J. R., Liu, C. C., Shinohara, M., Li, J., Schuler, D. R., et al. (2013). Neuronal clearance of amyloid-ß by endocytic receptor LRP1. *J. Neurosci.* 33, 19276–19283. doi: 10.1523/JNEUROSCI.3487-13.2013

Kanekiyo, T., Zhang, J., Liu, Q., Liu, C., Zhang, L., and Bu, G. (2011). Heparan sulfate proteoglycan and the low-density lipoprotein receptor-related protein 1 constitute major pathways for neuronal amyloid-beta uptake. *J. Neurosci.* 31, 1644–1651. doi: 10.1523/JNEUROSCI.5491-10.2011

Kang, D., Pietrzik, C., Baum, L., Chevallier, N., Merriam, D., Kounnas, M., et al. (2000). Modulation of amyloid beta-protein clearance and Alzheimer's disease susceptibility by the LDL receptor-related protein pathway. *J. Clin. Invest.* 106, 1159–1166. doi: 10.1172/JCI11013

Kang, D. E., Saitoh, T., Chen, X., Xia, Y., Masliah, E., Hansen, L. A., et al. (1997). Genetic association of the low-density lipoprotein receptor-related protein gene (LRP), and apolipoprotein E receptor, with late-onset Alzheimer's disease. *Neurology* 49, 56–61. doi: 10.1212/WNL.49.1.56

Kapustin, A., Stepanova, V., Aniol, N., Cines, D. B., Poliakov, A., Yarovoi, S., et al. (2012). Fibulin-5 binds urokinase-type plasminogen activator and mediates urokinase-stimulated β1-integrin-dependent cell migration. *Biochem. J.* 443, 491–503. doi: 10.1042/BJ20110348

Kasza, A., Petersen, H. H., Heegaard, C. W., Oka, K., Christensen, A., Dubin, A., et al. (1997). Specificity of serine proteinase/serpin complex binding to very- low-density lipoprotein receptor and alpha2-macroglobulin receptor/low-density-lipoprotein-receptor-related protein. *Eur. J. Biochem.* 248, 270–281. doi: 10.1111/j.1432-1033.1997.00270.x

Kinoshita, A., Shah, T., Tangredi, M. M., Strickland, D. K., and Hyman, B. T. (2003). The intracellular domain of the low density lipoprotein receptor-related protein modulates transactivation mediated by amyloid precursor protein and Fe65. *J. Biol. Chem.* 278, 41182–41188. doi: 10.1074/jbc.M306403200

Klug, W., Dietl, A., Simon, B., Sinning, I., and Wild, K. (2011). Phosphorylation of LRP1 regulates the interaction with Fe65. *FEBS Lett.* 585, 3229–3235. doi: 10.1016/j.febslet.2011.09.028

Knauer, D. J., Majumdar, D., Fong, P.-C., and Knauer, M. F. (2000). Serpin regulation of factor XIa. *J. Biol.Chem.* 275, 37340–37346. doi: 10.1074/jbc.M003909200

Knauer, M. F., Kridel, S. J., Hawley, S. B., and Knauer, D. J. (1997). The efficient catabolism of thrombin-protease nexin 1 complexes is a synergistic mechanism that requires both the LDL receptor-related protein and cell surface heparins. *J. Biol. Chem.* 272, 29039–29045. doi: 10.1074/jbc.272.46.29039

Knauer, M. F., Orlando, R. A., and Glabe, C. G. (1996). Cell surface APP751 forms complexes with protease nexin 2 ligands and is internalized via the low density lipoprotein receptor-related protein (LRP). *Brain Res.* 740, 6–14. doi: 10.1016/S0006-8993(96)00711-1

Komuro, H., and Rakic, P. (1992). Selective role of N-type calcium channels in neuronal migration. *Science* 257, 806–809. doi: 10.1126/science.1323145

Komuro, H., and Rakic, P. (1993). Modulation of neuronal migration by NMDA receptors. *Science* 260, 95–97. doi: 10.1126/science.8096653

Kounnas, M. Z., Argraves, W., and Strickland, D. (1992a). The 39-kDa receptor-associated protein interacts with two members of the low density lipoprotein receptor family, alpha 2-macroglobulin receptor and glycoprotein 330. *J. Biol. Chem.* 267, 21162–21166.

Kounnas, M. Z., Chappell, D. A., Wong, H., Argraves, W. S., and Strickland, D. K. (1995b). The cellular internalization and degradation of hepatic lipase is mediated by low density lipoprotein receptor-related protein and requires cell surface proteoglycans. *J. Biol. Chem.* 270, 9307–9312.

Kounnas, M. Z., Church, F. C., Argraves, W. S., and Strickland, D. K. (1996). Cellular internalization and degradation of antithrombin III-thrombin, heparin cofactor II-thrombin, and α1-antitrypsin- trypsin complexes is mediated by the low density lipoprotein receptor-related protein. *J. Biol. Chem.* 271, 6523–6529. doi: 10.1074/jbc.271.11.6523

Kounnas, M. Z., Henkin, J., Argraves, W. S., and Strickland, D. K. (1993). Low density lipoprotein receptor-related protein/alpha 2-macroglobulin receptor mediates cellular uptake of pro-urokinase. *J. Biol. Chem.* 268, 21862–21867.

Kounnas, M. Z., Moir, R. D., Rebeck, G. W., Bush, A. I., Argraves, W. S., Tanzi, R. E., et al. (1995a). LDL receptor-related protein, a multifunctional apoE receptor, binds secreted β -amyloid precursor protein and mediates its degradation. *Cell* 82, 331–340.

Kounnas, M. Z., Morris, R. E., Thompson, M. R., FitzGerald, D. J., Strickland, D. K., and Saelinger, C. B. (1992b). The alpha 2-macroglobulin receptor/low density lipoprotein receptor-related protein binds and internalizes *Pseudomonas* exotoxin A. *J. Biol. Chem.* 267, 12420–12423.

Kowal, R. C., Herz, J., Goldstein, J. L., Esser, V., and Brown, M. S. (1989). Low density lipoprotein receptor-related protein mediates uptake of cholesteryl esters derived from apoprotein E-enriched lipoproteins. *Proc. Natl. Acad. Sci. U.S.A.* 86, 5810–5814. doi: 10.1073/pnas.86.15.5810

Kozlova, N., Jensen, J., Chi, T., Samoylenko, A., and Kietzmann, T. (2015). PAI-1 modulates cell migration in a LRP1-dependent manner via β-catenin and ERK1/2. *Thromb. Haemost.* 113, 988–998. doi: 10.1160/TH14-08-0678

Kuiper, J., Otter, M., Rijken, D., and van Berkel, T. (1988). Characterization of the interaction in vivo of tissue-type plasminogen activator with liver cells. *J. Biol. Chem.* 263, 18220–18224.

Landowski, L. M., Pavez, M., Brown, L. S., Gasperini, R., Taylor, B. V., West, A. K., et al. (2016). Low-density lipoprotein receptor-related proteins in a novel mechanism of axon guidance and peripheral nerve regeneration. *J. Biol. Chem.* 291, 1092–1102. doi: 10.1074/jbc.M115.668996

Laudati, E., Gilder, A. S., Lam, M. S., Misasi, R., Sorice, M., Gonias, S. L., et al. (2016). The activities of LDL receptor-related protein-1 (LRP1) compartmentalize into distinct plasma membrane microdomains. *Mol. Cell. Neurosci.* 76, 42–51. doi: 10.1016/j.mcn.2016.08.006

Laurén, J., Gimbel, D. A., Nygaard, H. B., Gilbert, J. W., and Strittmatter, S. M. (2009). Cellular prion protein mediates impairment of synaptic plasticity by amyloid-β oligomers. *Nature* 457, 1128–1132. doi: 10.1038/nature07761

Lee, C. Y. D., and Landreth, G. E. (2010). The role of microglia in amyloid clearance from the AD brain. *J. Neural Transm.* 117, 949–960. doi: 10.1007/s00702-010-0433-4

Lee, S., Ko, H., Kwon, K., Lee, J., Han, S.-H., Han, D., et al. (2014). TPA regulates neurite outgrowth by phosphorylation of LRP5/6 in neural progenitor cells. *Mol. Neurobiol.* 49, 199–215. doi: 10.1007/s12035-013-8511-x

Lee, S. H., Suh, H. N., Lee, Y. J., Seo, B. N., Ha, J. W., and Han, H. J. (2012). Midkine prevented hypoxic injury of mouse embryonic stem cells through activation of Akt and HIV-1α via low-density lipoprotein receptor-related protein-1. *J. Cell. Physiol.* 227, 1731–1739. doi: 10.1002/jcp.22897

Lehti, K., Rose, N. F., Valavaara, S., Weiss, S. J., and Keski-Oja, J. (2009). MT1-MMP promotes vascular smooth muscle dedifferentiation through LRP1 processing. *J. Cell Sci.* 122, 126–135. doi: 10.1242/jcs.035279

Lemarchand, E., Maubert, E., Haelewyn, B., Ali, C., Rubio, M., and Vivien, D. (2016). Stressed neurons protect themselves by a tissue-type plasminogen activator-mediated EGFR-dependent mechanism. *Cell Death Differ.* 23, 123–131. doi: 10.1038/cdd.2015.76

Lensjø, K. K., Christensen, A. C., Tennøe, S., Fyhn, M., and Hafting, T. (2017). Differential expression and cell-type specificity of perineuronal nets in hippocampus, medial entorhinal cortex, and visual cortex examined in the rat and mouse. *eNeuro* 4:ENEURO.0379-16.2017. doi: 10.1523/ENEURO.0379-16.2017

Lenting, P. J., Neels, J. G., van den Berg, B. M., Clijsters, P. P., Meijerman, D. W., Pannekoek, H., et al. (1999). The light chain of factor VIII comprises a binding site for low density lipoprotein receptor-related protein. *J. Biol. Chem.* 274, 23734–23739. doi: 10.1074/jbc.274.34.23734

Lesept, F., Chevilley, A., Jezequel, J., Ladépêche, L., Macrez, R., Aimable, M., et al. (2016). Tissue-type plasminogen activator controls neuronal death by raising surface dynamics of extrasynaptic NMDA receptors. *Cell Death Dis.* 7:e2466. doi: 10.1038/cddis.2016.279

Li, S. S., Liu, Z., and Sundqvist, K.-G. (2006). Endogenous thrombospondin-1 is a cell-surface ligand for regulation of integrin-dependent T-lymphocyte adhesion. *Blood* 108, 3112–3120. doi: 10.1182/blood-2006-04-016832

Li, X., Herz, J., and Monard, D. (2006). Activation of ERK signaling upon alternative protease nexin-1 internalization mediated by syndecan-1. *J. Cell. Biochem.* 99, 936–951. doi: 10.1002/jcb.20881

Li, Y., Lu, W., Marzolo, M. P., and Bu, G. (2001). Differential functions of members of the low density lipoprotein receptor family suggested by their distinct endocytosis rates. *J. Biol. Chem.* 276, 18000–18006. doi: 10.1074/jbc.M101589200

Li, Y., Marzolo, M. P., van Kerkhof, P., Strous, G. J., and Bu, G. (2000). The YXXL motif, but not the two NPXY motifs, serves as the dominant endocytosis signal for low density lipoprotein receptor-related protein. *J. Biol. Chem.* 275, 17187–17194. doi: 10.1074/jbc.M000490200

Lillis, A., Mikhailenko, I., and Strickland, D. (2005). Beyond endocytosis: LRP function in cell migration, proliferation and vascular permeability. *J. Thromb. Haemost.* 3, 1884–1893. doi: 10.1111/j.1538-7836.2005.01371.x

Lillis, A., van Duyn, L., Murphy-Ullrich, J., and Strickland, D. (2008). LDL receptor-related protein 1: unique tissue-specific functions revealed by selective gene knockout studies. *Physiol. Rev.* 88, 887–918. doi: 10.1152/physrev.00033.2007

Lin, J., Mironova, Y. A., Shrager, P., and Giger, R. J. (2017). LRP1 regulates peroxisome biogenesis and cholesterol homeostasis in oligodendrocytes and is required for proper CNS myelin development and repair. *eLife* 6:e30498. doi: 10.7554/eLife.30498

Ling, T. Y., Chen, C. L., Huang, Y. H., Liu, I. H., Huang, S. S., and Huang, J. S. (2004). Identification and characterization of the acidic pH binding sites for growth regulatory ligands of low density lipoprotein receptor-related protein-1. *J. Biol. Chem.* 279, 38736–38748. doi: 10.1074/jbc.M310537200

Liu, C. C., Hu, J., Zhao, N., Wang, J., Wang, N., Cirrito, J. R., et al. (2017). Astrocytic LRP1 mediates brain Aβ clearance and impacts amyloid deposition. *J. Neurosci.* 37, 4023–4031. doi: 10.1523/JNEUROSCI.3442-16.2017

Liu, Q., Trotter, J., Zhang, J., Peters, M. M., Cheng, H., Bao, J., et al. (2010). Neuronal LRP1 knockout in adult mice leads to impaired brain lipid metabolism and progressive, age-dependent synapse loss and neurodegeneration. *J. Neurosci.* 30, 17068–17078. doi: 10.1523/JNEUROSCI.4067-10.2010

Liu, Q., Zerbinatti, C. V., Zhang, J., Hoe, H. S., Wang, B., Cole, S. L., et al. (2007). Amyloid precursor protein regulates brain apolipoprotein E and cholesterol metabolism through lipoprotein receptor LRP1. *Neuron* 56, 66–78. doi: 10.1016/j.neuron.2007.08.008

Liu, Q., Zhang, J., Zerbinatti, C., Zhan, Y., Kolber, B. J., Herz, J., et al. (2011). Lipoprotein receptor LRP1 regulates leptin signaling and energy homeostasis in the adult central nervous system. *PLoS Biol.* 9:e1000575. doi: 10.1371/journal.pbio.1000575

Liu, Y., Jones, M., Hingtgen, C. M., Bu, G., Laribee, N., Tanzi, R. E., et al. (2000). Uptake of HIV-1 tat protein mediated by low-density lipoprotein receptor-related protein disrupts the neuronal metabolic balance of the receptor ligands. *Nat. Med.* 6, 1380–1387. doi: 10.1038/82199

Lleo, A., Waldron, E., von Arnim, C. A., Herl, L., Tangredi, M. M., Peltan, I. D., et al. (2005). Low density lipoprotein receptor-related protein (LRP) interacts with presenilin 1 and is a competitive substrate of the amyloid precursor protein (APP) for gamma-secretase. *J. Biol. Chem.* 280, 27303–27309. doi: 10.1074/jbc.M413969200

Loukinova, E., Ranganathan, S., Kuznetsov, S., Gorlatova, N., Migliorini, M., Ulery, P. G., et al. (2002). Platelet-derived growth factor (PDGF)-induced tyrosine phosphorylation of the low density lipoprotein receptor-related protein (LRP). Evidence for integrated co-receptor function between LRP and the PDGF. *J. Biol. Chem.* 277, 15499–15506. doi: 10.1074/jbc.M200427200

Lu, Z., and Kipnis, J. (2010). Thrombospondin 1 - a key astrocyte-derived neurogenic factor. *FASEB J.* 24, 1925–1934. doi: 10.1096/fj.09-150573

Ma, Z., Thomas, K. S., Webb, D. J., Moravec, R., Salicioni, A. M., Mars, W. M., et al. (2002). Regulation of Rac1 activation by the low density lipoprotein receptor-related protein. *J. Cell Biol.* 159, 1061–1070. doi: 10.1083/jcb.200207070

Macrez, R., Bezin, L., Le Mauff, B., Ali, C., and Vivien, D. (2010). Functional occurrence of the interaction of tissue plasminogen activator with the NR1 subunit of N-methyl-D-aspartate receptors during stroke. *Stroke* 41, 2950–2955. doi: 10.1161/STROKEAHA.110.592360

Madani, R., Hulo, S., Toni, N., Madani, H., Steimer, T., Muller, D., et al. (1999). Enhanced hippocampal long-term potentiation and learning by increased neuronal expression of tissue-type plasminogen activator in transgenic mice. *EMBO J.* 18, 3007–3012. doi: 10.1093/emboj/18.11.3007

Mahley, R. W., and Huang, Y. (2007). Atherogenic remnant lipoproteins: role for proteoglycans in trapping, transferring, internalizing. *J. Clin. Invest.* 117, 94–98. doi: 10.1172/JCI30889

Makarova, A., Mikhailenko, I., Bugge, T. H., List, K., Lawrence, D. A., and Strickland, D. K. (2003). The low density lipoprotein receptor-related protein modulates protease activity in the brain by mediating the cellular internalization of both neuroserpin and neuroserpin-tissue-type plasminogen activator complexes. *J. Biol. Chem.* 278, 50250–50258. doi: 10.1074/jbc.M309150200

Mandrekar, S., Jiang, Q., Lee, C. Y., Koenigsknecht-Talboo, J., Holtzman, D. M., and Landreth, G. E. (2009). Microglia mediate the clearance of soluble Abeta through fluid phase macropinocytosis. *J. Neurosci.* 29, 4252–4262. doi: 10.1523/JNEUROSCI.5572-08.2009

Mantuano, E., Jo, M., Gonias, S. L., and Campana, W. M. (2010). Low density lipoprotein receptor-related protein (LRP1) regulates Rac1 and RhoA reciprocally to control Schwann cell adhesion and migration. *J. Biol. Chem.* 285, 14259–14266. doi: 10.1074/jbc.M109.085126

Mantuano, E., Lam, M., and Gonias, S. (2013). LRP1 assembles unique co-receptor systems to initiate cel signalling in response to tissue-type plasminogen activator and myelin-associated glycoprotein. *J. Biol. Chem.* 288, 34009–34018. doi: 10.1074/jbc.M113.509133

Mantuano, E., Lam, M., Shibayama, M., Campana, W., and Gonias, S. (2015). The NMDA receptor functions independently and as an LRP1 co-receptor to promote Schwann cell survival and migration. *J. Cell Sci.* 128, 3478–3488. doi: 10.1242/jcs.173765

Martin, A. M., Kuhlmann, C., Trossbach, S., Jaeger, S., Waldron, E., Roebroek, A., et al. (2008). The functional role of the second NPXY motif of the LRP1 β-chain in tissue-type plasminogen activator-mediated activation of N-methyl-D-aspartate receptors. *J. Biol. Chem.* 283, 12004–12013. doi: 10.1074/jbc.M707607200

Marzolo, M. P., von Bernhardi, R., Bu, G., and Inestrosa, N. C. (2000). Expression of alpha(2)- macroglobulin receptor/low density lipoprotein receptor-related protein (LRP) in rat microglial cells. *J. Neurosci. Res.* 60, 401–411. doi: 10.1002/(SICI)1097-4547(20000501)60:3<401::AID-JNR15>3.0.CO;2-L

May, P., Herz, J., and Bock, H. (2005). Molecular mechanisms of lipoprotein receptor signalling. *Cell. Mol. Life Sci.* 62, 2325–2338. doi: 10.1007/s00018-005-5231-z

May, P., Reddy, K., and Herz, J. (2002). Proteolytic processing of low density lipoprotein receptor-related protein mediates regulated release of its intracellular domain. *J. Biol. Chem.* 277, 18736–18743. doi: 10.1074/jbc.M201979200

May, P., Rohlmann, A., Bock, H. H., Zurhove, K., Marth, J. D., Schomburg, E. D., et al. (2004). Neuronal LRP1 functionally associates with postsynaptic proteins and is required for normal motor function in mice. *Mol. Cell. Biol.* 24, 8872–8883. doi: 10.1128/MCB.24.20.8872-8883.2004

McKeown-Longo, P. J., Hanning, R., and Mosher, D. F. (1984). Binding and degradation of platelet thrombospondin by cultured fibroblasts. *J. Cell Biol.* 98, 22–28. doi: 10.1083/jcb.98.1.22

Meijer, A., Rohlena, J., van der Zwaan, C., van Zonneveld, A., Boertjes, R., Lenting, P., et al. (2007). Functional duplication of ligand-binding domains within low-density lipoprotein receptor-related proten for interaction with receptor associated protein, alpha2-macroglobulin, factor IXa and factor VIII. *Biochim. Biophys. Acta* 1774, 714–722. doi: 10.1016/j.bbapap.2007.04.003

Meilinger, M., Gschwentner, C., Burger, I., Haumer, M., Wahrmann, M., Szollar, L., et al. (1999). Metabolism of activated complement component C3 is mediated by the low density lipoprotein receptor-related protein/alpha(2)-macroglobulin receptor. *J. Biol. Chem.* 274, 38091–38096. doi: 10.1074/jbc.274.53.38091

Meilinger, M., Haumer, M., Szakmary, K. A., Steinbock, F., Scheiber, B., Goldenberg, H., et al. (1995). Removal of lactoferrin from plasma is mediated by binding to low density lipoprotein receptor-related protein/α 2-macroglobulin receptor and transport to endosomes. *FEBS Lett.* 360, 70–74. doi: 10.1016/0014-5793(95)00082-K

Menezes, M. J., McClenahan, F. K., Leiton, C. V., Aranmolate, A., Shan, X., and Colognato, H. (2014). The extracellular matrix protein laminin α2 regulates the maturation and function of the blood-brain barrier. *J. Neurosci.* 34, 15260–15280. doi: 10.1523/JNEUROSCI.3678-13.2014

Meng, H., Zhang, X., Hankenson, K. D., and Wang, M. M. (2009). Thrombospondin 2 potentiates notch3/jagged1 signaling. *J. Biol. Chem.* 284, 7866–7874. doi: 10.1074/jbc.M803650200

Meng, H., Zhang, X., Lee, S. J., Strickland, D. K., Lawrence, D. A., and Wang, M. M. (2010). Low density lipoprotein receptor-related protein-1 (LRP-1) regulates thrombospondin-2 (TSP2) enhancement of Notch3 signaling. *J. Biol. Chem.* 285, 23047–23055. doi: 10.1074/jbc.M110.144634

Merle, B., Malaval, L., Lawler, J., Delmas, P., and Clezardin, P. (1997). Decorin inhibits cell attachment to thrombospondin-1 by binding to a KKTR-dependent cell adhesive site present within the N-terminal domain of thrombospondin-1. *J. Cell. Biochem.* 67, 75–83. doi: 10.1002/(SICI)1097-4644(19971001)67:1<75::AID-JCB8>3.0.CO;2-T

Mignatti, P., and Rifkin, D. B. (1993). Biology and biochemistry of proteinases in tumor invasion. *Physiol. Rev.* 73, 161–195. doi: 10.1152/physrev.1993.73.1.161

Mikhailenko, I., Kounnas, M. Z., and Strickland, D. K. (1995). Low density lipoprotein receptor-related protein/alpha 2-macroglobulin receptor mediates the cellular internalization and degradation of thrombospondin. A process facilitated by cell-surface proteoglycans. *J. Biol. Chem.* 270, 9543–9549. doi: 10.1074/jbc.270.16.9543

Mikhailenko, I., Krylov, D., Argraves, K. M., Roberts, D. D., Liau, G., and Strickland, D. K. (1997). Cellular internalization and degradation of thrombospondin-1 is mediated by the amino-terminal heparin binding domain (HBD): high affinity interaction of dimeric HBD with the low density lipoprotein receptor-related protein. *J. Biol. Chem.* 272, 6784–6791. doi: 10.1074/jbc.272.10.6784

Moestrup, S. K., Christensen, E. I., Sottrup-Jensen, L., and Gliemann, J. (1987). Binding and receptor-mediated endocytosis of pregnancy zone protein-proteinase complex in rat macrophages. *Biochim. Biophys. Acta* 930, 297–303. doi: 10.1016/0167-4889(87)90002-4

Moestrup, S. K., Cui, S., Vorum, H., Bregengard, C., Bjorn, S. E., Norris, K., et al. (1995). Evidence that epithelial glycoprotein 330/megalin mediates uptake of polybasic drugs. *J. Clin. Invest.* 96, 1404–1413. doi: 10.1172/JCI118176

Morikawa, S., Ikegaya, Y., Narita, M., and Tamura, H. (2017). Activation of perineuronal net-expressing excitatory neurons during associative memory encoding and retrieval. *Sci. Rep.* 7:46024. doi: 10.1038/srep46024

Muramatsu, H., Zou, K., Sakaguchi, N., Ikematsu, S., Sakuma, S., and Muramatsu, T. (2000). LDL-receptor-related protein as a component of the midkine receptor. *Biochem. Biophys. Res. Commun.* 270, 936–941. doi: 10.1006/bbrc.2000.2549

Muratoglu, S. C., Belgrave, S., Hampton, B., Migliorini, M., Coksaygan, T., Chen, L., et al. (2013). LRP1 protects the vasculature by regulating levels of connective tissue growth factor and HtrA1. *Arterioscler. Thromb. Vasc. Biol.* 33, 2137–2146. doi: 10.1161/ATVBAHA.113.301893

Muratoglu, S. C., Belgrave, S., Lillis, A. P., Migliorini, M., Robinson, S., Smith, E., et al. (2011). Macrophage LRP1 supresses neo-intima formation during vascular remodeling by modulating the TGF-β signaling pathway. *PLoS One* 6:e28846. doi: 10.1371/journal.pone.0028846

Murphy-Ullrich, J. E., Gurusiddappa, S., Frazier, W. A., and Hook, M. (1993). Heparin-binding peptides from thrombospondins 1 and 2 contain focal adhesion-labilizing activity. *J. Biol. Chem.* 268, 26784–26789.

Nakajima, C., Haffner, P., Goerke, S. M., Zurhove, K., Adelmann, G., Frotscher, M., et al. (2014). The lipoprotein receptor LRP1 modulates sphingosine-1-phosphate signaling and is essential for vascular development. *Development* 141, 4513–4525. doi: 10.1242/dev.109124

Nakajima, C., Kulik, A., Frotscher, M., Herz, J., Schäfer, M., Bock, H. H., et al. (2013). Low density lipoprotein receptor-related protein 1 (LRP1) modulates N-methyl-D-aspartate (n.d.) receptor-dependent intracellular signaling and NMDA-induced regulation of postsynaptic protein complexes. *J. Biol. Chem.* 288, 21909–21923. doi: 10.1074/jbc.M112.444364

Nazer, B., Hong, S., and Selkoe, D. J. (2008). LRP promotes endocytosis and degradation, but not transcytosis, of the amyloid-β peptide in a blood-brain barrier in vitro model. *Neurobiol. Dis.* 30, 94–102. doi: 10.1016/j.nbd.2007.12.005

Neels, J., van den Berg, B., Lookene, A., Olivecrona, G., Pannekoek, H., and van Zonneveld, A. (1999). The second and fourth cluster of class A cysteine-rich repeats of the low density lipoprotein receptor-related protein share ligand-binding properties. *J. Biol. Chem.* 274, 31305–31311. doi: 10.1074/jbc.274.44.31305

Ng, K.-S., Leung, H.-W., Wong, P. T.-H., and Low, C.-M. (2012). Cleavage of the NR2B subunit amino terminus of N-methyl-D-aspartate (n.d.) receptor by tissue plasminogen activator: identification of the cleavage site and characterization of ifenprodil and glycine affinities on truncated NMDA receptor. *J. Biol. Chem.* 287, 25520–25529. doi: 10.1074/jbc.M112.374397

Nicole, O., Docagne, F., Ali, C., Margaill, I., Carmeliet, P., MacKenzie, E. T., et al. (2001). The proteolytic activity of tissue-plasminogen activator enhances NMDA receptor-mediated signaling. *Nat. Med.* 7, 59–64. doi: 10.1038/83358

Niego, B., Freeman, R., Puschmann, T. B., Turnley, A. M., and Medcalf, R. L. (2012). T-PA-specific modulation of a human blood-brain barrier model involves plasmin-mediated activation of the Rho kinase pathway in astrocytes. *Blood* 119, 4752–4761. doi: 10.1182/blood-2011-07-369512

Nykjaer, A., Conese, M., Christensen, E. I., Olson, D., Cremona, O., Gliemann, J., et al. (1997). Recycling of the urokinase receptor upon internalization of the uPA:serpin complexes. *EMBO J.* 16, 2610–2620. doi: 10.1093/emboj/16.10.2610

Nykjaer, A., Kjoller, I., Cohen, R. I., Lawrence, D. A., Garni-Wagner, B. A., Todd, R. F., et al. (1994). Regions involved in binding of urokinase-type-1 inhibitor complex and pro-urokinase to the endocytic alpha 2-macroglobulin receptor/low density lipoprotein receptor-related protein. Evidence that the urokinase receptor protects pro-urokinase against binding to the endocytic receptor. *J. Biol. Chem.* 269, 25668–25676.

Nykjaer, A., Petersen, C. M., Moller, B., Jensen, P. H., Moestrup, S. K., Holtet, T. L., et al. (1992). Purified alpha 2- macroglobulin receptor/LDL receptor-related protein binds urokinase plasminogen activator inhibitor type-1 complex. Evidence that the alpha 2-macroglobulin receptor mediates cellular degradation of urokinase receptor-bound complexes. *J. Biol. Chem.* 267, 14543–14546.

Obiang, P., Macrez, R., Jullienne, A., Bertrand, T., Lesept, F., Ali, C., et al. (2012). GluN2D subunit-containing NMDA receptors control tissue plasminogen activator-mediated spatial memory. *J. Neurosci.* 32, 12726–12734. doi: 10.1523/JNEUROSCI.6202-11.2012

Okada, S. S., Grobmyer, S. R., and Barnathan, E. S. (1996). Contrasting effects of plasminogen activators, urokinase receptor, LDL receptor-related protein on smooth muscle cell migration and invasion. *Arterioscler. Thromb. Vasc. Biol.* 16, 1269–1276. doi: 10.1161/01.ATV.16.10.1269

Orr, A. W., Elzie, C. A., Kucik, D. F., and Murphy-Ullrich, J. E. (2003a). Thrombospondin signaling through the calreticulin/LDL receptor-related protein co-complex stimulates random and directed cell migration. *J. Cell Sci.* 116, 2917–2927.

Orr, A. W., Pedraza, C. E., Pallero, M. A., Elzie, C. A., Goicoechea, S., Strickland, D. K., et al. (2003b). Low density lipoprotein receptor-related protein is a calreticulin coreceptor that signals focal adhesion disassembly. *J. Cell Biol.* 161, 1179–1189.

Orr, A. W., Pallero, M. A., and Murphy-Ullrich, J. E. (2002). Thrombospondin stimulates focal adhesion disassembly through Gi- and phosphoinositide 3-kinase-dependent ERK activation. *J. Biol. Chem.* 277, 20453–20460. doi: 10.1074/jbc.M112091200

Orr, A. W., Pallero, M. A., Xiong, W. C., and Murphy-Ullrich, J. E. (2004). Thrombospondin induces RhoA inactivation through FAK-dependent signaling to stimulate focal adhesion disassembly. *J. Biol. Chem.* 279, 48983–48992. doi: 10.1074/jbc.M404881200

Orth, K., Madison, E. L., Gething, M. J., Sambrook, J. F., and Herz, J. (1992). Complexes of tissue-type plasminogen activator and its serpin inhibitor plasminogen-activator inhibitor type 1 are internalized by means of the low density lipoprotein receptor-related protein/alpha 2-macroglobulin receptor. *Proc. Natl. Acad. Sci. U.S.A.* 89, 7422–7426. doi: 10.1073/pnas.89.16.7422

Pan, L., North, H. A., Sahni, V., Jeong, S. J., Mcguire, T. L., Berns, E. J., et al. (2014). β1-integrin and integrin linked kinase regulate astroctic differentiation of neural stem cells. *PLoS One* 9:e104335. doi: 10.1371/journal.pone.0104335

Pan, L., Zhao, Y., Zhijie, Y., and Qin, G. (2016). Research advances on structure and biological functions of integrins. *Springerplus* 5:1094. doi: 10.1186/s40064-016-2502-0

Pang, P. T., and Lu, B. (2004). Regulation of late-phase LTP and long-term memory in normal and aging hippocampus: role of secreted proteins tPA and BDNF. *Ageing Res. Rev.* 3, 407–430. doi: 10.1016/j.arr.2004.07.002

Pang, P. T., Teng, H. K., Zaitsev, E., Woo, N. T., Sakata, K., Zhen, S., et al. (2004). Cleavage of proBDNF by tPA/plasmin is essential for long-term hippocampal plasticity. *Science* 306, 487–491. doi: 10.1126/science.1100135

Parcq, J., Bertrand, T., Montagne, A., Baron, A. F., Macrez, R., Billard, J. M., et al. (2012). Unveiling an exceptional zymogen: the single-chain form of tPA is a selective activator of NMDA receptor-dependent signaling and neurotoxicity. *Cell Death Differ.* 19, 1983–1991. doi: 10.1038/cdd.2012.86

Pasquet, N., Douceau, S., Naveau, M., Lesept, F., Louessard, M., Lebouvier, L., et al. (2018). Tissue-type plasminogen activator controlled corticogenesis through a mechanism dependent of NMDA receptors expressed on radial glial cells. *Cereb. Cortex* 119, 1–17. doi: 10.1093/cercor/bhy119

Pawlak, R., Melchor, J., Matys, T., Skrzypiec, A., and Strickland, S. (2005). Ethanol-withdrawal seizures are controlled by tissue plasminogen activator via modulation of NR2B-containing NMDA receptors. *Proc. Natl. Acad. Sci. U.S.A.* 102, 443–448. doi: 10.1073/pnas.0406454102

Pflanzner, T., Janko, M. C., André-Dohmen, B., Reuss, S., Weggen, S., Roebroek, A. J., et al. (2011). LRP1 mediates bidirectional transcytosis of amyloid-β across the blood-brain barrier. *Neurobiol. Aging* 32, 2323.e1–2323.e11. doi: 10.1016/j.neurobiolaging.2010.05.025

Pi, X., Schmitt, C. E., Xie, L., Portbury, A. L., Wu, Y., Lockyer, P., et al. (2012). LRP1-dependent endocytic mechanism governs the signaling output of the bmp system in endothelial cells and in angiogenesis. *Circ. Res.* 111, 564–574. doi: 10.1161/CIRCRESAHA.112.274597

Pietrzik, C., Busse, T., Merriam, D., Weggen, S., and Koo, E. (2002). The cytoplasmic domain of the LDL receptor-related protein regulates multiple steps in APP processing. *EMBO J.* 21, 5691–5700. doi: 10.1093/emboj/cdf568

Pietrzik, C., Yoon, I., Jaeger, S., Busse, T., Weggen, S., and Koo, E. (2004). FE65 constitutes the functional link between the low-density lipoprotein receptor-related protein and the amyloid precursor protein. *J. Neurosci.* 24, 4259–4265. doi: 10.1523/JNEUROSCI.5451-03.2004

Pitkänen, A., Ndode-Ekane, X. E., Łukasiuk, K., Wilczynski, G. M., Dityatev, A., Walker, M. C., et al. (2014). Neural ECM and epilepsy. *Prog. Brain Res.* 214, 229–262. doi: 10.1016/B978-0-444-63486-3.00011-6

Plump, A. S., Smith, J. D., Hayek, T., Aalto-Setäla, K., Walsh, A., Verstuyft, J. G., et al. (1992). Severe hypercholesterolemia and atherosclerosis in apolipoprotein E-deficient mice created by homologous recombination in ES cells. *Cell* 71, 343–353. doi: 10.1016/0092-8674(92)90362-G

Polavarapu, R., Gongora, M. C., Yi, H., Ranganthan, S., Lawrence, D. A., Strickland, D., et al. (2007). Tissue-type plasminogen activator-mediated shedding of astrocytic low-density lipoprotein receptor-related protein increases the permeability of the neurovascular unit. *Blood* 109, 3270–3278. doi: 10.1182/blood-2006-08-043125

Poller, W., Willnow, T. E., Hilpert, J., and Herz, J. (1995). Differential recognition of alpha 1-antitrypsin-elastase and alpha 1-antichymotrypsin-cathepsin G complexes by the low density lipoprotein receptor-related protein. *J. Biol. Chem.* 270, 2841–2845. doi: 10.1074/jbc.270.6.2841

Pyka, M., Wetzel, C., Aguado, A., Geissler, M., Hatt, H., and Faissner, A. (2011). Chondroitin sulfate proteoglycans regulate astrocyte-dependent synaptogenesis and modulate synaptic activity in primary embryonic hippocampal neurons. *Eur. J. Neurosci.* 33, 2187–2202. doi: 10.1111/j.1460-9568.2011.07690.x

Qian, Z., Gilbert, M. E., Colicos, M. A., Kandel, E. R., and Kuhl, D. (1993). Tissue-plasminogen activator is induced as an immediate-early gene during seizure, kindling and long-term potentiation. *Nature* 361, 453–457. doi: 10.1038/361453a0

Qiu, Z., Hyman, B. T., and Rebeck, G. W. (2004). Apolipoprotein E receptors mediate neurite outgrowth through activation of p44/42 mitogen-activated protein kinase in primary neurons. *J. Biol. Chem.* 279, 34948–34956. doi: 10.1074/jbc.M401055200

Qiu, Z., Strickland, D., Hyman, B., and Rebeck, G. (2002). Alpha 2-macroglobulin exposure reduces calcium responses to N -methyl-D-aspartate via low density lipoprotein receptor-related protein in cultured hippocampal neurons. *J. Biol. Chem.* 277, 14458–14466. doi: 10.1074/jbc.M112066200

Qiu, Z., Strickland, D. K., Hyman, B. T., and Rebeck, G. W. (1999). Alpha2-macroglogulin enhances the clearance of endogeneous soluble beta-amyloid-peptide via low-density lipoprotein receptor-related protein in cortical neurons. *J. Neurochem.* 73, 1393–1398. doi: 10.1046/j.1471-4159.1999.0731393.x

Rabiej, V., Pflanzner, T., Wagner, T., Goetze, K., Storck, S., Eble, J., et al. (2015). Low density lipoprotein receptor-related protein 1 mediated endocytosis of β1-integrin influences cell adhesion and cell migration. *Exp. Cell Res.* 340, 102–115. doi: 10.1016/j.yexcr.2015.11.020

Ramanathan, A., Nelson, A. R., Sagare, A. P., and Zlokovic, B. V. (2015). Impaired vascular-mediated clearance of brain amyloid beta in Alzheimer's disease: the role, regulation and restoration of LRP1. *Front. Aging Neurosci.* 7:136. doi: 10.3389/fnagi.2015.00136

Rastegarlari, G., Pegon, J. N., Casari, C., Odouard, S., Navarrete, A. M., Saint-Lu, N., et al. (2012). Macrophage LRP1 contributes to the clearance of von Willebrand factor. *Blood* 119, 2126–2134. doi: 10.1182/blood-2011-08-373605

Rebeck, G. W., Harr, S. D., Strickland, D. K., and Hyman, B. T. (1995). Multiple, diverse senile plaque-associated proteins are ligands of an apolipoproteinE receptor, the alpha 2-macroglobulin receptor/low-density-lipoprotein receptor related protein. *Ann. Neurol.* 37, 211–217. doi: 10.1002/ana.410370212

Reekmans, S. M., Pflanzner, T., Gordts, P. L., Isbert, S., Zimmermann, P., Annaert, W., et al. (2010). Inactivation of the proximal NPXY motif impairs early steps in LRP1 biosynthesis. *Cell. Mol. Life Sci.* 67, 135–145. doi: 10.1007/s00018-009-0171-7

Ribeiro, A., Balasubramanian, S., Hughes, D., Vargo, S., Powell, E. M., and Leach, J. B. (2013). β1-Integrin cytoskeletal signaling regulates sensory neuron response to matrix dimensionality. *Neuroscience* 248, 67–78. doi: 10.1016/j.neuroscience.2013.05.057

Robel, S., Buckingham, S. C., Boni, J. L., Campbell, S. L., Danbolt, N. C., Riedemann, T., et al. (2015). Reactive astrogliosis causes the development of spontaneous seizures. *J. Neurosci.* 35, 3330–3345. doi: 10.1523/JNEUROSCI.1574-14.2015

Robel, S., Mori, T., Zoubaa, S., Schlegel, J., Sirko, S., Faissner, A., et al. (2009). Conditional deletion of β1-integrin in astroglia causes partial reactive gliosis. *Glia* 57, 1630–1647. doi: 10.1002/glia.20876

Robinson, S. D., Lee, T. W., Christie, D. L., and Birch, N. P. (2015). Tissue plasminogen activator inhibits NMDA-receptor-mediated increases in calcium levels in cultured hippocampal neurons. *Front. Cell. Neurosci.* 9:404. doi: 10.3389/fncel.2015.00404

Roebroek, A. J., Reekmans, S., Lauwers, A., Feyaerts, N., Smeijers, L., and Hartmann, D. (2006). Mutant Lrp1 knock-in mice generated by recombinase-mediated cassette exchange reveal differential importance of the NPXY motifs in the intracellular domain of LRP1 for normal fetal development. *Mol. Cell. Biol.* 26, 605–616. doi: 10.1128/MCB.26.2.605-616.2006

Rohlmann, A., Gotthardt, M., Hammer, R. E., and Herz, J. (1998). Inducible inactivation of hepatic LRP gene by cre-mediated recombination confirms role of LRP in clearance of chylomicron remnants. *J. Clin. Invest.* 101, 689–695. doi: 10.1172/JCI1240

Rozanov, D. V., Hahn-Dantona, E., Strickland, D. K., and Strongin, A. Y. (2004). The low-density lipoprotein receptor-related protein LRP is regulated by membrane type-1 matrix metalloproteinase (MT1-MMP) proteolysis in malignant cells. *J. Biol. Chem.* 279, 4260–4268. doi: 10.1074/jbc.M311569200

Rushworth, J. V., Griffiths, H. H., Watt, N. T., and Hooper, N. M. (2013). Prion protein-mediated toxicity of amyloid-β oligomers requires lipid rafts and the transmembrane LRP1. *J. Biol. Chem.* 288, 8935–8951. doi: 10.1074/jbc.M112.400358

Sabeh, F., Ota, I., Holmbeck, K., Birkedal-Hansen, H., Soloway, P., Balbin, M., et al. (2004). Tumor cell traffic through the extracellular matrix is controlled by the membrane-anchored collagenase MT1-MMP. *J. Cel Biol.* 167, 769–781. doi: 10.1083/jcb.200408028

Sabeh, F., Shimizu-Hirota, R., and Weiss, S. J. (2009). Protease-dependent versus -independent cancer cell invasion programs: three-dimensional amoeboid movement revisited. *J. Cell Biol.* 185, 11–19. doi: 10.1083/jcb.200807195

Saenko, E. L., Yakhyaev, A. V., Mikhailenko, I., Strickland, D. K., and Sarafanov, A. G. (1999). Role of the low density lipoprotein-related protein receptor inmediation of factor VIII catabolism. *J. Biol. Chem.* 274, 37685–37692. doi: 10.1074/jbc.274.53.37685

Safina, D., Schlitt, F., Romeo, R., Pflanzner, T., Pietrzik, C. U., Narayanaswami, V., et al. (2016). Low-density lipoprotein receptor-related protein 1 is a novel modulator of radial glia stem cell proliferation, survival, and differentiation. *Glia* 64, 1363–1380. doi: 10.1002/glia.23009

Sagare, A., Deane, R., Bell, R. D., Johnson, B., Hamm, K., Pendu, R., et al. (2007). Clearance of amyloid-beta by circulating lipoprotein receptors. *Nat. Med.* 13, 1029–1031. doi: 10.1038/nm1635

Sagare, A. P., Bell, R. D., Zhao, Z., Ma, Q., Winkler, E. A., Ramanathan, A., et al. (2013). Pericyte loss influences Alzheimer-like neurodegeneration in mice. *Nat. Commun.* 4:2932. doi: 10.1038/ncomms3932

Sakimura, K., Kutsuwada, T., Ito, I., Manabe, T., Takayama, C., Kushiya, E., et al. (1995). Reduced hippocampal LTP and spatial learning in mice lacking NMDA receptor epsilon 1 subunit. *Nature* 373, 151–155. doi: 10.1038/373151a0

Salicioni, A., Gaultier, A., Brownlee, C., Cheezum, M., and Gonias, S. (2004). Low density lipoprotein receptor-related protein-1 promotes beta1 integrin maturation and transport to the cell surface. *J. Biol. Chem.* 279, 10005–10012. doi: 10.1074/jbc.M306625200

Salicioni, A. M., Mizelle, K. S., Loukinova, E., Mikhailenko, I., Strickland, D. K., and Gonias, S. L. (2002). The low density lipoprotein receptor-related protein mediates fibronectin catabolism and inhibits fibronectin accumulation on cell surfaces. *J. Biol. Chem.* 277, 16160–16166. doi: 10.1074/jbc.M201401200

Salza, R., Lethias, C., and Ricard-Blum, S. (2017). The multimerization state of the amyloid-β42 (Aβ 42) peptide governs its interaction network with the extracellular matrix. *J. Alzheimers Dis.* 56, 991–1005. doi: 10.3233/JAD-160751

Sanchez, M. C., Chiabrando, G. A., and Vides, M. A. (2001). Pregnancy zone protein-tissue-type plasminogen activator complexes bind to low-density lipoprotein receptor-related protein (LRP). *Arch. Biochem. Biophys.* 389, 218–222. doi: 10.1006/abbi.2001.2329

Sappino, A.-P., Madani, R., Huarte, J., Belin, D., Kiss, J. Z., Wohlwend, A., et al. (1993). Extracellular proteolysis in the adult murine brain. *J. Clin. Invest.* 92, 679–685. doi: 10.1172/JCI116637

Sarafanov, A. G., Ananyeva, N. M., Shima, M., and Saenko, E. L. (2001). Cell surface heparan sulfate proteoglycans participate in factor VIII catabolism mediated by low density lipoprotein receptor-related protein. *J. Biol. Chem.* 276, 11970–11979. doi: 10.1074/jbc.M008046200

Schorch, B., Song, S., van Diemen, F. R., Bock, H. H., May, P., Herz, J., et al. (2014). LRP1 is a receptor for *Clostridium perfringens* TpeL toxin indicating a two-receptor model of clostridial glycosylating toxins. *Proc Natl. Acad. Sci. U.S.A.* 111, 6431–6436. doi: 10.1073/pnas.1323790111

Schouwey, K., Delmas, V., Larue, L., Zimber-Strobl, U., Strobl, L. J., Radtke, F., et al. (2007). Notch1 and Notch2 receptors influence progressive hair graying in a dose-dependent manner. *Dev. Dyn.* 236, 282–289. doi: 10.1002/dvdy.21000

Scilabra, S. D., Troeberg, L., Yamamoto, K., Emonard, H., Thøgersen, I., Enghild, J. J., et al. (2013). Differential regulation of extracellular tissue inhibitor of metalloproteinases-3 levels by cell membrane-bound and shed low density

lipoprotein receptor-related protein 1. *J. Biol. Chem.* 288, 332–342. doi: 10.1074/jbc.M112.393322

Scilabra, S. D., Yamamoto, K., Pigoni, M., Sakamoto, K., Müller, S. A., Papadopoulou, A., et al. (2017). Dissecting the interaction between tissue inhibitor of metalloproteinases-3 (TIMP-3) and low density lipoprotein receptor-related protein-1 (LRP-1): development of a "TRAP" to increase levels of TIMP-3 in the tissue. *Matrix Biol.* 59, 69–79. doi: 10.1016/j.matbio.2016.07.004

Seeds, N. W., Basham, M., and Haffke, S. (1999). Neuronal migration is retarded in mice lacking the tissue plasminogen activator gene. *Proc. Natl. Acad. Sci. U.S.A.* 96, 14118–14123. doi: 10.1073/pnas.96.24.14118

Seeds, N. W., Friedman, G., Hayden, S. H., Thewke, D., Haffke, S., McGuire, P., et al. (1996). Plasminogen activators and their interaction with the extracellular matrix in neural development, plasticity and regeneration. *Semin. Neurosci.* 8, 405–412. doi: 10.1006/smns.1996.0049

Seeds, N. W., Williams, B. L., and Bickford, P. C. (1995). Tissue plasminogen activator induction in Purkinje neurons after cerebellar motor learning. *Science* 270, 1992–1994. doi: 10.1126/science.270.5244.1992

Segarini, P. R., Nesbitt, J. E., Li, D., Hays, L. G., Yates, J. R. III, and Carmichael, D. F. (2001). The low density lipoprotein receptor-related protein/alpha 2-macroglobulin receptor is a receptor for connective tissue growth factor. *J. Biol. Chem.* 276, 40659–40667. doi: 10.1074/jbc.M105180200

Selkoe, D. J. (2000). Toward a comprehensive theory for Alzheimer's disease. Hypothesis: alzheimer's disease is caused by the cerebral accumulation and cytotoxicity of amyloid beta-protein. *Ann. N.Y. Acad. Sci.* 924, 17–25. doi: 10.1111/j.1749-6632.2000.tb05554.x

Shakibaei, M., and Frevert, U. (1996). Dual interaction of the malaria circumsporozoite protein with the low density lipoprotein receptor-related protein (LRP) and heparan sulfate proteoglycans. *J. Exp. Med.* 184, 1699–1711. doi: 10.1084/jem.184.5.1699

Shibata, M., Yamada, S., Kumar, S. R., Calero, M., Bading, J., Frangione, B., et al. (2000). Clearance of Alzheimer's amyloid-β1-40 peptide from brain by LDL receptor-related protein-1 at the blood-brain barrier. *J. Clin. Invest.* 106, 1489–1499. doi: 10.1172/JCI10498

Shinohara, M., Tachibana, M., Kanekiyo, T., and Bu, G. (2017). Role of LRP1 in the pathogenesis of Alzheimer's disease: evidence from clinical and preclinical studies. *J. Lipid Res.* 58, 1267–1281. doi: 10.1194/jlr.R075796

Simons, K., and Toomre, D. (2000). Lipid rafts and signal transduction. *Nat. Rev. Mol. Cell Biol.* 1, 31–39. doi: 10.1038/35036052

Song, I., and Dityatev, A. (2018). Crosstalk between glia, extracellular matrix and neurons. *Brian Res. Bull.* 136, 101–108. doi: 10.1016/j.brainresbull.2017.03.003

Spijkers, P. P., Denis, C. V., Blom, A. M., and Lenting, P. J. (2008). Cellular uptake of C4b-binding protein is mediated by heparan sulfate proteoglycans and CD91/LDL receptor-related protein. *Eur. J. Immunol.* 38, 809–817. doi: 10.1002/eji.200737722

Spijkers, P. P. E. M., Costa Martins, P., Westein, E., Gahmberg, C. G., Zwaginga, J. J., and Lenting, P. J. (2005). LDL-receptor-related protein regulates β 2-integrin-mediated leukocyte adhesion. *Blood* 105, 170–177. doi: 10.1182/blood-2004-02-0498

Spires-Jones, T. L., and Hyman, B. T. (2014). The intersection of amyloid beta and tau at synapses in Alzheimer's disease. *Neuron* 82, 756–771. doi: 10.1016/j.neuron.2014.05.004

Staniszewska, I., Zaveri, S., Del Valle, L., Oliva, I., Rothman, V. L., Croul, S. E., et al. (2007). Interaction of alpha9beta1 integrin with thrombospondin-1 promotes angiogenesis. *Circ. Res.* 100, 1308–1316. doi: 10.1161/01.RES.0000266662.98355.66

Stefanitsch, C., Lawrence, A.-L., Olverling, A., Nilsson, I., and Fredriksson, L. (2015). tPA deficiency in mice leads to rearrangement in the cerebrovascular tree and cerebroventricular malformations. *Front. Cell. Neurosci.* 9:456. doi: 10.3389/fncel.2015.00456

Stefansson, S., Lawrence, D. A., and Argraves, W. S. (1996). Plasminogen activator inhibitor-1 and vitronectin promote the cellular clearance of thrombin by low density lipoprotein receptor-related proteins 1 and 2. *J. Biol. Chem.* 271, 8215–8220. doi: 10.1074/jbc.271.14.8215

Stefansson, S., Muhammad, S., Cheng, X. F., Battey, F. D., Strickland, D. K., and Lawrence, D. A. (1998). Plasminogen activator inhibitor-1 contains a cryptic high affinity binding site for the low density lipoprotein receptor-related protein. *J. Biol. Chem.* 273, 6358–6366. doi: 10.1074/jbc.273.11.6358

Stiles, T. L., Dickendesher, T. L., Gaultier, A., Fernandez-Castaneda, A., Mantuano, E., Giger, R. J., et al. (2013). LDL receptor-related protein-1 is a sialic-acid-independent receptor for myelin-associated glycoprotein that functions in neurite outgrowth inhibition by MAG and CNS myelin. *J. Cell Sci.* 126, 209–220. doi: 10.1242/jcs.113191

Storm, D., Herz, J., Trinder, P., and Loos, M. (1997). C1 inhibitor-C1s complexes are internalized and degraded by the low density lipoprotein receptor-related protein. *J. Biol. Chem.* 272, 31043–31050. doi: 10.1074/jbc.272.49.31043

Strickland, D. K., Ashcom, J. D., Williams, S., Burgess, W. H., Migliorini, M., and Argraves, W. S. (1990). Sequence identity between the alpha 2-macroglobulin receptor and low density lipoprotein receptor-related protein suggests that this molecule is a multifunctional receptor. *J. Biol. Chem.* 265, 17401–17404.

Strickland, D. K., Au, D. T., Cunfer, P., and Muratoglu, S. C. (2014). Low-density lipoprotein receptor-related protein-1: Role in the regulation of vascular integrity. *Arterioscler. Thromb. Vasc. Biol.* 34, 487–498. doi: 10.1161/ATVBAHA.113.301924

Strickland, D. K., Gonias, S. L., and Agraves, W. S. (2002). Diverse roles for the LDL receptor family. *Trends Endocrinol. Metab.* 13, 66–74. doi: 10.1016/S1043-2760(01)00526-4

Su, E. J., Fredriksson, L., Geyer, M., Folestad, E., Cale, J., Andrae, J., et al. (2008). Activation of PDGF-CC by tissue plasminogen activator impairs blood-brain barrier integrity during ischemic stroke. *Nat. Med.* 14, 731–737. doi: 10.1038/nm1787

Subramanian, M., Hayes, C. D., Thome, J. J., Thorp, E., Matsushima, G. K., Herz, J., et al. (2014). An AXL/LRP-1/RANBP9 complex mediates DC efferocytosis and antigen cross-presentation in vivo. *J. Clin. Invest.* 124, 1296–1308. doi: 10.1172/JCI72051

Sunyach, C., Jen, A., Deng, J., Fitzgerald, K. T., Frobert, Y., Grassi, J., et al. (2003). The mechanism of internalization of glycosylphosphatidylinositol-anchored prion protein. *EMBO J.* 22, 3591–3601. doi: 10.1093/emboj/cdg344

Swertfeger, D. K., Bu, G., and Hui, D. Y. (2002). Low density lipoprotein receptor-related protein mediates apolipoprotein E inhibition of smooth muscle cell migration. *J. Biol. Chem.* 277, 4141–4146. doi: 10.1074/jbc.M109124200

Takayama, Y., May, P., Anderson, R. G., and Herz, J. (2005). Low density lipoprotein receptor-related protein 1 (LRP1) controls endocytosis and c-CBL-mediated ubiquitination of the platelet-derived growth factor receptor beta (PDGFR beta). *J. Biol. Chem.* 280, 18504–18510. doi: 10.1074/jbc.M410265200

Talme, T., Bergdahl, E., and Sundqvist, K.-G. (2013). Regulation of T-lymphocyte motility, adhesion and de-adhesion by a cell surface mechanism directed by low density lipoprotein receptor-related protein 1 and endogenous thrombospondin-1. *Immunology* 142, 176–192. doi: 10.1111/imm.12229

Tan, M.-L., Ng, A., Pandher, P. S., Sashindranath, M., Hamilton, J. A., Davis, S. M., et al. (2012). Tissue plasminogen activator does not alter development of acquired epilepsy. *Epilepsia* 53, 1998–2004. doi: 10.1111/j.1528-1167.2012.03635.x

Taylor, D. R., and Hooper, N. M. (2007). The low-density lipoprotein receptor-related protein 1 (LRP1) mediates the endocytosis of the cellular prion protein. *Biochem. J.* 402, 17–23. doi: 10.1042/BJ20061736

Theret, L., Jeanne, A., Langlois, B., Hachet, C., David, M., Khrestchatisky, M., et al. (2017). Identification of LRP-1 as an endocytosis and recycling receptor for β1-integrin in thyroid cancer cells. *Oncotarget* 8, 78614–78632. doi: 10.18632/oncotarget.20201

Thevenard, J., Verzeaux, L., Devy, J., Etique, N., Jeanne, A., Schneider, C., et al. (2014). Low-density lipoprotein receptor-related protein-1 mediates endocytic clearance of tissue inhibitor of metalloproteinases-1 and promotes its cytokine-like activities. *PLoS One* 9:e103839. doi: 10.1371/journal.pone.0103839

Trommsdorff, M., Borg, J., Margolis, B., and Herz, J. (1998). Interaction of cytosolic adaptor proteins with neuronal apolipoprotein E receptors and the amyloid precursor protein. *J. Biol. Chem.* 273, 33556–33560. doi: 10.1074/jbc.273.50.33556

Trotter, J. H., Lussier, A. L., Psilos, K. E., Mahoney, H. L., Sponaugle, A. E., Hoe, H.-S., et al. (2014). Extracellular proteolysis of reelin by tissue plasminogen activator following synaptic potentiation. *Neuroscience* 274, 299–307. doi: 10.1016/j.neuroscience.2014.05.046

Tsen, F., Bhatia, A., O'Brien, K., Cheng, C.-F., Chen, M., Hay, N., et al. (2013). Extracellular heat shock protein 90 signals through subdomain II and the NPVY motif of LRP-1 receptor to Akt1 and Akt2: a circuit essential for promoting skin

cell migration in vitro and wound healing in vivo. *Mol. Cell. Biol.* 33, 4947–4959. doi: 10.1128/MCB.00559-13

Tsirka, S., Gualandris, A., Amaral, D., and Strickland, S. (1997). Excitotoxin-induced neuronal degeneration and seizure are mediated by tissue plasminogen activator. *Nature* 377, 340–344. doi: 10.1038/377340a0

Turner, P. M., and Lorand, L. (1989). Complexation of fibronectin with tissue transglutaminase. *Biochemistry* 28, 628–635. doi: 10.1021/bi00428a032

Ulery, P. G., Beers, J., Mikhailenko, I., Tanzi, R. E., Rebeck, G. W., Hyman, B. T., et al. (2000). Modulation of beta-amyloid precursor protein processing by the low density lipoprotein receptor-related protein (LRP). Evidence that LRP contributes to the pathogenesis of Alzheimer's disease. *J. Biol. Chem.* 275, 7410–7415. doi: 10.1074/jbc.275.10.7410

Vaillant, C., Michos, O., Orolicki, S., Brellier, F., Taieb, S., Moreno, E., et al. (2007). Protease nexin 1 and its receptor LRP modulate SHH signalling during cerebellar development. *Development* 134, 1745–1754. doi: 10.1242/dev.02840

Van Gool, B., Dedieu, S., Emonard, H., and Roebroek, A. J. (2015). The matricellular receptor LRP1 forms and interface for signaling and endocytosis in modulation of the extracellular tumor environment. *Front. Pharmacol.* 6:271. doi: 10.3389/fphar.2015.00271

van Horssen, J., Wesseling, P., van den Heuvel, L. P., de Waal, R. M., and Verbeek, M. M. (2003). Heparan sulfate proteoglycans in Alzheimer's disease and amyloid-related disorders. *Lancet Neurol.* 2, 482–492. doi: 10.1016/S1474-4422(03)00484-8

Venkatesan, C., Birch, D., Peng, C. Y., and Kessler, J. A. (2015). Astrocytic β1-integrin affects cellular composition of murine blood brain barrier in the cerebral cortex. *Int. J. Dev. Neurosci.* 44, 48–54. doi: 10.1016/j.ijdevneu.2015.05.005

Vierkotten, S., Muether, P. S., and Fauser, S. (2011). Overexpression of HTRA1 leads to ultrastructural changes in the elastic layer of Bruch's membrane via cleavage of extracellular matrix components. *PLoS One* 6:e22959. doi: 10.1371/journal.pone.0022959

von Arnim, C. A., Kinoshita, A., Peltan, I. D., Tangredi, M. M., Herl, L., Lee, B. M., et al. (2005). The low density lipoprotein receptor-related protein (LRP) is a novel beta-secretase (BACE1) substrate. *J. Biol. Chem.* 280, 17777–17785. doi: 10.1074/jbc.M414248200

von Einem, B., Schwanzar, D., Rehn, F., Beyer, A.-S., Weber, P., Wagner, M., et al. (2010). The role of low-density receptor-related protein 1 (LRP1) as a competitive substrate of the amyloid precursor protein (APP) for BACE1. *Exp. Neurol.* 225, 85–93. doi: 10.1016/j.expneurol.2010.05.017

Vreys, V., and David, G. (2007). Mammalian heparanase: what is the message? *J. Cell. Mol. Med.* 11, 427–452. doi: 10.1111/j.1582-4934.2007.00039.x

Vreys, V., Delande, N., Zhang, Z., Coomans, C., Roebroek, A., Dürr, J., et al. (2005). Cellular uptake of mammalian heparanase precursor involves low density lipoprotein receptor-related proteins, mannose 6-phosphate receptors and heparan sulfate proteoglycans. *J. Biol. Chem.* 280, 33141–33148. doi: 10.1074/jbc.M503007200

Waldron, E., Heilig, C., Schweitzer, A., Nadella, N., Jaeger, S., Martin, A. M., et al. (2008). LRP1 modulates APP trafficking along early compartments of the secretory pathway. *Neurobiol. Dis.* 31, 188–197. doi: 10.1016/j.nbd.2008.04.006

Wang, S., Herndon, M. E., Ranganathan, S., Godyna, S., Lawler, J., Argraves, W. S., et al. (2004). Internalization but not binding of thrombospondin-1 to low density lipoprotein receptor-related protein-1 requires heparan sulfate proteoglycans. *J. Cell. Biochem.* 91, 766–776. doi: 10.1002/jcb.10781

Wang, X., Gao, M., Schouteden, S., Roebroek, A., Eggermont, K., van Veldhoven, P. P., et al. (2014). Hematopoietic stem/progenitor cells directly contribute to arteriosclerotic progression via integrin β2. *Stem Cells* 33, 1230–1240. doi: 10.1002/stem.1939

Wang, X., Lee, S. R., Arai, K., Lee, S. R., Tsuji, K., Rebeck, G. W., et al. (2003). Lipoprotein receptor-mediated induction of matrix metalloproteinase by tissue plasminogen activator. *Nat. Med.* 10, 1313–1317. doi: 10.1038/nm926

Warshawsky, I., Broze, G. J. Jr., and Schwartz, A. L. (1994). The low density lipoprotein receptor-related protein mediates the cellular degradation of tissue factor pathway inhibitor. *Proc. Natl. Acad. Sci. U.S.A.* 91, 6664–6668. doi: 10.1073/pnas.91.14.6664

Weaver, A. M., Hussaini, I. M., Mazar, A., Henkin, J., and Gonias, S. L. (1997). Embryonic fibroblasts that are genetically deficient in low density lipoprotein receptor-related protein demonstrate increased activity of the urokinase receptor system and accelerated migration on vitronectin. *J. Biol. Chem.* 272, 14372–14379. doi: 10.1074/jbc.272.22.14372

Weaver, A. M., McCabe, M., Kim, I., Allietta, M. M., and Gonias, S. L. (1996). Epidermal growth factor and platelet-derived growth factor-BB induce a stable increase in the activity of low density lipoprotein receptor-related protein in vascular smooth muscle cells by altering receptor distribution and recycling. *J. Biol. Chem.* 271, 24894–24900. doi: 10.1074/jbc.271.40.24894

Werb, Z., Mainardi, C. L., Vater, C. A., and Harris, E. D. Jr. (1977). Endogenous activiation of latent collagenase by rheumatoid synovial cells. Evidence for a role of plasminogen activator. *N. Engl. J. Med.* 296, 1017–1023. doi: 10.1056/NEJM197705052961801

Werb, Z., Tremble, P. M., and Damsky, C. (1989). Signal transduction through the fibronectin receptor induces collagenase and stromelysin expression. *J. Cell Biol.* 109, 877–889. doi: 10.1083/jcb.109.2.877

Wijnberg, M. J., Quax, P. H., Nieuwenbroek, N. M., and Verheijen, J. H. (1997). The migration of human smooth muscle cells in vitro is mediated by plasminogen activation and can be inhibited by alpha2-macroglobulin receptor associated protein. *Thromb. Haemost.* 78, 880–886. doi: 10.1055/s-0038-1657646

Willnow, T. E., Goldstein, J. L., Orth, K., Brown, M. S., and Herz, J. (1992). Low density lipoprotein receptor-related protein and gp330 bind similar ligands, including plasminogen activator-inhibitor complexes and lactoferrin, an inhibitor of chylomicron remnant clearance. *J. Biol. Chem.* 267, 26172–26180.

Wilsie, L. C., and Orlando, R. A. (2003). The low density lipoprotein receptor-related protein complexes with cell surface heparan sulfate proteoglycan-mediated lipoprotein catabolism. *J. Biol. Chem.* 278, 15758–15764. doi: 10.1074/jbc.M208786200

Woo, J. A., Jung, A. R., Lakshmana, M. K., Bedrossian, A., Lim, Y., Bu, J. H., et al. (2012a). Pivotal role of the RanBP9-cofilin pathway in Abeta-induced apoptosis and neurodegeneration. *Cell Death Differ.* 19, 1413–1423. doi: 10.1038/cdd.2012

Woo, J. A., Roh, S. E., Lakshmana, M. K., and Kang, D. E. (2012b). Pivotal role of RanBP9 in integrin-dependent focal adhesion signaling and assembly. *FASEB J.* 26, 1672–1681. doi: 10.1096/fj.11-194423

Wu, F., Torre, E., Cuellar-Giraldo, D., Cheng, L., Yi, H., Bichler, E. K., et al. (2015). Tissue-type plasminogen activator triggers the synaptic vesicle cycle in cerebral cortical neurons. *J. Cereb. Blood Flow Metab.* 35, 1966–1976. doi: 10.1038/jcbfm.2015.155

Wu, L., and Gonias, S. L. (2005). The low-density lipoprotein-related protein-1 associates transiently with lipid rafts. *J. Cell. Biochem.* 96, 1021–1033. doi: 10.1002/jcb.20596

Wu, Y. P., Siao, C.-J., Lu, W., Sung, T.-C., Frohman, M. A., Milev, P., et al. (2000). The tissue plasminogen activator (tPA)/plasmin extracellular proteolytic system regulates seizure-induced hippocampal mossy fiber outgrowth through a proteoglycan substrate. *J. Cell Biol.* 148, 1295–1304. doi: 10.1083/jcb.148.6.1295

Wujak, L., Böttcher, R. T., Pak, O., Frey, H., El Agha, E., Chen, Y., et al. (2017). Low density lipoprotein receptor-related protein 1 couples β1 integrin activation to degradation. *Cell. Mol. Life Sci.* 75, 1671–1685. doi: 10.1007/s00018-017-2707-6

Yamada, K., Hashimoto, T., Yabuki, C., Nagae, Y., Tachikawa, M., Strickland, D. K., et al. (2008). The low density lipoprotein receptor-related protein 1 mediates uptake of amyloid β peptides in an in vitro model of the blood-brain barrier cells. *J. Biol. Chem.* 283, 34554–34562. doi: 10.1074/jbc.M801487200

Yamamoto, K., Owen, K., Parker, A. E., Scilabra, S. D., Dudhia, J., Strickland, D. K., et al. (2014). Low density lipoprotein receptor-related protein 1 (LRP1)-mediated endocytic clearance of a disintegrin and metalloproteinase with thrombospondin motifs-4 (ADAMTS-4): functional differences of non-catalytic domains of ADAMTS-4 and ADAMTS-5 in LRP1 binding. *J. Biol. Chem.* 289, 6462–6474. doi: 10.1074/jbc.M113.545376

Yanagisawa, H., Davis, E. C., Starcher, B. C., Ouchi, T., Yanagisawa, M., Richardson, J. A., et al. (2002). Fibulin-5 is an elastin-binding protein essential for elastic fibre development in vivo. *Nature* 415, 168–171. doi: 10.1038/415168a

Yang, D. S., Small, D. H., Seydel, U., Smith, J. D., Hallmayer, J., Gandy, S. E., et al. (1999). Apolipoprotein E promotes the binding and uptake of beta-amyloid into Chinese hamster ovary cells in an isoform-specific manner. *Neuroscience* 90, 1217–1226. doi: 10.1016/S0306-4522(98)00561-2

Yang, Z., Strickland, D. K., and Bornstein, P. (2001). Extracellular matrix metalloproteinase 2 levels are regulated by the low density lipoprotein-related scavenger receptor and thrombospondin 2. *J. Biol. Chem.* 276, 8403–8408. doi: 10.1074/jbc.M008925200

Yepes, M., and Lawrence, D. A. (2004). Neuroserpin: a selective inhibitor of tissue-type plasminogen activator in the central nervous system. *Thromb. Haemost.* 91, 457–464. doi: 10.1160/TH03-12-0766

Yepes, M., Sandkvist, M., Moore, E. G., Bugge, T. H., Strickland, D. K., and Lawrence, D. A. (2003). Tissue-type plasminogen activator induces opening of the blood-brain barrier via the LDL receptor-related protein. *J. Clin. Invest.* 112, 1533–1540. doi: 10.1172/JCI200319212

Yepes, M., Wu, F., Torre, E., Cuellar-Giraldo, D., Jia, D., and Cheng, L. (2016). Tissue-type plasminogen activator induces synaptic vesicle endocytosis in cerebral cortical neurons. *Neuroscience* 319, 69–78. doi: 10.1016/j.neuroscience.2016.01.046

Yin, K. J., Cirrito, J. R., Yan, P., Hu, X., Xiao, Q., Pan, X., et al. (2006). Matrix metalloproteinases expressed by astrocytes mediate extracellular amyloid-beta peptide catabolism. *J. Neurosci* 26, 10939–10948. doi: 10.1523/JNEUROSCI.2085-06.2006

Yu, C., Nwabuisi-Heath, E., Laxton, K., and Ladu, M. J. (2010). Endocytic pathways mediating oligomeric Aβ42 neurotoxicity. *Mol. Neurodegener.* 5:19. doi: 10.1186/1750-1326-5-19

Yuan, H., Vance, K. M., Junge, C. E., Geballe, M. T., Snyder, J. P., Hepler, J. R., et al. (2009). The serine protease plasmin cleaves the amino-terminal domain of the NR2A subunit to relieve zinc inhibition of the N-methyl-D-aspartate receptors. *J. Biol. Chem.* 284, 12862–12873. doi: 10.1074/jbc.M805123200

Zemskov, E. A., Mikhailenko, I., Strickland, D. K., and Belkin, A. M. (2007). Cell-surface transglutaminase undergoes internalization and lysosomal degradation: an essential role for LRP1. *J. Cell Sci.* 120, 3188–3199. doi: 10.1242/jcs.010397

Zhang, C., An, J., Haaile, W. B., Echeverry, R., Strickland, D. K., and Yepes, M. (2009). Microglial low-density lipoprotein receptor-related protein 1 mediates the effect of tissue-type plasminogen activator on matrix metalloproteinase-9 activity in the ischemic brain. *J. Cereb. Blood Flow Metab.* 29, 1946–1954. doi: 10.1038/jcbfm.2009.174

Zhang, H., Links, P. H., Ngsee, J. K., Tran, K., Cui, Z., Ko, K. W. S., et al. (2004). Localization of low density lipoprotein receptor-related protein 1 to caveolae in 3T3-L1 adipocytes in response to insulin treatment. *J. Biol. Chem.* 279, 2221–2230. doi: 10.1074/jbc.M310679200

Zhang, S. H., Reddick, R. L., Burkey, B., and Maeda, N. (1994). Diet-induced atherosclerosis in mice heterozygous and homozygous for apolipoprotein E gene disruption. *J. Clin. Invest.* 94, 937–945. doi: 10.1172/JCI117460

Zhang, X., Polavarapu, R., She, H., Mao, Z., and Yepes, M. (2007). Tissue-type plasminogen activator and the low-density lipoprotein receptor-related protein mediate cerebral ischemia-induced nuclear factor-kappaB pathway activation. *Am. J. Pathol.* 171, 1281–1290. doi: 10.2353/ajpath.2007.070472

Zhou, L., Takayama, Y., Boucher, P., Tallquist, M. D., and Herz, J. (2009). LRP1 regulates architecture of the vascular wall by controlling PDGFRβ -dependent phosphatidylinositol 3-kinase activation. *PLoS One* 4:e6922. doi: 10.1371/journal.pone.0006922

Zhu, Y., and Hui, D. Y. (2003). Apolipoprotein E binding to low density lipoprotein receptor-related protein-1 inhibits cell migration via activation of cAMP-dependent protein kinase A. *J. Biol. Chem.* 278, 36257–36263. doi: 10.1074/jbc.M303171200

Zhuo, M., Holtzman, D. M., Li, Y., Osaka, H., DeMaro, J., Jacquin, M., et al. (2000). Role of tissue plasminogen activator receptor LRP in hippocampal long-term potentiation. *J. Neurosci.* 20, 542–549. doi: 10.1523/JNEUROSCI.20-02-00542.2000

Zilberberg, A., Yaniv, A., and Gazit, A. (2004). The low density lipoprotein receptor-1, LRP1, interacts with the human frizzled-1 (HFz1) and down-regulates the canonical Wnt signaling pathway. *J Biol. Chem.* 279, 17535–17542. doi: 10.1074/jbc.M311292200

Zurhove, K., Nakajima, C., Herz, J., Bock, H. H., and May, P. (2008). Gamma-secretase limits the inflammatory response through the processing of LRP1. *Sci. Signal.* 1:ra15. doi: 10.1126/scisignal.1164263

Conflict of Interest Statement: The authors declare that the research was conducted in the absence of any commercial or financial relationships that could be construed as a potential conflict of interest.

The reviewer DL declared a shared affiliation, with no collaboration, with the authors to the handling Editor at the time of review.

frontiers in Cell and Developmental Biology

ORIGINAL RESEARCH
published: 28 March 2019
doi: 10.3389/fcell.2019.00035

Avian Primordial Germ Cells Contribute to and Interact With the Extracellular Matrix During Early Migration

*David J. Huss[1,2], Sasha Saias[1], Sevag Hamamah[1], Jennifer M. Singh[3,4], Jinhui Wang[3,4], Mohit Dave[1], Junhyong Kim[4,5], James Eberwine[3,4] and Rusty Lansford[1,2]**

[1] Department of Radiology, Children's Hospital Los Angeles, Los Angeles, CA, United States, [2] Translational Imaging Center, University of Southern California, Los Angeles, CA, United States, [3] Department of Pharmacology, University of Pennsylvania, Philadelphia, PA, United States, [4] Penn Genome Frontiers Institute, University of Pennsylvania, Philadelphia, PA, United States, [5] Department of Biology, University of Pennsylvania, Philadelphia, PA, United States

During early avian development, primordial germ cells (PGC) are highly migratory, moving from the central area pellucida of the blastoderm to the anterior extra-embryonic germinal crescent. The PGCs soon move into the forming blood vessels by intravasation and travel in the circulatory system to the genital ridges where they participate in the organogenesis of the gonads. This complex cellular migration takes place in close association with a nascent extracellular matrix that matures in a precise spatio-temporal pattern. We first compiled a list of quail matrisome genes by bioinformatic screening of human matrisome orthologs. Next, we used single cell RNA-seq analysis (scRNAseq) to determine that PGCs express numerous ECM and ECM-associated genes in early embryos. The expression of select ECM transcripts and proteins in PGCs were verified by fluorescent *in situ* hybridization (FISH) and immunofluorescence (IF). Live imaging of transgenic quail embryos injected with fluorescent antibodies against fibronectin and laminin, showed that germinal crescent PGCs display rapid shape changes and morphological properties such as blebbing and filopodia while surrounded by, or in close contact with, an ECM fibril meshwork that is itself in constant motion. Injection of anti-β1 integrin CSAT antibodies resulted in a reduction of mature fibronectin and laminin fibril meshwork in the germinal crescent at HH4-5 but did not alter the active motility of the PGCs or their ability to populate the germinal crescent. These results suggest that integrin β1 receptors are important, but not required, for PGCs to successfully migrate during embryonic development, but instead play a vital role in ECM fibrillogenesis and assembly.

Keywords: primordial germ cells, extracellular matrix, transcriptome, germinal crescent, quail, matrisome

OPEN ACCESS

Edited by:
Claudia Tanja Mierke, Leipzig University, Germany

Reviewed by:
Mike McGrew, University of Edinburgh, United Kingdom
Elena P. Moiseeva, Retired, Leicester, United Kingdom

***Correspondence:**
Rusty Lansford
lansford@usc.edu

Specialty section:
This article was submitted to Cell Adhesion and Migration, a section of the journal Frontiers in Cell and Developmental Biology

Received: *23 December 2018*
Accepted: *26 February 2019*
Published: *28 March 2019*

Citation:
Huss DJ, Saias S, Hamamah S, Singh JM, Wang J, Dave M, Kim J, Eberwine J and Lansford R (2019) Avian Primordial Germ Cells Contribute to and Interact With the Extracellular Matrix During Early Migration. Front. Cell Dev. Biol. 7:35. doi: 10.3389/fcell.2019.00035

INTRODUCTION

The extracellular matrix (ECM) plays a vital role in the timing, speed and direction of embryonic cell movements (Dufour et al., 1988; Loganathan et al., 2016). In addition to its importance in cell migration, the ECM also provides signaling cues that regulate cell behaviors and coordinate cell functions in tissue formation and homeostasis. The ECM is known to impart structure and stiffness to the developing embryo, and maintain proper tissue tension (Sato et al., 2017). The ECM helps

establish and maintain stem cell niches and serves as a ligand for soluble growth factors and a system for communication between cells and tissues (Hynes, 2009; Watt and Huck, 2013; Ahmed and Ffrench-Constant, 2016; de Almeida et al., 2016). The composition of the ECM, its three-dimensional organization and proteolytic renovations are critical factors in the microenvironmental signaling that regulates cell shape, motility, growth, survival, and differentiation. At the tissue level, the ECM is known to play a dynamic role in shaping large-scale movements during early morphogenesis in Xenopus (Boucaut et al., 1990; Davidson et al., 2006), zebrafish (Latimer and Jessen, 2010), chick (Sanders, 1984), and quail (Zamir et al., 2006). The integrin receptors are a key component in a cell's ability to interact with the ECM during embryogenesis and cell migration (Beauvais-Jouneau and Thiery, 1997; Darribère et al., 2000). In addition to changing cell behavior, the binding of integrins to the ECM has a profound effect upon the ECM itself by changing the rate and timing of fibrillogenesis, assembly and breakdown (Darribère et al., 1990; Danen et al., 2002; Leiss et al., 2008).

Primordial germ cells (PGCs) represent the founder cells of the germline lineage. During amniote embryonic development the PGCs undergo a long and complex migration that moves through embryonic and extra-embryonic tissues. For example, avian PGCs are initially detected in the epiblast layer in the center of the blastoderm at the freshly laid developmental stage EGK-X (Eyal-Giladi et al., 1981). Avian PGCs then delaminate from the dorsal epiblast and move ventrally where they associate with hypoblast cells. They move with the hypoblast during gastrulation toward the anterior extra-embryonic end of the embryo to the germinal crescent (Swift, 1914). The germinal crescent is a semi-circular shaped extra-embryonic region that lies roughly along the area opaca/area pellucida (AO/AP) border anterior to the embryo (Clawson and Domm, 1969; Fujimoto et al., 1976). After ∼2 days of incubation, the PGCs enter the newly formed vascular plexus and move via the circulatory system throughout the embryonic and extra-embryonic regions. PGCs leave the blood vessels around day 3 and travel along the gut mesentery to colonize the developing gonadal anlage (Nakamura et al., 2007; De Melo Bernardo et al., 2012). While there are differences between species in the routes, timing, and guidance mechanisms involved, the ability of PGCs to eventually colonize the genital ridges and produce functional sex cells is critical to reproductive success (Richardson and Lehmann, 2010; Tarbashevich and Raz, 2010; Barton et al., 2016; Cant and Laird, 2017).

Several studies have shown that migrating PGCs intimately interact with the emerging ECM as they migrate to the gonadal anlage. The migration of PGCs in relation to the spatio-temporal expression pattern of particular ECM glycoproteins has been investigated using fixed tissue histochemical and immunofluorescent approaches in mice (Soto-Suazo et al., 1999, 2002). The location and role of fibronectin along the PGC migratory route, in particular, has been examined in detail (Heasman et al., 1981; Fujimoto et al., 1985; Ffrench-Constant et al., 1991). In avians, Urven et al. (1989) described the distribution of fibronectin, laminin, chondroitin sulfate and collagen IV along the PGC migratory pathway during the first 5 days of development. PGCs may shift their adhesiveness to the different ECM substrate molecules that they encounter during their migration (García-Castro et al., 1997). Loss-of-function assays have been used to identify the roles played by individual components of the complex PGC/ECM relationship. For example, the elimination of the integrin β1 receptors in null mouse lines led to poor colonization of the gonad by migratory PGCs (Anderson et al., 1999). Knockout mouse lines lacking the Msx1/2 transcription factors showed abnormal PGC migration along with increased amounts of fibronectin (Sun et al., 2016). These previous studies have led to an increasing understanding of PGC-ECM interactions particularly during the later migratory period; however, the early migratory stages have received less study.

Direct visualization of PGC/ECM interactions in real time *in vivo* may provide new insights into the early migratory phase of PGCs. Unfortunately, imaging PGC migration in early mouse embryos is technically challenging (Molyneaux et al., 2001). We have previously demonstrated the utility of fluorescently labeled transgenic quail for imaging early developmental processes (Sato et al., 2010; Huss et al., 2015a; Bénazéraf et al., 2017). Recently, we have developed a novel transgenic quail line that is a useful model system for studying early cell motility and migration. A shared characteristic of all of the ubiquitously expressing transgenic quail lines is that slowly dividing cells, such as PGCs, show a higher level of fluorescence compared to rapidly dividing cells. This unique feature allows us to follow the movement of PGCs *in vivo* (Huss et al., 2015a). The injection of fluorescently labeled anti-glycoprotein antibodies into live embryos makes following the highly dynamic ECM possible (Little and Drake, 2000; Filla et al., 2004). By combining these approaches, we can now visualize the interactions of PGCs with their surrounding ECM in real time.

Interpreting these PGC-ECM interactions will require a thorough understanding of the molecular profile of these unique stem cells. The previously published PGC mRNA abundance data have primarily been obtained from stem cell culture (Macdonald et al., 2010; Jean et al., 2015). Knowing which ECM genes are expressed in avian PGCs and their surrounding somatic cells at different stages along their migratory pathway will be vital in understanding *in vivo* PGC/ECM interactions.

Numerous "matrisomes" have recently been compiled that list all of the genes that code for the structural ECM components in a particular species. Using domain-based organization, genes that code for proteins that directly interact with or remodel the ECM have been included (Naba et al., 2016). These lists also include genes that have the potential to interact with

Abbreviations: AF, auto-fluorescence; AO, area opaca; AP, area pellucida; CSAT, cell substrate attachment antibody; ECM, extra-cellular matrix; EGK, Eyal-Giladi and Kochav stage; EMB, embryo; FISH, fluorescence *in situ* hybridization; FN, fibronectin; FP, fluorescent protein; GC, germinal crescent; H2B, histone 2B; HH Hamburger Hamilton stage; HCR, hybridization chain reaction; hUbC, human ubiquitin C promoter; IF, immunofluorescence; ITG, integrin receptor; LAM, laminin; NA, numerical aperture; NSA, non-specific amplification; PGC, primordial germ cell; PGK, phosphoglycerate kinase promoter; scRNAseq, single cell RNA sequencing; Tg, transgene.

the structural ECM (Naba et al., 2012). To account for these broad categories, Hynes and Naba (2012) defined the Core Matrisome to include all of the ECM glycoproteins, collagens, proteoglycans and a second category as matrisome associated genes that includes ECM-affiliated proteins, ECM regulators, and secreted factors. Extensive transcriptome and proteome data have been included within the searchable human and mouse matrisomes. To date, *D. rerio*, *C. elegans*, and *D. melanogaster* matrisomes have also been compiled, but avian matrisomes are lacking (http://matrisome.org/).

Here, we fill the gaps in knowledge concerning certain aspects of PGC-ECM interactions by using several methodologies. First, we compiled a quail matrisome and used it to analyze the transcriptome from individual PGCs manually isolated from early embryonic stage transgenic quail. The single cell RNA-seq (scRNA-seq) data shows that PGCs express a complex mixture of ECM and ECM-affiliated genes including fibronectin and numerous members of the collagen, laminin, and integrin gene families. To confirm the scRNA-seq results, whole mount mRNA fluorescent *in situ* hybridization (FISH) and immunofluorescence (IF) of selected genes were combined with confocal imaging to localize these transcripts and proteins to the PGCs and the surrounding cells of the germinal crescent. Live imaging of transgenic quail injected with anti-fibronectin or laminin antibodies showed rapid cell shape changes of PGCs in the germinal crescent and their active interplay with a dynamic ECM. Perturbation of the β1 integrin receptor/ECM interaction had no discernable effect on PGC cell motility, but resulted in a dramatic reduction in the abundance of the matrix fibril meshwork in the germinal crescent.

MATERIALS AND METHODS

Transgenic Quail

Three separate transgenic Japanese quail (*Coturnix japonica*) lines were utilized in this study. We previously reported the [Tg(PGK1:H2B-cherryFP)] or [PGK1] line that fluorescently labels all cell nuclei and allows cell proliferation rates to be determined (Huss et al., 2015a). The [Tg(UbC.H2B-cerFP-2A-Dendra2)] or [UbC.CerD2] quail line ubiquitously co-expresses histone 2B-ceruleanFP (H2B-cerFP) and Dendra2. Dendra2 is a photoconvertible green fluorophore that efficiently converts to red after exposure to near-UV light (Gurskaya et al., 2006). Details on the molecular cloning, lentivirus production and EGK-X blastoderm injections have been reported (Huss and Lansford, 2017). The [Tg(hUbC:Membrane-eGFP)] quail line was a kind gift from Dr. Jerome Gros (Pasteur Institute, Paris, France) (Saadaoui et al., 2018) and labels the plasma membrane of all cells. All animal procedures were carried out in accordance with approved guidelines from the Children's Hospital Los Angeles and the University of Southern California Institutional Animal Care and Use Committees.

Japanese Quail Genome

For these studies we used the *Coturnix japonica* genome (https://www.ncbi.nlm.nih.gov/genome/?term=coturnix).

Quail Matrisome

We screened the human matrisome genes against the *Coturnix japonica* genome to identify gene orthologs that could be considered as the Quail matrisome. The matching quail genes were divided into (1) "Core matrisome" and (2) "Matrisome-associated" genes similar to the human matrisome (Naba et al., 2016). Categories within groups—(1) Core matrisome: ECM, Collagens, and Proteoglycans; (2) Matrisome-associated: ECM-related, Regulators, and Secreted Factors.

Transcriptome Analysis of Individual PGCs

[Tg(PGK1:H2B-mCherry)] quail embryos were incubated until HH3, HH6, or HH12 and harvested on paper rings into PBS. Tissue areas containing PGCs were excised using fine iris scissors (**Figure S1**). The tissues were dissociated at 37°C using TrypLE Express (ThermoFisher), pipet triturated and diluted in PBS. A drop of diluted cell suspension was placed on a plastic petri dish on the stage of an Olympus MVX10 epi-fluorescent stereomicroscope. Using a micro manipulator and alternating between bottom white light illumination and CY3 filtered fluorescence, single cells were visually aspirated into glass needles with a tip opening of ∼40 μm. Once aspirated, the glass pipet was quickly withdrawn from the suspension. The tip of the glass pipet containing the single cell was crushed into the bottom of a 1.5 ml RNase/DNase free microfuge tube. Twenty cells from each developmental stage were collected based on their H2B-mCherry brightness and overall size. Amplification of the mRNA population was then carried out according to the protocol outlined in Morris et al. (2011). Deep sequencing of the prepared single cell libraries was performed at the University of Pennsylvania Genomics Center. Bioinformatics processing was carried out in the laboratory of Dr. Junhyong Kim using their software platform Interactive Data Visualization [KimLabIDV, v1.03, now PIVOT] (Zhu et al., 2018). RNAseq reads were aligned to the reference *Coturnix* and *Gallus* genomes using Bowtie2 (Langmead and Salzberg, 2012) or the Star software package (Dobin et al., 2013). Outlier cells were excluded based on cell library read depth (<50 million reads/cell) and overall percentage sequence alignment. Unsupervised clustering analysis of the scRNAseq data was used to define cell types and stable states (Kim and Eberwine, 2010). Cells were categorized using principle component analysis and assigned unique molecular identifiers (UMI). DDX4 and DAZL were used as PGC marker genes to screen the 20 picked cells from each developmental stage. We identified 12 PGCs from HH3 (60%), 13 PGCs from HH6 (65%), and 8 PGCs from HH12 (40%). Quail gene orthologs to the mouse and human core matrisome genes (Naba et al., 2016) were identified and used to assign scRNAseq reads to particular genes. Gene sets were analyzed and graphed using Microsoft Excel.

Immunofluorescence and Static Imaging

Anti-fibronectin (B3/D6), anti-laminin (31-2), anti-fibronectin/laminin receptor (JG-22), anti-integrin β1 subunit (CSAT), anti-fibrillin 2 (JB-3), anti-collagen type IV (M3F7) and anti-chondroitin sulfate (9BA12) monoclonal antibodies were purchased from the Developmental Studies Hybridoma Bank at the University of Iowa (DSHB, Iowa City, IA). Directly

conjugated B3/D6 (AlexaFluor 594) and 31-2 (AlexaFluor 555) were kind gifts from Dr. Charles Little (University of Kansas Medical School, Kansas City, MO). Anti-CVH polyclonal antibody (also known as VASA or DDX4) was a kind gift of Dr. Toshiaki Noce, Keio University School of Medicine, Tokyo, Japan). The anti-DAZL rabbit monoclonal antibody (ab215718) was purchased from Abcam (Cambridge, MA). Before use, the CSAT antibody serum was concentrated from 20 to 174 μg/ml by centrifugation through a 30,000 mw cutoff Amicon Ultra-15 cellulose filter column (Millipore) at 4,000 × g for 1 h at 4°C.

Eggs were grown in a forced air humidified incubator at 37°C until the proper age. Quail embryos were staged according to Eyal-Giladi and Kochav (1976), Hamburger and Hamilton (1951) and Ainsworth et al. (2010) with additional detailed descriptions of primitive streak morphology and staging from Streit and Stern (2008). Embryos were harvested from the yolk using a filter paper ring (Chapman et al., 2001), washed in PBS (phosphate buffered saline) and fixed in 4% formaldehyde/PBS made from a 36% stock solution (Sigma, F8775). Embryos were dissected free of the paper ring, washed in PBST (0.1% Triton X-100), blocked in PBST containing 1% bovine serum albumin and 5% normal donkey serum and incubated in primary antibodies in blocking solution overnight at 4°C. DSHB antibodies were diluted to 5 μg/ml. Anti-CVH and DAZL were diluted to 1:500. After washing, the embryos were blocked in PBSTW (0.1% Tween-20) and incubated in 1:1,000 dilutions of appropriate donkey secondary antibodies conjugated to AlexaFluor fluorophores (Thermo-Fisher) overnight at 4°C. After washing in PBST, embryos were incubated in PBST + 0.05 μg/ml DAPI for 1 h at 4°C, washed again and cleared in ScaLe U2 solution (Hama et al., 2011). Controls in which the primary antibody was eliminated failed to show specific labeling. Embryos were stored in the dark at 4°C until imaging. Static imaging was conducted with the cleared embryos placed dorsal side down on No. 0 glass bottom petri dishes (Mattek, Ashland, MA) and covered with a thin layer of ScaLe U2. Imaging was performed on a Zeiss 780 inverted confocal microscope with 5x/0.16NA, 10x/0.45NA, 20x/0.8NA, 63x/1.4NA oil Plan-Apochromat objectives or a 40x/1.1NA water LD C-Apochromat water immersion objective. Images were processed using the Zeiss Zen software along with NIH Image J (PMID 22743772). Slight adjustments to the contrast and brightness of the entire image were occasionally made.

Hybridization Chain Reaction

In situ hybridization was carried out on whole-mount quail embryos using the hybridization chain reaction (HCR) technique (Choi et al., 2014, 2016; Huss et al., 2015b). Oligonucleotide antisense probes (30 or 50 nt) against quail or chicken target sequences were commercially synthesized (IDT or ThermoFisher, see **Video S4** for the exact sequences). Probes sets contained between 4 and 11 probes and included unique initiator sequences to allow for simultaneous multiplex hybridizations. Probes were hybridized to the embryonic mRNA target sequences overnight at 37°C. After washing, fluorescently conjugated hairpin amplifiers were hybridized to the probes overnight at RT. Controls included the elimination of both probes and hairpins to test the inherent fluorescence of the embryonic tissue and the use of only hairpins to judge whether they were contributing to non-specific signal production. All HCR-treated embryos were imaged similar to the aforementioned IF-treated embryos.

Time-Lapse Imaging and Microinjection

Fertilized Tg[hUbC:H2B-Cerulean-2A-Dendra2] quail eggs were incubated on their sides until HH3 then windowed. Injections of directly conjugated anti-fibronectin (abB3/D6) or anti-laminin (ab31-2) antibodies [1 mg/ml] were made into 3 locations around the anterior area opaca/area pellucida boundary (Little and Drake, 2000). The window was then sealed with parafilm and the egg incubated 2 h until being harvested on a paper ring. Embryos were cultured dorsal side down on No. 0 glass bottom 35 mm petri dishes that had been covered by a thin layer of agar/albumin (Sato and Lansford, 2013). A ring of moist Kimwipe (Kimtech Science) was wrapped around the inside perimeter of the dish and the top sealed with a thin strip of parafilm. The cultured embryo was allowed to settle for 1 h in the microscope stage mounted incubator at 37°C before imaging. Confocal Z stacks were taken at 1.5 min time intervals in order to capture short-term cell morphology changes. In the CSAT live imaging experiments, the embryos were first imaged as above then were removed from the microscope incubator, injected with CSAT [174 μg/ml] antibodies just under the epiblast, lateral to the primitive streak at the level of Hensen's node and returned to the heated stage for 1–2 h before additional imaging.

RESULTS

Quail Matrisome

To generate a Quail Matrisome (**Table S1**), we used a bioinformatic approach to screen the *Coturnix* genome for ECM and ECM-associated genes modeled after the human matrisome (Naba et al., 2016). Approximately 706 quail matrisome genes were identified compared to 1,026 in the human (**Figure 1**). The quail Core matrisome category contains 167 ECM glycoprotein, 31 proteoglycan, and 40 collagen genes. The quail Matrisome-associated category consists of 99 ECM-affiliated proteins, 155 ECM regulators and 214 secreted factors. Full bioinformatics information for the quail matrisome genes can be found in **Table S1**.

ECM and ECM-Associated Transcripts Are Expressed by PGCs

Since avian PGCs undergo a long and complex migratory pathway across the first three days of post-laying development, we hoped to understand how their ECM transcriptome changed during this time. The inherent brightness of PGC nuclei in the Tg(PGK1:H2B-mCherry) quail line along with their unique morphology (large diameter, globular shape with internal glycogen vesicles) allowed us to pick single cells from enzymatically dissociated tissue. PGCs from HH3, HH6, and HH12 embryos were collected at distinct morphological regions of the embryos that included the germinal crescent (**Figure S1**). Amplification of the mRNA was performed according to the protocol described by Morris et al. (2011). Next generation sequencing produced a transcriptome that was analyzed based on

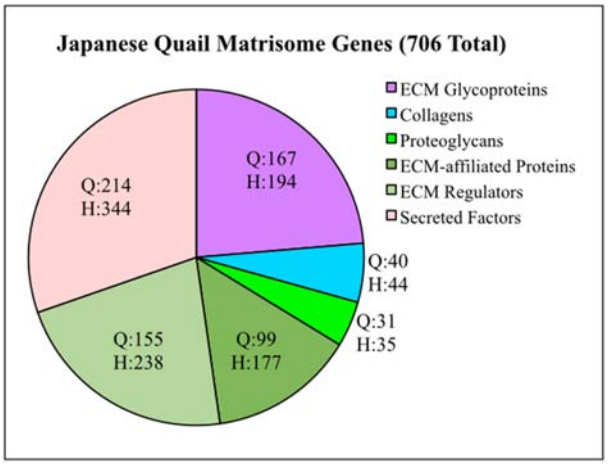

FIGURE 1 | Quail matrisome categorized according to the human matrisome results of Naba et al. (2016). Q = Quail genes (706 total). H = Human genes (1,026 total). ECM Glycoproteins, Collagens and Proteoglycans make up the Core Matrisome. ECM-affiliated Proteins, ECM Regulators and Secreted Factors are Matrisome Associated genes.

the newly generated quail matrisome. The scRNAseq raw data for the quail matrisome genes are provided in **Table S2**.

While not strictly quantitative, the number of sequencing reads, likely provides a rough indication of overall mRNA abundance. The genes DAZL (deleted in azoospermia like) and DDX4 (DEAD-box helicase 4, also referred to as chicken vasa homolog or CVH) were used as markers for PGCs. The number of reads for matrix glycoproteins, collagens and integrin receptor subunits was compared for PGCs across three developmental time points (**Table S2** and **Figures 2**, **3**). PGCs express many of the core matrisome glycoproteins with fibronectin 1 (FN1), laminin α1 subunit (LAMA1), laminin β1 subunit (LAMB1), and laminin γ1 subunit (LAMC1) showing the highest average number of reads per PGC. With the exception of FN1 at HH6, the abundance of these glycoprotein transcripts does not change markedly across developmental time points (**Figure 2A**). Additional matrix mRNA transcripts (shown in **Figure S5D**) such as the fibulin (FBN) and fibrillin (FBLN) families and heparan sulfate glycoprotein (HSPG) are clearly present but appear at much reduced levels compared to fibronectin and laminin. Many types of collagen mRNA transcripts were also detected in PGCs (**Figure 2B**). COL4A1, COL4A5, and COL26A1 were elevated slightly in expression while COL18A1 showed an increased number of reads at HH6 (**Figure 2B**).

The integrin ITGA2, ITGA4, and ITGA6 alpha subunits are detected at high levels in PGCs across the three time points examined (**Figure 3A**). ITGA2 shows a distinct increase in abundance between HH3 and HH6. Among the integrin β subunits, ITGB1subunit transcripts appear most numerous, with the ITGB7 and ITGB8 subunit showing lower, but consistent expression at the three developmental stages examined (**Figure 3B**). The integrin receptor subunits that showed lower relative levels of expression are shown in **Figure S5**. ITGA1 and ITGAV subunits were present, but at much reduced levels compared to ITGA2, ITGA4, and ITGA6 (**Figure S5A**). ITGB2, ITGB3, ITGB4, ITGB5, and ITGB6 subunit transcripts were amplified at the highest relative numbers at HH6 although, overall, these subunits were at lower levels than ITGB1 (**Figure S5B**). Note the change in the y-axis scale between **Figure 3B** and **Figure S5B**.

While integrin receptors, especially those containing the ITGB1 subunit, are highly abundant at the mRNA transcript level in PGCs, non-integrin receptors may also play important roles in cell/ECM interactions. Transcript levels for non-integrin receptors are shown in **Figure S5C**. Syndecan (SDC2), hyaluronan mediated motility receptor (HMMR) and CD47 were present in levels comparable to the most common integrin receptors. Dystroglycan (DAG1) was particularly abundant in PGCs at HH6 (**Figure S5C**).

PGCs Associate Closely With Fibronectin and Laminin

Individual PGCs strongly express FN1, LAMA1, LAMB1, and LAMC1 transcripts at developmental stages HH3, HH6, and HH12. To investigate the intimate associations between nascent, migrating PGCs and these ECM components, we used immunofluorescence (IF) to detect extracellular fibronectin using the B3/D6 antibody on whole-mount quail embryos ranging from stage HH3 to HH6 (**Figure 4A**). Confocal 3D (x, y, z) imaging across the entire embryo revealed that fibronectin protein expression was most highly concentrated at the border of the area opaca (AO) and area pellucida (AP) in all four stages shown. Expression at the anterior (rostral) end of the AO/AP border in the germinal crescent where PGCs congregate contained a dense meshwork of FN fibrils (**Figures 4A**, **5A**). In agreement with earlier studies, the expression pattern of FN in the embryonic tissue layers was less dense than at the AO/AP border, consisting of short, scattered fibrils and puncta (Duband and Thiery, 1982; Raddatz et al., 1991).

Anti-FN IF revealed an intricate mesh of FN fibrils in the HH6 germinal crescent (**Figure 5A**). IF using an antibody against the cytoplasmic PGC marker chick vasa homolog (CVH) shows that a large number of PGCs had migrated into the same region. In addition to IF, PGCs were also localized by the bright cell nuclei of [PGK1] transgenic embryos. Within the germinal crescent of some embryos, bulges, or folds, of the tissue layers created open spaces devoid of most cells (Sanders, 1982). An area such as this is shown in **Figure 5B**. Interestingly, PGCs were often found in these spaces while neither fibronectin nor laminin was present. Antibodies against fibrillin-2 (JB-3), collagen type IV (M3F7) and chondroitin sulfate (9BA12) also failed to label these spaces (data not shown), yet PGCs can be seen migrating throughout these germinal crescent spaces. The ECM component within these spaces remains to be determined. CVH IF showed a high proportion of PGCs, whether inside of these spaces or not, as having morphological characteristics consistent with active cell motility such as blebs (yellow arrow) and long cellular processes (white arrow, **Figure 5C**. See also **Video S1**). At stage HH12, PGCs in the germinal crescent continue to be in close contact with the FN fibril meshwork (**Figures S2**).

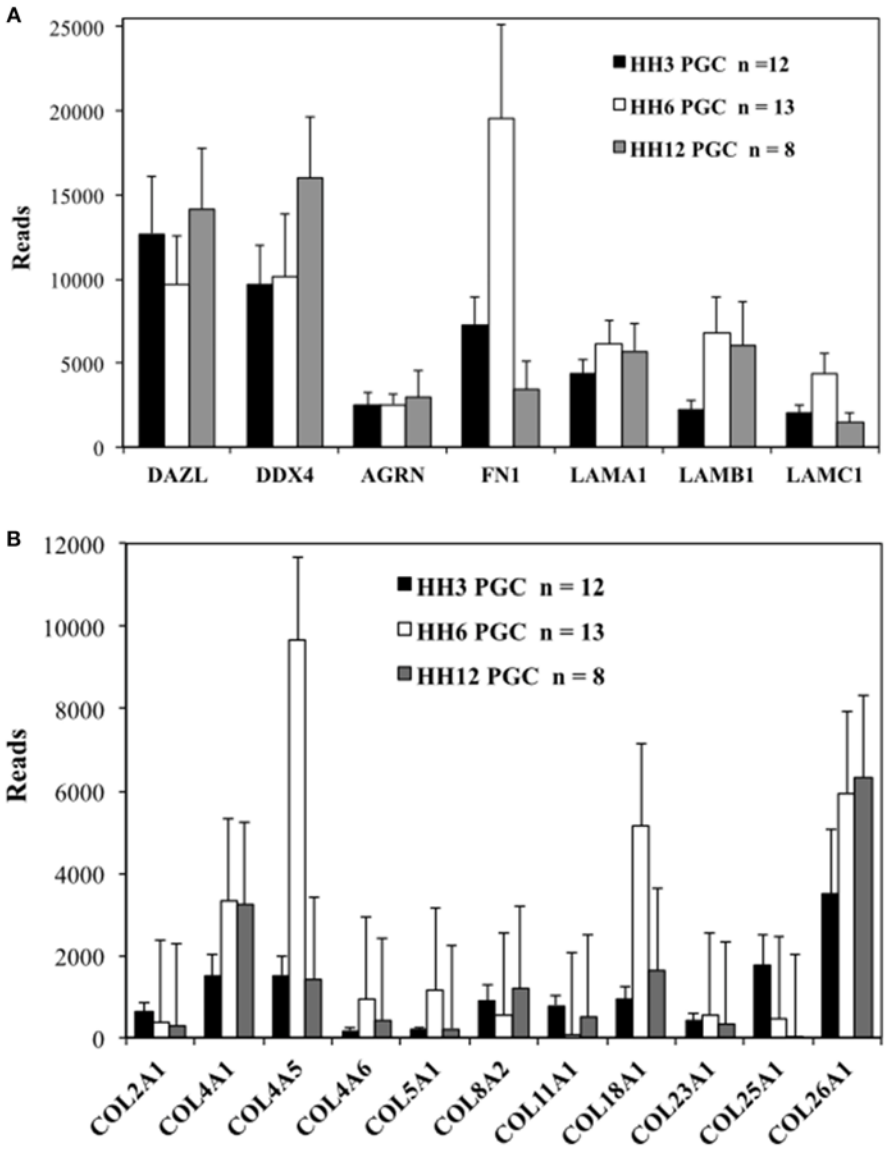

FIGURE 2 | Quail PGCs express mRNA for a diverse set of matrix glycoprotein and collagen genes. scRNAseq of select ECM transcripts in PGCs at HH3, HH6, and HH12. **(A)** Matrix genes along with PGC markers DAZL and DDX4. DAZL = Deleted in azoospermia-like. DDX4 = (Dead-box helices 4 or chicken vasa homolog (CVH). AGRN, Agrin; FN, Fibronectin; LAMA1, Laminin alpha subunit 1; LAMB1, Laminin beta subunit 1; LAMBC1, Laminin gamma subunit 1. **(B)** Collagen genes. Y axis scaling has been adjusted separately in **(A,B)**. Bars represent the mean + s.e.m. The number of single cells in each group are shown in the legend.

The pattern of laminin glycoprotein expression was assayed in HH3-HH6 whole-mount quail embryos using the 31-2 antibody (**Figure 4B**). Like FN, laminin expression was most abundant at the AO/AP border and within the germinal crescent (**Figure 4B**). Laminin was also detected in the basal lamina, or basement membrane, on the ventral surface of the epiblast layer lateral to the primitive streak at HH5, which agrees with previous reports (Bortier et al., 1989; Zagris et al., 2000). The majority of PGCs in the germinal crescent closely associated with the areas highest in laminin fibril density (**Figure 6**, Merge). Much like fibronectin, laminin fibrils formed a tight meshwork in the HH5 germinal crescent and surrounded or enclosed, some PGCs (**Figure 6C** white arrows). PGCs were seen clustered together in clumps or individually, many with smooth, globular morphology.

Validation of PGC Transcriptome Results With IF and FISH in Embryos

We used whole-mount immunofluorescence and *in situ* hybridization to validate the scRNAseq expression data of select ECM genes in migratory stage PGCs. JG-22 is an antibody specific for the integrin β1 subunit that makes up part of the heterodimeric cell surface receptors that bind laminin and fibronectin (Greve and Gottlieb, 1982). This antibody showed ubiquitous expression across all embryonic and extra-embryonic

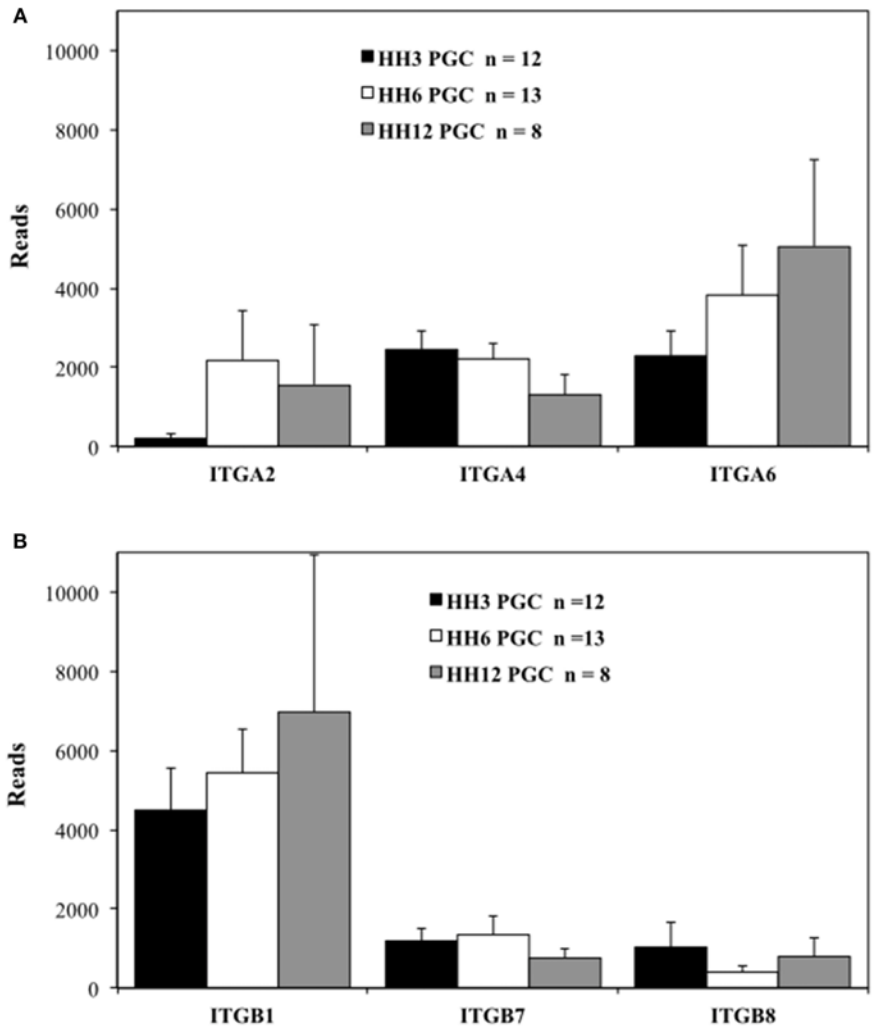

FIGURE 3 | Migratory quail PGCs express multiple integrin alpha and beta subunits. scRNAseq of integrin receptor subunit mRNA transcripts from PGCs across 3 developmental time points. **(A)** Integrin alpha subunits (ITGA2, 4, and 6). **(B)** Integrin beta subunits (ITGB1, 7, and 8). Bars represent the mean + s.e.m. The number of single cells in each group are shown in the legend.

tissues in primitive streak stage embryos (**Figure 7C**). Dazl+ PGCs in HH4 [Tg(hUbC:Membrane-eGFP)] quail embryos showed strong co-localization of integrin β1 with their GFP+ cell membranes (white arrows, **Figures 7A,B,D,E**). Somatic cells in close proximity to the PGCs in the germinal crescent were also strongly positive for integrin β1 subunit protein (**Figures 7A,B,D,E**).

The fluorescent *in situ* hybridization chain reaction (HCR) technique allows for multiple target mRNA transcripts to be detected simultaneously in whole-mount embryos (Choi et al., 2014). The anti-sense probe set sequences for quail FN1, LAMA1, LAMB1, ITGB1, and DAZL can be found in **Figure S3**. FN1 mRNA was widely detected across the embryo but showed particularly high expression in the anterior embryonic/extra-embryonic border area (**Figure 8A**). DAZL labeling localized a large concentration of PGCs in this region as well. LAMB1 was also ubiquitously expressed but was most prominent in the embryonic tissues, likely due to its abundance in the basement membrane on the ventral surface of the epiblast layer (**Figure 8A**; Zagris et al., 2000). Stage HH4-5 germinal crescent PGCs, and the nearby somatic cells, showed co-localized punctate labeling of FN1 with LAMB1 and LAMA1 (**Figures 8B–E**).

Likewise, FN1 mRNA was co-expressed along with ITGB1 transcripts in germinal crescent PGCs (**Figures 9A–D**). Cells surrounding the PGCs also showed strong expression of fibronectin and integrin β1 mRNA transcripts. Control embryos incubated without probes and amplifying hairpins (**Figure 9E**) or hairpins alone (**Figure 9F**) failed to show the expression pattern of the experimental embryos.

Time-Lapse Imaging of PGC-ECM Interactions

Fluorescently conjugated anti-glycoprotein antibodies were injected into the anterior AO/AP boundary of HH3

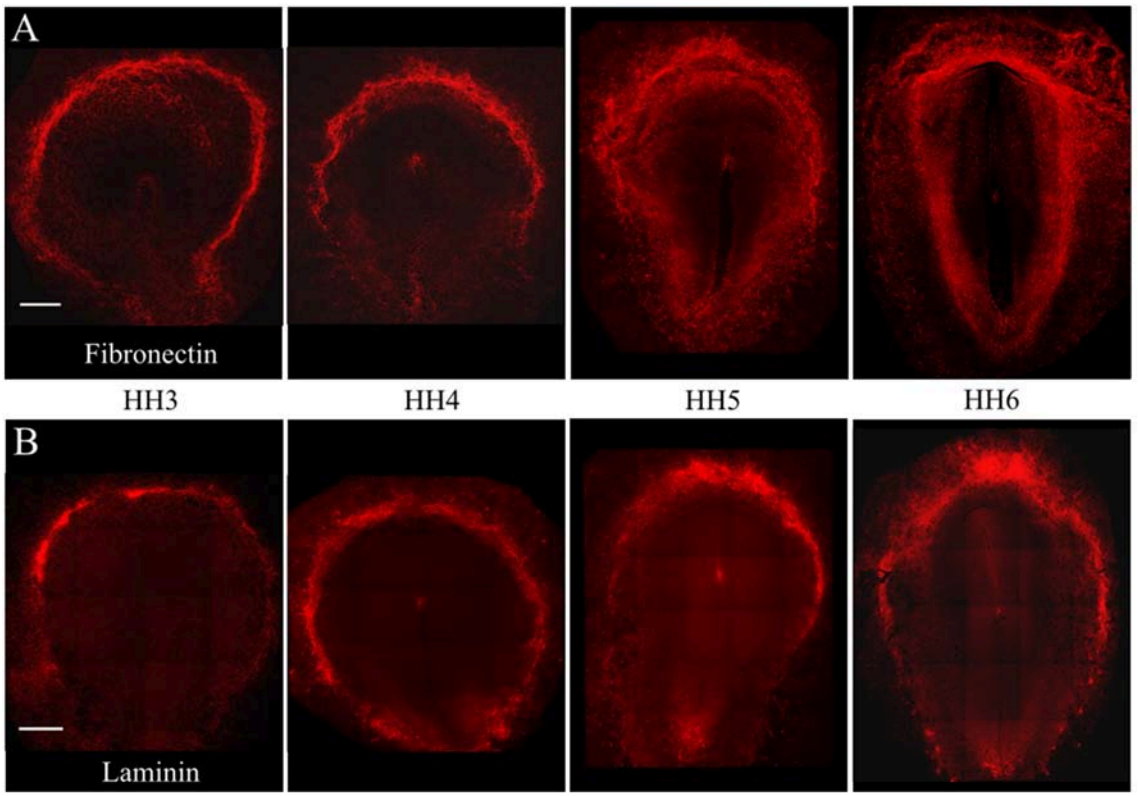

FIGURE 4 | Fibronectin and Laminin protein is highly expressed at the AO/AP border and germinal crescent at stages HH3-6. Wholemount immunofluorescence for fibronectin (abB3/D6) and laminin (ab31-2) in 4 developmental stages. **(A)** Fibronectin (red), **(B)** Laminin (red). Images are maximum intensity projections of 10x tiled confocal Z stacks taken from the dorsal aspect. Anterior (rostral) to top. Scale bars = 500 um.

[Tg(hUbC:H2B-Cerulean-2A-Dendra2)] quail embryos in order to dynamically image PGC/ECM interactions in real time (Little and Drake, 2000). **Figure 10** shows 9 captured time points (90 s intervals) from the germinal crescent of an HH5 transgenic embryo injected with anti-fibronectin (abB3/D6, AlexaFluor 594). The fibronectin matrix appears as bright red puncta and fibrils, cells are displayed with blue nuclei (H2B-Cerulean) and green cytoplasm (Dendra2 fluorescent protein). While the overall tissue and fibronectin fibrils move smoothly to the lower left, toward the embryo, the PGCs (large bright cells indicated with a white arrow, 0 min) show a rapid, constantly shifting cellular morphology (see **Video S1**). Blebs can be seen in most time points. Fibronectin fibrils surround the outside of the PGC cell closely, with the PGC cell body moving around and between fibrils.

Injected anti-laminin antibodies (ab31-2, AlexaFluor 555) show a similar pattern when injected into the germinal crescent region of an HH4 transgenic embryo (**Figure 11** and **Video S2**). The PGCs are mostly clustered and show the same fast morphology changes seen in **Figure 10** and **Video S1**. The laminin ECM matrix can be seen shifting, expanding and contracting along with the large-scale tissue motion. The bounding boxes, starting at minute 47 (yellow arrow in Movie 2), highlight a small region of condensed laminin fibrils that begin in a relaxed, smooth wave-like configuration. The fibrils then seem to undergo a compression which forces the smooth wave into a sharp peak (minute 57). Next, the ECM and tissue seem to expand, bringing the laminin fibrils back into a smooth wave appearance by minute 71. All along, the PGCs move with the tissue flow but continue their independent, seemingly random shape changes.

Video S3 was taken from the lateral germinal crescent region of a single HH4 embryo injected with anti-fibronectin fluorescent antibodies. In this short example, the fibronectin fibrils can be seen as forming a loose band running roughly in the anterio-posterior direction (the embryo is toward the lower right, out of view). The PGCs, which are clustered to the medial side of the FN, move with the overall tissue/ECM flow laterally with only a few PGCs interacting closely with the ECM. A yellow arrow highlights a rapidly moving PGC that moves around the end of a FN fibril and comes to a stop along a second FN band. **Video S4** begins a short time later at the same location of **Video S5**. Here, the impression is one of the FN forming a structural boundary, or demarcation line, across which the PGCs are not readily crossing, at least in the time frame imaged (about 60 min total). **Video S5** shows a digitally zoomed view of a region from **Video S4**. The constant and sometimes erratic movements of individual PGCs can be seen, all occurring against the large-scale tissue and ECM

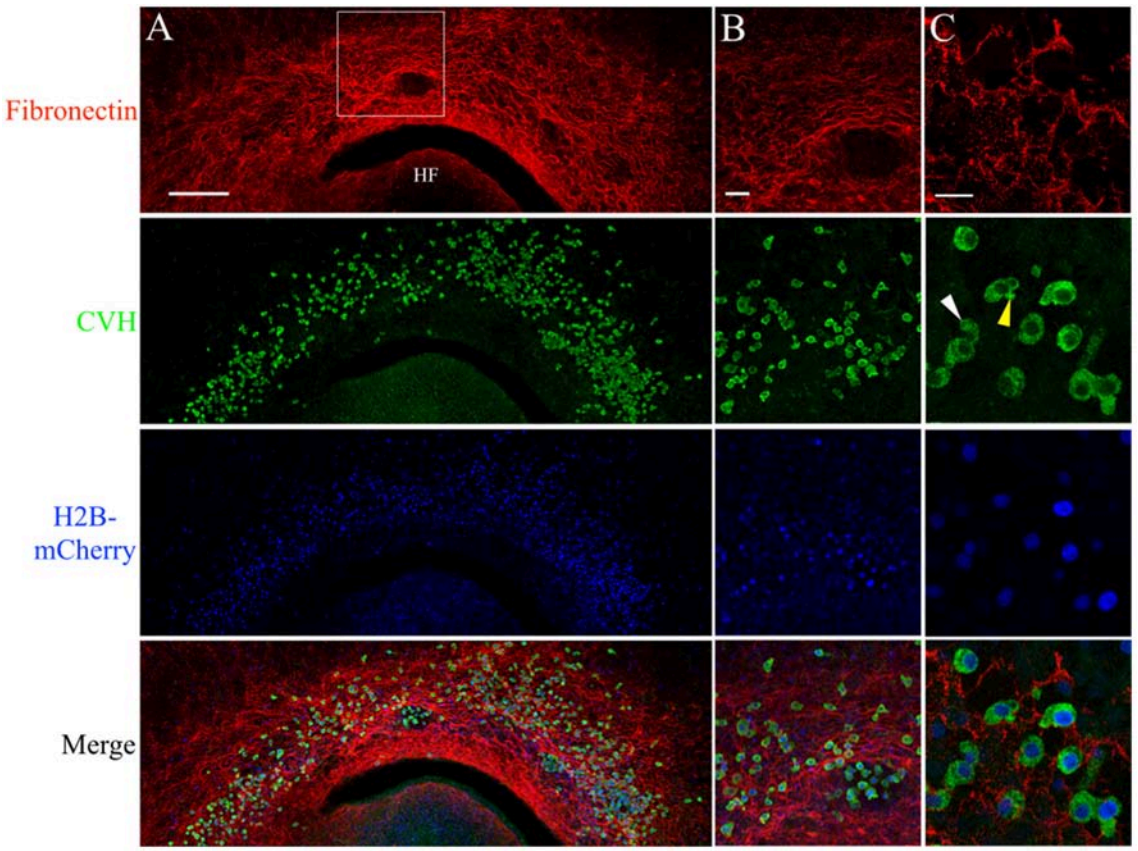

FIGURE 5 | PGCs are closely associated with the complex fibronectin fibril meshwork in the germinal crescent. Wholemount immunofluorescence for fibronectin (abB3/D6) and CVH across the germinal crescent of HH5 and HH6 [Tg(PGK1:H2B-mCherry)] quail embryos. **(A)** Fibronectin red, CVH (PGC marker, green), H2B-mCherry (blue) and merged maximum intensity projections of 10x tiled confocal Z stacks taken from the dorsal aspect of an HH6 embryo germinal crescent. Anterior (rostral) to top. HF = head fold. **(A)** Scale bar = 250 μm. Images in **(B)** are maximum intensity projections of 20x tiled confocal Z stacks taken from the dorsal aspect at the location of the bounding box in **(A)**. **(B)** Scale bar = 50 μm. **(C)** Images are maximum intensity projections of 4 × 2.1 μm optical sections from 63x confocal Z stacks taken in an HH5 embryo. Yellow arrow in the CVH image highlights a bleb on a PGC. White arrow indicates a long cellular process. Scale bar = 25 μm.

flow. Lastly, **Video S6** shows a dynamically moving meshwork of FN fibrils and puncta in the germinal crescent of an HH4 embryo demonstrating the fluid-like capacity of the ECM to shift, expand and contract with the large-scale tissue movements of the growing embryo.

Perturbation of PGC Migration and ECM Expression by CSAT

To elucidate the functional roles that integrin receptors play in PGC movements, we introduced the CSAT (cell substrate attachment) antibody, which blocks the ability of integrin β1 containing receptors to bind their ECM components including laminin and fibronectin (Drake and Little, 1991; Drake et al., 1991). CSAT antibodies, or control medium, was injected under the epiblast of HH3 embryos, incubated for 6 h until HH5 and fixed. Detection of the CSAT antibody with fluorescently labeled secondary antibodies showed that the integrin β1 blocking immunoglobulins had spread across the entire embryonic and extra-embryonic area (**Figures 12A,B**). Control embryos, which lacked CSAT antibodies, showed no fluorescent signal. IF using anti-FN (abB3/D6) or laminin (ab31-2) antibodies revealed that CSAT injection had noticeably decreased the expression of both FN and laminin fibrils in the AO/AP boundary, particularly in the germinal crescent (**Figures 12A,B**, yellow arrows in CSAT embryos, white arrows in control embryos). In addition, the pattern of FN expression was altered in the CSAT injected embryos themselves. The fibronectin-free zone that typically surrounds the primitive streak was significantly wider in the CSAT treated embryos (**Figures 12A,D**, white line. $P > 0.001$, paired Student's T-Test). This result suggests that the mesodermal cells migrating laterally away from the primitive streak had not assembled mature FN fibrils as normal. Surprisingly, in both control and CSAT embryos, PGCs similarly moved from the embryonic regions to the extra-embryonic germinal crescent as in normal development (data not shown).

To rule out the possibility that these observed changes in ECM distribution were simply the result of overall delayed development caused by the CSAT antibody injection procedure, we made a series of measurements from bright-field

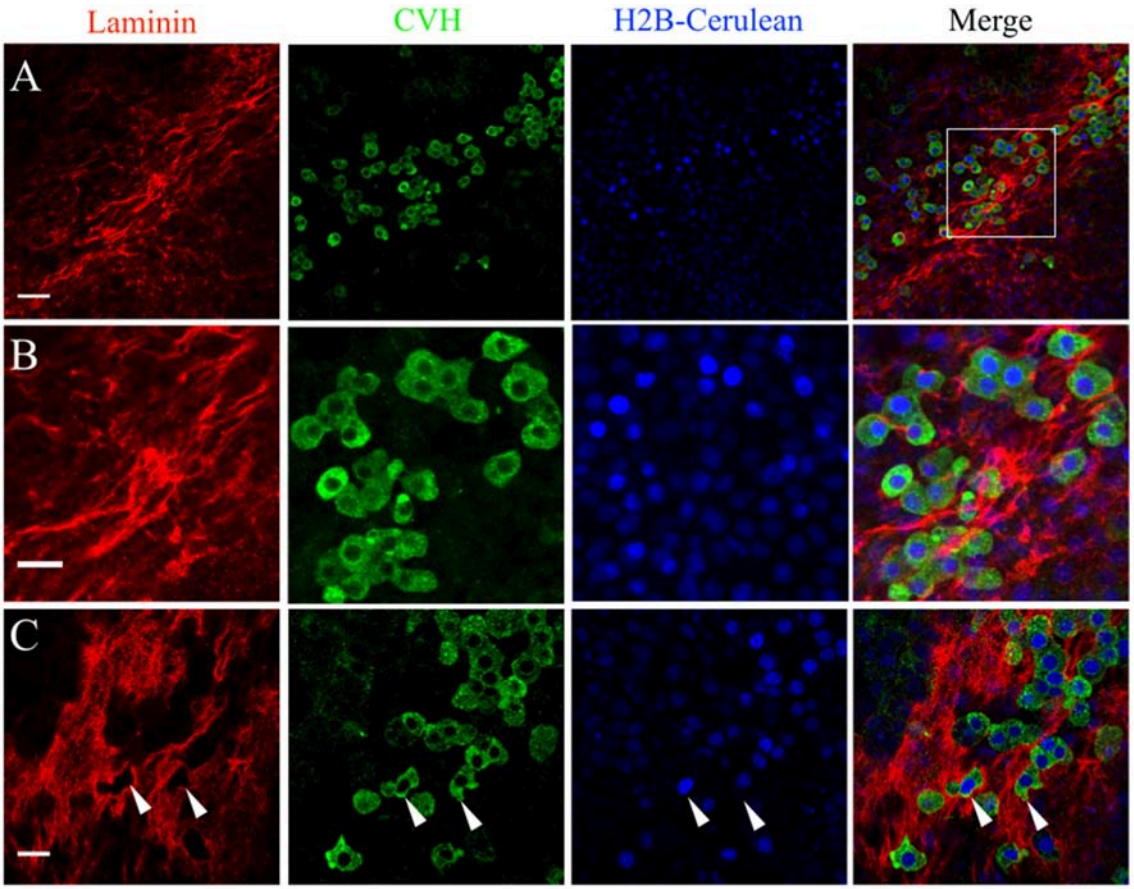

FIGURE 6 | PGCs in the germinal crescent are intimately associated with the laminin fibril meshwork. Whole-mount immunofluorescence for laminin (ab31-2) and CVH from two locations in the lateral germinal crescent of an HH5 [Tg(hUbC:H2B-Cerulean-2A-Dendra2)] quail embryo. Images in **(A)** are single optical sections (3.2 μm Z depth) taken at a lateral region of the germinal crescent using a 20x 0.8NA objective. Scale bar = 50 um. The bounding box in the merge indicates the region shown in **(B)** at increased magnification. Scale bar = 25 μm. **(C)** Images are maximum intensity projections of 3 optical sections (2.3 μm each) from 40x confocal Z stacks taken from the dorsal aspect of the embryo at the lateral germinal crescent. White arrows in **(C)** highlight regions of laminin that appear completely displaced by a PGC. Scale bar = 25 μm.

stereomicroscope images of both the experimental and control embryos (**Figure 12C**). Both the overall area of the area pellucida (AP) and the width of the AP taken at Hensen's node were significantly smaller in the CSAT embryos ($P > 0.001$, paired Student's *T*-Test. **Figure 12E**). Overall AP length was also reduced in the CSAT embryos, as was primitive streak (PS) length (**Figure S4**). However, a careful staging of the embryos using the morphological landmarks described by Streit and Stern (2008) showed that all embryos, from both groups, had reached between HH4- and HH5- (**Figures S4A,B**). The ratio between AP length/PS length were also not different. Therefore, it appears that the CSAT treated embryos were not simply developmentally younger and hence, smaller. Adhesion between tissue layers was compromised, as evidenced by the frequent areas of tissue layer separation in CSAT treated embryos (magenta arrow, **Figure 12B**).

Interestingly, the overall distribution of PGCs, as detected by anti-DAZL antibodies, was not altered by CSAT when compared to serum-injected controls. To further test whether the CSAT antibodies could affect the cell motility and rapid cell morphology changes of PGCs, which were evident in our initial time-lapse images (**Videos S4**–**S8**), we conducted a second CSAT injection experiment. Five HH3 [UbC.CerD2] quail embryos were first injected with fluorescent anti-FN antibodies along the anterior AP/AO border and allowed to develop *in ovo* for 3 h. The embryos were then mounted on paper rings, cultured dorsal side down on a thin bed of agar-albumin and dynamically imaged to record the pre-CSAT PGC movements (**Figure 12F** and **Video S7**). CSAT antibodies were then injected into the mesodermal space at three locations along the germinal crescent. A small amount of fast green mixed with the serum allowed the visualization of the antibodies as they spread. The embryo was allowed to recover for 2 h before imaging again (**Figure 12G** and **Video S8**). A qualitative assessment of the PGC cell motility movements determined that the rapid shape changes and the appearances and disappearances of putative blebs, filopodia etc., had not been altered by the CSAT antibody (compare the movies in **Videos S7**, **S8**).

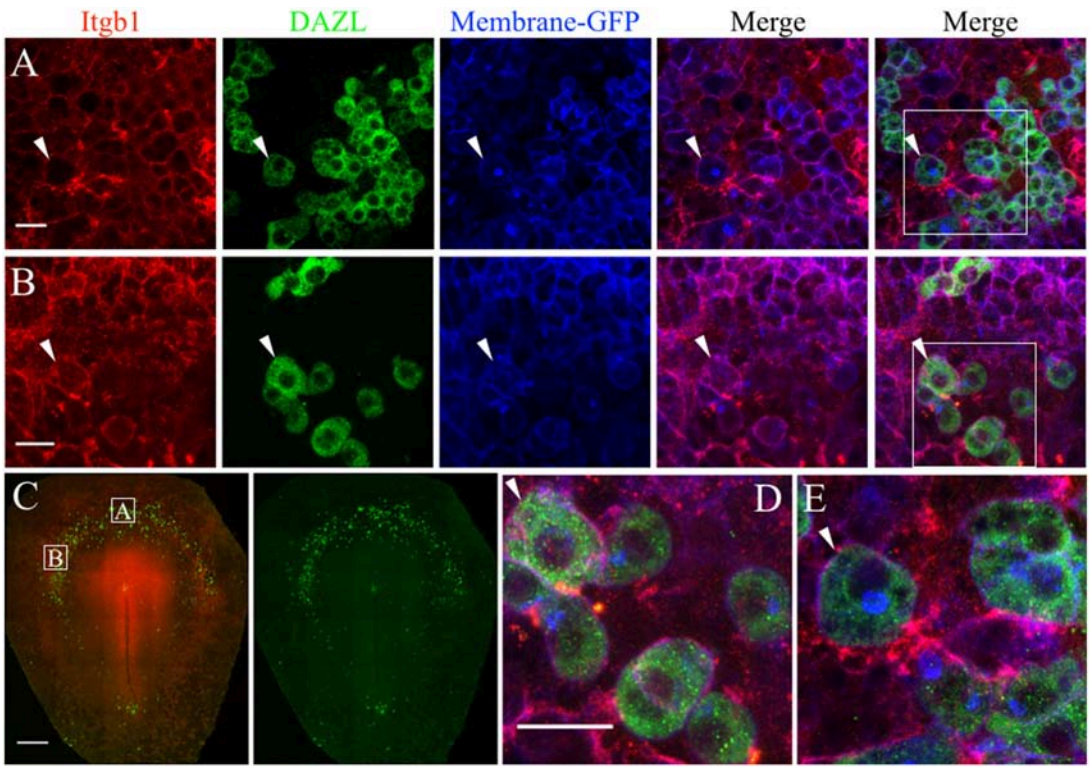

FIGURE 7 | PGCs and their surrounding cells in the germinal crescent express integrin beta 1 subunit protein on their cell surfaces. Whole-mount immunofluorescence for fibronectin and laminin receptors (integrin beta 1 subunit, abJG-22) and PGC-specific Dazl at two separate locations within an HH4 [Tg(hUbC:Membrane-eGFP)] quail embryo germinal crescent. **(A)** Central germinal crescent (see panel C for location). Left to right: Integrin beta 1 subunit (Itgb1, abJG-22, red), Dazl (PGC marker, green), membrane-GFP (blue), Itgb1 and membrane-GFP merge, Itgb1, membrane-GFP, Dazl merge (bounding box shown at higher magnification in E). White arrows indicate one PGC imaged in cross section with a clearly defined perimeter of Itgb1. 20x 0.8x zoom. **(B)** Lateral germinal crescent (see panel C for location). Left to right: Integrin beta 1 subunit (Itgb1, abJG-22, red), Dazl (PGC marker, green), membrane-GFP (blue), Itgb1 and membrane-GFP merge, Itgb1, membrane-GFP, DAZL merge (bounding box shown at higher magnification in D). White arrows indicate one PGC with a clearly defined perimeter of Itgb1 that was imaged at an oblique angle. 20x 1.0x zoom. **(C)** Tiled 10x confocal Z stack maximum intensity projections of the whole-mount HH4 embryo. Bounding boxes indicate location of images in **(A,B)**. Itgb1 (red), Dazl (green). Scale bar C = 500μm. **(D,E)** Images are digital zooms of bounding boxes in **(B,A)** Merge. White arrows in **(D,E)** highlight particular PGCs with integrin beta 1 subunit receptor labeled puncta on the cell surface which was imaged in oblique **(D)** or in cross-section **(E)** by the confocal optical slice. Scale bar A, B, D, E = 25 μm.

DISCUSSION

Germinal Crescent as a Stem Cell Niche

We have shown that the complexity of the ECM fibril meshwork in the germinal crescent increases from HH3 to HH6, which corresponds with the arrival and concentration of PGCs in this anterior AP/AO border area (**Figures 4–6**; Critchley et al., 1979). Our results indicate that PGCs are actively contributing to the ECM in the germinal crescent. Whether the germinal crescent could be considered a stem cell niche is an open question. Certainly, the ECM has been shown to be important for determining the structural microenvironment of adult stem cell niches (reviewed in Watt and Huck, 2013). Our immunofluorescence and live imaging data suggest that this may be the case for the embryonic germinal crescent as well.

Unlike adult stem cell niches that are sometimes maintained for years, the embryonic germinal crescent is a highly transitory morphological space that is maintained from roughly HH3 to HH9, a time period of about 16 h. During this time, the vast majority of PGCs gather in this avascular region and closely interact with one another. By HH9 the vascular plexus, which has been concurrently forming by vasculogenesis in a posterior to anterior direction in both the left and right lateral extra-embryonic tissues, begins to converge toward the midline of the germinal crescent. By HH12, this process is complete and most PGCs have intravasated from the germinal crescent into the newly formed blood vessels. There is a multifaceted array of direct and indirect stem cell/ECM interactions that occur in an adult stem cell niche that regulate many processes including stem cell proliferation and differentiation (Rozario and DeSimone, 2010; Ahmed and Ffrench-Constant, 2016; Cant et al., 2016). It will be interesting to explore whether this bi-directional communication system is also present in the embryonic germinal crescent. In particular, whether or not the germinal crescent ECM is binding morphogens, chemokines or growth factors as a way of attracting the PGCs to the "correct" location, maintaining their pluripotency and contributing to the expansion of the vascular plexus is unknown.

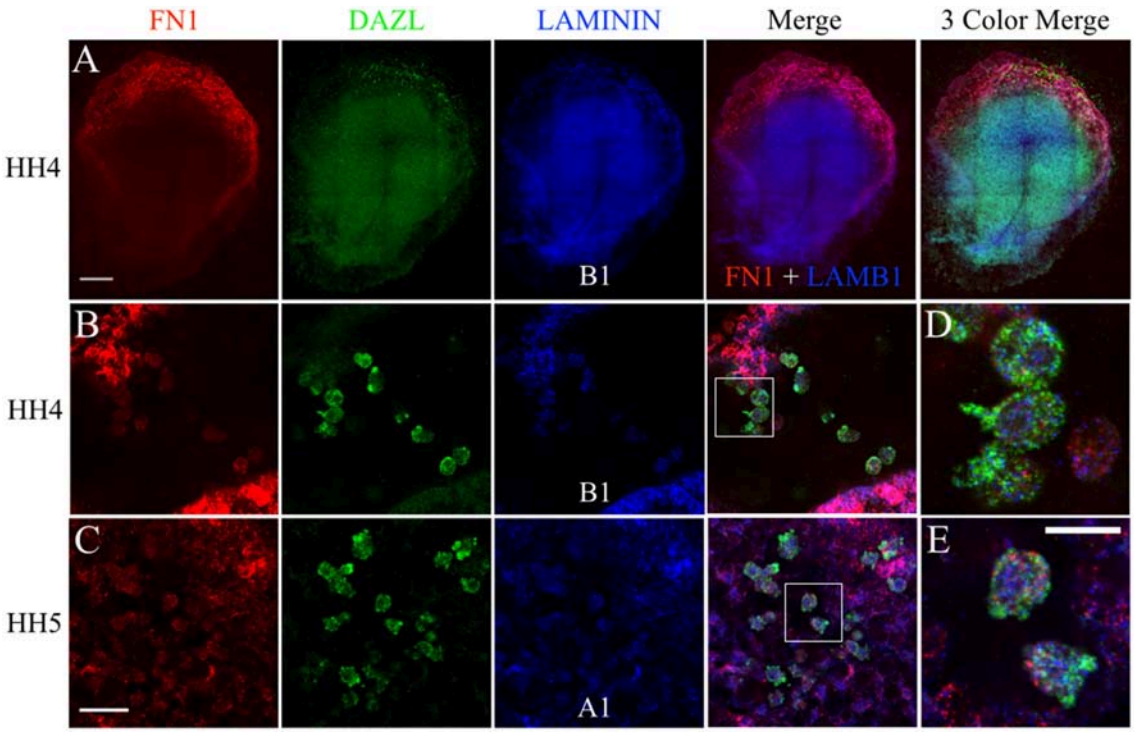

FIGURE 8 | PGCs and their surrounding cells in the germinal crescent co-express transcripts for fibronectin and 2 subunits of laminin. mRNA transcripts for FN1, DAZL, LAMA1, and LAMB1 are expressed by PGCs and their surrounding cells within the germinal crescent of HH4 quail embryos. Wholemount multiplex hybridization chain reaction (HCR) for fibronectin1 (FN1), laminin alpha1 (LAMA1), laminin beta1 (LAMB1), and DAZL mRNA transcripts in HH4-5 quail embryos. **(A)** HH4. Tiled 10x confocal Z stack maximum intensity projections. From left to right: FN1 (red), DAZL (PGC marker, green), LAMB1 (blue), FN1 and LAMB1 Merge, FN1, DAZL, LAMB1 Merge. Scale bar = 500 μm. **(B,C)** Images are single optical sections (3.2 um each) from 20x confocal Z stacks with 2x zoom of HH4 **(B)** and HH5 **(C)** quail germinal crescent. From left to right: FN1 (red) DAZL (green) LAMB1 or LAMA1 (blue), 3 Color Merge of FN1, DAZL, and LAMB1. Scale bar = 25 μm. **(D)** Bounding box from B merge, at higher magnification. **(E)** Bounding box from C merge, at higher magnification. Scale bar = 20 μm.

If so, it would lend additional support to the idea of Gu et al. (2009) that PGCs migrate along a "traveling niche" during embryogenesis.

Flexibility of ECM/Integrin Interactions

The inability of the CSAT perturbation experiment to alter either the short-term cell motility or long-term migration of PGCs to the germinal crescent was surprising (**Figure 12**, and **Videos S7**, **S8**). Pertubation of integrin receptor binding to the ECM has led to reduced chicken neural crest cell migration (Bronner-Fraser, 1985). CSAT antibodies have also been shown to alter somite morphology and their lateral displacement from the neural tube in quail embryos (Drake and Little, 1991). In addition, CSAT antibodies reduced the embryo's normal rate of expansion, and the pattern of fibronectin expression around the primitive streak. Harrisson et al. (1993) found that microinjection of integrin receptor binding antibodies into early stage chicken embryos disrupted the ability of ingressing epiblast cells to spread laterally, resulting in an abnormal thickening of the primitive streak. Davidson et al. (2002) reported a similar lack of mesendoderm extension in *Xenopus laevis* explants treated with blocking antibodies to fibronectin or α5β1 integrin receptors. It is likely that the CSAT perturbation assay had a similar affect here and yet the PGCs continued their migration to the germinal crescent with no apparent delay.

By blocking the β1 integrin receptors' ability to bind either fibronectin or laminin we have likely demonstrated the inherent flexibility and redundancy of the integrin receptor/ECM system (Rozario and DeSimone, 2010). It is possible that other integrin receptor subunits may have compensated for the loss of β1 activity. Our PGC scRNAseq data show that after β1, the highest number of reads at HH3 and HH6 are subunits β7 and β8 (**Figure 3B**). At HH6, just after our CSAT experimental timeline, the expression levels of integrin β2–β6 subunits are low and highly variable from cell to cell, yet are at detectable levels. This expression appears transient, as these transcripts fail to appear in the other time points examined (**Figure S5B**). As for the integrin α subunits that can pair with non-β1 subunits, α4, and α6 show the highest expression levels with αV being detected at much lower levels (**Figure S5A**). Taken together, this would leave the possible compensating integrin receptors that bind fibronectin and/or laminin as α4β7, αVβ3, αVβ6, αVβ8, and α6β4. mRNA for α4β7 receptor subunits are consistently present in migrating avian PGCs at all ages studied (**Figure 3**). However, the α4β7 subunit has previously been described primarily in leukocytes and endothelial cells (Brezinschek et al., 1996), so its presence

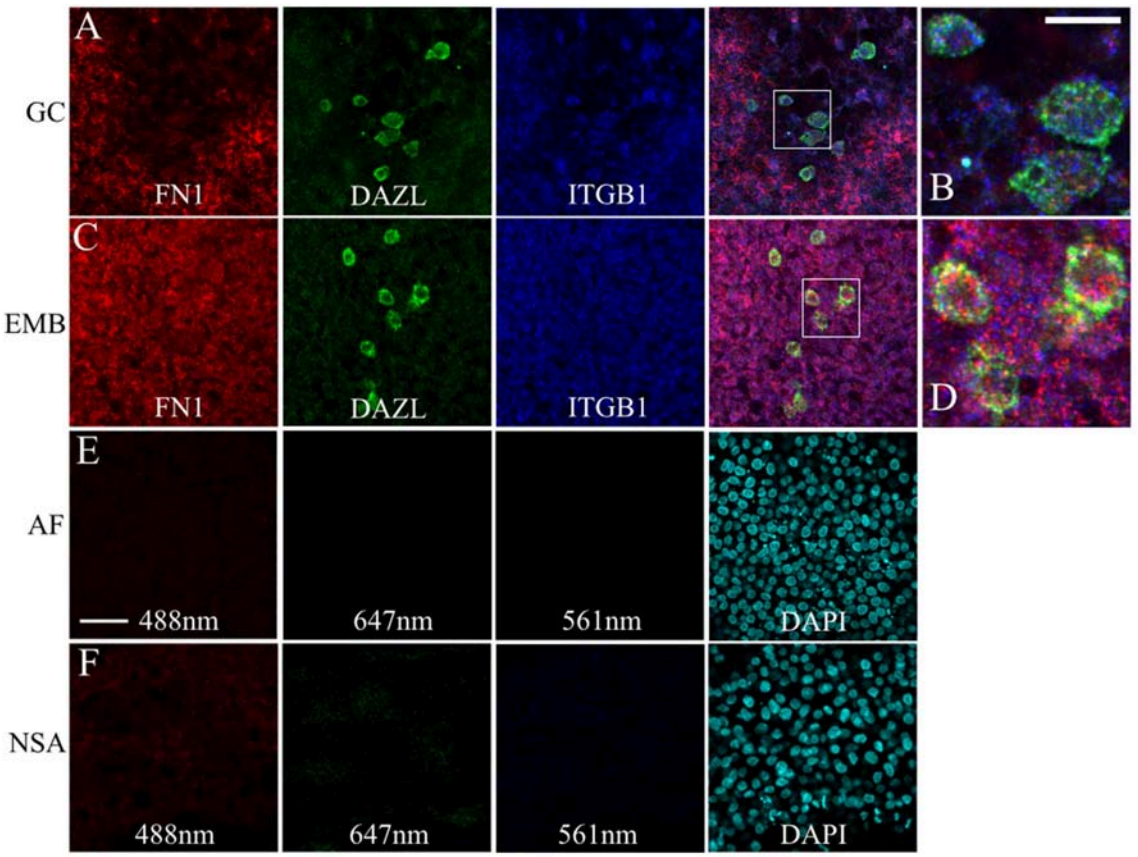

FIGURE 9 | PGCs and their surrounding cells in the germinal crescent co-express transcripts for fibronectin and integrin beta 1. mRNA for fibronectin, DAZL and integrin beta1 receptor subunit are localized to PGCs and their surrounding cells in both the extra-embryonic germinal crescent and in the embryo proper. Whole-mount multiplex hybridization chain reaction (HCR) for Fibronectin1 (FN1, red), Integrin beta1 subunit (ITGB1, blue), and DAZL (green) mRNA transcripts in HH4 quail embryos. All images are single optical sections (3.2 μm each) from 20x confocal Z stacks with 2x zoom. **(A,B)** GC = germinal crescent. **(C,D)** EMB = Embryo. Mesoderm/hypoblast in the mid-lateral region of the embryo containing PGCs that have not yet reached the germinal crescent. **(B)** Bounding box from A at higher magnification. **(D)** Bounding box from **(C)** at higher magnification. 20 μm scale bar in **(B)** also applies to **(D)**. **(E)** AF = Auto-fluorescence control and **(F)** NSA = Non-specific amplification controls using the indicated laser lines. Control imaging conditions were identical to those used in **(A–D)**. Twenty five micrometer scale bar in **(E)** also applies to **(A,C,F)**.

in our early time-point PGC transcriptome was un-expected and its potential role in PGC motility and migration is unknown. Likewise, the expression pattern and functionality of the other putative integrin receptors on migratory PGCs will have to be determined empirically.

Interestingly, integrin α5 subunit mRNA was not detected in the PGC transcriptome. This gene is expressed in early stage chicken embryos as shown in Muschler and Horwitz (1991) and Endo et al. (2013). Although chicken integrin α5 subunit was fully sequenced in 2013, the less complete nature of the *Coturnix* genome annotation has likely made integrin α5 subunit mRNA difficult to locate with automatic genomic algorithms (Endo et al., 2013). In this case, a directed BLAST search of the quail genome using the chicken sequence for ITGA5 failed to locate this gene. The *Coturnix* genome was recently sequenced and is currently being annotated based largely on the *Gallus* genome. It is likely that some genes found in chicken but not quail may simply be due to incomplete sequencing or lack of proper gene annotations in the nascent *Coturnix* genome. In other cases, the differences in genomes will reflect the true genetic diversity between these species. Discerning between these two possibilities will require additional investigation on a gene by gene basis.

Loss-of-function experiments can be difficult to interpret given the enormous complexity of the ECM/integrin receptor system, and other explanations for our CSAT perturbation results are equally plausible. It has been argued that PGCs initially utilize a passive mechanism of cell migration from EGK-X to HH2 and only when reaching the final anterior one-third of the embryo at HH3 do they employ active migration to reach the germinal crescent (Ginsburg and Eyal-Giladi, 1986; Kang et al., 2015). Perhaps by HH4-5, the stages examined in our perturbation assay, the PGCs were simply not actively utilizing integrin β1 receptors and fibronectin/laminin ECM fibrils as migratory and cell motility substrates. Injecting the CSAT at earlier stages may be a more effective strategy for blocking the ability of PGCs to populate the germinal crescent. Although it

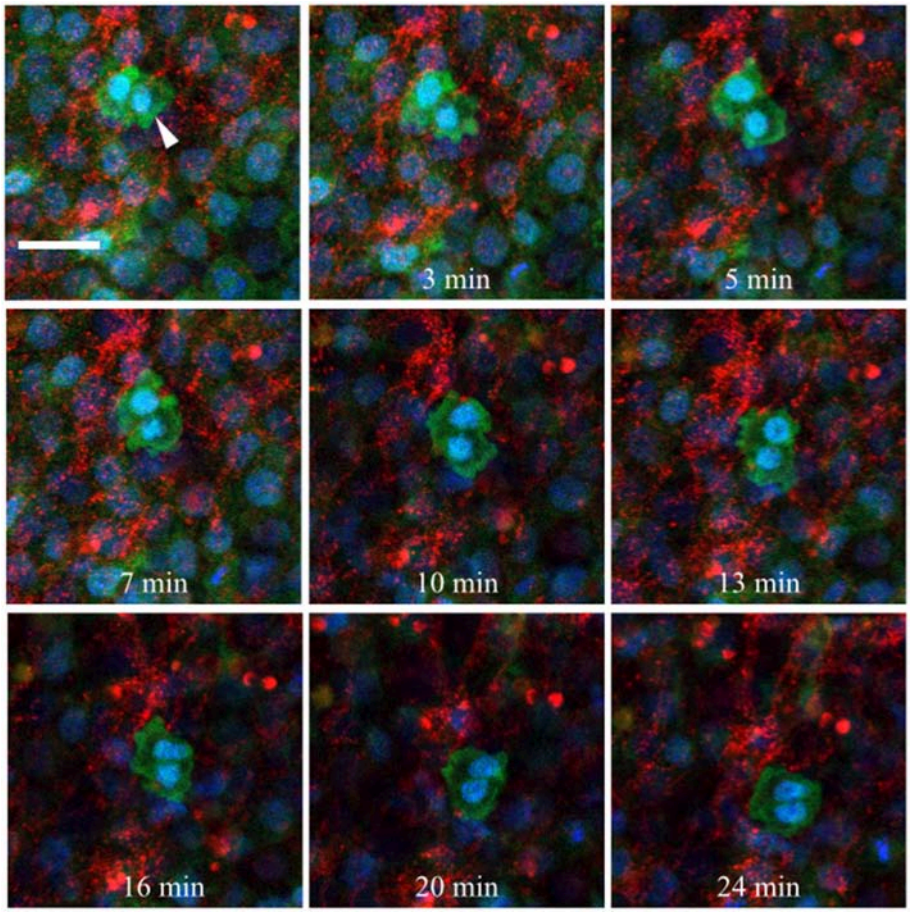

FIGURE 10 | Germinal crescent PGCs are actively motile in the presence of fibronectin. Captured frames from live confocal microscope imaging of an HH5 [Tg(hUbC:H2B-Cerulean-2A-Dendra2)] quail embryo that was injected with an antibody against fibronectin (abB3/D6). This antibody was directly conjugated to AlexaFluor 594, red). The 20x images, with 2x optical zoom, are maximum intensity projections of 3 optical slices (2.3 μm each) taken from the dorsal aspect at 1.5 min intervals. Cell nuclei = H2B-Cerulean (blue), cell bodies = Dendra2 (green). While the cells are ubiquitously labeled by the transgene, those with low proliferation rates, such as PGCs (white arrow), are brighter than the surrounding cells. Scale bar = 25 μm. View the full movie in **Video S1**.

seems likely, whether the PGCs contributed to the reduction in laminin and fibronectin fibril meshwork in the germinal crescent after CSAT perturbation was not definitively shown in our current experiments. Performing scRNAseq after perturbation would help elucidate whether the transcriptome of the PGCs was altered, thus contributing to the re-modeling of the ECM in the germinal crescent.

Based on the Kyoto Encyclopedia of Genes and Genomes (KEGG) Pathway ECM-Receptor Interaction 04512 (www.kegg.jp) it is clear that non-integrin cell surface receptors in the proteoglycan, glycoprotein and immunoglobulin superfamily classes may play a significant role in PGC motility and migration. Transcript levels for non-integrin receptor genes with at least moderate levels of expression in the majority of PGCs are shown in **Figure S5C**. Syndecan2, DAG1 (dystroglycan associated glycoprotein 1), HMMR (hyaluronan mediated motility receptor) and CD47 all show significant transcript levels in PGCs. In addition, matrix proteins besides fibronectin and laminin such as agrin (AGRN, **Figure 2A**) may be involved in PGC motility and migration (Wei and Liu, 2014). Mean transcript numbers for additional matrix genes that showed at least moderate levels of expression in most of the sampled PGCs are reported in **Figure S5D**. While scRNAseq gives us a valuable snapshot of which mRNA transcripts are present in a cell at any given time, no insight into RNA processing, translation, post-translational modification or the level of functional protein is gained. Determining precisely which of these receptors and matrix proteins play an active role in PGC motility and migration will require additional experimentation. For instance, it has been shown that the syndecan family of membrane-intercalated proteoglycan receptors cooperate closely with integrin receptors and the ECM through multiple molecular signaling pathways to control cell adhesion, angiogenesis, axon guidance, wound healing, and cell migration (Morgan et al., 2007). The presence of Syndecan2 and multiple integrin receptor heterodimer subunits in our scRNAseq data suggests that integrin-syndecan functional synergy may play an important role in PGC directional migration as well.

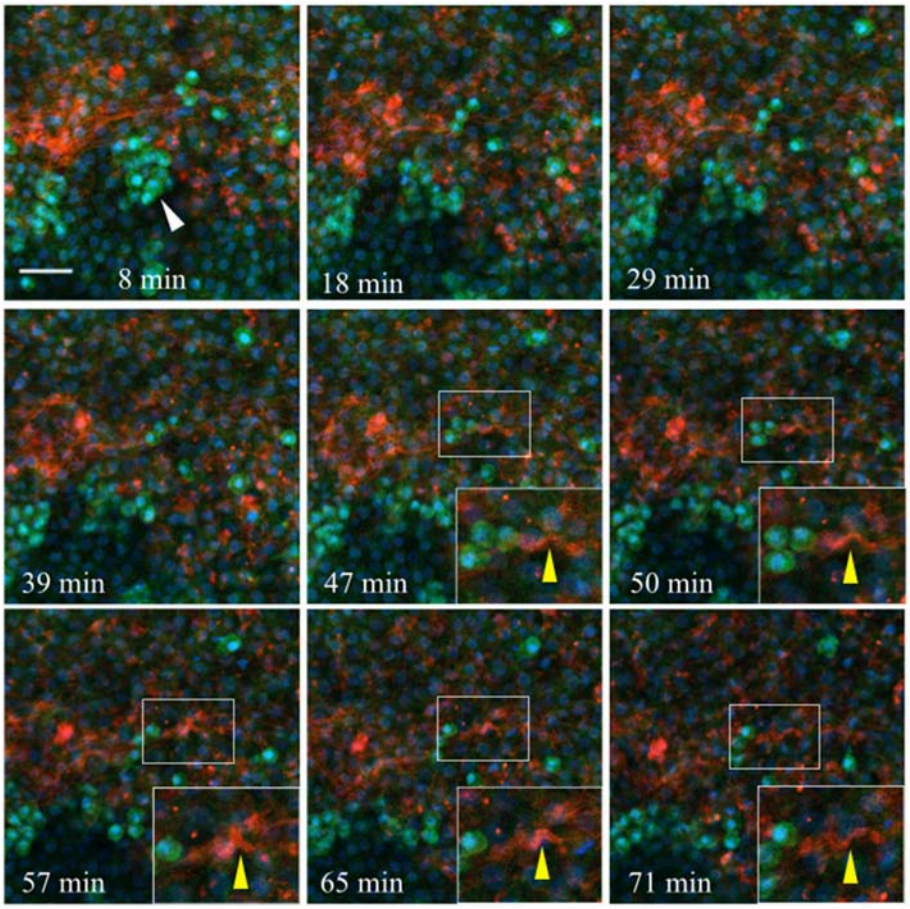

FIGURE 11 | Germinal crescent PGCs are actively motile in the presence of laminin. Captured frames from live confocal microscope imaging of an HH4 [Tg(hUbC:H2B-Cerulean-2A-Dendra2)] quail embryo that was injected with an antibody against laminin (ab31-2). This antibody was directly conjugated to AlexaFluor 555, red). The 20x images are maximum intensity projections of 3 optical slices (3.2 μm each) taken from the dorsal aspect at 1.5 min intervals. Cell nuclei = H2B-Cerulean (blue), cell bodies = Dendra2 (green). PGCs (clump, white arrow), are brighter than the surrounding cells. Bounding box indicates the region shown in the lower right corner of the last five frames. The laminin fibril bundle (yellow arrow) has a smooth wave shape at 47 min. At 50–57 min the fibril bundle is condensed, pushing it upwards into a sharp peak. Later, as the tissue expands from 65 to 71 min, the bundle resumes its prior form. Scale bar = 25 μm. View the full movie in **Video S2**.

The clear reduction of mature fibronectin and laminin fibrils in the germinal crescent of CSAT injected embryos highlights the role of integrin β1 subunit receptors in fibrillogenesis and matrix assembly (**Figure 12**). Loss-of-function experiments in cell lines have established the role that integrin β1 and β3 play in fibronectin matrix assembly (Darribère et al., 1990; Danen et al., 2002). We have shown that blocking integrin β1 subunit receptors reduces the fibronectin fibril meshwork pattern on a tissue-wide scale as well. How the β1 integrin receptors affect laminin assembly in the germinal crescent may be an interesting line of investigation given the presence of DAG1 and HSPG2 (heparan sulfate proteoglycan 2 or perlecan) in germinal crescent PGCs (**Figures S5CD**). Dystroglycan and perlecan are known to modify the assembly of laminin basement membrane in association with integrin β1 receptors (Henry et al., 2001; Soulintzi and Zagris, 2007; Nakaya et al., 2011). Whether these molecular interactions are contributing to assembly and modification of the laminin fibril meshwork in the germinal crescent during early development remains to be proven. Overall, the CSAT perturbation experiment has clearly highlighted the ability of cells and tissues to actively remodel their surrounding ECM using a diverse set of matrix molecules and receptors.

ECM as an Autocrine/Paracrine System

Cells secret soluble fibronectin dimers into their extracellular environment. Fibronectin is then assembled into fibrils or basement membrane after binding to integrin receptors. These two processes can occur in the same cells (autocrine) or in different cells (paracrine), and are regulated in a spatio-temporal manner during development. It has been suggested by de Almeida et al. (2016) that fibronectin matrix assembly during early chick embryogenesis may function as either an autocrine or paracrine system depending on the germ layer and stage of development examined. This idea is based on growth factor

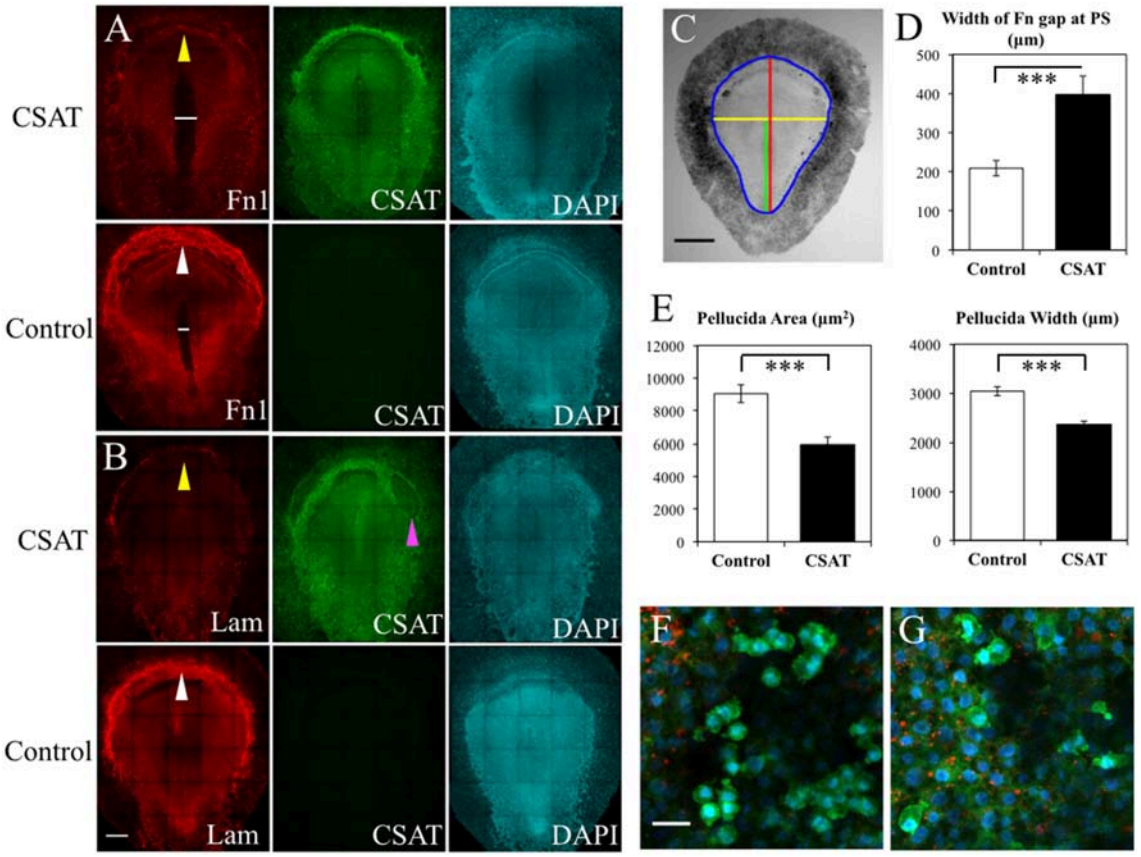

FIGURE 12 | CSAT antibody decreases the amount of fibronectin in the germinal crescent. Whole-mount immunofluorescence for fibronectin (abB3/D6), and laminin (ab31-2) in HH5 quail embryos following injection of CSAT antibodies or control serum. All images are maximum intensity projections of tiled 10x confocal Z stacks taken from the dorsal aspect. **(A)** From left to right: fibronectin, CSAT antibody and DAPI cell nucleus marker of a CSAT injected (first row) and a serum injected control embryo (second row). The line in A indicates the region around the primitive streak that lacks fibronectin compared to the same region in the control embryo below. **(B)** Same pattern as **(A)** but with laminin immunofluorescence. White arrows in control fibronectin and laminin labeled embryos indicate the germinal crescent region with widespread mature ECM fibrils compared to the same regions in CSAT injected embryos (yellow arrows). The magenta arrow in **(B)** CSAT indicates a region where the ectoderm/epiblast has separated from the underlying mesoderm, a pattern which was seen in several CSAT injected embryos. Scale bar = 500 μm. **(C)** Bright-field stereomicroscope image of a control embryo showing the histomorphometry parameters measured. Blue = area pellucida and area opaca perimeter. Red = length of the area pellucida along the central axis. Yellow = width of the area pellucida at Hensen's node. Green = length of the primitive streak (PS) from Hensen's node to the caudal boundary of the area opaca. Scale bar = 1 mm. **(D–E)** Control vs. CSAT embryo group means ± standard error of the mean for histomorphometry measurements. **(D)** width between the fibronectin rich areas lateral to the PS in the tissue layers ventral to the epiblast. **(E)** Pellucida area (left) and pellucida width (right). Two tailed, paired Student's *T*-Test. ***$P < 0.001$. For additional measures, see **Video S5**. **(F)** Captured frame from time-lapse imaging of a HH5 [Tg(hUbC:H2B-Cerulean-2A-Dendra2)] before injection with CSAT antibodies. **(G)** Same embryo as in D, imaged post-CSAT antibody injection. Fibronectin (red), Dendra2 (green), H2B-Cerulean (blue). See **Videos S7**, **S8** for the full time-lapse movies. PGC motility morphology appears unchanged after CSAT antibody injection. Scale bar = 25 μm.

signaling in which one tissue secretes the soluble factor and another tissue, the growth factor target tissue which may be located some distance away, expresses the receptor for it. In order to explore this question for migratory PGCs, we examined fibronectin protein and mRNA expression in PGCs taken from the first 2 days of development. scRNAseq shows that PGCs of all three stages (HH3, HH6, and HH12) are producing mRNA transcripts for both fibronectin and various integrin receptor subunits (**Figures 2**, **3**). *In situ* hybridization by HCR imaging confirms that PGCs have similar expression patterns of fibronectin and integrin receptor mRNA transcripts as their neighboring somatic cells (**Figures 8**, **9**). PGCs that are migrating within the mesodermal space of the embryo, and PGCs that have previously reached the extra-embryonic germinal crescent show similar expression patterns (**Figures 9A–D**). Likewise, both PGCs and their neighboring cells express integrin β1 receptor protein as shown in our IF data (**Figure 7**). Thus, consistent with an autocrine system of matrix regulation, PGCs not only produce soluble fibronectin but they also express the integrin receptors needed to initiate fibril assembly. It is likely that PGCs interact in a bi-directional way with their surrounding cells in order to secrete, assemble and re-model the fibronectin matrix dynamically during all phases of their migratory journey.

DATA AVAILABILITY

All datasets generated for this study are included in the manuscript and/or the **Supplementary Files**.

ETHICS STATEMENT

This study was carried out in accordance with the recommendations in the Guide for the Care and Use of Laboratory Animals of the National Institutes of Health. The protocol was approved by the University of Southern California (Protocol # 11944-CR001) and the Children's Hospital Los Angeles (Protocol # 351-16) Institutional Animal Care and Use Committees.

AUTHOR CONTRIBUTIONS

RL and JE planned the experiments. RL and SS prepared the quail matrisome. DH, MD, SS, SH, JW, and JS performed the experiments. RL, JK, JS, DH, and JE analyzed the scRNAseq dataset. DH and RL wrote the manuscript.

FUNDING

This work was supported in part by a 2017 Wright Foundation Pilot Award to RL.

ACKNOWLEDGMENTS

We thank Dr. Bertrand Benazeraf, Dr. Robert Mecham, Dr. Charles Little, and Dr. Scott Fraser for helpful insights into this work. This work was supported in part by a 2017 Wright Foundation Pilot Award to RL.

SUPPLEMENTARY MATERIAL

The Supplementary Material for this article can be found online at: https://www.frontiersin.org/articles/10.3389/fcell.2019.00035/full#supplementary-material

Figure S1 | Freshly harvested [Tg(PGK1:H2B-mCherry)] quail embryos at the 3 developmental stages used for single cell mRNA isolation. Bright-field (BF, left) and red epi-fluorescence (right) stereomicroscope images. Dashed bounding boxes represent the approximate area of the embryo excised for tissue dissociation followed by single cell picking, mRNA amplification and sequencing. PS, primitive streak; HF, head fold. Rostral (anterior) to the top in all images. Scale bars = 1 mm.

Figure S2 | Whole-mount immunofluorescence for fibronectin (B3/D6) and CVH in the germinal crescent and head region of an HH12 [Tg(PGK1:H2B-mCherry)] quail embryo. **(A)** Fibronectin. **(B)** CVH (PGC marker). **(C)** Fibronectin and CVH merged and **(D)** DAPI. Images are maximum intensity projections of 5x tiled confocal Z stacks taken from the dorsal aspect. Anterior (rostral) to top. **(A–D)** Scale bar = 500 μm. **(E–H)** taken at location of bounding box in **(B)**. **(E)** Fibronectin. **(F)** CVH. **(G)** H2B-mCherry. **(H)** Fibronectin, H2B-mCherry and CVH merged. Images are maximum intensity projections of 40x confocal Z stacks taken from the dorsal aspect. Anterior (rostral) to top. **(E–H)** Scale bar = 50 μm.

Figure S3 | Anti-sense oligonucleotide sequences used for hybridization chain reaction (HCR) probes. This *in-situ* hybridization technique uses a unique initiator sequence for each probe set to allow for simultaneous multiplex hybridizations.

Figure S4 | Measurements of quail embryos following injection of CSAT antibodies or control serum. **(A)** Embryos were staged based on the Hamilton-Hamburger chicken developmental series for both CSAT antibody injected ($n = 11$) and control embryos ($n = 7$). **(B)** Numerical values were assigned to the stages as follows: HH4– = 3.667, HH4 = 4, HH4+ = 4.333, HH5– = 4.667, HH5 = 5. Control vs. CSAT injected embryo group means ± standard error of the mean for histomorphometry measurements of area pellucida length/width ratio, primitive streak (PS) length and pellucida length/PS length ratio. Two tailed, paired Student's *T*-Test. $*P < 0.05$. NS = not significantly different.

Figure S5 | Transcriptome of less abundant ECM mRNA transcripts in PGCs across 3 developmental time points based on the KEGG Pathway ECM-Receptor Interaction 04512 for Japanese quail. **(A)** Integrin alpha subunit receptors. **(B)** Integrin beta subunits. **(C)** Non-integrin receptors. SDC, Syndecan (proteoglycan); DAG, Dystroglycan (glycoprotein); HMMR, Hyaluronan Mediated Motility Receptor and CD47 (immunoglobulin superfamily genes). **(D)** Matrix genes. HSPG, Heparan Sulfate Proteoglycan; FBLN, Fibrillin; FBN3, Fibulin. Bars represent the mean + s.e.m. The number of single cells in each group are shown in the legend.

Table S1 | Japanese quail matrisome.

Table S2 | Quail PGC transcriptome.

Video S1 | Live confocal microscope imaging of the germinal crescent region of an HH5 [Tg(hUbC:H2B-Cerulean-2A-Dendra2)] quail embryo that was injected with an antibody against fibronectin (abB3/D6). The antibody was directly conjugated to AlexaFluor 594, red). The 20x images, with 2x optical zoom, are maximum intensity projections of 3 optical slices (2.3 μm each) taken from the dorsal aspect at 1.5 min intervals. Total elapsed time is 26 min. Cell nuclei = H2B-Cerulean (blue), cell bodies = Dendra2 (green). While the cells are ubiquitously labeled by the transgene, those with low proliferation rates, such as PGCs, are brighter than the surrounding tissue. Anterior to top. Embryonic tissue to the lower right. Extra-embryonic tissue to the upper left. Scale bar = 25 μm.

Video S2 | Live confocal microscope imaging of the central germinal crescent region of an HH4 [Tg(hUbC:H2B-Cerulean-2A-Dendra2)] quail embryo that was injected with an antibody against laminin (ab31-2). This antibody was directly conjugated to AlexaFluor 555 (red). The 20x images are maximum intensity projections of 3 optical slices (3.2 μm each) taken from the dorsal aspect at 1.5 min intervals. Total elapsed time is 71 min. Cell nuclei = H2B-Cerulean (blue), cell bodies = Dendra2 (green). The PGCs are typically larger and brighter than the surrounding cells. Scale bar = 50 μm.

Video S3 | Live confocal microscope imaging of the lateral germinal crescent region of an HH4 [Tg(hUbC:H2B-Cerulean-2A-Dendra2)] quail embryo that was injected with an antibody against fibronectin (abB3/D6). The antibody was directly conjugated to AlexaFluor 594, red). The 20x images are maximum intensity projections of 3 optical slices (2.3 um each) taken from the dorsal aspect at 1.5 min intervals. Total elapsed time is 18 min. Cell nuclei = H2B-Cerulean (blue), cell bodies = Dendra2 (green). PGCs are larger and brighter than the surrounding tissue and appear in clusters and individually. Anterior to top, mediolateral midline to the right out of view. Embryonic tissue to the lower right. Extra-embryonic tissue to the left and upper left. Yellow arrow denotes a PGC that moves rapidly around a FN fibril. Scale bar = 50 um.

Video S4 | Live confocal microscope imaging of the lateral germinal crescent region of an HH4 [Tg(hUbC:H2B-Cerulean-2A-Dendra2)] quail embryo that was injected with an antibody against fibronectin (abB3/D6). The antibody was directly conjugated to AlexaFluor 594 (red). The 20x images are maximum intensity projections of 3 optical slices (2.3 μm each) taken from the dorsal aspect at 1.5 min intervals. Total elapsed time is 43 min. Cell nuclei = H2B-Cerulean (blue), cell bodies = Dendra2 (green). PGCs are larger and brighter than the surrounding tissue and appear in clusters and individually. Anterior to top, mediolateral midline to the right out of view. Embryonic tissue to the lower right. Extra-embryonic tissue to the left and upper left. Scale bar = 50 μm.

Video S5 | Cropped area from the lower left region of the movie in **Video S2** shown with increased magnification. Live confocal microscope imaging of the lateral germinal crescent region of an HH4 [Tg(hUbC:H2B-Cerulean-2A-Dendra2)] quail embryo that was injected with an antibody against fibronectin (abB3/D6). The antibody was directly conjugated to AlexaFluor 594 (red). The 20x images are maximum intensity projections of 3 optical slices (2.3 μm each) taken from the dorsal aspect at 1.5 min intervals. Total elapsed time is 43 min. Cell nuclei = H2B-Cerulean (blue), cell bodies = Dendra2 (green). PGCs are larger and brighter

than the surrounding tissue and appear in clusters and individually. Anterior to top, mediolateral midline to the right out of view. Embryonic tissue to the lower right. Extra-embryonic tissue to the left and upper left. Scale bar = 25 μm.

Video S6 | Live confocal microscope imaging of the central germinal crescent region of an HH4 [Tg(hUbC:H2B-Cerulean-2A-Dendra2)] quail embryo that was injected with an antibody against fibronectin (abB3/D6). The antibody was directly conjugated to AlexaFluor 594 (red). The 20x images are maximum intensity projections of 3 optical slices (2.3 μm each) taken from the dorsal aspect at 1.5 min intervals. Total elapsed time is 46 min. Cell nuclei = H2B-Cerulean (blue), cell bodies = Dendra2 (green). PGCs are larger and brighter than the surrounding tissue and appear in clusters and individually. Anterior to the top. Embryonic tissue toward the bottom. Extra-embryonic tissue at the top. Scale bar = 50 μm.

Video S7 | Pre-CSAT antibody injection movie for embryo 2. Time-lapse confocal microscope imaging of the central germinal crescent region of an HH5 [Tg(hUbC:H2B-Cerulean-2A-Dendra2)] quail embryo that was injected with an antibody against fibronectin (abB3/D6). The antibody was directly conjugated to AlexaFluor 594 (red). After incubation, the germinal crescent region was live imaged to establish the baseline movement of the PGCs. The 20x images, with 1.5x optical zoom are maximum intensity projections of 3 optical slices (2.3 μm each) taken from the dorsal aspect at 1.5 min intervals. Total elapsed time is 28 min. Cell nuclei = H2B-Cerulean (blue), cell bodies = Dendra2 (green). PGCs are larger and brighter than the surrounding tissue and appear individually and in clumps in this movie. Anterior to the top. Embryonic tissue toward the bottom. Extra-embryonic tissue at the top. Scale bar = 50 μm.

Video S8 | Post-CSAT antibody injection movie for embryo 2. See **Video S7** for pre-CSAT injection cell movements. CSAT antibodies against integrin β1 subunits fail to affect the cell motility and morphology of PGCs in HH5 embryos. Time-lapse confocal microscope imaging of the central germinal crescent region of an HH5 [Tg(hUbC:H2B-Cerulean-2A-Dendra2)] quail embryo that was injected with an antibody against fibronectin (abB3/D6). The antibody was directly conjugated to AlexaFluor 594 (red). After incubation, the germinal crescent region was injected again, this time with CSAT antibodies (174 ug/ml) and imaged live. The 20x images, with 2x optical zoom are maximum intensity projections of 3 optical slices (2.3 μm each) taken from the dorsal aspect at 1.5 min intervals. Total elapsed time is 24 min. Cell nuclei = H2B-Cerulean (blue), cell bodies = Dendra2 (green). PGCs are larger and brighter than the surrounding tissue and appear individually and in clumps in this movie. Anterior to the top. Embryonic tissue toward the bottom. Extra-embryonic tissue at the top. Scale bar = 25 μm.

REFERENCES

Ahmed, M., and Ffrench-Constant, C. (2016). Extracellular matrix regulation of stem cell behavior. *Curr. Stem. Cell. Rep*. 2, 197–206. doi: 10.1007/s40778-016-0056-2

Ainsworth, S. J., Stanley, R. L., and Evans, D. J. (2010). Developmental stages of the Japanese quail. *J. Anat*. 216, 3–15. doi: 10.1111/j.1469-7580.2009.01173.x

Anderson, R., Fässler, R., Georges-Labouesse, E., Hynes, R. O.,Bader, B. L.,Kreidberg, J. A., et al. (1999). Mouse primordial germ cells lacking beta1 integrins enter the germline but fail to migrate normally to the gonads. *Development* 126, 1655–1664.

Barton, L. J., LeBlanc, M. G., and Lehmann, R. (2016). Finding their way: themes in germ cell migration. *Curr. Opin. Cell. Biol*. 42, 128–137. doi: 10.1016/j.ceb.2016.07.007

Beauvais-Jouneau, A., and Thiery, J. P. (1997). Multiple roles for integrins during development. *Biol. Cell*. 89, 5–11.

Bénazéraf, B., Beaupeux, M., Tchernookov, M., Wallingford, A., Salisbury, T., Shirtz, A., et al. (2017). Multi-scale quantification of tissue behavior during amniote embryo axis elongation. *Development* 144, 4462–4472. doi: 10.1242/dev.150557

Bortier, H., De Bruyne, G., Espeel, M., and Vakaet, L. (1989). Immunohistochemistry of laminin in early chicken and quail blastoderms. *Anat. Embryol*. 180, 65–69.

Boucaut, J. C., Johnson, K. E.,Darribère, T., Shi, D. L.,Riou, J. F.,Bache, H. B., et al. (1990). Fibronectin-rich fibrillar extracellular matrix controls cell migration during amphibian gastrulation. *Int. J. Dev. Biol*. 34, 139–147.

Brezinschek, R. I., Brezinschek, H. P.,Lazarovits, A. I.,Lipsky, P. E., Oppenheimer-Marks N., (1996). Expression of the beta 7 integrin by human endothelial cells. *Am. J. Pathol*. 149, 1651–1660.

Bronner-Fraser, M. (1985). Alterations in neural crest migration by a monoclonal antibody that affects cell adhesion. *J. Cell. Biol*. 101, 610–617.

Cant,ú, A. V., Altshuler-Keylin, S., and Laird, D. J. (2016). Discrete somatic niches coordinate proliferation and migration of primordial germ cells via Wnt signaling. *J. Cell. Biol*. 214, 215–229. doi: 10.1083/jcb.201511061

Cant,ú, A. V., and Laird, D. J. (2017). A pilgrim's progress: seeking meaning in primordial germ cell migration. *Stem Cell. Res*. 24:181–187. doi: 10.1016/j.scr.2017.07.017

Chapman, S. C., Collignon, J., Schoenwolf, G. C., and Lumsden, A. (2001). Improved method for chick whole-embryo culture using a filter paper carrier. *Dev. Dyn*. 220, 284–289. doi: 10.1002/1097-0177(20010301)220:3<284::AID-DVDY1102>3.0.CO;2-5

Choi, H. M., Beck, V. A., and Pierce, N. A. (2014). Next-generation *in situ* hybridization chain reaction: higher gain, lower cost, greater durability. *ACS Nano* 8, 4284–4294. doi: 10.1021/nn405717p

Choi, H. M., Calvert, C. R.,Husain, N., Huss, D., Barsi, J. C.,Deverman, B. E., et al. (2016). Mapping a multiplexed zoo of mRNA expression. *Development* 143, 3632–3637. doi: 10.1242/dev.140137

Clawson, R. C., and Domm, L. V. (1969). Origin and early migration of primordial germ cells in the chick embryo: a study of the stages definitive primitive streak through eight somites. *Am. J. Anat*. 125, 87–111. doi: 10.1002/aja.1001250105

Critchley, D. R., England, M. A.,Wakely, J., and Hynes, R. O. (1979). Distribution of fibronectin in the ectoderm of gastrulating chick embryos. *Nature* 280, 498–500.

Danen, E. H., Sonneveld, P., Brakebusch, C., Fassler, R., and Sonnenberg, A. (2002). The fibronectin-binding integrins alpha5beta1 and alphavbeta3 differentially modulate RhoA-GTP loading, organization of cell matrix adhesions, and fibronectin fibrillogenesis. *J. Cell. Biol*. 159, 1071–1086. doi: 10.1083/jcb.200205014

Darribère, T., Guida, K., Larjava, H., Johnson, K. E.,Yamada, K. M.,Thiery, J. P., et al. (1990). *In vivo* analyses of integrin beta 1 subunit function in fibronectin matrix assembly. *J. Cell. Biol*. 110, 1813–1823.

Darribère, T., Skalski, M., Cousin, H. L.,Gaultier, A., Montmory, C., and Alfandari, D. (2000). Integrins: regulators of embryogenesis. *Biol. Cell*. 92, 5–25. doi: 10.1016/S0248-4900(00)88760-2

Davidson, L. A., Hoffstrom, B. G.,Keller, R., and DeSimone, D. W. (2002). Mesendoderm extension and mantle closure in Xenopus laevis gastrulation: combined roles for integrin alpha(5)beta(1), fibronectin, and tissue geometry. *Dev. Biol*. 242, 109–129. doi: 10.1006/dbio.2002.0537

Davidson, L. A., Marsden, M., Keller, R., and Desimone, D. W. (2006). Integrin alpha5beta1 and fibronectin regulate polarized cell protrusions required for Xenopus convergence and extension. *Curr. Biol*. 16, 833–844. doi: 10.1016/j.cub.2006.03.038

de Almeida, P. G., Pinheiro, G. G.,Nunes, A. M.,Gonçalves, A. B., and Thorsteinsdóttir, S. (2016). Fibronectin assembly during early embryo development: a versatile communication system between cells and tissues. *Dev. Dyn*. 245, 520–535. doi: 10.1002/dvdy.24391

De Melo Bernardo, A., Sprenkels, K., Rodrigues, G., Noce, T., and Chuva De Sousa Lopes S. M., (2012). Chicken primordial germ cells use the anterior vitelline veins to enter the embryonic circulation. *Biol. Open*. 1, 1146–1152. doi: 10.1242/bio.20122592

Dobin, A., David, C. A., Schlesinger, F., Drenkow, J., Zaleski, C., Jha, S., et al. (2013). STAR: ultrafast universal RNA-seq aligner. Bioinformatics 29, 15–21. doi: 10.1093/bioinformatics/bts635

Drake, C. J., Davis, L. A., Hungerford, J. E., and Little, C. D. (1991). Pertubation of Beta1 integrin-mediated adhesions results in altered somite cell shape and behavior. *Dev. Biol*. 149:327–338.

Drake, C. J., and Little, C. D. (1991). Integrins play an essential role in somite adhesion to the embryonic axis. *Dev. Biol*. 143, 418–421.

Duband, J. L., and Thiery, J. P. (1982). Appearance and distribution of fibronectin during chick embryo gastrulation and neurulation. *Dev. Biol.* 94, 337–350.

Dufour, S., Duband, J. L.,Kornblihtt, A. R., and Thiery, J. P. (1988). The role of fibronectins in embryonic cell migrations. *Trends Genet.* 4, 198–203.

Endo, Y., Ishiwata-Endo, H., and Yamada, K. M. (2013). Cloning and characterization of chicken α5 integrin: endogenous and experimental expression in early chicken embryos. *Matrix Biol.* 32, 381–386. doi: 10.1016/j.matbio.2013.04.002

Eyal-Giladi, H., Ginsburg, M., and Farbarov, A. (1981). Avian primordial germ cells are of epiblastic origin. *J. Embryol. Exp. Morphol.* 65:139–147.

Eyal-Giladi, H., and Kochav, S. (1976). From cleavage to primitive streak formation: a complementary normal table and a new look at the first stages of the development of the chick. *I. General morphology. Dev. Biol.* 49, 321–337.

Ffrench-Constant, C., Hollingsworth, A., Heasman, J., and Wylie, C. C. (1991). Response to fibronectin of mouse primordial germ cells before, during and after migration. *Development* 113, 1365–1373.

Filla, M. B., Czirók, A., Zamir, E. A.,Little, C. D.,Cheuvront, T. J., and Rongish, B. J. (2004). Dynamic imaging of cell, extracellular matrix, and tissue movements during avian vertebral axis patterning. *Birth Defects Res. C. Embryo Today* 72, 267–276. doi: 10.1002/bdrc.20020

Fujimoto, T., Ukeshima, A., and Kiyofuji, R. (1976). The origin, migration and morphology of the primordial germ cells in the chick embryo. *Anat. Rec.* 185, 139–145. doi: 10.1002/ar.1091850203

Fujimoto, T., Yoshinaga, K., and Kono, I. (1985). Distribution of fibronectin on the migratory pathway of primordial germ cells in mice. *Anat. Rec.* 211, 271–278. doi: 10.1002/ar.1092110307

García-Castro, M. I., Anderson, R., Heasman, J., and Wylie, C. (1997). Interactions between germ cells and extracellular matrix glycoproteins during migration and gonad assembly in the mouse embryo. *J. Cell. Biol.* 138, 471–480.

Ginsburg, M., and Eyal-Giladi, H. (1986). Temporal and spatial aspects of the gradual migration of primordial germ cells from the epiblast into the germinal crescent in the avian embryo. *J. Embryol. Exp. Morphol.* 95, 53–71.

Greve, J. M., and Gottlieb, D. I. (1982). Monoclonal antibodies which alter the morphology of cultured chick myogenic cells. *J. Cell. Biochem.* 18, 221–229. doi: 10.1002/jcb.1982.240180209.

Gu, Y., Runyan, C., Shoemaker, A., Surani, A., and Wylie, C. (2009). Steel factor controls primordial germ cell survival and motility from the time of their specification in the allantois, and provides a continuous niche throughout their migration. *Development* 136, 1295–1303. doi: 10.1242/dev.030619

Gurskaya, N. G., Verkhusha, V. V.,Shcheglov, A. S.,Staroverov, D. B.,Chepurnykh, T. V.,Fradkov, A. F., et al. (2006). Engineering of a monomeric green-to-red photoactivatable fluorescent protein induced by blue light. *Nat. Biotechnol.* 24, 461–465. doi: 10.1038/nbt1191

Hama, H., Kurokawa, H., Kawano, H., Ando, R., Shimogori, T., Noda, H., et al. (2011). Scale: a chemical approach for fluorescence imaging and reconstruction of transparent mouse brain. *Nat. Neurosci.* 14, 1481–1488. doi: 10.1038/nn.2928

Hamburger, V., and Hamilton, H. L. (1951). A series of normal stages in the development of the chick embryo. *J. Morphol.* 88, 49–92.

Harrisson, F., Van Nassauw, L., Van Hoof, J., and Foidart, J. M. (1993). Microinjection of antifibronectin antibodies in the chicken blastoderm: inhibition of mesoblast cell migration but not of cell ingression at the primitive streak. *Anat. Rec.* 236, 685–696. doi: 10.1002/ar.1092360413

Heasman, J., Hynes, R. O.,Swan, A. P.,Thomas, V., and Wylie, C. C. (1981). Primordial germ cells of Xenopus embryos: the role of fibronectin in their adhesion during migration. *Cell* 27(3 Pt 2):437–447.

Henry, M. D., Satz, J. S.,Brakebusch, C., Costell, M., Gustafsson, E., Fässler, R., et al. (2001). Distinct roles for dystroglycan, beta1 integrin and perlecan in cell surface laminin organization. *J. Cell. Sci.* 114(Pt. 6):1137–1144.

Huss, D., Benazeraf, B., Wallingford, A., Filla, M., Yang, J., Fraser, S. E., et al. (2015a). A transgenic quail model that enables dynamic imaging of amniote embryogenesis. *Development* 142, 2850–2859. doi: 10.1242/dev.121392

Huss, D., Choi, H. M.,Readhead, C., Fraser, S. E.,Pierce, N. A., and Lansford, R. (2015b). Combinatorial analysis of mRNA expression patterns in mouse embryos using hybridization chain reaction. *Cold Spring Harb. Protoc.* 2015, 259–268. doi: 10.1101/pdb.prot083832

Huss, D., and Lansford, R. (2017). Fluorescent quail: a transgenic model system for the dynamic study of avian development. *Methods Mol. Biol.* 1650, 125–147. doi: 10.1007/978-1-4939-7216-6_8

Hynes, R. O. (2009). The extracellular matrix: not just pretty fibrils. *Science* 326, 1216–1219. doi: 10.1126/science.1176009

Hynes, R. O., and Naba, A. (2012). Overview of the matrisome–an inventory of extracellular matrix constituents and functions. *Cold Spring Harb. Perspect. Biol.* 4:a004903. doi: 10.1101/cshperspect.a004903

Jean, C., Oliveira, N. M.,Intarapat, S., Fuet, A., Mazoyer, C., De Almeida, I., et al. (2015). Transcriptome analysis of chicken ES, blastodermal and germ cells reveals that chick ES cells are equivalent to mouse ES cells rather than EpiSC. *Stem Cell Res.* 14, 54–67. doi: 10.1016/j.scr.2014.11.005

Kang, K. S., Lee, H. C.,Kim, H. J.,Lee, H. G.,Kim, Y. M.,Lee, H. J., et al. (2015). Spatial and temporal action of chicken primordial germ cells during initial migration. *Reproduction* 149, 179–187. doi: 10.1530/REP-14-0433

Kim, J., and Eberwine, J. (2010). RNA: state memory and mediator of cellular phenotype. *Trends Cell. Biol.* 20, 311–318. doi: 10.1016/j.tcb.2010.03.003

Langmead, B., and Salzberg, S. L. (2012). Fast gapped-read alignment with Bowtie 2. *Nat. Methods* 9, 357–359. doi: 10.1038/nmeth.1923

Latimer, A., and Jessen, J. R. (2010). Extracellular matrix assembly and organization during zebrafish gastrulation. *Matrix Biol.* 29, 89–96. doi: 10.1016/j.matbio.2009.10.002

Leiss, M., Beckmann, K., Girós, A., Costell, M., and Fässler, R. (2008). The role of integrin binding sites in fibronectin matrix assembly *in vivo*. *Curr. Opin. Cell. Biol.* 20, 502–507. doi: 10.1016/j.ceb.2008.06.001

Little, C. D., and Drake, C. J. (2000). "Whole-mount immunolabeling of embryos by microinjection. Increased detection levels of extracellular and cell surface epitopes," in *Developmental Biology Protocols, Vol. 1*., eds R. S. Tuan, and C. W. Lo (Totowa, NJ: Humana Press). doi: 10.1385/1-59259-685-1:183

Loganathan, R., Rongish, B. J.,Smith, C. M.,Filla, M. B.,Czirok, A., Bénazéraf, B., et al. (2016). Extracellular matrix motion and early morphogenesis. *Development* 143, 2056–2065. doi: 10.1242/dev.127886

Macdonald, J., Glover, J. D.,Taylor, L., Sang, H. M., and McGrew, M. J. (2010). Characterisation and germline transmission of cultured avian primordial germ cells. *PLoS ONE* 5:e15518. doi: 10.1371/journal.pone.0015518

Molyneaux, K. A., Stallock, J., Schaible, K., and Wylie, C. (2001). Time-lapse analysis of living mouse germ cell migration. *Dev. Biol.* 240, 488–498. doi: 10.1006/dbio.2001.0436

Morgan, M.R., Humphries, M. J., and Bass, M. D. (2007). Synergistic control of cell adhesion by integrins and syndecans. *Nat. Rev. Mol. Cell. Biol.* 8, 957–969. doi: 10.1038/nrm2289

Morris, J., Singh, J. M., and Eberwine, J. H. (2011). Transcriptome analysis of single cells. *J. Vis. Exp.* 50:2634. doi: 10.3791/2634

Muschler, J. L., and Horwitz, A. F. (1991). Down-regulation of the chicken alpha 5 beta 1 integrin fibronectin receptor during development. *Development* 113, 327–337.

Naba, A., Clauser, K. R.,Ding, H., Whittaker, C. A.,Carr, S. A., and Hynes, R. O. (2016). The extracellular matrix: tools and insights for the omics era. *Matrix Biol.* 49, 10–24. doi: 10.1016/j.matbio.2015.06.003

Naba, A., Hoersch, S., and Hynes, R. O. (2012). Towards definition of an ECM parts list: an advance on GO categories. *Matrix Biol.* 31, 371–372. doi: 10.1016/j.matbio.2012.11.008

Nakamura, Y., Yamamoto, Y., Usui, F., Mushika, T., Ono, T., Setioko, A. R., et al. (2007). Migration and proliferation of primordial germ cells in the early chicken embryo. *Poult. Sci.* 86, 2182–2193. doi: 10.1093/ps/86.10.2182

Nakaya, Y., Sukowati, E. W.,Alev, C., Nakazawa, F., and Sheng, G. (2011). Involvement of dystroglycan in epithelial-mesenchymal transition during chick gastrulation. *Cells Tissues Organs.* 193, 64–73. doi: 10.1159/000320165

Raddatz, E., Monnet-Tschudi, F., Verdan, C., and Kucera, P. (1991). Fibronectin distribution in the chick embryo during formation of the blastula. *Anat. Embryol.* 183, 57–65.

Richardson, B. E., and Lehmann, R. (2010). Mechanisms guiding primordial germ cell migration: strategies from different organisms. *Nat. Rev. Mol. Cell. Biol.* 11, 37–49. doi: 10.1038/nrm2815

Rozario, T., and DeSimone, D. W. (2010). The extracellular matrix in development and morphogenesis: a dynamic view. *Dev. Biol.* 341, 126–140. doi: 10.1016/j.ydbio.2009.10.026

Saadaoui, M., Corson, F., Rocancourt, D., Roussel, J., and Gros, J. (2018). A tensile ring drives tissue flows to shape the gastrulating amniote embryo. *bioRxiv [preprint]*. bioRxiv:412767. doi: 10.1101/412767

Sanders, E. J. (1982). Ultrastructural immunocytochemical localization of fibronectin in the early chick embryo. *J. Embryol. Exp. Morphol*. 71:155–170.

Sanders, E. J. (1984). Labelling of basement membrane constituents in the living chick embryo during gastrulation. *J. Embryol. Exp. Morphol*. 79:113–123.

Sato, Y., and Lansford, R. (2013). Transgenesis and imaging in birds, and available transgenic reporter lines. *Dev. Growth. Differ*. 55, 406–421. doi: 10.1111/dgd.12058

Sato, Y., Nagatoshi, K., Hamano, A., Imamura, Y., Huss, D., Uchida, S., et al. (2017). Basal filopodia and vascular mechanical stress organize fibronectin into pillars bridging the mesoderm-endoderm gap. *Development* 144, 281–291. doi: 10.1242/dev.141259

Sato, Y., Poynter, G., Huss, D., Filla, M. B.,Czirok, A., Rongish, B. J., et al. (2010). Dynamic analysis of vascular morphogenesis using transgenic quail embryos. *PLoS ONE* 5:e12674. doi: 10.1371/journal.pone.0012674

Soto-Suazo, M., Abrahamsohn, P. A.,Pereda, J., and Zorn, T. M. (1999). Distribution and space-time relationship of proteoglycans in the extracellular matrix of the migratory pathway of primordial germ cells in mouse embryos. *Tissue Cell*. 31, 291–300. doi: 10.1054/tice.1999.0041

Soto-Suazo, M., San Martin, S., Ferro, E. S., and Zorn, T. M. (2002). Differential expression of glycosaminoglycans and proteoglycans in the migratory pathway of the primordial germ cells of the mouse. *Histochem. Cell. Biol*. 118, 69–78. doi: 10.1007/s00418-002-0414-2

Soulintzi, N., and Zagris, N. (2007). Spatial and temporal expression of perlecan in the early chick embryo. *Cells Tissues Organs*. 186, 243–256. doi: 10.1159/000107948.

Streit, A., and Stern, C. D. (2008). Operations on primitive streak stage avian embryos. *Methods Cell. Biol*. 87, 3–17. doi: 10.1016/S0091-679X(08)0 0201-X

Sun, J., Ting, M. C.,Ishii, M., and Maxson, R. (2016). Msx1 and Msx2 function together in the regulation of primordial germ cell migration in the mouse. *Dev. Biol*. 417, 11–24. doi: 10.1016/j.ydbio.2016.07.013

Swift, Charles H. (1914). Origin and early history of the primordial germ-cells in the chick. *Am. J. Anat*. 18, 483–516. doi: 10.1002/aja.1000150404

Tarbashevich, K., and Raz, E. (2010). The nuts and bolts of germ-cell migration. *Curr. Opin. Cell. Biol*. 22, 715–721. doi: 10.1016/j.ceb.2010.09.005

Urven, L. E., Abbott, U. K., and Erickson, C. A. (1989). Distribution of extracellular matrix in the migratory pathway of avian primordial germ cells. *Anat. Rec*. 224, 14–21. doi: 10.1002/ar.1092240104

Watt, F. M., and Huck, W. T. (2013). Role of the extracellular matrix in regulating stem cell fate. *Nat. Rev .Mol. Cell. Biol*. 14, 467–473. doi: 10.1038/ nrm3620

Wei, K. H., and Liu, I. H. (2014). Heparan sulfate glycosaminoglycans modulate migration and survival in zebrafish primordial germ cells. *Theriogenology* 81, 1275–85.e1-2. doi: 10.1016/j.theriogenology.2014.02.009

Zagris, N., Chung, A. E., and Stavridis, V. (2000). Differential expression of laminin genes in early chick embryo. *Int. J. Dev. Biol*. 44, 815–818.

Zamir, E. A., Czirók, A., Cui, C., Little, C. D., and Rongish, B. J. (2006). Mesodermal cell displacements during avian gastrulation are due to both individual cell-autonomous and convective tissue movements. *Proc. Natl. Acad. Sci. U. S. A*. 103, 19806–19811. doi: 10.1073/pnas.0606100103

Zhu, Q., Fisher, S. A.,Dueck, H., Middleton, S., Khaladkar, M., and Kim, J. (2018). PIVOT: platform for interactive analysis and visualization of transcriptomics data. *BMC Bioinform*. 19:6. doi: 10.1186/s12859-017-1994-0

Conflict of Interest Statement: The authors declare that the research was conducted in the absence of any commercial or financial relationships that could be construed as a potential conflict of interest.

frontiers in Cell and Developmental Biology

ORIGINAL RESEARCH
published: 18 September 2019
doi: 10.3389/fcell.2019.00178

Collagen Dynamics During the Process of Osteocyte Embedding and Mineralization

Lora A. Shiflett[1], LeAnn M. Tiede-Lewis[1], Yixia Xie[1], Yongbo Lu[2], Eleanor C. Ray[1] and Sarah L. Dallas[1]†*

[1] Department of Oral and Craniofacial Sciences, School of Dentistry, University of Missouri-Kansas City, Kansas City, MO, United States, [2] Department of Biomedical Sciences, Texas A&M University College of Dentistry, Dallas, TX, United States

Bone formation, remodeling and repair are dynamic processes, involving cell migration, ECM assembly, osteocyte embedding, and bone resorption. Using live-cell imaging, we previously showed that osteoblast assembly of the ECM proteins fibronectin and collagen is highly dynamic and is integrated with cell motility. Additionally, osteoblast-to-osteocyte transition involved arrest of cell motility, followed by dendrite extension and retraction that may regulate positioning of embedding osteocytes. To further understand how osteocytes differentiate and embed in collagen, mice were generated that co-expressed GFP*topaz*-tagged collagen with a Dmp1-Cre-inducible tdTomato reporter targeted to preosteocytes/osteocytes. Dual live-cell imaging of collagen and osteocyte dynamics in mineralizing primary calvarial cell cultures showed that Dmp1-Cre/tdTomato turned on in early bone nodule forming regions, demarcated by foci of concentrated GFP-collagen bundles that appeared structurally distinct from the surrounding collagen. Dmp1-Cre/tdTomato-positive cells were post-mitotic and were continuously induced throughout the 2 week timecourse, whereas the majority of collagen was assembled by day 7. GFP-collagen fibrils showed global (tissue-level) motions, suggesting coordinated cell layer movement, and local fibril motions mediated by cell-generated forces. Condensation of collagen fibril networks occurred within bone nodules prior to mineralization. Intravital imaging confirmed a similar structural appearance of GFP-collagen in calvarial bone, with analogous global motions of mineralizing areas adjacent to sutures. In early (unmineralized) calvarial cell cultures, Dmp1-Cre/tdTomato-positive cells were motile (mean velocity 4.8 μm/h), moving freely in and around the forming bone nodule, with a small number of these cells embedded in collagen, constraining their motion. In mineralizing cultures, the average velocity of Dmp1-Cre/tdTomato-positive cells was significantly reduced (0.7 μm/h), with many immobilized in the mineralizing nodule. Three apparent mechanisms for embedding of Dmp1-Cre/tdTomato-positive cells were observed. In some cases, a previously motile Dmp1-Cre/tdTomato-positive cell became immobilized in collagen fibril networks that were newly assembled around the cell, thereby entrapping it. In other cases, a motile Dmp1-Cre/tdTomato-positive cell moved into an already formed "collagen lacuna,"

OPEN ACCESS

Edited by:
Rajprasad Loganathan, Johns Hopkins University, United States

Reviewed by:
Jean Aaron, University of Leeds, United Kingdom
Elena P. Moiseeva, Retired, Leicester, United Kingdom

***Correspondence:**
Sarah L. Dallas
dallass@umkc.edu

†ORCID:
Sarah L. Dallas
orcid.org/0000-0002-5197-891X

Specialty section:
This article was submitted to Cell Adhesion and Migration, a section of the journal Frontiers in Cell and Developmental Biology

Received: *01 July 2019*
Accepted: *15 August 2019*
Published: *18 September 2019*

Citation:
Shiflett LA, Tiede-Lewis LM, Xie Y, Lu Y, Ray EC and Dallas SL (2019) Collagen Dynamics During the Process of Osteocyte Embedding and Mineralization. Front. Cell Dev. Biol. 7:178. doi: 10.3389/fcell.2019.00178

arrested its motility and became embedded. Alternatively, some cells switched on tdTomato expression *in situ* within a lacuna. These data provide new insight into the dynamic process of bone collagen assembly and suggest multiple mechanisms for osteocyte entrapment in collagen matrix.

Keywords: osteocytes, collagen, extracellular matrix, live cell imaging, motility, bone mineralization, embedding

INTRODUCTION

Our understanding of mineralized tissue biology has come predominantly from static imaging approaches, such as histology/histomorphometry, light and electron microscopy and micro computed tomography, combined with chemical, biochemical, protein and molecular biological analyses, together with manipulation of mouse genetics (Halloran et al., 2002; Faibish et al., 2005; Mckee et al., 2005; Murshed et al., 2005; Huitema and Vaandrager, 2007; Pacureanu et al., 2012). These approaches have led to an in depth understanding of many of the molecular pathways controlling development and postnatal growth of the skeleton as well as skeletal aging and various bone pathologies. However, the biological processes that occur in bone tissues, such as bone formation, remodeling and repair are highly coordinated dynamic processes, involving cell migration and embedding, extracellular matrix (ECM) assembly, and bone resorption. Static imaging approaches do not convey the dynamic nature of these events and may therefore fall short in providing a comprehensive understanding of the underlying biology. In contrast, live cell imaging allows us to visualize active processes in living cells, organs, whole embryos and whole animals from a temporospatial perspective and enables cellular, subcellular and tissue behavior to be quantified as a function of time. Live cell imaging is increasingly being used in various model systems to obtain quantitative insight into intracellular and extracellular processes, such as organelle transport, mitochondrial function, autophagy and energy metabolism, assembly and reorganization of the ECM as well as to study embryonic development/morphogenesis and stem cell function (Eils and Athale, 2003; Friedl, 2004; Kulesa, 2004; Dallas et al., 2006; Sivakumar et al., 2006; Zamir et al., 2008; Lo Celso et al., 2009; Tiede et al., 2009; Xie et al., 2009; Appelhans and Busch, 2017; Bell, 2017; Bigley et al., 2017; Ratnayake and Currie, 2017; Lu et al., 2018).

Important insights into the dynamic process of extracellular matrix assembly and organization have come from live cell imaging of ECM proteins, such as fibronectin, collagen, elastin, fibrillins and latent transforming growth factor beta binding proteins (LTBPs) (Czirok et al., 2004; Davidson et al., 2004; Filla et al., 2004; Dallas et al., 2006; Kozel et al., 2006; Sivakumar et al., 2006; Aleksandrova et al., 2012; Lu et al., 2018). A common theme emerging from these studies is that assembly of many of these ECM proteins is highly dynamic and appears to be integrated with cell motility. These cell motions exert forces on the fibrils, which stretch and distort them as they are being assembled. Our laboratory has recently developed GFP*topaz*- and mCherry-tagged type I collagen fusion protein constructs and stably transfected them into MLO-A5 osteoblast-like cells and fibronectin-null mouse embryonic fibroblasts (Lu et al., 2018). Live cell imaging using these cell models revealed the dynamic nature of type I collagen assembly and showed its dependence on fibronectin assembly (Lu et al., 2018). A particularly interesting observation from these studies was that osteoblasts were able to physically reshape the collagen fibrillar network by pushing collagen outwards to form hole-like structures. We hypothesized that this reshaping of the collagen ECM to form holes in the network may provide a mechanism for formation of a nascent osteocyte lacuna in bone.

Osteocytes make up over 90% of the cells in bone, but because they are embedded within a mineralized matrix, they have been challenging to study. These terminally differentiated cells are derived from osteoblasts that become embedded within the ECM they produce, termed osteoid, which then becomes mineralized (reviewed in Dallas et al., 2013; Jilka and O'brien, 2016; Prideaux et al., 2016). The transition from osteoblast to osteocyte involves a dramatic change in morphology from a polygonal cell to a cell with a reduced cytoplasmic volume and a highly dendritic morphology, reminiscent of neuronal cells. Differentiation from osteoblast to osteocyte is associated with downregulation of osteoblast expressed genes, such as type I collagen (*COL1A1* and *COL1A2*), alkaline phosphatase (*TNSALP*), and RUNX family transcription factor 2 (*RUNX2*), concomitant with upregulation of osteocyte marker genes including E11/gp38/podoplanin (*PDPN*), dentin matrix protein 1 (*DMP1*), matrix extracellular phosphoglycoprotein (*MEPE*), phosphate-regulating gene with homologies to endopeptidases on the X chromosome (*PHEX*), and fibroblast growth factor 23 (*FGF23*) (Schulze et al., 1999; Toyosawa et al., 2001; Igarashi et al., 2002; Franz-Odendaal et al., 2006; Ubaidus et al., 2009; reviewed in Dallas et al., 2013). Differentiation to the mature osteocyte phenotype is associated with expression of the *SOST* gene, which encodes the protein, sclerostin (Winkler et al., 2003).

Various mechanisms have been proposed to explain how osteoblasts embed to become osteocytes. One theory proposes that embedding is a passive process in which osteoblasts slow down their production of extracellular matrix and then become "buried alive" in the osteoid produced by neighboring osteoblasts (Palumbo et al., 1990; Nefussi et al., 1991; Franz-Odendaal et al., 2006). However, other researchers have proposed that osteocyte embedding is an active, invasive process, involving proteolytic degradation of the extracellular matrix to form the osteocyte lacuna and canaliculi (Zhao et al., 2000; Holmbeck et al., 2005). To further understand the dynamic mechanisms by which osteocytes differentiate and embed in collagen, this study set out to perform dual imaging of osteocyte differentiation

using a lineage reporter, together with imaging collagen using a fluorescently tagged collagen fusion protein. To accomplish this, transgenic mice were generated that co-expressed a GFP*topaz*-tagged type I collagen fusion protein, together with a Dmp1-Cre-inducible tdTomato reporter targeted to preosteocytes/osteocytes. Dual live cell imaging of collagen fibril assembly dynamics and osteocyte differentiation and embedding was performed in mineralizing primary bone cells isolated from these mice and intravital imaging was also performed in these mice. The findings reveal the dynamic nature of collagen assembly by mineralizing bone cells and suggest multiple mechanisms for osteocyte entrapment in collagen matrix.

MATERIALS AND METHODS

Reagents

Unless stated otherwise, standard reagents and chemicals were from Sigma Aldrich (St. Louis, MO, United States), or Thermo Fisher Scientific (Waltham, MA, United States). Rat tail collagen was from Becton-Dickinson (Franklin Lakes, NJ, United States). L-ascorbic acid phosphate magnesium salt n-hydrate was from Wako Chemicals USA, Inc., Richmond, VA, United States.

Animals

The Ai9 mouse, hereafter referred to as tdTomato, was from the Jackson Laboratory, Bar Harbor, ME, United States [B6.Cg-Gt(ROSA)26Sor$^{TM9(CAG-tdTomato)Hze}$, JAX Stock #007909] and is a Cre reporter mouse with a STOP cassette flanked by LoxP sites (Madisen et al., 2010). The STOP cassette blocks transcription of the tdTomato red fluorescent protein variant and tdTomato fluorescence is induced following Cre-mediated recombination. The 10 kb Dmp1-Cre mouse was kindly provided by Dr. Jian Q. Feng (Texas A&M College of Dentistry) and has been described previously (Lu et al., 2007). GFP-collagen transgenic mice were generated in our laboratory by inserting a GFP*topaz* tag into the mouse proα2(I) collagen N-terminus under control of the 3.6 kb type I collagen promoter (Kamel-Elsayed et al., 2015 and manuscript in preparation). These transgenic mice were generated on a C57BL/6N background by pronuclear injection at the Transgenic Technology Center at the University of Texas Southwestern Medical Center, Dallas, TX, United States. Mice were bred to generate GFP-col$^{+/-}$/Dmp1-Cre$^{+/-}$/tdTomato$^{+/-}$ mice, which have green fluorescent collagen and a red fluorescent lineage reporter for preosteocytes/osteocytes. The mice were genotyped by PCR of tail DNA samples. For tdTomato mice, PCR was performed according to the Jackson Laboratory protocol. Genotyping of Dmp1-Cre transgenic mice was performed using forward primer, 5′-CCAAGCCCTGAAAATCACAGA-3′ and reverse primer, 5′-CCTGGCGATCCCTGAACATG-3′. Genotyping of GFP-collagen transgenic mice was performed using forward primer 5′-TCATCTGCACCACCGGCAAGC-3′ and reverse primer 5′-AGCAGGACCATGTGATCGCGC-3′. Expression of the fluorescent transgenes was confirmed by examining tail clip biopsies under a Nikon TE300 widefield epifluorescence microscope. Animal experiments and euthanasia were performed under an approved IACUC protocol at the University of Missouri Kansas City (UMKC), and conformed to relevant federal guidelines. The UMKC animal facility is AAALAC approved and animal care and husbandry meets requirements in the Guide for the Care and use of Laboratory Animals (8th Ed.), National Research Council. Animals were group housed on a 12 h light/dark cycle with *ad libitum* food and water at 22°C constant temperature and 45–55% humidity.

Fluorescent Bone Histology

Femurs from 8 week old GFP-collagen transgenic mice or Dmp1-Cre$^{+/-}$/tdTomato$^{+/-}$ mice were prepared for cryosectioning as described previously (Kamel-Elsayed et al., 2015). Briefly, after fixation in 4% paraformaldehyde in PBS, the femurs were decalcified in 10% EDTA, pH 7.4 for 1–2 weeks, then equilibrated in 15% then 30% sucrose in PBS before embedding and freezing in Tissue-Tek O.C.T compound (Sakura Finetek USA Inc., Torrence, CA, United States). 6μm longitudinal sections were cut on a Leica CM3050S cryomicrotome (Leica Microsystems, Wetzlar, Germany). Slides were either viewed without staining or the nuclei were stained using a 5 min incubation in 4 μg/ml 4′-6-Diamidino-2-phenylindole (DAPI) (Thermo Fisher Scientific, Waltham, MA, United States) in PBS. Sections were coverslip mounted in 1:1 glycerol:PBS with 1 mM $MgCl_2$. Sections were imaged using a 20x 0.75 NA or 10x 0.45 NA objective on a Nikon E800 widefield epifluorescence microscope (Nikon Instruments Inc., Mellville, NY, United States) with filter sets optimized for each fluorophore. Digital photographs were taken using an Optronics CCD color camera (Optronics, Goleta, CA, United States) interfaced with the AnalySIS software (Soft Imaging System GmbH, Muenster, Germany).

Cell Culture

Unless stated otherwise tissue culture reagents were from Gibco (Life Technologies Inc., Grand Island, NY, United States), GE Healthcare Life Sciences (Marlborough, MA, United States), or Mediatech Inc. (Herndon, VA, United States). Heat inactivated fetal bovine serum (FBS) was from Hyclone Laboratories (GE Healthcare Life Sciences) or Atlanta Biologicals (Flowery Branch, GA, United States). Primary calvarial cells were routinely maintained in growth medium consisting of α-Minimum Essential Medium (α-MEM) containing 10% heat inactivated FBS, 2 mM L-glutamine (LG) and 100 U/ml penicillin/streptomycin (P/S) in a humidified 5% CO_2 incubator at 37°C. The preparation of these primary cells is described below. For experiments, the cells were plated onto rat tail collagen-coated Lab-Tek coverglass chamber slides (Thermo Fisher Scientific, Waltham, MA, United States) at 4×10^4 cells/cm^2 growth area in growth medium. At confluence (day 0), the medium was changed to osteogenic medium consisting of α-MEM supplemented with 5% FBS, 100 U/ml P/S, 2 mM LG, 5 mM β-Glycerophosphate (βGP) and 50 μg/ml ascorbic acid, to promote osteogenic differentiation. In some experiments 0.5 mM βGP was used for days 0–5 and then 5 mM βGP was used from day 5 onwards. The cells were cultured for up to 14–21 days, with media refreshed every 3 days. Imaging was initiated at various times as indicated in the results section. During imaging

100 μg/ml L-ascorbic acid phosphate magnesium salt n-hydrate was used in place of standard ascorbic acid, since it is more stable under imaging conditions.

Primary Calvarial Cell Isolation

Primary mouse calvarial cells were isolated from 7 to 8 day old neonatal mouse calvaria by sequential trypsin and collagenase digestions using a modification of methods described previously for fetal rats (Harris et al., 1994; Dallas et al., 1995). Briefly, the parietal and frontal bones were aseptically dissected and subjected to four 20 min sequential digests in 0.2% collagenase/0.05% trypsin in α-MEM (no additives) on a shaker plate at 37°C. Digests 2–4 were kept as the osteoblast-enriched cell population and first or second passage cells were plated for experiments.

Live Cell Imaging

For live cell imaging, cells were plated onto collagen-coated Lab-Tek coverglass chamber slides (Thermo Fisher Scientific, Waltham, MA, United States) and differentiated as described above. On the day of imaging, the media was refreshed with additives as above, but with 100 μg/ml L-ascorbic acid phosphate magnesium salt n-hydrate (a more stable form of ascorbic acid). Live cell imaging was performed on an automated Nikon TE 2000E widefield epifluorescence microscope with precision motorized x, y, and z stage using a 20x 0.75 NA objective with filter sets optimized for each fluorophore. The "Metamorph" software (Molecular Devices, LLC, Sunnyvale, CA, United States) controlled the microscope and multidimensional imaging parameters. Temperature was held constant at 37°C using a microscope incubator cabinet ("The Box" with "The Cube," Life Imaging Systems, Reinach, Switzerland) and a humidified 5% CO_2 atmosphere was maintained using a gas mixer ("The Brick," Life Imaging Systems) in conjunction with a humidified stage top incubation chamber. Images were acquired for each time point under epifluorescent illumination using a Photometrics Coolsnap HQ cooled CCD camera with 12-bit gray scale resolution. Fields of 450 × 335μm were imaged at a spatial resolution of 696 × 520 pixels (with 2 × 2 binning) every 30 min for up to 14 days from 5 optical planes, with media refreshed every 48 h. Image stacks were processed in Metamorph using the "best focus" algorithm or by manually selecting the best focus plane and then exported as image stack (.stk) files. Post-acquisition image processing including contrast adjustments, color merging, conversion to 8-bit or RGB stacks, stack processing and compilation into movies was done using ImageJ software. Image stacks were registered using the "stackreg" plugin in ImageJ (translation mode) (Thevenaz et al., 1998) to align the time series stacks and correct for misaligned image frames. Aligned image stacks were assembled into movies using ImageJ. Gamma adjustments were applied to some of the collagen-GFP movies to allow visualization of collagen fibrils at early time points due to the large dynamic range of fluorescence intensity between early and late time points and to some of the Dmp1-Cre/tdTomato movies to allow better visualization of low intensity pixels at the cell boundaries. These are indicated in the legends for the **Supplementary Movies**.

Intravital Imaging

Intravital imaging was performed on 2 week old mice. The mice were anesthetized with 75 mg/Kg ketamine and 0.5 mg/Kg dexmedetomidine (Henry Schein Animal Health, Dublin, OH). Once under a deep plane of anesthesia, the surgical site was prepared by shaving the fur on the top of the head with an electric clipper and cleaning with betadyne followed by 70% ethanol (repeated three times). The skin overlying the calvarium was then aseptically dissected using iris scissors and reflected to expose the surface of the calvarium (mainly the parietal and frontal bones). Loose adherent connective tissue was gently dissected from the bone surface with sterile forceps under a dissection microscope. The mouse was then immobilized using a custom stereotaxic holder designed for the inverted confocal microscope platform, with the mouse lain ventral side upwards and the exposed calvarial surface apposed to a sterile glass coverslip window, allowing imaging from below. To maintain hydration of the exposed calvarial surface, an imaging gel consisting of 300 mM D-sorbitol and 0.5% carbomer940 pH 7.4 (Rothstein et al., 2006) was placed between the exposed calvarial surface and the glass coverslip. To ensure that deep anesthesia was maintained, the animals were monitored throughout the imaging period by assessment of toe pinch reflex, respiratory rate, and checking for spontaneous movement or other signs of discomfort. Deep anesthesia was maintained by administering an additional half dose of ketamine/dexmedetomidine if needed. Sterile saline was injected subcutaneously prior to surgery to maintain hydration (500 μl/10 g body weight). To prevent hypothermia, the air temperature in the microscope incubation cabinet was held at 30°C. At the end of the imaging period, while still under deep anesthesia, the animals were humanely euthanized.

Intravital imaging was performed using a Leica TCS Sp5 II scanning confocal microscope in resonant scanner mode interfaced with the LAS-AF software (Leica Microsystems, Wetzlar, Germany). Images were acquired at a spatial resolution of 1024 × 1024 pixels using a 20x 0.7 NA objective with 4x digital zoom, a pinhole size of 1.2 AU and using line averaging of 48. Images were acquired for GFP-collagen and tdTomato fluorescence from 7 optical planes with a step size of 2 μm. The 488 nm laser (15% output) was used for excitation of GFP-collagen and the 543nm laser (20% output) was used for excitation of tdTomato. Collection windows were optimized for each fluorophore using the Leica SP prism and tunable slider system and signal was collected using HyD detectors. Post-acquisition image processing was done using ImageJ software, as described above.

Cell Tracking and Quantitation of Collagen-GFP and tdTomato Assembly Dynamics

For tracking of cell velocities and cell motions, registered image stacks were used and the motion trajectories for individual cells within each movie field were plotted using the MTrackJ Plugin in ImageJ (Meijering et al., 2012). As an additional analysis, cells that had their motion trajectories plotted were scored according to whether they arose by directly switching on tdTomato expression

or via mitotic division of a cell expressing tdTomato (note: cells that were already tdTomato-positive at the start of the movies were excluded from this scoring analysis). To quantify collagen-GFP and tdTomato fluorescence over time in long-term timelapse movies, background subtracted movie stacks were thresholded in ImageJ and the collagen fibril area or tdTomato fluorescence area was quantified from thresholded stacks using the Analyze Particles Plugin in ImageJ (Meijering et al., 2012).

RESULTS

Expression of Fluorescent Transgenes in GFP-Collagen/Dmp1-Cre/tdTomato Mice

Figure 1A shows expression of the tdTomato transgene in the femur of Dmp1-Cre$^{+/-}$/tdTomato$^{+/-}$ transgenic mice. In this model, the tdTomato reporter is expressed following Cre-mediated recombination driven by the 10 kb *Dmp1* promoter. This promoter was originally thought to be expressed in preosteocytes, osteocytes, odontoblasts and some pulp cells (Toyosawa et al., 2001; Feng et al., 2003; Kalajzic et al., 2004; Lu et al., 2007). However, subsequent studies have shown that it is expressed in some late osteoblasts as well (Kalajzic et al., 2013; Dallas et al., 2018), which may be due to the sensitivity of the tdTomato reporter in the Ai9 mouse line, even to extremely low levels of Cre recombinase (reviewed in Dallas et al., 2018). In our hands, in bone tissue, the tdTomato transgene was strongly expressed in the majority of embedded osteocytes, preosteocytes, and some late osteoblasts on the bone surface when used with the 10 kb Dmp1 Cre driver (**Figure 1A**) (a Cre negative littermate control is shown at right). **Figure 1B** shows the localization of GFP-tagged collagen in the femur of a GFP-collagen transgenic mouse. Bright GFP-collagen fluorescence was observed in the extracellular matrix of the bone (a GFP negative littermate control is shown at right). **Figure 1C** shows still frames from intravital imaging in a GFP-collagen$^{+/-}$/Dmp1-Cre$^{+/-}$/tdTomato$^{+/-}$ triple transgenic mouse to illustrate the expression of GFP-collagen and tdTomato at the suture region of the parietal bone (see left image of a mouse skull for the location of the imaged region). GFP-collagen fiber bundles could be clearly visualized in the suture area, with a much more densely packed appearance of the GFP-collagen in the mineralized bone regions on either side of the suture. Many tdTomato-positive cells were found embedded in lacunae in the GFP-collagen bone matrix (E-OCY). Additionally, larger tdTomato-positive cells were observed on the bone at the edges of the suture and on the bone surface (M-OCY), presumably representing cells that retain properties of osteoblasts, but are transitioning toward becoming future osteocytes. These cells were also found to be motile (data not shown). tdTomato-positive cells were not observed in the suture region.

Dynamics of Collagen Assembly in Mineralizing Primary Calvarial Cell Cultures

Having established that the GFP-collagen and Dmp1-Cre/tdTomato transgenes showed the expected localizations in bone, primary calvarial cells were isolated from these transgenic mice and differentiated *in vitro* to form mineralized bone nodules using osteogenic media containing ascorbic acid and β-GP. This culture system was used as an *in vitro* model to determine the dynamics of collagen assembly as well as the dynamic process by which osteocytes become embedded in bone collagen matrix. Long-term timelapse imaging was performed for up to 14 days. First, the GFP-collagen movies were examined, which allowed visualization of collagen assembly over time as the primary calvarial cells formed foci that progressed to form mineralized bone nodules. **Figures 2A,B** show a series of still frames from live imaging of a developing bone nodule starting at 3 days of culture in osteogenic media and continuing to 16.7 days. **Supplementary Movie 1** shows the entire movie sequence from the initial condensation of cells at around 3 days to form an early nodule through expansion and maturation of the nodule and its mineralization. Since this movie represents a full 2 weeks of live cell imaging, we have also divided the movie into shorter segments to better illustrate the dynamic events at different stages throughout the differentiation and mineralization process.

Supplementary Movie 2 shows the time period from d3 to d4, representing the early stages of differentiation (also see still frames in **Figure 2A**). At these early stages, the initial formation of a future bone nodule is seen in the DIC images as a condensation of cells in a focal area where the cells became rounded/multilayered. GFP-collagen was deposited throughout the cell layer, but was brighter and more concentrated in these foci of condensed cells that would become future bone nodules. Many of these GFP-collagen containing foci underwent expansion/stretching whereby the collagen was pushed outwards from the center of the forming nodule, as shown in **Supplementary Movie 2**. This expansion appeared to be mediated by coordinated movement of cells outwards from the center of the nodule and further condensation of cells to increase the nodule size. In addition, there was considerable assembly of new collagen in both the forming nodule and the adjacent cell layer. The cells participating in nodule formation appeared more rounded and showed extensive membrane ruffling (visible in the movies as bright hair-like features on the cells) compared to the cells in the surrounding monolayer. Additionally, the cells in both the forming nodule and surrounding monolayer were constantly in motion, which exerted forces on the forming fibrils, resulting in continual stretching/small deformations of the fibrils during the assembly and expansion process.

Supplementary Movie 3 depicts the time period from d4 to d8 (also see still frames in **Figure 2A**). Over this period, the foci continued to expand outwards and assembled brighter and thicker GFP-collagen fibril networks. As the collagen fiber network matured, the collagen in the nodule forming foci appeared structurally distinct from the surrounding collagen and by day 7 had a honeycomb-like appearance, with well-defined "holes" in the collagen network that probably represent future osteocyte lacunae. These presumptive lacunae appeared to be initially formed by cells pushing collagen fibrils outwards to form a hole, followed by new assembly of collagen fibrils around the periphery and compaction of the newly assembled collagen fibrils around the lacunae. An

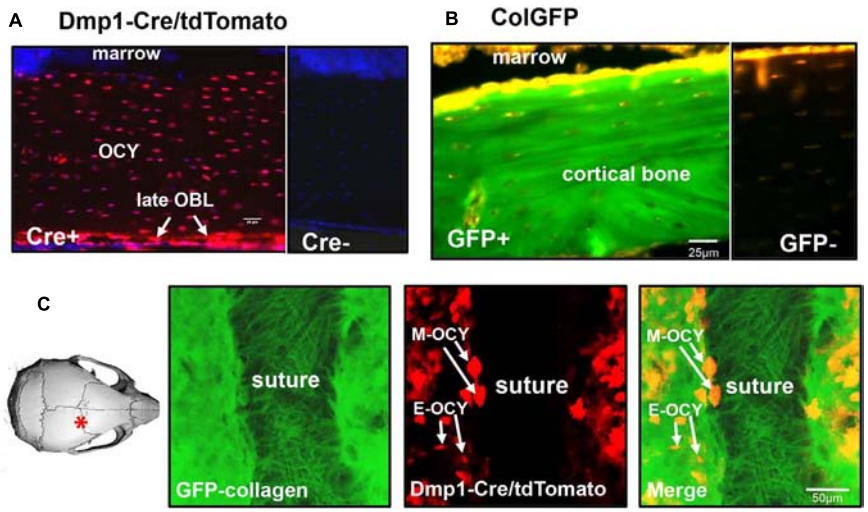

FIGURE 1 | Expression of fluorescent transgenes in GFP-collagen and Dmp1-Cre/tdTomato mice. **(A)** tdTomato expression in the femur (longitudinal section) of an 8 week old Dmp1Cre/tdTomato transgenic mouse (Cre+). A Cre negative littermate control is shown at right for comparison (Cre-). tdTomato expression is shown in red and DAPI nuclear stain is shown in blue. (OCY, osteocytes; late OBL, late osteoblasts), bar = 50 μm. **(B)** GFP-collagen expression in the femur (longitudinal section) an 8 week old GFP-collagen transgenic mouse (GFP+). A GFP-negative littermate is shown at right for comparison (GFP-). GFP-collagen is shown in green and tissue autofluorescence appears yellow/orange, bar = 25 μm. **(C)** Still frame from intravital imaging in a 15 day old GFP-collagen/Dmp1-Cre/tdTomato transgenic mouse. The image on the left illustrates the location of the imaging field. GFP collagen is shown in green and tdTomato is shown in red. (E-OCY, embedded osteocytes; M-OCY, larger tdTomato-positive cells that are motile, located at the edge of the suture), bar = 50 μm. Panel **(A)** is modified from Dallas et al. (2018) with permission.

example of this is shown by the two lacunae in **Supplementary Movie 3** that are indicated by arrowheads. **Figure 2C** shows still frames of the same two forming lacunae from the boxed region indicated in **Figure 2A**. Note that between 5 and 5.4 days, the holes indicated by arrowheads are formed within the collagen fibril network. This occurs by cell(s) physically pushing the collagen fibrils outward to form an initial hole, followed by assembly of more collagen around the periphery of the lacunae and compaction of the collagen into a dense fibril network. During the time period from d4 to d8, there was still continuous cell movement and fibril stretching as well as some condensation of fibrils occurring in certain regions, especially between days 6 and 8 (see **Supplementary Movie 3**).

Supplementary Movie 4 shows the time period from d8 to d16.7 (also see still frames in **Figures 2A,B**). Please note from this movie that the mature collagen matrix at d8 appears relatively stable, with little motion compared to earlier time points. The first sign of mineral deposition can be seen in the DIC movie panel and still frames at around day 9, with rapid mineral deposition occurring between days 10 and 12. After mineralization, as would be predicted, there was very little movement of collagen within the mineralized nodule area. However, there was continued fibril motion in areas that were not mineralized. **Figure 2B** shows still frame images of GFP-collagen, DIC and a merged GFP-collagen/DIC image at day 16.7. The outline of the mineralized nodule is indicated in yellow and it is clear that mineral was deposited only in areas containing bright, dense, GFP-collagen that appears distinct from the collagen in the non-mineralized areas.

In many cases, when mineralized bone nodules were forming, global (tissue-level) motions were observed in which the forming nodules moved relative to each other, suggesting coordinated movement of sheets of cells between the nodules. This is best appreciated by viewing **Supplementary Movie 5** and is illustrated by the still images in **Figure 3A**. When viewing **Supplementary Movie 5**, note that the bone nodule foci marked by asterisks in **Figure 3A** show motions relative to each other and that the one at the bottom of the image field moves up and down relative to the other nodules. This is further illustrated by the merged color image in **Figure 3A** in which still frames from 7, 8, and 9 days are pseudocolored in red, green and blue, respectively, and merged. Areas that appear white indicate no change, but areas that are red, green or blue indicate motions of the forming nodules relative to each other.

Intravital imaging in the calvaria of GFP-collagen expressing mice provided analogous observations whereby the collagen in the mineralizing bone matrix appeared structurally distinct from the collagen fibers in the sutures. Global motions of the mineralizing bone fronts on either side of the suture relative to each other were observed, apparently due to contraction of collagen in the sutures, presumably due to underlying cell and tissue-level motions (see **Supplementary Movie 6**). Interestingly, the structural appearance of bone collagen in the calvarial bone in the live mice resembled that in the mature *in vitro* bone nodules after mineralization (compare **Supplementary Movie 6** with the GFP-collagen image in **Figure 2B**). However, our intravital imaging studies in mice have so far been limited to timescales of up to 8 h and this was not sufficiently long to see significant new collagen deposition.

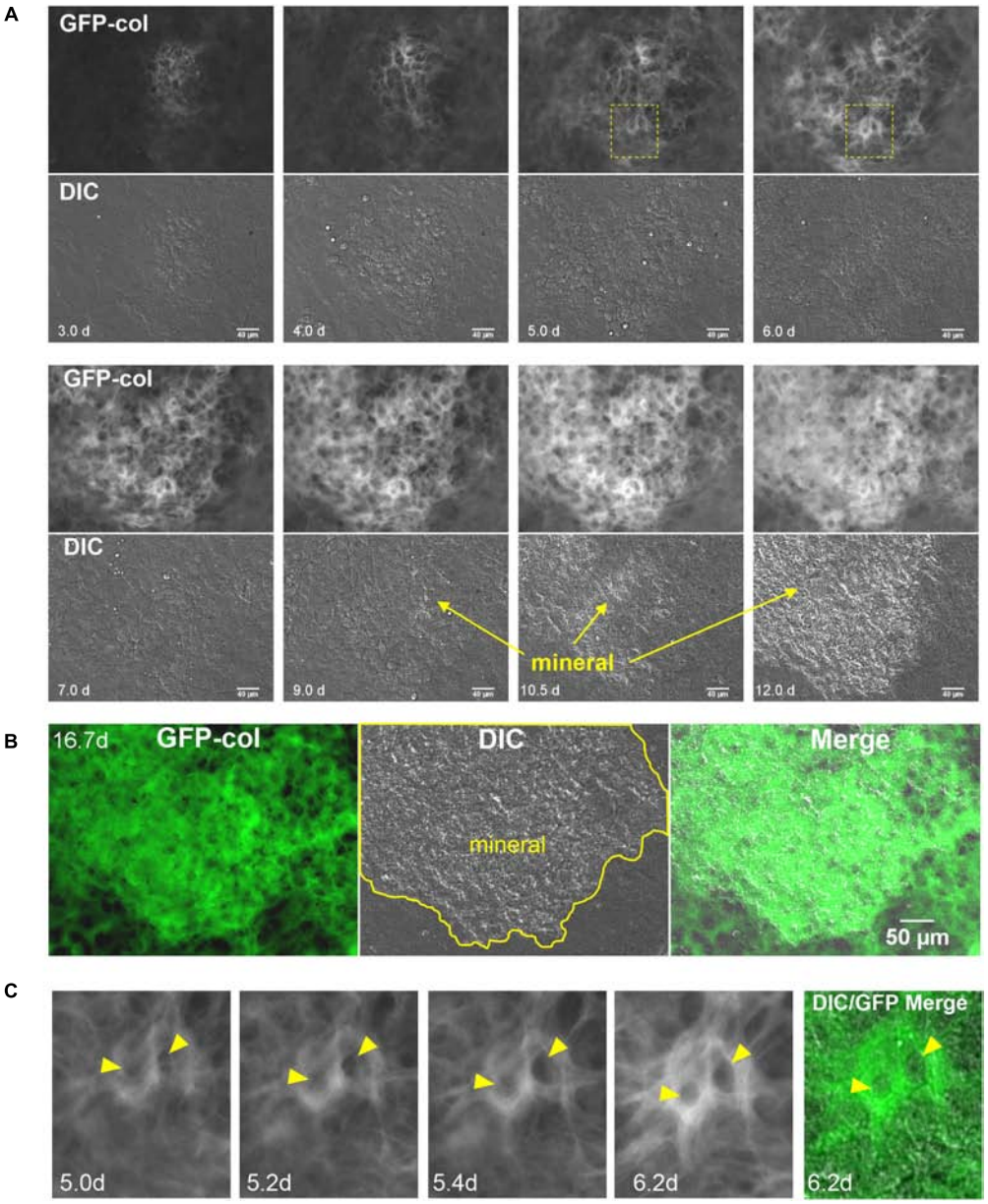

FIGURE 2 | Live cell imaging of collagen assembly dynamics in long-term osteogenic calvarial cell cultures. **(A)** Still frames from timelapse imaging showing formation of a mineralized bone nodule from its initial condensation at day 3 to mineralization by day 12. GFP-collagen is shown in the upper panels and DIC images are shown in the lower panels. Mineral deposition can be seen on the DIC images and is initiated around day 9 (bar = 40 μm). To appreciate the dynamic nature of this collagen assembly please view **Supplementary Movies 1**–**4**. **(B)** Still frames from day 16.7 in the same timelapse series showing GFP-collagen, DIC and merged images. Note that the mineral is deposited exclusively in the collagen-rich focal area (bar = 50 μm). **(C)** Still frames showing an enlargement of the boxed area in **(**A), illustrating GFP-collagen dynamics during the formation of two osteocyte lacunae (arrowheads) within the bone matrix over days 5.0–6.2. A merged GFP-collagen/DIC image is shown at right for the 6.2 h time point. To view this dynamically, please see **Supplementary Movie 3**, arrowheads.

As well as motions of bone nodules relative to each other, compaction/condensation of collagen within mineralizing foci was frequently observed prior to the onset of mineralization. This is best appreciated by viewing **Supplementary Movie 7** in which compaction of collagen in the nodule can be observed at around days 7–8, preceding mineral deposition, which starts at around day 9. This is further illustrated by the still images in **Figure 3B** in which the forming bone nodule is outlined in yellow at day 6. The day 6 outline is superimposed on the 8, 10, and 12 day images, showing that the contours of the nodule are reduced relative to day 6, as indicated by the light blue distance bars. DIC images show mineral deposition at 10 and 12 day.

In addition to global motions of fibrils and condensation of fibril networks prior to mineral deposition, localized motions of individual fibrils were also frequently observed. An example of this is shown in **Supplementary Movie 8**, in which the fibril

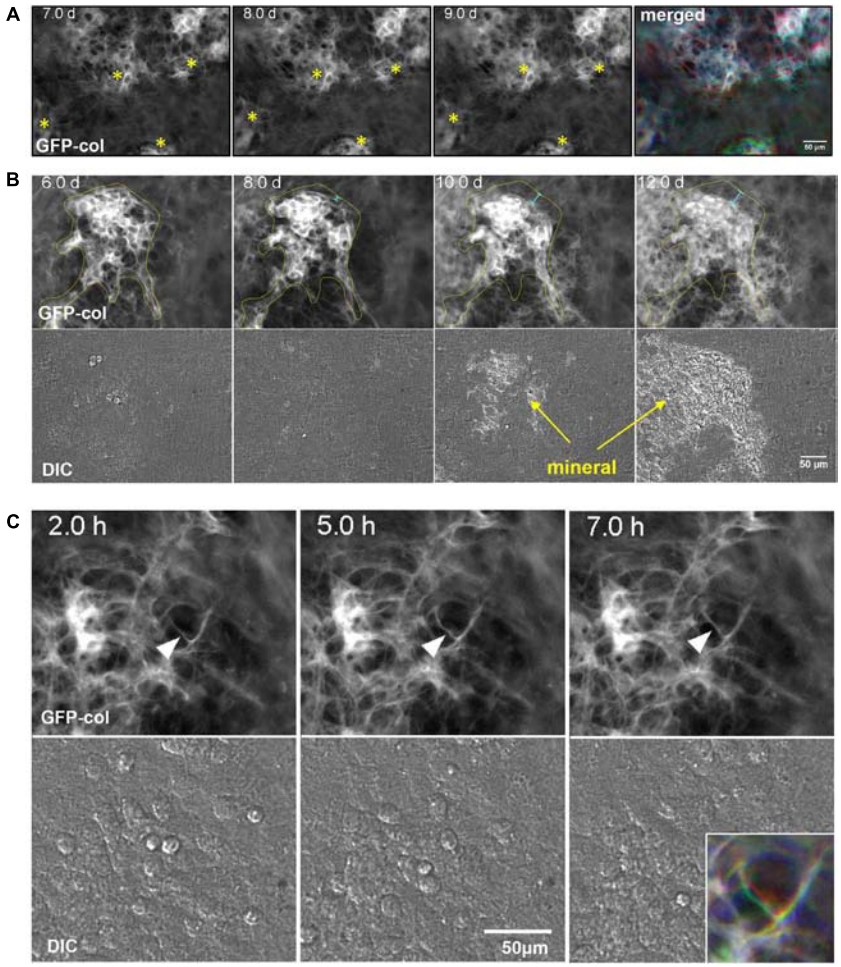

FIGURE 3 | Dynamic events during collagen assembly. **(A)** Still frames from timelapse imaging of bone nodules forming in long-term osteogenic calvarial cell cultures. Note the nodules marked with the asterisks that move relative to each other. This is best appreciated by viewing **Supplementary Movie 5**. The RGB color image on the right shows the 7, 8, and 9 day images merged into the red, green, and blue channels respectively. **(B)** Still frames from timelapse imaging of a bone nodule mineralizing. The collagen in the osteogenic nodule is outlined in yellow at day 6 and the same outline is superimposed on the images at days 8, 10, and 12. The light blue distance bars indicate compaction of the collagen relative to the original contours of the nodule. This is best appreciated by viewing **Supplementary Movie 7**. **(C)** Still frames from a timelapse movie illustrating local motions of an individual fibril marked with an arrowhead. The fibril starts out straight at 2 h and is deformed by local cell motion at 5 h before becoming straightened again at 7 h. These local fibril dynamics are best appreciated by viewing **Supplementary Movie 8**, where you can see this and other fibrils repeatedly being stretched and distorted by local cell motions. The colored inset image in the lower right shows the same fibril from the 2, 5, and 7 h images merged into the red, green, or blue channels respectively. In all panels, bar = 50 μm.

marked by the arrowhead is repeatedly distorted relative to those around it, presumably due to local cell motion/protrusive activity. Still images in **Figure 3C** illustrate motions of the fibril in **Supplementary Movie 8**. The motion of this fibril is best appreciated by the merged color image shown in the lower right inset, in which still frames from 2, 5, and 7 h are pseudocolored blue, green and red, respectively and merged. Areas that appear white indicate no change, but areas that are red, green or blue indicate motions of the fibril.

Dmp1-Cre/tdTomato Cell Dynamics During Collagen Assembly

Next, to visualize how osteocyte differentiation is dynamically integrated with bone collagen assembly, two-color movies of GFP-collagen were examined together with Dmp1-Cre/tdTomato to visualize preosteocytes/osteocytes. Interestingly, the tdTomato reporter turned on almost exclusively in the same foci of concentrated GFP-collagen fibers that demarcate where mineralized nodules will form (**Figure 4A** and **Supplementary Movie 9**) with very little expression of tdTomato in regions between bone nodule foci. As can be seen in **Supplementary Movie 9**, the tdTomato turns on first in cells that are motile, but as the forming bone nodule matures, many of them become embedded in lacunae within the collagen matrix. Quantitation of the area of GFP-collagen and tdTomato fluorescence showed that over the 2 week osteogenic differentiation time course, the majority of collagen assembled within the first 7 days, whereas the number of Dmp1-Cre/tdTomato cells continuously increased throughout the time

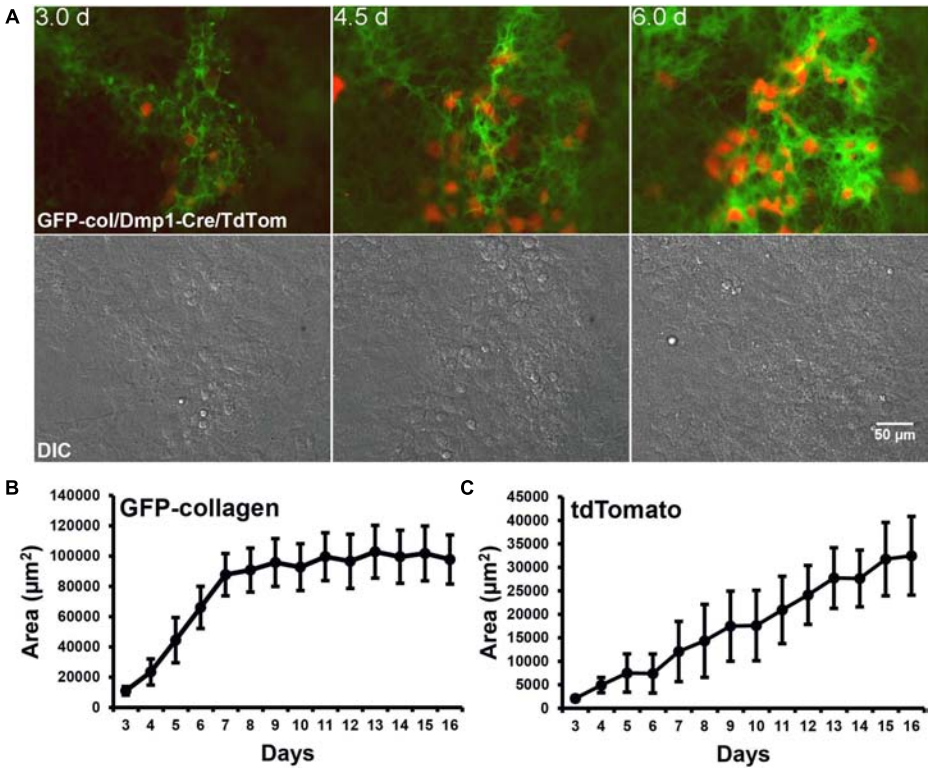

FIGURE 4 | Dmp1-Cre/tdTomato cell dynamics during collagen assembly. **(A)** Still frames from timelapse dual imaging of GFP-collagen (green) and Dmp1-Cre/tdTomato (red) in primary calvarial osteoblast cultures between days 3 and 6 (upper panels). DIC images of the cell cultures are shown in the lower panels. Bar = 50 μm. To appreciate the dynamic process of collagen assembly together with tdTomato cell dynamics please view **Supplementary Movie 9**. **(B,C)** Quantitative analysis of the area of GFP-collagen **(B)** and area of tdTomato-positive cells **(C)** in long-term osteogenic calvarial cell cultures over days 3–17. Data are mean ± SEM from n = 4 independent movies.

course (**Figures 4B,C**). Interestingly, a more detailed analysis with measurements taken at every time point revealed small spikes in the area of GFP-collagen fluorescence that appeared to correspond to media changes every 48 h (**Supplementary Figure S1A**). This probably reflects initial rapid assembly and intracellular accumulation of collagen upon changing the media and adding fresh ascorbate. A similar detailed analysis showed a stepwise increase in tdTomato fluorescence area that also seemed to correspond with changes in media every 48 h (**Supplementary Figure S1B**). These kinetics are missed in most standard types of experiments that do not have the increased temporal resolution provided by time lapse imaging with images acquired every 30 min.

The dramatic increase in tdTomato-positive cells that occurred throughout the differentiation process (**Figures 4A,C**, **5A**) could either be due to mitosis of tdTomato-positive cells or due to individual cells switching on tdTomato expression during differentiation. Quantitative analysis from 5 independent movies (total of 103 cells analyzed) showed that 100% of these tdTomato-positive cells arose by cells switching on tdTomato and no instances were recorded of cells arising through mitosis of a tdTomato-positive cell. This is illustrated in **Supplementary Movie 10**, where numerous cells can be observed to turn on tdTomato expression without originating from a cell division. **Supplementary Movie 10** is formatted so that after playing once through, it plays back in reverse. The cell marked with the arrowhead in the reverse movie segment is an example of a cell that can be tracked back to its origin to confirm that it arose by switching on tdTomato rather than from a cell division. These data show that the Dmp1-Cre/tdTomato cells are post-mitotic. These post-mitotic tdTomato-positive cells make up a relatively small fraction of the entire population in the calvarial cell cultures and their numbers increase over time as more mineralized nodules are formed. Within the mineralizing nodule regions themselves, quantitative analysis indicated that the tdTomato positive cells occupy 28–30% of the nodule area (data not shown). In a typical differentiated primary calvarial cell culture, the mineralized bone nodule area occupies about 25–40% of the culture plate area. Therefore, the overall percentage of tdTomato-positive cells is estimated to be around 7–12% of the total population.

Motility tracking analysis was performed on tdTomato-positive cells from long-term time lapse movie stacks (**Figure 5B**). This showed that in early (d3–5) cultures the cells moved freely in and around the bone forming nodules prior to mineralization. Quantitative analysis showed that they had a mean velocity of 4.8 μm/h (**Figure 5C**). At this early time, only a few cells were embedded in collagen, constraining their motion. However, in

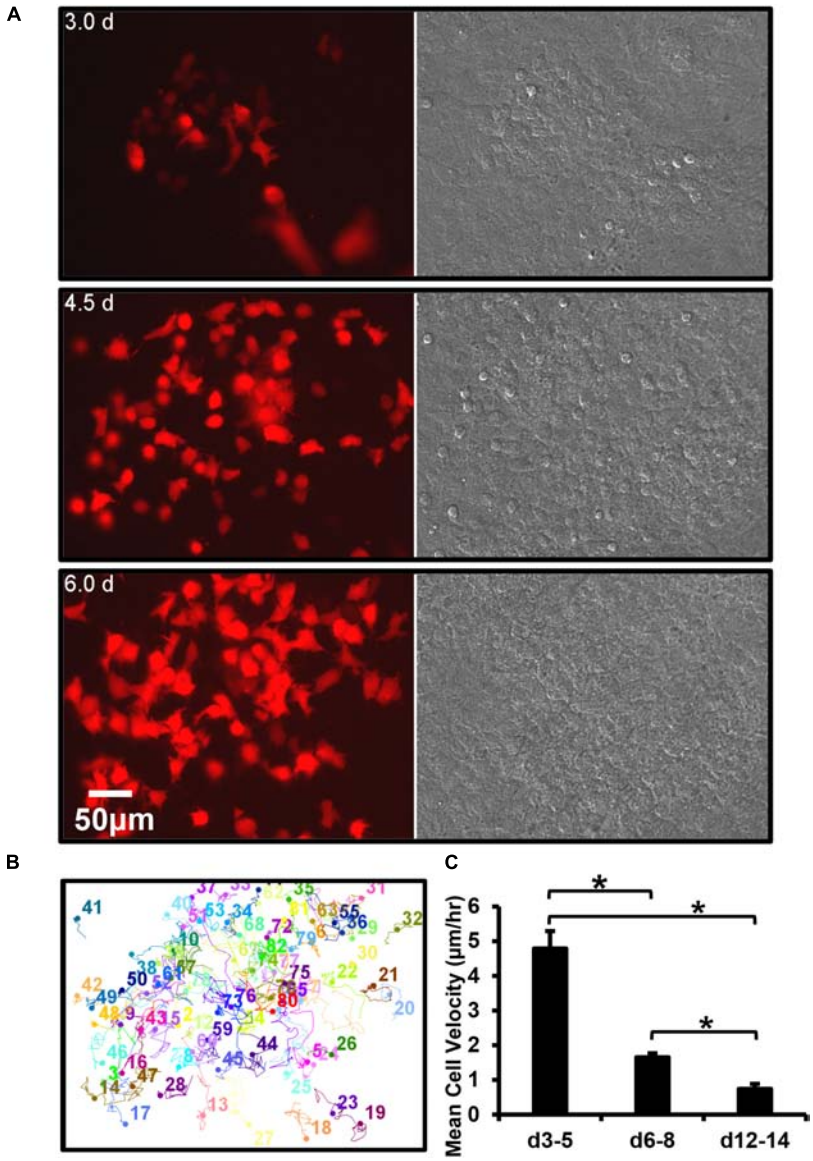

FIGURE 5 | Dmp1-Cre/tdTomato reporter switches on in a post-mitotic cell that is initially motile and then embeds. **(A)** Still frames from a timelapse movie showing the dramatic increase in tdTomato-positive cells over time in osteogenic calvarial cell cultures from Dmp1-Cre/tdTomato transgenic mice, bar = 50 μm. The tdTomato-positive cells arise exclusively from new cells switching on tdTomato rather than from mitotic division of cells already expressing tdTomato, which is best appreciated by viewing **Supplementary Movie 10**. **(B)** Motion trajectory plots for individual cells within the movie field. **(C)** Graph showing the average velocities of tdTomato-positive cells over 3–5, 6–8, and 12–14 days. Data are mean ± SEM from $n = 9$ independent movies for d3–5 and $n = 10$ for d6–8 and d12–14. *$p < 0.05$ (ANOVA/Student Newman Keul's).

more mature (d6–8), cultures the mean velocity was significantly reduced to 1.7 μm/h and in mineralizing (d12–14) cultures it was further reduced to 0.7 μm/h, as many cells became immobilized in the mineralized nodule (**Figure 5C**).

Osteocyte Embedding Behavior Prior to Mineralization

Dual imaging of GFP-collagen and Dmp1-Cre/tdTomato provided novel insight into how osteocytes may embed into their lacunae. Interestingly, three distinct mechanisms for embedding were observed. In some instances, previously motile tdTomato-positive cells became trapped and immobilized in collagen fibril networks that were newly assembled around the cell. An example of this is shown in **Figure 6A** and **Supplementary Movie 11**. Note the cell marked with the arrowhead that is freely motile at the start of the movie. By around 8 days, the motility of the cell is arrested as it is trapped in a network of new collagen fibers assembled around it. In other cases, cells appeared to switch on tdTomato expression *in situ* within an already formed presumptive lacuna in the collagen matrix. An example of this is shown in **Figure 6B** and **Supplementary Movie 12**. Note

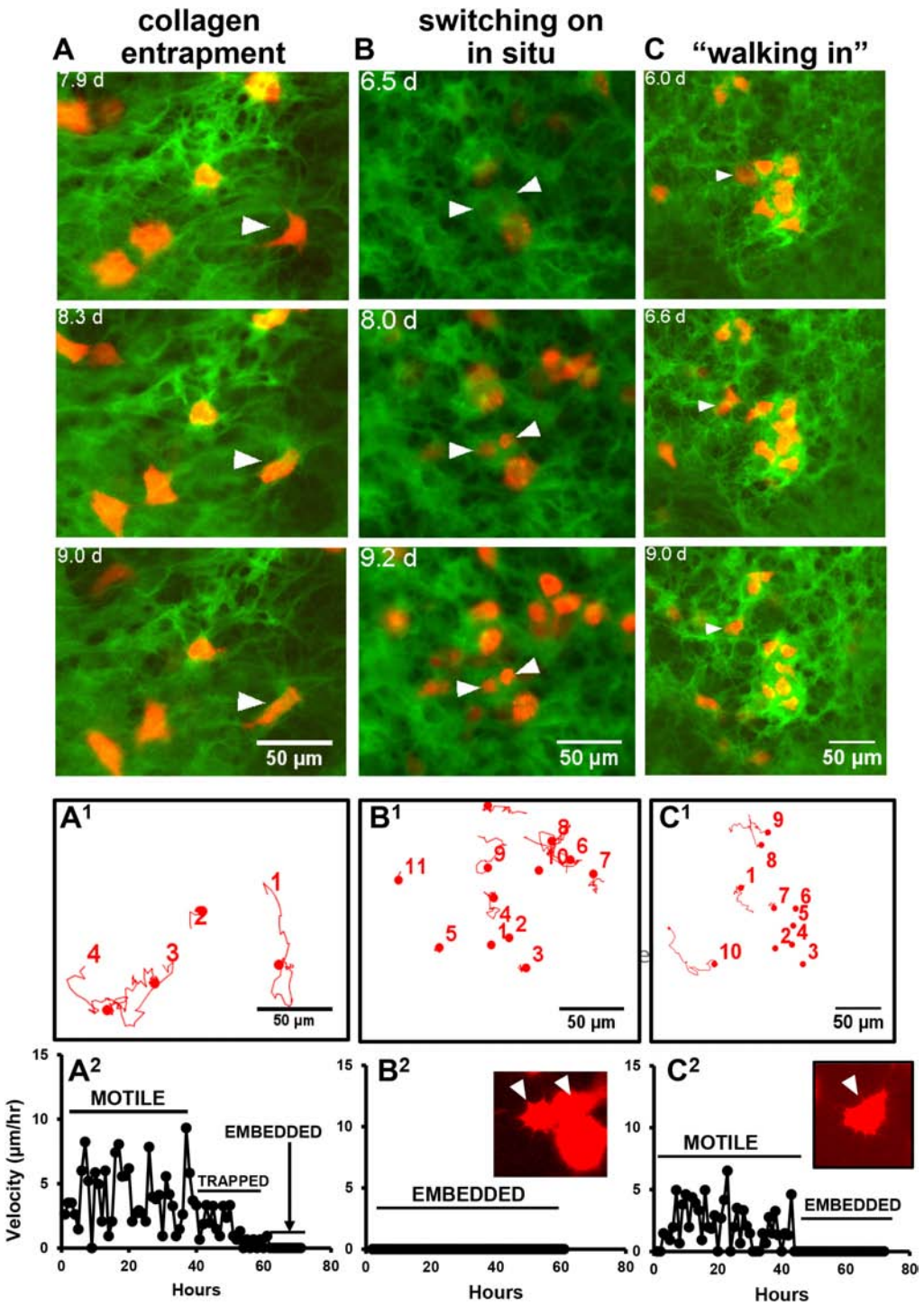

FIGURE 6 | Multiple mechanisms for osteocyte embedding. **(A–C)** Still frames from timelapse movies that illustrate the different mechanisms of embedding of tdTomato-positive cells in osteogenic calvarial cell cultures from GFP-collagen/Dmp1-Cre/tdTomato transgenic mice. **(A)** shows a tdTomato-positive cell (arrowhead) becoming embedded via collagen entrapment. This cell initially shows motile activity until around 8 days, when a network of collagen fibers is assembled around the cell, thereby immobilizing it. This is best visualized dynamically by viewing **Supplementary Movie 11**; **(B)** shows two cells (arrowheads) that switch on tdTomato expression *in situ* while already located within a lacuna. This is best visualized dynamically by viewing **Supplementary Movie 12**; **(C)** shows a tdTomato-positive cell (arrowhead) that shows motile activity and "walks into" an already formed lacuna in the collagen matrix. The contours of the cell then conform to the contours of the lacuna. This is best visualized dynamically by viewing **Supplementary Movie 13**. **(A^1–C^1)** Show motion trajectory plots for the cells in movies **(A–C)**, respectively. **(A^2–C^2)** Show the motility profiles for the featured cells in **(A–C)**, respectively, that exemplify the different embedding behaviors. The inset images show that the morphology of the embedded cells in movies **(B,C)** at the end of the movie resemble the dendritic morphology of osteocytes. In all panels, bar = 50 µm.

the two cells marked with arrowheads that turn on tdTomato expression when they are already located within a presumptive lacuna, suggesting that the cells were already present in the lacunae prior to differentiating to express Dmp1. A third mechanism was observed in which tdTomato-positive cells appeared to "walk" into an already formed hole/lacuna in the collagen network. Once immobilized, the cell then adopted a morphology conforming to the contours of the lacuna. An example of this is shown in **Figure 6C** and **Supplementary Movie 13**. Motion trajectory plots of the cells in each movie are shown in **Figure 6** in the corresponding panels A^1, B^1, and C^1. The cell motility profiles of the featured cells showing "collagen entrapment," "switching on *in situ*" and "walking into lacunae" behaviors are shown in **Figure 6** in the corresponding panels A^2, B^2, and C^2. As expected, the cell motility plots paralleled the behavior of the cells observed in the timelapse movies, with the "collagen entrapped" cell (A^2) initially showing motile behavior, followed by a reduction in motility after entrapment and a further reduction to zero once the cell is fully embedded. The "switching on *in situ*" cell (B^2) showed no motile behavior at all, consistent with the observation that it appeared to differentiate from a cell that was already located within a lacuna. The inset image shows that one of these two cells also adopts a dendritic osteocyte morphology. The third type of cell that "walks into a lacuna" (C^2) shows a period of motility before it "walks" into the lacuna and then shows no further motile behavior after it is embedded. In another variation on the "walking into a lacuna" embedding style, several cells were observed that appeared to move into and out of more than one presumptive lacunae before finally embedding. An example is shown in **Supplementary Figure S2** and **Supplementary Movie 14**. Here, two lacunae are marked by the yellow arrowheads and the moving cell is marked by the white arrowhead. The motion trajectory plot of this cell shows a period of motility, then a period of inactivity while the cell is temporarily located in lacuna L1. This is followed by another period of motility while the cell moves to the second lacuna and finally the motility is reduced to zero when the cell embeds in lacuna L2. **Supplementary Figures S3–S5** show 10 examples of individual cell motility profiles for each category of embedding cell, including the "collagen entrapped" (**Supplementary Figure S3**), "switching on *in situ*" (**Supplementary Figure S4**) and "walking into a lacuna" (**Supplementary Figure S5**) embedding types as well as a graph showing the mean velocities of the 10 cells of each type. Although there is some variation in the profiles amongst individual cells, the cells within each category show similar motility profiles that parallel their embedding behaviors. Comparisons of the mean velocities of these cells over the first 40 h of tracking showed that the "collagen entrapped" cells had a significantly higher velocity (4.621 μm/h $\pm$ 0.418) compared to either the "switching on *in situ*" (0.014 μm/h $\pm$ 0.005) or "walking into a lacuna" cells (2.599 μm/h $\pm$ 0.0.499) ($p < 0.05$, ANOVA/Tukeys).

Quantitation of the overall percentages of cells embedding by each type of mechanism showed that the majority of the cells (49%) embedded by collagen entrapment, with 30% turning on tdTomato expression *in situ* and 21% embedding by "walking into" an already formed lacuna (see **Figure 7A**). When the average day of embedding was determined for each of these categories, it was found that the collagen entrapment mechanism tended to be used by cells that embedded significantly earlier (average around 8 days), compared to the other two mechanisms, which tended to be used by cells that embedded later (average around 12–13 days) (see **Figure 7B**).

DISCUSSION

In this study, long-term timelapse imaging was performed in mineralizing bone cell cultures, which has provided novel insight into the dynamic process of collagen assembly and mineralization and has revealed three independent mechanisms by which osteocytes can embed within bone matrix. This timelapse imaging was performed using primary calvarial cell cultures from transgenic mice expressing GFP-collagen together with a tdTomato lineage reporter for differentiation toward the osteocyte phenotype. Long-term live imaging of collagen deposition in this osteogenic culture model showed that, while collagen is assembled throughout the cell layer, mineral deposition is restricted to regions demarcated by foci of concentrated GFP-collagen bundles that appear structurally distinct from the surrounding collagen. These foci are associated with cell condensations that demarcate where the bone nodule will form. The assembly of collagen within these foci was highly dynamic, with global (tissue level) motions of the collagen, including an outward expansion of collagen that appeared to be mediated by coordinated movement of cells outwards from the center of the nodule, as well as motions of the forming bone nodules relative to each other, suggesting coordinated movement of sheets of cells between the nodules. In addition, there were local motions of individual fibrils that were stretched/distorted, presumably by local cell motions or protrusive activity. These observations on collagen assembly dynamics show parallels with the work of Rongish and co-workers, who examined fibrillin and fibronectin fibril dynamics in early avian embryos (Filla et al., 2004; Czirok et al., 2006; Aleksandrova et al., 2012). Their work identified two distinct types of motion of ECM filaments, one in which the filaments are moved by large-scale tissue motions due to folding of tissue layers during embryonic morphogenesis and a second type whereby the motion of individual filaments is driven by motility/protrusive activity of neighboring cells. Snapping and recoil of fibronectin fibrils by local cell-mediated forces has also been demonstrated using live cell imaging (Ohashi et al., 1999; Sivakumar et al., 2006; Davidson et al., 2008). We have also recently reported on the generation of GFP*topaz* and mCherry-tagged type I collagen fusion protein constructs that were stably transfected into MLO-A5 osteoblast-like cells and fibronectin-null mouse embryonic fibroblasts (Lu et al., 2018). Timelapse imaging in these cell models over timeframes of up to 2 days revealed the dynamic nature of type I collagen assembly and showed that collagen assembly was dependent on and temporally integrated with fibronectin assembly (Lu et al., 2018). These studies also showed that the cells were able to physically reshape their assembled collagen fiber networks by pushing collagen outwards to form

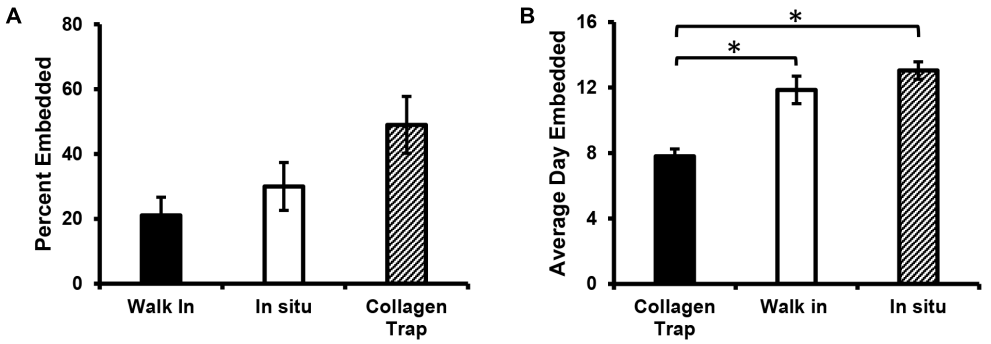

FIGURE 7 | Mechanism of osteocyte embedding may be dependent on the maturation of the bone nodule. **(A)** Quantitation of the percentage of Dmp1-Cre/tdTomato-positive cells that embed via the three different mechanisms identified, including collagen entrapment, switching on tdTomato *in situ* and "walking" into an already formed collagen lacuna. **(B)** Graph showing the average day on which embedding occurred for cells in the three embedding categories. Data in **(A,B)** are mean ± SEM from $n = 4$ independent movies (86 individual embedding cells analyzed). **(B)** $^*p < 0.05$, ANOVA/Tukeys.

holes that may represent early lacunae. Similar physical reshaping of the collagen matrix was observed in the current study and the formation of future osteocyte lacunae appeared to be mediated by cells pushing collagen fibrils outwards from the center of the forming lacuna, accompanied by deposition of more collagen and compaction of the collagen fibril networks around the lacuna. A further overall condensation of the collagen fibrils in the forming bone nodule was observed that preceded mineral deposition.

A key issue to consider is how the dynamic collagen assembly events observed in the current study in an osteogenic cell culture model can be extrapolated to assembly and mineralization of collagen *in vivo*. In the long bones, which contain mostly lamellar bone, collagen is deposited in a highly organized manner by osteoblasts aligned on a mineralization front, and the collagen fibers are predominantly oriented longitudinally. The osteogenic primary cell culture model used in the current studies is derived from calvarial bone, which is formed developmentally by intramembranous ossification. Therefore, this model is probably more relevant to intramembranous and/or woven bone formation, where collagen is deposited rapidly, with a less organized and more random orientation. In the current study, intravital imaging was performed in GFP-collagen transgenic mice and it was observed that the structural and organizational appearance of collagen in calvarial bone in the growth regions adjacent to the sutures is very similar to its organization in mineralizing calvarial cell cultures and that the collagen in the mineralizing bone matrix appeared structurally distinct from the collagen fibers in the sutures. Similar to data from the *in vitro* osteogenesis model, global motions of the mineralizing bone fronts on either side of the suture relative to each other were observed, apparently due to cell-mediated contraction of collagen in the sutures. However, in our experience the collagen assembly process is relatively slow and our intravital imaging in mice has so far been limited to timescales of up to 8 h, which is not sufficiently long to visualize significant assembly of new collagen. Intravital imaging using transgenic mice co-expressing GFP-collagen and Dmp1-Cre/tdTomato also did not enable us to visualize osteocyte embedding events, due to the limited timescales for intravital imaging (data not shown). In contrast, the *in vitro* osteogenic cell culture model enables tracking of multiple embedding events that take place over the extended timescales of 7–14 days that can be imaged using this model system.

In the current study, time lapse imaging in osteogenic calvarial cell cultures showed that the Dmp1-Cre/tdTomato reporter turned on in the same foci of concentrated GFP-collagen bundles that progress to form mineralized bone nodules, with very little expression in regions between bone nodules. The number of Dmp1-Cre/tdTomato-positive cells continuously increased throughout the 2 week timecourse, whereas the majority of collagen was assembled by day 7. In early forming bone nodules, the tdTomato reporter was expressed initially in a motile cell type. Timelapse imaging allowed observation of the fate of these Dmp1-Cre/tdTomato-positive cells over a long timecourse and this revealed that cells which turned on tdTomato expression almost invariably became embedded within "lacunae" in the collagen matrix, which later mineralized. The Dmp1-Cre transgene therefore appears to mark a cell type that is already committed to becoming a future osteocyte. This observation is important, as when initially developed, the Dmp1-Cre deleter strain was thought to specifically target gene deletion to osteocytes (Lu et al., 2007). Later studies showed apparent off target expression in bone in a subpopulation of cells on the bone surface that by their location would be viewed as osteoblasts (Kalajzic et al., 2013; Dallas et al., 2018). However, the current studies suggest that these cells represent a late osteoblast/preosteocyte that is already committed to becoming an embedded osteocyte. The fact that the tdTomato-positive cells arose exclusively by new cells turning on tdTomato expression rather than from mitosis of tdTomato-positive cells further supports this, by demonstrating that the Dmp1-Cre/tdTomato-positive cells are a post-mitotic, committed cell.

Although we have virtually never observed the tdTomato-positive cells to divide in this osteogenesis culture model, it was reported recently that Dmp1-expressing osteocyte-like cells have the capacity to dedifferentiate into osteoblasts and proliferate. These observations were made using an *in vitro*

assay in which the cells migrate out from bone chips onto a plastic culture surface (Torreggiani et al., 2013). In considering this data together with the findings of the current study, a likely explanation is that the Dmp1-expressing cell will retain its post-mitotic state as long as it remains surrounded by bone extracellular matrix, which provides signaling cues to the cell to maintain its differentiated state. The dedifferentiation of osteocyte-like cells most likely occurs only if the cell is removed from its microenvironment and is separated from these environmental cues, for example by migrating out onto plastic. It remains unclear whether such dedifferentiation of osteocytes can occur *in vivo*.

Long term time lapse imaging in the current study has shed new light on the unresolved question of how osteoblasts embed to become osteocytes. A widely accepted theory proposes that embedding is a passive process in which specific surface osteoblasts slow down their production of extracellular matrix and then become "buried alive" in the osteoid produced by adjacent cells (Palumbo et al., 1990; Nefussi et al., 1991; Franz-Odendaal et al., 2006). A competing theory proposes that osteocyte embedding is an active, invasive process, involving proteolytic degradation of the extracellular matrix to excavate the osteocyte lacuna and canaliculi (Zhao et al., 2000; Holmbeck et al., 2005). Our data suggest that there may be more than one mechanism for osteocytes to become embedded in bone extracellular matrix. In some cases, a motile Dmp1-Cre/tdTomato-positive cell, presumably representing a late osteoblast/preosteocyte, became entrapped in a network of collagen fibers that was newly assembled around the cell. The probable source of this newly assembled collagen appears to be the adjacent cells, as GFP-collagen was not observed inside tdTomato-positive cells. Therefore, this seems to agree with theories of osteoblasts being "buried alive" in the extracellular matrix produced by neighboring cells (Palumbo et al., 1990; Nefussi et al., 1991; Franz-Odendaal et al., 2006). A second intriguing mechanism observed was one in which a motile tdTomato-positive late osteoblast/preosteocyte cell "walked in" to an already formed collagen lacuna in the developing nodule. This was followed by arrest of cell motility and the cell morphology adopting a shape conforming to the boundaries of the lacuna. There were also variations on this theme in which cells were seen to move from one lacuna to another before finally settling into a lacuna. Since the current study was limited to imaging the collagen matrix and Dmp1-Cre\tdTomato-positive cells, it is unclear whether another cell that is tdTomato-negative would have to vacate the lacuna to allow the tdTomato-positive cell to occupy it. Future studies using multiplexed imaging with an osteoblast reporter in addition to imaging collagen and Dmp1-Cre/tdTomato-positive osteocytes are needed to address this question. The third mechanism for osteocyte embedding involved cells that were already located within a lacuna differentiating *in situ* to turn on expression of Dmp1-Cre/tdTomato. Therefore, cells that fell into this category showed no motility after switching on tdTomato.

Which of these three mechanisms is used appears to be time-sensitive and/or dependent on the maturation state of the forming bone nodule, with the collagen entrapment mechanism being favored at earlier stages of bone nodule formation, when more of the cells were motile, rapid collagen deposition was occurring and the collagen fibrillar networks showed more motion. The other two mechanisms were more predominant at later stages of bone nodule formation when the collagen fibril networks were more mature and more rigid, collagen assembly had plateaued and mineral deposition had begun. At these later stages, the presumptive osteocyte lacunae were also well demarcated. In extrapolating these observations to bone formation *in vivo*, it seems likely that different embedding mechanisms could operate depending on the maturation state of the forming bone matrix and/or the rapidity with which the bone is being formed. For example, in early stages of bone formation and in the rapid type of bone formation that produces woven bone, when copious amounts of collagen are quickly being assembled, entrapment of osteocytes within newly assembled collagen matrix may be the predominant mechanism. In contrast, in formation of lamellar bone or later stages of woven bone formation when collagen assembly is slower, the other two mechanisms may predominate. Regardless of the mechanism, osteocyte embedding appears to be a systematic rather than a random process, as osteocytes have a regular spacing within the bone matrix when viewed in three dimensions, with approximately equal distances between neighboring osteocytes.

In summary, we present for the first time, long-term timelapse dual imaging of collagen assembly dynamics and osteocyte embedding using an *in vitro* osteogenic cell culture model. These data have revealed the highly dynamic nature of collagen assembly and maturation and provided new insight into the dynamic process of osteocyte differentiation and embedding. Rather than a single mechanism for osteocyte embedding, the data suggest multiple mechanisms for osteocyte entrapment in collagen matrix that may be time and matrix maturation dependent.

DATA AVAILABILITY

The raw data supporting the conclusions of this manuscript will be made available by the authors, without undue reservation, to qualified researcher.

ETHICS STATEMENT

The animal study was reviewed and approved by UMKC Animal Care and Use Committee.

AUTHOR CONTRIBUTIONS

SD, LS, and YL designed the study and interpreted the data. LS, LT-L, YX, and ER collected and analyzed the data. LS and SD drafted the manuscript. LT-L, YX, YL, and ER revised and approved the manuscript. SD took responsibility for the integrity of the data.

FUNDING

This work was supported by the NIH grants P01AG039355, R21AR054449, R21AR062346, and R01AR051517.

ACKNOWLEDGMENTS

We acknowledge use of the UMKC Confocal Microscopy Core supported by NIH grants S10RR027668 and S10OD021665, the UMKC Office of Research Services, and UMKC Center of Excellence in Dental and Musculoskeletal Tissues.

SUPPLEMENTARY MATERIAL

The Supplementary Material for this article can be found online at: https://www.frontiersin.org/articles/10.3389/fcell.2019.00178/full#supplementary-material

REFERENCES

Aleksandrova, A., Czirok, A., Szabo, A., Filla, M. B., Hossain, M. J., Whelan, P. F., et al. (2012). Convective tissue movements play a major role in avian endocardial morphogenesis. *Dev. Biol.* 363, 348–361. doi: 10.1016/j.ydbio.2011.12.036

Appelhans, T., and Busch, K. B. (2017). Dynamic imaging of mitochondrial membrane proteins in specific sub-organelle membrane locations. *Biophys. Rev.* 9, 345–352. doi: 10.1007/s12551-017-0287-1

Bell, D. M. (2017). Imaging morphogenesis. *Philos. Trans. R. Soc. Lond. B. Biol. Sci.* 372:20150511. doi: 10.1098/rstb.2015.0511

Bigley, R. B., Payumo, A. Y., Alexander, J. M., and Huang, G. N. (2017). Insights into nuclear dynamics using live-cell imaging approaches. *Wiley Interdiscip. Rev. Syst. Biol. Med.* 9:e1372. doi: 10.1002/wsbm.1372

Czirok, A., Rongish, B. J., and Little, C. D. (2004). Extracellular matrix dynamics during vertebrate axis formation. *Dev. Biol.* 268, 111–122. doi: 10.1016/j.ydbio.2003.09.040

Czirok, A., Zach, J., Kozel, B. A., Mecham, R. P., Davis, E. C., and Rongish, B. J. (2006). Elastic fiber macro-assembly is a hierarchical, cell motion-mediated process. *J. Cell. Physiol.* 207, 97–106. doi: 10.1002/jcp.20573

Dallas, S. L., Chen, Q., and Sivakumar, P. (2006). Dynamics of assembly and reorganization of extracellular matrix proteins. *Curr. Top. Dev. Biol.* 75, 1–24. doi: 10.1016/s0070-2153(06)75001-3

Dallas, S. L., Miyazono, K., Skerry, T. M., Mundy, G. R., and Bonewald, L. F. (1995). Dual role for the latent transforming growth factor-beta binding protein in storage of latent TGF-beta in the extracellular matrix and as a structural matrix protein. *J. Cell Biol.* 131, 539–549. doi: 10.1083/jcb.131.2.539

Dallas, S. L., Prideaux, M., and Bonewald, L. F. (2013). The osteocyte: an endocrine cell...and more. *Endocr. Rev.* 34, 658–690. doi: 10.1210/er.2012-1026

Dallas, S. L., Xie, Y., Shiflett, L. A., and Ueki, Y. (2018). Mouse Cre models for the study of bone diseases. *Curr. Osteoporos. Rep.* 16, 466–477. doi: 10.1007/s11914-018-0455-7

Davidson, L. A., Dzamba, B. D., Keller, R., and Desimone, D. W. (2008). Live imaging of cell protrusive activity, and extracellular matrix assembly and remodeling during morphogenesis in the frog, Xenopus laevis. *Dev. Dyn.* 237, 2684–2692. doi: 10.1002/dvdy.21600

Davidson, L. A., Keller, R., and Desimone, D. W. (2004). Assembly and remodeling of the fibrillar fibronectin extracellular matrix during gastrulation and neurulation in Xenopus laevis. *Dev. Dyn.* 231, 888–895. doi: 10.1002/dvdy.20217

Eils, R., and Athale, C. (2003). Computational imaging in cell biology. *J. Cell Biol.* 161, 477–481. doi: 10.1083/jcb.200302097

Faibish, D., Gomes, A., Boivin, G., Binderman, I., and Boskey, A. (2005). Infrared imaging of calcified tissue in bone biopsies from adults with osteomalacia. *Bone* 36, 6–12. doi: 10.1016/j.bone.2004.08.019

Feng, J. Q., Huang, H., Lu, Y., Ye, L., Xie, Y., Tsutsui, T. W., et al. (2003). The Dentin matrix protein 1 (Dmp1) is specifically expressed in mineralized, but not soft, tissues during development. *J. Dent. Res.* 82, 776–780. doi: 10.1177/154405910308201003

Filla, M. B., Czirok, A., Zamir, E. A., Little, C. D., Cheuvront, T. J., and Rongish, B. J. (2004). Dynamic imaging of cell, extracellular matrix, and tissue movements during avian vertebral axis patterning. *Birth Defects Res. C Embryo Today* 72, 267–276. doi: 10.1002/bdrc.20020

Franz-Odendaal, T. A., Hall, B. K., and Witten, P. E. (2006). Buried alive: how osteoblasts become osteocytes. *Dev. Dyn.* 235, 176–190. doi: 10.1002/dvdy.20603

Friedl, P. (2004). Dynamic imaging of cellular interactions with extracellular matrix. *Histochem. Cell Biol.* 122, 183–190. doi: 10.1007/s00418-004-0682-0

Halloran, B. P., Ferguson, V. L., Simske, S. J., Burghardt, A., Venton, L. L., and Majumdar, S. (2002). Changes in bone structure and mass with advancing age in the male C57BL/6J mouse. *J. Bone Miner. Res.* 17, 1044–1050. doi: 10.1359/jbmr.2002.17.6.1044

Harris, S. E., Bonewald, L. F., Harris, M. A., Sabatini, M., Dallas, S., Feng, J. Q., et al. (1994). Effects of transforming growth factor beta on bone nodule formation and expression of bone morphogenetic protein 2, osteocalcin, osteopontin, alkaline phosphatase, and type I collagen mRNA in long-term cultures of fetal rat calvarial osteoblasts. *J. Bone Miner. Res.* 9, 855–863. doi: 10.1002/jbmr.5650090611

Holmbeck, K., Bianco, P., Pidoux, I., Inoue, S., Billinghurst, R. C., Wu, W., et al. (2005). The metalloproteinase MT1-MMP is required for normal development and maintenance of osteocyte processes in bone. *J. Cell Sci.* 118, 147–156. doi: 10.1242/jcs.01581

Huitema, L. F., and Vaandrager, A. B. (2007). What triggers cell-mediated mineralization? *Front. Biosci.* 12, 2631–2645.

Igarashi, M., Kamiya, N., Ito, K., and Takagi, M. (2002). In situ localization and in vitro expression of osteoblast/osteocyte factor 45 mRNA during bone cell differentiation. *Histochem. J.* 34, 255–263.

Jilka, R. L., and O'brien, C. A. (2016). The role of osteocytes in age-related bone loss. *Curr. Osteoporos. Rep.* 14, 16–25. doi: 10.1007/s11914-016-0297-0

Kalajzic, I., Braut, A., Guo, D., Jiang, X., Kronenberg, M. S., Mina, M., et al. (2004). Dentin matrix protein 1 expression during osteoblastic differentiation, generation of an osteocyte GFP-transgene. *Bone* 35, 74–82. doi: 10.1016/j.bone.2004.03.006

Kalajzic, I., Matthews, B. G., Torreggiani, E., Harris, M. A., Divieti Pajevic, P., and Harris, S. E. (2013). In vitro and in vivo approaches to study osteocyte biology. *Bone* 54, 296–306. doi: 10.1016/j.bone.2012.09.040

Kamel-Elsayed, S. A., Tiede-Lewis, L. M., Lu, Y., Veno, P. A., and Dallas, S. L. (2015). Novel approaches for two and three dimensional multiplexed imaging of osteocytes. *Bone* 76, 129–140. doi: 10.1016/j.bone.2015.02.011

Kozel, B. A., Rongish, B. J., Czirok, A., Zach, J., Little, C. D., Davis, E. C., et al. (2006). Elastic fiber formation: a dynamic view of extracellular matrix assembly using timer reporters. *J. Cell Physiol.* 207, 87–96. doi: 10.1002/jcp.20546

Kulesa, P. M. (2004). Developmental imaging: insights into the avian embryo. *Birth Defects Res. C Embryo Today* 72, 260–266. doi: 10.1002/bdrc.20021

Lo Celso, C., Wu, J. W., and Lin, C. P. (2009). *In vivo* imaging of hematopoietic stem cells and their microenvironment. *J. Biophotonics* 2, 619–631. doi: 10.1002/jbio.200910072

Lu, Y., Kamel-El Sayed, S. A., Wang, K., Tiede-Lewis, L. M., Grillo, M. A., Veno, P. A., et al. (2018). Live imaging of type I collagen assembly dynamics in osteoblasts stably expressing gfp and mcherry-tagged collagen constructs. *J. Bone Miner. Res.* 33, 1166–1182. doi: 10.1002/jbmr.3409

Lu, Y., Xie, Y., Zhang, S., Dusevich, V., Bonewald, L. F., and Feng, J. Q. (2007). DMP1-targeted Cre expression in odontoblasts and osteocytes. *J. Dent. Res.* 86, 320–325. doi: 10.1177/154405910708600404

Madisen, L., Zwingman, T. A., Sunkin, S. M., Oh, S. W., Zariwala, H. A., Gu, H., et al. (2010). A robust and high-throughput Cre reporting and characterization

system for the whole mouse brain. *Nat. Neurosci.* 13, 133–140. doi: 10.1038/nn.2467

Mckee, M. D., Addison, W. N., and Kaartinen, M. T. (2005). Hierarchies of extracellular matrix and mineral organization in bone of the craniofacial complex and skeleton. *Cells Tissues Organs.* 181, 176–188. doi: 10.1159/000091379

Meijering, E., Dzyubachyk, O., and Smal, I. (2012). Methods for cell and particle tracking. *Methods Enzymol.* 504, 183–200. doi: 10.1016/B978-0-12-391857-4.00009-4

Murshed, M., Harmey, D., Millan, J. L., Mckee, M. D., and Karsenty, G. (2005). Unique coexpression in osteoblasts of broadly expressed genes accounts for the spatial restriction of ECM mineralization to bone. *Genes Dev.* 19, 1093–1104. doi: 10.1101/gad.1276205

Nefussi, J. R., Sautier, J. M., Nicolas, V., and Forest, N. (1991). How osteoblasts become osteocytes: a decreasing matrix forming process. *J. Biol. Buccale* 19, 75–82.

Ohashi, T., Kiehart, D. P., and Erickson, H. P. (1999). Dynamics and elasticity of the fibronectin matrix in living cell culture visualized by fibronectin-green fluorescent protein. *Proc. Natl. Acad. Sci. U.S.A.* 96, 2153–2158. doi: 10.1073/pnas.96.5.2153

Pacureanu, A., Langer, M., Boller, E., Tafforeau, P., and Peyrin, F. (2012). Nanoscale imaging of the bone cell network with synchrotron X-ray tomography: optimization of acquisition setup. *Med. Phys.* 39, 2229–2238. doi: 10.1118/1.3697525

Palumbo, C., Palazzini, S., Zaffe, D., and Marotti, G. (1990). Osteocyte differentiation in the tibia of newborn rabbit: an ultrastructural study of the formation of cytoplasmic processes. *Acta Anat.* 137, 350–358. doi: 10.1159/000146907

Prideaux, M., Findlay, D. M., and Atkins, G. J. (2016). Osteocytes: the master cells in bone remodelling. *Curr. Opin. Pharmacol.* 28, 24–30. doi: 10.1016/j.coph.2016.02.003

Ratnayake, D., and Currie, P. D. (2017). Stem cell dynamics in muscle regeneration: insights from live imaging in different animal models. *Bioessays* 39:1700011. doi: 10.1002/bies.201700011

Rothstein, E. C., Nauman, M., Chesnick, S., and Balaban, R. S. (2006). Multiphoton excitation microscopy in intact animals. *J. Microsc.* 222, 58–64. doi: 10.1111/j.1365-2818.2006.01570.x

Schulze, E., Witt, M., Kasper, M., Lowik, C. W., and Funk, R. H. (1999). Immunohistochemical investigations on the differentiation marker protein E11 in rat calvaria, calvaria cell culture and the osteoblastic cell line ROS 17/2.8. *Histochem. Cell Biol.* 111, 61–69. doi: 10.1007/s004180050334

Sivakumar, P., Czirok, A., Rongish, B. J., Divakara, V. P., Wang, Y. P., and Dallas, S. L. (2006). New insights into extracellular matrix assembly and reorganization from dynamic imaging of extracellular matrix proteins in living osteoblasts. *J. Cell Sci.* 119, 1350–1360. doi: 10.1242/jcs.02830

Thevenaz, P., Ruttimann, U. E., and Unser, M. (1998). A pyramid approach to subpixel registration based on intensity. *IEEE Trans. Image Process.* 7, 27–41. doi: 10.1109/83.650848

Tiede, L., Steyger, P. S., Nichols, M. G., and Hallworth, R. (2009). Metabolic imaging of the organ of corti–a window on cochlea bioenergetics. *Brain Res.* 1277, 37–41. doi: 10.1016/j.brainres.2009.02.052

Torreggiani, E., Matthews, B. G., Pejda, S., Matic, I., Horowitz, M. C., Grcevic, D., et al. (2013). Preosteocytes/osteocytes have the potential to dedifferentiate becoming a source of osteoblasts. *PLoS One* 8:e75204. doi: 10.1371/journal.pone.0075204

Toyosawa, S., Shintani, S., Fujiwara, T., Ooshima, T., Sato, A., Ijuhin, N., et al. (2001). Dentin matrix protein 1 is predominantly expressed in chicken and rat osteocytes but not in osteoblasts. *J. Bone Miner. Res.* 16, 2017–2026. doi: 10.1359/jbmr.2001.16.11.2017

Ubaidus, S., Li, M., Sultana, S., De Freitas, P. H., Oda, K., Maeda, T., et al. (2009). FGF23 is mainly synthesized by osteocytes in the regularly distributed osteocytic lacunar canalicular system established after physiological bone remodeling. *J. Electron. Microsc.* 58, 381–392. doi: 10.1093/jmicro/dfp032

Winkler, D. G., Sutherland, M. K., Geoghegan, J. C., Yu, C., Hayes, T., Skonier, J. E., et al. (2003). Osteocyte control of bone formation via sclerostin, a novel BMP antagonist. *EMBO J.* 22, 6267–6276. doi: 10.1093/emboj/cdg599

Xie, Y., Yin, T., Wiegraebe, W., He, X. C., Miller, D., Stark, D., et al. (2009). Detection of functional haematopoietic stem cell niche using real-time imaging. *Nature* 457, 97–101. doi: 10.1038/nature07639

Zamir, E. A., Rongish, B. J., and Little, C. D. (2008). The ECM moves during primitive streak formation–computation of ECM versus cellular motion. *PLoS Biol.* 6:e247. doi: 10.1371/journal.pbio.0060247

Zhao, W., Byrne, M. H., Wang, Y., and Krane, S. M. (2000). Osteocyte and osteoblast apoptosis and excessive bone deposition accompany failure of collagenase cleavage of collagen. *J. Clin. Invest.* 106, 941–949. doi: 10.1172/jci10158

Conflict of Interest Statement: The authors declare that the research was conducted in the absence of any commercial or financial relationships that could be construed as a potential conflict of interest.

frontiers in Cell and Developmental Biology

REVIEW
published: 19 July 2019
doi: 10.3389/fcell.2019.00135

Mechanochemical Signaling of the Extracellular Matrix in Epithelial-Mesenchymal Transition

*Lewis E. Scott, Seth H. Weinberg and Christopher A. Lemmon**

Department of Biomedical Engineering, Virginia Commonwealth University, Richmond, VA, United States

Epithelial-Mesenchymal Transition (EMT) is a critical process in embryonic development in which epithelial cells undergo a transdifferentiation into mesenchymal cells. This process is essential for tissue patterning and organization, and it has also been implicated in a wide array of pathologies. While the intracellular signaling pathways that regulate EMT are well-understood, there is increasing evidence that the mechanical properties and composition of the extracellular matrix (ECM) also play a key role in regulating EMT. In turn, EMT drives changes in the mechanics and composition of the ECM, creating a feedback loop that is tightly regulated in healthy tissues, but is often dysregulated in disease. Here we present a review that summarizes our understanding of how ECM mechanics and composition regulate EMT, and how in turn EMT alters ECM mechanics and composition.

Keywords: extracellular matrix (ECM), epithelial-mesenchymal transition (EMT), mechanobiology, cellular signaling, epithelial phenotype

OPEN ACCESS

Edited by:
Charles D. Little, University of Kansas Medical Center, United States

Reviewed by:
Lidija Radenovic, University of Belgrade, Serbia
Parthasarathy Chandrakesan, University of Oklahoma Health Sciences Center, United States

****Correspondence:***
Christopher A. Lemmon
clemmon@vcu.edu

Specialty section:
This article was submitted to Cell Adhesion and Migration, a section of the journal Frontiers in Cell and Developmental Biology

Received: *18 January 2019*
Accepted: *04 July 2019*
Published: *19 July 2019*

Citation:
Scott LE, Weinberg SH and Lemmon CA (2019) Mechanochemical Signaling of the Extracellular Matrix in Epithelial-Mesenchymal Transition. Front. Cell Dev. Biol. 7:135. doi: 10.3389/fcell.2019.00135

1. INTRODUCTION

Epithelial-Mesenchymal Transition (EMT) is a transdifferentiation process in which epithelial cells progressively lose key hallmarks of the phenotype, including strong cell-cell contacts, an apicobasal polarity, a cobblestone morphology, and collective migration. Loss of the epithelial phenotype corresponds with an acquisition of a mesenchymal one, with hallmarks including front-back polarity, independent migration, and an elongated cell shape. This process, along with the inverse process, Mesenchymal-Epithelial Transition, is absolutely critical to tissue patterning and organization in developing embryos. However, the past three decades have revealed that dysregulation of EMT is associated with a wide array of pathologies, including fibrotic diseases and cancer. Maintenance of the epithelial phenotype, and subsequent loss of the phenotype during EMT, are highly influenced and controlled by the surrounding extracellular matrix (ECM).

This review summarizes the myriad interactions between the ECM, epithelial polarization, cell migration, and EMT, and details the following progression of ECM/EMT interactions, illustrated in **Figure 1**: the composition of the basal lamina drives epithelial differentiation; during routine tissue remodeling, MMPs activate migration through structural changes to the ECM, release of bioactive fragments, and shedding of cell-bound receptors. Each of these events, intended to maintain healthy tissue, prevents an avenue for dysregulation. Conversion to a fibrillar matrix upregulates mesenchymal transcription factors and represses epithelial markers to drive EMT. In a feed-forward process, EMT in turn upregulates many of these fibrillar ECM components. In addition to presenting an ECM composition which facilitates the mesenchymal phenotype, fibrillar ECM also drives changes in tissue stiffness, which further add to epithelial repression and

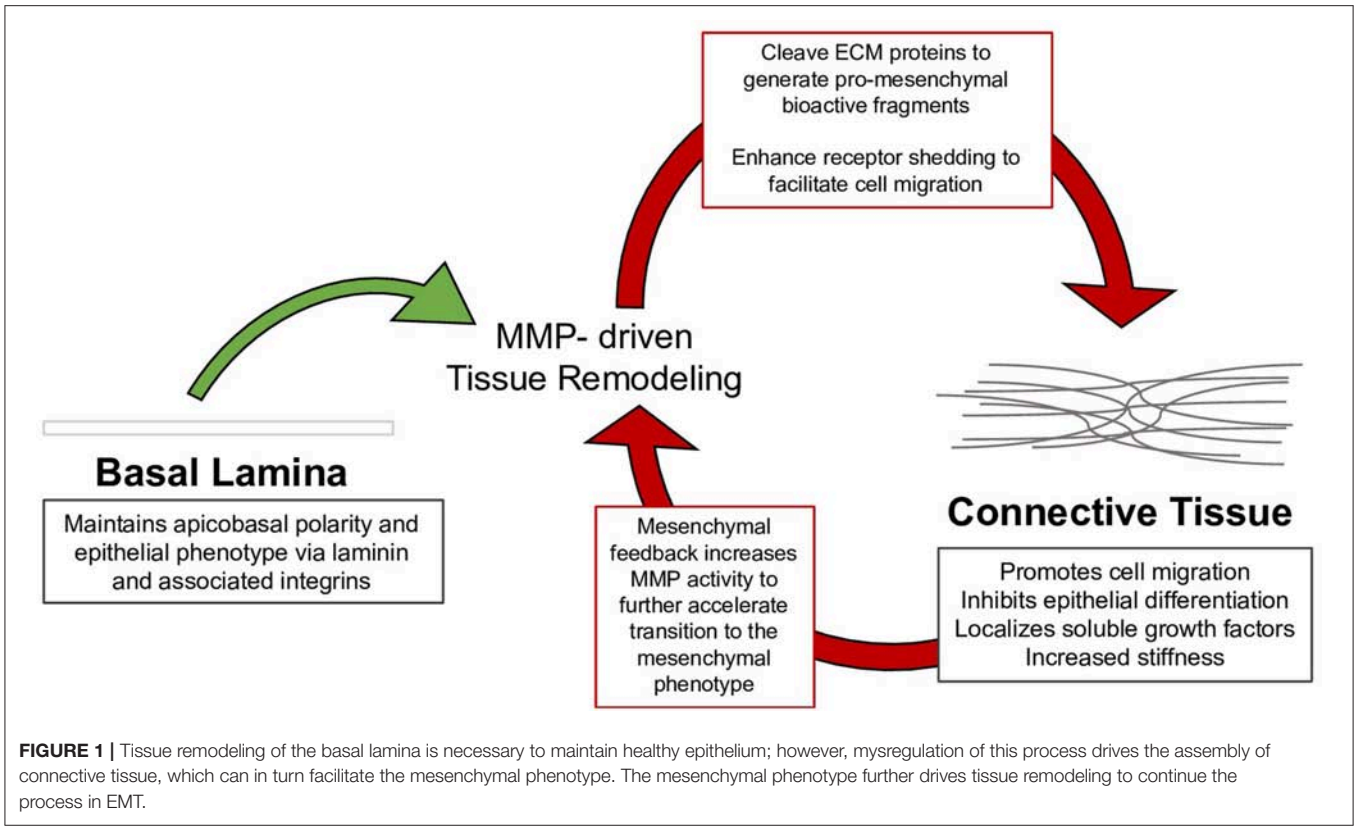

FIGURE 1 | Tissue remodeling of the basal lamina is necessary to maintain healthy epithelium; however, mysregulation of this process drives the assembly of connective tissue, which can in turn facilitate the mesenchymal phenotype. The mesenchymal phenotype further drives tissue remodeling to continue the process in EMT.

mesenchymal differentiation. Finally, a host of matricellular proteins modify the ECM response to further regulate EMT. Pathways involved in these processes are summarized in **Figure 2**.

2. THE BASAL LAMINA AND EPITHELIAL DIFFERENTIATION

In a polarized epithelium, attachment to the ECM orients the apicobasal axis by defining the basal surface (Morrissey and Sherwood, 2015). Basement membranes are thin, dense specialized ECM that self-assemble at the basal surface of the epithelial sheet as a structural scaffolding for epithelial attachment (McKee et al., 2007). The innermost layers of the basement membrane are the cell-adherent layers, and include the laminin-rich *lamina lucida* and the collagen IV-rich *lamina densa*. Together these layers, joined by glycoprotein nidogen and heparan sulfate proteoglycans perlecan, agrin, and collagen VII, comprise a supramolecular, reticular structure known as the basal lamina (Hohenester and Yurchenco, 2013).

2.1. Basal Lamina Establishes the Epithelial Apicobasal Polarity

Laminins are a family of glycoproteins consisting of an α-β-γ heterotrimer that forms three separate short arms (laminin-$\alpha_A\beta_B\gamma_G$) and an extended triple helical coiled-coil long arm arranged in a cross-like confirmation. Overlapping lateral interactions along the triple-helical domain and N- and C-terminal domains provides stability to the collagen IV network (Khoshnoodi et al., 2008). Collagen VII (Rousselle et al., 1997) and microfibril collagen VI (Yurchenco, 2011) stabilize the *lamina densa* and link it to the reticular lamina. Mammary epithelia exhibit normal physiological function when in contact with laminin, but lose this when exposed to fibrillar matrix components, such as collagen I and fibronectin. Developmental studies indicate that laminin not only maintains epithelial differentiation but is also the progenitor of the basement membrane and epithelial polarization during gastrulation (reviewed in Li et al., 2003), suggesting laminin contributes to epithelial differentiation rather than mesenchymal suppression (Zutter et al., 1995; Ramirez et al., 2011).

Laminins form a cell-adherent sheet-like matrix at the cell surface through interactions with its receptors. The laminin G domain located at the α-chain C-terminus of the long arm, together with adjacent coiled-coil domains, mediates cell attachment to integrin, dystroglycan, sulfated glycolipids, and heparan sulfate chains (Yurchenco and Patton, 2009). While laminin deposition and organization at the cell surface requires attachment to dystroglycan (Henry and Campbell, 1998; Henry et al., 2001) and β_1 integrin (Li et al., 2002), assembly of laminin into sheets occurs spontaneously (Hamill et al., 2009). The laminin specific integrin receptors $\alpha_3\beta_1$ and $\alpha_6\beta_4$ additionally contribute to the integrity of the epithelium by reinforcing cell-cell junctions: integrin $\alpha_3\beta_1$ is localized to the cytoplasmic plaque of cell-cell junctions, where it forms a complex with α-actinin and links the subcortical actin network to the catenin complex of cell-cell junctions (Wang et al., 1999); integrin $\alpha_6\beta_4$ is localized to a multiprotein complex known as the hemidesmosome,

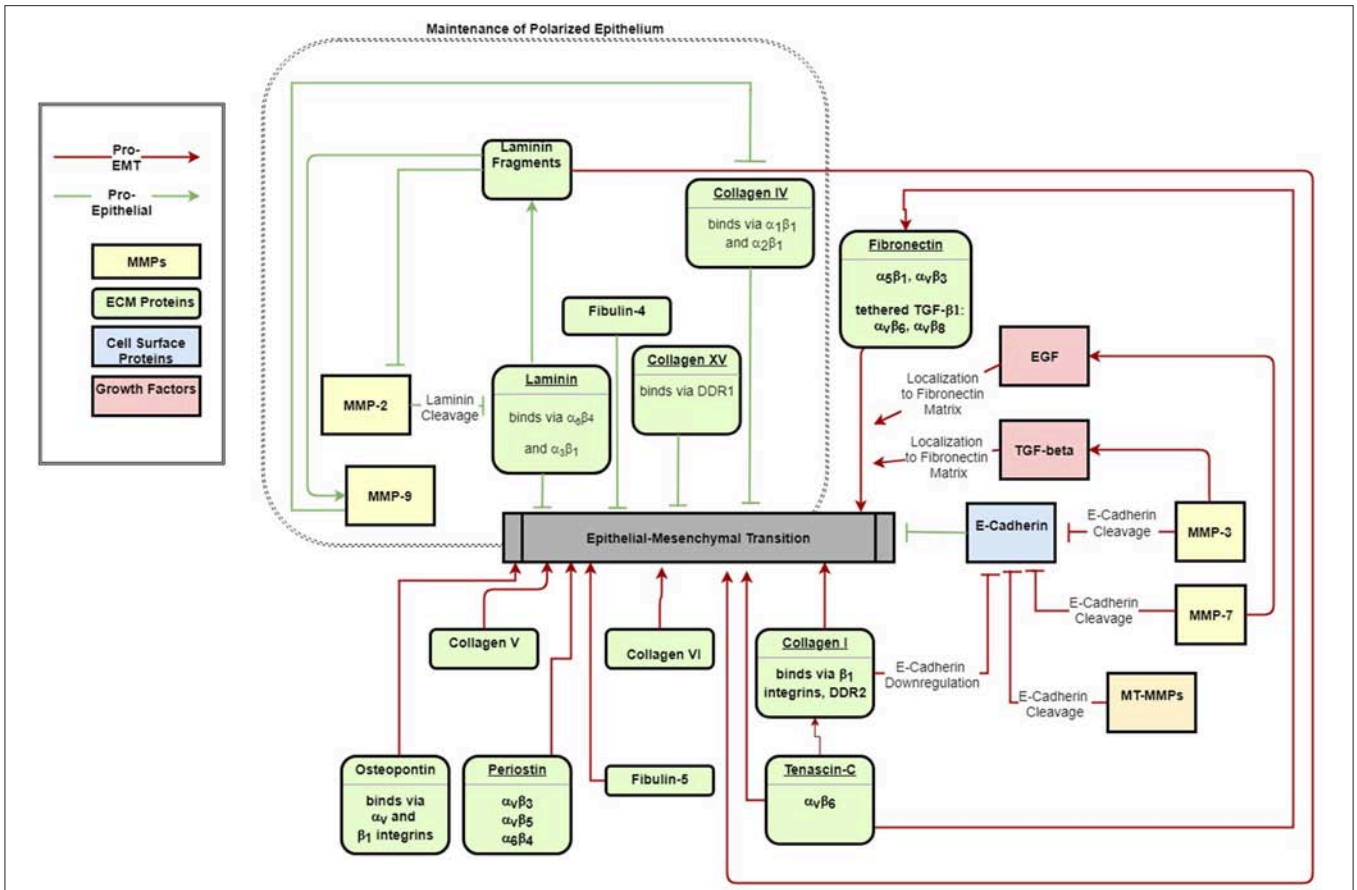

FIGURE 2 | ECM signals both maintain epithelial polarization (green arrows) and drive EMT (red arrows). The schematic indicates major ECM components that have been identified to activate or inhibit EMT.

which anchors the cytoskeleton to the basal lamina, provides attachment for intermediate filaments, and confers tensile strength to the epithelium (Borradori and Sonnenberg, 1999). Though not necessary for assembly, laminin-integrin ligation does stimulate small GTPases to restructure the cytoskeleton to support epithelial polarization (reviewed in Lee and Streuli, 2014). Integrin receptors for collagen and laminin were further shown to have a dynamic role in sensing the basal cue through distinct GTPase activity (Myllymäki et al., 2011): while $\alpha_6\beta_4$ (along with collagen receptor $\alpha_2\beta_1$) activates Rac-mediated actin cytoskeleton reorganization that guides apicobasal polarity, $\alpha_3\beta_1$ stimulates Cdc42-mediated microtubule rearrangement, which guides polarity complexes to the respective apical and basolateral domain. These contacts, together with a basement membrane linked to connective tissue, form a cohesive and mechanically coupled structure.

2.2. Basal Lamina Components Regulate EMT

Despite its role in maintaining epithelial differentiation, elements of the basal lamina can also promote EMT and tumor growth. For example, laminin receptors $\alpha_3\beta_1$ and $\alpha_6\beta_4$ have been implicated in EMT and cancer progression. In a study of keratinocytes, $\alpha_3\beta_1$ and $\alpha_6\beta_4$ integrin ligation was sufficient to form tumors despite abnormal cell attachment (Waterman et al., 2007). Deletion of the $\alpha_3\beta_1$ gene itga3 deletion prevented tumor initiation with an associated decrease in downstream activation of EMT-linked FAK, Rac1, MAPK, and JNK pathways (Cagnet et al., 2014). Studies of alveolar epithelium (Kim et al., 2009a,b) and hepatocellular carcinoma (Giannelli et al., 2005) demonstrate cooperative activity between $\alpha_3\beta_1$ and transforming growth factor β_1 (TGF-β1) to suppress the epithelial phenotype. Colocalization and endocytosis of $\alpha_3\beta_1$ with the TGF-β receptor type I (TGFβRI) receptor led to phosphorylation of Smad2 and of β-catenin on Y654, resulting in formation of a pSmad2-Y654-β-catenin complex, though it is unclear how this complex suppresses the epithelial phenotype. A separate study in immortalized mouse keratinocytes demonstrated that $\alpha_3\beta_1$-TGF-β1 cooperativity induces tissue remodeling of the basal lamina by stimulating MMP9 (Sugiura and Berditchevski, 1999; Morini et al., 2000) and induces epithelial transcriptional suppressors, Snail and Slug (Zhang et al., 2003). Hepatocellular carcinomas overexpressing $\alpha_6\beta_4$ exhibit aberrant cell proliferation and invasion associated with downregulation of the epithelial phenotype by PI3K/Akt signaling dependent upregulation of Slug (Li et al., 2017).

In addition, collagen IV, which is a primary component of the basement membrane, can suppress epithelial differentiation and induce expression of the EMT transcription factors Snail and Slug. Hepatocellular carcinomas express collagen IV receptors $\alpha_1\beta_1$ and $\alpha_2\beta_1$ to facilitate local invasion across the basal lamina and lamina reticularis (Yang et al., 2003). In mammary epithelial cells, collagen IV induces epithelial repressors Snail and Slug by upstream FAK/ERK signaling and NFκB activation (Espinosa Neira and Salazar, 2012).

Another component of the basement membrane is Collagen XV, which forms an unusual supramolecular structure resembling a figure-of-eight/pretzel configuration (Myers et al., 2007). This structure links banded fibrils in the basement membrane (Amenta et al., 2005) to provide tensile strength and join the basement membrane to connective tissue. Collagen receptor discoidin domain receptor 1 (DDR1) is distributed to the lateral membrane of epithelium to stabilize cell-cell junctions. This suppresses Cdc42 activity (Wang et al., 2009) and prevents $\alpha_2\beta_1$-DDR1 cooperative activation of migration. In pancreatic adenocarcinoma cells, collagen XV was shown to stabilize cell-cell junctions by DDR1, suggesting antagonistic EMT potential (Clementz et al., 2013).

3. TISSUE REMODELING AND EMT

Tissue remodeling in development (Brauer, 2006) and tissue repair (Page-McCaw et al., 2007; Rodríguez et al., 2010) requires fine spatiotemporal control over ECM degradation, which is often dysregulated in fibrosis (Giannandrea and Parks, 2014; Craig et al., 2015; Pardo et al., 2016) and cancer progression (Nabeshima et al., 2002; Têtu et al., 2006; Kessenbrock et al., 2010; Deryugina and Quigley, 2015). Through ECM and growth factor proteolysis, matrix metalloproteinases (MMPs) modify the molecular and mechanical characteristics of the extracellular microenvironment to facilitate cellular migration (Sternlicht and Werb, 2001). MMPs consist of a catalytic domain, an autoinhibitory prodomain, and hemopexin domain. The six classifications of MMPs–collagenase, gelatinase, stromelysin, matrilysin, membrane-type and non-classified MMPs–delineate substrate specificity that is further tied to cellular and extracellular localization (Nagase et al., 2006). Functionally, MMPs regulate motility motifs by proteolytically processing ECM components and its sequestered latent signals, as well as membrane receptor docking and shedding (Sternlicht and Werb, 2001). Receptor docking spatially confines remodeling, whereas proteolytic byproducts act as soluble signals to engage feedback loops that temporally maintain ECM degradation.

3.1. Growth Factors and Bioactive Fragments Activate EMT

Beyond the structural effects on ECM, MMP proteolytic processing of the basal lamina produces bioactive fragments (Horejs, 2016), many of which regulate angiogenesis (Xu et al., 2001) and migration (Horejs et al., 2014) in a paracrine fashion. For example: Collagen IV fragment α_5(IV) binds collagen receptor DDR1, preventing distribution to cell-cell junctions, and activates ERK (Xiao et al., 2015), a downstream signal of TGF-β1-induced EMT (Xie et al., 2004; Buonato and Lazzara, 2014), and a laminin-111 β-chain fragment competitively binds $\alpha_3\beta_1$ integrin to upregulate mesenchymal markers and switch gelatinase A (MMP2) production in the inner lamina lucida to gelatinase B (MMP9) in the outer lamina densa and reticular lamina.

Additionally, MMPs dock with cell adhesion receptors, facilitating proteolytic activation of latent signaling molecules sequestered within the ECM and inducing survival and migratory signaling pathways (Illman et al., 2006; Chaturvedi and Hass, 2011; Mori et al., 2013). Redistribution of MMPs to the migratory front mediates focal proteolysis that is spatially confined to the invadopodia (reviewed in Jacob and Prekeris, 2015): gelatinases (Yu and Stamenkovic, 2000), stromelysin (MMP3) (Maeda et al., 2002), and membrane type (MT)-MMPs (Mu et al., 2002) each proteolytically activate latent form of TGF-β1, and the subsequent TGF-β1 signaling upregulates gelatinases, creating a self-sustaining loop of matrix remodeling (Krstic and Santibanez, 2014). To this point, knockdown of MMP9 abrogated mesenchymal markers and inhibited TGF-β1-induced invasion and migration in a study of esophageal squamous cell carcinoma (Bai et al., 2017).

3.2. Receptor Shedding Enhances Mobility

Another means by which tissue remodeling drives EMT is through MMP-mediated receptor shedding. MT-MMP (Rozanov et al., 2004), MMP3 (Yamashita et al., 2011), MMP9, and matrilysin (MMP7) (McGuire et al., 2003) localize to adherens junctions to shed the E-cadherin ectodomain, producing a soluble fragment frequently increased in the serum of cancer patients (Repetto et al., 2014). The 80 kDa ectodomain fragment acts as a paracrine/autocrine signal that reduces cell aggregation by competitive homophilic binding with E-cadherin (Noe et al., 2001) and promotes MMP production via EGFR (David and Rajasekaran, 2012). MMP3 additionally cleaves E-cadherin, which specifically activates Rac1 splice variant Rac1b that in turn activates ROS/Snail (Radisky et al., 2005).

3.3. EMT Induces MMP Production

Soluble factors released during tissue remodeling can induce EMT, which in turn stimulates MMP production to sustain remodeling of the ECM for migration (reviewed in Gilles et al., 2013 and Bonnans et al., 2014). Activation of EMT transcription factors corresponds with an increased secretion of gelatinases in human mammary breast cancer epithelium (Octavio et al., 2015) and oral squamous cell carcinoma (Qiao et al., 2010). Specifically, Slug directly enhances MMP1 transcription in breast cancer cells (Shen et al., 2017a) as well as MMP9 in oral squamous cell carcinoma (Joseph et al., 2009), and Snail upregulates MMP9 in MDCKs (Jordà et al., 2005). Additionally, Kruppel-like factor 8 (KLF8), a downstream transcription factor of TGF-β1 signaling, upregulates MMP9 (Wang et al., 2011) and MT1-MMP, both directly (by activating MT1-MMP promoter) and indirectly (through β-catenin nuclear translocation and TCF1 upregulation) (Lu et al., 2014). Proteolytically activated growth

factors induce these transcription factors, resulting in a positive feedback loop. TGF-β1-dependent EMT triggers gelatinases in oral squamous cell carcinoma by upregulated Snail (Qiao et al., 2010) and MMP10 in keratinocytes (Wilkins-Port and Higgins, 2007). Wnt stimulates MMP production that amplifies tissue remodeling and cell mobility. For example, MT3-MMP is a soluble and membrane bound proteinase that cleaves pro-MMP2 and is associated with progression of hepatocellular (Wu et al., 2007) and colorectal (Shen et al., 2017b) carcinomas.

4. CONNECTIVE TISSUE AND MESENCHYMAL DIFFERENTIATION

4.1. Fibrous Matrix Promotes Attachment and Migration

Unlike the basal lamina, the ECM of connective tissue is fibrillar and primarily deposited by activated fibroblasts (Hosper et al., 2013). Assembly of fibrillar matrix on the basement membrane plays a significant role in repressing the epithelial phenotype and inducing EMT. The primary component of connective tissue, fibrillar collagen, is crudely aligned parallel to the basal lamina to provide mechanical support by resisting tensile forces. Non-fibrillar collagens, proteoglycans, and glycoproteins organize the fibrillar matrix and link the connective tissue to the basement membrane. Fibronectin, a 230–270 kDa fibrous homodimer glycoprotein, provides a scaffold for cell attachment and *de novo* fibrillogenesis (Hynes, 1982). Secreted as a soluble dimer, maturation of the fibronectin matrix requires integrin attachment and cell contractility for polymerization into an insoluble fibrillar matrix (Mao and Schwarzbauer, 2005; Weinberg et al., 2017). Integrin binding facilitates fibronectin stretch, which exposes additional binding sites for ECM deposition and growth factor binding (Singh et al., 2010). As a scaffold for *de novo* ECM assembly, polymerized fibronectin provides binding sites for collagenous matrix deposition (Sottile et al., 2002). However, in a negative feedback loop that halts *de novo* ECM synthesis, maturation of collagenous matrix stabilizes polymerized fibronectin but shields it from cell contractility (Kubow et al., 2015).

Integrin and syndecan receptors link the fibronectin matrix to the cytoskeleton and signaling pathways during migration (Elfenbein and Simons, 2013). Integrins $\alpha_5\beta_1$ and $\alpha_v\beta_3$ dynamically bind to the fibronectin matrix to extend pseudopodia and form contractile filaments via small GTPases (Morgan et al., 2009). Fibronectin binding organizes nascent cell contacts into stable focal adhesions that activate the conventional integrin signaling pathways associated with growth and motility. Antagonistic $\alpha_5\beta_1$ recycling to the migratory front maintains cell-matrix adhesion whereas $\alpha_v\beta_3$ is recycled to the migratory front to form nascent focal adhesions to fibronectin and stimulate Rac-mediated cytoskeletal rearrangement (White et al., 2007; Lawson and Burridge, 2014). The sustained β_1 integrin signaling stimulates Rho-mediated contractility as the nascent adhesion moves peripherally to centrally and matures to a fibrillar adhesion near the center and posterior of the cell. Syndecan, as a co-receptor for cell attachment, facilitates integrin clustering into focal adhesions (Woods et al., 2000); mediates small GTPase activity (Bass et al., 2007; Brooks et al., 2012); regulates extracellular matrix assembly (Klass et al., 2000); and, specifically, binds to the fibronectin type III_{12-14} heparin-binding domain adjacent to $\alpha_5\beta_1$ to facilitate cell attachment (Tumova et al., 2000).

Collagens form the bulk of connective tissue, consisting of a family of 28 members classified as either fibril forming or network forming (Ricard-Blum, 2011). Three polypeptide α-chains of repeating gly-X-Y sequence and interrupting non-collagenous domains form a helical trimer, which is stabilized by glycine, proline and hydroxyproline, hydrogen bonds, and electrostatic interactions, allowing collagen to assemble unique structures and participate in biological activity (Shoulders and Raines, 2009). Collagen receptors β_1 integrin heterodimers (α_1, α_2, α_{10}, and α_{11}) and DDRs relay adhesion signals at the cell-cell and cell-matrix interface to exert transcriptional regulation of migration and survival signaling pathways (Boraschi-Diaz et al., 2017). DDR1 stabilizes adherens junctions in the stable epithelium but redistributes to cell-matrix focal adhesions to regulate motility (Huang et al., 2009; Chen et al., 2016). Minor collagens, elastic fibers, and proteoglycans support fibrillar collagens to confer structural integrity to connective tissues (Frantz et al., 2010). Collagen V associates with fibrillar collagens I and III to regulate assembly, and collagen VI to stabilize the ECM (Mak et al., 2016). Collagen VI forms beaded filament networks at the stroma-basement membrane interface and organizes three-dimensional tissue architecture by linking connective tissue with collagen IV (Kuo et al., 1997) and laminin (Cescon et al., 2015) of the basal lamina.

Proteoglycans, owing largely to their glycosaminoglycan polysaccharide chains, hydrate tissues and provide mechanical support by resisting compression. Hyaluronan, a glycosaminoglycan synthesized by hyaluronan synthase (HAS), is secreted in a high molecular weight form consisting of N-acetylglucosamine and glucuronic acid repeats. The hyaluronan receptor CD44 activates Src, Rho, and Ras signaling pathways to alter cytoskeletal arrangement and promote motility (Turley et al., 2002). CD44 in particular regulates mobility by interacting with and stimulating production of MMPs. For example, hyaluronan-CD44 binding stimulates gelatinase secretion to regulate cancer invasion (Park et al., 2002; Zhang et al., 2002; Guo et al., 2012) and MMP9 docks with CD44 to remodel the ECM at the invasive front (Peng et al., 2007). Thus, hyaluronan and its receptors mediate mobility through connective tissue.

4.2. Fibrillar Matrix Inhibits Epithelial Differentiation

Dysregulation of fibrillar matrix is widely implicated in fibrosis (Karsdal et al., 2017) and cancer progression (Fang et al., 2014; Kaushik et al., 2016; Wang and Hielscher, 2017), owing to the suppression of epithelial differentiation (Shintani et al., 2008b). As a downstream target of Wnt (Gradl et al., 1999) and TGF-β1 (Kolosova et al., 2011) signaling, fibronectin is a marker of mesenchymal differentiation (Petrini et al., 2016). Fibronectin accumulation at cleft-forming sites during salivary gland and lung branching morphogenesis induces Slug to suppress the

epithelial phenotype (Onodera et al., 2010). At the invadopodia, $\alpha_v\beta_3$ ligation induces Slug expression (Knowles et al., 2013) and $\alpha_5\beta_1$ integrin stimulates Rho-mediated contractility (Mierke et al., 2011).

Fibrillar collagens, acting through canonical β_1 integrin/FAK/Src signaling, suppress epithelial differentiation at the transcriptional level and disrupt the cadherin complex to enhance cell mobility (reviewed in Imamichi and Menke, 2007). In ovarian and prostate cancer cells, collagen-β_1 binding alters E-cadherin expression through both PI3K- (Cheng and Leung, 2011) and Src-dependent mechanisms (Menke et al., 2001). Collagen I promotes Snail and LEF1 through ILK-dependent activation of NF-κB and inhibition of GSK3β, which drives transcriptional activation of Snail (Medici and Nawshad, 2010). In a separate study of pancreatic carcinoma cells, DDR1 and β1 integrin concomitant activation converges on JNK signaling to increase expression of N-cadherin (Shintani et al., 2008a), which is a marker of EMT. However, H-Ras-induced Zeb reduces DDR1 expression in mammary epithelial cells, suggesting a negative feedback loop during EMT (Koh et al., 2015).

Given its role in maintaining adherens junctions, collagen-DDR signaling may indicate a switch from cell-cell to cell-matrix adhesion. Switching from epithelial-associated to mesenchymal-associated DDR drives mesenchymal differentiation by activating and stabilizing EMT transcription factors Snail and Zeb, and by inducing gelatinases to promote invasion (reviewed in Rammal et al., 2016). Collagen I-DDR2 ligation induces invasion of metastatic mammary epithelium *in vivo* and *in vitro* by activating Src/ERK signaling to phosphorylate Snail, which facilitates stabilization and nuclear translocation (Zhang et al., 2013). Similarly, in human renal proximal tube epithelial cells, increased DDR2 expression by TGF-β1 suppresses epithelial differentiation via NF-κB and LEF-1 activation (Walsh et al., 2011). As a result, fibrillar collagens, specifically type I and III, are potent suppressors of epithelial differentiation, reducing cell aggregation by transcriptional regulation and disrupting junctions.

Reinforcing other collagenous components of connective tissue also regulates EMT. As a gene target of TGF-β1, aberrant collagen V expression is characteristic of fibrosis and cancer in various tissues (Mak et al., 2016). Overexpression of collagen V in idiopathic pulmonary fibrosis is driven via both a Twist-dependent mechanism (Lei et al., 2016) and STIM1, an endoplasmic reticulum Ca^{2+} sensor that regulates Ca^{2+} influx and promotes invasion of colorectal cancer (Zhang et al., 2015, 2017). Co-immunoprecipitation identified TGF-β1 and MMP2 as binding partners of collagen V (Symoens et al., 2011), suggesting collagen V sequesters TGF-β1 and MMP2 in the ECM to restrict bioavailability and exert spatiotemporal control over tissue remodeling. Collagen VI and its non-integrin receptor NG2, a transmembrane chondroitin sulfate proteoglycan, are highly expressed in tumors (reviewed in Chen et al., 2013) and at the invasive front (Park and Scherer, 2012) where they synergize with canonical TGF-β1 signaling to enhance EMT. NG2 stabilizes cytoplasmic β-catenin and phosphorylates GSK3β downstream of β_1 integrin-induced Akt (Chekenya et al., 2008), resulting in activation of TCF/LEF and nuclear accumulation of β-catenin (Iyengar et al., 2005).

Hyaluronan is another key component of the connective tissue ECM that stimulates EMT. CD44 mediates hyaluronan-induced invasion through interactions with MMPs that result in focal proteolysis and CD44 cleavage: CD44 ligation localizes MMP9 to the migratory front where it remodels the ECM and cleaves CD44 (Chetty et al., 2012). MT1-MMP additionally localizes to invadopodia where it sheds the CD44 ectodomain to promote motility (Kajita et al., 2001). Aberrant expression of hyaluronan is observed in the tumor stroma of breast, lung, and prostate cancer; urine of bladder cancer; and serum of ovarian, head and neck, and prostate cancer(reviewed in Chanmee et al., 2016) where it primes the cell and microenvironment for invasion(reviewed in Toole, 2004). Hyaluronan induces LOX-mediated matrix stiffening, FAK/Erk signaling, and Twist downstream of CD44 in the progression of breast carcinoma (El-Haibi et al., 2012). In addition, downstream PI3K/Akt and GSK3β phosphorylation results in β-catenin nuclear translocation (Zoltan-Jones et al., 2003), suggesting hyaluronan regulates the epithelial phenotype by inhibiting the catenin complex formation. Despite accumulation in the tumor microenvironment and association with aggressiveness, neither hyaluronan nor CD44 are required to induce mesenchymal transcriptional promoters. Instead, hyaluronan synthase 2 (HAS2) regulates TGF-β1-induced EMT in normal murine mammary gland cells independent of hyaluronan synthesizing activity (Porsch et al., 2013). Knockdown of HAS2 resulted in decreased TGF-β1-induced migration, suggesting a potential role downstream of TGF-β1 signaling. Thus, hyaluronan, along with its synthase and CD44 receptor, not only create a microenvironment to support migration, but also actively suppress epithelial proteins to promote EMT.

4.3. Connective Tissue Regulates Soluble Factor Localization

Just as in the basal lamina, proteoglycans of connective tissue sequester soluble factors as a means to regulate bioavailability or to spatially confine activation. Neighboring the primary cell attachment domain of fibronectin, a growth factor binding domain localizes growth factor signaling near the cell attachment for simultaneous activation of signaling pathways that promote survival and migration (Vega and Schwarzbauer, 2016). One example of this in EMT is the latent TGF-β-binding protein (LTBP), which binds to fibronectin at the type III12-14 repeat and sequesters TGF-β1 in a conformationally latent form until mechanically or proteolytically activated (Zilberberg et al., 2012; Robertson et al., 2015). Confining TGF-β1 to the ECM in this latent form allows for spatial and temporal control over TGF-β1 activation (Rifkin, 2005). In the ECM-bound latent form, TGF-β1 is activated through cell contractility or proteolytic cleavage. The α_v integrins, namely $\alpha_v\beta_6$ and $\alpha_v\beta_8$, bind to the RGD sequences in fibronectin and latent TGF-β complex LAP to conformationally alter LAP and activate TGF-β1 (Mamuya and Duncan, 2012).

Taken together, conventional integrin signaling and growth factor availability regulation represent two distinct but interacting mechanisms by which fibrillar ECM regulates

EMT (Hynes, 2009). Previous studies of mammary breast epithelium suggest fibronectin, but not laminin, is necessary for TGF-β1-induced EMT, likely due to binding the fibronectin receptor $\alpha_5\beta_1$ integrin and latent TGF-β1 localization (Park and Schwarzbauer, 2014; Griggs et al., 2017). Fibronectin receptor $\alpha_v\beta_3$ integrin has also been shown to phosphorylate TGFβRII at Y284 to activate p38/MAPK signaling, separately from canonical Smad signaling, and promote tumor invasion (Galliher and Schiemann, 2007).

4.4. Tissue Mechanics Inhibit Epithelial Differentiation

In addition to the compositional aspects of ECM-EMT regulation, the mechanical properties of the ECM play a key role in regulating epithelial differentiation and EMT. Prior studies have demonstrated that induction of EMT is dependent on the mechanical properties of the underlying tissue; *in vitro*, TGF-β induces EMT on surfaces with a high elastic modulus, but induces apoptosis on surfaces with a lower elastic modulus (Leight et al., 2012). Inherent tension within a tissue also induces EMT; areas of higher stress within a colony of epithelial cells correlates with EMT, while ares of lower stress maintain the epithelial phenotype (Gomez et al., 2010). As such, the mechanics of the ECM play a critical role in driving EMT.

Mechanical coupling between a cell and its environment allows for rapid signal transduction and propagation across the tissue. Mechanotransducers, the cell adhesion receptors and focal adhesion proteins that link the ECM to the cytoskeleton and intracellular signaling cascades, reorient the cytoskeleton to mitigate anisotropic tension (Tseng et al., 2012). Expression of the EMT marker vimentin, which is assembled into intermediate filaments, has been shown to enhance mechanotransduction (Conway and Schwartz, 2014) and mediate growth of focal adhesions (Liu et al., 2015); similarly, organization of the microtubule network regulates both contractile and propulsive force generation (Kent and Lele, 2016), which facilitates migration and protrusion during EMT (Whipple et al., 2010; Gu et al., 2016). Although connective tissue lacks the inherent organization of self-assembled basal lamina, tension pulls the fibers into alignment, parallel to the direction of applied force. The fibrillar components stiffen the ECM and shift cell adhesion and cytoskeletal arrangement toward a migratory scheme.

Deposition and organization of the ECM is sensitive to substrate stiffness (Eisenberg et al., 2011). Fibronectin assembly correlates with substrate stiffness (Williams et al., 2008; Scott et al., 2015), which is not the case with self-assembled laminin in basal lamina. A proposed mechanism suggests stretch of fibronectin type III repeats exposes additional growth factor and ECM binding sites (Weinberg et al., 2017). Stiffer matrices promote greater fibrillogenesis, which in turn facilitates excessive matrix deposition, growth factor tethering, and further stiffening of the ECM (Kubow et al., 2015). It has been proposed that one possible role for collagen in fibronectin deposition is to provide a rigid collagen network that increases tension in the matrix to facilitate fibronectin assembly (Singh et al., 2010). This mechanism would be similar to the tensional effects of cell-cell interactions on fibronectin assembly in Xenopus embryos (Dzamba et al., 2009).

Mechanical feedback at cell-matrix interfaces is an important regulator of EMT (Le Bras et al., 2012). In addition to matrix deposition, the effects of matrix stiffening may enhance signaling of tethered growth factors. In alveolar epithelial cells, fibronectin facilitates stiffness-dependent EMT induced by TGF-β. The requirement for integrin α_v that binds both fibronectin and the TGF-β1 complex suggests cell contractility mediates the substrate stiffness response to TGF-β1-induced EMT (Markowski et al., 2012; Brown et al., 2013). The α_v integrin activates latent TGF-β, which in turn induces LOX production (Sethi et al., 2011; Voloshenyuk et al., 2011), crosslinks collagen, and stiffens the ECM. Together, these findings suggest integrin receptors mediate the stiffness trends of fibronectin-TGF-β1 activation of EMT in a contractility-dependent manner. In NMuMG cells, matrix rigidity regulates the switch between TGF-β1 induced apoptosis and EMT via FAK/PI3K/Akt signaling (Leight et al., 2012). Additionally, ECM stiffness plays a role in nuclear signaling: nuclear localization of Twist is observed with increased substrate stiffness due to β_1 integrin activation (Wei et al., 2015); Yes-associated protein (YAP) and transcriptional co-activator with PDZ binding motif (TAZ) are nuclear relays of matrix rigidity downstream of Rho GTPase (Dupont et al., 2011); and nuclear translocation of Hippo effectors YAP and TAZ regulate a RhoA-dependent feedforward mechanism (Calvo et al., 2013) of cell spreading that controls focal adhesion assembly (Nardone et al., 2017). Mechanical feedback also drives rearrangement of cytoskeletal components in EMT, which in turn, can drive EMT (reviewed in Sun et al., 2015).

Similarly, mechanical signaling facilitates events at the cell-cell junction. Cadherin complexes transduce tension between adjacent cells during early epithelialization (Huang et al., 2012). Adherens junctions recruit actin to reinforce adhesion on substrates of high traction stress and strain (Collins et al., 2017). Tensile forces that are exerted on cadherin complexes result in the unfolding of α-catenin to reveal cryptic vinculin-binding sites, which nucleate polymerization of new actin microfilaments (Yonemura et al., 2010). G-actin depletion from the cytoplasmic pool stimulates nuclear accumulation of myocardin-related transcription factor (MRTF)-A, a regulator of actin alignment, to promote cellular contraction (O'Connor et al., 2015). MRTF-A activity also regulates myogenic features (Seifert and Posern, 2017), and is a downstream mediator of TGF-β1-induced EMT (Gomez et al., 2010).

5. THE FUNCTIONAL ROLE OF ECM MATRICELLULAR PROTEINS

In addition to the specific ECM components discussed here, there are a host of non-structural matricellular proteins that play a role in EMT signaling. A functional role is observed both in the extracellular environment, by soluble signal sequestering and receptor binding, and the intracellular environment, by orchestrating cytoskeletal arrangement or

activating mesenchymal transcriptional promoters. Matricellular proteins also are involved in the cellular mechanical response, as mechanosensor integrins are receptors for many of the proteins.

5.1. Osteopontin

Osteopontin is a 44 kDa aspartic acid rich, N-linked glycosylated phosphoprotein with widespread expression across tissues. The osteopontin receptors, integrins α_v and β_1, and CD44, stimulate tissue remodeling, inflammation, and biomineralization signaling pathways. Due to its role in tissue remodeling and inflammation, aberrant expression is frequently associated with fibrosis and cancer (reviewed in Zhao et al., 2018), owing to induction of the mesenchymal pathways PI3K and MAPK and canonical transcriptional regulators Twist, Snail, and Zeb (Kothari et al., 2016). Together, these suggest osteopontin potently elicits EMT, further supported by the interaction with TGF-β1 to activate fibroblasts for tissue remodeling.

5.2. SPARC

Secreted protein acidic and rich in cysteine (SPARC) is a glycoprotein consisting of Ca^{2+} binding domains and a disulfide, copper binding follistatin domain. SPARC influences collagen I and IV organization, and sequesters growth factors to inhibit receptor binding (reviewed in Murphy-Ullrich and Sage, 2014). Overexpression is observed in a number of cancers (Arnold and Brekken, 2009) and is accompanied by increased expression of mesenchymal markers. Epidermal melanocytes exhibit E-cadherin suppression as a result of increased expression of Snail (Robert et al., 2006) and Slug dependent on PI3K/Akt signaling (Fenouille et al., 2012).

5.3. Periostin

Periostin consists of four alternatively spliced isoforms that consist of a small cysteine-rich module, fasciclin-like domains, and a hydrophilic carboxy terminal. The fasciclin-like domains mediate cell adhesion, while the hydrophilic carboxy terminal binds ECM proteins, such as collagen, fibronectin, tenascin-C, and heparin. Periostin is both a marker and promoter of EMT, which contributes to the progression of a number of tumor types (Morra and Moch, 2011). Expression is regulated by EMT transcription factor Twist and growth factors TGF-β1, BMP-2, PDGF, bFGF, TNFα, IL-4, IL-13, angiotensin II, and oncostatin (González-González and Alonso, 2018). Studies indicate periostin elicits a pronounced EMT response by downregulating miR-381, a Twist and Snail repressor, via MAPK (Hu et al., 2017).

5.4. Tenascin

Tenascins are a four member family of ECM glycoproteins consisting of N-terminal heptad repeats, EGF-like repeats, fibronectin type III repeats, and a C-terminal fibrinogen-like globular domain (Hsia and Schwarzbauer, 2005). Tenascin-C assembles into hexamers that regulate integrin, proteoglycan, and immunoglobulin binding to the ECM, primarily through interactions with fibronectin. FAK phosphorylation and Src activity together with β-catenin nuclear localization suggest tenascin induces EMT by integrin binding (Yoshida et al., 2015). TGF-β1 stimulates significantly greater tenascin-C secretion for mesenchymal cells relative to epithelial cells via ERK/MAPK but not PI3K signaling (Maschler et al., 2004).

5.5. Fibulin

Fibulins are a five isoform family of alternatively spliced anaphylatoxin-like repeats, calcium binding EGF-like repeats, and a fibulin-type carboxyl terminus. Calcium ligation confers structural stability to fibulin and elasticity to the ECM. Fibulins assemble into microfibrils that bind with other components of the ECM. Fibulin-4 knockdown significantly decreased expression of E-cadherin and increased expression of N-cadherin, vimentin, Snail, Slug, and Twist. Endometrial fibroblasts also exhibited a significant decrease in vimentin and α-smooth muscle actin when co-cultured with fibulin-4 expressing endometrial epithelial cells (Wang et al., 2017). Fibulin-5 contains an RGD-motif, and mediates binding to integrin receptors $\alpha_4\beta_1$, $\alpha_5\beta_1$, $\alpha_9\beta_5$, $\alpha_v\beta_3$, and $\alpha_v\beta_5$ (Yanagisawa et al., 2009). Fibulin-5 initiates EMT and is also a gene target of TGF-β1, indicated by Twist expression. In addition, fibulin-5 stimulated gelatinase proteolytic activity (Lee et al., 2008).

6. COMMENTARY AND OUTLOOK

In this review, we have summarized work that highlights the important role of healthy epithelial ECM in maintaining epithelial polarization, while also investigating how fibrillar ECM drives EMT, with a focus on the roles of both soluble signals embedded in the ECM and the mechanical properties of the ECM. We have also discussed how the EMT process itself remodels the ECM to enable EMT progression.

While many aspects of the bidirectional regulation between the ECM and EMT signaling are well-understood, there are also key aspects of these signaling processes that remain to be fully elucidated. Although many individual pieces of these physiological puzzles have been studied in isolation, the emergent responses *in vivo* are inherently more complicated to understand. For example, which mechanochemical interactions that drive dynamics are critical for epithelial polarization and EMT, and which signaling pathways act in parallel and provide redundancy? Further, what are the mechanisms driving these individual interactions between mechanics and composition at the molecular and biophysical level? Additionally, what processes and features are cell type and/or species dependent, which is a critical question to understand ultimately what aspects of epithelial maintenance and EMT suppression can be critically translated? Studies that probe these questions represent the next steps forward in understanding the complex interactions between ECM and EMT.

AUTHOR CONTRIBUTIONS

LS, SW, and CL collectively formulated the structure and content of the review paper, wrote sections of the manuscript, and collectively edited the final manuscript.

ACKNOWLEDGMENTS

This work was supported through the National Institutes of Health/National Institute of General Medical Sciences via Grant R01-GM115678 (CL, SW) and R01-GM122855 (CL, SW, LS). The authors would like to acknowledge Nadiah Hassan for thoughtful and thorough reading and comments.

REFERENCES

Amenta, P. S., Scivoletti, N. A., Newman, M. D., Sciancalepore, J. P., Li, D., and Myers, J. C. (2005). Proteoglycan-collagen XV in human tissues is seen linking banded collagen fibers subjacent to the basement membrane. *J. Histochem. Cytochem.* 53, 165–176. doi: 10.1369/jhc.4A6376.2005

Arnold, S. A., and Brekken, R. A. (2009). SPARC: a matricellular regulator of tumorigenesis. *J. Cell Commun. Signal.* 3, 255–273. doi: 10.1007/s12079-009-0072-4

Bai, X., Li, Y.-y., Zhang, H.-y., Wang, F., He, H.-l., Yao, J.-c., et al. (2017). Role of matrix metalloproteinase-9 in transforming growth factor-β1-induced epithelial-mesenchymal transition in esophageal squamous cell carcinoma. *Oncotargets Ther.* 10, 2837–2847. doi: 10.2147/OTT.S134813

Bass, M. D., Roach, K. A., Morgan, M. R., Mostafavi-Pour, Z., Schoen, T., Muramatsu, T., et al. (2007). Syndecan-4'dependent Rac1 regulation determines directional migration in response to the extracellular matrix. *J. Cell Biol.* 177, 527–538. doi: 10.1083/jcb.200610076

Bonnans, C., Chou, J., and Werb, Z. (2014). Remodelling the extracellular matrix in development and disease. *Nat. Rev. Mol. Cell Biol.* 15, 786–801. doi: 10.1038/nrm3904

Boraschi-Diaz, I., Wang, J., Mort, J. S., and Komarova, S. V. (2017). Collagen type I as a ligand for receptor-mediated signaling. *Front. Phys.* 5:12. doi: 10.3389/fphy.2017.00012

Borradori, L., and Sonnenberg, A. (1999). Structure and function of hemidesmosomes: more than simple adhesion complexes. *J. Invest. Dermatol.* 112, 411–418. doi: 10.1046/j.1523-1747.1999.00546.x

Brauer, P. R. (2006). MMPs–role in cardiovascular development and disease. *Front. Biosci. J. Virt. Libr.* 11, 447–478. doi: 10.2741/1810

Brooks, R., Williamson, R. C., and Bass, M. D. (2012). Syndecan-4 independently regulates multiple small GTPases to promote fibroblast migration during wound healing. *Small GTPases* 3, 73–79. doi: 10.4161/sgtp.19301

Brown, A. C., Fiore, V. F., Sulchek, T. A., and Barker, T. H. (2013). Physical and chemical microenvironmental cues orthogonally control the degree and duration of fibrosis-associated epithelial-to-mesenchymal transitions. *J. Pathol.* 229, 25–35. doi: 10.1002/path.4114

Buonato, J. M., and Lazzara, M. J. (2014). ERK1/2 blockade prevents epithelial–mesenchymal transition in lung cancer cells and promotes their sensitivity to EGFR inhibition. *Cancer Res.* 74, 309–319. doi: 10.1158/0008-5472.CAN-12-4721

Cagnet, S., Faraldo, M. M., Kreft, M., Sonnenberg, A., Raymond, K., and Glukhova, M. A. (2014). Signaling events mediated by $\alpha 3\beta 1$ integrin are essential for mammary tumorigenesis. *Oncogene* 33, 4286–4295. doi: 10.1038/onc.2013.391

Calvo, F., Ege, N., Grande-Garcia, A., Hooper, S., Jenkins, R. P., Chaudhry, S. I., et al. (2013). Mechanotransduction and YAP-dependent matrix remodelling is required for the generation and maintenance of cancer-associated fibroblasts. *Nat. Cell Biol.* 15, 637–646. doi: 10.1038/ncb2756

Cescon, M., Gattazzo, F., Chen, P., and Bonaldo, P. (2015). Collagen VI at a glance. *J. Cell Sci.* 128, 3525–3531. doi: 10.1242/jcs.169748

Chanmee, T., Ontong, P., and Itano, N. (2016). Hyaluronan: a modulator of the tumor microenvironment. *Cancer Lett.* 375, 20–30. doi: 10.1016/j.canlet.2016.02.031

Chaturvedi, S., and Hass, R. (2011). Extracellular signals in young and aging breast epithelial cells and possible connections to age-associated breast cancer development. *Mech. Ageing Dev.* 132, 213–219. doi: 10.1016/j.mad.2011.04.002

Chekenya, M., Krakstad, C., Svendsen, A., Netland, I. A., Staalesen, V., Tysnes, B. B., et al. (2008). The progenitor cell marker NG2/MPG promotes chemoresistance by activation of integrin-dependent PI3k/Akt signaling. *Oncogene* 27, 5182–5194. doi: 10.1038/onc.2008.157

Chen, H.-R., Yeh, Y.-C., Liu, C.-Y., Wu, Y.-T., Lo, F.-Y., Tang, M.-J., et al. (2016). DDR1 promotes E-cadherin stability via inhibition of integrin-β1-Src activation-mediated E-cadherin endocytosis. *Sci. Rep.* 6:36336. doi: 10.1038/srep36336

Chen, P., Cescon, M., and Bonaldo, P. (2013). Collagen VI in cancer and its biological mechanisms. *Trends Mol. Med.* 19, 410–417. doi: 10.1016/j.molmed.2013.04.001

Cheng, J.-C., and Leung, P. C. K. (2011). Type I collagen down-regulates E-cadherin expression by increasing PI3kca in cancer cells. *Cancer Lett.* 304, 107–116. doi: 10.1016/j.canlet.2011.02.008

Chetty, C., Vanamala, S. K., Gondi, C. S., Dinh, D. H., Gujrati, M., and Rao, J. S. (2012). MMP-9 induces CD44 cleavage and CD44 mediated cell migration in glioblastoma xenograft cells. *Cell. Signal.* 24, 549–559. doi: 10.1016/j.cellsig.2011.10.008

Clementz, A. G., Mutolo, M. J., Leir, S.-H., Morris, K. J., Kucybala, K., Harris, H., et al. (2013). Collagen XV inhibits epithelial to mesenchymal transition in pancreatic adenocarcinoma cells. *PLoS ONE* 8:e72250. doi: 10.1371/journal.pone.0072250

Collins, C., Denisin, A. K., Pruitt, B. L., and Nelson, W. J. (2017). Changes in E-cadherin rigidity sensing regulate cell adhesion. *Proc. Natl. Acad. Sci. U.S.A.* 114, E5835–E5844. doi: 10.1073/pnas.1618676114

Conway, D. E., and Schwartz, M. A. (2014). Mechanotransduction of shear stress occurs through changes in VE-cadherin and PECAM-1 tension: implications for cell migration. *Cell Adhes. Migr.* 9, 335–339. doi: 10.4161/19336918.2014.968498

Craig, V. J., Zhang, L., Hagood, J. S., and Owen, C. A. (2015). Matrix metalloproteinases as therapeutic targets for idiopathic pulmonary fibrosis. *Am. J. Respir. Cell Mol. Biol.* 53, 585–600. doi: 10.1165/rcmb.2015-0020TR

David, J. M., and Rajasekaran, A. K. (2012). Dishonorable discharge: the oncogenic roles of cleaved E-cadherin fragments. *Cancer Res.* 72, 2917–2923. doi: 10.1158/0008-5472.CAN-11-3498

Deryugina, E. I., and Quigley, J. P. (2015). Tumor angiogenesis: MMP-mediated induction of intravasation- and metastasis-sustaining neovasculature. *Matrix Biol.* 44–46, 94–112. doi: 10.1016/j.matbio.2015.04.004

Dupont, S., Morsut, L., Aragona, M., Enzo, E., Giulitti, S., Cordenonsi, M., et al. (2011). Role of YAP/TAZ in mechanotransduction. *Nature* 474, 179–183. doi: 10.1038/nature10137

Dzamba, B. J., Jakab, K. R., Marsden, M., Schwartz, M. A., and DeSimone, D. W. (2009). Cadherin adhesion, tissue tension, and noncanonical Wnt signaling regulate fibronectin matrix organization. *Dev Cell* 16, 421–432. doi: 10.1016/j.devcel.2009.01.008

Eisenberg, J. L., Safi, A., Wei, X., Espinosa, H. D., Budinger, G. S., Takawira, D., et al. (2011). Substrate stiffness regulates extracellular matrix deposition by alveolar epithelial cells. *Res. Rep. Biol.* 2011, 1–12. doi: 10.2147/RRB.S13178

Elfenbein, A., and Simons, M. (2013). Syndecan-4 signaling at a glance. *J. Cell Sci.* 126, 3799–3804. doi: 10.1242/jcs.124636

El-Haibi, C. P., Bell, G. W., Zhang, J., Collmann, A. Y., Wood, D., Scherber, C. M., et al. (2012). Critical role for lysyl oxidase in mesenchymal stem cell-driven breast cancer malignancy. *Proc. Natl. Acad. Sci. U.S.A.* 109, 17460–17465. doi: 10.1073/pnas.1206653109

Espinosa Neira, R., and Salazar, E. P. (2012). Native type IV collagen induces an epithelial to mesenchymal transition-like process in mammary epithelial cells MCF10a. *Int. J. Biochem. Cell Biol.* 44, 2194–2203. doi: 10.1016/j.biocel.2012.08.018

Fang, M., Yuan, J., Peng, C., and Li, Y. (2014). Collagen as a double-edged sword in tumor progression. *Tumour Biol.* 35, 2871–2882. doi: 10.1007/s13277-013-1511-7

Fenouille, N., Tichet, M., Dufies, M., Pottier, A., Mogha, A., Soo, J. K., et al. (2012). The epithelial-mesenchymal transition (EMT) regulatory factor SLUG (SNAI2) is a downstream target of SPARC and AKT in promoting melanoma cell invasion. *PLoS ONE* 7:e40378. doi: 10.1371/journal.pone.0040378

Frantz, C., Stewart, K. M., and Weaver, V. M. (2010). The extracellular matrix at a glance. *J. Cell Sci.* 123, 4195–4200. doi: 10.1242/jcs.023820

Galliher, A. J., and Schiemann, W. P. (2007). Src phosphorylates Tyr284 in TGF-beta type II receptor and regulates TGF-beta stimulation of p38 MAPK during breast cancer cell proliferation and invasion. *Cancer Res.* 67, 3752–3758. doi: 10.1158/0008-5472.CAN-06-3851

Giannandrea, M., and Parks, W. C. (2014). Diverse functions of matrix metalloproteinases during fibrosis. *Dis. Models Mech.* 7, 193–203. doi: 10.1242/dmm.012062

Giannelli, G., Bergamini, C., Fransvea, E., Sgarra, C., and Antonaci, S. (2005). Laminin-5 with transforming growth factor-β1 induces epithelial to mesenchymal transition in hepatocellular carcinoma. *Gastroenterology* 129, 1375–1383. doi: 10.1053/j.gastro.2005.09.055

Gilles, C., Newgreen, D. F., Sato, H., and Thompson, E. W. (2013). *Matrix Metalloproteases and Epithelial-to-Mesenchymal Transition: Implications for Carcinoma Metastasis*. Austin, TX: Landes Bioscience.

Gomez, E. W., Chen, Q. K., Gjorevski, N., and Nelson, C. M. (2010). Tissue geometry patterns epithelial-mesenchymal transition via intercellular mechanotransduction. *J. Cell. Biochem.* 110, 44–51. doi: 10.1002/jcb.22545

González-González, L., and Alonso, J. (2018). Periostin: a matricellular protein with multiple functions in cancer development and progression. *Front. Oncol.* 8:225. doi: 10.3389/fonc.2018.00225

Gradl, D., Kühl, M., and Wedlich, D. (1999). The Wnt/Wg signal transducer β-Catenin controls fibronectin expression. *Mol. Cell. Biol.* 19, 5576–5587. doi: 10.1128/MCB.19.8.5576

Griggs, L. A., Hassan, N. T., Malik, R. S., Griffin, B. P., Martinez, B. A., Elmore, L. W., et al. (2017). Fibronectin fibrils regulate TGF-β1-induced epithelial-mesenchymal transition. *Matrix Biol.* 60–61, 157–175. doi: 10.1016/j.matbio.2017.01.001

Gu, S., Liu, Y., Zhu, B., Ding, K., Yao, T.-P., Chen, F., et al. (2016). Loss of α-tubulin acetylation is associated with TGF-β-induced epithelial-mesenchymal transition. *J. Biol. Chem.* 291, 5396–5405. doi: 10.1074/jbc.M115.713123

Guo, M.-S., Wu, Y.-Y., and Liang, Z.-B. (2012). Hyaluronic acid increases MMP-2 and MMP-9 expressions in cultured trabecular meshwork cells from patients with primary open-angle glaucoma. *Mol. Vis.* 18, 1175–1181. doi: 10.1167/iovs.13-13088

Hamill, K. J., Kligys, K., Hopkinson, S. B., and Jones, J. C. R. (2009). Laminin deposition in the extracellular matrix: a complex picture emerges. *J. Cell Sci.* 122, 4409–4417. doi: 10.1242/jcs.041095

Henry, M. D., and Campbell, K. P. (1998). A role for dystroglycan in basement membrane assembly. *Cell* 95, 859–870. doi: 10.1016/S0092-8674(00)81708-0

Henry, M. D., Satz, J. S., Brakebusch, C., Costell, M., Gustafsson, E., Fassler, R., et al. (2001). Distinct roles for dystroglycan, (β)1 integrin and perlecan in cell surface laminin organization. *J. Cell Sci.* 114, 1137–1144.

Hohenester, E., and Yurchenco, P. D. (2013). Laminins in basement membrane assembly. *Cell Adhes. Migr.* 7, 56–63. doi: 10.4161/cam.21831

Horejs, C.-M. (2016). Basement membrane fragments in the context of the epithelial-to-mesenchymal transition. *Eur. J. Cell Biol.* 95, 427–440. doi: 10.1016/j.ejcb.2016.06.002

Horejs, C.-M., Serio, A., Purvis, A., Gormley, A. J., Bertazzo, S., Poliniewicz, A., et al. (2014). Biologically-active laminin-111 fragment that modulates the epithelial-to-mesenchymal transition in embryonic stem cells. *Proc. Natl. Acad. Sci. U.S.A.* 111, 5908–5913. doi: 10.1073/pnas.1403139111

Hosper, N. A., van den Berg, P. P., de Rond, S., Popa, E. R., Wilmer, M. J., Masereeuw, R., et al. (2013). Epithelial-to-mesenchymal transition in fibrosis: Collagen type I expression is highly upregulated after EMT, but does not contribute to collagen deposition. *Exp. Cell Res.* 319, 3000–3009. doi: 10.1016/j.yexcr.2013.07.014

Hsia, H. C., and Schwarzbauer, J. E. (2005). Meet the Tenascins: multifunctional and mysterious. *J. Biol. Chem.* 280, 26641–26644. doi: 10.1074/jbc.R500005200

Hu, W.-W., Chen, P.-C., Chen, J.-M., Wu, Y.-M., Liu, P.-Y., Lu, C.-H., et al. (2017). Periostin promotes epithelial-mesenchymal transition via the MAPK/miR-381 axis in lung cancer. *Oncotarget* 8, 62248–62260. doi: 10.18632/oncotarget.19273

Huang, R. Y.-J., Guilford, P., and Thiery, J. P. (2012). Early events in cell adhesion and polarity during epithelial-mesenchymal transition. *J. Cell Sci.* 125, 4417–4422. doi: 10.1242/jcs.099697

Huang, Y., Arora, P., McCulloch, C. A., and Vogel, W. F. (2009). The collagen receptor DDR1 regulates cell spreading and motility by associating with myosin IIA. *J. Cell Sci.* 122, 1637–1646. doi: 10.1242/jcs.046219

Hynes, R. O. (1982). Fibronectins: multifunctional modular glycoproteins. *J. Cell Biol.* 95, 369–377. doi: 10.1083/jcb.95.2.369

Hynes, R. O. (2009). Extracellular matrix: not just pretty fibrils. *Science* 326, 1216–1219. doi: 10.1126/science.1176009

Illman, S. A., Lehti, K., Keski-Oja, J., and Lohi, J. (2006). Epilysin (MMP-28) induces TGF-β mediated epithelial to mesenchymal transition in lung carcinoma cells. *J. Cell Sci.* 119, 3856–3865. doi: 10.1242/jcs.03157

Imamichi, Y., and Menke, A. (2007). Signaling pathways involved in collagen-induced disruption of the E-cadherin complex during epithelial-mesenchymal transition. *Cells Tissues Organs* 185, 180–190. doi: 10.1159/000101319

Iyengar, P., Espina, V., Williams, T. W., Lin, Y., Berry, D., Jelicks, L. A., et al. (2005). Adipocyte-derived collagen VI affects early mammary tumor progression *in vivo*, demonstrating a critical interaction in the tumor/stroma microenvironment. *J. Clin. Invest.* 115, 1163–1176. doi: 10.1172/JCI200523424

Jacob, A., and Prekeris, R. (2015). The regulation of MMP targeting to invadopodia during cancer metastasis. *Front. Cell Dev. Biol.* 3:4. doi: 10.3389/fcell.2015.00004

Jordà, M., Olmeda, D., Vinyals, A., Valero, E., Cubillo, E., Llorens, A., et al. (2005). Upregulation of MMP-9 in MDCK epithelial cell line in response to expression of the Snail transcription factor. *J. Cell Sci.* 118, 3371–3385. doi: 10.1242/jcs.02465

Joseph, M. J., Dangi-Garimella, S., Shields, M. A., Diamond, M. E., Sun, L., Koblinski, J. E., et al. (2009). Slug is a downstream mediator of transforming growth factor-β1-induced matrix metalloproteinase-9 expression and invasion of oral cancer cells. *J. Cell. Biochem.* 108, 726–736. doi: 10.1002/jcb.22309

Kajita, M., Itoh, Y., Chiba, T., Mori, H., Okada, A., Kinoh, H., et al. (2001). Membrane-type 1 matrix metalloproteinase cleaves Cd44 and promotes cell migration. *J. Cell Biol.* 153, 893–904. doi: 10.1083/jcb.153.5.893

Karsdal, M. A., Nielsen, S. H., Leeming, D. J., Langholm, L. L., Nielsen, M. J., Manon-Jensen, T., et al. (2017). The good and the bad collagens of fibrosis–their role in signaling and organ function. *Adv. Drug Deliv. Rev.* 121, 43–56. doi: 10.1016/j.addr.2017.07.014

Kaushik, S., Pickup, M. W., and Weaver, V. M. (2016). From transformation to metastasis: deconstructing the extracellular matrix in breast cancer. *Cancer Metastasis Rev.* 35, 655–667. doi: 10.1007/s10555-016-9650-0

Kent, I. A., and Lele, T. P. (2016). Microtubule-based force generation. *Wiley Interdiscip. Rev. Nanomed. Nanobiotechnol.* 9, 1–11. doi: 10.1002/wnan.1428

Kessenbrock, K., Plaks, V., and Werb, Z. (2010). Matrix metalloproteinases: regulators of the tumor microenvironment. *Cell* 141, 52–67. doi: 10.1016/j.cell.2010.03.015

Khoshnoodi, J., Pedchenko, V., and Hudson, B. (2008). Mammalian collagen IV. *Microsc. Res. Tech.* 71, 357–370. doi: 10.1002/jemt.20564

Kim, K. K., Wei, Y., Szekeres, C., Kugler, M. C., Wolters, P. J., Hill, M. L., et al. (2009a). Epithelial cell $\alpha 3\beta 1$ integrin links β-catenin and Smad signaling to promote myofibroblast formation and pulmonary fibrosis. *J. Clin. Invest.* 119, 213–224. doi: 10.1172/JCI36940

Kim, Y., Kugler, M. C., Wei, Y., Kim, K. K., Li, X., Brumwell, A. N., et al. (2009b). Integrin $\alpha 3\beta 1$-dependent β-catenin phosphorylation links epithelial Smad signaling to cell contacts. *J. Cell Biol.* 184, 309–322. doi: 10.1083/jcb.200806067

Klass, C. M., Couchman, J. R., and Woods, A. (2000). Control of extracellular matrix assembly by syndecan-2 proteoglycan. *J. Cell Sci.* 113, 493–506.

Knowles, L. M., Gurski, L. A., Engel, C., Gnarra, J. R., Maranchie, J. K., and Pilch, J. (2013). Integrin $\alpha v\beta 3$ and fibronectin upregulate Slug in cancer cells to promote clot invasion and metastasis. *Cancer Res.* 73, 6175–6184. doi: 10.1158/0008-5472.CAN-13-0602

Koh, M., Woo, Y., Valiathan, R. R., Jung, H. Y., Park, S. Y., Kim, Y. N., et al. (2015). Discoidin domain receptor 1 is a novel transcriptional target of ZEB1 in breast epithelial cells undergoing H-Ras-induced epithelial to mesenchymal transition. *Int. J. Cancer* 136, E508–E520. doi: 10.1002/ijc.29154

Kolosova, I., Nethery, D., and Kern, J. A. (2011). Role of Smad2/3 and p38 MAP kinase in TGF-β1-induced epithelial-mesenchymal transition of pulmonary epithelial cells. *J. Cell. Physiol.* 226, 1248–1254. doi: 10.1002/jcp.22448

Kothari, A. N., Arffa, M. L., Chang, V., Blackwell, R. H., Syn, W.-K., Zhang, J., et al. (2016). Osteopontin–a master regulator of epithelial-mesenchymal transition. *J. Clin. Med.* 5:39. doi: 10.3390/jcm5040039

Krstic, J., and Santibanez, J. F. (2014). Transforming growth factor-beta and matrix metalloproteinases: functional interactions in tumor stroma-infiltrating myeloid cells. *ScientificWorldJournal* 2014:521754. doi: 10.1155/2014/521754

Kubow, K. E., Vukmirovic, R., Zhe, L., Klotzsch, E., Smith, M. L., Gourdon, D., et al. (2015). Mechanical forces regulate the interactions of fibronectin and collagen I in extracellular matrix. *Nat. Commun.* 6:8026. doi: 10.1038/ncomms9026

Kuo, H.-J., Maslen, C. L., Keene, D. R., and Glanville, R. W. (1997). Type VI collagen anchors endothelial basement membranes by interacting with type IV collagen. *J. Biol. Chem.* 272, 26522–26529. doi: 10.1074/jbc.272.42.26522

Lawson, C. D., and Burridge, K. (2014). The on-off relationship of Rho and Rac during integrin-mediated adhesion and cell migration. *Small GTPases* 5:e27958. doi: 10.4161/sgtp.27958

Le Bras, G. F., Taubenslag, K. J., and Andl, C. D. (2012). The regulation of cell-cell adhesion during epithelial-mesenchymal transition, motility and tumor progression. *Cell Adhes. Migr.* 6, 365–373. doi: 10.4161/cam.21326

Lee, J. L., and Streuli, C. H. (2014). Integrins and epithelial cell polarity. *J. Cell Sci.* 127, 3217–3225. doi: 10.1242/jcs.146142

Lee, Y.-H., Albig, A. R., Regner, M., Schiemann, B. J., and Schiemann, W. P. (2008). Fibulin-5 initiates epithelial-mesenchymal transition (EMT) and enhances EMT induced by TGF-β in mammary epithelial cells via a MMP-dependent mechanism. *Carcinogenesis* 29, 2243–2251. doi: 10.1093/carcin/bgn199

Lei, G.-S., Kline, H. L., Lee, C.-H., Wilkes, D. S., and Zhang, C. (2016). Regulation of collagen V expression and epithelial-mesenchymal transition by miR-185 and miR-186 during idiopathic pulmonary fibrosis. *Am. J. Pathol.* 186, 2310–2316. doi: 10.1016/j.ajpath.2016.04.015

Leight, J. L., Wozniak, M. A., Chen, S., Lynch, M. L., Chen, C. S., and Wang, Y.-L. (2012). Matrix rigidity regulates a switch between TGF-β1-induced apoptosis and epithelial-mesenchymal transition. *Mol. Biol. Cell* 23, 781–791. doi: 10.1091/mbc.e11-06-0537

Li, S., Edgar, D., Fässler, R., Wadsworth, W., and Yurchenco, P. D. (2003). The role of laminin in embryonic cell polarization and tissue organization. *Dev. Cell* 4, 613–624. doi: 10.1016/S1534-5807(03)00128-X

Li, S., Harrison, D., Carbonetto, S., Fässler, R., Smyth, N., Edgar, D., et al. (2002). Matrix assembly, regulation, and survival functions of laminin and its receptors in embryonic stem cell differentiation. *J. Cell Biol.* 157, 1279–1290. doi: 10.1083/jcb.200203073

Li, X.-L., Liu, L., Li, D.-D., He, Y.-P., Guo, L.-H., Sun, L.-P., et al. (2017). Integrin β4 promotes cell invasion and epithelial-mesenchymal transition through the modulation of Slug expression in hepatocellular carcinoma. *Sci. Rep.* 7:40464. doi: 10.1038/srep40464

Liu, C.-Y. Y., Lin, H.-H. H., Tang, M.-J. J., and Wang, Y.-K. K. (2015). Vimentin contributes to epithelial-mesenchymal transition cancer cell mechanics by mediating cytoskeletal organization and focal adhesion maturation. *Oncotarget* 6, 15966–15983. doi: 10.18632/oncotarget.3862

Lu, H., Hu, L., Yu, L., Wang, X., Urvalek, A. M., Li, T., et al. (2014). KLF8 and FAK cooperatively enrich the active MMP14 on the cell surface required for the metastatic progression of breast cancer. *Oncogene* 33, 2909–2917. doi: 10.1038/onc.2013.247

Maeda, S., Dean, D., Gomez, R., Schwartz, Z., and Boyan, B. (2002). The first stage of transforming growth factor β1 activation is release of the large latent complex from the extracellular matrix of growth plate chondrocytes by matrix vesicle stromelysin-1 (MMP-3). *Calcif. Tissue Int.* 70, 54–65. doi: 10.1007/s002230010032

Mak, K. M., Png, C. Y. M., and Lee, D. J. (2016). Type V collagen in health, disease, and fibrosis. *Anat. Rec.* 299, 613–629. doi: 10.1002/ar.23330

Mamuya, F. A., and Duncan, M. K. (2012). aV integrins and TGF-β-induced EMT: a circle of regulation. *J. Cell. Mol. Med.* 16, 445–455. doi: 10.1111/j.1582-4934.2011.01419.x

Mao, Y., and Schwarzbauer, J. E. (2005). Fibronectin fibrillogenesis, a cell-mediated matrix assembly process. *Matrix Biol.* 24, 389–399. doi: 10.1016/j.matbio.2005.06.008

Markowski, M. C., Brown, A. C., and Barker, T. H. (2012). Directing epithelial to mesenchymal transition through engineered microenvironments displaying orthogonal adhesive and mechanical cues. *J. Biomed. Mater. Res. A* 100A, 2119–2127. doi: 10.1002/jbm.a.34068

Maschler, S., Grunert, S., Danielopol, A., Beug, H., and Wirl, G. (2004). Enhanced tenascin-C expression and matrix deposition during Ras/TGF-β-induced progression of mammary tumor cells. *Oncogene* 23, 3622–3633. doi: 10.1038/sj.onc.1207403

McGuire, J. K., Li, Q., and Parks, W. C. (2003). Matrilysin (matrix metalloproteinase-7) mediates E-cadherin ectodomain shedding in injured lung epithelium. *Am. J. Pathol.* 162, 1831–1843. doi: 10.1016/S0002-9440(10)64318-0

McKee, K. K., Harrison, D., Capizzi, S., and Yurchenco, P. D. (2007). Role of laminin terminal globular domains in basement membrane assembly. *J. Biol. Chem.* 282, 21437–21447. doi: 10.1074/jbc.M702963200

Medici, D., and Nawshad, A. (2010). Type I collagen promotes epithelial-mesenchymal transition through ILK-dependent activation of NF-κB and LEF-1. *Matrix Biol.* 29, 161–165. doi: 10.1016/j.matbio.2009.12.003

Menke, A., Philippi, C., Vogelmann, R., Seidel, B., Lutz, M. P., Adler, G., et al. (2001). Down-regulation of E-cadherin gene expression by collagen type I and type III in pancreatic cancer cell lines. *Cancer Res.* 61, 3508–3517.

Mierke, C. T., Frey, B., Fellner, M., Herrmann, M., and Fabry, B. (2011). Integrin $\alpha5\beta1$ facilitates cancer cell invasion through enhanced contractile forces. *J. Cell Sci.* 124, 369–383. doi: 10.1242/jcs.071985

Morgan, M., Byron, A., Humphries, M., and Bass, M. (2009). Giving off mixed signals–distinct functions of $\alpha5\beta1$ and $\alpha V\beta3$ integrins in regulating cell behaviour. *IUBMB Life* 61, 731–738. doi: 10.1002/iub.200

Mori, H., Lo, A. T., Inman, J. L., Alcaraz, J., Ghajar, C. M., Mott, J. D., et al. (2013). Transmembrane/cytoplasmic, rather than catalytic, domains of Mmp14 signal to MAPK activation and mammary branching morphogenesis via binding to integrin $\beta1$. *Development* 140, 343–352. doi: 10.1242/dev.084236

Morini, M., Mottolese, M., Ferrari, N., Ghiorzo, F., Buglioni, S., Mortarini, R., et al. (2000). The $\alpha3\beta1$ integrin is associated with mammary carcinoma cell metastasis, invasion, and gelatinase B (mmp-9) activity. *Int. J. Cancer* 87, 336–342. doi: 10.1002/1097-0215(20000801)87:3<336::AID-IJC5>3.0.CO;2-3

Morra, L., and Moch, H. (2011). Periostin expression and epithelial-mesenchymal transition in cancer: a review and an update. *Virchows Arch.* 459, 465–475. doi: 10.1007/s00428-011-1151-5

Morrissey, M. A., and Sherwood, D. R. (2015). An active role for basement membrane assembly and modification in tissue sculpting. *J. Cell Sci.* 128, 1661–1668. doi: 10.1242/jcs.168021

Mu, D., Cambier, S., Fjellbirkeland, L., Baron, J. L., Munger, J. S., Kawakatsu, H., et al. (2002). The integrin $\alpha v\beta8$ mediates epithelial homeostasis through MT1-MMP-dependent activation of TGF-$\beta1$. *J. Cell. Biol.* 157, 493–507. doi: 10.1083/jcb.200109100

Murphy-Ullrich, J. E., and Sage, E. H. (2014). Revisiting the matricellular concept. *Matrix Biol.* 37, 1–14. doi: 10.1016/j.matbio.2014.07.005

Myers, J. C., Amenta, P. S., Dion, A. S., Sciancalepore, J. P., Nagaswami, C., Weisel, J. W., et al. (2007). The molecular structure of human tissue type XV presents a unique conformation among the collagens. *Biochem. J.* 404, 535–544. doi: 10.1042/BJ20070201

Myllymäki, S. M., Teräväinen, T. P., and Manninen, A. (2011). Two distinct integrin-mediated mechanisms contribute to apical lumen formation in epithelial cells. *PLoS ONE* 6:e19453. doi: 10.1371/journal.pone.0019453

Nabeshima, K., Inoue, T., Shimao, Y., and Sameshima, T. (2002). Matrix metalloproteinases in tumor invasion: role for cell migration. *Pathol. Int.* 52, 255–264. doi: 10.1046/j.1440-1827.2002.01343.x

Nagase, H., Visse, R., and Murphy, G. (2006). Structure and function of matrix metalloproteinases and TIMPs. *Cardiovasc. Res.* 69, 562–573. doi: 10.1016/j.cardiores.2005.12.002

Nardone, G., Oliver-De La Cruz, J., Vrbsky, J., Martini, C., Pribyl, J., Skládal, P., et al. (2017). YAP regulates cell mechanics by controlling focal adhesion assembly. *Nat. Commun.* 8:15321. doi: 10.1038/ncomms15321

Noe, V., Fingleton, B., Jacobs, K., Crawford, H. C., Vermeulen, S., Steelant, W., et al. (2001). Release of an invasion promoter E-cadherin fragment by matrilysin and stromelysin-1. *J. Cell Sci.* 114, 111–118.

O'Connor, J. W., Riley, P. N., Nalluri, S. M., Ashar, P. K., and Gomez, E. W. (2015). Matrix rigidity mediates TGF$\beta1$-induced epithelial-myofibroblast transition by

controlling cytoskeletal organization and MRTF-A localization. *J. Cell. Physiol.* 230, 1829–1839. doi: 10.1002/jcp.24895

Octavio, G.-H., Cristina, G.-V., Pedro, C.-R., Emmanuel, R.-U., Sonia, C.-O., Octavio, R.-H., et al. (2015). Extracellular vesicles from women with breast cancer promote an epithelial-mesenchymal transition-like process in mammary epithelial cells MCF10a. *Tumour Biol.* 36, 9649–9659. doi: 10.1007/s13277-015-3711-9

Onodera, T., Sakai, T., Hsu, J. C.-f., Matsumoto, K., Chiorini, J. A., and Yamada, K. M. (2010). Btbd7 regulates epithelial cell dynamics and branching morphogenesis. *Science* 329, 562–565. doi: 10.1126/science.1191880

Page-McCaw, A., Ewald, A. J., and Werb, Z. (2007). Matrix metalloproteinases and the regulation of tissue remodelling. *Nat. Rev. Mol. Cell Biol.* 8, 221–233. doi: 10.1038/nrm2125

Pardo, A., Cabrera, S., Maldonado, M., and Selman, M. (2016). Role of matrix metalloproteinases in the pathogenesis of idiopathic pulmonary fibrosis. *Respir. Res.* 17:23. doi: 10.1186/s12931-016-0343-6

Park, J., and Scherer, P. E. (2012). Adipocyte-derived endotrophin promotes malignant tumor progression. *J. Clin. Invest.* 122, 4243–4256. doi: 10.1172/JCI63930

Park, J., and Schwarzbauer, J. E. (2014). Mammary epithelial cell interactions with fibronectin stimulate epithelial-mesenchymal transition. *Oncogene* 33, 1649–1657. doi: 10.1038/onc.2013.118

Park, M.-J., Kim, M.-S., Park, I.-C., Kang, H.-S., Yoo, H., Park, S. H., et al. (2002). PTEN suppresses hyaluronic acid-induced matrix metalloproteinase-9 expression in U87mg glioblastoma cells through focal adhesion kinase dephosphorylation. *Cancer Res.* 62, 6318–6322.

Peng, S.-T., Su, C.-H., Kuo, C.-C., Shaw, C.-F., and Wang, H.-S. (2007). CD44 crosslinking-mediated matrix metalloproteinase-9 relocation in breast tumor cells leads to enhanced metastasis. *Int. J. Oncol.* 31, 1119–1126. doi: 10.3892/ijo.31.5.1119

Petrini, I., Barachini, S., Carnicelli, V., Galimberti, S., Modeo, L., Boni, R., et al. (2016). ED-B fibronectin expression is a marker of epithelial-mesenchymal transition in translational oncology. *Oncotarget* 8, 4914–4921. doi: 10.18632/oncotarget.13615

Porsch, H., Bernert, B., Mehić, M., Theocharis, A. D., Heldin, C.-H., and Heldin, P. (2013). Efficient TGFβ-induced epithelial-mesenchymal transition depends on hyaluronan synthase HAS2. *Oncogene* 32, 4355–4365. doi: 10.1038/onc.2012.475

Qiao, B., Johnson, N. W., and Gao, J. (2010). Epithelial-mesenchymal transition in oral squamous cell carcinoma triggered by transforming growth factor-beta1 is Snail family-dependent and correlates with matrix metalloproteinase-2 and -9 expressions. *Int. J. Oncol.* 37, 663–668. doi: 10.3892/ijo_00000715

Radisky, D. C., Levy, D. D., Littlepage, L. E., Liu, H., Nelson, C. M., Fata, J. E., et al. (2005). Rac1b and reactive oxygen species mediate MMP-3-induced EMT and genomic instability. *Nature* 436, 123–127. doi: 10.1038/nature03688

Ramirez, N. E., Zhang, Z., Madamanchi, A., Boyd, K. L., O'Rear, L. D., Nashabi, A., et al. (2011). The $\alpha_2\beta_1$ integrin is a metastasis suppressor in mouse models and human cancer. *J. Clin. Invest.* 121, 226–237. doi: 10.1172/JCI42328

Rammal, H., Saby, C., Magnien, K., Van-Gulick, L., Garnotel, R., Buache, E., et al. (2016). Discoidin domain receptors: potential actors and targets in cancer. *Front. Pharmacol.* 7:55. doi: 10.3389/fphar.2016.00055

Repetto, O., De Paoli, P., De Re, V., Canzonieri, V., and Cannizzaro, R. (2014). Levels of soluble E-cadherin in breast, gastric, and colorectal cancers. *Biomed. Res. Int.* 2014:408047. doi: 10.1155/2014/408047

Ricard-Blum, S. (2011). The collagen family. *Cold Spring Harbor Perspect. Biol.* 3:ea004978. doi: 10.1101/cshperspect.a004978

Rifkin, D. B. (2005). Latent transforming growth factor-β (TGF-β) binding proteins: orchestrators of TGF-β availability. *J. Biol. Chem.* 280, 7409–7412. doi: 10.1074/jbc.R400029200

Robert, G., Gaggioli, C., Bailet, O., Chavey, C., Abbe, P., Aberdam, E., et al. (2006). SPARC represses E-cadherin and induces mesenchymal transition during melanoma development. *Cancer Res.* 66, 7516–7523. doi: 10.1158/0008-5472.CAN-05-3189

Robertson, I. B., Horiguchi, M., Zilberberg, L., Dabovic, B., Hadjiolova, K., and Rifkin, D. B. (2015). Latent TGF-β-binding proteins. *Matrix Biol.* 47, 44–53. doi: 10.1016/j.matbio.2015.05.005

Rodríguez, D., Morrison, C. J., and Overall, C. M. (2010). Matrix metalloproteinases: what do they not do? New substrates and biological roles identified by murine models and proteomics. *Biochim. Biophys. Acta* 1803, 39–54. doi: 10.1016/j.bbamcr.2009.09.015

Rousselle, P., Keene, D. R., Ruggiero, F., Champliaud, M.-F., van der Rest, M., and Burgeson, R. E. (1997). Laminin 5 binds the NC-1 domain of type VII collagen. *J. Cell Biol.* 138, 719–728. doi: 10.1083/jcb.138.3.719

Rozanov, D. V., Deryugina, E. I., Monosov, E. Z., Marchenko, N. D., and Strongin, A. Y. (2004). Aberrant, persistent inclusion into lipid rafts limits the tumorigenic function of membrane type-1 matrix metalloproteinase in malignant cells. *Exp. Cell Res.* 293, 81–95. doi: 10.1016/j.yexcr.2003.10.006

Scott, L. E., Mair, D. B., Narang, J. D., Feleke, K., and Lemmon, C. A. (2015). Fibronectin fibrillogenesis facilitates mechano-dependent cell spreading, force generation, and nuclear size in human embryonic fibroblasts. *Integr. Biol.* 7, 1454–1465. doi: 10.1039/c5ib00217f

Seifert, A., and Posern, G. (2017). Tightly controlled MRTF–a activity regulates epithelial differentiation during formation of mammary acini. *Breast Cancer Res.* 19:68. doi: 10.1186/s13058-017-0860-3

Sethi, A., Mao, W., Wordinger, R. J., and Clark, A. F. (2011). Transforming growth factor-β induces extracellular matrix protein cross-linking lysyl oxidase (LOX) genes in human trabecular meshwork cells. *Invest. Ophthal. Vis. Sci.* 52, 5240–5250. doi: 10.1167/iovs.11-7287

Shen, C.-J., Kuo, Y.-L., Chen, C.-C., Chen, M.-J., and Cheng, Y.-M. (2017a). MMP1 expression is activated by slug and enhances multi-drug resistance (MDR) in breast cancer. *PLoS ONE* 12:e0174487. doi: 10.1371/journal.pone.0174487

Shen, Z., Wang, X., Yu, X., Zhang, Y., and Qin, L. (2017b). MMP16 promotes tumor metastasis and indicates poor prognosis in hepatocellular carcinoma. *Oncotarget* 8, 72197–72204. doi: 10.18632/oncotarget.20060

Shintani, Y., Fukumoto, Y., Chaika, N., Svoboda, R., Wheelock, M. J., and Johnson, K. R. (2008a). Collagen I-mediated up-regulation of N-cadherin requires cooperative signals from integrins and discoidin domain receptor 1. *J. Cell Biol.* 180, 1277–1289. doi: 10.1083/jcb.200708137

Shintani, Y., Maeda, M., Chaika, N., Johnson, K. R., and Wheelock, M. J. (2008b). Collagen I promotes epithelial-to-mesenchymal transition in lung cancer cells via transforming growth factor-β signaling. *Am. J. Respir. Cell Mol. Biol.* 38, 95–104. doi: 10.1165/rcmb.2007-0071OC

Shoulders, M. D., and Raines, R. T. (2009). Collagen structure and stability. *Annu. Rev. Biochem.* 78, 929–958. doi: 10.1146/annurev.biochem.77.032207.120833

Singh, P., Carraher, C., and Schwarzbauer, J. E. (2010). Assembly of fibronectin extracellular matrix. *Annu. Rev. Cell Dev. Biol.* 26, 397–419. doi: 10.1146/annurev-cellbio-100109-104020

Sottile, J., Hocking, D. C., and Schwartz, M. (2002). Fibronectin polymerization regulates the composition and stability of extracellular matrix fibrils and cell-matrix adhesions. *Mol. Biol. Cell* 13, 3546–3559. doi: 10.1091/mbc.e02-01-0048

Sternlicht, M. D., and Werb, Z. (2001). How matrix metalloproteinases regulate cell behavior. *Annu. Rev. Cell Dev. Biol.* 17, 463–516. doi: 10.1146/annurev.cellbio.17.1.463

Sugiura, T., and Berditchevski, F. (1999). Function of $\alpha3\beta1$-tetraspanin protein complexes in tumor cell invasion. Evidence for the role of the complexes in production of matrix metalloproteinase 2 (Mmp-2). *J. Cell Biol.* 146, 1375–1389. doi: 10.1083/jcb.146.6.1375

Sun, B., Fang, Y., Li, Z., Chen, Z., and Xiang, J. (2015). Role of cellular cytoskeleton in epithelial-mesenchymal transition process during cancer progression. *Biomed. Rep.* 3, 603–610. doi: 10.3892/br.2015.494

Symoens, S., Renard, M., Bonod-Bidaud, C., Syx, D., Vaganay, E., Malfait, F., Ricard-Blum, S., et al. (2011). Identification of binding partners interacting with the α1-N-propeptide of type V collagen. *Biochem. J.* 433, 371–381. doi: 10.1042/BJ20101061

Têtu, B., Brisson, J., Wang, C. S., Lapointe, H., Beaudry, G., Blanchette, C., et al. (2006). The influence of MMP-14, TIMP-2 and MMP-2 expression on breast cancer prognosis. *Breast Cancer Res.* 8:R28. doi: 10.1186/bcr1503

Toole, B. P. (2004). Hyaluronan: from extracellular glue to pericellular cue. *Nat. Rev. Cancer* 4, 528–539. doi: 10.1038/nrc1391

Tseng, Q., Duchemin-Pelletier, E., Deshiere, A., Balland, M., Guillou, H., Filhol, O., et al. (2012). Spatial organization of the extracellular matrix regulates cell–cell junction positioning. *Proc. Natl. Acad. Sci. U.S.A.* 109, 1506–1511. doi: 10.1073/pnas.1106377109

Tumova, S., Woods, A., and Couchman, J. R. (2000). Heparan sulfate chains from glypican and syndecans bind the Hep II domain of fibronectin similarly despite minor structural differences. *J. Biol. Chem.* 275, 9410–9417. doi: 10.1074/jbc.275.13.9410

Turley, E. A., Noble, P. W., and Bourguignon, L. Y. W. (2002). Signaling properties of hyaluronan receptors. *J. Biol. Chem.* 277, 4589–4592. doi: 10.1074/jbc.R100038200

Vega, M. E., and Schwarzbauer, J. E. (2016). Collaboration of fibronectin matrix with other extracellular signals in morphogenesis and differentiation. *Curr. Opin. Cell Biol.* 42, 1–6. doi: 10.1016/j.ceb.2016.03.014

Voloshenyuk, T. G., Landesman, E. S., Khoutorova, E., Hart, A. D., and Gardner, J. D. (2011). Induction of cardiac fibroblast lysyl oxidase by TGF-β1 requires PI3k/Akt, Smad3, and MAPK signaling. *Cytokine* 55, 90–97. doi: 10.1016/j.cyto.2011.03.024

Walsh, L. A., Nawshad, A., and Medici, D. (2011). Discoidin domain receptor 2 is a critical regulator of epithelial-mesenchymal transition. *Matrix Biol.* 30, 243–247. doi: 10.1016/j.matbio.2011.03.007

Wang, C.-Z., Yeh, Y.-C., and Tang, M.-J. (2009). DDR1/E-cadherin complex regulates the activation of DDR1 and cell spreading. *Am. J. Physiol. Cell Physiol.* 297, C419–C429. doi: 10.1152/ajpcell.00101.2009

Wang, J. P., and Hielscher, A. (2017). Fibronectin: how its Aberrant expression in tumors may improve therapeutic targeting. *J. Cancer* 8, 674–682. doi: 10.7150/jca.16901

Wang, T., Wang, M., Fang, S., Wang, Q., Fang, R., and Chen, J. (2017). Fibulin-4 is associated with prognosis of endometrial cancer patients and inhibits cancer cell invasion and metastasis via Wnt/β-catenin signaling pathway. *Oncotarget* 8, 18991–19012. doi: 10.18632/oncotarget.15086

Wang, X., Lu, H., Urvalek, A. M., Li, T., Yu, L., Lamar, J., et al. (2011). KLF8 promotes human breast cancer cell invasion and metastasis by transcriptional activation of MMP9. *Oncogene* 30, 1901–1911. doi: 10.1038/onc.2010.563

Wang, Z., Symons, J. M., Goldstein, S. L., McDonald, A., Miner, J. H., and Kreidberg, J. A. (1999). (Alpha)3(beta)1 integrin regulates epithelial cytoskeletal organization. *J. Cell Sci.* 112, 2925–2935.

Waterman, E. A., Sakai, N., Nguyen, N. T., Horst, B. A. J., Veitch, D. P., Dey, C. N., et al. (2007). A laminin-collagen complex drives human epidermal carcinogenesis through phosphoinositol-3-kinase activation. *Cancer Res.* 67, 4264–4270. doi: 10.1158/0008-5472.CAN-06-4141

Wei, S. C., Fattet, L., Tsai, J. H., Guo, Y., Pai, V. H., Majeski, H. E., et al. (2015). Matrix stiffness drives epithelial-mesenchymal transition and tumour metastasis through a TWIST1-G3bp2 mechanotransduction pathway. *Nat. Cell Biol.* 17, 678–688. doi: 10.1038/ncb3157

Weinberg, S. H., Mair, D. B., and Lemmon, C. A. (2017). Mechanotransduction dynamics at the cell-matrix interface. *Biophys. J.* 112, 1962–1974. doi: 10.1016/j.bpj.2017.02.027

Whipple, R. A., Matrone, M. A., Cho, E. H., Balzer, E. M., Vitolo, M. I., Yoon, J. R., et al. (2010). Epithelial-to-mesenchymal transition promotes tubulin detyrosination and microtentacles that enhance endothelial engagement. *Cancer Res.* 70, 8127–8137. doi: 10.1158/0008-5472.CAN-09-4613

White, D. P., Caswell, P. T., and Norman, J. C. (2007). αvβ3 and α5β1 integrin recycling pathways dictate downstream Rho kinase signaling to regulate persistent cell migration. *J. Cell. Biol.* 177, 515–525. doi: 10.1083/jcb.200609004

Wilkins-Port, C. E., and Higgins, P. J. (2007). Regulation of extracellular matrix remodeling following transforming growth factor-β1/epidermal growth factor-stimulated epithelial-mesenchymal transition in human premalignant keratinocytes. *Cells Tissues Organs* 185, 116–122. doi: 10.1159/000101312

Williams, C. M., Engler, A. J., Slone, R. D., Galante, L. L., and Schwarzbauer, J. E. (2008). Fibronectin expression modulates mammary epithelial cell proliferation during acinar differentiation. *Cancer Res.* 68, 3185–3192. doi: 10.1158/0008-5472.CAN-07-2673

Woods, A., Longley, R. L., Tumova, S., and Couchman, J. R. (2000). Syndecan-4 binding to the high affinity heparin-binding domain of fibronectin drives focal adhesion formation in fibroblasts. *Arch. Biochem. Biophys.* 374, 66–72. doi: 10.1006/abbi.1999.1607

Wu, B., Crampton, S. P., and Hughes, C. C. W. (2007). Wnt signaling induces matrix metalloproteinase expression and regulates T cell transmigration. *Immunity* 26, 227–239. doi: 10.1016/j.immuni.2006.12.007

Xiao, Q., Jiang, Y., Liu, Q., Yue, J., Liu, C., Zhao, X., et al. (2015). Minor type IV collagen α5 chain promotes cancer progression through Discoidin domain receptor-1. *PLoS Genet.* 11:e1005249. doi: 10.1371/journal.pgen.1005249

Xie, L., Law, B. K., Chytil, A. M., Brown, K. A., Aakre, M. E., and Moses, H. L. (2004). Activation of the Erk pathway is required for TGF-β1-induced EMT *in vitro*. *Neoplasia* 6, 603–610. doi: 10.1593/neo.04241

Xu, J., Rodriguez, D., Petitclerc, E., Kim, J. J., Hangai, M., Yuen, S. M., et al. (2001). Proteolytic exposure of a cryptic site within collagen type IV is required for angiogenesis and tumor growth *in vivo*. *J. Cell Biol.* 154, 1069–1080. doi: 10.1083/jcb.200103111

Yamashita, C. M., Dolgonos, L., Zemans, R. L., Young, S. K., Robertson, J., Briones, N., et al. (2011). Matrix metalloproteinase 3 is a mediator of pulmonary fibrosis. *Am. J. Pathol.* 179, 1733–1745. doi: 10.1016/j.ajpath.2011.06.041

Yanagisawa, H., Schluterman, M. K., and Brekken, R. A. (2009). Fibulin-5, an integrin-binding matricellular protein: its function in development and disease. *J. Cell Commun. Signal.* 3, 337–347. doi: 10.1007/s12079-009-0065-3

Yang, C., Zeisberg, M., Lively, J. C., Nyberg, P., Afdhal, N., and Kalluri, R. (2003). Integrin $\alpha1\beta1$ and $\alpha2\beta1$ are the key regulators of hepatocarcinoma cell invasion across the fibrotic matrix microenvironment. *Cancer Res.* 63, 8312–8317. doi: 10.1186/1755-1536-6-17

Yonemura, S., Wada, Y., Watanabe, T., Nagafuchi, A., and Shibata, M. (2010). Alpha-catenin as a tension transducer that induces adherens junction development. *Nat. Cell Biol.* 12, 533–542. doi: 10.1038/ncb2055

Yoshida, T., Akatsuka, T., and Imanaka-Yoshida, K. (2015). Tenascin-C and integrins in cancer. *Cell Adhes. Migr.* 9, 96–104. doi: 10.1080/19336918.2015.1008332

Yu, Q., and Stamenkovic, I. (2000). Cell surface-localized matrix metalloproteinase-9 proteolytically activates TGF-β and promotes tumor invasion and angiogenesis. *Genes Dev.* 14, 163–176. doi: 10.1101/gad.14.2.163

Yurchenco, P. D. (2011). Basement membranes: cell scaffoldings and signaling platforms. *Cold Spring Harbor Perspect. Biol.* 3:a004911. doi: 10.1101/cshperspect.a004911

Yurchenco, P. D., and Patton, B. L. (2009). Developmental and pathogenic mechanisms of basement membrane assembly. *Curr. Pharm. Des.* 15, 1277–1294. doi: 10.2174/138161209787846766

Zhang, F., Tom, C. C., Kugler, M. C., Ching, T.-T., Kreidberg, J. A., Wei, Y., et al. (2003). Distinct ligand binding sites in integrin $\alpha3\beta1$ regulate matrix adhesion and cell–cell contact. *J. Cell Biol.* 163, 177–188. doi: 10.1083/jcb.200304065

Zhang, K., Corsa, C. A., Ponik, S. M., Prior, J. L., Piwnica-Worms, D., Eliceiri, K. W., et al. (2013). The collagen receptor discoidin domain receptor 2 stabilizes SNAIL1 to facilitate breast cancer metastasis. *Nat. Cell Biol.* 15, 677–687. doi: 10.1038/ncb2743

Zhang, S., Miao, Y., Zheng, X., Gong, Y., Zhang, J., Zou, F., et al. (2017). STIM1 and STIM2 differently regulate endogenous Ca^{2+} entry and promote TGF-β-induced EMT in breast cancer cells. *Biochem. Biophys. Res. Commun.* 488, 74–80. doi: 10.1016/j.bbrc.2017.05.009

Zhang, Y., Thant, A. A., Machida, K., Ichigotani, Y., Naito, Y., Hiraiwa, Y., et al. (2002). Hyaluronan-CD44s signaling regulates matrix metalloproteinase-2 secretion in a human lung carcinoma cell line QG90. *Cancer Res.* 62, 3962–3965.

Zhang, Z., Liu, X., Feng, B., Liu, N., Wu, Q., Han, Y., et al. (2015). STIM1, a direct target of microRNA-185, promotes tumor metastasis and is associated with poor prognosis in colorectal cancer. *Oncogene* 34, 4808–4820. doi: 10.1038/onc.2014.404

Zhao, H., Chen, Q., Alam, A., Cui, J., Suen, K. C., Soo, A. P., et al. (2018). The role of osteopontin in the progression of solid organ tumour. *Cell Death Dis.* 9:356. doi: 10.1038/s41419-018-0391-6

Zilberberg, L., Todorovic, V., Dabovic, B., Horiguchi, M., Couroussé, T., Sakai, L. Y., et al. (2012). Specificity of latent TGF-β binding protein (LTBP) incorporation into matrix: role of fibrillins and fibronectin. *J. Cell. Physiol.* 227, 3828–3836. doi: 10.1002/jcp.24094

Zoltan-Jones, A., Huang, L., Ghatak, S., and Toole, B. P. (2003). Elevated Hyaluronan production induces mesenchymal and transformed properties in epithelial cells. *J. Biol. Chem.* 278, 45801–45810. doi: 10.1074/jbc.M308168200

Zutter, M. M., Santoro, S. A., Staatz, W. D., and Tsung, Y. L. (1995). Re-expression of the alpha 2 beta 1 integrin abrogates the malignant phenotype of breast carcinoma cells. *Proc. Natl. Acad. Sci. U.S.A.* 92, 7411–7415. doi: 10.1073/pnas.92.16.7411

Conflict of Interest Statement: The authors declare that the research was conducted in the absence of any commercial or financial relationships that could be construed as a potential conflict of interest.

frontiers in Cell and Developmental Biology

ORIGINAL RESEARCH
published: 16 October 2019
doi: 10.3389/fcell.2019.00224

Dynamic Assembly of Human Salivary Stem/Progenitor Microstructures Requires Coordinated $\alpha_1\beta_1$ Integrin-Mediated Motility

Danielle Wu[1,2], *Robert L. Witt*[3,4], *Daniel A. Harrington*[1,2] *and Mary C. Farach-Carson*[1,2]*

[1] Department of Diagnostic and Biomedical Sciences, The University of Texas Health Science Center at Houston, Houston, TX, United States, [2] Department of BioSciences, Rice University, Houston, TX, United States, [3] Center for Translational Cancer Research, Helen F. Graham Cancer Center & Research Institute, Christiana Care Health Center, Newark, DE, United States, [4] Department of Otolaryngology-Head and Neck Surgery, Thomas Jefferson University, Philadelphia, PA, United States

OPEN ACCESS

Edited by:
Charles D. Little,
University of Kansas Medical Center,
United States

Reviewed by:
Patrick Sachs,
Old Dominion University, United States
Jon Humphries,
University of Manchester,
United Kingdom

***Correspondence:**
Mary C. Farach-Carson
mary.c.farachcarson@uth.tmc.edu

Specialty section:
This article was submitted to Cell Adhesion and Migration, a section of the journal Frontiers in Cell and Developmental Biology

Received: 15 December 2018
Accepted: 20 September 2019
Published: 16 October 2019

Citation:
Wu D, Witt RL, Harrington DA and Farach-Carson MC (2019) Dynamic Assembly of Human Salivary Stem/Progenitor Microstructures Requires Coordinated $\alpha_1\beta_1$ Integrin-Mediated Motility. Front. Cell Dev. Biol. 7:224. doi: 10.3389/fcell.2019.00224

A tissue engineering approach can provide replacement salivary gland structures to patients with hyposalivation disorders and xerostomia. Salivary human stem/progenitor cells (hS/PCs) were isolated from healthy regions of parotid glands of head and neck surgery patients, expanded, then encapsulated in biocompatible hyaluronate (HA)-based hydrogels. These bioactive hydrogels provide a surrogate territorial matrix suitable for the dynamic assembly, growth and reorganization of salivary gland components. This study examined the dynamics of salivary microstructure formation, growth, and reorganization using time-lapse imaging over 15 h. Immunofluorescence detection monitored production of individual basement membrane components forming around developing microstructures, and Ki67 assessed proliferation. Dynamic movements in hydrogels were quantified by measuring angular velocity (ω) of rotating salivary microstructures and changes in basement membrane architecture during microstructure growth. Integrin involvement in the dynamic reassembly was assessed using knockdown and inhibitor approaches. Single hS/PCs expanded over 5 days into spherical microstructures typically containing 3–10 cells. In larger macrostructures, proliferation occurred near the peripheral basement membrane that underwent growth-associated cycles of thinning and collapse. *De novo* secretion of laminin/collagen IV from reorganizing hS/PCs preceded that of perlecan/HSPG2. Microstructures routinely expressed β_1 integrin-containing complexes at basement membrane-associated regions and exhibited spontaneous and coordinated rotation during basement membrane maturation. β_1 integrin siRNA knockdown at the single-cell state prevented hS/PC microstructure growth. After microstructure formation, β_1 integrin knockdown reduced rotation and mean ω by 84%. Blockade of the α_1 integrin subunit (CD49a) that associates with β_1 reduced mean ω by 66%. Studies presented here show that initial hS/PC structure growth and basement membrane maturation depends on $\alpha_1\beta_1$-integrin mediated

signaling. Coordinated cellular motility during neotissue reorganization reminiscent of salivary gland acini was critically dependent both on hS/PC-secretion of laminin,collagen type-IV, and perlecan/HSPG2 and the force-driven interactions of $\alpha_1\beta_1$-integrin activation. We conclude that $\alpha_1\beta_1$-integrin plays a critical role in establishing human salivary gland coordinated structure and function, and that its activation in tissue engineered systems is essential to tissue assembly.

Keywords: basement membrane, integrin, mechanotransduction, salivary gland, human, stem/progenitor cells

INTRODUCTION

The long-term focus of work in our lab is to devise tissue engineering approaches to fully reestablish salivary function in patients suffering from hyposalivation disorders related to cancer treatment, aging, disease, or injury. Salivary gland engineering is a challenge because the gland is a complex physiological system in which multiple cell types, including several distinct epithelia, comprise an intact functional gland. These epithelia natively form in direct contact with the underlying mesenchyme, which provides biological cues to direct differentiation and development. This work builds upon observations in salivary gland development that point to the critical role of the $\alpha_1\beta_1$-integrin and associated extracellular matrix (ECM) in salivary morphogenesis (Larsen et al., 2006; Daley et al., 2011). We investigated the dynamic reorganization of primary human salivary stem/progenitor cells (hS/PCs) that we characterized previously (Srinivasan et al., 2017) after encapsulation within a biomimetic hyaluronate (HA) hydrogel designed to mimic native tissue mesenchyme. The hydrogel culture system offers optical clarity, preservation of 3D architecture, and control of the microenvironment representing the natural mesenchyme that surrounds a developing exocrine gland, allowing us to explore the early events that occur during hS/PC reorganization as they mimic events in salivary gland morphogenesis.

In tissue, the basement membrane is the link between the epithelium and the underlying mesenchyme, providing orientation and organization, allowing selective filtration of nutrients and waste, and establishing survival cues. Integrins, present on epithelial cells including those in salivary glands (Togarrati et al., 2018), initiate cytoskeletal reorganization and associated cell signaling processes in development, homeostasis, and regeneration. Adhesion-dependent processes enhance responses to growth factors present in the environment to initiate cellular processes (Chen et al., 1994; Miyamoto et al., 1996) including cellular proliferation and differentiation, signal transduction activation, cell survival signals, and gene expression occurring as early as 6 h post-adhesion (Royce et al., 1993; Hoffman et al., 1996; Bouhadir and Mooney, 1998; Lafrenie et al., 1998; Overeem et al., 2015). Integrin ligands in the basement membrane including laminin (Virtanen et al., 2000), collagen IV, and perlecan/HSPG2 surround ductal and acinar compartments in salivary glands. Each component of the basement membrane has unique functions. Laminin directly interacts with integrins (Nishiuchi et al., 2006) expressed by epithelial cells to induce cell polarity and organization of developing structures and tissues (Li et al., 2003; Patel et al., 2006; Daley et al., 2012). Collagen IV fibers in the basement membrane interact primarily with the underlying mesenchyme in connective tissue to provide tensile strength critical for regulating integrin turnover during dynamic cell movements and tissue maintenance (Pines et al., 2012). Another critical component, perlecan/HSPG2, is essential because of its complex repertoire of adhesive motifs (Yurchenco et al., 1987; Hayashi et al., 1992; Battaglia et al., 1993; Brown et al., 1997; Ettner et al., 1998), its ability to serve as a growth factor depot (Chen et al., 2007), and its innate compressive strength and flexibility as a proteoglycan with long flexible core and hydrophilic glycosaminoglycan chains (Wijeratne et al., 2016). Perlecan also mechanically stabilizes the basement membrane (Farach-Carson et al., 2014), because perlecan's core protein anchors to laminin while its heparan sulfate chain containing domains integrate with collagen IV in a "spot-weld" fashion (Behrens et al., 2012).

We hypothesized that dynamic interactions between integrins present on hS/PCs and their matrix ligands in the basement membrane mediate salivary hS/PC microstructure growth and dynamic reorganization. Using a variety of techniques including quantitative time lapse imaging, immunostaining, RNA knockdown, and direct inhibition, we investigated the role of $\alpha_1\beta_1$-integrin in early events during hS/PC microstructure formation and basement membrane assembly. The temporal and spatial organization of *de novo* microstructures was analyzed to reveal how physical and biological morphogenic cues direct salivary gland architecture, reorganization, and growth dynamics, all needed to support development of tissue engineered replacements to provide a permanent solution for hyposalivation disorders.

MATERIALS AND METHODS

Human Subjects Research

This study was carried out in accordance with the recommendations of the Christiana Care Health System Institutional Review Board (IRB)-approved protocols with written informed consent from all subjects. All subjects gave written informed consent in accordance with the Declaration of Helsinki. The protocol was approved by the IRBs at CCHS, Rice University and UTHealth as well as by the Committee for the Protection of Human Subjects at UTHealth.

Tissue Culture

Patients undergoing scheduled surgery at Christiana Care Health System (Newark, DE) consented for an unaffected portion of their parotid gland tissue to be transferred to Rice University or the University of Texas Health Science Center at Houston under IRB-approved protocols. The fresh parotid gland tissue was prepared in agreement with a standard operating protocol for generating hS/PCs (Wu et al., 2018). hS/PCs were cultured in Hepato-STIM™ medium supplemented with 10 ng/mL EGF (355056; Corning) and 1% (v/v) penicillin-streptomycin (15140122; Life Technologies/ThermoFisher), and maintained at 37°C in a 5% (v/v) CO_2 incubator as described previously (Pradhan et al., 2009). The studies in this article used samples from three female donors age, 22, 57 and 63. hS/PCs expressed biomarkers, K5, K14, and p63 and were encapsulated in hydrogels and cultured in complete Hepato-STIM™ medium for these studies. A full characterization of these cells appeared in Srinivasan et al. (2017) and they were fully sequenced in the functional annotation of the mammalian genome 5 (FANTOM5) project (FANTOM Consortium the RIKEN PMI CLST et al., 2014).

Encapsulation and Hydrogel Culture

Early passages (between 3 and 6) of hS/PC cells were encapsulated at 3×10^6 cell/mL in HyStem® hydrogel (GS311; BioTime/Ascendance Biotechnology). According to manufacturer's instructions, hydrogels were formed by mixing reconstituted thiol-modified hyaluronic acid (5.9 mM) and polyethylene glycol diacrylate (1.5 mM) at a 4:1 volume ratio, and plated on microscope glass slides fitted with pre-sterilized arrays of 50 μL wells made from laser-cut polydimethylsiloxane (PDMS; Sylgard™ 184; Dow Corning) sheets (**Figure S1**). Hydrogels were removed from the mold then each transferred into individual wells of a 48-well plate and cultured as described above. A typical hydrogel formed a low-profile cylinder measuring 6 mm in diameter and 2 mm in height. Hydrogels also were formed directly on confocal glass bottom dishes (P50G1.54F; MatTek) for live-cell imaging. 3D cultures were maintained until microstructures reached up to ∼50 μm in diameter (between 6 and 16 days), a time when most live-tracking experiments were initiated. Viability assays using Calcein AM (80011-3; Biotium) and Ethidium Homodimer-III (40050; Biotium) in accordance with manufacturer guidelines were performed in cell-laden hydrogel cultures. IMARIS 9.2 software (Bitplane) was used to separate and quantify objects (**Movie S1**).

Immunocytochemistry

Human parotid gland tissue cryosections embedded in CRYO-OCT Compound (Tissue-Tek) or cells encapsulated in hydrogels were fixed with 4% (w/v) paraformaldehyde (A11313; Alfa Aesar), permeabilized with 0.2–3% (v/v) Triton® X-100 (A16046; Alfa Aesar), and blocked with 3–10% (v/v) goat serum (5058835; EMD Millipore). Samples were incubated with primary antibodies against basement membrane proteins: laminin (NB300-144; Novus Biologicals, 1:200), collagen IV (NBP1-97716, 1:200; Novus Biologicals), perlecan/HSPG2 (NBP1-05170, 1:200; Novus Biologicals), or β_1 integrin (NB100-63255, 1:200; Novus Biologicals), followed by appropriate secondary antibodies conjugated to Alexa Fluor 488 (A11029; Life Technologies/ThermoFisher), Alexa Fluor 568 (A11011; Life Technologies/ThermoFisher) to tag proteins of interest. Nuclear [4′,6-diamidino-2-phenylindole (DAPI); 40011; Biotium] and filamentous actin (A22287; Life Technologies/ThermoFisher) counterstains were used prior to mounting (P36930; Life Technologies/ThermoFisher), if necessary, and confocal imaging (A1; Nikon Instruments) of specimens.

Western Blots

Cells transfected with siRNA in 6 well-plate were harvested with and lysed in RIPA buffer containing: 150 mM NaCl, 5 mM EDTA, 1% (v/v) NP-40, 24 mM sodium deoxycholate, 3.5 mM SDS, and supplemented with protease inhibitors (Halt™ Protease Inhibitor Cocktail (100X), 78430; Thermo Scientific). Proteins were separated by SDS-PAGE and transferred to nitrocellulose membranes for immunoblotting with antibodies. Primary antibodies were monoclonal mouse anti-integrin β1 (NB100-63255, 1:500, Novus Biologicals) and polyclonal rabbit GAPDH (PA1-980, 1:1000; Invitrogen). Secondary antibodies were horseradish peroxidase-conjugated sheep anti-mouse (515-035-062, 1:25,000) or goat anti-rabbit (111-035-144, 1:50,000) from Jackson ImmunoResearch Laboratories Inc. For β_1 integrin knockdown studies in 2D, cells were either transfected with scrambled siRNA or ITGB1 siRNA and collected at 72 h post-transfection.

Time-Lapse Imaging and Image Analysis

For brightfield live imaging experiments, hydrogels were transferred to glass bottom culture dishes and placed within a temperature controlled heated stage set to 37°C during 15 h live-imaging experiments (Eclipse TE300 and A1R MP+ microscopes, Nikon Instruments). Angular velocities (ω) (rev/h) of organizing hS/PC microstructures (diameters of 20–52 μm) were calculated manually from time-lapse imaging videos where images were acquired every 5 min. Time-lapse recordings and confocal micrographs were analyzed using NIS Elements AR (Nikon Instruments). Dimensional and positional information was extracted from individual frames in each time-lapse recording. For fluorescence image analysis, fluorescence intensities were divided into four groups: $I = 0$, $I > 500$, $I > 1000$, and $I > 3000$. The baseline-background intensities (I_b) were calculated from confocal images of secondary only control hydrogels used in the analysis and are 188 ± 4 (A.U.), 221 ± 2 (A.U.), and 48 ± 2 (A.U.) for laminin, collagen IV, and perlecan, respectively. Timestamps of fluorescence micrographs or movies of hS/PCs in hydrogels will be in the form of days (D) or hours. Dimensional, colocalization, and surface analysis of fluorescence images was performed on confocal micrograph stacks using IMARIS 9.2 (Bitplane). Image preparation and visualization required NIS Elements AR, IMARIS, Fiji (Schindelin et al., 2012), ImageJ (NIH), and Adobe Photoshop (Adobe).

Integrin Analysis

Published literature was consulted to identify the integrin subunits reported to be present in normal human salivary tissue. The summary of these findings is presented in **Table S1**, along with key studies establishing binding interactions between integrins and their ligands expressed in human salivary tissue: laminin, collagen IV, and perlecan/HSPG2. This analysis implicated the β_1 integrin as a likely player in salivary reassembly, thus immediate efforts were focused on this integrin subunit. Integrin subunits that form dimers with β_1 integrin expressed in human salivary tissue include α_1, α_3, α_5, and α_6. Integrin subunits α_3 and α_6 are expressed at lower levels than α_1, and α_5 is essential during branching morphogenesis via fibronectin interactions. The integrin subunit α_1 is abundant in the epithelial compartments of the salivary gland and a prime candidate for interacting with basement membrane components secreted by hS/PCs: laminin, collagen IV, and perlecan/HSPG2, during early reorganization.

Small Interfering RNA and Transfections

Knockdown of the expression of β_1 integrin was accomplished using an siRNA approach (*Silencer*® Select siRNA, 4390825; Life Technologies/ThermoFisher). ITGB1 siRNA (s7574) labeled with Cy3 (AM1632; Ambion), or *Silencer*® Cy™3-labeled Negative Control No. 1 siRNA (AM4621; Ambion) was used to identify structures transfected with siRNA or scrambled siRNA. Cells in hydrogels were transfected with a final concentration of 192 nM of each siRNA sequence under rotating culture conditions using Lipofectamine RNAiMAX Transfection Reagent (13778150; Invitrogen) for 6 h. Quantification of knockdown using siRNA targeting ITGB1 in hS/PC microstructures (hydrogels) and in monolayers (6-well plate) was, respectively, performed by immunocytochemistry 46 h post-transfection and Western blot 72 h post-transfection. A coverage index (I_C) in Equation 1 was developed to quantify the amount of β_1 integrin expression surrounding a microstructure to evaluate the effectiveness of siRNA treatment in hydrogels.

$$I_C = \frac{A_{\beta 1\ integrin}}{A_s} \tag{1}$$

I_C is dimensionless and defined by the area occupied by β_1 integrin at the surface of the microstructure ($A_{\beta 1\ integrin}$) normalized to the theoretical surface area (A_s) in Equation 2 of the microstructure determined by respective microstructure radii.

$$A_s = 4\pi r^2 \tag{2}$$

$A_{\beta 1\ integrin}$ is quantified from confocal z-stacks using the IMARIS image analysis software. Surfaces are generated from immunofluorescence intensities of β_1 integrin expression for microstructures treated with scrambled siRNA ($n = 10$) or ITGB1 siRNA ($n = 10$). Calculations of $A_{\beta 1\ integrin}$ are generated and normalized by A_s to determine I_C for both treatment groups ($n = 10$). $A_{\beta 1\ integrin}$ universally was greater since surface area calculations for each β_1 integrin plaque were summed and contributed to an observed inflation of I_C. However, relative differences remain true since each confocal z-stack was subjected to the same image analysis algorithm.

Loss of Function Studies

Loss of function studies were conducted between 3 and 7 days after encapsulation, to ensure structure sizes were similar at the time of treatment and time-lapse imaging studies were performed within 36 h post-transfection. Treatments were performed the same way for all hydrogels regardless of encapsulated cell/cluster size. The ω of Cy3-labeled ITGB1 siRNA$^+$ microstructures ($n = 37$) compared to Cy3-labeled scrambled siRNA controls ($n = 25$) was measured.

Next, CD49a blocking antibody (anti-CD49a, Clone 5E8D9, NBP2-29757; Novus Biologicals) was used to stabilize the inactive conformation of β_1 integrin subunits with their α_1 subunit partners, effectively blocking functional interactions with matrix ligands (Forsyth et al., 2002). Culture media without blocking antibody as well as a non-blocking CD49a antibody (anti-CD49a, Clone CL7207, NBP2-76478; Novus Biologicals) served as controls. CD49a antibodies (25 μg/mL) were added for 1 h prior to time-lapse imaging to allow full diffusional access to cells in hydrogels (Du et al., 2011). The ω of antibody-blocked structures moving in hydrogels ($n = 32$) was calculated and analyzed as described above and compared to no treatment ($n = 24$) and non-blocking ($n = 14$) controls.

Statistical Analysis

All quantified values are shown as mean ± SEM, with n = number of events. Unpaired Student's t-tests were used to identify differences between control and treated groups. One-way ANOVA followed by a post-test was used to identify differences between groups >2. No significant differences were identified when comparing cells from three donors ($p = 0.55$) (**Figure S2**), so data from control and treated conditions from all sources was analyzed together to increase sample size. Asterisks indicate significant differences when compared with reference controls ($^{***}p < 0.001$). Prism 7.0 (Graph Pad) was used for statistical analyses.

RESULTS

Cell Encapsulation and Microstructure Formation

Encapsulated hS/PCs in HA-hydrogel systems readily formed multicellular 3D microstructures. Most cell death observed at day 2 (D2) occurred during the encapsulation process or in the period immediately after encapsulation. EthD-III$^+$ dead cells remained as single cells and had not divided nor co-localized with other viable single-cells or clusters (not shown). These non-viable cells at D2 post-encapsulation accounted for 24% of cells, and they remained in the single-cell state. By day 5 post-encapsulation (D5), 74.3 ± 0.3% of the total viable cells were either clustered or remained at the single-cell state (**Figures 1A,B**). Furthermore, all single hS/PCs after 5 days in culture express laminin and 32% express perlecan (**Figure S3**), when a representative region

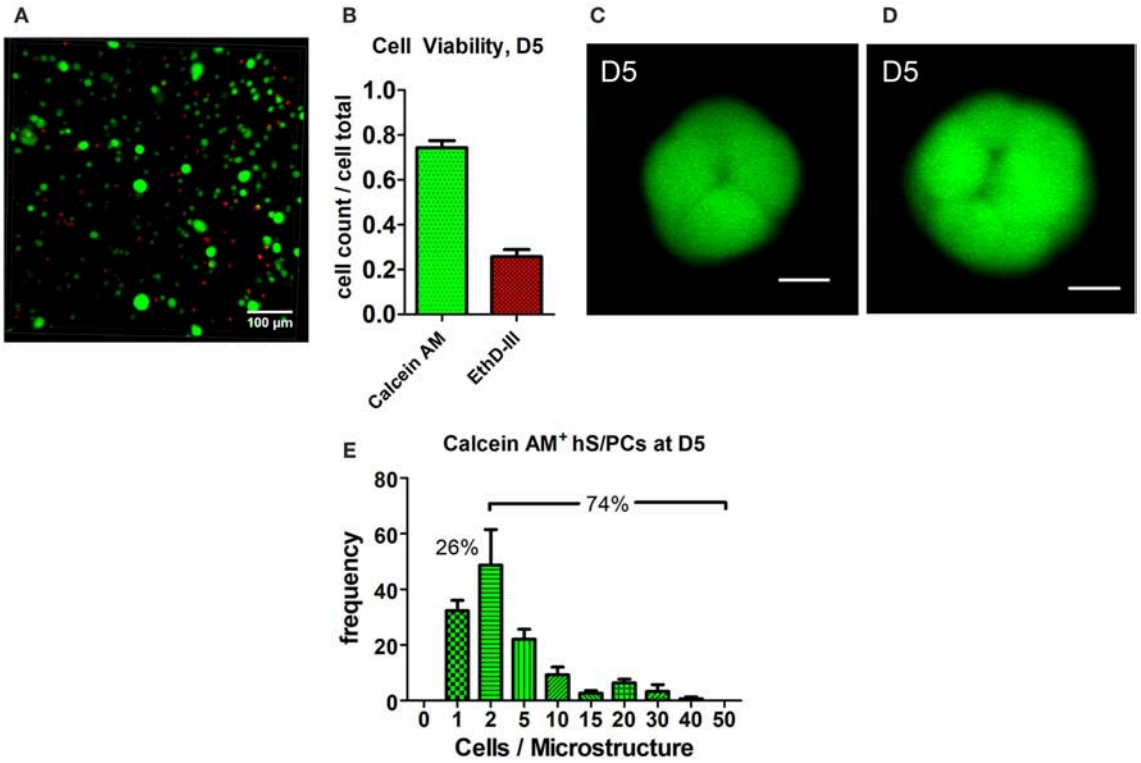

FIGURE 1 | Cluster formation and analysis of microstructure size. hS/PCs cultured for 5 days in HA-based hydrogels formed clusters up to 35 µm in diameter **(A)** with 74.3% viability **(B)** determined by Live/Dead assays. Confocal micrographs were used to quantify cell viability from regions of interest (ROI) of equivalent volumes. Organizing microstructures of 30–35 µm containing 8 and 16 cells, respectively (**C,D**, scale bar = 10 µm), are readily seen. The distribution of the number of hS/PCs within each microstructure encapsulated in HA-based hydrogel at D5 was measured with respect to microstructure diameter. Approximately 74% of viable cells were in clusters and 26% of viable cells remained single cells **(E)**.

of interest is evaluated. Two examples of viable microstructures at D5 had diameters of 30 and 37 µm and contained 8 and 16 cells, respectively (**Figures 1C,D**). Analysis of the total viable population showed that cluster volumes at D5 averaged 9465 $\pm$ 985 μm^3 with mean diameters of 26 µm and containing 5–6 cells. Of the viable cells, ∼74% were in clusters and 26% remained as single cells (**Figure 1E**). In **Figure 1E**, values within each group are binned to include quantities between an interval beginning and including the group value to and excluding the larger group value, i.e., group 1 contains the cell count between $1 < 2$, including 1 but excluding 2. Structure sizes varied throughout the entire hydrogel, and did not track with location. Larger structures (>40 µm in diameter) were found distributed throughout the hydrogel as well as in the hydrogel center, indicating that nutrient diffusion was not limited near the center of the hydrogel.

Dynamics of Basement Membrane Formation

The optical clarity of HA-based hydrogels made visualization of dynamics of basement membrane formation in 3D feasible. Single-cell and multicellular motility of cells and microstructures was captured using time-lapse microscopy and production of basement membrane components in time-matched specimens was analyzed using immunocytochemistry (ICC). We initially observed that the interactions involved in hS/PC microstructure formation, growth and basement membrane maturation preceded polarization and lumen formation that occurred only later in larger structures. The synthesis and secretion of basement membrane proteins began shortly after encapsulation in cultured hS/PCs in 3D HA-hydrogel cultures, evident even in single cells (**Figures 2A,D,G**). Encapsulated hS/PCs at the single-cell state initially secreted basement membrane proteins laminin (**Figure 2A**) and collagen IV (**Figure 2D**), and some perlecan/HSPG2 (**Figure 2G**) at the periphery to form *de novo* basement membranes surrounding larger individual salivary microstructures. All single hS/PCs in culture express laminin and 32% express perlecan when evaluated after 5 days in culture (**Figure S3**), and shows laminin is routinely deposited at the single-cell state. Collagen IV was seen in both the secretory pathway and at the periphery in single cells and larger clusters (**Figures 2D–F**). Both laminin and collagen IV surrounded larger structures (**Figures 2B,C,E,F**), but perlecan expression was discontinuous at the structure periphery, regardless of cluster size (**Figures 2H,I**). Laminin, collagen IV, and perlecan proteins surrounding single hS/PCs and hS/PC microstructures were quantified with respect to structure diameters and fluorescence intensities (**Figure S4**). Basement membrane proteins are present

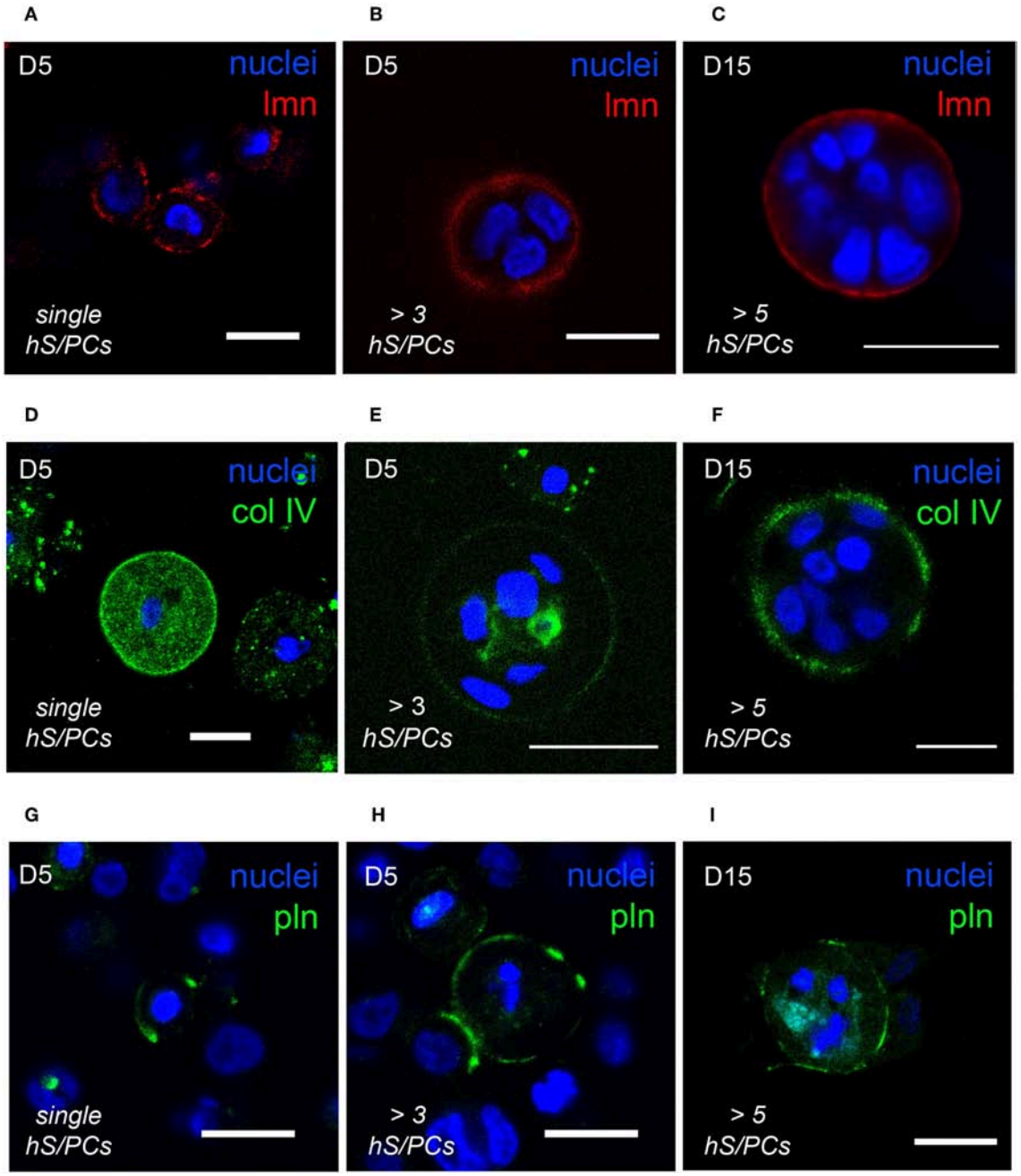

FIGURE 2 | hS/PCs sequentially secrete basement membrane proteins during microstructure reorganization and function. Encapsulated hS/PCs in HA-PEGDA hydrogels initially produce laminin (red) **(A–C)** and collagen IV (green) **(D–F)** even at the single-cell state **(A,D)**. Perlecan (green) **(G–I)** secretion follows to stabilize the laminin and collagen IV networks. Scalebar = 20 μm in all confocal micrographs.

at early and later growth stages. Laminin and collagen IV are secreted by single hS/PCs by D5 (**Figures S5A–C**) and by D15, laminin remains at the periphery of the multicellular cluster accompanied by perlecan (**Figures S5D–F**). Production of individual basement membrane components was similar to that seen in native tissue, where laminin, collagen IV, and perlecan surround and separate individual acini, co-located with β1 integrin on the basal cell surfaces of acinar cells (**Figure S6**).

Microstructures "Spin" as They Deposit Basement Membrane

Microstructures containing two or more cells were observed to generate enough traction to begin to rotate or "spin" in the HA-based hydrogels during the same time period when deposition of basement membrane components was occurring (**Movie S2**). Adhesive interactions between integrins on cells and matrix or hydrogel networks surrounding them

can generate traction forces large enough to drive observed revolutions of entire multicellular structures, and this behavior was observed in **Figures 3A–D**. Cells within microstructures moved together in a coordinated manner yielding a net directional rotation whose angular velocity (ω) could be measured. Microstructures were observed to move both in a clockwise or a counterclockwise fashion, even within the same gel. The coordinated motion of cells within microstructures was quantified by their rotation where ω was calculated from time-lapse imaging micrographs. In cases where the surrounding *de novo* basement membrane was not completely formed and/or exhibited border irregularity, neither the rotation nor coordination were quantifiable. Therefore, only angular velocities of smooth, multicellular structures exhibiting coordinated rotations were included in the analysis. Analysis of 118 spinning structures meeting these criteria showed that untreated microstructures $33.9 \pm 1.06\,\mu m$ in diameter rotated at 0.28 ± 0.02 rev/h, $n = 49$. An example of this is shown in **Figure 3** where a $30\,\mu m$ microstructure rotates at 92°/h ($\omega = 0.26$ rev/h).

If cells in a microstructure were seen to move independently from one other within its structure, net rotations were never observed. This lack of coordination was seen periodically in clusters of 3–4 cells during early stages of organization. Immunocytochemistry revealed cell-secreted laminin and collagen IV surrounded individual cells within microstructures of comparable size (not shown).

Growth of Microstructures After Basement Membrane Formation

Dynamic growth and organization of microstructures that had formed in hydrogels were tracked using time-lapse imaging to identify how various dynamic processes affected microstructure growth and basement membrane maturation in HA-hydrogels. Coordinated multicellular movements on the micron-order were observed to occur in virtually all viable structures. Motion analysis at the cell- and microstructure-level was performed at discrete timepoints to examine both cell-cell and cell-basement membrane dynamics of hS/PC-derived microtissues during microstructure organization. A surprising observation was that the size of salivary microstructures did not increase linearly, rather the motion and expansion of the cells within the structure appeared to exert a force on the basement membrane that first led to its thinning, and then its "popping" to assume a larger diameter (**Movie S3**). **Movie S4** captures expansion events of a pair of salivary microstructures. For example, the basement membrane of a larger microstructures ($\geq 100\,\mu m$ in diameter) underwent cyclical contractile and tensile phases, evident as "thick" or "thin" basement membranes (**Figures 4A,B**). A typical "popping cycle" lasted 0.67 ± 0.34 h and led to a volumetric expansion of $42.8 \pm 8.3\%$ ($n = 3$) that was assessed by taking measurements of the major and minor axes in individual frames acquired from time-lapse imaging for each microstructure. To determine how microstructures grow at a cellular level, we examined Ki67 expression and found that the vast majority of dividing cells reside at the periphery of the multicellular structures, immediately adjacent to the basement membrane where they are expected to apply compressive force (**Figure 4C**).

Figure 4D shows how the thickening and thinning phases of the basement membrane changed with time. Contractile or "thick" phases (noted as 1: shaded red) alternated with tensile or "thin" phases (noted as 2,3: shaded blue). Prior to "popping," a progressive thinning of the basement membrane was seen, eventually leading to its failure and a yielding of its tensile strength as the structure expanded volumetrically. **Figure 4E** is a schematic that illustrates proposed interactions between the basement membrane and integrin subunits during contractile (phase 1) and tensile events (phases 2–3). Forces exerted on the basement membrane are large enough to break perlecan spot-welds between laminin and collagen IV networks causing subsequent remodeling of the basement membrane.

Cell-Basement Membrane Interactions: Dependence on $\alpha_1\beta_1$ Integrin

To investigate the dependence on integrin interactions for dynamic behavior of microstructures within a hydrogel microenvironment, we used a Cy3-tagged siRNA specifically targeted to β_1 integrin. Not surprisingly, early β_1 integrin siRNA treatment on single-cells in hydrogel prevented hS/PC microstructures from forming, while scrambled Cy3-tagged siRNA treatment on single-cells in hydrogel yielded microstructure formation through days 7–8 post-treatment (**Figure S7**). To study the role of β_1 integrin in microstructure motility, loss of function experiments was undertaken after microstructure formation had already occurred and time-lapse recordings were performed for various treatment groups.

Quantification of knockdown of β_1 integrin in hS/PC microstructures treated with scrambled siRNA or ITGB1 siRNA was performed in hydrogels using immunocytochemistry to capture spatial distribution of β_1 integrin expression. In the scrambled siRNA group, β_1 integrin expression was continuous and surrounded each microstructure's surface (**Figure 5A**). A discontinuous or "patchy" distribution of β_1 integrin surrounded each microstructure in the β_1 integrin knockdown group (**Figure 5B**). A 63% reduction in β_1 integrin expression at the surface of hS/PC microstructures was achieved from ITGB1 siRNA treatment in hydrogels ($I_C = 0.80 \pm 0.13$, $n = 10$) compared to the group treated with scrambled siRNA ($I_C = 2.22 \pm 0.16$, $n = 10$) (**Figure 5C**). Quantification of knockdown using siRNA targeting ITGB1 in hS/PC monolayers was also performed by Western blot (**Figure S8**). Immunocytochemistry proved to be the more sensitive approach for quantifying β_1 integrin knockdown and is consistent with the loss of function results obtained from time-lapse imaging experiments.

Angular velocities were calculated in both treated knockdown and scrambled control conditions. Organized hS/PC structures treated with β_1 integrin siRNA demonstrated an 84% mean reduction in ω ($\omega = 0.04 \pm 0.01$ rev/h, $n = 37$) compared to the scrambled control ($p < 0.0001$) (**Figures 6A,B**). Complete arrest of motility was not apparent because a few cells were still motile within the microstructures. **Figure S9** shows distribution of Cy3-tagged siRNA in hS/PC microstructures

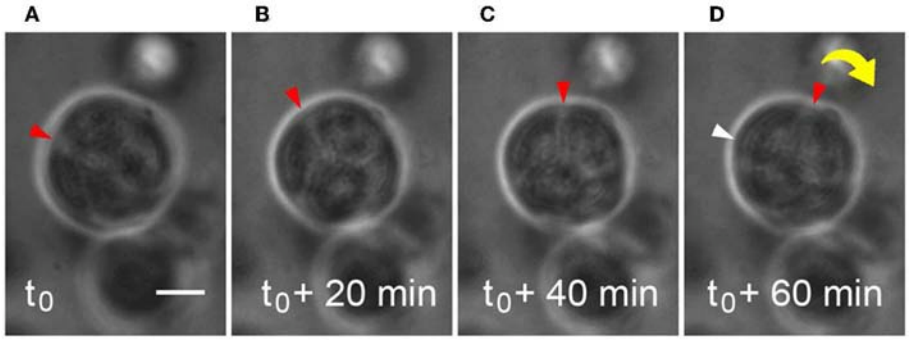

FIGURE 3 | Microstructure dynamics during rotation in HA-based hydrogel. Movement of a 30 μm microstructure was measured and found to rotate ~92°/h during basement membrane deposition. Still frames are extracted from time-lapse movies of microstructure motility at 20 min intervals **(A–D)**. Scale bar = 10 μm.

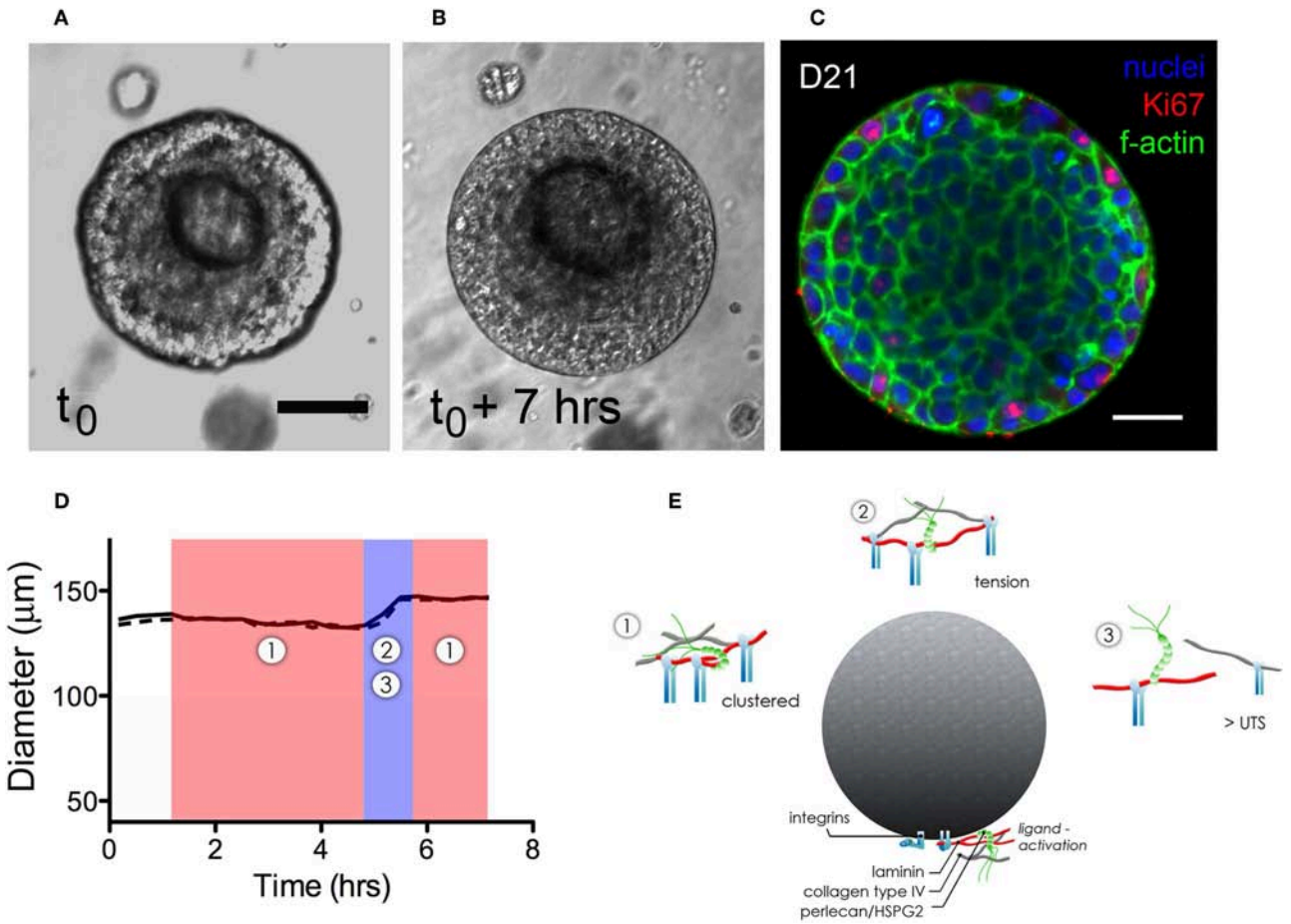

FIGURE 4 | Dynamics of expansion of an hS/PC microstructure in HA-based hydrogel. Non-linear structural expansion was observed over a 7 h period **(A,B)**. Total expansion increased structure volume by 33%. Ki67 staining revealed proliferative cells at the periphery of the microstructure, adjacent to the basement membrane **(C)**. Dimensional analysis measuring major and minor axes (x-dotted line, y-solid line) in **(D)** reveals microstructure contraction during phase 1 followed by a growth and tensile phase (2–3) for <1.5 h that visibly stretched and thinned the basement membrane. Schematics of phases 1–3 in **(E)** focus on integrin-basement membrane interactions. During phase 1, integrins are more tightly spaced when associated with laminin and collagen IV in the basement membrane. Expansion-induced tension on the basement membrane in phase 2 increased periodicity of in-tact integrin attachments reaching tensions large enough to break perlecan spot-welds between laminin and collagen IV networks. Ultimate tensile strength (UTS) of proteins in the basement membrane are approached during phase 3-expansion causing reorganization and subsequently remodeling of the basement membrane as contractile events during phase 1 began. Scalebar = 25 μm.

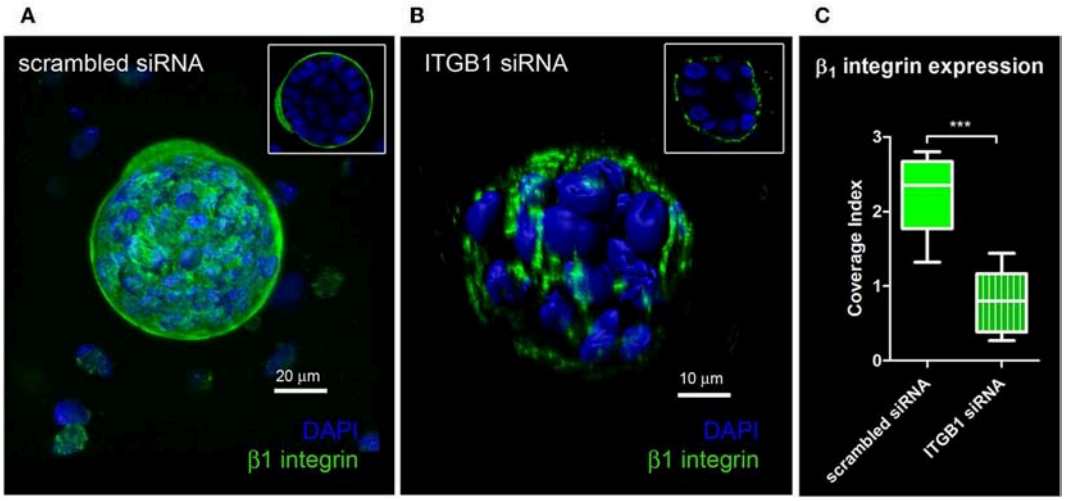

FIGURE 5 | Quantification of knockdown of β_1 integrin in hS/PC microstructures. hS/PC microstructures formed in HA-based hydrogels and were transfected with scrambled siRNA or ITGB1 siRNA. Immunocytochemistry was used to determine β_1 integrin expression and spatial distribution of β_1 integrin 46 h post-transfection. Image analysis software was used to quantify β_1 integrin expression at microstructure surfaces from confocal micrographs and coverage indices were calculated for scrambled siRNA **(A)** and ITGB1 siRNA **(B)** groups where a 63% reduction in β_1 integrin expression at microstructure surfaces was quantified **(C)**.

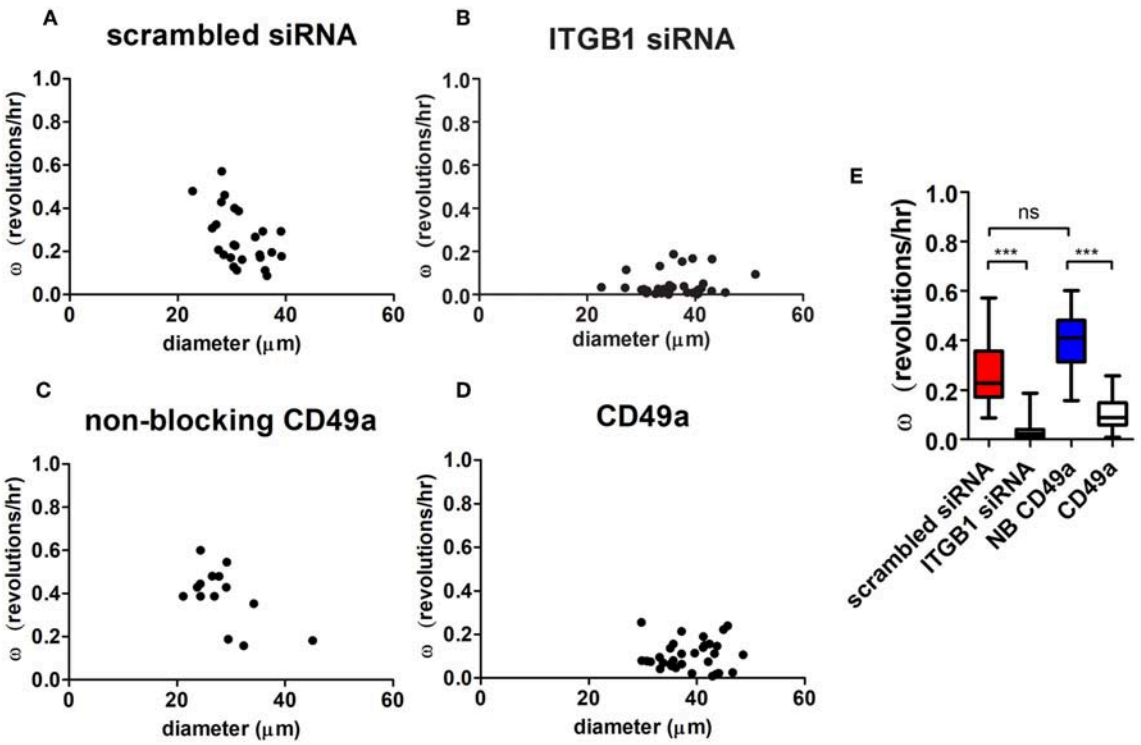

FIGURE 6 | Integrin inhibition diminishes microstructure motility in HA-based hydrogels. Angular velocities (ω) of hS/PC microstructures were plotted with respect to size **(A–D)**. The ω of hS/PC structures treated with siRNA targeting β_1 integrin demonstrated an 84% mean reduction in ω compared to its control ($p < 0.0001$). Organized hS/PC structures treated with integrin blocking antibody CD49a resulted in a 73% reduction in ω when compared to its non-blocking CD49a control ($p < 0.0001$) **(E)**. The ω of hS/PC structures treated with scrambled siRNA and non-blocking CD49a control groups were not significantly different from each other, $p = 0.23$.

before time-lapse experiments. Acute treatment on hS/PC microstructures with either scrambled siRNA (**Figure S9A**) or ITGB1 siRNA (**Figure S9B**) yielded high transfection efficiency where each cell within all microstructures contained Cy3-tagged siRNA. These images were taken prior to each siRNA live-imaging experiment to ensure presence of siRNA in each hS/PC microstructure.

To further define the integrin involved in spinning behavior, hS/PC clusters were treated with a blocking antibody that stabilizes the inactive conformation of α_1 integrin subunit (CD49a) its partner β_1 integrin, which would normally complex with laminin and collagen IV. This treatment resulted in a 73% reduction in ω ($\omega = 0.11 \pm 0.01$ rev/h, $n = 32$) when compared to the non-blocking CD49a control ($p < 0.0001$), (**Figures 6C–E**). The reduction of β_1 integrin activation with blocking α_1 integrin subunits and direct interactions with the basement membrane significantly reduced the rotational motion observed by the perturbed microstructures. Treatment with Volociximab, a clinically used high-affinity monoclonal antibody that specifically binds to $\alpha_5\beta_1$ integrin (Ricart et al., 2008), decreased ω ($\omega = 0.11 \pm 0.01$ rev/h, $n = 54$) to levels similar to those observed when α_1 integrin subunit was targeted. The ω of hS/PC structures treated with scrambled siRNA and without treatment were not significantly different from each other, $p = 0.23$, nor were the non-treated and non-blocking CD49a control groups (**Figure 6E**).

DISCUSSION

Microstructure Assembly and Basement Membrane Formation

The pattern and sequence of basement membrane protein production that we observed for hS/PC microstructures in HA-hydrogels was comparable to that seen in embryonic development, wherein laminin is secreted before collagen IV or perlecan (Huang et al., 2003). This finding helps validate the use of the HA-hydrogel platform for study of cell and matrix dynamics as they occur in salivary gland development. Interactions between cells and basement membrane depend on adhesion molecules and surface receptors, primarily integrins (Loducca et al., 2003; Lourenço and Kapas, 2005; Laine et al., 2008), and thus these molecules typically are expressed concordantly with the basement membrane components during embryogenesis (Li et al., 2003). Unlike in the salivary gland, where formation of the gland involves growth and branching morphogenesis originating from a rudimentary salivary bud, in HA hydrogels, microstructures originate from growth from a single hS/PC or merging of adjacent hS/PC microclusters (Pradhan-Bhatt et al., 2013). In HA hydrogels, hS/PCs secrete ligands including laminin, collagen IV, and perlecan that together direct matrix-mediated signaling to establish the apical-basal axis in polarizing secretory epithelium similar to that which forms *in vivo* (Yu et al., 2005; Overeem et al., 2015). This signal transduction is initiated by HA receptors (Spicer and Tien, 2004) and integrins (Hynes, 2002) interacting with their respective ligands to regulate cell cycle, adhesion, differentiation, as well as motility during microstructure growth and organization. These integrin-mediated interactions with basement membrane proteins precede both epithelial morphogenesis (Rebustini et al., 2007) and polarity in developing epithelial tissues (Haigo and Bilder, 2011; Lerner et al., 2013). The observation that hS/PCs secrete their own ECM to promote homeostasis and survival, in a hydrogel naïve of murine extracellular matrix proteins and growth-factors, further supports hS/PCs' role in human tissue engineering applications. Key understanding of hS/PCs ability to maintain key cell machinery for secretory function (Baker et al., 2010) in modifiable hydrogel culture systems (Shubin et al., 2015, 2017) is now of critical importance and continues to challenge us in the field of translational tissue engineering.

A survey of integrins previously reported to be expressed in salivary gland led us to examine the role of β_1 integrin that is known to be involved in acquisition of polarity in dynamic microstructure formation (Akhtar and Streuli, 2013). A key finding from our work was that the initial deposition of matrix proteins, first laminin, then collagen IV, and finally perlecan, along with expression of the β_1 integrin, is required for *de novo* basement membrane maturation, and precedes epithelial cell polarization and lumen formation needed for vectorial secretion of salivary components.

In microstructures, perlecan/HSPG2 was deposited with the laminin and collagen IV networks of the organizing *de novo* basement membrane similarly to the way it would in salivary compartments in native tissue (**Figure S6**). The perlecan distribution that we observed within the basement membrane was not as continuous, seen in **Figures 2G–I**, as *de novo* laminin or collagen IV networks. Regions of discontinuity could offer spatial opportunities for branching morphogenesis, cleft formation, and interactions with stromal elements to occur. Access to hS/PC derived epithelial microstructures attached to the basement membrane could also encourage integration with connective tissue or support cells, i.e., vascular, neuronal, or immune cells after hydrogel implantation. During salivary microstructure maturation, assembled basement membrane proteins recruit β_1 integrin-mediated adhesion complexes to the cell surface where they provide survival signals, support motility, and favor additional ECM secretion. Lacking these signals, it is thus not surprising that the majority of cell death that we observed after cells were encapsulated occurred within the single cell population shortly after encapsulation. Once matrix secretion commenced, high viability was observed throughout the rest of the culture period.

"Spinning" as a Way to Deposit Basement Membrane

Within our tunable HA-based hydrogel system (G' range ∼60–300 Pa) (Ghosh et al., 2005; Prestwich, 2011), basement membrane deposition and organization was found to be dynamic and restricted to the microstructure's periphery in 3D. Basement membrane proteins are actively secreted on planar culture systems (E∼3 GPa) (Callister, 2000), but do not provide organizational cues and are nine orders of magnitude stiffer when contrasted with most hydrogel systems. However, a laminin- or

elastin-modified synthetic 2D scaffold system (E∼1–20 MPa), although 10^6 times stiffer than our hydrogels, triggered tight junction formation and polarization in monolayers of acinar and ductal cells (Cantara et al., 2012; Foraida et al., 2017) reinforcing the role of spatial cues from the basement membrane on reorganizing salivary epithelium.

As salivary hS/PC microstructures matured and were enveloped by an organizing basement membrane, spontaneous global revolutions were observed. Other hydrogel culture systems used by others to encourage epithelial cell growth and organization also revealed coordinated dynamics during cellular reorganization. For example, primary breast cancer cells harvested from murine tumor cells were cultured in rodent Matrigel™. Matrigel™-based culture systems consist of self-assembling basement membrane networks, and these primary murine tumor cells produced multicellular assemblies (Tanner et al., 2012) visibly similar to those produced in our HA-hydrogels. A key difference between our HA-hydrogels and Matrigel™ systems is that our HA-hydrogels are protein-free, thus any proteins present in the basement membrane were produced *de novo* by the encapsulated cells themselves, and were not supplied by the hydrogel system.

3D assembly of mammary and kidney cells in Matrigel™ were reported to exhibit full revolutions of mammary gland acini and MDCK cell cysts (Tanner et al., 2012; Wang et al., 2013). Revolutions were tracked during the fibrillar organization of the surrounding basement membrane. A separate study confined MDCK cell cysts to a micropatterned array, to show they rotated when soluble Matrigel™ components were made available (Rodríguez-Fraticelli et al., 2012). Those MDCK cell "cysts" established basement membranes and formed lumens post-rotation indicating that basement membrane formation and organization preceded polarization. In developing *Drosophila* eggs, global revolutions established a polarized corset of collagen IV matrix to govern elongation (Haigo and Bilder, 2011). Thus, this coordinated multicellular motility and likely mechanical feedback from the microenvironment is likely to be associated with secretion and organization of *de novo* basement membranes surrounding multicellular structures. It should be noted that unlike the process of salivary gland formation during embryonic development, where the bud is "anchored" to the stalk and full range of rotation is limited, the unanchored hS/PC derived microstructures in hydrogels are capable of full 360° rotations.

Features of Basement Membrane That Support Tissue Expansion and Morphogenesis

We found that HA-hydrogels encouraged the dynamic assembly and movement of microstructures exhibiting coordinated cell-cell and cell-matrix adhesion behavior reminiscent of salivary cell movements during morphogenesis (Lafrenie and Yamada, 1998). This movement is thought to occur via mechano-chemical coupling similar to that previously reported in other systems (Ringer et al., 2017). The basement membranes of larger, mature microstructures were evident at the boundaries between cluster and hydrogel directly interacting with the outermost hS/PCs. This connected hS/PC cell complex could participate in propagating intercellular signals either directly or indirectly using co-signaling mechanisms established throughout the entire microstructure. These hS/PC cell complexes in HA hydrogels are not restricted by the organized basement membrane and will continue to grow into larger structures within growth permissive hydrogel matrices. The hydrogels used to study reorganization dynamics (G' ∼ 200 Pa, E∼0.6 kPa) had mechanical properties comparable to embryonic tissue (E ∼ 0.1 kPa) (Peters et al., 2015), where $\nu = 0.5$ and $E = 2G'(1+\nu)$. All microstructures exhibited a tightly organized basement membrane and rarely exceeded diameters >50 μm, similar to dimensions of acinar structures in normal human tissue (E ∼ 2 kPa) where acinar diameters range between 30 and 60 μm (not shown). These mechanosensitive interactions thus directly influence the size and shape of these reorganizing salivary microstructures. We have shown salivary hS/PCs require specific integrin binding complexes to achieve the coordinated reorganization within HA-based hydrogel culture systems. With increased knowledge of the effect of stiffness and bioactive potential of our tunable hydrogel on hS/PC growth and reorganization, we may now further design the hydrogel composition to encourage and reveal hierarchical complexities of the growing salivary epithelium.

Interactions Between Growing Structures and Basement Membranes Favor Non-linear Expansion

In **Figure 7**, we present a proposed model to describe the observed interactions of the basement membrane components that can produce changes in local tensile and adhesive interactions with surface integrins that can occur during microstructure rotation and expansion. Integrin-mediated complexes with basement membrane components generate forces that influence all adjacent cells within the microstructure. If the basement membrane surrounding the microstructure is treated as a thin walled vessel under internal pressure from increasing cell numbers, the increase in compressive force on the structure would generate strain on the basement membrane, enough to cause a "thinning" and potential breakage of the basement membrane fabric at its weakest adhesion points, described in **Figure 4** and **Movie S3**. In the case of this basement membrane network, we propose that the relatively low affinity linkages involving perlecan's heparan sulfate chains may be those weakest links because of its mechanical behavior in tension (Wijeratne et al., 2016) and its role as a crosslinker rather than a true part of the polymeric meshwork of the basement membrane. The rupture of the "spot welds" (Behrens et al., 2012) involving perlecan thus are likely to be those sites first to break during the "pop," allowing for the observed rapid expansion and initiating a new round of basement membrane formation to surround the larger structure.

Critical Role of Integrin $\alpha_1\beta_1$ in Supporting Dynamic Movements of Salivary Microstructures

In this study, β_1 integrin was found to be essential to both the formation and organization of hS/PC microstructures, evidenced

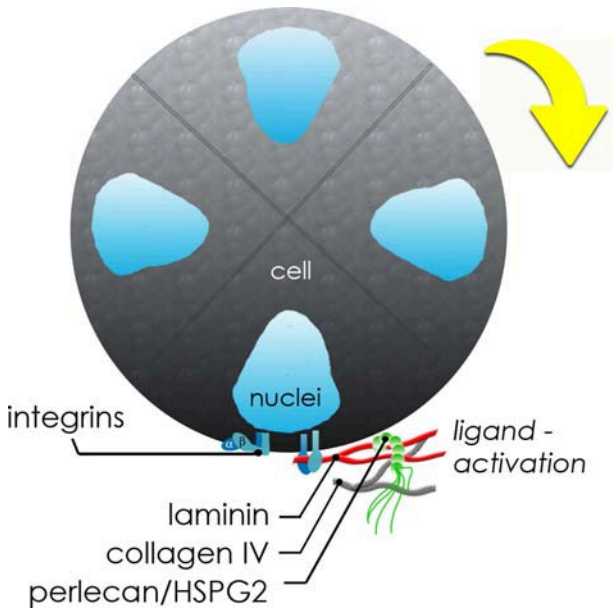

FIGURE 7 | Schematic of molecular interplay during *de novo* microstructure organization. Secreted basement membrane proteins are directionally secreted and organized by hS/PCs at the periphery of the growing microstructure. The initial growth and coordinated movement during this maturation phase depends on β_1 integrin activation by hS/PC-secreted ligands: laminin, collagen IV, and perlecan/HSPG2. Adhesive interactions between integrins on cells and matrix or hydrogel networks surrounding them can generate traction forces large enough to drive coordinated revolutions of entire multicellular structures.

by our finding that knockdown cells lacking normal amounts of β_1 integrin failed to form multi-cellular microstructures. Additionally, even though single hS/PCs could secrete individual matrix proteins prior to microstructure assembly, activated integrins were required to initiate formation of multicellular structures. We specifically found that β_1 integrin is a key driver of early microstructure assembly and growth. The role of β_1 integrins, primarily $\alpha_1\beta_1$, in dynamic movements of formed structures also was clear for spinning and associated deposition of basement membrane components. Knockdown and antibody-blocked microstructures failed to exhibit the dynamic behaviors of normal microstructures. This is entirely consistent with the appearance of this integrin during salivary development during times of peak glandular growth, morphogenesis and expansion (Lafrenie and Yamada, 1998).

In addition to integrins, salivary hS/PCs possess integrin-independent CD44 and RHAMM receptors for HA (Pradhan-Bhatt et al., 2014) and interact directly with HA to promote cell-cell and cell-matrix adhesion during morphogenesis (Spicer and Tien, 2004). Early studies of the basement membrane in murine embryonic salivary glands showed that hyaluronan accounted for ∼50% of newly synthesized glycosaminoglycans (GAGs) in the basal lamina (Cohn et al., 1977). The high presence of hyaluronan during development tracks with the abundance of HA-receptor, CD44, expression in human embryonic parotid glands that persist during adulthood (Franchi et al., 2001). These non-integrin signaling receptors influence cell adhesion, proliferation, invasion, and matrix assembly; however, deletion of these receptors does not result in embryonic lethality (Tammi et al., 2002). Likewise, although these receptors can mediate similar processes to those that integrins regulate (Toole, 2001), their expression in our system alone was not sufficient to encourage growth and maturation of hS/PC microstructures, which required production of basement membrane components and associated integrins.

Although this study primarily focused on laminin, collagen IV and perlecan/HSPG2 as major components of the basement membrane, the presence and role of fibronectin in HA-based hydrogel systems also must be explored in future work. Demonstration that coordinated motility of organizing hS/PC microstructures is partially mediated by $\alpha_5\beta_1$ integrin, which is known to interact with fibronectin, provides evidence that specific cellular machinery required for branching morphogenesis is preserved in hS/PC microstructures cultured in biocompatible and GMP-ready hydrogels. To drive and establish the hierarchical architecture of the salivary gland, a clearer understanding of basement membrane dynamics in the context of maintaining boundaries during homeostasis and breaking boundaries during growth and morphogenesis is desired.

Fibronectin's role during bulk and local reorganization of the basement membrane triggers branching morphogenesis events in developing salivary glands (Larsen et al., 2006; Harunaga et al., 2014). The basement membrane dynamics at the periphery of larger microstructures would encourage cryptic self-assembly sites within fibronectin to be exposed by tension (Zhong et al., 1998) to encourage local morphological changes. Of particular interest, high-affinity binding of fibronectin by β_1 integrin (Faull et al., 1993) and β_1 integrin's role in the mechano-chemical "check-point" of salivary gland cleft formation (Daley et al., 2011), highlights the potential formation of sophisticated glandular geometries within our hydrogel systems, an area of current investigation in our laboratory.

ETHICS STATEMENT

This study was carried out in accordance with the recommendations of the Christiana Care Health System Institutional Review Board (IRB)-approved protocols with written informed consent from all subjects. All subjects gave written informed consent in accordance with the Declaration of Helsinki during their pre-operation consultation. The protocol was approved by the IRBs at CCHS, Rice University and UTHealth as well as by the Committee for the Protection of Human Subjects at UTHealth.

AUTHOR CONTRIBUTIONS

DW designed and performed experiments and prepared manuscript. RW provided cell source and clinical advisor.

DW, RW, DH, and MF-C provided scientific and manuscript writing contributions.

FUNDING

The authors would like to acknowledge that grant support was provided by NIH/NIDCR R01DE022969 to MF-C and F32DE024697 to DW, private philanthropic funding from the Helen F. Graham Cancer Center and Research Institute to RW, as well as the UTHealth System Faculty STARs Program Award to MF-C.

SUPPLEMENTARY MATERIAL

The Supplementary Material for this article can be found online at: https://www.frontiersin.org/articles/10.3389/fcell.2019.00224/full#supplementary-material

REFERENCES

Akhtar, N., and Streuli, C. H. (2013). An integrin–ILK–microtubule network orients cell polarity and lumen formation in glandular epithelium. *Nat. Cell Biol.* 15, 17–27. doi: 10.1038/ncb2646

Baker, O. J., Schulz, D. J., Camden, J. M., Liao, Z., Peterson, T. S., Seye, C. I., et al. (2010). Rat Parotid Gland Cell Differentiation in Three-Dimensional Culture. *Tissue Eng. Part C* 16, 1135–1144. doi: 10.1089/ten.tec.2009.0438

Battaglia, C., Aumailley, M., Mann, K., Mayer, U., and Timpl, R. (1993). Structural basis of β1 integrin-mediated cell adhesion to a large heparan sulfate proteoglycan from basement membranes. *Eur. J. Cell Biol.* 61, 92–9.

Behrens, D. T., Villone, D., Koch, M., Brunner, G., Sorokin, L., Robenek, H., et al. (2012). The epidermal basement membrane is a composite of separate laminin- or collagen IV-containing networks connected by aggregated perlecan, but not by nidogens. *J. Biol. Chem.* 287, 18700–18709. doi: 10.1074/jbc.M111.336073

Bouhadir, K. H., and Mooney, D. J. (1998). *In vitro* and *in vivo* models for the reconstruction of intercellular signaling. *Annal. N. York Acad. Sci.* 842, 188–194. doi: 10.1111/j.1749-6632.1998.tb09647.x

Brown, J. C., Sasaki, T., Göhring, W., Yamada, Y., and Timpl, R. (1997). The C-terminal domain V of perlecan promotes β1 integrin-mediated cell adhesion, binds heparin, nidogen and fibulin-2 and can be modified by glycosaminoglycans. *Eur. J. Biochem.* 250, 39–46. doi: 10.1111/j.1432-1033.1997.t01-1-00039.x

Callister, W. (2000). *Fundamentals of Material Science and Engineering: An Interactive E-Text*. Somerset, NJ: John Wiley & Sons.

Cantara, S. I., Soscia, D.,. A., Sequeira, S. J., Jean-Gilles, R. P., Castracane, J., and Larsen, M. (2012). Selective functionalization of nanofiber scaffolds to regulate salivary gland epithelial cell proliferation and polarity. *Biomaterials* 33, 8372–8382. doi: 10.1016/j.biomaterials.2012.08.021

Chen, Q., Kinch, M. S., Lin, T. H., Burridge, K., and Juliano, R. L. (1994). Integrin-mediated cell adhesion activates mitogen-activated protein kinases. *J. Biol. Chem.* 269, 26602–26605.

Chen, Q., Sivakumar, P., Barley, C., Peters, D. M., Gomes, R. R., Farach-Carson, M. C., et al. (2007). Potential role for heparan sulfate proteoglycans in regulation of transforming growth factor-β (TGF-β) by modulating assembly of latent TGF-β-binding protein-1. *J. Biol. Chem.* 282, 26418–26430. doi: 10.1074/jbc.M703341200

Cohn, R. H., Banerjee, S. D., and Bernfield, M. R. (1977). Basal lamina of embryonic salivary epithelia. Nature of glycosaminoglycan and organization of extracellular materials. *J. Cell Biol.* 73, 464–478. doi: 10.1083/jcb.73.2.464

Daley, W. P., Gervais, E. M., Centanni, S. W., Gulfo, K. M., Nelson, D. A., and Larsen, M. (2012). ROCK1-directed basement membrane positioning coordinates epithelial tissue polarity. *Development* 139, 411–422. doi: 10.1242/dev.075366

Daley, W. P., Kohn, J.,. M., and Larsen, M. (2011). A focal adhesion protein-based mechanochemical checkpoint regulates cleft progression during branching morphogenesis. *Dev. Dynam.* 240, 2069–2083. doi: 10.1002/dvdy.22714

Du, J., Chen, X., Liang, X., Zhang, G., Xu, J., He, L., et al. (2011). Integrin activation and internalization on soft ECM as a mechanism of induction of stem cell differentiation by ECM elasticity. *Proc. Natl. Acad. Sci. U.S.A.* 108, 9466–9471. doi: 10.1073/pnas.1106467108

Ettner, N., Göhring, W., Sasaki, T., Mann, K., and Timpl, R. (1998). The N-terminal globular domain of the laminin α1 chain binds to α1β1 and α2β1 integrins and to the heparan sulfate-containing domains of perlecan. *FEBS Lett.* 430, 217–221. doi: 10.1016/S0014-5793(98)00601-2

FANTOM Consortium and the RIKEN PMI and CLST, Forrest, A. R., Kawaji, H., Rehli, M., Baillie, J. K., de Hoon, M. J., et al. (2014). A promoter-level mammalian expression atlas. *Nature* 507, 462–470. doi: 10.1038/nature13182

Farach-Carson, M. C., Warren, C.,. R., Harrington, D. A., and Carson, D. D. (2014). Border patrol: insights into the unique role of perlecan/heparan sulfate proteoglycan 2 at cell and tissue borders. *Matrix Biol.* 34 (Suppl. C), 64–79. doi: 10.1016/j.matbio.2013.08.004

Faull, R. J., Kovach, N.,. L., Harlan, J. M., and Ginsberg, M. H. (1993). Affinity modulation of integrin alpha 5 beta 1: regulation of the functional response by soluble fibronectin. *J. Cell Biol.* 121, 155–162. doi: 10.1083/jcb.121.1.155

Foraida, Z. I., Kamaldinov, T., Nelson, D. A., Larsen, M., and Castracane, J. (2017). Elastin-PLGA hybrid electrospun nanofiber scaffolds for salivary epithelial cell self-organization and polarization. *Acta Biomater.* 62, 116–127. doi: 10.1016/j.actbio.2017.08.009

Forsyth, C. B., Pulai, J., and Loeser, R.,. F. (2002). Fibronectin fragments and blocking antibodies to α2β1 and α5β1 integrins stimulate mitogen-activated protein kinase signaling and increase collagenase 3 (matrix metalloproteinase 13) production by human articular chondrocytes. *Arthritis Rheum.* 46, 2368–2376. doi: 10.1002/art.10502

Franchi, A., Moroni, M., Paglierani, M., and Santucci, M. (2001). Expression of CD44 standard and variant isoforms in parotid gland and parotid gland tumours. *J. Oral Pathol. Med.* 30, 564–568. doi: 10.1034/j.1600-0714.2001.300910.x

Ghosh, K., Shu, X. Z., Mou, R., Lombardi, J., Prestwich, G. D., Rafailovich, M. H., et al. (2005). Rheological characterization of *in situ* cross-linkable hyaluronan hydrogels. *Biomacromolecules* 6, 2857–2865. doi: 10.1021/bm050361c

Haigo, S. L., and Bilder, D. (2011). Global tissue revolutions in a morphogenetic movement controlling elongation. *Science* 331, 1071–1074. doi: 10.1126/science.1199424

Harunaga, J. S., Doyle, A. D., and Yamada, K. M. (2014). Local and global dynamics of the basement membrane during branching morphogenesis require protease activity and actomyosin contractility. *Dev. Biol.* 394, 197–205. doi: 10.1016/j.ydbio.2014.08.014

Hayashi, K., Madri, J. A., and Yurchenco, P. D. (1992). Endothelial cells interact with the core protein of basement membrane perlecan through beta 1 and beta 3 integrins: an adhesion modulated by glycosaminoglycan. *J. Cell Biol.* 119, 945–959. doi: 10.1083/jcb.119.4.945

Hoffman, M. P., Kibbey, M. C., Letterio, J. J., and Kleinman, H. K. (1996). Role of laminin-1 and TGF-beta 3 in acinar differentiation of a human submandibular gland cell lie (HSG). *J. Cell Sci.* 109, 2013–2021.

Huang, C.-C., Hall, D. H., Hedgecock, E. M., Kao, G., Karantza, V., Vogel, B. E., et al. (2003). Laminin α subunits and their role in *C. elegans* development. *Development* 130, 3343–3358. doi: 10.1242/dev.00481

Hynes, R. O. (2002). Integrins: bidirectional, allosteric signaling machines. *Cell* 110, 673–687. doi: 10.1016/S0092-8674(02)00971-6

Lafrenie, R. M., Bernier, S. M., and Yamada, K. M. (1998). Adhesion to fibronectin or collagen I gel induces rapid, extensive, biosynthetic alterations in epithelial cells. *J. Cell. Physiol.* 175, 163–173. doi: 10.1002/(SICI)1097-4652(199805)175:2<163::AID-JCP6>3.0.CO;2-M

Lafrenie, R. M., and Yamada, K. M. (1998). Integrins and matrix molecules in salivary gland cell adhesion, signaling, and gene expression. *Ann. N. York Acad. Sci.* 842, 42–48. doi: 10.1111/j.1749-6632.1998.tb09630.x

Laine, M., Virtanen, I., Porola, P., Rotar, Z., Rozman, B., Poduval, P., et al. (2008). Acinar epithelial cell laminin-receptors in labial salivary glands in Sjogren's syndrome. *Clin. Exp. Rheumatol.* 26, 807–813. Available online at: http://www.clinexprheumatol.org/default.asp

Larsen, M., Wei, C., and Yamada, K. M. (2006). Cell and fibronectin dynamics during branching morphogenesis. *J. Cell Sci.* 119, 3376–3384. doi: 10.1242/jcs.03079

Lerner, D. W., McCoy, D., Adam Isabella, J., Anthony Mahowald, P., Gary Gerlach, F., Thymur Chaudhry, A., et al. (2013). A Rab10-dependent mechanism for polarized basement membrane secretion during organ morphogenesis. *Dev. Cell* 24, 159–168. doi: 10.1016/j.devcel.2012.12.005

Li, S., Edgar, D., Fässler, R., Wadsworth, W., and Yurchenco, P. D. (2003). The role of laminin in embryonic cell polarization and tissue organization. *Dev. Cell* 4, 613–624. doi: 10.1016/S1534-5807(03)00128-X

Loducca, S. V. L., Mantesso, A., Kapas, S., Williams, D. M., Araújo, N. S., and Araújo, V. C. (2003). Salivary gland tumours: immunoexpression of integrins β1, β3 and β4. *J. Oral Pathol. Med.* 32, 305–309. doi: 10.1034/j.1600-0714.2003.00114.x

Lourenço, S., and Kapas, S. (2005). Integrin expression in developing human salivary glands. *Histochem. Cell Biol.* 124, 391–399. doi: 10.1007/s00418-005-0784-3

Miyamoto, S., Teramoto, H., Gutkind, J.,. S., and Yamada, K. M. (1996). Integrins can collaborate with growth factors for phosphorylation of receptor tyrosine kinases and MAP kinase activation: roles of integrin aggregation and occupancy of receptors. *J. Cell Biol.* 135(6 Pt 1), 1633–1642. doi: 10.1083/jcb.135.6.1633

Nishiuchi, R., Takagi, J., Hayashi, M., Ido, H., Yagi, Y., Sanzen, N., et al. (2006). Ligand-binding specificities of laminin-binding integrins: a comprehensive survey of laminin–integrin interactions using recombinant α3β1, α6β1, α7β1 and α6β4 integrins. *Matrix Biol.* 25, 189–197. doi: 10.1016/j.matbio.2005.12.001

Overeem, A. W., Bryant, D. M., and van Ijzendoorn, S. C. D. (2015). Mechanisms of apical–basal axis orientation and epithelial lumen positioning. *Trends Cell Biol.* 25, 476–485. doi: 10.1016/j.tcb.2015.04.002

Patel, V. N., Rebustini, I. T., and Hoffman, M. P. (2006). Salivary gland branching morphogenesis. *Differentiation* 74, 349–364. doi: 10.1111/j.1432-0436.2006.00088.x

Peters, S. B., Nelson, D. A., Kwon, H. R., Koslow, M., DeSantis, K. A., and Larsen, M. (2015). TGFβ signaling promotes matrix assembly during mechanosensitive embryonic salivary gland restoration. *Matrix Biol.* 43, 109–124. doi: 10.1016/j.matbio.2015.01.020

Pines, M., Das, R., Ellis, S. J., Morin, A., Czerniecki, S., Yuan, L, et al. (2012). Mechanical force regulates integrin turnover in Drosophila *in vivo*. *Nat. Cell Biol.* 14, 935–943. doi: 10.1038/ncb2555

Pradhan, S., Zhang, C., Jia, X., Carson, D. D., Witt, R. L., and Farach-Carson, M. C. (2009). Perlecan domain IV peptide stimulates salivary gland cell assembly *in vitro*. *Tissue Eng. Part A* 15, 3309–3320. doi: 10.1089/ten.tea.2008.0669

Pradhan-Bhatt, S., Harrington, D., Duncan, R., Jia, X., Witt, R., and Farach-Carson, M. (2013). Implantable three-dimensional salivary spheroid assemblies demonstrate fluid and protein secretory responses to neurotransmitters. *Tissue Eng. Part A* 19, 1610–1620. doi: 10.1089/ten.tea.2012.0301

Pradhan-Bhatt, S., Harrington, D. A., Duncan, R. L., Farach-Carson, M. C., Jia, X., and Witt, R. L. (2014). A novel *in vivo* model for evaluating functional restoration of a tissue-engineered salivary gland. *Laryngoscope* 124, 456–461. doi: 10.1002/lary.24297

Prestwich, G. D. (2011). Hyaluronic acid-based clinical biomaterials derived for cell and molecule delivery in regenerative medicine. *J. Control. Release* 155, 193–199. doi: 10.1016/j.jconrel.2011.04.007

Rebustini, I. T., Patel, V. N., Stewart, J. S., Layvey, A., Georges-Labouesse, E., Miner, J. H., et al. (2007). Laminin α5 is necessary for submandibular gland epithelial morphogenesis and influences FGFR expression through β1 integrin signaling. *Dev. Biol.* 308, 15–29. doi: 10.1016/j.ydbio.2007.04.031

Ricart, A. D., Tolcher, A. W., Liu, G., Holen, K., Schwartz, G., Albertini, M., et al. (2008). Volociximab, a chimeric monoclonal antibody that specifically binds a_5b_1 integrin: a phase I, pharmacokinetic, and biological correlative study. *Clin. Cancer Res.* 14, 7924–7929. doi: 10.1158/1078-0432.CCR-08-0378

Ringer, P., Colo, G., Fässler, R., and Grashoff, C. (2017). Sensing the mechano-chemical properties of the extracellular matrix. *Matrix Biol.* 64, 6–16. doi: 10.1016/j.matbio.2017.03.004

Rodríguez-Fraticelli, A. E., Auzan, M., Alonso, M. A., Bornens, M., and Martín-Belmonte, F. (2012). Cell confinement controls centrosome positioning and lumen initiation during epithelial morphogenesis. *J. Cell Biol.* 198, 1011–1023. doi: 10.1083/jcb.201203075

Royce, L. S., Kibbey, M. C., Mertz, P., Kleinman, H. K., and Baum, B. J. (1993). Human neoplastic submandibular intercalated duct cells express an acinar phenotype when cultured on a basement membrane matrix. *Differentiation* 52, 247–255. doi: 10.1111/j.1432-0436.1993.tb00637.x

Schindelin, J., Arganda-Carreras, I., Frise, E., Kaynig, V., Longair, M., Pietzsch, T., et al. (2012). Fiji: an open-source platform for biological-image analysis. *Nature Methods* 9, 676–682. doi: 10.1038/nmeth.2019

Shubin, A. D., Felong, T. J., Graunke, D., Ovitt, C. E., and Benoit, D. S. W. (2015). Development of Poly(Ethylene Glycol) hydrogels for salivary gland tissue engineering applications. *Tissue Eng. Part A* 21, 1733–1751. doi: 10.1089/ten.tea.2014.0674

Shubin, A. D., Felong, T. J., Schutrum, B. E., Joe, D. S. L., Ovitt, C. E., and Benoit, D. S. W. (2017). Encapsulation of primary salivary gland cells in enzymatically degradable poly(ethylene glycol) hydrogels promotes acinar cell characteristics. *Acta Biomater.* 50, 437–449. doi: 10.1016/j.actbio.2016.12.049

Spicer, A. P., and Tien, J. Y. L. (2004). Hyaluronan and morphogenesis. *Birth Defects Res. Part C* 72, 89–108. doi: 10.1002/bdrc.20006

Srinivasan, P. P., Patel, V. N., Liu, S., Harrington, D. A., Hoffman, M. P., Jia, X., et al. (2017). Primary salivary human stem/progenitor cells undergo microenvironment-driven acinar-like differentiation in hyaluronate hydrogel culture. *Stem Cells Transl. Med.* 6, 110–120. doi: 10.5966/sctm.2016-0083

Tammi, M. I., Day, A. J., and Turley, E. A. (2002). Hyaluronan and homeostasis: a balancing act. *J. Biol. Chem.* 277, 4581–4584. doi: 10.1074/jbc.R100037200

Tanner, K., Mori, H., Mroue, R., Bruni-Cardoso, A., and Bissell, M. J. (2012). Coherent angular motion in the establishment of multicellular architecture of glandular tissues. *Proc. Natl. Acad. Sci. U.S.A.* 109, 1973–1978. doi: 10.1073/pnas.1119578109

Togarrati, P. P., Dinglasan, N., Desai, S., Ryan, W. R., and Muench, M. O. (2018). CD29 is highly expressed on epithelial, myoepithelial, and mesenchymal stromal cells of human salivary glands. *Oral Dis.* 24, 561–572. doi: 10.1111/odi.12812

Toole, B. P. (2001). Hyaluronan in morphogenesis. *Semin. Cell Dev. Biol.* 12, 79–87. doi: 10.1006/scdb.2000.0244

Virtanen, I., Gullberg, D., Rissanen, J., Kivilaakso, E., Kiviluoto, T., Laitinen, L., et al. (2000). Laminin α1-chain shows a restricted distribution in epithelial basement membranes of fetal and adult human tissues. *Exp. Cell Res.* 257, 298–309. doi: 10.1006/excr.2000.4883

Wang, H., Lacoche, S., Huang, L., Xue, B., and Muthuswamy, S. K. (2013). Rotational motion during three-dimensional morphogenesis of mammary epithelial acini relates to laminin matrix assembly. *Proc. Natl. Acad. Sci. U.S.A.* 110, 163–168. doi: 10.1073/pnas.1201141110

Wijeratne, S. S., Martinez, J. R., Grindel, B. J., Frey, E. W., Li, J., Wang, L., et al. (2016). Single molecule force measurements of perlecan/HSPG2: A key component of the osteocyte pericellular matrix. *Matrix Biol.* 50 (Suppl. C), 27–38. doi: 10.1016/j.matbio.2015.11.001

Wu, D., Chapela, P., and Farach-Carson, M. C. (2018). Reassembly of functional human stem/progenitor cells in 3D culture. *Methods Mol. Biol.* 1817, 19–32. doi: 10.1007/978-1-4939-8600-2_3

Yu, W., Datta, A., Leroy, P., O'Brien, L. E., Mak, G., Jou, T.-S., et al. (2005). β1-integrin orients epithelial polarity via Rac1 and laminin. *Mol. Biol. Cell* 16, 433–445. doi: 10.1091/mbc.e04-05-0435

Yurchenco, P. D., Cheng, Y. S., and Ruben, G. C. (1987). Self-assembly of a high molecular weight basement membrane heparan sulfate proteoglycan into dimers and oligomers. *J. Biol. Chem.* 262, 17668–17676.

Zhong, C., Chrzanowska-Wodnicka, M., Brown, J., Shaub, A., Belkin, A.,. M., and Burridge, K. (1998). Rho-mediated contractility exposes a cryptic site in fibronectin and induces fibronectin matrix assembly. *J. Cell Biol.* 141, 539–551. doi: 10.1083/jcb.141.2.539

Conflict of Interest: The authors declare that the research was conducted in the absence of any commercial or financial relationships that could be construed as a potential conflict of interest.

frontiers in Physiology

REVIEW
published: 22 August 2019
doi: 10.3389/fphys.2019.01011

Imaging the Dynamic Interaction Between Sprouting Microvessels and the Extracellular Matrix

*Adam Rauff[1,2], Steven A. LaBelle[1,2], Hannah A. Strobel[3], James B. Hoying[3] and Jeffrey A. Weiss[1,2]**

[1]Department of Biomedical Engineering, University of Utah, Salt Lake City, UT, United States, [2]Scientific Computing and Imaging Institute, University of Utah, Salt Lake City, UT, United States, [3]Innovations Laboratory, Advanced Solutions Life Sciences, Manchester, NH, United States

Thorough understanding of growth and evolution of tissue vasculature is fundamental to many fields of medicine including cancer therapy, wound healing, and tissue engineering. Angiogenesis, the growth of new vessels from existing ones, is dynamically influenced by a variety of environmental factors, including mechanical and biophysical factors, chemotactic factors, proteolysis, and interaction with stromal cells. Yet, dynamic interactions between neovessels and their environment are difficult to study with traditional fixed time imaging techniques. Advancements in imaging technologies permit time-series and volumetric imaging, affording the ability to visualize microvessel growth over 3D space and time. Time-lapse imaging has led to more informative investigations of angiogenesis. The environmental factors implicated in angiogenesis span a wide range of signals. Neovessels advance through stromal matrices by forming attachments and pulling and pushing on their microenvironment, reorganizing matrix fibers, and inducing large deformations of the surrounding stroma. Concurrently, neovessels secrete proteolytic enzymes to degrade their basement membrane, create space for new vessels to grow, and release matrix-bound cytokines. Growing neovessels also respond to a host of soluble and matrix-bound growth factors, and display preferential growth along a cytokine gradient. Lastly, stromal cells such as macrophages and mesenchymal stem cells (MSCs) interact directly with neovessels and their surrounding matrix to facilitate sprouting, vessel fusion, and tissue remodeling. This review highlights how time-lapse imaging techniques advanced our understanding of the interaction of blood vessels with their environment during sprouting angiogenesis. The technology provides means to characterize the evolution of microvessel behavior, providing new insights and holding great promise for further research on the process of angiogenesis.

Keywords: angiogenesis, neovessels, vascular networks, time-series imaging, extracellular matrix

OPEN ACCESS

Edited by:
Charles D. Little, University of Kansas Medical Center, United States

Reviewed by:
Aurora Hernandez-Machado, University of Barcelona, Spain
Nor Eddine Sounni, University of Liège, Belgium

***Correspondence:**
Jeffrey A. Weiss
jeff.weiss@utah.edu

Specialty section:
This article was submitted to Biophysics, a section of the journal Frontiers in Physiology

Received: *20 February 2019*
Accepted: *22 July 2019*
Published: *22 August 2019*

Citation:
Rauff A, LaBelle SA, Strobel HA, Hoying JB and Weiss JA (2019) Imaging the Dynamic Interaction Between Sprouting Microvessels and the Extracellular Matrix. Front. Physiol. 10:1011. doi: 10.3389/fphys.2019.01011

INTRODUCTION

An understanding of the growth and evolution of tissue vasculatures is fundamental to many fields of medicine including cancer therapy, wound healing, and tissue engineering (Carmeliet, 2005). Blood vessels are dynamic structures that provide tissues with oxygen and nutrients, endocrine signals, and immune access (Carmeliet and Jain, 2011). Changes in vascular growth

within tissues occur in response to changing metabolic needs and tissue repair. Angiogenesis, the growth of new vessels from existing ones, is dynamically influenced by a variety of environmental factors, including the tissue matrix. For example, growing vessels form adhesions that can transmit force to the extracellular matrix (ECM) and sense forces from the ECM. They also degrade the ECM around them by secretion of proteases and respond to growth factors for directional growth. Lastly, cells communicate *via* paracrine and juxtacrine signaling to regulate angiogenesis. These factors affect neovessel growth and guidance through the tissue stroma.

Despite our relatively deep knowledge of the process of angiogenesis and its regulation, there remains a gap in our understanding of the interactions between growing neovessels and the tissue microenvironment leading to deterministic vascular patterning. Angiogenesis is highly sensitive to chemical and mechanical factors present in the microenvironment, and distinct modes of interaction between vessels and the ECM are largely known from qualitative experiments (Ingber, 2002; Shiu et al., 2005; Li et al., 2005b). However, quantitative measurements of a signal or combination of multiple signals and the corresponding change in vessel behavior, such as migration direction or elongation rate, are difficult to obtain. Chemical signals such as cytokines and proteases are difficult to visualize over space and time near a growing microvessel. Spatiotemporal mechanical signals associated with ECM properties such as structure, composition, and boundary conditions are also difficult to obtain. However, recent studies that used new imaging technologies to capture the interplay of these signals and microvessels have helped elucidate the dynamics of mechanisms modulating angiogenesis.

Several image-based experimental methodologies enable the study of microvascular networks in space and time. Advancements in imaging technologies permit time-series and volumetric imaging of *in vitro* experiments. Time-series imaging involves capturing a sequence of images at defined locations and times, allowing observation of the dynamic evolution of vascular networks, instead of a single "snapshot" of a complex behavior. In microscopy, volumetric imaging acquires pictures of three-dimensional (3D) space by capturing a sequence of two-dimensional (2D) images at spaced focal planes. These volumetric imaging techniques enable extraction of more physiologically relevant information, as vessels reside in 3D environments *in vivo*, and behave differently on 2D substrates (Friedl and Wolf, 2003; Yamada and Cukierman, 2007). Thus, the ability to visualize microvessel growth over 3D space and time has led to more informative investigations of angiogenesis. Furthermore, experiments involving 3D time-series often require custom design and fabrication to devise a system that sustains culture conditions and enables imaging of both microvessels and their environment. Still, the technology offers unique measurements such as rates of growth and changes in network topology that are physiologically significant and are necessary for advancement of our understanding of angiogenesis.

This review describes how time-series microscopy has been used to study the interactions between growing microvessels and the ECM. First, we review mechanical and biophysical factors known to modulate angiogenic growth and the structure of new microvascular networks. Then, we consider proteolysis by neovessels as they degrade their surrounding matrix with matrix metalloproteases (MMPs). Next, we discuss chemotaxis, the migration of microvessels in response to a gradient of cytokines. Then, we look at the effect of stromal cells, including macrophages and mesenchymal stem cells (MSCs), on sprouting microvessels. Finally, we identify future directions for time-series-based research.

MECHANICAL AND BIOPHYSICAL SIGNALS

The development of the microvasculature during angiogenesis is regulated by mechanical and biophysical signals between growing neovessels and their local environment (Ingber, 2002; Rivron et al., 2012). Neovessel sprouts migrate through a complex environment of cells and ECM in the tissue, commonly referred to as the stroma. To advance through stromal matrices, neovessels use both pulling and pushing forces, which reorganize matrix fibers, while contracting and migrating cells can induce large deformations of the surrounding stroma (Shiu et al., 2005; Kirkpatrick et al., 2007; Krishnan et al., 2007; Underwood et al., 2014). Yet, dynamic interactions between neovessels and the stroma are difficult to study with traditional fixed time imaging techniques. Traditional techniques cannot directly observe behaviors such as migration, anastomosis, network elongation, and regression (Mammoto et al., 2009). This is primarily due to the limited number of model systems that permit observation of interactions in 3D space and time under physiologically relevant conditions, and the inherent nonlinearity of the integration of biochemical, biophysical, and mechanical signals (Ingber et al., 1995; Ingber, 2002). Studying the reciprocal relationship (**Figure 1**) of sprouting neovessels on their surrounding stromal matrix is crucial to determining the morphogenic control of developing vasculature, an important aspect of organ development (Ingber, 2002; Carmeliet, 2005), tissue engineering (Krishnan et al., 2013; Park et al., 2014), and wound healing (Kilarski et al., 2009; Hoying et al., 2014). Biophysical and mechanical factors such as ECM density and stiffness (Shiu et al., 2005; Krishnan et al., 2007; Edgar et al., 2014), fiber orientation (Kirkpatrick et al., 2007; McCoy et al., 2018), and tissue deformation (Underwood et al., 2014) are known to affect sprouting angiogenesis. Time-series microscopy has helped elucidate the dynamic behavior of microvessels in response to these biophysical signals, including the quantification of rates of neovessel elongation and matrix deformation, and new characterization of migratory behavior.

Effects of Extracellular Matrix Density

Microvessels are influenced by the density of their ECM substrate, which is related to the stiffness and porosity of the ECM (LaValley and Reinhart-King, 2014). Sieminski et al. found that capillary morphogenesis of human umbilical vein endothelial cells (HUVECs) and human blood outgrowth

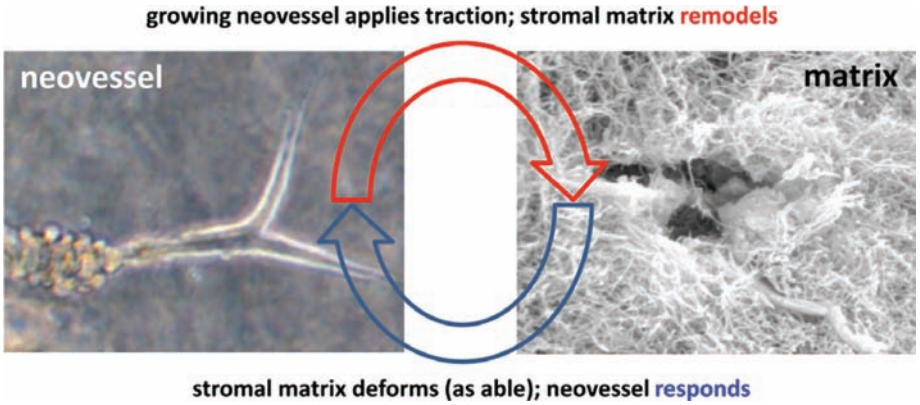

FIGURE 1 | Schematic highlighting the interplay between the growing neovessel and the surrounding matrix structure. Obtained with permission from Hoying et al. (1996).

endothelial cells (HBOEC) is affected by changes of apparent ECM stiffness (Sieminski et al., 2004). Three-dimensional (3D) cultures with type I collagen ECM were subjected to either a change in collagen density or constrained culture edges. At a lower collagen concentration (1.5 mg/ml), vascular networks exhibited greater luminal fractional area and no significant difference between constrained and floating cultures. At higher collagen concentration (3.0 mg/ml), constrained cultures showed decreased luminal fractional area compared with floating cultures. Ghajar et al. embedded HUVECs in varying concentrations of fibrin (2.5–10 mg/ml) and observed that higher fibrin concentrations reduced the growth of capillary networks (Ghajar et al., 2008). However, they also found that the increased density increased stiffness and altered diffusive transport of molecules, which may have contributed to the reduced growth. Edgar et al. used an *in vitro* culture of intact microvessels suspended in type I collagen and a computational model of angiogenesis and found that higher matrix density led to decreased microvessel growth (**Figure 2**; Edgar et al., 2014). When cultured in type I collagen concentrations of 3–4 mg/ml, microvessels exhibited shorter networks with decreased connectivity compared to a concentration of 2.0 mg/ml. These results were obtained using static measurements extracted from images of a confocal microscope. The vascular network was skeletonized, meaning the fluorescent vessels were segmented and an image processing algorithm was implemented to give a thin version of the vessel network. The skeletons of the network allowed measurement of total vascular length, interconnectivity, branch points, and normalized number of endpoints (**Figure 2**). The study suggests that for certain density ranges of a particular ECM composition, higher ECM density decreases growth rate, anastomosis, and pruning. Nevertheless, alteration of ECM density is often accompanied by changes in stiffness that can independently affect microvessel growth.

Studying the effects of matrix stiffness and density requires hydrogels with tunable stiffness. Cross-linked collagen gels created by reducing sugar content during polymerization (glycation) have increased stiffness with the same density. Mason et al. embedded spheroids of bovine aortic ECs (BAECs) embedded within type I collagen of varying mechanical properties according to initial ribose concentration. Increasing ECM stiffness independent of density resulted in increased formation of branched cord-like outgrowths from embedded spheroids (Mason et al., 2013). In another study, Bordeleau et al. used an *in vitro* model of BAEC and HUVEC spheroids embedded in type I collagen gel of varying mechanical properties. The study also included an *in vivo* model of tumor angiogenesis, where mice were treated with an inhibitor of the matrix crosslinking enzyme lysyl oxidase to alter tissue stiffness. The study demonstrated that increasing stiffness of the *in vitro* model altered the growth, integrity, and structure of EC vessels structures. Additionally, mice treated with the matrix crosslinking inhibitor had decreased tumor stiffness compared with controls, and the decreased stiffness correlated with significant decrease in the number of microvessel branches (Bordeleau et al., 2017). Alternatively, Sun et al. created hydrogels of varying stiffness and similar densities by adding different concentrations of PEG-dextran to Matrigel. HUVECs were then seeded on the hydrogel surface. The stiffest hydrogels (1,331 Pa) were shown to contain the most dense vascular network with the most branching and smallest cord length, compared to gels of lower stiffness (444 and 8,091 Pa) (Sun et al., 2014). These studies show that increasing ECM stiffness independently of density increases microvessel branching and growth. Nevertheless, studies that increased ECM density, and thereby stiffness, showed decreased microvessel branching and growth (Ghajar et al., 2008; Edgar et al., 2014). This inconsistency could arise because of lack of experimental data, as microvessels have not been observed to grow on stiff enough substrates that cause decrease in vessel growth. Alternatively, both stiffness and density affect microvessel growth in different ways that we do not yet understand. This is partly because previous experiments that observed microvascular network growth quantified global parameters of a vascular network and the entire ECM substrates using images of fixed cultures, which offer limited insight of microvessel behavior.

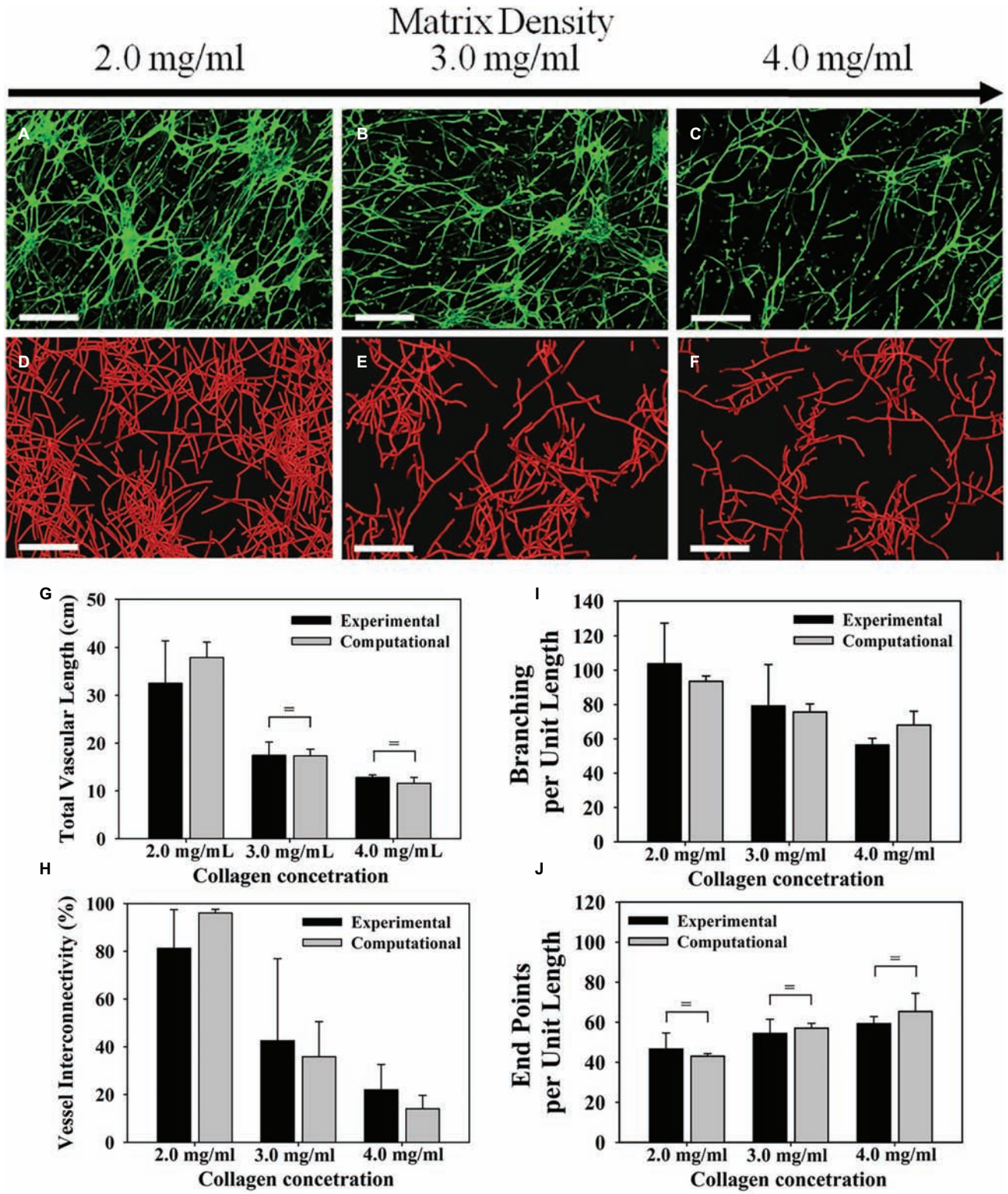

FIGURE 2 | Microvascular networks observed at different levels of collagen density, and associated measurements about the network. Increasing the density of the ECM reduced neovascularization in both the experiments and computational simulations. Top row **(A–C)**: Z-projection mosaic of 3D confocal image data showing vascularized collagen gels taken at Day 6 with different initial collagen concentration. **(D–F)** Results of comparable computational simulations, presented as renderings of the line segment data. **(G)** The total vascular length decreased as matrix density increased. Experimental measurements presented in black and

(Continued)

FIGURE 2 | computational predictions presented in gray. **(H)** Vessel interconnectivity, measuring percentage of microvessels that are connected into the largest continuous vascular network, decreased as a function of matrix density. **(I)** Branching point, defined as a node that connected to three or more vessel segments, was created by either a new vessel sprout (branching) or two separate vessels fusing into one (anastomosis). The number of branch points was normalized by the total vascular length to isolate the tendency of microvessels to branch as they grow. Branching per unit length decreased as matrix density increased. **(J)** An end point was defined as a node that was associated with only one vessel segment and represents the terminal end of a vessel. Normalizing the number of end points by the total vascular length revealed that the number of free ends per unit length increased with matrix density. There was a significant effect of matrix density on total vascular length, network connectivity, branch points, and free ends per unit length for both experimental and computational results (one-way ANOVA, $p < 0.05$ in all four cases). Modified with permission from Edgar et al. (2014).

Imaging microvessel cultures of varying ECM density over time has allowed the observation of evolution of a microvascular network, providing measurements of network regression, maturation and rate of growth. Park et al. used an *in vitro* model with a microfluidic device, time-lapse microscopy, and HUVECs to study the effect of ECM density on microvessel growth. HUVECs were polymerized in type I collagen with initial concentrations varied between 2.0 and 3.0 mg/ml. By measuring regression of vessels, that is the decrease in number of vessel segments over time from 90 to 720 min after seeding, microvessels were found to undergo decreased regression at the lower ECM density. This indicates that lower ECM density is more conductive to formation of a vascular network. Additionally, primitive metrics of network maturation were obtained by measuring the number of connected branches, junctions, and lumen formation of the same microvascular network over 7 days (Park et al., 2014). In another study, Shamloo et al. used a microfluidic device and varied type I collagen concentration between 0.7 and 2.7 mg/ml, while growing human dermal microvascular ECs (HMVECs) on beads. Microvessels exhibited longer sprouts in ECM densities of 1.2 and 1.9 mg/ml, while those grown on higher densities of 2.7 mg/ml formed fewer and shorter viable microvessels sprouts. Using time-lapse imaging, the authors observed the effect of ECM density on sprout elongation and branching over time. This led to the novel observation that HUVEC sprouts formed on beads elongate at a faster rate and undergo more branching events in ECM density ranges between 1.2 and 1.9 mg/ml (Shamloo et al., 2016). These studies were consistent with previous studies observing vascular formation while altering ECM density (Sieminski et al., 2004; Edgar et al., 2014). Even though these studies did not elucidate the effect of matrix stiffness on cellular responses, they introduced novel measurements relevant to neovessel behavior that could not be previously characterized. To understand microvessel response to differential ECM densities and stiffness, we must characterize vascular behavior over time. In addition to density and stiffness, ECM structure affects microvessel growth and evolves in response to vascular growth (**Figure 1**).

Microstructural Organization of the Extracellular Matrix

Actively growing neovessels move through the stroma and both reorganize matrix fibers and respond to the matrix structure (Korff and Augustin, 1999; Kirkpatrick et al., 2007; Edgar et al., 2014; Gjorevski et al., 2015). Most stromal matrices are heterogeneous interstitial gels composed of fibrillar collagen, chondroitin sulfates, hyaluronic acid, and other biomolecules (Hughes, 2008; Lu et al., 2011; McGettrick et al., 2012). The reorientation and remodeling of collagen fibrils influences the direction of neovessel migration through a contact guidance mechanism. Korff et al. embedded spheroids of endothelial cells in type I collagen gels, and observed sprouting by two nearby spheroids (Korff and Augustin, 1999). Tensional forces in the matrix generated by the endothelial cell sprouts between nearby cell spheroids remodeled ECM fiber orientation. Additionally, cells from each spheroid sprouted toward each other leading to sprout interactions. This interaction was shown to depend on adhesion to the collagen fibril RGD peptides, as addition of soluble RGD prevented directional sprout growth. In collectively migrating cell populations, similar tension forces resulted in alignment of the matrix fibrils, creating micro-tracks within the matrix. The direction of cell movements correlated with the direction of matrix alignment, indicating that migrating cells directly influence the matrix and exert spatially oriented forces to align matrix elements to navigate through the stroma (Gjorevski et al., 2015).

Substrate microstructural characteristics, including fiber orientation, length, and thickness influence cell behavior (Ingber et al., 1995). Mudera et al. embedded fibroblasts in collagen and exposed them to dual cues of contact guidance and mechanical load (Mudera et al., 2000). Differing degrees of orientation of fibronectin strands provided contact guidance that aligned cells. Cells that were not aligned during the applied loads remodeled their surrounding matrix more rapidly using MMPs (MMP-1, 2, and 3). This suggests matrix remodeling occurs to suit the co-existing mechanical stimuli. In another study, Lai et al. fabricated ECMs of aligned collagen fibrils and cultured human dermal microvascular ECs on aligned and unaligned collagen strips on a glass slide. Migration of ECs on aligned collagen substrates occurred primarily along the direction of fibers, while migration on unaligned substrates occurred randomly in all directions (Lai et al., 2012). Moreover, the shape of the cytoskeleton, as visualized by immunofluorescence, was extended along the direction of the fibers. In addition to directed migration from contact guidance, matrix fiber thickness, and length also influence EC network formation. McCoy et al. embedded human cerebral microvascular endothelial cells (hCMECs) in type I collagen, and allowed collagen polymerization at two different temperatures, 4 or 37°C (McCoy et al., 2016). Hydrogels polymerized in colder conditions contained thicker and longer collagen fibrils. The temperature-induced alteration of fiber size did not influence migration direction. However,

polymerization temperature did influence network maturity, as more lumen formation was observed in cold hydrogels.

Sprouting vessels in a 3D environment are assumed to be affected by local fiber orientation of the surrounding ECM, yet experimental observations of 3D matrix fibers by growing neovessels are scarce. Local fiber distribution contributes to the local mechanical response of the vessel microenvironment and the transmission of forces from cell-induced tractions (Guillabert-Gourgues et al., 2016; Hall et al., 2016). Forces from neighboring cells, vessels, or constraints imposed on the tissue boundaries distort the cytoskeleton and surrounding ECM environment (Hall et al., 2016), alter intracellular signaling pathways (Ingber et al., 1995; Mammoto et al., 2009; Rivron et al., 2012), and govern neovessel growth direction and final network shape (Krishnan et al., 2013; Edgar et al., 2014; Underwood et al., 2014). Neovessels growing in denser collagen gels produce less deformation and thus decreased fiber reorganization. Importantly, and consistent with a contact guidance-based mechanism, neovessels grow slower in these high-density matrices (Edgar et al., 2014). Furthermore, neovessels actively remodel their environment as tip cells actively contract, compact, and reorganize matrix structures (Rivron et al., 2012; Gjorevski et al., 2015). The extent of ECM deformation depends on vascular traction and substrate material properties, and also on the distribution of matrix fibers, which in turn influence neovessel growth and organization (Krishnan et al., 2007; Rivron et al., 2012; Underwood et al., 2014). Notwithstanding, physiological mechanisms involved with microvessel migration through 3D matrices remain incomplete. Previous experiments using traditional, fixed-culture methods report observations of an entire vessel network at one time point, rather than evolution of individual microvessels. While ECM structure, including fiber orientations, thickness, and length are known to affect microvessel growth, characterizing ECM microstructure during microvessel behavior remains a challenge. To study the dynamic interaction between microvessels and the structure of their microenvironment we need to observe the evolution of ECM structures along with sprouting angiogenesis.

Time-lapse imaging allows quantification of active ECM fiber orientation simultaneously with neovessel behavior during angiogenesis. Kirkpatrick et al. used second harmonic generation (SHG) imaging, a nonlinear microscopic imaging technique that can image collagen without use of exogenous labels (Campagnola et al., 2001), to noninvasively visualize changes to fibril organization around angiogenic sprouts and growing neovessels in real time (Kirkpatrick et al., 2007). The investigation utilized an *in vitro* model of angiogenesis that uses intact vessel fragments that recapitulate all aspects of *in vivo* sprouting angiogenesis (**Figure 3**; Hoying et al., 1996). Higher densities of collagen fibrils formed preferentially around microvascular segments. Increases in collagen fibril density occurred simultaneously with neovessel growth. By using time-lapse imaging, preferential fibril formation around microvessels was demonstrated to be a biologically active event. Moreover, microvessels exerted contractile forces on their surrounding environment that induced local fiber alignment, exhibiting a fan-like structure (**Figure 4**). The alignment of fibrils by neovessels was quantified by measuring fibril orientation distributions over multiple days in a region adjacent to neovessel tips. Neovessels were found to significantly modify ECM fiber structures throughout the culturing period data. In a later study, McCoy et al. used two different EC types, hCMECs and HUVECs, to study the effects of collagen fiber orientation on vascular formation (McCoy et al., 2018). Varying levels of pre-strain were applied

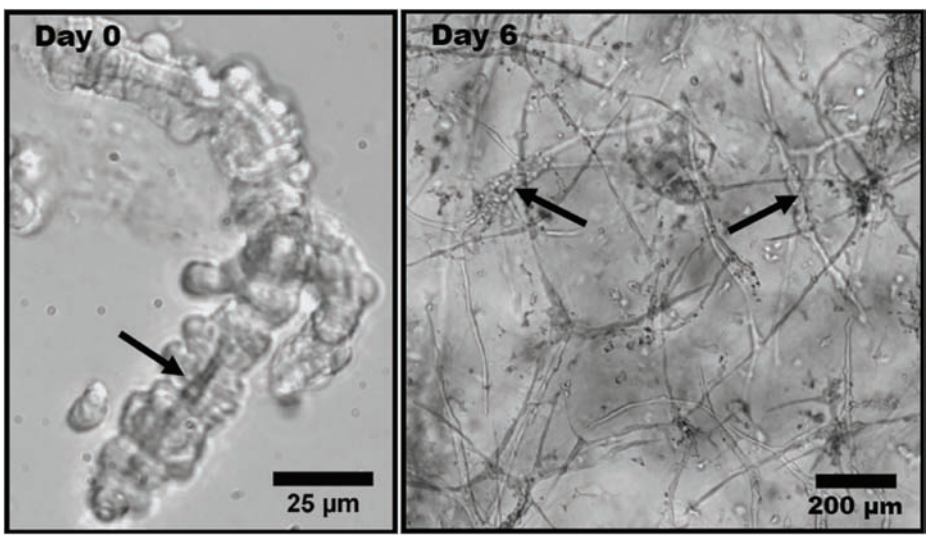

FIGURE 3 | Phase contrast light micrographs of rat microvessel fragments embedded in type I collagen matrix. This experimental model is used to represent angiogenesis *in vitro*. (Left) Isolated microvessel fragment at Day 0 with a visible lumen, indicated by the arrow. (Right) Angiogenic microvessel fragments at Day 6 of growth. The thicker initial fragments are indicated by the arrows. The thinner protrusions extending from the initial fragments are neovessels formed through angiogenesis. Obtained with permission from Edgar et al. (2014).

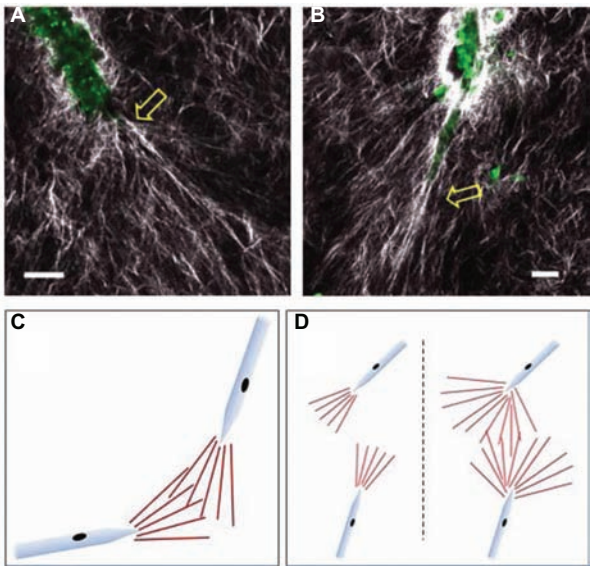

FIGURE 4 | Experimental images and schematics of collagen fibril reorientation by the tips of growing neovessels. **(A,B)** Collagen fibrils (white) and endogenous endothelial cell fluorescence were visualized using SHG/two-photon microscopy. Scale bar = 20 μm. Yellow arrows point to new sprouts arising from the parent microvessel (green). **(C,D)** Schematics of collagen fibril orientation by neovessel tips, and potential mechanism of contact guidance. The "fan" of aligned matrix fibrils (red lines) in front of each growing neovessel would act to "track" the neovessels toward each other when overlapping. **(D)** Consequences to neovessel location due to differences in the size of the fibril-alignment zone. A small fibril-alignment zone would not readily overlap, while a larger zone (due to a less stiff matrix) would make overlapping of these tracks between neighboring neovessels more likely. Modified with permission from Edgar et al. (2014).

to microwells filled with type I collagen to create alignment of collagen fibrils prior to cell seeding. The results demonstrated that aligned collagen hydrogels promote aligned and thicker microvascular networks with elevated deposition of type IV collagen. Time-lapse imaging was implemented using a bright field microscope placed inside a conventional culturing incubator. Vessel sprouts aligned along pre-existing microstructure. Moreover, when used with pharmacological inhibitors of cell mechanosignaling, inhibition of focal adhesion kinase and myosin II was shown to disrupt the ability of ECs to align along the fibrils. However, inhibition of Rho-associated protein kinase had a significantly decreased effect, a trend that was not observed in cultures with unaligned ECM. This suggests that distinct intracellular signaling pathways of mechanotransduction are involved. These studies characterized biologically relevant information of microvessel growth along with adjacent ECM microstructure. Previously, microstructural characteristics of the fibrous ECM were known to give rise to deterministic microvascular patterning. Using time-lapse imaging we could record the evolution of microvessels and their surrounding stroma. These observations are crucial to the advancement of knowledge on microvessel migration, as it offers direct inspection of 3D migration that could not be investigated previously.

Forces and Deformation of the Extracellular Matrix

Traction forces applied to the ECM by microvascular endothelial cells modulate vascular growth and capillary morphogenesis (Sieminski et al., 2004; Kniazeva and Putnam, 2009). As neovessels migrate, they form ECM adhesions and use these connections with the ECM to exert traction on the ECM components, resulting in local deformation of the microenvironment (Jakobsson et al., 2010). Migrating neovessels locally degrade the ECM by proteolysis, synthesize ECM and basement membrane, and create matrix deformations by exerting traction forces (Korff and Augustin, 1999; Krishnan et al., 2007; Lee et al., 2009; Edgar et al., 2014; Underwood et al., 2014).

Neovessel tractional forces and matrix stiffness have been studied by imposing fixed boundary conditions on the edges of microvessel cultures. Sieminski et al. cultured ECs on type I collagen in a floating culture by loosening gels from their wells using a spatula (Sieminski et al., 2004). Constrained gels that remained attached to their wells exhibited vessel-like structures with greater accumulation of actin stress fibers. All ECs formed vessel-like structures, but constrained cultures exhibited different network morphologies characterized by shorter total vascular length, smaller vessel-like structures, decreased branching, and larger lumens. Underwood et al. seeded intact microvessels in 3D collagen gels and investigated several different constraint conditions on the boundaries of gels with rectangular and circular cross-sections (Underwood et al., 2014). Traction forces imposed by growing neovessels caused compressive strain that led to realignment of ECM fibers, and large deformation of the entire gel. Hence, cellular traction forces can deform the ECM, realign collagen fibrils, and result in anisotropic material properties for the matrix. Measurements of microvessel network topology, including total vascular length, segment length, and branch points, were quantified by skeletonizing 3D confocal images. Sprouting neovessel growth was demonstrated along a direction perpendicular to compressive strain. Thus, the ability of the sprouting neovessels to deform the matrix resulted in realignment of collagen fibrils, and the neovessels then grew along these aligned fibrils, creating a highly aligned microvascular network.

Neovessel tractions on the ECM can also be studied by confining gel substrates to specific shapes. Nelson et al. seeded bovine pulmonary artery ECs on islands of fibronectin that adhered to a glass slides in circular, rectangular, and square shapes (Nelson et al., 2005). On the circular islands, ECs were quiescent except at the perimeter, where cells continued to proliferate. ECs grown on square islands proliferated toward the island corners with higher preference. Hence, proliferation showed a dependence on substrate geometry, but it also correlated with areas of high stress, as the perimeter of a circle and corners of a square have higher effective local stiffness because of their shapes. Inhibition of molecules that participate in signaling pathways of cellular traction, including Rho kinase (ROCK) and myosin light chain kinase, reduced proliferation. Thus, the study suggests cytoskeletal generated forces are associated with proliferation. In a different study, Sun et al.

cultured HUVECs on Matrigel substrates of simple shapes including circle, square, star, and triangle (Sun et al., 2014). The HUVEC networks had longer segments in the center of the substrate compared with areas closer to the substrate boundary for all shapes. Cellular traction forces were also modulated by inhibiting ROCK, which significantly decreased the length of vessel-like segments. This finding suggests that vessels closer to the feature boundaries encounter higher matrix stiffness, and exert greater forces to elongate, migrate, and create a network. Collectively, these studies investigate tractional forces by probing individual proteins associated with the entire culture, measuring deformation of whole gels, or fabricating substrates of confined shapes. These are global measurements that reflect entire vascular networks, but these measurements do not reveal information about local interaction of vessels with the ECM.

Time-lapse imaging enables tracking of individual vessel behavior during interaction with the surrounding environment, allowing quantification of matrix deformations over time. The forces exerted by the vessels are difficult to measure, but deformations of a local environment can elucidate information about the induced stress. Kniazeva et al. fabricated an experimental system of cultured ECs on microcarrier beads embedded in fibrin gels. Using this system, the authors observed that higher matrix densities impeded sprouting (Kniazeva et al., 2012). Using time-lapse imaging, the authors further observed the extent of sprouting increased with the rate ECs deformed the fibrin fibers (Kniazeva et al., 2012). This offers direct evidence that neovessel migration and elongation are associated with traction on the ECM. Moreover, the dependence on the rate of deformation means that the cellular induced forces may need to be balanced with the mechanical response of ECM for angiogenic sprouting. In another study, Utzinger et al. used an *in vitro* model of angiogenesis where microvessel fragments were suspended in type I collagen, and SHG imaging was used to investigate microvessel-ECM interactions (Utzinger et al., 2015). Dynamic 3D multiphoton imaging of the gels was performed hourly over 3 days. The study demonstrated that sprouting neovessels dynamically interact with the ECM to deform their surroundings and episodically switch between elongation and regression (**Figure 5**). Distinct collagen fibril structures were observed around tip cells, suggesting greater

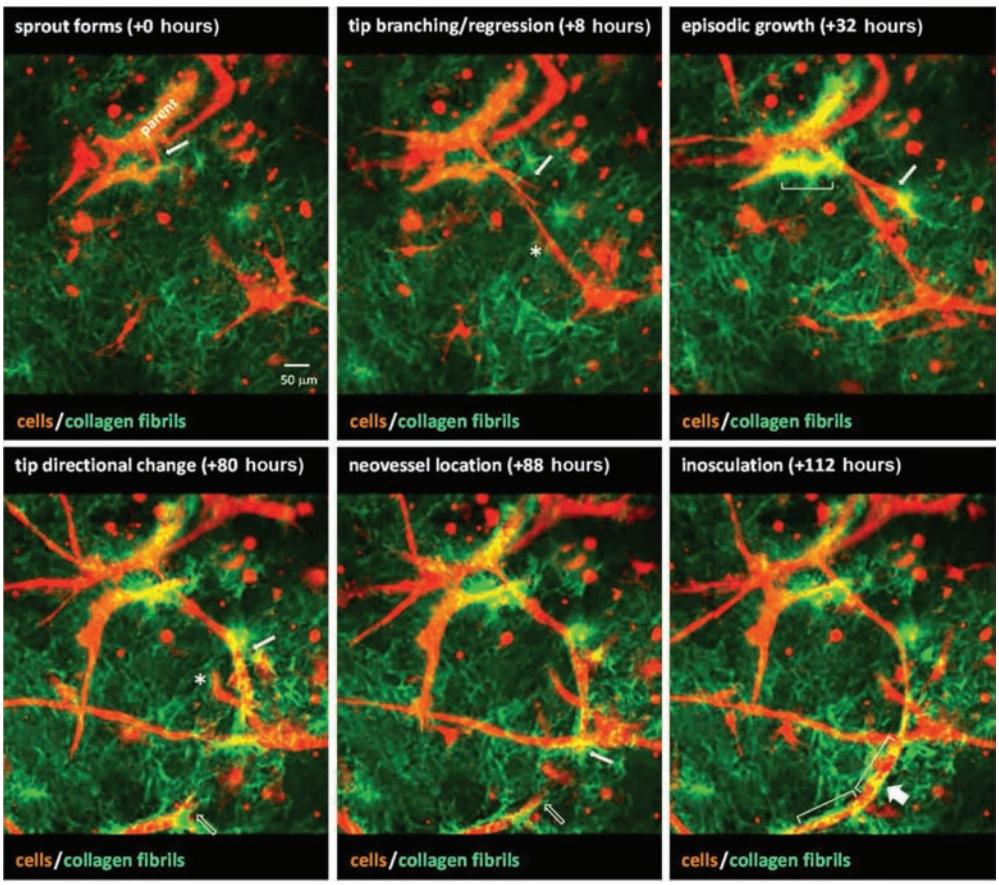

FIGURE 5 | A sequence of images from time-lapse video of neovessel sprouting, growth, and inosculation within a collagen gel stroma. Microvessels (red) were imaged *via* confocal microscopy and collagen fibril structure (green) was visualized using SHG imaging. Over the course of ~4.5 days, a neovessel sprout (white arrow) forms, grows, and changes direction to eventually inosculate (wide arrow) with a second neovessel (open arrow) that appears from out of the field of view. Brackets indicate areas of collagen condensation occurring at neovessel walls. The asterisk marks a neovessel sprout that forms and then regresses approximately 3 days later. Obtained with permission from Edgar et al. (2014).

traction forces by advancing tips. Du et al. suspended ECs in type I collagen mixed with beads (Du et al., 2016). By tracking beads over time, deformation fields were resolved around the sprouting tips of neovessels. The use of time-lapse imaging, vessel tracking, and deformation field evolution led to a new characterization of microvessel migratory behavior. As a vessel advances it exhibits a "pull," relating to contractile forces transmitted by adhesion complexes, "release," "protrusion-related push," and "retraction-related push." These studies demonstrate dynamic interaction of growing neovessels with their surroundings that cannot be observed using traditional techniques. Additionally, they offer information about individual microvessels as they navigate the ECM, rather than global parameters of the entire vascular network. The findings from these studies offer new paradigms of sprouting, as forces imparted on the ECM during sprouting involve rates of deformation, local deformation fields, and fiber structures adjacent to microvessels.

PROTEOLYSIS

Proteases play several critical roles in the process of angiogenesis. These roles include degradation of the basement membrane that surrounds the vessel, degradation of the fibrin gel that is leaked from the vascular bed, degradation of the ECM in locations where new vessels are sprouting, creation of space for the new vessels to grow, and release of matrix-bound cytokines or membrane-anchored cytokine receptors. It is important to maintain a balance of protease secretion, as too much matrix degradation can also impair cellular migration (Bacharach et al., 1998) and degrade the mechanical properties of the extracellular matrix (Krishnan et al., 2007).

During angiogenesis, quiescent ECs take on an invasive phenotype and produce proteases that locally degrade their basement membrane at the location of sprouting. Specifically, MMPs MMP-2 and MMP-9 are fundamentally important for this process (Bergers et al., 2000; Fang et al., 2000). MMPs are produced by ECs, and target the major components of the basement membrane, including type IV collagen, type XV collagen, type XVIII collagen, laminins, and heparin sulfate proteoglycans (Roy et al., 2006). MMP production is regulated by growth factors such as VEGF and FGF (Lamoreaux et al., 1998; Zucker et al., 1998; Partridge et al., 2000; Ardi et al., 2009), although MMPs are in turn able to regulate the functionality and availability of these growth factors.

In addition to degrading the basement membrane, ECs must navigate through the ECM, which is primarily composed of Types I and III collagen, elastin, and proteoglycans, depending on the particular tissue type. MMP-2, MMP-9, and MT-MMP-1 (MMP-14) are produced by ECs during angiogenesis (Taraboletti et al., 2002), and they all target the major collagens found in the ECM (Roy et al., 2006). The degradation of ECM can release matrix-bound growth factors that may be necessary for stimulating sprouting and vessel growth (Houck et al., 1992; Plouet et al., 1997). Proteases can also regulate angiogenesis by degrading growth factors and diminishing their activity (Ito et al., 1996).

A handful of innovative methods have been developed for imaging protease activity, and there are several excellent review articles and protocols that describe the methods for imaging of protease activity and proteolysis (Sameni et al., 2000; Jedeszko et al., 2008; Moin et al., 2012; Chalasani et al., 2017). In general, protease activity can be detected by using probes that are based on either monitoring the activity of proteases on the substrate, or by probes that inhibit the protease by binding covalently to the active site of a protease (activity-based probes, or ABPs). For both approaches, a fluorogenic probe is commonly used for detection, although other options have been used such as chromogenic substrates (Van Noorden, 2010). Fluorogenic substrates often use quenched substrates, which combine a nonfluorescent quencher held in close proximity to a reporting fluorophore by a linker peptide that can be degraded by proteases. After degradation of the linker, the reporting fluorophore is separated from the nonfluorescent quencher, yielding a fluorescent signal. A second approach for fluorescent substrates is the use of proteolytic beacons (McIntyre and Matrisian, 2009). These protease substrates use fluorescence resonance energy transfer (FRET) to provide detection due to protease activity (e.g., Scherer et al., 2008). ABPs report the active sites of specific enzymes rather than the proteolytic activity (Blum et al., 2005). Since these probes bind to the active site of the enzyme, they essentially inactivate the enzyme at the time of reporting. All of these approaches to visualizing active enzymes or proteolytic activity are amenable to confocal, multiphoton, and structured illumination microscopy. Live imaging experiments are needed to assess changes in protease activity over time.

Only a handful of studies have examined the distribution of active proteases or protease activity in the context of neovessel growth during angiogenesis, and we found only one study that used true time-series imaging of protease activity during angiogenesis. Most of the proteolysis assays that are available for live imaging have been developed for the study of tumor invasion and metastasis, and thus most of the applications in the literature are related to cancer cells. One of the first studies to use quenched substrates to image proteolysis in living cells was published in 2000 (Sameni et al., 2000). The investigators focused on the study of living human breast cancer cells and used quenched fluorogenic substrates, specifically DQ-BAS or DQ-collagen IV (Thermo Fisher Scientific, Waltham, MA). The quenched substrate was mixed with gelatin and used to coat class coverslips. Cells were plated and observed over 48 h for fluorescence, representing proteolytic degradation of the fluorogenic substrates, using a laser scanning confocal microscope. Finger-like pits or tunnels were observed in the gelatin under the cells at the sites of fluorescence. Although the study reported that time series imaging was used, only a single set of images were presented, acquired 48 h after seeding. A number of subsequent studies were published by the same investigative group, applying the technique to the study of colorectal, prostate, and endothelial

progenitor cells (Sameni et al., 2003; Cavallo-Medved et al., 2005; Podgorski et al., 2005; Urbich et al., 2005). All of these studies used single timepoint imaging, typically 48 h after the start of culture.

In recent years, a major focus in angiogenesis research has been the influence of other cell populations on EC sprouting. This has included the study of primarily MSCs and stromal cells. Ghajar et al. examined the mechanisms by which MSCs stimulate capillary morphogenesis from endothelial cells in 3D culture (Ghajar et al., 2010). They used ECs cultured on microcarrier beads, and these were mixed with MSCs in a 3D fibrin matrix. The 3D constructs were doped with a small amount of DQ Collagen I at day 7 prior to imaging. ECs cultured alone resulted in a focal appearance of the fluorescence signal from the DQ collagen substrate. By contrast, EC-MSC cultures showed a very strong fluorescence signal primarily associated with the ECs. RT-PCR revealed that the primary differences in protease message between ECs cultured alone and EC-MSC cultures was increased expression of MT3-MMP and MM-9.

We were only able to find a single study that incorporated time-series imaging of proteolysis during angiogenesis. The study focused on understanding the role of compartmentalization of proteases to caveolae and the dynamics of ECM degradation (Cavallo-Medved et al., 2009). Among other assays, the investigators performed live cell proteolysis assays in 4D during tube formation by endothelial cells. HUVECs were seeded onto DQ-Collagen IV and imaged every 10 min over 16 h. The time series imaging demonstrated that by 4 h the cells had started to align and form small tubular networks. Notably, degradation products of the DQ-Collagen IV were visible pericellularly. By 14 and 16 h, degradation products were observed adjacent to the tubular structures, and at the rear of one of the cells that was migrating toward a developing tubular structure. This study demonstrates the unique ability of fluorogenic substrates to both localize degradation and subsequently track degradation products.

CHEMOTACTIC FACTORS

Angiogenesis is initiated and regulated by a host of soluble and matrix-bound growth factors. The coordination and phenotypic regulation of ECs in growing neovessels are controlled in part by chemotaxis, the growth of cells along a cytokine gradient. Chemotaxis is distinguished from chemokinesis, which is a change in migratory behavior due to the concentration of a cytokine-independent of spatial heterogeneity (**Figures 6A,B**). *In vivo*, cytokine gradients are formed by cellular secretions, interstitial flow, and differential sequestration of growth factors by ECM proteins. Angiogenic activity progresses over temporal scales that vary from minutes to days and spatial scales that span from the intracellular space to the microvascular network ensemble. Commonly studied angiogenic growth factors include vascular endothelial growth factor (VEGF), fibroblast growth factor (FGF), platelet-derived growth factor (PDGF), tumor necrosis factor alpha (TNF-α), transforming growth factor beta (TGF-β), and angiopoietins (Ang). Angiogenic growth factors participate in numerous signaling pathways including VEGF, Delta-Notch, Rho Rac, and Wnt signaling.

Several types of chemotaxis assays have been used to study the role of chemotaxis in angiogenesis. One of the earliest reported chemotaxis assays is the Boyden (transwell) chamber (Boyden, 1962), and it remains as one of the most commonly used assays for chemotaxis. The assay consists of a reservoir containing chemoattractants separated from a reservoir containing the cells of interest by a permeable membrane (**Figure 6C**). The permeable membrane is fixed after cell migration to determine the number of cells crossing the membrane. Endpoint chemotaxis assays such as the Boyden chamber do not distinguish chemotaxis from chemokinesis, describe cellular trajectories, or capture the evolution of morphogenic events associated with the development of the microvascular network. Thus, they provide limited information about microvessel growth in response to a cytokine gradient. Time-lapse imaging provides time-series descriptions of cellular trajectories and behavior that can determine the effects of chemotaxis on isolated ECs and microvasculatures. This section reviews early attempts to study the effects of chemotaxis during angiogenesis using time-lapse imaging and more recent methods that allow for qualitative determination of spatiotemporal gradients of soluble and matrix-bound cytokines. Several excellent review articles can be consulted for specific details of chemotaxis assays (Keenan and Folch, 2008; Chung and Choo, 2010; Lee et al., 2018).

Studies of Chemotaxis Using Chambers and Transwell Migration Assays

Both single cell (e.g., HUVEC studies) and sprouting angiogenic assays (e.g., retina, microvessel studies) have been used to gauge cellular and microvascular responses to chemotaxis *in vitro*. Although these methods do not provide fine control over gradient formation and evolution, they have revealed interactions between growth factors, target cells, cell receptors, and signaling network members.

Commercially available Boyden chamber assays (and transwell migration assays) have been used to determine chemotactic behaviors of ECs. For these assays, a top chamber containing ECs is separated from a chamber containing a chemotactic factor by a permeable barrier, allowing soluble gradients to form between the chambers (**Figure 6C**; Boyden, 1962). Quantitative counts of cells that pass through the membrane can be made at the end of the assay, but quantitative measurements of cellular trajectories and gradient distribution are not available. Further, gradients within the assay equilibrate in approximately the same time period that it takes for ECs to migrate through the membrane. Thus, the gradient magnitude decreases during the time period that is used to collect migration data until it becomes negligible (Zantl and Horn, 2011). To overcome these limitations, bridge chambers, for example, the Zigmond (rectangular) (Zigmond, 1977) and Dunn (concentric) (Zicha et al., 1991) chambers, were developed (**Figure 6D**). The improved chambers connect the cell-containing chamber and the cytokine-containing chamber by a thin bridge, with the top of the chamber covered by a

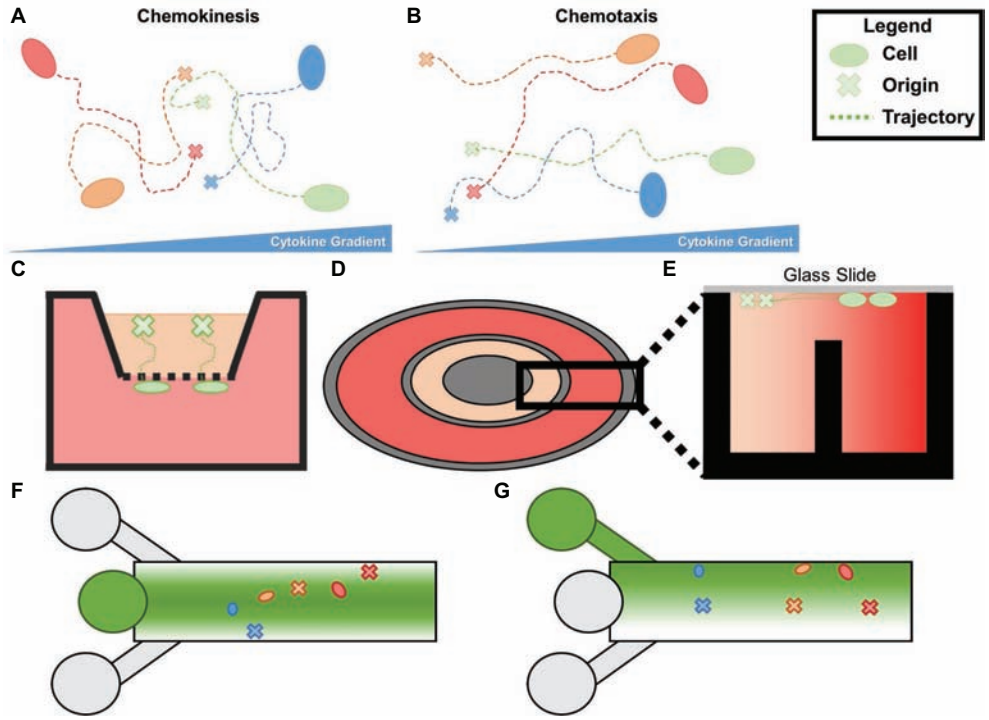

FIGURE 6 | (A) Chemokinesis is increase in cellular movement proportional to cytokine concentration without oriented trajectories. **(B)** Chemotaxis is an increase in orientation of a cell's trajectory in the presence of a cytokine gradient. **(C)** Boyden (transwell) chambers. The bottom chamber containing the chemoattractant and the top chamber containing the cells of interest are separated by a permeable membrane which can be removed and fixed to analyze chemotaxis. **(D)** Top view of a Dunn chamber. **(E)** Profile of Dunn chamber. The outer well containing chemoattractant and the inner well containing controlled media are separated by a central post, allowing a gradient to form between the two. Cells are seeded on glass slides flush with the innermost and outermost rings. **(F)** Simplified schematic of typical microfluidic chemotaxis chamber. A central source well (center left) is flanked by sink channels which form a gradient of chemoattractant from the centerline. Cells are seeded downstream and migrate to the centerline during chemotaxis. **(G)** Alternative schematic in which the top inlet contains the chemoattractant, the middle contains cells and media, and the bottom is a sink.

glass slide to allow time-lapse imaging (**Figure 6E**). In one study, HMVECs seeded in the center of a Dunn chamber were imaged every 5 min for 9 h in the presence of bone morphogenic protein 2 (BMP-2), VEGF, pleiotrophin (PTN), a synthetic thrombin mimic (TP508), or control media (Li et al., 2005a). Cells cultured in control media migrated randomly. By contrast, cells cultured in each of the cytokines grew toward the cytokine gradients. Using time-lapse imaging, migration speed was measured, and TP508 was found to induce the highest HMVEC speed of all cytokines. Although the cytokine concentration along the gradients is unknown in bridge chamber assays, they provide a simple method to compare cellular behavior in response to various cytokines.

In vitro and *in vivo* assays for angiogenic sprouting can result in gradients in cytokines due to autocrine signaling. Investigators have developed novel ways to eliminate these gradients to study baseline chemotactic behaviors. For instance, soluble fms-like tyrosine kinase-1 (sFlt-1) is a receptor that sequesters VEGF from ECs. In a time-lapse study of an aortic ring sprouting assay, sFlt-1 was used to remove VEGF gradients that developed from the aortic ring in the absence of externally added cytokines (Gerhardt et al., 2003). Filopodia were found to retract after treatment with sFlt-1. By contrast, there was not any filopodia retraction when cultures were treated with VEGF receptor-IgG fusion proteins, which creates dimerized Flt that cannot bind VEGF. Time-lapse imaging allowed measurement of vascular migration and growth, including filopodia and lamellipodia activity, tip cell migration, and sprout elongation, which all decreased in the presence of sFlt-1. Stalk cell proliferation, however, remained unchanged. This information in combination with results from non-time-lapse studies, helped distinguish tip and sprout behavior in the absence of autocrine gradients. In particular, tip cell migration relies on VEGF gradients, while proliferation is a concentration-dependent activity characteristic of stalk cells. Thus, precise gradient control and quantification is not necessary to obtain time-lapse chemotaxis data capable of delineating tip cell migration and stalk cell proliferation.

Studies of Soluble Chemotaxis Using Microfluidic Devices

The advent of microfluidic devices has permitted quantification and precise, reproducible spatiotemporal control of soluble cytokine distributions. Generally, cells are seeded in a channel that may be coated with matrix proteins (e.g., fibrin or collagen).

The culture chamber can be flanked by another chamber that may contain a chemoattractant. While flow through the chamber continuously supplies media and cytokines, gradients form between the flanking chambers in the direction perpendicular to the flow (**Figures 6F,G**). Finite element analysis and numerical solutions to the convection-diffusion equation have been used to predict solute distributions. Computational predictions have been validated *in vitro* with fluorescent molecules that have diffusive properties similar to VEGF such as conjugated dextran (Barkefors et al., 2008; Shamloo et al., 2008; Vickerman et al., 2008; Chung et al., 2009; Huang et al., 2015; Shirure et al., 2017) and AlexaFluor 488 (Zengel et al., 2011). A major advantage of these microfluidic devices is that they facilitate time-series imaging.

Barkefors et al. designed a single channel microfluidic device to study the rate of chemotactic growth along a hill-shaped diffusive gradient (Barkefors et al., 2008). HUVECs or human umbilical artery ECs (HUAECs) were cultured with two VEGF splice variants $VEGF_{165}$, $VEGF_{121}$, or FGF-2 supplemented ubiquitously or as a gradient and imaged every 5 min for 200 min. Chemotaxis and chemokinesis effects were delineated by measuring the net distance of migration toward the growth factor (chemotaxis) and the total cell migration distance (chemokinesis). Both VEGF splice variant gradients induced chemotaxis, but not chemokinesis. HUVECs were slightly influenced by FGF-2 chemotaxis, but HUAECs were not affected, suggesting that ECs from different origins may exhibit different behavior. They also noted that cells near the peak concentration migrated negligibly compared to regions of sharper gradients, indicating that cells near growth factor sources become non-migratory. A follow-up study investigated the role of FGD5, a guanine nucleotide exchange factor found in endosomes containing VEGF receptor 2 (Heldin et al., 2017). HMVECs were analyzed in the same microfluidic device used by Barkefors et al. or were transfected with siRNA to knockdown FGD5. HMVECs lacking FGD5 were found to have reduced chemotactic response to VEGF gradients and accelerated VEGFR2 degradation and signaling.

Fibrous matrices have been included in microfluidic assays to better represent soft tissue mechanics and facilitate sprouting chemotactic studies. Shamloo et al. adhered ECs to microbeads embedded in a collagen-fibronectin mix in the cell culture channel of their microfluidic device (Shamloo et al., 2012). A VEGF gradient was established across the culture chamber and growth was imaged daily. Time-lapse images showed initial EC organization into sprouts, which later grew from the bead surface into the collagen-fibronectin matrix and finally up the VEGF gradient. By adjusting the collagen concentration and magnitude of the VEGF gradient, they observed that denser matrices (1.9 mg/ml) impaired alignment of sprouting cells along the VEGF gradient. However, alignment of sprouts was observed in lower ECM density (1.2 mg/ml). Notwithstanding, alignment could be achieved at lower densities without changing VEGF gradient, but increasing minimum VEGF concentration. This suggests that both cytokine gradient and concentration influence microvessel migration. Furthermore, sprout trajectories were tracked over time to determine how quickly cells aligned along the VEGF gradient. Sprouts in denser matrices took more time to align than sprouts cultured in less dense matrices. The time for an initial sprout to form and grow from the microbead also increased with increasing matrix density. In a follow-up study, daily images informed metrics such as the number of cells per sprout, sprout length, thickness, and elongation rate over time (Shamloo et al., 2016). This information was used to create a computational model of sprouting angiogenesis that was validated with time-lapse data.

In addition to gradients formed from cytokine supplemented media, gradients can be established *via* coculture. Vickerman et al. stimulated cellular migration first along synthesized recombinant cytokine gradients then along coculture-derived cytokine gradients in the same device (Vickerman et al., 2008; Takuwa et al., 2010). For the first study they established a gradient of sphingosine-1-phosphate (S1P) – a lipid mediator associated with EC proliferation, migration, lumen formation, and endothelial barrier function (Takuwa et al., 2010). Time-lapse imaging of migrating HMVECs demonstrated filopodial extension and retraction, chemotaxis along S1P gradients, and lumen formation (Vickerman et al., 2008). For the second study, the source channel was seeded with MTLn3 cancer cells, U87MG cancer cells, or smooth muscle cells to serve as a source of cell-secreted growth factors. MTLn3 cells induced chemotaxis at a rate lower than VEGF alone while U887MG failed to induce chemotaxis. By contrast, SMC coculture reduced migration and had a slight negative chemotactic effect on HMVECs in which cells migrated away from the source of cytokines. They also investigated the timing of VEGF administration on chemotaxis. Migration was strongest when VEGF gradients were established 1 day after seeding HMVECs and was reduced when the VEGF gradient was introduced after 3 days (Chung et al., 2009).

In addition to custom microfluidic devices, a few commercial options have emerged such as the μSlide chemotaxis assay (Zantl and Horn, 2011). In one coculture time-lapse study using this assay, HUVECs were cultured with VEGF producing carcinomic FaDu cells. Surprisingly, adding supernatant from FaDu cells to the chemoattractant source reservoir did not induce chemotaxis, but culturing FaDu cells in the reservoir elicited chemotaxis (Zengel et al., 2011). In another time-lapse study using the μSlide assay, HUVECs migrated toward a Wnt3a gradient while knockdown of Kif26b, a kinesin associated with microtubules, lead to longer and more scattered trajectories. These results provided evidence that Kif26b interacts with disheveled 3 (Dvl3) Daam1 complexes that could regulate microtubule stability during the formation of polarized cell edges during angiogenesis (Guillabert-Gourgues et al., 2016).

Microfluidic-based approaches can be optimized to reduce confounding variables. Further, precise gradient control improves reproducibility during time-series evaluation of chemotaxis. Custom and commercial microfluidic devices have enabled simple studies that accommodate diverse *in vitro* culture models and improve on the Boyden bridge chamber methods by easing gradient quantification and providing long-term gradient stability.

Assessment of Chemotaxis by Matrix-Bound Cytokines

Cytokine splice variants have different binding affinities for matrix proteins, which can result in unique spatial distributions of each splice variant (Vempati et al., 2011). For example, the longer isoforms of VEGF, $VEGF_{165}$, and $VEGF_{189}$ can be sequestered by heparan sulfate proteoglycans (HSPGs), while $VEGF_{121}$ lacks the binding domain contained by the longer isoforms. Investigators have exploited this effect to generate gradients in cell culture. For instance, Liu et al. electrochemically immobilized gradients of fibronectin, $VEGF_{165}$, or both onto slides (Liu et al., 2007). The gradient profiles ranged between the hill and step profiles. All gradients triggered an increase in EC migration, with VEGF gradients causing more migration than fibronectin. Combining gradients resulted in a larger increase in migration, indicating that both growth factors and the ECM affect cellular migration, and their integration can be additive.

Approaching matrix-bound chemotaxis from a different angle, Li et al. investigated the role of cell surface receptors (Li et al., 2016). Syndecan-4 (Synd4) is a heparan sulfate proteoglycan (HSPG) cell surface receptor that has previously been implicated in haptotaxis during angiogenesis (Bass et al., 2007) as well as chemotaxis due to its ability to act as a co-receptor and independent receptor for FGFs. HUVECs were transfected with null and knockout genes for Synd4 then seeded in μSlide chemotaxis assays. A locally linear bFGF gradient was introduced and imaged every 30 min for 18 h. There was a linear relationship between the initial position of a cell along the gradient and the accumulated distance the cell moved, allowing prediction of the distance a cell would travel based on its initial position. Synd4 knockdown was associated with reduced accumulated distance and Euclidean distance, although there was no difference in proliferation (Elfenbein and Simons, 2013).

STROMAL CELL INTERACTIONS

Stromal cells are a broad classification of cells located in the ECM surrounding the microvasculature, including fibroblasts, pericytes, macrophages, MSCs, and others. Macrophages and MSCs play critical roles throughout angiogenesis, interacting directly with both microvessels and their surrounding matrix to facilitate sprouting, growth, vessel fusion, and tissue remodeling. The role of stromal cells in angiogenesis is shown graphically in **Figure 7**. Here, we will discuss the dynamic interactions of these cells with microvessels and matrix through all phases of angiogenesis, and how different imaging techniques have increased our understanding of the temporal behavior of these cells.

Macrophages

While the spectrum of reported macrophage phenotypes has broadened considerably in recent years, macrophages are often discussed in terms of two, general phenotypes related to inflammation and tissue repair: the "classically activated" M1 and "alternatively activated" M2 phenotypes. M1 macrophages are strongly present in regions of inflammation and have historically been considered anti-angiogenic (Kodelja et al., 1997; Jetten et al., 2014). However, recent reports suggest they may directly influence early stages of angiogenesis (Spiller et al., 2014; Gurevich et al., 2018). The M2 phenotype is more typically associated with healing and angiogenesis (Kodelja et al., 1997; Jetten et al., 2014). These two general phenotypes can be broken down into a spectrum of sub-phenotypes with distinct chemokine profiles (reviewed in Mantovani et al., 2004). Assessing the spatial and temporal role of different macrophage phenotypes and sub-phenotypes is critical for understanding and controlling angiogenesis.

Spiller et al. compared the effects of M0 (unactivated), M1, M2a, and M2c macrophages over time during angiogenesis, using traditional *in vitro* sprouting assays and *in vivo* scaffold implantation (Spiller et al., 2014). They found that M1 macrophages may play a critical role in early stages of angiogenesis by secreting VEGF, FGF, and other growth factors to stimulate neovessel sprouting, and M2c macrophages secreted high levels of MMP-9. MMPs locally degrade the basement membrane of the parent vessel, enabling sprout formation. M2a macrophages then secrete PDGF to recruit pericytes and MSCs to stabilize vessels, and TIMP3 to halt the effects of M1 macrophages (Spiller et al., 2014). When scaffolds were implanted in mice, they found that incorporating both M1 and M2 phenotypes were necessary for vascularization, although the balance of each phenotype could not be quantified during early and late stages of neovessel growth (Spiller et al., 2014). Still, this study demonstrates the critical role of macrophage phenotypic shifts throughout angiogenesis.

While this information is a critical step toward understanding the spatiotemporal role of macrophage phenotype, an inability to perform time-series analyses in these mouse studies limited potential insight. Because animals must be sacrificed at each time point, the same sample cannot be evaluated continuously over time. Thus, it is difficult to determine if and when macrophage phenotypic changes are occurring in the tissues. Techniques that allow for dynamic analysis of samples over time may be key to unlocking the mechanisms driving macrophage behavior and phenotypic transition over time during angiogenesis.

Zebrafish eggs have become a popular tool for studying angiogenesis with dynamic imaging. Because zebrafish eggs are clear, live imaging techniques can be used to examine how microvessels and macrophages, or other stromal cells, behave over time during development. Gurevich et al. utilized zebrafish eggs from a transgenic fish line with fluorescent macrophages and blood vessels to study macrophage behavior following injury (Gurevich et al., 2018). They observed that M1 macrophages were most predominant at the sprouting stage of angiogenesis, where they localized at neovessel tips. Non-M1 macrophages had a higher presence in mid-late stage angiogenesis, and associated more randomly with vessels, sometimes wrapping around the vessel similarly to pericytes. At the remodeling stage, macrophages appeared to reduce the number of neovessels by inducing endothelial apoptosis, which is necessary after the damaged tissue has healed and metabolic demands are decreased. A decrease in M1 macrophages is critical for this remodeling (Gurevich et al., 2018). Overall, M2 macrophages appeared to have less of an

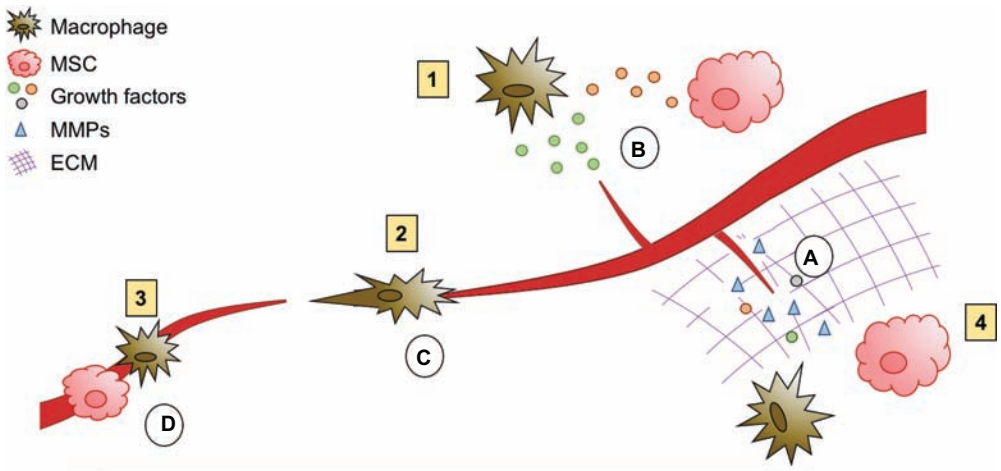

	Dynamic and time series imaging has enabled visualization of:
1	Macrophage movement mechanism through different types of ECM
2	Macrophages bridging two tip cells to facilitate fusion
3	Macrophages migrating to neovessels and wrapping around them as pericytes
4	Protease secretion profile of MSCs affects neovessel structure

FIGURE 7 | Role of stromal cells in angiogenesis. Macrophages and MSCs secrete MMPs, which degrade the matrix to allow sprouts to form and grow, and releases matrix bound growth factors. **(A)** Macrophages and MSCs secrete growth factors to stimulate sprouting and guide growing neovessels, and MSCs secrete factors to attract macrophages and modulate their phenotype. **(B)** Macrophages can facilitate neovessel fusion by bridging two tip cells. **(C)** Macrophages and MSCs can also act as pericytes to stabilize newly developed blood vessels. **(D)** MSCs also aid in lumen formation.

effect on neovascular density than M1 macrophages (Gurevich et al., 2018), which is contrary to earlier studies (Kodelja et al., 1997; Jetten et al., 2014). It is possible that these discrepancies over the effects of M1 macrophages may be due to further sub-phenotype differences within both M1 and M2 macrophages that may have varied between studies. In this case, live imaging was able to confirm the results of previous studies, and establish a more precise timeline and deeper understanding of macrophage movement and behavior.

Live imaging has also enabled researchers to gain an understanding of how macrophages are moving through the extracellular matrix. Van Goethem et al. observed macrophage migration in both fibrillar and non-fibrillar collagen matrices using a 3D *in vitro* migration assay (Van Goethem et al., 2010). They observed that macrophages perform amoeboid movement through fibrillar collagen, which is when the cell extends protrusions forward and "crawls" through the matrix using pseudopodia. When cultured in Matrigel or non-fibrillar gelled collagen, the macrophages adapted their movement to mesenchymal, meaning that the cell extends a larger protrusion forward, secretes proteases to degrade the extracellular matrix, and creates a path through which it can travel. This was an important observation, as it indicates that macrophages can adapt their migration mechanism to move through different tissue types throughout the body (Van Goethem et al., 2010).

Live imaging has also been used to study macrophage movement *in vivo* in Takeda fish. Grabher et al. observed that macrophages become more motile as they mature, switching from a rounded shape typical of amoeboid migration to a flattened phenotype with long protrusions as their motility increased (Grabher et al., 2007). When the PI3K signaling pathway was inhibited, the authors observed reduced macrophage migration, suggesting it plays a critical role in macrophage movement (Grabher et al., 2007).

Macrophages are critical for the process of forming vessel intersections. Fantin et al. observed the developing mouse brain and found that macrophages appear to bridge two tip cells growing toward each other just prior to fusion (Fantin et al., 2010). The authors then used live imaging of zebrafish to confirm the role of macrophages in this process. They were able to observe in real-time that macrophages migrate to areas of vessel fusion and spread between two vessels, interacting with both tip cells until they fused (Fantin et al., 2010). However, the exact mechanisms for vessel fusion, and the role of macrophages, remain to be determined. A similar effect was observed in a zebrafish model of brain vascular ruptures, where live imaging enabled the visualization of macrophages extending their filopodia to form physical contacts between two disconnected endothelial cells and pulling them together (Liu et al., 2016). It is possible that a similar mechanism is causing two tip cells to come together during the fusion of two growing neovessels.

Macrophages play distinct roles in angiogenesis by secreting cytokines and degrading the ECM to enable sprouting; they guide neovessel growth, recruit stabilizing cells, facilitate vessel fusion, and trigger apoptosis to remodel tissues. Macrophage phenotypic transition may play a critical role in moving from

one stage of vessel growth to the next, as each phenotype and sub-phenotype is activated by and produces a different combination of signaling factors. It has also been suggested that matrix degradation products can trigger a phenotypic switch from M1 to M2 phenotype (Sicari et al., 2014). However, further understanding is still needed of the environmental factors that trigger macrophage phenotypic transition and the role of each sub-phenotype on angiogenesis. Future advancements in live imaging to track macrophage phenotypic changes may help answer some of these key questions.

Mesenchymal Stem Cells

MSCs are a type of stromal cell found in several different tissues. They can differentiate into a variety of cell types, including smooth muscle cells and pericytes. MSCs are known to have a broad range of tissue healing functions, including a critical role in angiogenesis. They secrete growth factors, such as VEGF, PDGF, and Ang-1, to stimulate angiogenesis (Chen et al., 2008). MSCs also recruit and activate macrophages and modulate macrophage phenotype (Chen et al., 2008; Nakajima et al., 2012; Cho et al., 2014; Wise et al., 2014). Like macrophages, they secrete MMPs, which are critical for MSC-mediated vessel sprouting, neovessel assembly, and tissue remodeling (Collen et al., 2003; Chun et al., 2004; Ghajar et al., 2006, 2010; Kachgal and Putnam, 2011; Wise et al., 2014).

Kachgal-Putnam et al. showed in an *in vitro* model that MSCs from different tissue types, specifically bone marrow and adipose tissue, secrete different profiles of proteases to modulate angiogenesis (Kachgal and Putnam, 2011). Bone marrow-derived MSCs primarily secrete MMPs, while adipose-derived MSCs secrete more plasmin. This suggests that the protease secretion profile of MSCs may be specific to the ECM compositions of different tissues, to best support neovessel growth through the matrix. They also found that selectively inhibiting different proteases affects neovessel phenotype. Inhibiting MMPs resulted in distended vessels, although it did not affect vessel length. This suggests that MSC protease secretion profile may play a role in determining vessel phenotype and structure in different tissues (Kachgal and Putnam, 2011). Others have shown that MMPs play a larger role in angiogenesis, halting EC tube formation altogether if inhibited (Collen et al., 2003; Ghajar et al., 2010). These discrepancies suggest that other environmental factors may be playing a role in MSC-mediated angiogenesis that are not yet understood.

Further studies are needed to characterize the complex interactions between the cell types in the stroma and the microvascular network. *In vitro* studies do not sufficiently replicate the dynamic multi-cellular *in vivo* environment. However, studying angiogenesis in animals can be challenging, due to the need to sacrifice animals at each time point, the reproducibility, and the decreased access to imaging. The ability to track the same sample over time may allow for a more accurate understanding of the progression of angiogenesis. Above, we discussed transparent zebrafish as a tool for acquiring live videos of angiogenesis. Bioluminescence imaging is another alternative that allows for *in vivo* imaging of an anesthetized animal. Implanted cells can be engineered to contain luciferase, a protein that will emit light when activated. Luciferase can be activated at multiple time points by injection of luciferin, enabling time-series imaging of a single sample following implantation.

Sanz et al. used bioluminescent imaging to monitor the formation of vascular networks in mice (**Figure 8**; Sanz et al., 2008). They

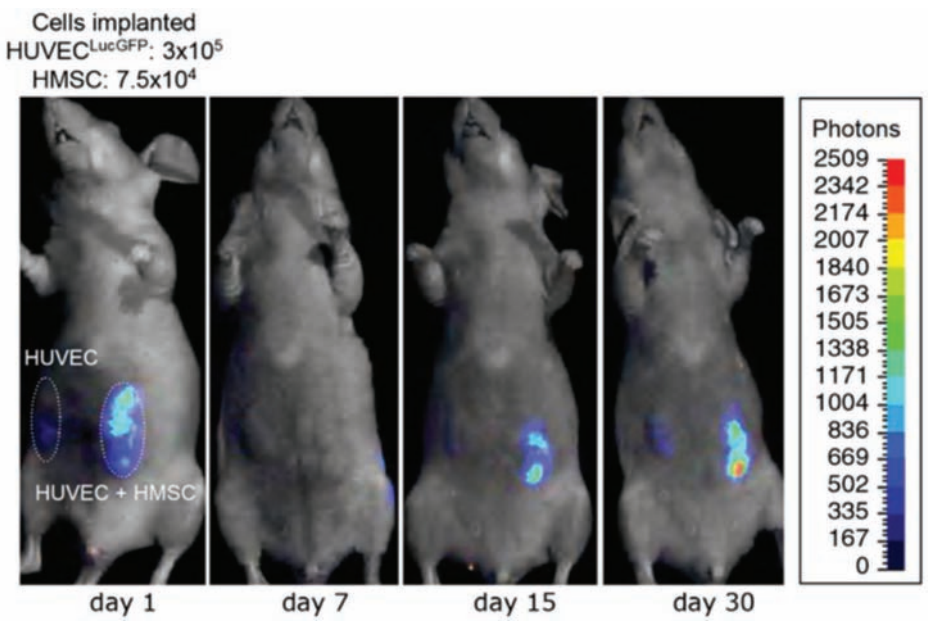

FIGURE 8 | Time-lapse bioluminescence imaging of rats with implanted HUVECs or HUVECs + HMSCs. After an initial drop, the number of luciferin-activated cells increases over time to a greater extent in the HUVEC + HMSC group compared to the HUVEC only group. This suggests increased vascular network formation in the implant with HMSCs, compared to HUVECs alone. This figure was reproduced with permission from Elsevier (Sanz et al., 2008).

implanted scaffolds with HUVECs (expressing luciferase) alone or HUVECs and MSCs together and imaged the constructs periodically for 120 days. Constructs with MSCs, most notably at later time points, measured a higher number of photons per second, indicating that a higher number of HUVECs were exposed to the luciferin in those samples. It is difficult to determine if this was due to the presence of a more mature vascular network, exposing more of the construct to the luciferin, or if there were simply changes in the number of HUVECs. The authors used other methods, including histological and immunohistochemical analysis, to verify that more mature vascular networks (vessels containing erythrocytes) were the cause of the increased bioluminescent signal in scaffolds containing MSCs (Sanz et al., 2008). Using bioluminescent imaging in live mice, others have demonstrated that MSCs enhance vascular network formation (Roura et al., 2012; Todeschi et al., 2015). While bioluminescent imaging is a useful tool for establishing time courses of increased vascularization, it is limited in its ability to evaluate vessel structure and function.

MSCs and macrophages are key examples of stromal cells that are involved in multiple stages of angiogenesis. Due to their spatiotemporal roles throughout angiogenesis, they are ideal targets for dynamic imaging. However, other cell types may also benefit from this approach. Pericytes are recruited during angiogenesis to wrap around the endothelium and stabilize the neovessel, and have also been shown to enhance microvessel elongation and directed migration using time-lapse imaging (Arima et al., 2011). In tumors, cancer-associated fibroblasts also play a role in stimulating angiogenesis by secreting angiogenic cytokines. Dynamic imaging methods may provide insights into the behavior of these other cell types as well.

DISCUSSION

This review highlights how time-lapse imaging techniques have advanced our understanding of the interaction of blood vessels with their environment during sprouting angiogenesis. Angiogenesis is dynamically influenced by a variety of environmental factors of the surrounding tissue matrix, as vessels interact with the ECM. Hence, the role of the ECM is vast and includes biophysical, mechanical factors, and chemotactic factors. The imaging techniques have provided the means to observe, characterize, and quantify the evolution of microvessel behavior, providing new insights on the process of angiogenesis and the interaction of microvessels with the ECM. Thus, data derived from time-lapse imaging experiments holds great promise to further elucidate angiogenic responses and advance the field. For example, the information could be observation and quantification of multiple signals experienced by microvessels. This will help determine how signals are integrated to promote a functional microvascular network, a key problem of angiogenesis (Ingber et al., 1995). It could also help bridge our understanding between extracellular signals and intracellular events such as EC metabolic pathways (Eelen et al., 2018), and EC phenotypic behaviors such as tip cell overtaking (Jakobsson et al., 2010; Arima et al., 2011). Lastly, as time-series imaging techniques improve to *in vivo* in mammals, we could gain better insight into angiogenic invasion in tumors, treatment efficacy, and graft acceptance.

Despite advances in our understanding of the biophysical and mechanical interaction of angiogenic microvessels with the ECM (**Figure 9**), there are a number of areas that warrant further investigation. The stiffness, density, and microstructure of the ECM, and forces exerted by microvessels alter angiogenic behavior (Krishnan et al., 2007; Han et al., 2018). However, most of the available experimental data focuses on global measures of vascular network morphometry. Little is known about the effects of local perturbations in biophysical properties on microvessel behavior. For instance, the *in vivo* mechanotransductive signaling cascades that lead to deterministic vessel behavior by nonlinear integration of biophysical signals remain unknown. However, other studies that did not investigate angiogenesis have introduced techniques to measure local ECM stiffness and focal adhesion complexes using time-lapse imaging (Han et al., 2018; Kang et al., 2018). The gap in our knowledge about microvessel interaction with

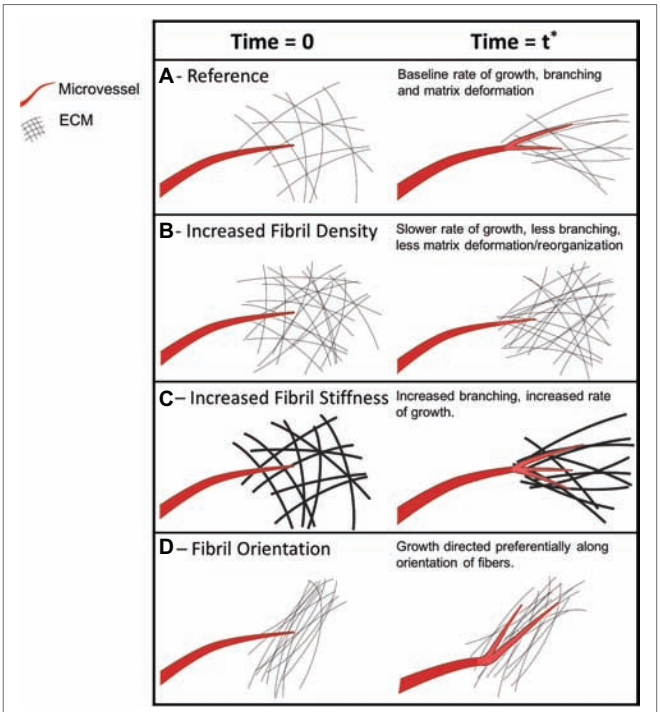

FIGURE 9 | Mechanical and biophysical signals of a microvessel as it interacts with its microenvironment during growth. Microvessels are shown in red, new microvessel growth is shown in brighter red on the right column, and extracellular matrix fibers are shown in black. The first column of each section shows an arbitrary initial point in time when a vessel is first observed. The vessel remains the same across the rows but ECM conditions are altered. The second column represents a later point in time of the same vessel and its ECM microenvironment. **(A)** A microvessel forms cell-ECM adhesions, exerts pulling forces, and deforms the ECM during growth. **(B)** Higher ECM density, along with increased stiffness, causes microvessels to induce decreased deformation and decreased growth. **(C)** Stiffer ECM independent of fibril density leads to increased branching. **(D)** Pre-existing ECM fiber alignment induces directed neovessel growth.

its environment stems from lack of experimental data on the local interaction of microvessels with their stromal environment and capturing the dynamic interplay over time. This information could be provided by experiments utilizing time-series imaging, and these data are necessary to advance our understanding of angiogenesis.

The role of chemotaxis in angiogenesis has been only partly understood, as traditional chemotaxis assays were unable to describe cellular migration, vessel elongation, or the development of the microvascular network. Time-series imaging techniques helped distinguish tip and sprout behavior in the absence of autocrine gradients (Gerhardt et al., 2003), and established on what day of culturing VEGF gradients were most influential on cell (Chung et al., 2009). Microfluidic devices and computational methods have enabled the precise control and quantification of soluble and matrix-bound cytokine gradients. The methods could potentially be modified to incorporate multicellular sprouting assays that recapitulate angiogenesis more closely. This would enable a more holistic study of angiogenesis by accounting for intercellular interactions and tip-stalk cell dynamics. In conjunction with time-lapse imaging, these approaches could advance understanding of the effects of spatiotemporal cytokine gradients on sprouting microvascular networks.

The effects and role of protease activity during angiogenesis have been largely discovered, yet the exact role of proteases over time and space is not well understood. The available methods based on fluorogenic substrates show great promise, but they have seen limited use in the study of angiogenesis to date. There are some notable limitations of these techniques, however. The two common approaches to their application have been to include a fluorogenic enzyme substrate either during polymerization of a surrogate ECM such as collagen and Matrigel or as an additive to a culture containing proliferating ECs or angiogenic microvessels. In the former approach, fluorescence from the substrate continues to increase over time in culture and at some point, and becomes the limiting factor for performing time series imaging over longer periods. In the case of spiking the culture, the approach relies on diffusive transport of the fluorogenic substrate throughout the culture. There is a time constant associated with this diffusive process, which can limit temporal resolution and, thus, utility of the approach. In both cases, fluorescence produced by protease activity on a fluorogenic substrate represents a "high water mark" of protease activity, as the fluorescent signal continues to accumulate over time. Thus, there is certainly room for improved techniques for times-series imaging of protease activity.

Another key problem of angiogenesis is determining the role of stromal cells to facilitate sprouting, growth, vessel fusion, and tissue remodeling. Stromal cells are essential for many angiogenic processes, and dynamic imaging has helped to uncover the interaction of stromal cells with both microvessels and their surrounding matrix. Dynamic imaging has provided knowledge about more precise macrophage phenotype activity throughout the timeline of angiogenesis (Gurevich et al., 2018), macrophages migration mechanisms by tissue type (Grabher et al., 2007, p. #81; Grabher et al., 2007; Van Goethem et al., 2010), the role of macrophages in vessel fusion (Fantin et al., 2010; Liu et al., 2016), enhanced vascular network formation and maturation in the presence of MSCs (Sanz et al., 2008). However, improved technology is needed to visualize the real-time behavior of MSCs throughout angiogenesis *in vivo*. Imaging *in vivo* is particularly important, as *in vitro* experiments as of yet do not replicate the complexity of the *in vivo* environment. Angiogenesis is a complex process that relies on communication between multiple cell types and vessels, secretion of precise profiles of chemokines and proteases, and the controlled degradation of the extracellular matrix. Advancements in real-time imaging may help understand the complex interplay between these components during different stages of angiogenesis. Bioluminescence imaging has enabled time-series imaging of mammals *in vivo* without the need for sacrifice. However, it has a limited scope and can only be used for indirect quantification of vascular network development. While this technology is a major advancement, we are still unable to visualize specific cellular behaviors over time in mammals. Technologies addressing this limitation have enormous potential to advance our understanding of cellular behavior throughout angiogenesis. Moving forward, more work is needed toward understanding the complex relationship between stromal cells and other factors that support angiogenesis, such as mechanical, biophysical, and biochemical stimuli. Imaging methodologies that allow us to monitor stromal cell behavior along with ECM biophysical, mechanical, and chemotactic factors would provide a more comprehensive understanding of angiogenesis.

AUTHOR CONTRIBUTIONS

All authors contributed to the conception and writing of this review article.

FUNDING

Funding from NIH #R01HL131856, R01AR069297, and R01GM083925 is gratefully acknowledged. JW and JH are principle investigators on the grants. HS is a postdoctoral fellow, and SL and AR are graduate student researchers.

REFERENCES

Ardi, V. C., Van Den Steen, P. E., Opdenakker, G., Schweighofer, B., Deryugina, E. I., and Quigley, J. P. (2009). Neutrophil MMP-9 proenzyme, unencumbered by TIMP-1, undergoes efficient activation in vivo and catalytically induces angiogenesis via a basic fibroblast growth factor (FGF-2)/FGFR-2 pathway. *J. Biol. Chem.* 284, 25854–25866. doi: 10.1074/jbc.M109.033472

Arima, S., Nishiyama, K., Ko, T., Arima, Y., Hakozaki, Y., Sugihara, K., et al. (2011). Angiogenic morphogenesis driven by dynamic and heterogeneous collective endothelial cell movement. *Development* 138, 4763–4776. doi: 10.1242/dev.068023

Bacharach, E., Itin, A., and Keshet, E. (1998). Apposition-dependent induction of plasminogen activator inhibitor type 1 expression: a mechanism for balancing pericellular proteolysis during angiogenesis. *Blood* 92, 939–945.

Barkefors, I., Le Jan, S., Jakobsson, L., Hejll, E., Carlson, G., Johansson, H., et al. (2008). Endothelial cell migration in stable gradients of vascular endothelial growth factor A and fibroblast growth factor 2: effects on chemotaxis and chemokinesis. *J. Biol. Chem.* 283, 13905–13912. doi: 10.1074/jbc.M704917200

Bass, M. D., Roach, K. A., Morgan, M. R., Mostafavi-Pour, Z., Schoen, T., Muramatsu, T., et al. (2007). Syndecan-4-dependent Rac1 regulation determines directional migration in response to the extracellular matrix. *J. Cell Biol.* 177, 527–538. doi: 10.1083/jcb.200610076

Bergers, G., Brekken, R., McMahon, G., Vu, T. H., Itoh, T., Tamaki, K., et al. (2000). Matrix metalloproteinase-9 triggers the angiogenic switch during carcinogenesis. *Nat. Cell Biol.* 2, 737–744. doi: 10.1038/35036374

Blum, G., Mullins, S. R., Keren, K., Fonovic, M., Jedeszko, C., Rice, M. J., et al. (2005). Dynamic imaging of protease activity with fluorescently quenched activity-based probes. *Nat. Chem. Biol.* 1, 203–209. doi: 10.1038/nchembio728

Bordeleau, F., Mason, B. N., Lollis, E. M., Mazzola, M., Zanotelli, M. R., Somasegar, S., et al. (2017). Matrix stiffening promotes a tumor vasculature phenotype. *Proc. Natl. Acad. Sci. USA* 114, 492–497. doi: 10.1073/pnas.1613855114

Boyden, S. (1962). The chemotactic effect of mixtures of antibody and antigen on polymorphonuclear leucocytes. *J. Exp. Med.* 115, 453–466. doi: 10.1084/jem.115.3.453

Campagnola, P. J., Clark, H. A., Mohler, W. A., Lewis, A., and Loew, L. M. (2001). Second-harmonic imaging microscopy of living cells. *J. Biomed. Opt.* 6, 277–286. doi: 10.1117/1.1383294

Carmeliet, P. (2005). Angiogenesis in life, disease and medicine. *Nature* 438, 932–936. doi: 10.1038/nature04478

Carmeliet, P., and Jain, R. K. (2011). Molecular mechanisms and clinical applications of angiogenesis. *Nature* 473, 298–307. doi: 10.1038/nature10144

Cavallo-Medved, D., Mai, J., Dosescu, J., Sameni, M., and Sloane, B. F. (2005). Caveolin-1 mediates the expression and localization of cathepsin B, pro-urokinase plasminogen activator and their cell-surface receptors in human colorectal carcinoma cells. *J. Cell Sci.* 118, 1493–1503. doi: 10.1242/jcs.02278

Cavallo-Medved, D., Rudy, D., Blum, G., Bogyo, M., Caglic, D., and Sloane, B. F. (2009). Live-cell imaging demonstrates extracellular matrix degradation in association with active cathepsin B in caveolae of endothelial cells during tube formation. *Exp. Cell Res.* 315, 1234–1246. doi: 10.1016/j.yexcr.2009.01.021

Chalasani, A., Ji, K., Sameni, M., Mazumder, S. H., Xu, Y., Moin, K., et al. (2017). Live-cell imaging of protease activity: assays to screen therapeutic approaches. *Methods Mol. Biol.* 1574, 215–225. doi: 10.1007/978-1-4939-6850-3_16

Chen, L., Tredget, E. E., Wu, P. Y., and Wu, Y. (2008). Paracrine factors of mesenchymal stem cells recruit macrophages and endothelial lineage cells and enhance wound healing. *PLoS One* 3:e1886. doi: 10.1371/journal.pone.0003946

Cho, D. I., Kim, M. R., Jeong, H. Y., Jeong, H. C., Jeong, M. H., Yoon, S. H., et al. (2014). Mesenchymal stem cells reciprocally regulate the M1/M2 balance in mouse bone marrow-derived macrophages. *Exp. Mol. Med.* 46:e70. doi: 10.1038/emm.2014.36

Chun, T. H., Sabeh, F., Ota, I., Murphy, H., McDonagh, K. T., Holmbeck, K., et al. (2004). MT1-MMP-dependent neovessel formation within the confines of the three-dimensional extracellular matrix. *J. Cell Biol.* 167, 757–767. doi: 10.1083/jcb.200405001

Chung, B. G., and Choo, J. (2010). Microfluidic gradient platforms for controlling cellular behavior. *Electrophoresis* 31, 3014–3027. doi: 10.1002/elps.201000137

Chung, S., Sudo, R., Mack, P. J., Wan, C. R., Vickerman, V., and Kamm, R. D. (2009). Cell migration into scaffolds under co-culture conditions in a microfluidic platform. *Lab Chip* 9, 269–275. doi: 10.1039/b807585a

Collen, A., Hanemaaijer, R., Lupu, F., Quax, P. H., Van Lent, N., Grimbergen, J., et al. (2003). Membrane-type matrix metalloproteinase-mediated angiogenesis in a fibrin-collagen matrix. *Blood* 101, 1810–1817. doi: 10.1182/blood-2002-05-1593

Du, Y., Herath, S. C., Wang, Q.-G., Wang, D.-A., Asada, H. H., and Chen, P. C. (2016). Three-dimensional characterization of mechanical interactions between endothelial cells and extracellular matrix during angiogenic sprouting. *Sci. Rep.* 6:21362. doi: 10.1038/srep21362

Edgar, L. T., Underwood, C. J., Guilkey, J. E., Hoying, J. B., and Weiss, J. A. (2014). Extracellular matrix density regulates the rate of neovessel growth and branching in sprouting angiogenesis. *PLoS One* 9:e85178. doi: 10.1371/journal.pone.0101767

Eelen, G., De Zeeuw, P., Treps, L., Harjes, U., Wong, B. W., and Carmeliet, P. (2018). Endothelial cell metabolism. *Physiol. Rev.* 98, 3–58. doi: 10.1152/physrev.00001.2017

Elfenbein, A., and Simons, M. (2013). Syndecan-4 signaling at a glance. *J. Cell Sci.* 126, 3799–3804. doi: 10.1242/jcs.124636

Fang, J., Shing, Y., Wiederschain, D., Yan, L., Butterfield, C., Jackson, G., et al. (2000). Matrix metalloproteinase-2 is required for the switch to the angiogenic phenotype in a tumor model. *Proc. Natl. Acad. Sci. USA* 97, 3884–3889. doi: 10.1073/pnas.97.8.3884

Fantin, A., Vieira, J. M., Gestri, G., Denti, L., Schwarz, Q., Prykhozhij, S., et al. (2010). Tissue macrophages act as cellular chaperones for vascular anastomosis downstream of VEGF-mediated endothelial tip cell induction. *Blood* 116, 829–840. doi: 10.1182/blood-2009-12-257832

Friedl, P., and Wolf, K. (2003). Tumour-cell invasion and migration: diversity and escape mechanisms. *Nat. Rev. Cancer* 3, 362–374. doi: 10.1038/nrc1075

Gerhardt, H., Golding, M., Fruttiger, M., Ruhrberg, C., Lundkvist, A., Abramsson, A., et al. (2003). VEGF guides angiogenic sprouting utilizing endothelial tip cell filopodia. *J. Cell Biol.* 161, 1163–1177. doi: 10.1083/jcb.200302047

Ghajar, C. M., Blevins, K. S., Hughes, C. C., George, S. C., and Putnam, A. J. (2006). Mesenchymal stem cells enhance angiogenesis in mechanically viable prevascularized tissues via early matrix metalloproteinase upregulation. *Tissue Eng.* 12, 2875–2888. doi: 10.1089/ten.2006.12.2875

Ghajar, C. M., Chen, X., Harris, J. W., Suresh, V., Hughes, C. C., Jeon, N. L., et al. (2008). The effect of matrix density on the regulation of 3-D capillary morphogenesis. *Biophys. J.* 94, 1930–1941. doi: 10.1529/biophysj.107.120774

Ghajar, C. M., Kachgal, S., Kniazeva, E., Mori, H., Costes, S. V., George, S. C., et al. (2010). Mesenchymal cells stimulate capillary morphogenesis via distinct proteolytic mechanisms. *Exp. Cell Res.* 316, 813–825. doi: 10.1016/j.yexcr.2010.01.013

Gjorevski, N., Piotrowski, A. S., Varner, V. D., and Nelson, C. M. (2015). Dynamic tensile forces drive collective cell migration through three-dimensional extracellular matrices. *Sci. Rep.* 5:11458. doi: 10.1038/srep11458

Grabher, C., Cliffe, A., Miura, K., Hayflick, J., Pepperkok, R., Rorth, P., et al. (2007). Birth and life of tissue macrophages and their migration in embryogenesis and inflammation in medaka. *J. Leukoc. Biol.* 81, 263–271. doi: 10.1189/jlb.0806526

Guillabert-Gourgues, A., Jaspard-Vinassa, B., Bats, M.-L., Sewduth, R. N., Franzl, N., Peghaire, C., et al. (2016). Kif26b controls endothelial cell polarity through the dishevelled/Daam1-dependent planar cell polarity-signaling pathway. *Mol. Biol. Cell* 27, 941–953. doi: 10.1091/mbc.E14-08-1332

Gurevich, D. B., Severn, C. E., Twomey, C., Greenhough, A., Cash, J., Toye, A. M., et al. (2018). Live imaging of wound angiogenesis reveals macrophage orchestrated vessel sprouting and regression. *EMBO J.* 37:e97786. doi: 10.15252/embj.201797786

Hall, M. S., Alisafaei, F., Ban, E., Feng, X., Hui, C.-Y., Shenoy, V. B., et al. (2016). Fibrous nonlinear elasticity enables positive mechanical feedback between cells and ECMs. *Proc. Natl. Acad. Sci. USA* 113, 14043–14048. doi: 10.1073/pnas.1613058113

Han, Y. L., Ronceray, P., Xu, G., Malandrino, A., Kamm, R. D., Lenz, M., et al. (2018). Cell contraction induces long-ranged stress stiffening in the extracellular matrix. *Proc. Natl. Acad. Sci. USA* 115, 4075–4080. doi: 10.1073/pnas.1722619115

Heldin, J., O'callaghan, P., Hernandez Vera, R., Fuchs, P. F., Gerwins, P., and Kreuger, J. (2017). FGD5 sustains vascular endothelial growth factor A (VEGFA) signaling through inhibition of proteasome-mediated VEGF receptor 2 degradation. *Cell. Signal.* 40, 125–132. doi: 10.1016/j.cellsig.2017.09.009

Houck, K. A., Leung, D. W., Rowland, A. M., Winer, J., and Ferrara, N. (1992). Dual regulation of vascular endothelial growth factor bioavailability by genetic and proteolytic mechanisms. *J. Biol. Chem.* 267, 26031–26037.

Hoying, J. B., Boswell, C. A., and Williams, S. K. (1996). Angiogenic potential of microvessel fragments established in three-dimensional collagen gels. *In Vitro Cell. Dev. Biol. Anim.* 32, 409–419.

Hoying, J. B., Utzinger, U., and Weiss, J. A. (2014). Formation of microvascular networks: role of stromal interactions directing angiogenic growth. *Microcirculation* 21, 278–289. doi: 10.1111/micc.12115

Huang, P. H., Chan, C. Y., Li, P., Nama, N., Xie, Y., Wei, C. H., et al. (2015). A spatiotemporally controllable chemical gradient generator via acoustically oscillating sharp-edge structures. *Lab Chip* 15, 4166–4176. doi: 10.1039/c5lc00868a

Hughes, C. C. (2008). Endothelial–stromal interactions in angiogenesis. *Curr. Opin. Hematol.* 15, 204–209. doi: 10.1097/MOH.0b013e3282f97dbc

Ingber, D. E. (2002). Mechanical signaling and the cellular response to extracellular matrix in angiogenesis and cardiovascular physiology. *Circ. Res.* 91, 877–887. doi: 10.1161/01.res.0000039537.73816.e5

Ingber, D. E., Prusty, D., Sun, Z., Betensky, H., and Wang, N. (1995). Cell shape, cytoskeletal mechanics, and cell cycle control in angiogenesis. *J. Biomech.* 28, 1471–1484. doi: 10.1016/0021-9290(95)00095-X

Ito, A., Mukaiyama, A., Itoh, Y., Nagase, H., Thogersen, I. B., Enghild, J. J., et al. (1996). Degradation of interleukin 1beta by matrix metalloproteinases. *J. Biol. Chem.* 271, 14657–14660. doi: 10.1074/jbc.271.25.14657

Jakobsson, L., Franco, C. A., Bentley, K., Collins, R. T., Ponsioen, B., Aspalter, I. M., et al. (2010). Endothelial cells dynamically compete for the tip cell position during angiogenic sprouting. *Nat. Cell Biol.* 12, 943–953. doi: 10.1038/ncb2103

Jedeszko, C., Sameni, M., Olive, M. B., Moin, K., and Sloane, B. F. (2008). Visualizing protease activity in living cells: from two dimensions to four dimensions. *Curr. Protoc. Cell Biol.* 39, 4–20, Chapter 4, Unit-4.20. doi: 10.1002/0471143030.cb0420s39

Jetten, N., Verbruggen, S., Gijbels, M. J., Post, M. J., De Winther, M. P., and Donners, M. M. (2014). Anti-inflammatory M2, but not pro-inflammatory M1 macrophages promote angiogenesis in vivo. *Angiogenesis* 17, 109–118. doi: 10.1007/s10456-013-9381-6

Kachgal, S., and Putnam, A. J. (2011). Mesenchymal stem cells from adipose and bone marrow promote angiogenesis via distinct cytokine and protease expression mechanisms. *Angiogenesis* 14, 47–59. doi: 10.1007/s10456-010-9194-9

Kang, Y. G., Jang, H., Yang, T. D., Notbohm, J., Choi, Y., Park, Y., et al. (2018). Quantification of focal adhesion dynamics of cell movement based on cell-induced collagen matrix deformation using second-harmonic generation microscopy. *J. Biomed. Opt.* 23, 1–8. doi: 10.1117/1.JBO.23.6.065001

Keenan, T. M., and Folch, A. (2008). Biomolecular gradients in cell culture systems. *Lab Chip* 8, 34–57. doi: 10.1039/b711887b

Kilarski, W. W., Samolov, B., Petersson, L., Kvanta, A., and Gerwins, P. (2009). Biomechanical regulation of blood vessel growth during tissue vascularization. *Nat. Med.* 15, 657–664. doi: 10.1038/nm.1985

Kirkpatrick, N. D., Andreou, S., Hoying, J. B., and Utzinger, U. (2007). Live imaging of collagen remodeling during angiogenesis. *Am. J. Physiol. Heart Circ. Physiol.* 292, H3198–H3206. doi: 10.1152/ajpheart.01234.2006

Kniazeva, E., and Putnam, A. J. (2009). Endothelial cell traction and ECM density influence both capillary morphogenesis and maintenance in 3-D. *Am. J. Phys. Cell Phys.* 297, C179–C187. doi: 10.1152/ajpcell.00018.2009

Kniazeva, E., Weidling, J. W., Singh, R., Botvinick, E. L., Digman, M. A., Gratton, E., et al. (2012). Quantification of local matrix deformations and mechanical properties during capillary morphogenesis in 3D. *Integr. Biol.* 4, 431–439. doi: 10.1039/c2ib00120a

Kodelja, V., Muller, C. A., Tenorio, S., Schebesch, C., Orfanos, C. E., and Goerdt, S. (1997). Differences in angiogenic potential of classically vs alternatively activated macrophages. *Immunobiology* 197, 478–493. doi: 10.1016/S0171-2985(97)80080-0

Korff, T., and Augustin, H. G. (1999). Tensional forces in fibrillar extracellular matrices control directional capillary sprouting. *J. Cell Sci.* 112, 3249–3258.

Krishnan, L., Chang, C. C., Nunes, S. S., Williams, S. K., Weiss, J. A., and Hoying, J. B. (2013). Manipulating the microvasculature and its microenvironment. *Crit. Rev. Biomed. Eng.* 41, 91–123. doi: 10.1615/critrevbiomedeng.2013008077

Krishnan, L., Hoying, J. B., Nguyen, H., Song, H., and Weiss, J. A. (2007). Interaction of angiogenic microvessels with the extracellular matrix. *Am. J. Physiol. Heart Circ. Physiol.* 293, H3650–H3658. doi: 10.1152/ajpheart.00772.2007

Lai, E. S., Huang, N. F., Cooke, J. P., and Fuller, G. G. (2012). Aligned nanofibrillar collagen regulates endothelial organization and migration. *Regen. Med.* 7, 649–661. doi: 10.2217/rme.12.48

Lamoreaux, W. J., Fitzgerald, M. E., Reiner, A., Hasty, K. A., and Charles, S. T. (1998). Vascular endothelial growth factor increases release of gelatinase A and decreases release of tissue inhibitor of metalloproteinases by microvascular endothelial cells in vitro. *Microvasc. Res.* 55, 29–42. doi: 10.1006/mvre.1997.2056

LaValley, D. J., and Reinhart-King, C. A. (2014). Matrix stiffening in the formation of blood vessels. *Adv. Regener. Biol.* 1:25247. doi: 10.3402/arb.v1.25247

Lee, S., Ko, J., Park, D., Lee, S. R., Chung, M., Lee, Y., et al. (2018). Microfluidic-based vascularized microphysiological systems. *Lab Chip* 18, 2686–2709. doi: 10.1039/c8lc00285a

Lee, P.-F., Yeh, A. T., and Bayless, K. J. (2009). Nonlinear optical microscopy reveals invading endothelial cells anisotropically alter three-dimensional collagen matrices. *Exp. Cell Res.* 315, 396–410. doi: 10.1016/j.yexcr.2008.10.040

Li, G., Cui, Y., McIlmurray, L., Allen, W. E., and Wang, H. (2005a). rhBMP-2, rhVEGF(165), rhPTN and thrombin-related peptide, TP508 induce chemotaxis of human osteoblasts and microvascular endothelial cells. *J. Orthop. Res.* 23, 680–685. doi: 10.1016/j.orthres.2004.12.005

Li, S., Huang, N. F., and Hsu, S. (2005b). Mechanotransduction in endothelial cell migration. *J. Cell. Biochem.* 96, 1110–1126. doi: 10.1002/jcb.20614

Li, R., Wu, H., Xie, J., Li, G., Gu, R., Kang, L., et al. (2016). Syndecan-4 regulates the bFGF-induced chemotactic migration of endothelial cells. *J. Mol. Histol.* 47, 503–509. doi: 10.1007/s10735-016-9693-0

Liu, L., Ratner, B. D., Sage, E. H., and Jiang, S. (2007). Endothelial cell migration on surface-density gradients of fibronectin, VEGF, or both proteins. *Langmuir* 23, 11168–11173. doi: 10.1021/la701435x

Liu, C., Wu, C., Yang, Q., Gao, J., Li, L., Yang, D., et al. (2016). Macrophages mediate the repair of brain vascular rupture through direct physical adhesion and mechanical traction. *Immunity* 44, 1162–1176. doi: 10.1016/j.immuni.2016.03.008

Lu, P., Takai, K., Weaver, V. M., and Werb, Z. (2011). Extracellular matrix degradation and remodeling in development and disease. *Cold Spring Harb. Perspect. Biol.* 3:a005058. doi: 10.1101/cshperspect.a005058

Mammoto, A., Connor, K. M., Mammoto, T., Yung, C. W., Huh, D., Aderman, C. M., et al. (2009). A mechanosensitive transcriptional mechanism that controls angiogenesis. *Nature* 457, 1103–1108. doi: 10.1038/nature07765

Mantovani, A., Sica, A., Sozzani, S., Allavena, P., Vecchi, A., and Locati, M. (2004). The chemokine system in diverse forms of macrophage activation and polarization. *Trends Immunol.* 25, 677–686. doi: 10.1016/j.it.2004.09.015

Mason, B. N., Starchenko, A., Williams, R. M., Bonassar, L. J., and Reinhart-King, C. A. (2013). Tuning three-dimensional collagen matrix stiffness independently of collagen concentration modulates endothelial cell behavior. *Acta Biomater.* 9, 4635–4644. doi: 10.1016/j.actbio.2012.08.007

McCoy, M. G., Seo, B. R., Choi, S., and Fischbach, C. (2016). Collagen I hydrogel microstructure and composition conjointly regulate vascular network formation. *Acta Biomater.* 44, 200–208. doi: 10.1016/j.actbio.2016.08.028

McCoy, M. G., Wei, J. M., Choi, S., Goerger, J. P., Zipfel, W., and Fischbach, C. (2018). Collagen fiber orientation regulates 3D vascular network formation and alignment. *ACS Biomater Sci. Eng.* 4, 2967–2976. doi: 10.1021/acsbiomaterials.8b00384

McGettrick, H. M., Butler, L. M., Buckley, C. D., Ed Rainger, G., and Nash, G. B. (2012). Tissue stroma as a regulator of leukocyte recruitment in inflammation. *J. Leukoc. Biol.* 91, 385–400. doi: 10.1189/jlb.0911458

McIntyre, J. O., and Matrisian, L. M. (2009). Optical proteolytic beacons for in vivo detection of matrix metalloproteinase activity. *Methods Mol. Biol.* 539, 155–174. doi: 10.1007/978-1-60327-003-8_9

Moin, K., Sameni, M., Victor, B. C., Rothberg, J. M., Mattingly, R. R., and Sloane, B. F. (2012). 3D/4D functional imaging of tumor-associated proteolysis: impact of microenvironment. *Methods Enzymol.* 506, 175–194. doi: 10.1016/B978-0-12-391856-7.00034-2

Mudera, V., Pleass, R., Eastwood, M., Tarnuzzer, R., Schultz, G., Khaw, P., et al. (2000). Molecular responses of human dermal fibroblasts to dual cues: contact guidance and mechanical load. *Cell Motil. Cytoskeleton* 45, 1–9. doi: 10.1002/(SICI)1097-0169(200001)45:1<1::AID-CM1>3.0.CO;2-J

Nakajima, H., Uchida, K., Guerrero, A. R., Watanabe, S., Sugita, D., Takeura, N., et al. (2012). Transplantation of mesenchymal stem cells promotes an alternative pathway of macrophage activation and functional recovery after spinal cord injury. *J. Neurotrauma* 29, 1614–1625. doi: 10.1089/neu.2011.2109

Nelson, C. M., Jean, R. P., Tan, J. L., Liu, W. F., Sniadecki, N. J., Spector, A. A., et al. (2005). Emergent patterns of growth controlled by multicellular form and mechanics. *Proc. Natl. Acad. Sci. USA* 102, 11594–11599. doi: 10.1073/pnas.0502575102

Park, Y. K., Tu, T.-Y., Lim, S. H., Clement, I. J., Yang, S. Y., and Kamm, R. D. (2014). In vitro microvessel growth and remodeling within a three-dimensional microfluidic environment. *Cell. Mol. Bioeng.* 7, 15–25. doi: 10.1007/s12195-013-0315-6

Partridge, C. R., Hawker, J. R. Jr., and Forough, R. (2000). Overexpression of a secretory form of FGF-1 promotes MMP-1-mediated endothelial cell migration. *J. Cell. Biochem.* 78, 487–499. doi: 10.1002/1097-4644(20000901)78:3<487::aid-jcb13>3.0.co;2-z

Plouet, J., Moro, F., Bertagnolli, S., Coldeboeuf, N., Mazarguil, H., Clamens, S., et al. (1997). Extracellular cleavage of the vascular endothelial growth factor 189-amino acid form by urokinase is required for its mitogenic effect. *J. Biol. Chem.* 272, 13390–13396. doi: 10.1074/jbc.272.20.13390

Podgorski, I., Linebaugh, B. E., Sameni, M., Jedeszko, C., Bhagat, S., Cher, M. L., et al. (2005). Bone microenvironment modulates expression and activity of cathepsin B in prostate cancer. *Neoplasia* 7, 207–223. doi: 10.1593/neo.04349

Rivron, N. C., Vrij, E. J., Rouwkema, J., Le Gac, S., Van Den Berg, A., Truckenmüller, R. K., et al. (2012). Tissue deformation spatially modulates VEGF signaling and angiogenesis. *Proc. Natl. Acad. Sci. USA* 109, 6886–6891. doi: 10.1073/pnas.1201626109

Roura, S., Bago, J. R., Soler-Botija, C., Pujal, J. M., Galvez-Monton, C., Prat-Vidal, C., et al. (2012). Human umbilical cord blood-derived mesenchymal stem cells promote vascular growth in vivo. *PLoS One* 7:e49447. doi: 10.1371/journal.pone.0049447

Roy, R., Zhang, B., and Moses, M. A. (2006). Making the cut: protease-mediated regulation of angiogenesis. *Exp. Cell Res.* 312, 608–622. doi: 10.1016/j.yexcr.2005.11.022

Sameni, M., Dosescu, J., Moin, K., and Sloane, B. F. (2003). Functional imaging of proteolysis: stromal and inflammatory cells increase tumor proteolysis. *Mol. Imaging* 2, 159–175. doi: 10.1162/153535003322556903

Sameni, M., Moin, K., and Sloane, B. F. (2000). Imaging proteolysis by living human breast cancer cells. *Neoplasia* 2, 496–504. doi: 10.1038/sj.neo.7900116

Sanz, L., Santos-Valle, P., Alonso-Camino, V., Salas, C., Serrano, A., Vicario, J. L., et al. (2008). Long-term in vivo imaging of human angiogenesis: critical role of bone marrow-derived mesenchymal stem cells for the generation of durable blood vessels. *Microvasc. Res.* 75, 308–314. doi: 10.1016/j.mvr.2007.11.007

Scherer, R. L., Vansaun, M. N., McIntyre, J. O., and Matrisian, L. M. (2008). Optical imaging of matrix metalloproteinase-7 activity in vivo using a proteolytic nanobeacon. *Mol. Imaging* 7, 118–131. doi: 10.2310/7290.2008.00010

Shamloo, A., Ma, N., Poo, M. M., Sohn, L. L., and Heilshorn, S. C. (2008). Endothelial cell polarization and chemotaxis in a microfluidic device. *Lab Chip* 8, 1292–1299. doi: 10.1039/b719788h

Shamloo, A., Mohammadaliha, N., Heilshorn, S. C., and Bauer, A. L. (2016). A comparative study of collagen matrix density effect on endothelial sprout formation using experimental and computational approaches. *Ann. Biomed. Eng.* 44, 929–941. doi: 10.1007/s10439-015-1416-2

Shamloo, A., Xu, H., and Heilshorn, S. (2012). Mechanisms of vascular endothelial growth factor-induced pathfinding by endothelial sprouts in biomaterials. *Tissue Eng. A* 18, 320–330. doi: 10.1089/ten.tea.2011.0323

Shirure, V. S., Lezia, A., Tao, A., Alonzo, L. F., and George, S. C. (2017). Low levels of physiological interstitial flow eliminate morphogen gradients and guide angiogenesis. *Angiogenesis* 20, 493–504. doi: 10.1007/s10456-017-9559-4

Shiu, Y.-T., Weiss, J. A., Hoying, J. B., Iwamoto, M. N., Joung, I. S., and Quam, C. T. (2005). The role of mechanical stresses in angiogenesis. *Crit. Rev. Biomed. Eng.* 33, 431–510. doi: 10.1615/CritRevBiomedEng.v33.i5.10

Sicari, B. M., Dziki, J. L., Siu, B. F., Medberry, C. J., Dearth, C. L., and Badylak, S. F. (2014). The promotion of a constructive macrophage phenotype by solubilized extracellular matrix. *Biomaterials* 35, 8605–8612. doi: 10.1016/j.biomaterials.2014.06.060

Sieminski, A., Hebbel, R., and Gooch, K. (2004). The relative magnitudes of endothelial force generation and matrix stiffness modulate capillary morphogenesis in vitro. *Exp. Cell Res.* 297, 574–584. doi: 10.1016/j.yexcr.2004.03.035

Spiller, K. L., Anfang, R. R., Spiller, K. J., Ng, J., Nakazawa, K. R., Daulton, J. W., et al. (2014). The role of macrophage phenotype in vascularization of tissue engineering scaffolds. *Biomaterials* 35, 4477–4488. doi: 10.1016/j.biomaterials.2014.02.012

Sun, J., Jamilpour, N., Wang, F.-Y., and Wong, P. K. (2014). Geometric control of capillary architecture via cell-matrix mechanical interactions. *Biomaterials* 35, 3273–3280. doi: 10.1016/j.biomaterials.2013.12.101

Takuwa, Y., Du, W., Qi, X., Okamoto, Y., Takuwa, N., and Yoshioka, K. (2010). Roles of sphingosine-1-phosphate signaling in angiogenesis. *World J. Biol. Chem.* 1, 298–306. doi: 10.4331/wjbc.v1.i10.298

Taraboletti, G., D'ascenzo, S., Borsotti, P., Giavazzi, R., Pavan, A., and Dolo, V. (2002). Shedding of the matrix metalloproteinases MMP-2, MMP-9, and MT1-MMP as membrane vesicle-associated components by endothelial cells. *Am. J. Pathol.* 160, 673–680. doi: 10.1016/S0002-9440(10)64887-0

Todeschi, M. R., El Backly, R., Capelli, C., Daga, A., Patrone, E., Introna, M., et al. (2015). Transplanted umbilical cord mesenchymal stem cells modify the in vivo microenvironment enhancing angiogenesis and leading to bone regeneration. *Stem Cells Dev.* 24, 1570–1581. doi: 10.1089/scd.2014.0490

Underwood, C. J., Edgar, L. T., Hoying, J. B., and Weiss, J. A. (2014). Cell-generated traction forces and the resulting matrix deformation modulate microvascular alignment and growth during angiogenesis. *Am. J. Physiol. Heart Circ. Physiol.* 307, H152–H164. doi: 10.1152/ajpheart.00995.2013

Urbich, C., Heeschen, C., Aicher, A., Sasaki, K., Bruhl, T., Farhadi, M. R., et al. (2005). Cathepsin L is required for endothelial progenitor cell-induced neovascularization. *Nat. Med.* 11, 206–213. doi: 10.1038/nm1182

Utzinger, U., Baggett, B., Weiss, J. A., Hoying, J. B., and Edgar, L. T. (2015). Large-scale time series microscopy of neovessel growth during angiogenesis. *Angiogenesis* 18, 219–232. doi: 10.1007/s10456-015-9461-x

Van Goethem, E., Poincloux, R., Gauffre, F., Maridonneau-Parini, I., and Le Cabec, V. (2010). Matrix architecture dictates three-dimensional migration modes of human macrophages: differential involvement of proteases and podosome-like structures. *J. Immunol.* 184, 1049–1061. doi: 10.4049/jimmunol.0902223

Van Noorden, C. J. (2010). Imaging enzymes at work: metabolic mapping by enzyme histochemistry. *J. Histochem. Cytochem.* 58, 481–497. doi: 10.1369/jhc.2010.955518

Vempati, P., Popel, A. S., and Mac Gabhann, F. (2011). Formation of VEGF isoform-specific spatial distributions governing angiogenesis: computational analysis. *BMC Syst. Biol.* 5:59. doi: 10.1186/1752-0509-5-59

Vickerman, V., Blundo, J., Chung, S., and Kamm, R. (2008). Design, fabrication and implementation of a novel multi-parameter control microfluidic platform for three-dimensional cell culture and real-time imaging. *Lab Chip* 8, 1468–1477. doi: 10.1039/b802395f

Wise, A. F., Williams, T. M., Kiewiet, M. B., Payne, N. L., Siatskas, C., Samuel, C. S., et al. (2014). Human mesenchymal stem cells alter macrophage phenotype and promote regeneration via homing to the kidney following ischemia-reperfusion injury. *Am. J. Physiol. Renal Physiol.* 306, F1222–F1235. doi: 10.1152/ajprenal.00675.2013

Yamada, K. M., and Cukierman, E. (2007). Modeling tissue morphogenesis and cancer in 3D. *Cell* 130, 601–610. doi: 10.1016/j.cell.2007.08.006

Zantl, R., and Horn, E. (2011). Chemotaxis of slow migrating mammalian cells analysed by video microscopy. *Methods Mol. Biol.* 769, 191–203. doi: 10.1007/978-1-61779-207-6_13

Zengel, P., Nguyen-Hoang, A., Schildhammer, C., Zantl, R., Kahl, V., and Horn, E. (2011). Mu-slide chemotaxis: a new chamber for long-term chemotaxis studies. *BMC Cell Biol.* 12:21. doi: 10.1186/1471-2121-12-21

Zicha, D., Dunn, G. A., and Brown, A. F. (1991). A new direct-viewing chemotaxis chamber. *J. Cell Sci.* 99, 769–775.

Zigmond, S. H. (1977). Ability of polymorphonuclear leukocytes to orient in gradients of chemotactic factors. *J. Cell Biol.* 75, 606–616. doi: 10.1083/jcb.75.2.606

Zucker, S., Mirza, H., Conner, C. E., Lorenz, A. F., Drews, M. H., Bahou, W. F., et al. (1998). Vascular endothelial growth factor induces tissue factor and matrix metalloproteinase production in endothelial cells: conversion of prothrombin to thrombin results in progelatinase A activation and cell proliferation. *Int. J. Cancer* 75, 780–786. doi: 10.1002/(SICI)1097-0215(19980302)75:5<780::AID-IJC19>3.0.CO;2-A

Conflict of Interest Statement: The authors declare that the research was conducted in the absence of any commercial or financial relationships that could be construed as a potential conflict of interest.

frontiers in Cell and Developmental Biology

BRIEF RESEARCH REPORT
published: 31 August 2020
doi: 10.3389/fcell.2020.00674

Viscoelastic Properties of ECM-Rich Embryonic Microenvironments

Zsuzsa Akos[1], Dona Greta Isai[2], Sheeja Rajasingh[3], Edina Kosa[4], Saba Ghazvini[5†], Prajnaparamita Dhar[5] and Andras Czirok[2,6]*

[1] Division of Biology and Biological Engineering, California Institute of Technology, Pasadena, CA, United States, [2] Department of Anatomy & Cell Biology, University of Kansas Medical Center, Kansas City, KS, United States, [3] Department of Bioscience Research, University of Tennessee Health Science Center, Memphis, TN, United States, [4] Department of Research, Kansas City University of Medicine and Biosciences, Kansas City, MO, United States, [5] Chemical & Petroleum Engineering, The University of Kansas, Lawrence, KS, United States, [6] Department of Biological Physics, Eotvos University, Budapest, Hungary

OPEN ACCESS

Edited by:
Shamik Sen, Indian Institute of Technology Bombay, India

Reviewed by:
Abhijit Majumder, Indian Institute of Technology Bombay, India
Gang Xu, University of Central Oklahoma, United States

***Correspondence:**
Andras Czirok
aczirok@gmail.com

†Present address:
Saba Ghazvini, Dosage Form Design and Development, AstraZeneca, Gaithersburg, MD, United States

Specialty section:
This article was submitted to Cell Adhesion and Migration, a section of the journal Frontiers in Cell and Developmental Biology

Received: *16 November 2019*
Accepted: *02 July 2020*
Published: *31 August 2020*

Citation:
Akos Z, Isai DG, Rajasingh S, Kosa E, Ghazvini S, Dhar P and Czirok A (2020) Viscoelastic Properties of ECM-Rich Embryonic Microenvironments. Front. Cell Dev. Biol. 8:674. doi: 10.3389/fcell.2020.00674

The material properties of tissues and their mechanical state is an important factor in development, disease, regenerative medicine and tissue engineering. Here we describe a microrheological measurement technique utilizing aggregates of microinjected ferromagnetic nickel particles to probe the viscoelastic properties of embryonic tissues. Quail embryos were cultured in a plastic incubator chamber located at the center of two pairs of crossed electromagnets. We found a pronounced viscoelastic behavior within the ECM-rich region separating the mesoderm and endoderm in Hamburger Hamilton stage 10 quail embryos, consistent with a Zener (standard generalized solid) model. The viscoelastic response is about 45% of the total response, with a characteristic relaxation time of 1.3 s.

Keywords: ECM, quail embryo, microrheology, elasticity, Young's modulus, Zener solid, magnetic, nanorods

1. INTRODUCTION

Tissues are physical bodies, thus their formation necessarily involves controlled generation and relaxation of mechanical stresses (Preziosi et al., 2010). Tissue cells are known to generate mechanical stresses by actin-myosin contractility, specifically relying on non-muscle Myosin II, with upstream regulators coordinated through a spatial and temporal activity of rho GTPases such as RhoA (Ridley et al., 2003). The relaxation of mechanical stresses involves the disruption of cell-cell connections, often accompanied by changes in cell neighbors (Forgacs et al., 1998; Smutny et al., 2017; Petridou et al., 2019). While this process is less understood on the molecular level than acto-myosin contractility, the spatio-temporal regulation for both force generation and relaxation are equally important to shape the embryonic tissues. Embryonic tissues are thus plastic, with their stress-free shapes deforming through the development process.

A cell-resolved mechanism underlying tissue plasticity was first resolved in flies, where studies indicated a pulsatile, ratchet-like contraction mechanism (Martin et al., 2009). Thus, instead of a uniformly distributed contractile activity across the tissue, individual cells were observed to undergo (asynchronously) a repeating cycle of contraction, stiffening and relaxation by cytoskeletal rearrangements. The pulsatile nature of tissue movements is also evident in the ECM displacements recorded within avian embryos (Szabó et al., 2011).

While measures for tissue deformation (strain) became recently possible to obtain during development (Rozbicki et al., 2015), estimates for tissue stress and material properties are still

very challenging to determine. A FRET-based molecular sensor has been recently developed (Meng and Sachs, 2011) and used to measure tension *in vivo* (Cai et al., 2014), however its applicability in living tissues is still controversial (Eder et al., 2017). Instead, estimates of mechanical stress within tissues rely on mechanical perturbations (Hutson et al., 2003; Varner et al., 2010; Varner and Taber, 2012; Aleksandrova et al., 2015). In such experiments an introduced discontinuity alters the local mechanical balance of the tissue. As the tissue deforms to obtain a new mechanical equilibrium, this response can be recorded and evaluated. While precise stress measurements would require detailed knowledge about the spatial distribution of material parameters, such data are usually not available. Instead, the existence of tension or compression is deduced from the equilibrium shape of the wound (Varner et al., 2010); the wound opens up more if the stress component perpendicular to the cut is tensile.

The biophysical tool set measuring embryonic tissue rheology, however, is growing together with the interest to determine the material properties of the tissue (Petridou and Heisenberg, 2019). Microrheology, an especially promising approach, involves the analysis of the motion of colloidal tracer particles that are embedded into the sample of interest. The motion can be either a Brownian motion as in passive microrheology (Mason et al., 1997; Crocker et al., 2000; Baker et al., 2009), or driven by external forces as in active microrheology (Mizuno et al., 2008; Waigh, 2016; Vaclaw et al., 2018). These approaches can yield information on the local micro-mechanical properties (both viscous and elastic) of complex biopolymer networks like actin filaments, microtubules or intermediate filaments—both *in vitro*, and in live cells (Chen et al., 2010; Celedon et al., 2011; Nishizawa et al., 2017). The application of microrheology to extracellular matrix (ECM) materials has been rather limited so far (Waigh, 2016) and to the best of our knowledge has not been used to study the mechanical properties of cell-ECM assemblies that are of our interest. Yet, the ability to deduce the material properties prevalent in a microenvironment comparable with the size of the utilized probe, presents microrheology as a logical tool to explore tissues within a developing organism such as described in this study.

2. METHODS

2.1. Nanorod Preparation

Nanorods 3 μm long and 300 nm in diameter were synthesized by electrochemical deposition of nickel into alumina templates as described previously (Paxton et al., 2004; Dhar et al., 2010; Ghazvini et al., 2015). The magnetized nickel nanorods were dispersed in a 90% isopropyl alcohol, 10% water solution.

2.2. Microrheology

For magnetic microrheology we have custom built electromagnets (**Figure 1A**) using 5 inches long iron cores (Ed Fagan Inc., alloy 79, 0.750″ diameter) wrapped around with multiple layers of magnet wire (Tech Fixx Inc., 22 awg).

The theory of elasticity measurement follows (Wilhelm et al., 2002; Celedon et al., 2011). Let ϕ and θ denote the direction of the magnetic moment of the particle and the external field in the xy plane, respectively. The torque $T_{magnetic}$ of the magnetic field B_0 acting on a particle with magnetization m is

$$T_{magnetic} = mB_0 \sin(\theta - \phi). \tag{1}$$

Within an elastic material, the torque $T_{elastic}$ resisting the rotation of the particle in the x-y plane is

$$T_{elastic} = -\mu f(\phi - \phi_0) \tag{2}$$

where $\mu = E/[2(1+\nu)]$ is the shear modulus, $f = \pi\ell^3/[3\ln(\ell/4r)]$ is a geometric factor and ϕ_0 denotes the particle's direction in the absence of external forces or fields (Wilhelm et al., 2002; Celedon et al., 2011). Similarly, the torque associated with a viscous drag is

$$T_{visc} = -\eta f\dot{\phi} \tag{3}$$

where η is the viscosity, and $\dot{\phi}$ is the angular velocity of the nanorod.

In the Kelvin-representation of the standard linear solid (SLS), an elastic and a Kelvin-Voigt material are in series: the short term response is hence elastic, followed by a slower viscoelastic relaxation to a new elastic equilibrium. In this approximation the rotation of the material $\Delta\phi = \phi - \phi_0$ is decomposed into the sum $\Delta\phi = \phi_1 + \phi_2$, where the terms indicate the initial elastic and the subsequent viscoelastic responses, respectively. Thus, the torque balance for a magnetic particle embedded in an SLS material is

$$T_{magnetic} = \mu_1 f\phi_1 = \mu_2 f\phi_2 + \eta f\dot{\phi_2} \tag{4}$$

For small deformations $\Delta\phi \ll 1$, we approximate $T_{magnetic}$ as a Taylor series:

$$T_{magnetic} = mB_0 \sin(\theta - \phi_0) - mB_0 \cos(\theta - \phi_0)\Delta\phi + ... \tag{5}$$

Unless ϕ_0 and θ are parallel, $|\sin(\theta - \phi_0)| \gg |\cos(\theta - \phi_0)\Delta\phi|$, thus $T_{magnetic}$ remains a constant during small deformations. Under such conditions, the solutions of Equation (4) are:

$$\phi_1 = \frac{T_{magnetic}}{\mu_1 f} \tag{6}$$

and

$$\phi_2 = A[1 - \exp(-t/\tau)] \tag{7}$$

where $A = T_{magnetic}/(\mu_2 f)$ and the characteristic relaxation time is

$$\tau = \eta/\mu_2. \tag{8}$$

In the steady state elastic torques resists all the externally imposed $T_{magnetic}$ in the Kelvin-Voigt unit, hence

$$T_{magnetic} = \mu_2 f\phi_2^{max}. \tag{9}$$

Thus, the ratio of the viscoelastic and pure elastic response is obtained as

$$\frac{\phi_1}{\phi_2^{max}} = \frac{\mu_2}{\mu_1}. \tag{10}$$

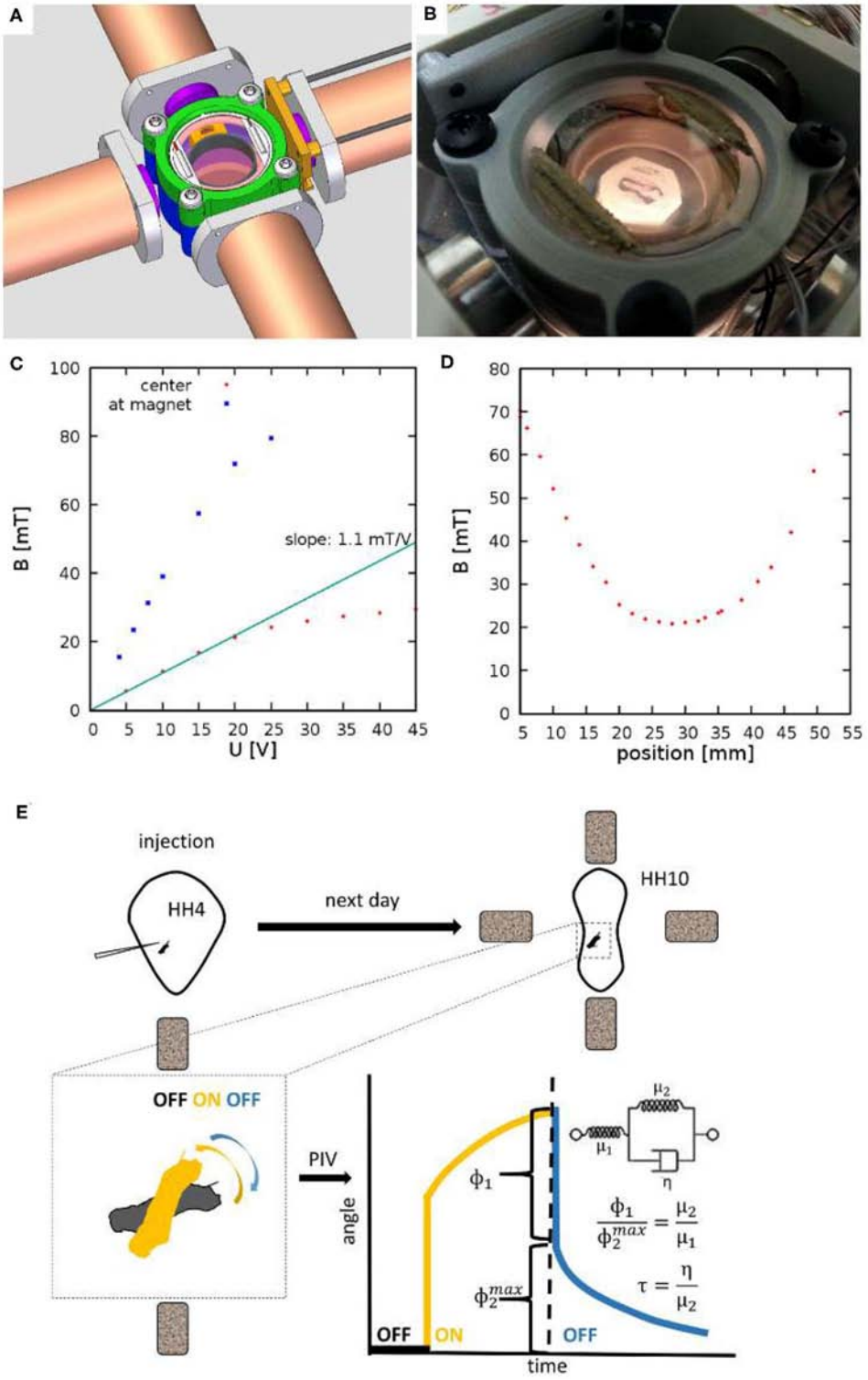

FIGURE 1 | Experimental setup to measure viscoelastic properties of embryonic tissues. **(A)** CAD drawing showing four electromagnets and a 3D-printed incubator chamber in the center. **(B)** The incubator is heated by ITO coated glass windows at the top and bottom of the chamber. **(C)** The measured magnetic field as a function of the voltage across the electromagnets. Red and Blue symbols indicate measured values at the center of the incubation chamber and in the proximity of an iron core, respectively. **(D)** Spatial profile of the magnetic field, measured at $U = 20$V. **(E)** Schematic of measurement: HH Stage 4 quail embryos are microinjected with ferromagnetic nanorod aggregates. After an overnight incubation the specimen is placed between the electromagnets. Switching the magnetic fields on and off exerts a torque on the aggregate. Its rotation and that of the adjacent tissue is recorded by live imaging. Angle of rotation, as a function of time, was extracted using a Particle Image Velocimetry (PIV) method. The rotation response is evaluated in terms of a standard linear solid model, as described in the text.

2.3. Embryo Culture

Fertile wild type quail (Coturnix coturnix japonica) eggs (Ozark Egg Co., Stover, MO) were incubated for varying periods of time (from 20 to 36 h) at 37°C to reach Hamburger and Hamilton (HH) stage 4 (Hamburger and Hamilton, 1951). Embryos were then isolated, injected and cultured as in (Aleksandrova et al., 2015), modified from (Chapman et al., 2001) to reach HH10 when they were subjected to experimental analysis.

2.4. Microinjection and ECM Labeling

Monoclonal antibodies directed against fibrillin-2 and fibronectin ECM proteins (JB3, B3D6; DSHB, Iowa City, IA) were directly conjugated to AlexaFluor 488, 555, or 647 (Molecular Probes) according to the manufacturer's instructions (Czirok et al., 2006). The direct conjugates were injected into the lateral plate mesoderm as 5–40 nl boluses using a PLI-100 (Harvard Instruments) microinjector as described in Little and Drake (2000). Microinjections were performed 30–60 min prior to the beginning of the image acquisition to allow for antibody diffusion and antigen binding.

2.5. Preparation of Transverse Plastic Sections

The embryos were dehydrated through graded ethanol series, placed in acrylamide containing infiltration solution for an hour under vacuum, and embedded in an acrylamide-agarose resin. Subsequently, 100 um sections were cut using a vibratome (Germroth et al., 1995).

2.6. Microscopy

Microrheological measurements were performed on the powered stage of a dissecting microscope (Leica M205FA) equipped with epifluorescence illumination and a Planapo 2.0x objective. The imaging system recorded 1,392 × 1,040 pixel images at a rate of 15.44 frames/s and at a resolution of 0.4 μm /pixel.

2.7. Optical Flow-Based Analysis of Local Tissue Rotation

To characterize tissue deformation, we first apply our non-invasive, optical flow-based method described in Czirok et al. (2017) for each image of the recording. The displacement field $\vec{u}(t,\vec{x})$, calculated relative to the first image as a reference, provides the basis to calculate local tissue rotation. We approximate the local vorticity as

$$|\nabla \times \vec{u}(t,\vec{x})| = \frac{\partial u_y}{\partial x} - \frac{\partial u_x}{\partial y} \approx \frac{u_y(x+h,y) - u_y(x-h,y) - u_x(x,y+h) + u_x(x,y-h)}{2h} \quad (11)$$

where h is the resolution of the optical flow-derived grid.

3. RESULTS

3.1. Magnetic Microrheometer

To facilitate microrheology measurements in live embryos, we built a plastic incubator chamber surrounded by two, orthogonal pairs of electromagnets (**Figure 1**). The plastic construction of the incubator chamber minimizes perturbations of the magnetic field. The incubator chamber consists of two heated indium tin oxide (ITO) glass surfaces that enclose a 35mm dish (**Figures 1A,B**). In the dish a 3D-printed ring (Gulyas et al., 2018) delineates an inner chamber, filled by low melting point agarose, while the outer chamber is filled with sterile distilled water to provide humidity. Temperature was controlled by heating currents within the ITO surfaces, feedback was provided by a thermometer probe immersed in the water bath surrounding the agarose bed. Quail embryos were cultured at the surface of the agarose bed.

The magnetic field within the incubator chamber could be gradually adjusted up to a value of 30 mT by setting the voltage across the electromagnets (**Figure 1C**). The approximate Helmholtz pair-like configuration of the electromagnets was designed to provide a spatial homogeneous magnetic field. According to our measurements, within a 10 mm diameter region around the symmetry center the magnetic field changes less than 5% (**Figure 1D**).

3.2. Microinjection of Ferromagnetic Nickel Nanorod Probes

To measure the material properties of embryonic tissues, we microinjected ferromagnetic nanorods into HH stage 4 quail embryos. In the confined space of the injector capillary, the particles formed aggregates, which incorporated into the tissue, and were detectable by transmitted light microscopy for the entire length of ex ovo development (**Figures 2A,B**). The aggregates also appear as dark areas against the background of ECM immunofluorescence (**Figure 2C**). As subsequent physical sectioning of the microinjected embryos revealed, most nanorod aggregates were delivered into the ECM rich space separating the mesoderm and the endoderm (**Figure 2D**).

3.3. Tissue Deformation Forced by External Fields

Microrheological recordings were performed in HH10 embryos—by which time the injury associated with microinjection completely healed. As high framerate transmitted light live imaging reveals, alternating magnetic fields readily induce rotation of the embedded aggregates, accompanied by a profound deformation of the surrounding tissue microenvironment (**Figure 3**, **Supplementary Movie 1**). The deformation of the ECM was established by live imaging of fibronectin and fibrillin immunofluorescence (**Supplementary Movie 2**, **Figure 2C**). As kymogrphs demonstrate by visualizing movement along the perimeter of a 50 μm radius circle centered at an aggregate, the external force-induced deformation of the ECM and the tissue was similar both in magnitude and timing (**Figures 3B,C**).

To quantify the tissue deformations induced by the rotation of ferromagnetic aggregates, we modified our image analysis tools used to characterize cardiomyocyte beating activity (Czirok et al., 2017). We compared a sequence of images to a common reference frame by PIV analysis, yielding a displacement field

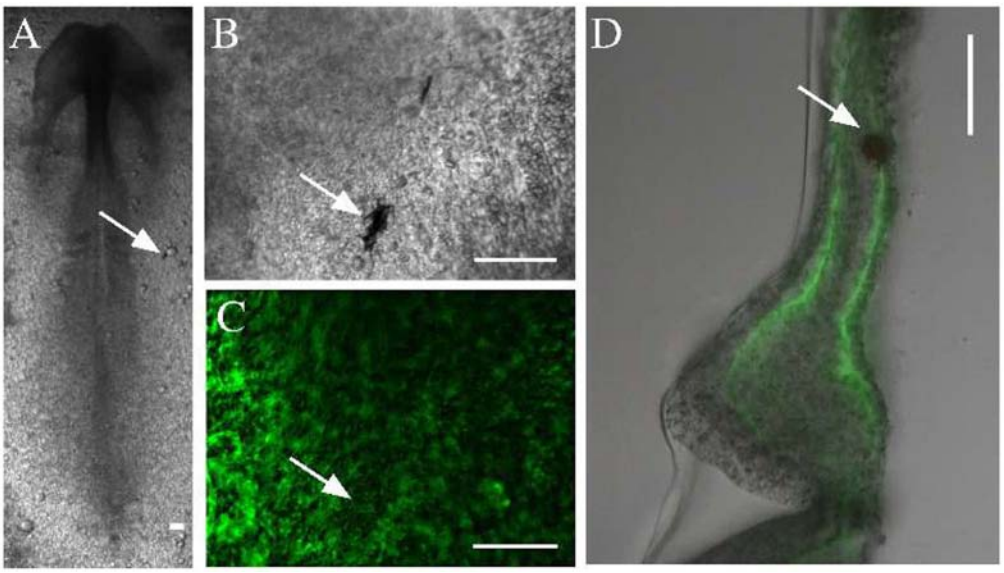

FIGURE 2 | Microinjected ferromagnetic rod aggregates in quail embryos. **(A,B)** An embryo, microinjected with ferromagnetic aggregates at HH stage 4 and healed during an overnight incubation (shown at HH stage 7). Scale bars indicate 100 μm, white arrows point to the same aggregate. **(C)** The ECM microenvironment is visualized by fluorescently labeled antibodies (JB3 anti-fibrillin, B3D6 anti-fibronectin mixture) microinjected into the extracellular space. **(D)** A 100 μm thick transverse cross section of the same embryo locates the aggregate between the endoderm and the lateral plate mesoderm.

(u). The time-dependent spatial average of u indicates a gradually increasing baseline, upon which the magnetic field-induced changes are superimposed (**Figure 4A**). The increasing baseline reflects deformations intrinsic to the developing tissue.

Tissue rotation was specifically characterized by calculating vorticity (**Figure 4C**), the amount of local spinning motion that would be seen by a local observer moving with the tissue. The overall rotation was established based on Stokes' theorem: the sum total of vorticity within an area gives the amount of circulation along the perimeter. Thus, by calculating the sum of vorticity over circles of various sizes, we can determine the spatial extent of the tissue deformation as well as the magnitude of the rotation (**Figure 4B**).

While we do not know the net magnetic moment of the aggregates, the temporal behavior of tissue rotation allows the characterization of the local viscoelastic response of the tissue using Equations (7) and (8). As **Figure 4B** shows, the response of the tissue is biphasic: a very fast (less than 0.2 s) adjustment is followed by a slow, creep-like behavior lasting for several seconds. As a quantitative measure of the response, we fitted an exponential function

$$\phi(t) = a\exp(-t/\tau) + \phi_\infty \tag{12}$$

to each of the recorded responses—both in the creep and relaxation phases—and then transformed the data so that the asymptotic value ϕ_∞ was shifted to zero. The average time-dependent difference from the estimated equilibrium value $|\phi(t) - \phi_\infty|$ indeed validates the presence of a slow, exponential relaxation with a characteristic time of 1.3 ± 0.2 s (**Figures 4D,E**). The presence of a faster and a slower response thus suggest that the ECM-containing early embryonic tissue is well-described as a Zener material (Mainardi and Spada, 2011), represented with a spring in series with a Kelvin-Voigt unit (**Figure 4D** inset). By fitting the Zener model to data extracted from HH10 embryos ($n = 4$) we calculated $\mu_2/\mu_1 = 0.45 \pm 0.1$ and found that the ratio of the viscoelastic and pure elastic response is 45:55%.

4. DISCUSSION

Compression of cell aggregates yielded the first insight into the viscoelastic properties of cell assemblies (Forgacs et al., 1998; Khalilgharibi et al., 2016). These studies established a biphasic elastoplastic response: when aggregates are compressed, there is an initial reversible elastic deformation. When the compressed state is sustained, the forces required to maintain the deformation diminish. For most cell types the force relaxation exhibits an initial fast decay with a characteristic time of around 2 s. This initial decay is followed by a slower exponential process with a characteristic time of 20 s. This late stage process involves a plastic change of the stress free shape of the aggregate: when the external compression is removed, the aggregates did not return to their initial spherical shape for almost a day. The plastic deformation is accompanied by cellular rearrangement in the bulk: by exchanging neighbors cells restored their cuboidal shape. Our measurements remained in the elastic regime: the stress free state of the tissue did not change as evidenced by the diminishing rotation angle upon turning the external magnetic fields off. The tissue response, however, was viscoelastic: an initial elastic response followed by an exponential creep. The characteristic time scale of the creep was consistent with the time scale of the

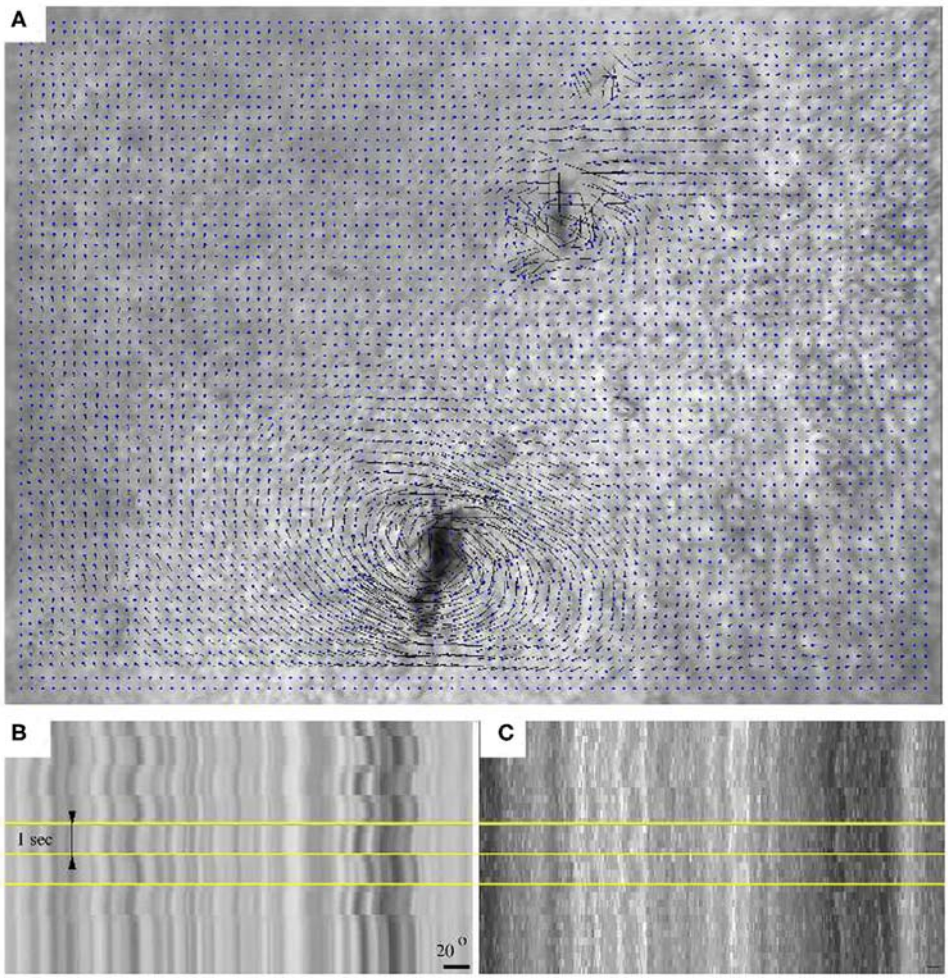

FIGURE 3 | Switching the direction of the external magnetic field rotates an aggregate of magnetic rods and the tissue environment within a HH 10 quail embryo. **(A)** Tissue displacement, calculated using Particle Image Velocimetry (PIV). **(B)** A kymograph representation of the tissue movements reveals the extent of magnetic field-induced rotation. **(C)** Kymograph of the corresponding immunofluorescence recording. Horizontal yellow lines indicate changes in magnetic field direction, timed at 1 s intervals. The scale bar indicates a rotation of 20°.

fast phase in (Forgacs et al., 1998). We suspect that the viscous component arises by movements of cytoskeletal and ECM components in the presence of drag forces from the cytosol and the interstitial fluid inside and outside of the cells, respectively.

Our measurements did not cover the plastic regime as at longer time scales tissue deformations intrinsic to developmental processes interfere with the analysis. The microaspiration technique on *Xenopus laevis* embryos measure material properties on larger scales, and found power law stress relaxation (von Dassow et al., 2010), i.e., a remodeling process fundamentally slower than those found in cell aggregates. Interestingly the creep response was still linear: thus no evidence for active mechanical feedback was observed.

Previous measurement on the chick embryo lateral plate mesoderm found $E = 1,300$ Pa for the Young's modulus when evaluated the tissue deformation caused by a cantilever beam (Agero et al., 2010). This value, together with a Poisson number of 0.2 (Wilhelm et al., 2002; Celedon et al., 2011) yields a shear modulus $\mu_1 + \mu_2 = E/2.4 \approx 550$ Pa. Thus, from our measurements $\mu_2 \approx 250$Pa and $\eta = \mu_2\tau \approx 300$ Pa s, a value consistent with behavior observed in ECM hydrogels *in vitro* (Massensini et al., 2015).

Since cantilever beam probing encompasses a larger area, a more local measurement would be useful to determine local material parameters (E and η) inside the embryo. This could be potentially achieved with the same method presented here, but using magnetic beads where magnetization can be determined and small enough to inject. Further studies can take this direction to explore additional local internal tissue properties.

The importance of tissue material properties on stem cell differentiation (Charrier et al., 2018) generated renewed interest in the mechanical testing of the embryonic (D'Angelo et al.,

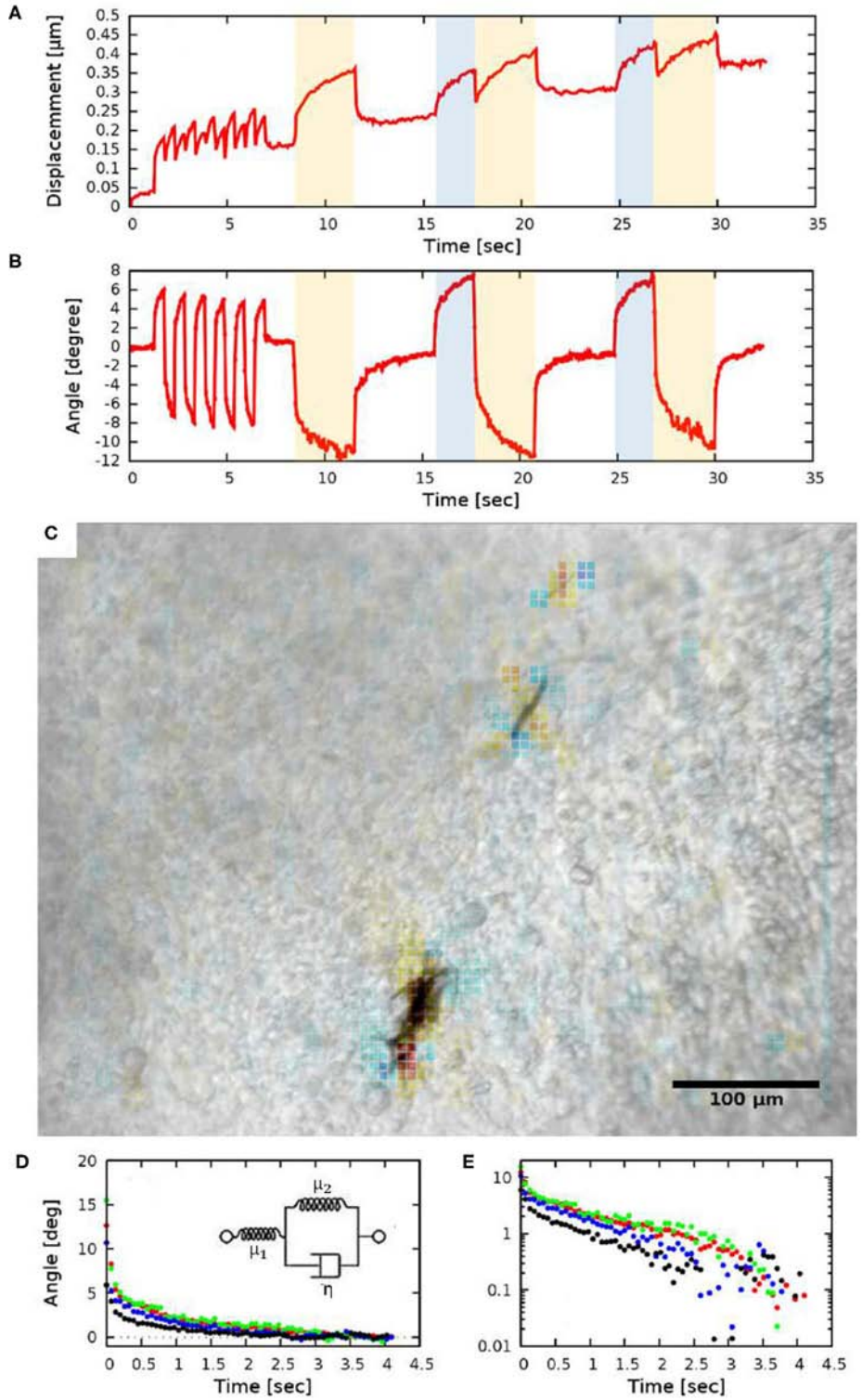

FIGURE 4 | Quantitative measures of tissue rotation obtained from live recordings. **(A)** Average displacements relative to a reference frame. Shaded areas indicate the time while the electromagnets were turned on (the two orthogonal electromagnet pairs are indicated with distinct colors, blue and yellow). **(B)** Angle of rotation calculated from the vorticity (curl) of the displacement field. **(C)** Vorticity of the PIV displacement field, superimposed on a corresponding brightfield image. **(D,E)** Viscoelastic creep of the embryonic tissue. Difference between the current angle and the estimated equilibrium value $|\phi(t) - \phi_\infty|$, as a function of time elapsed since the switch in magnetic field direction. The distinct colors indicate four HH 10 embryos, each injected at the lateral plate mesoderm. The data set presented with black symbols was obtained with a magnetic field of 21 mT (2.35 A coil current), while the other data sets were obtained using a magnetic field of 26 mT (3.4 A coil current). The exponential decay on a linear axis **(D)** appear as straight lines on a logarithmic axis **(E)**. The observed behavior is consistent with a Zener solid (inset **D**).

2019) and organotypic tissues (Chevalier et al., 2016; Charrier et al., 2018) and cells. We trust that the magnetic microrheology method reported here will be a valuable tool to probe tissues at the intermediate length scales, between that of cells and whole organs.

DATA AVAILABILITY STATEMENT

The datasets generated for this study are available on request to the corresponding author.

AUTHOR CONTRIBUTIONS

ZA, SG, PD, and AC designed experiments and the microrheological instrument. PD provided nanorods and designed the calibration experiment. ZA, SG, and EK performed the calibration. EK and SR injected quail embryos and performed measurements. ZA, DI, and AC analyzed data and wrote the manuscript.

FUNDING

The authors would like to acknowledge that grant support was provided by the NIH (R01GM102801) to AC and PD, the American Heart Association (19IPLOI34760594) to AC and the Hungarian Scholarship Board's Eotvos Scholarship to ZA.

ACKNOWLEDGMENTS

We thank Miklos Csiszer for his help in building the experimental apparatus and Michael B. Filla for his initial help with experiments.

SUPPLEMENTARY MATERIAL

The Supplementary Material for this article can be found online at: https://www.frontiersin.org/articles/10.3389/fcell.2020.00674/full#supplementary-material

REFERENCES

Agero, U., Glazier, J. A., and Hosek, M. (2010). Bulk elastic properties of chicken embryos during somitogenesis. *Biomed. Eng. Online* 9:19. doi: 10.1186/1475-925X-9-19

Aleksandrova, A., Czirok, A., Kosa, E., Galkin, O., Cheuvront, T. J., and Rongish, B. J. (2015). The endoderm and myocardium join forces to drive early heart tube assembly. *Dev. Biol.* 404, 40–54. doi: 10.1016/j.ydbio.2015.04.016

Baker, E. L., Bonnecaze, R. T., and Zaman, M. H. (2009). Extracellular matrix stiffness and architecture govern intracellular rheology in cancer. *Biophys. J.* 97, 1013–1021. doi: 10.1016/j.bpj.2009.05.054

Cai, D., Chen, S.-C., Prasad, M., He, L., Wang, X., Choesmel-Cadamuro, V., et al. (2014). Mechanical feedback through E-cadherin promotes direction sensing during collective cell migration. *Cell* 157, 1146–1159. doi: 10.1016/j.cell.2014.03.045

Celedon, A., Hale, C. M., and Wirtz, D. (2011). Magnetic manipulation of nanorods in the nucleus of living cells. *Biophys. J.* 101, 1880–1886. doi: 10.1016/j.bpj.2011.09.008

Chapman, S., Collignon, J., Schoenwolf, G., and Lumsden, A. (2001). Improved method for chick whole-embryo culture using a filter paper carrier. *Dev. Dyn.* 220, 284–289. doi: 10.1002/1097-0177(20010301)220:3<284::AID-DVDY1102>3.0.CO;2-5

Charrier, E. E., Pogoda, K., Wells, R. G., and Janmey, P. A. (2018). Control of cell morphology and differentiation by substrates with independently tunable elasticity and viscous dissipation. *Nat. Commun.* 9:449. doi: 10.1038/s41467-018-02906-9

Chen, D., Wen, Q., Janmey, P., Crocker, J., and Yodh, A. (2010). Rheology of soft materials. *Annu. Rev. Condens. Matter Phys.* 1, 301–322. doi: 10.1146/annurev-conmatphys-070909-104120

Chevalier, N. R., Gazquez, E., Dufour, S., and Fleury, V. (2016). Measuring the micromechanical properties of embryonic tissues. *Methods* 94, 120–128. doi: 10.1016/j.ymeth.2015.08.001

Crocker, J. C., Valentine, M. T., Weeks, E. R., Gisler, T., Kaplan, P. D., Yodh, A. G., et al. (2000). Two-point microrheology of inhomogeneous soft materials. *Phys. Rev. Lett.* 85, 888–891. doi: 10.1103/PhysRevLett.85.888

Czirok, A., Isai, D. G., Kosa, E., Rajasingh, S., Kinsey, W., Neufeld, Z., et al. (2017). Optical-flow based non-invasive analysis of cardiomyocyte contractility. *Sci. Rep.* 7:10404. doi: 10.1038/s41598-017-10094-7

Czirok, A., Zamir, E. A., Filla, M. B., Little, C. D., and Rongish, B. J. (2006). Extracellular matrix macroassembly dynamics in early vertebrate embryos. *Curr. Top. Dev. Biol.* 73, 237–258. doi: 10.1016/S0070-2153(05)73008-8

D'Angelo, A., Dierkes, K., Carolis, C., Salbreux, G., and Solon, J. (2019). *In vivo* force application reveals a fast tissue softening and external friction increase during early embryogenesis. *Curr. Biol.* 29, 1564.e6–1571.e6. doi: 10.1016/j.cub.2019.04.010

Dhar, P., Cao, Y., Fischer, T. M., and Zasadzinski, J. A. (2010). Active interfacial shear microrheology of aging protein films. *Phys. Rev. Lett.* 104:016001. doi: 10.1103/PhysRevLett.104.016001

Eder, D., Basler, K., and Aegerter, C. M. (2017). Challenging FRET-based E-cadherin force measurements in Drosophila. *Sci. Rep.* 7:13692. doi: 10.1038/s41598-017-14136-y

Forgacs, G., Foty, R. A., Shafrir, Y., and Steinberg, M. S. (1998). Viscoelastic properties of living embryonic tissues: a quantitative study. *Biophys. J.* 74, 2227–2234. doi: 10.1016/S0006-3495(98)77932-9

Germroth, P. G., Gourdie, R. G., Thompson, R. P. (1995) Confocal microscopy of thick sections from acrylamide gel embedded embryos. *Microsc. Res. Tech.* 30, 513–520. doi: 10.1002/jemt.1070300608

Ghazvini, S., Ricke, B., Zasadzinski, J. A., and Dhar, P. (2015). Monitoring phases and phase transitions in phosphatidylethanolamine monolayers using active interfacial microrheology. *Soft Matter* 11, 3313–3321. doi: 10.1039/c4sm02900c

Gulyas, M., Csiszer, M., Mehes, E., and Czirok, A. (2018). Software tools for cell culture-related 3D printed structures. *PLoS ONE* 13:e0203203. doi: 10.1371/journal.pone.0203203

Hamburger, V., and Hamilton, H. (1951). A series of normal stages in the development of the chick embryo. *J. Morphol.* 88, 49–92.

Hutson, M. S., Tokutake, Y., Chang, M.-S., Bloor, J. W., Venakides, S., Kiehart, D. P., et al. (2003). Forces for morphogenesis investigated with laser microsurgery and quantitative modeling. *Science* 300, 145–149. doi: 10.1126/science.1079552

Khalilgharibi, N., Fouchard, J., Recho, P., Charras, G., and Kabla, A. (2016). The dynamic mechanical properties of cellularised aggregates. *Curr. Opin. Cell Biol.* 42, 113–120. doi: 10.1016/j.ceb.2016.06.003

Little, C. D., and Drake, C. J. (2000). Whole-mount immunolabeling of embryos by microinjection. Increased detection levels of extracellular and cell surface epitopes. *Methods Mol. Biol.* 135, 183–189. doi: 10.1385/1-59259-685-1:183

Mainardi, F., and Spada, G. (2011). Creep, relaxation and viscosity properties for basic fractional models in rheology. *Eur. Phys. J. Spec. Top.* 193, 133–160. doi: 10.1140/epjst/e2011-01387-1

Martin, A. C., Kaschube, M., and Wieschaus, E. F. (2009). Pulsed contractions of an actin-myosin network drive apical constriction. *Nature* 457, 495–499. doi: 10.1038/nature07522

Mason, T., Ganesan, K., van Zanten, J., Wirtz, D., and Kuo, S. (1997). Particle tracking microrheology of complex fluids. *Phys. Rev. Lett.* 79, 3282–3286.

Massensini, A. R., Ghuman, H., Saldin, L. T., Medberry, C. J., Keane, T. J., Nicholls, F. J., et al. (2015). Concentration-dependent rheological properties of ECM hydrogel for intracerebral delivery to a stroke cavity. *Acta Biomater.* 27, 116–130. doi: 10.1016/j.actbio.2015.08.040

Meng, F., and Sachs, F. (2011). Visualizing dynamic cytoplasmic forces with a compliance-matched FRET sensor. *J. Cell. Sci.* 124, 261–269. doi: 10.1242/jcs.071928

Mizuno, D., Head, D., MacKintosh, F., and Schmidt, C. (2008). Active and passive microrheology in equilibrium and nonequilibrium systems. *Macromolecules* 41, 7194–7202.

Nishizawa, K., Bremerich, M., Ayade, H., Schmidt, C. F., Ariga, T., and Mizuno, D. (2017). Feedback-tracking microrheology in living cells. *Sci. Adv.* 3:e1700318. doi: 10.1126/sciadv.1700318

Paxton, W. F., Kistler, K. C., Olmeda, C. C., Sen, A., Angelo, S. K. S., Cao, Y., et al. (2004). Catalytic nanomotors: autonomous movement of striped nanorods. *J. Am. Chem. Soc.* 126, 13424–13431. doi: 10.1021/ja047697z

Petridou, N. I., Grigolon, S., Salbreux, G., Hannezo, E., and Heisenberg, C.-P. (2019). Fluidization-mediated tissue spreading by mitotic cell rounding and non-canonical Wnt signalling. *Nat. Cell Biol.* 21, 169–178. doi: 10.1038/s41556-018-0247-4

Petridou, N. I., and Heisenberg, C.-P. (2019). Tissue rheology in embryonic organization. *EMBO J.* 38:e102497. doi: 10.15252/embj.2019102497

Preziosi, L., Ambrosi, D., and Verdier, C. (2010). An elasto-visco-plastic model of cell aggregates. *J. Theor. Biol.* 262, 35–47. doi: 10.1016/j.jtbi.2009.08.023

Ridley, A. J., Schwartz, M. A., Burridge, K., Firtel, R. A., Ginsberg, M. H., Borisy, G., et al. (2003). Cell migration: integrating signals from front to back. *Science* 302, 1704–1709. doi: 10.1126/science.1092053

Rozbicki, E., Chuai, M., Karjalainen, A. I., Song, F., Sang, H. M., Martin, R., et al. (2015). Myosin-II-mediated cell shape changes and cell intercalation contribute to primitive streak formation. *Nat. Cell Biol.* 17, 397–408. doi: 10.1038/ncb3138

Smutny, M., Akos, Z., Grigolon, S., Shamipour, S., Ruprecht, V.,Capek, D., et al. (2017). Friction forces position the neural anlage. *Nat. Cell Biol.* 19, 306–317. doi: 10.1038/ncb3492

Szabó, A., Rupp, P. A., Rongish, B. J., Little, C. D., and Czirók, A. (2011). Extracellular matrix fluctuations during early embryogenesis. *Phys. Biol.* 8:045006. doi: 10.1088/1478-3975/8/4/045006

Vaclaw, M. C., Sprouse, P. A., Dittmer, N. T., Ghazvini, S., Middaugh, C. R., Kanost, M. R., et al. (2018). Self-assembled coacervates of chitosan and an insect cuticle protein containing a Rebers-Riddiford Motif. *Biomacromolecules* 19, 2391–2400. doi: 10.1021/acs.biomac.7b01637

Varner, V. D., and Taber, L. A. (2012). Not just inductive: a crucial mechanical role for the endoderm during heart tube assembly. *Development* 139, 1680–90. doi: 10.1242/dev.073486

Varner, V. D., Voronov, D. A., and Taber, L. A. (2010). Mechanics of head fold formation: investigating tissue-level forces during early development. *Development* 137, 3801–3811. doi: 10.1242/dev.054387

von Dassow, M., Strother, J. A., and Davidson, L. A. (2010). Surprisingly simple mechanical behavior of a complex embryonic tissue. *PLoS ONE* 5:e15359. doi: 10.1371/journal.pone.0015359

Waigh, T. A. (2016). Advances in the microrheology of complex fluids. *Rep. Prog. Phys.* 79:074601. doi: 10.1088/0034-4885/79/7/074601

Wilhelm, C., Elias, F., Browaeys, J., Ponton, A., and Bacri, J.-C. (2002). Local rheological probes for complex fluids: application to Laponite suspensions. *Phys. Rev. E Stat. Nonlinear Soft Matter Phys.* 66:021502. doi: 10.1103/PhysRevE.66.021502

Conflict of Interest: The authors declare that the research was conducted in the absence of any commercial or financial relationships that could be construed as a potential conflict of interest.

frontiers in Cell and Developmental Biology

REVIEW
published: 12 April 2019
doi: 10.3389/fcell.2019.00053

The Expression and Possible Functions of Tenascin-W During Development and Disease

Richard P. Tucker[1] and Martin Degen[2]*

[1] Department of Cell Biology and Human Anatomy, University of California, Davis, Davis, CA, United States, [2] Laboratory for Oral Molecular Biology, Department of Orthodontics and Dentofacial Orthopedics, University of Bern, Bern, Switzerland

Tenascins are a family of multifunctional glycoproteins found in the extracellular matrix of chordates. Two of the tenascins, tenascin-C and tenascin-W, form hexabrachions. In this review, we describe the discovery and domain architecture of tenascin-W, its evolution and patterns of expression during embryogenesis and in tumors, and its effects on cells in culture. In avian and mammalian embryos tenascin-W is primarily expressed at sites of osteogenesis, and in the adult tenascin-W is abundant in certain stem cell niches. In primary cultures of osteoblasts tenascin-W promotes cell migration, the formation of mineralized foci and increases alkaline phosphatase activity. Tenascin-W is also prominent in many solid tumors, yet it is missing from the extracellular matrix of most adult tissues. This makes it a potential candidate for use as a marker of tumor stroma and a target for anti-cancer therapies.

Keywords: tenascin-W, extracellular matrix, development, osteogenesis, stem cells, tumor stroma

OPEN ACCESS

Edited by:
Charles D. Little,
The University of Kansas Medical Center, United States

Reviewed by:
Daniel Graf,
University of Alberta, Canada
Eva Turley,
The University of Western Ontario, Canada

****Correspondence:***
Richard P. Tucker
rptucker@ucdavis.edu

Specialty section:
This article was submitted to Cell Adhesion and Migration, a section of the journal Frontiers in Cell and Developmental Biology

Received: *28 November 2018*
Accepted: *20 March 2019*
Published: *12 April 2019*

Citation:
Tucker RP and Degen M (2019) The Expression and Possible Functions of Tenascin-W During Development and Disease. Front. Cell Dev. Biol. 7:53. doi: 10.3389/fcell.2019.00053

INTRODUCTION

Tenascins are extracellular matrix glycoproteins that have a characteristic domain organization. At the N-terminus tenascins have a region that permits trimerization through coiled–coil interactions, and some tenascins have N-terminal cysteines that can support the covalent linking of two trimers to form a hexabrachion. From N-terminal to C-terminal this multimerization region is followed by one or more epidermal growth factor (EGF)-like domains, a series of fibronectin type III (FNIII) domains, and a fibrinogen-related domain (Chiquet-Ehrismann and Tucker, 2011).

In tetrapods there are four tenascin genes that encode tenascin-C, tenascin-R, tenascin-X, and tenascin-W (Chiquet-Ehrismann and Tucker, 2011). The best studied of these is tenascin-C, which was also the first tenascin to be discovered (Chiquet-Ehrismann and Tucker, 2011; Midwood et al., 2016). Tenascin-C is widely expressed in the embryo at sites of epithelial–mesenchymal interactions and around motile cells, including neural crest cells and migrating neuroblasts and glial precursors. It is also found at sites of branching morphogenesis and in developing smooth muscle, bone and cartilage. In the adult, the expression of tenascin-C is more limited, but it is still expressed at high levels in tendons and in some stem cell niches (Chiquet-Ehrismann et al., 2014). Tenascin-R has a more restricted pattern of expression. It is primarily found around subsets of glia and in perineural nets in the developing and adult central nervous system (Dzyubenko et al., 2016). Tenascin-X is found widely in loose connective tissue in both the late stages of embryonic development and in the adult, often displaying expression that is mostly complementary to that of tenascin-C (Valcourt et al., 2015).

This review will concentrate on the fourth and final member of the tenascin gene family to be identified: tenascin-W. We will summarize its discovery and domain architecture, patterns of expression, effects on cells in culture, relationships to other tenascins, as well as its roles in cancer and potential for translational use.

TENASCIN-W BASICS

Discovery and Domain Organization

Tenascin-W was first identified in the zebrafish (Weber et al., 1998). The "W" is most likely an eponymous reference to the last name of its discoverer. *In situ* hybridization with zebrafish embryos demonstrated that tenascin-W is expressed by migrating sclerotome cells and neural crest cells, together with tenascin-C. The zebrafish tenascin-W described by Weber et al. (1998) has 4 EGF-like domains and 5 FNIII domains, and a predicted molecular weight of 103 kDa. A sixth predicted FNIII domain is found in the genomic sequence of zebrafish tenascin-W which may be available for alternative splicing (Tucker et al., 2006), though alternative splicing of tenascin-W has not been reported.

The homolog of tenascin-W in the mouse was originally named tenascin-N (Neidhardt et al., 2003), which explains why this term and its abbreviation TNN is still encountered in the literature and sequence repositories. The murine homolog was assumed to be a novel tenascin since it has 12 FNIII domains instead of the 5 previously reported in the zebrafish. However, sequence alignment studies reveal that the third FNIII domain of tenascin-W, which is encoded on a single exon, has duplicated repeatedly over the course of evolution (Tucker et al., 2006). Consequently, the number of FN III domains, and hence the size of tenascin-W, can vary significantly from species to species (**Figure 1**). Synteny also supports the argument that murine tenascin-N is, in fact, tenascin-W: in fish, birds and mammals the tenascin-W gene is found adjacent to the tenascin-R gene (Tucker et al., 2006). In the years that followed the publication of these observations, all peer-reviewed studies focusing on this form of tenascin refer to it as "tenascin-W," and not tenascin-N. Like tenascin-C, and unlike other tenascins, tenascin-W forms hexabrachions (Scherberich et al., 2004). There is no evidence supporting the formation of tenascin-C/tenascin-W heteromers.

The functions of some of the domains of tenascin-W have been determined experimentally, and potential roles can also be hypothesized from published work with tenascin-C. For example, the FNIII domains appear to contain integrin binding sites (see below), and the fibrinogen-related domains of tenascin-W and tenascin-C share significant similarities and are able to bind and activate Toll-like receptor 4 (Zuliani-Alvarez et al., 2017). Tenascin-W, like tenascin-C, can bind Wnt3a (Hendaoui et al., 2014), but the domain where this binding takes place is unknown. Finally, the EGF-like domains of tenascin-W are nearly identical to those of tenascin-C, and the latter have been shown to be able to activate EGF receptors (Swindle et al., 2001; Fujimoto et al., 2016). Future studies should be directed to see if these properties are unique to tenascin-C, or if tenascin-W may share these and other functional domains with its larger paralog.

Evolution

While some extracellular matrix molecules like collagens and thrombospondins evolved with the first metazoans (Özbek et al., 2010), others evolved more recently. Tenascins are an example of a family of extracellular matrix molecules that evolved with the first chordates; they are not present in echinoderms, ecdysozoa, or lophotrochozoa (Tucker and Chiquet-Ehrismann, 2009a). A single tenascin gene is found in amphioxus and tunicates,

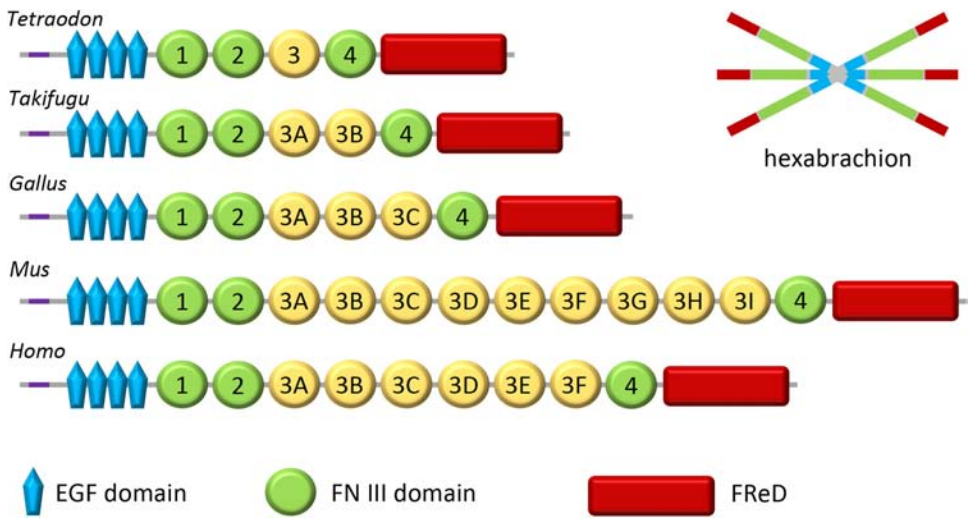

FIGURE 1 | Domain organization of tenascin-W. Tenascin-W has a region near its N-terminus that promotes trimerization (purple); two trimers become covalently linked to form a hexabrachion. Tenascin-W from different species can have different molecular weights as the third FNIII domain (yellow), which is encoded on a single exon, has been duplicated a number of times over the course of evolution. *Tetraodon* and *Takifugu* are genera of pufferfish. *Gallus* is the genus of the chicken and *Mus* is the genus of the mouse. FReD, fibrinogen-related domain.

yet neither of these groups has a fibronectin gene (Adams et al., 2015). In lampreys and cartilaginous fish there are two tenascins, and in the latter group these are clearly tenascin-C and tenascin-R. But in bony fish the full complement of four tenascins are seen, including tenascin-W. Thus, tenascin-W apparently evolved together with a bony skeleton, which is intriguing considering its primary sites of expression and its effects on cells *in vitro* (see below).

Expression at Sites of Osteogenesis and Around Smooth Muscle

Following the pioneering study of tenascin-W expression in the zebrafish described above, the expression of tenascin-W was studied in the mouse and chicken. In contrast to tenascin-C, tenascin-W is detected by immunohistochemistry at relatively late stages of development in the chicken. Starting around embryonic day (E) 8, tenascin-W immunostaining is found in areas of osteogenesis and around a subset of smooth muscles in the developing gut (Meloty-Kapella et al., 2006). Later in development it is seen in the cartilaginous skeleton of the heart. Antibodies to tenascin-W label fibrils in the extracellular matrix and it usually, but not always, co-localizes with tenascin-C in these fibrils. Co-localization with tenascin-C is nicely illustrated in developing scleral ossicles in the E10 eye (**Figure 2A**). The tenascin-W found at sites of osteogenesis likely comes from the osteoblasts themselves, as cultured primary chicken osteoblasts elaborate tenascin-W matrices in the presence of bone morphogenetic protein (BMP) 2 (**Figure 2B**). The literature lacks, however, detailed descriptions of where tenascin-W is found *in situ*: is it made by osteoblasts only, or is it made by osteoblast precursor cells as well? The latter is possible, and

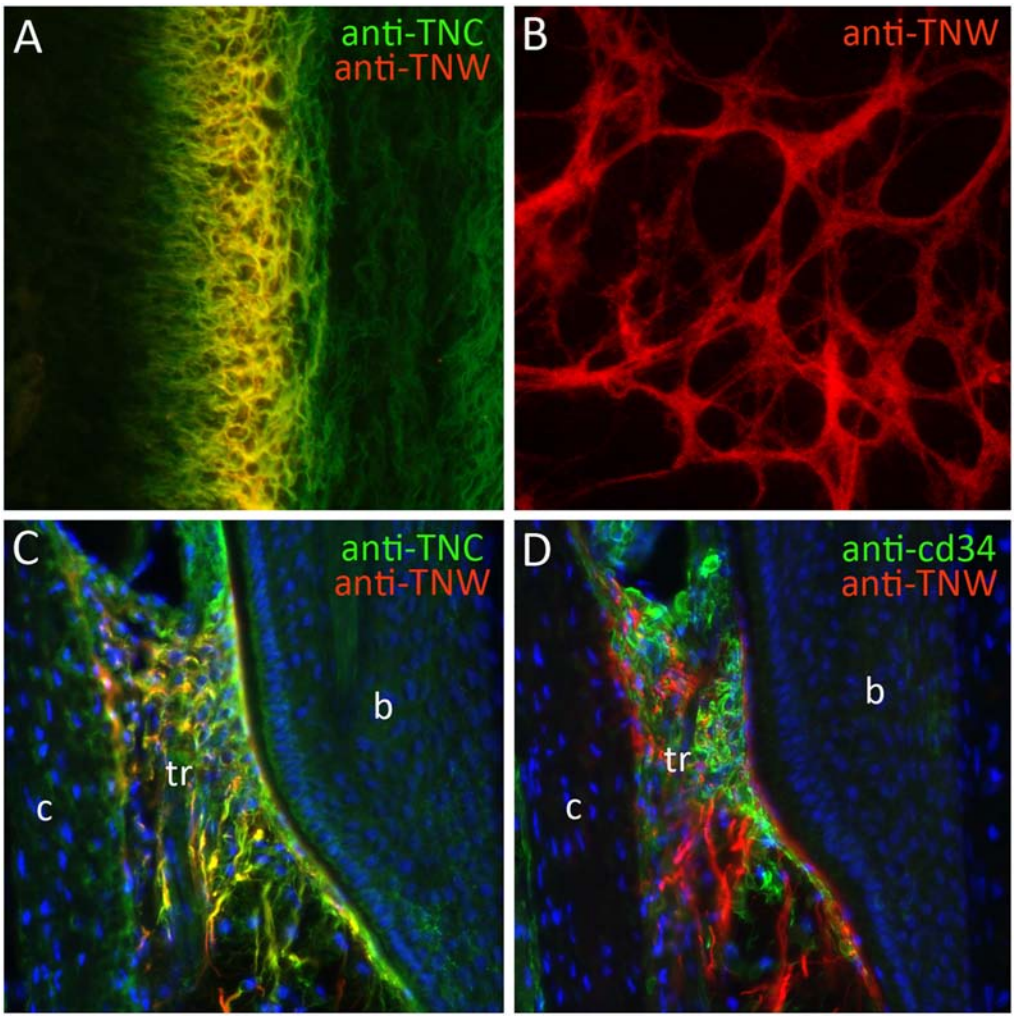

FIGURE 2 | The expression of tenascin-W (TNW). **(A)** Double-label immunohistochemical localization of tenascin-C (TNC) and TNW in the scleral ossicles of an E10 chicken. TNW is commonly expressed at sites of osteogenesis, where it is typically found in the subset of the extracellular matrix labeled with antibodies to TNC. **(B)** After 6 days in culture primary chicken osteoblasts elaborate a TNW-rich extracellular matrix in the presence of BMP2. **(C)** Anti-TNC and anti-TNW both label fibrils in the trabecular region (tr) of adult mouse whisker follicles between the bulge (b) and the capsule (c). TNW-positive fibrils are typically, but not always, a subset of the TNC-positive fibrils. **(D)** The TNW-rich trabecular region contains cd34-positive stem cells.

tenascin-W transcripts are detected in MC3T3-E1 preosteoblasts (Schroeder et al., 2007).

During mouse development tenascin-W expression has been studied with both *in situ* hybridization and immunohistochemistry. As in the chicken, tenascin-W in the mouse is expressed at sites of osteogenesis and in subsets of smooth and skeletal muscle during development (Scherberich et al., 2004). It is first seen in the maxillary processes at E11.5. While its expression at sites of osteogenesis typically overlaps extensively with the expression of tenascin-C, its expression in smooth muscle sometimes overlaps and sometimes does not. For example, both tenascin-C and tenascin-W are found in the muscularis mucosa of the stomach at E15.5, but at this stage of development only tenascin-W is found in the muscularis externa. As in the chicken, tenascin-W expression is not observed in the developing nervous system of the mouse (Scherberich et al., 2004). The expression of tenascin-W in a subset of skeletal muscles is evident both from immunohistochemistry (Scherberich et al., 2004) and microarray studies (Fischer et al., 2005). In the mouse, tenascin-W is expressed in developing teeth (Scherberich et al., 2004), and this has been confirmed by microarray analysis of RNA from laser-captured tissues (Sun et al., 2012).

In the adult chicken tenascin-W is detected in the interstitial matrix of the testis and lining brain ventricles (Meloty-Kapella et al., 2006). The latter immunostaining is the only expression of tenascin-W that is related to the nervous system. In the adult mouse tenascin-W expression is observed in periostea, kidney, spleen (Neidhardt et al., 2003; Scherberich et al., 2004) and stem cell niches (see below). Tenascin-W is also seen in some adult human periostea (Tucker et al., 2016).

Expression in Stem Cell Niches

The first evidence that tenascin-W might play a role in stem cell niches came from studies of its expression in the adult mouse by Scherberich et al. (2004). They observed anti-tenascin-W immunostaining in the corneal limbus and at the base of the cusps of the aortic valves. The limbus niche contains corneal epithelial stem cells (Castro-Muñozledo, 2013), and the cusp base is a potential site of islet1-expressing neural crest-derived stem cells (Engleka et al., 2012). The expression of tenascin-W in bone may also be related to stem cell niches, but this will require more detailed studies for confirmation. Tenascin-W is not detected with immunohistochemistry in the stem cell niche of intestinal crypts (Scherberich et al., 2004; Meloty-Kapella et al., 2006).

One of the most prominent sites of tenascin-W expression in the adult mouse is in hair and whisker follicles (Tucker et al., 2013). In hair follicles tenascin-W is found in a ring just proximal and immediately adjacent to the keratin-15-positive bulge. This region corresponds to the location of nestin-positive stem cells (Amoh et al., 2010) that take part in the cyclic regeneration of hair shafts. In the much larger whisker follicle, tenascin-W-positive fibrils are found in the trabecular region. Tenascin-C is also found in this region, and there is extensive, but not complete, overlap in the tenascin-W and tenascin-C-positive fibrils (**Figure 2C**). The region inside the whisker follicle capsule where tenascin-W is found is filled with cd34-positive stem cells (**Figure 2D**). These cells may be mast cell progenitors, or they may be a population of stem cells like those near the keratin-15-positive bulge of hair follicles.

Tenascin-W expression has been found to be up- or downregulated in many studies using microarrays. A search of the 2913 datasets published on the GEO website[1] found by searching for "TNN and tenascin" (TNN is the genetic shorthand for both tenascin-W and troponins) revealed 33 examples where tenascin-W was consistently up- or downregulated (**Supplementary Table S1**). Many of these are related to tenascin-W expression in dense connective tissue and in stem cell niches; others are related to tenascin-W in cancer (see below).

THE CELL BIOLOGY OF TENASCIN-W

Tenascin-W as an Adhesion Modulatory Protein

Adhesion modulation can influence cell motility, proliferation and differentiation. Tenascin-C is a classic adhesion modulatory protein (Chiquet-Ehrismann and Tucker, 2011). *In vitro*, cells can attach to tenascin-C, but they typically fail to spread and form focal adhesions. Similarly, cells that have formed focal adhesions on a substratum coated with fibronectin will lose their focal adhesions if tenascin-C is added to the medium. Tenascin-W also has the potential to act as an adhesion modulatory protein. For example, the myoblast-derived osteogenic mouse cell line C2C12 spread and form focal adhesions and stress fibers on fibronectin, but C2C12 cells remain rounded or stellate and fail to form focal adhesions or stress fibers when cultured in the presence of tenascin-W (Scherberich et al., 2004; Brellier et al., 2012a). Moreover, C2C12 cells remain stellate when cultured on fibronectin if tenascin-W is in the culture medium or if they are cultured on a mixed fibronectin/tenascin-W substratum (Brellier et al., 2012a). Similarly, primary osteoblasts cultured from chicken embryo calvarias spread and form stress fibers on fibronectin but fail to spread on combinations of fibronectin and tenascin-W (Meloty-Kapella et al., 2006). Tenascin-W does not demonstrate adhesion modulation with all cell types. For example, the human breast cancer cell line T47D does not adhere to a tenascin-W-coated substratum, in contrast to dermal fibroblast Detroit551 cells, which attach to human tenascin-W in an integrin β1-dependent manner (Degen et al., 2007). In addition, T47D cells are still able to adhere to a mixed fibronectin/tenascin-W substratum, which is not the case for fibronectin/tenascin-C substrata (Degen et al., 2007).

Effects of Tenascin-W on Cultured Osteoblasts

Tenascin-W may have evolved in bony fish, and a prominent and phylogenetically conserved site of tenascin-W expression is periosteum and other sites of osteogenesis. One way of studying the effects of tenascin-W on bone maturation is to measure alkaline phosphatase activity in cultured osteoblasts in

[1] https://www.ncbi.nlm.nih.gov/geo/

the presence of tenascin-W. When cultured in dishes coated with 1–10 μg/ml of tenascin-W there is a significant increase in alkaline phosphatase activity in primary calvarial osteoblasts from the chicken (Meloty-Kapella et al., 2008). Interestingly, no increase in activity is seen when higher concentrations of tenascin-W are used to coat the dishes. Over time, cultured primary osteoblasts make mineralized foci called rosettes. In the presence of tenascin-W, significantly more rosettes form. Tenascin-W also influences osteoblast motility in culture. When primary osteoblasts are cultured on tenascin-W-coated filters, significantly more cells migrate across the filter when compared with uncoated filters or filters coated with tenascin-C. Unlike tenascin-C, tenascin-W has no effect on primary osteoblast proliferation.

Regulation of Tenascin-W Expression

In contrast to the other tenascins relatively little is known about how tenascin-W expression is regulated (Chiovaro et al., 2015a). The UCSC Genome Browser reveals a high degree of conservation between the first non-coding exons of human and murine tenascin-W, as well as in the region extending up to 600 bp 5′ to the first exon. This indicates that there are likely conserved promoters in this region, but more experimental research is clearly needed. This region contains both a TATA box (conserved with tenascin-C) and predicted SMAD-binding elements, and both appear to be active (Chiovaro et al., 2015b). Some potential transcriptional regulators and regulatory pathways are suggested by microarray analyses, including sonic hedgehog, Wilms tumor protein 1, and Notch 1 (**Supplementary Table S1**). *In vitro*, transforming growth factor (TGF) β1 upregulates tenascin-W in bone marrow stem cells (Chiovaro et al., 2015b), and BMP2 induces tenascin-W in both C2C12 (Scherberich et al., 2004) and HC11 cells (Scherberich et al., 2005).

Effects of Tenascin-W on Stem Cells *in vitro*

Stem cells can be cultured from their niche in the trabecular region of whisker follicles by stripping the follicle of its capsule, cutting the whisker on either side of the niche, and putting the whisker with the attached niche onto coated plastic dishes. Over time, the stem cells migrate away from the niche and their behavior and morphology can be studied (Sieber-Blum and Hu, 2008). As seen earlier with primary osteoblasts and C2C12 cells, these stem cells will spread and form focal adhesion and stress fibers on fibronectin, but the cells are less spread and have significantly fewer focal adhesions when they migrate onto a mixed fibronectin/tenascin-W substratum (Tucker et al., 2013). The stem cells proliferate at a greater rate in the presence of tenascin-C, but not tenascin-W. What might the role of tenascin-W be in the whisker follicle, and other, stem cell niche? One might be to anchor and concentrate factors like Wnt3a that can influence proliferation and differentiation. Another could be to form a substratum that supports migration: stem cells leaving the trabecular region need to migrate over a millimeter to the whisker follicle bulb, and their pathway is lined with tenascin-W. Insight may come from careful analysis of the tenascin-W knockout mouse, which has yet to be characterized.

Tenascin-W Signaling

Tenascin-W may be an integrin ligand, and some of its effects on cells in culture may be the results of integrin-based signaling. Scherberich et al. (2004) cultured human T98G glioblastoma-derived cells on murine tenascin-W and assayed the ability of function-blocking antibodies against specific integrin subunits to inhibit this adhesion. The only antibody to block the adhesion was an anti-β1. As a function-blocking anti-α8 was not available, Scherberich et al. (2004) next transfected a cell line that does not normally adhere to tenascin-W with an α8 cDNA, and found that this induced adhesion to tenascin-W. In addition, antibodies to the α8 integrin subunit show expression in many of the same tissues where tenascin-W is found, including periosteum (Scherberich et al., 2004). These observations were expanded upon with 3T3 cells. 3T3 cells normally do not adhere to tenascin-W, but transfecting 3T3 cells with the α8 integrin subunit increases both their adhesion to, and motility on, tenascin-W-coated substrata (Scherberich et al., 2005). The drawback of such studies is that they do not show direct interactions between the ligand and the receptor. α8β1 integrin recognizes the tripeptide motif RGD, and an RGD is found in an exposed loop of the second FNIII domain of mouse tenascin-W. Accordingly, RGD-containing peptides, but not scrambled peptides, block the adhesion of T98G cells to murine tenascin-W-coated substrata (Scherberich et al., 2004). However, an exposed RGD is not found in human or chicken tenascin-W. Interestingly, human and chicken tenascin-C have an RGD motif in the third FNIII, but the third FNIII of mouse tenascin-C does not (Adams et al., 2015). Perhaps tenascin-C and tenascin-W share come integrin-mediated functions and can compensate for each other. Future studies should consider the use of murine tenascin-W with the RGD mutated to another sequence to see if this is, in fact, the sequence recognized by α8β1 integrin.

In summary, studies of cell-tenascin-W interactions *in vitro* indicate that tenascin-W can influence cell adhesion, migration and differentiation, but unlike tenascin-C, tenascin-W does not appear to influence cell proliferation. Tenascin-W seems to modulate cell adhesion in a highly cell type-specific and integrin-dependent way, which might have relevance in the dissemination process of cancer cells during tumor progression (see below).

TENASCIN-W IN CANCER

Tenascin-W Expression in Solid Human Tumors

Tumor development has traditionally been viewed as a cell-autonomous process and research was greatly focused on neoplastic cells and the understanding of cancer cell transformation. However, this reductionist vision has changed over the last couple of years. It is now well established that for the full malignant manifestation, tumor cells require a tumor-permissive microenvironment, which is created by a complex

interplay between cancer cells and their local environment. Among the proteins known to be specifically expressed in tumor-associated stroma are tenascin-C and tenascin-W. Initially, tenascin-W was found to be overexpressed in the stroma around murine breast tumor lesions having a high likelihood to form metastases (Scherberich et al., 2005). Prompted by these first observations, additional studies on the expression pattern of tenascin-W in human biopsies followed. These analyses revealed complete absence of tenascin-W in most normal adult human tissues and prominent *de novo* expression in all tumors investigated. Tenascin-W is overexpressed in the tumor stroma of breast (Degen et al., 2007), colorectal (Degen et al., 2008), brain (oligodendroglioma, astrocytoma, and glioblastoma) (Martina et al., 2010), kidney (clear cell carcinoma, papillary carcinoma, chromophobe renal carcinoma, and oncocytoma), ovarian, prostate, pancreas, and lung cancers as well as in melanomas (Brellier et al., 2012b; **Figure 3**). In metastatic melanoma patients, tenascin-W is not only expressed in the primary tumor, but it is also detected in 25% of biopsies received from metastases from diverse locations (i.e., spleen, lung, and skin) as well as in 38% of lymph node metastasis samples (Brellier et al., 2012b). In the tumor stroma, tenascin-W is often found adjacent to blood vessels co-localizing with the endothelial cell markers cd31 and von-Willebrand-factor (Martina et al., 2010; Brellier et al., 2012b; **Figure 3**).

The cellular source of tenascin-W expression in the tumor stroma remains to be clarified. So far, all available data suggest that tenascin-W expression is restricted to stromal cells. In a xenograft model of breast cancer cells with bone-specific metastatic potential, the bone marrow-derived stromal cells exclusively expressed tenascin-W when co-cultured with the malignant cells (Chiovaro et al., 2015b). Confirming the concept of tenascin-W production by stromal cells, tenascin-W is neither detectable in epithelial-derived cancer cells by immunohistochemistry nor in various human cancer cell lines analyzed and screened by *in vitro* assays. This contrasts with tenascin-C, which can be expressed by stromal as well as cancer cells (e.g., in gliomas) (Sivasankaran et al., 2009).

It is well established that tenascin-C is subject to alternative splicing within its FNIII domains. Certain tenascin-C splice variants containing additional FNIII domains are more tumor-specific than the shortest isoform, and isoform-specific antibodies against tenascin-C can be used as tumor markers. Although tenascin-W shares the modular structure of tenascin-C including a (shorter) stretch of FNIII domains, there is no evidence so far that tenascin-W undergoes alternative splicing in physiological as well tumorigenic conditions.

While tenascin-C and tenascin-W are often co-expressed in the stroma of various solid tumors, certain cancers selectively express only one of the two extracellular matrix proteins (Degen et al., 2007, 2008). These observations suggest the existence of common as well as independent regulatory mechanisms responsible for tenascin-C and tenascin-W expression (Chiquet-Ehrismann and Tucker, 2011). Numerous regulatory

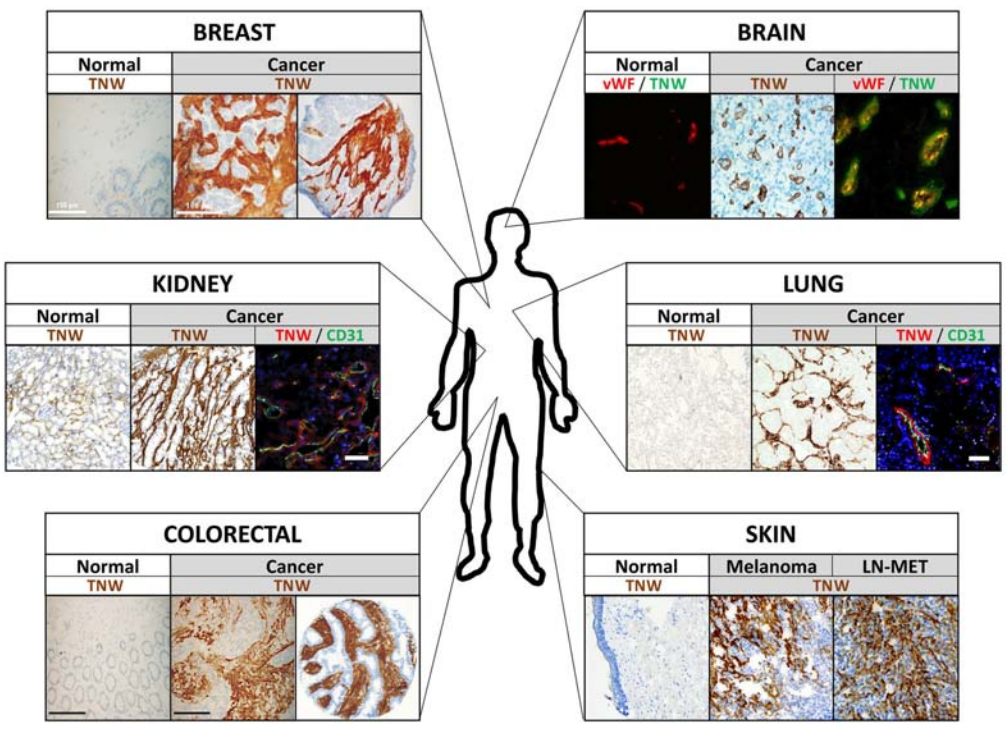

FIGURE 3 | Tenascin-W (TNW) expression in human tumors. Examples of immunohistochemical analyses of TNW in various human tumors and adjacent normal tissue are shown. Note that TNW is prominently expressed in the tumor stroma, often co-localizing with blood vessel markers (see kidney, brain, and lung cancer pictures) and mostly not detectable in the corresponding normal tissue. vWF, von Willebrand factor; cd31, blood vessel marker; LN-MET, lymph node metastasis.

mechanisms have been identified for tenascin-C, which include regulation by patterning genes during development, growth factors and inflammatory mediators, hypoxic conditions, mechanical stress, activated signaling pathways, as well as microRNAs (Tucker and Chiquet-Ehrismann, 2009b; Chiquet-Ehrismann and Tucker, 2011; Chiovaro et al., 2015a). Several of these stimuli might be relevant for the tumor-specific expression of tenascin-C. For example, active Notch signaling has been linked to tenascin-C expression during gliomagenesis (Sivasankaran et al., 2009). Knowledge of tenascin-W regulation remains sparse and mostly restricted to mouse and chicken studies. BMP2, BMP7, and tumor necrosis factor (TNF) α induce tenascin-W expression in cultured murine cells, such as mouse embryonic fibroblasts, cranial fibroblasts, C2C12 cells, and HC11 normal mammary gland epithelial cells (Scherberich et al., 2004, 2005; Kimura et al., 2007; d'Amaro et al., 2012) and primary chicken osteoblast cultures. However, this seems to be different in human cells, in which none of the growth factors tested are able to induce endogenous tenascin-W expression. Only recently, TGFβ1 was identified as a first transcriptional regulator of tenascin-W in the metastatic bone marrow niche. *De novo* deposition of tenascin-W by stromal cells was induced via cancer-mesenchymal cell interactions in a TGFβ1-dependent manner (Chiovaro et al., 2015b). Clearly, more research is required for the identification of additional differences (e.g., TGFβ vs. BMPs) or similarities (e.g., negative regulation by glucocorticoids) in the control of *tenascin-C* and *tenascin-W* genes, especially elucidating their abundant *de novo* expression in neoplastic conditions.

Tenascin-W Promotes Tumor Cell Migration

The first evidence that tenascin-W influences cancer cell migration was provided in transwell migration assays using murine mammary cells plated on inserts coated with mouse tenascin-W. While the normal mouse mammary gland epithelial cell line HC11 failed to migrate across filters coated with tenascin-W, tenascin-W as substrata stimulated the migratory behavior of the highly metastatic 4T1 mouse mammary cancer cell line (Scherberich et al., 2005). This specific response to the presence of tenascin-W was related to the expression of integrin α8, a potential tenascin-W receptor (see above), in 4T1 cells and its absence in HC11 cells (Scherberich et al., 2005). Confirming the motility-promoting activity of tenascin-W, addition of soluble human tenascin-W to the lower side of a transwell migration chamber stimulated cell migration of T47D breast cancer cells toward the fibronectin substratum (Degen et al., 2007). Hence, presence of tenascin-W in the tumor microenvironment stimulates migration of at least breast cancer cells.

Tenascin-W Promotes Angiogenesis

The observation that tenascin-W co-localizes with endothelial cell markers in the tumor stroma of brain (Martina et al., 2010), kidney, colon, breast, ovary, and prostate cancer (Brellier et al., 2012b), but is completely absent in corresponding normal tissues, encouraged additional studies to determine a possible function of tenascin-W in promoting tumor angiogenesis. Indeed, presence of tenascin-W induces an elongated morphology in human umbilical vein endothelial cells (HUVEC) correlating with increased motility, two characteristic features of angiogenic endothelial cells (Martina et al., 2010). To gain further evidence for a role of tenascin-W in stimulating angiogenesis, a collagen gel-embedded spheroid-based *in vitro* angiogenesis assay was performed. A significant induction of endothelial cell sprouts was observed in HUVEC spheroids embedded in a collagen/tenascin-W gel compared to collagen gels alone (Martina et al., 2010). These data point toward an important role for tenascin-W in stimulating tumor angiogenesis.

Promotion of Metastasis by Tenascin-W

Recent data suggest that tenascin-C represents an important component of various physiological as well as pathological stem cell niches, playing fundamental roles in stem cell maintenance and renewal (Chiquet-Ehrismann et al., 2014). Since tenascin-W often shares physiological and tumor-associated expression, as well as functional similarities with tenascin-C, it was not surprising to learn that tenascin-W is present in stem cell niches as well (e.g., corneal limbus and whisker follicles; see above) (Scherberich et al., 2004; Tucker et al., 2013). Similar to tenascin-C, which is part of the lung-metastatic niche for breast cancer cells (Oskarsson et al., 2011), evidence emerged recently that tenascin-W is a component of the congenial metastatic niche in breast cancer cells disseminating to bone (Chiovaro et al., 2015b). After homing of breast cancer cells to bone marrow the malignant cells secrete TGFβ1, which acts in a paracrine fashion to modulate the bone marrow niche, including the *de novo* deposition of tenascin-W. As a specific component of this metastatic niche, tenascin-W promotes metastatic progression by stimulating growth and migration of the cancer cells (Chiovaro et al., 2015b). These data reveal that tenascin-W can be induced in stem cell niches in the bone by breast cancer cell-secreted factors, ultimately leading to an increased risk of bone metastasis. This and other potential roles for tenascin-W in cancer are summarized in **Figure 4**.

POTENTIAL TRANSLATIONAL USE OF TENASCIN-W

Cancer Detection

Although tenascin-C and tenascin-W are often overexpressed in tumor stroma, there is now good evidence that the expression of tenascin-W is much more tumor-specific than the expression of tenascin-C (Brellier et al., 2012b). Tenascin-C is readily expressed in certain healthy tissues and it is well established that it can be re-expressed under pathological conditions other than cancers, such as inflammation, healing wounds, infections, and asthma (Orend and Chiquet-Ehrismann, 2006; Brellier et al., 2009; Midwood et al., 2016). Tenascin-W, however, mostly shows no detectable expression in normal tissues adjacent to tumors (Degen et al., 2007, 2008; Brellier et al., 2012b), and so far, there is no *in situ* evidence that it can be induced under conditions other than tumors. For instance, tenascin-W is neither detected in biopsies

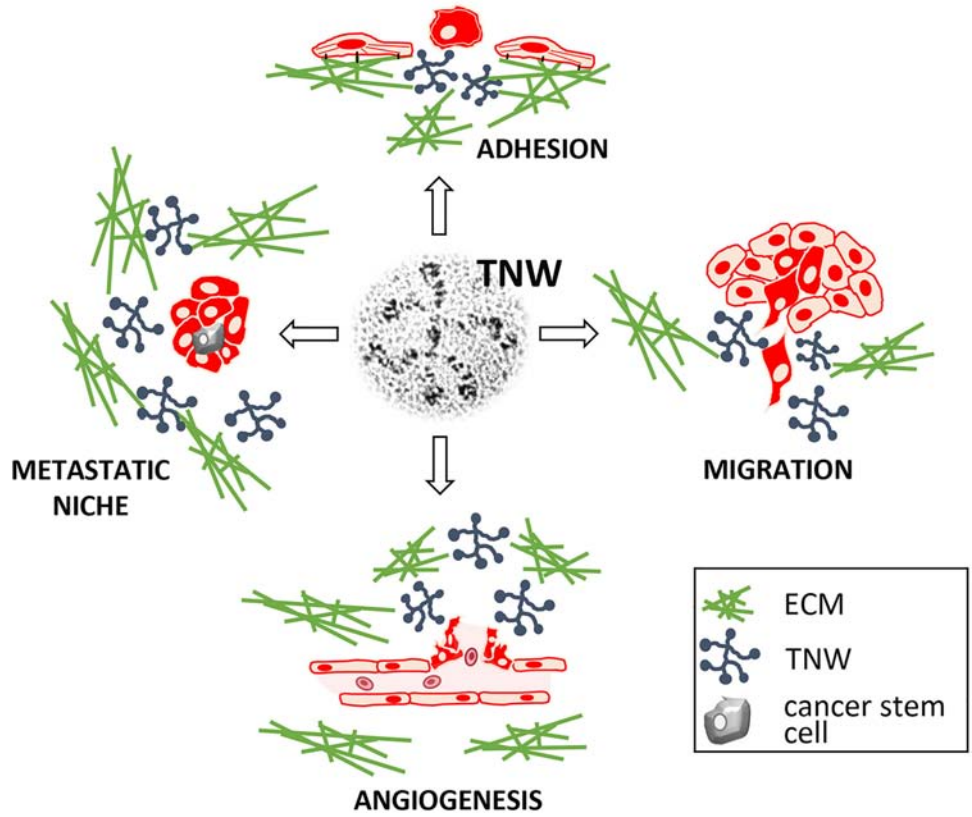

FIGURE 4 | Described functions of tenascin-W (TNW). As a matricellular protein, TNW regulates the interplay between stromal and epithelial cells, and between cells and other extracellular matrix (ECM) components, thereby influencing cancer cell behavior and promoting tumor formation.

from patients with inflammatory bowel diseases displaying strong tenascin-C expression (unpublished data) nor in healing wounds in mice (Brellier et al., 2012a). Hence, its prominent and highly tumor-specific expression establish tenascin-W as a potential diagnostic tumor biomarker candidate. Tenascin-W can also be detected in liquid biopsies, making it even more convenient and attractive as a biomarker. Elevated levels of serum tenascin-W have been reported in breast and colon cancer patients compared to controls using a sensitive tenascin-W-specific sandwich ELISA (Degen et al., 2008).

Prediction of Metastatic Potential

Tenascin-W expression is higher in mouse models of mammary cancer that metastasize compared to non-metastasizing tumors (Scherberich et al., 2005). Up to now, such a correlation was not observed in human breast cancer where tenascin-W expression is enriched in low-grade tumors (Degen et al., 2007). However, in lung cancer, the average expression levels of tenascin-W appear to correlate with tumor grade (Brellier et al., 2012b) and in colorectal cancer, tenascin-W may correlate with the aggressiveness of the disease. Mean serum tenascin-W levels in non-metastatic colorectal cancer patients is 1.5-fold higher in those patients suffering from recurrence compared to non-recurrent patients (Degen et al., 2008). These data suggest that tenascin-W might have potential value as a predictive biomarker. Clearly, these initial studies are too small to draw any conclusive conclusions. Nevertheless, these data warrant more studies to determine the predictive value of tenascin-W in certain malignancies.

Targeting Therapies

Given its tumor-specific expression and its proximity to blood vessels, we speculate that tenascin-W might be used as a potential candidate for identifying stromal areas with tumors and as a potential target for therapies. Such therapies could include selective delivery of anticancer medicine via tenascin-W specific antibody-drug conjugates. Similar approaches are successfully ongoing with tenascin-C-specific antibodies. In particular, the F16 monoclonal human antibody specifically recognizing the alternatively spliced A1 domain of tenascin-C is being evaluated in clinical trials in combination with approved anti-tumor drugs in patients with solid tumors and metastatic breast cancer (Catania et al., 2015). Since tenascin-W seems to a be a more specific tumor marker than tenascin-C (Brellier et al., 2012b), tenascin-W might represent an additional tumor antigen that could be used as target for antibody-based therapies.

Diverse pro-tumorigenic activities have been attributed to tenascin-W in the tumor stroma. Hence, specifically knocking-down tenascin-W via RNA interference approaches in tumors

could interfere with various crucial stages during the malignant progression and could be beneficial for cancer patients. In this regard, it is noteworthy that such strategies are being developed for tenascin-C. Tenascin-C expression was successfully targeted in aggressive brain tumors with a double stranded RNA homologous to tenascin-C triggering its degradation. Glioma patients treated with such an approach benefited from a better quality of life as well from an increase in overall survival. However, the treatment only provided a very short survival advantage (Wyszko et al., 2008).

CONCLUSION AND FUTURE DIRECTIONS

Since its discovery in zebrafish 21 years ago (Weber et al., 1998), we have gained significant insight into the structure, evolution, function, and expression of tenascin-W, the final member of the tenascin family. Tenascin-W appears to have evolved together with bone, and a phylogenetically conserved site of tenascin-W expression is at sites of osteogenesis. Tenascin-W is also part of certain adult stem cell niches and is prominent in tumor stroma. In contrast to tenascin-C, tenascin-W is generally absent from normal adult tissue. Cell cultures studies reveal that tenascin-W is an adhesion modulatory protein that can promote bone development, angiogenesis, cell adhesion and cell migration. These observations may be related to the widespread expression of tenascin-W in solid tumors, where tenascin-W may also promote angiogenesis, cell adhesion and cell migration. Whether or not this information will lead to the development of novel cancer diagnosis opportunities or even intervention therapies remains speculative at this point. To make use of tenascin-W as a potential therapeutic entry point we first need to greatly advance our understanding about the impact of the tumor microenvironment on disease progression and about the complexity and multi-functionality of tenascin-W. Compared with tenascin-C, relatively little is known about tenascin-W, but there are some clear directions for future research. The tenascin-W promoter, for example, still needs serious attention. In addition, while the adhesion modulatory properties of tenascin-C have been described in detail, the molecular mechanisms of how tenascin-W affects adhesion remain elusive. For instance, is tenascin-W able to bind to fibronectin, which would be similar to tenascin-C, and which integrins and signaling pathways are involved in regulating the adhesion-modulating characteristics of tenascin-W? Surprisingly, no one has published a characterization of the tenascin-W knockout mouse. This may be partly due to the legacy of the tenascin-C knockout mouse, which was notorious for having a "null phenotype" and the possibility that tenascin-C and tenascin-W might compensate for each other's absence in certain tissues. However, more detailed studies of the tenascin-C knockout mouse revealed significant defects in behavior that are likely related to abnormal neural stem cell niches, as well as other phenotypes related to abnormal responses to trauma and inflammation. Similarly, detailed studies of the tenascin-W knockout mouse may also prove fruitful.

AUTHOR CONTRIBUTIONS

RT wrote the first draft of the Sections "Introduction," "Tenascin-W Basics," and "The Cell Biology of Tenascin-W," and prepared the **Figures 1**, **2**. MD wrote the first draft of Sections "Tenascin-W in Cancer," "Potential Translational Use of Tenascin-W," and "Conclusion," and prepared the **Figures 3**, **4**. Both authors contributed to the final draft and figures.

FUNDING

Some funding for open access publication fees can be paid for by the Library of the University of California.

SUPPLEMENTARY MATERIAL

The Supplementary Material for this article can be found online at: https://www.frontiersin.org/articles/10.3389/fcell.2019.00053/full#supplementary-material

REFERENCES

Adams, J. C., Chiquet-Ehrismann, R., and Tucker, R. P. (2015). The evolution of tenascins and fibronectin. *Cell Adh. Migr.* 9, 22–33. doi: 10.4161/19336918.2014.970030

Amoh, Y., Li, L., Katsuoka, K., and Hoffman, R. M. (2010). Embryonic development of hair follicle pluripotent stem (hfPS) cells. *Med. Mol. Morphol.* 43, 123–127. doi: 10.1007/s00795-010-0498-z

Brellier, F., Martina, E., Chiquet, M., Ferralli, J., Van Der Heyden, M., Orend, G., et al. (2012a). The adhesion modulating properties of tenascin-W. *Int. J. Biol. Sci.* 8, 187–194.

Brellier, F., Martina, E., Degen, M., Heuze-Vourc'h, N., Petit, A., Kryza, T., et al. (2012b). Tenascin-W is a better cancer biomarker than tenascin-C for most human solid tumors. *BMC Clin. Pathol.* 12:14. doi: 10.1186/1472-6890-12-14

Brellier, F., Tucker, R. P., and Chiquet-Ehrismann, R. (2009). Tenascins and their implications in diseases and tissue mechanics. *Scand. J. Med. Sci. Sports* 19, 511–519. doi: 10.1111/j.1600-0838.2009.00916.x

Castro-Muñozledo, F. (2013). Review: corneal epithelial stem cells, their niche and wound healing. *Mol. Vis.* 19, 1600–1613.

Catania, C., Maur, M., Berardi, R., Rocca, A., Giacomo, A. M., Spitaleri, G., et al. (2015). The tumor-targeting immunocytokine F16-IL2 in combination with doxorubicin: dose escalation in patients with advanced solid tumors and expansion into patients with metastatic breast cancer. *Cell Adh. Migr.* 9, 14–21. doi: 10.4161/19336918.2014.983785

Chiovaro, F., Chiquet-Ehrismann, R., and Chiquet, M. (2015a). Transcriptional regulation of tenascin genes. *Cell Adh. Migr.* 9, 34–47. doi: 10.1080/19336918.2015.1008333

Chiovaro, F., Martina, E., Bottos, A., Scherberich, A., Hynes, N. E., and Chiquet-Ehrismann, R. (2015b). Transcriptional regulation of tenascin-W by TGF-beta signaling in the bone metastatic niche of breast cancer cells. *Int. J. Cancer* 137, 1842–1854. doi: 10.1002/ijc.29565

Chiquet-Ehrismann, R., Orend, G., Chiquet, M., Tucker, R. P., and Midwood, K. S. (2014). Tenascins in stem cell niches. *Matrix Biol.* 37, 112–123. doi: 10.1016/j.matbio.2014.01.007

Chiquet-Ehrismann, R., and Tucker, R. P. (2011). Tenascins and the importance of adhesion modulation. *Cold Spring Harb. Perspect. Biol.* 3:a004960. doi: 10.1101/cshperspect.a004960

d'Amaro, R., Scheidegger, R., Blumer, S., Pazera, P., Katsaros, C., Graf, D., et al. (2012). Putative functions of extracellular matrix glycoproteins in secondary palate morphogenesis. *Front. Physiol.* 3:377. doi: 10.3389/fphys.2012.00377

Degen, M., Brellier, F., Kain, R., Ruiz, C., Terracciano, L., Orend, G., et al. (2007). Tenascin-W is a novel marker for activated tumor stroma in low-grade human breast cancer and influences cell behavior. *Cancer Res.* 67, 9169–9179. doi: 10.1158/0008-5472.CAN-07-0666

Degen, M., Brellier, F., Schenk, S., Driscoll, R., Zaman, K., Stupp, R., et al. (2008). Tenascin-W, a new marker of cancer stroma, is elevated in sera of colon and breast cancer patients. *Int. J. Cancer* 122, 2454–2461. doi: 10.1002/ijc.23417

Dzyubenko, E., Gottschling, C., and Faissner, A. (2016). Neuron-glia interactions in neural plasticity: contributions of neural extracellular matrix and perineuronal nets. *Neural Plast.* 2016:5214961. doi: 10.1155/2016/5214961

Engleka, K. A., Manderfield, L. J., Brust, R. D., Li, L., Cohen, A., Dymecki, S. M., et al. (2012). Islet1 derivatives in the heart are of both neural crest and second heart field origin. *Circ. Res.* 110, 922–926. doi: 10.1161/CIRCRESAHA.112.266510

Fischer, M. D., Budak, M. T., Bakay, M., Gorospe, J. R., Kjellgren, D., Pedrosa-Domellöf, F., et al. (2005). Definition of the unique human extraocular muscle allotype by expression profiling. *Physiol. Genomics* 22, 283–291. doi: 10.1152/physiolgenomics.00158.2004

Fujimoto, M., Shiba, M., Kawakita, F., Liu, L., Nakasaki, A., Shimojo, N., et al. (2016). Epidermal growth factor-like repeats of tenascin-C-induced constriction of cerebral arteries via activation of epidermal growth factor receptors in rats. *Brain Res.* 1642, 436–444. doi: 10.1016/j.brainres.2016.04.034

Hendaoui, I., Tucker, R. P., Zingg, D., Bichet, S., Schittny, J., and Chiquet-Ehrismann, R. (2014). Tenascin-C is required for normal Wnt/β-catenin signaling in the whisker follicle stem cell niche. *Matrix Biol.* 40, 46–53. doi: 10.1016/j.matbio.2014.08.017

Kimura, H., Akiyama, H., Nakamura, T., and De Crombrugghe, B. (2007). Tenascin-W inhibits proliferation and differentiation of preosteoblasts during endochondral bone formation. *Biochem. Biophys. Res. Commun.* 356, 935–941. doi: 10.1016/j.bbrc.2007.03.071

Martina, E., Degen, M., Ruegg, C., Merlo, A., Lino, M. M., Chiquet-Ehrismann, R., et al. (2010). Tenascin-W is a specific marker of glioma-associated blood vessels and stimulates angiogenesis in vitro. *FASEB J.* 24, 778–787. doi: 10.1096/fj.09-140491

Meloty-Kapella, C. V., Degen, M., Chiquet-Ehrismann, R., and Tucker, R. P. (2006). Avian tenascin-W: expression in smooth muscle and bone, and effects on calvarial cell spreading and adhesion in vitro. *Dev. Dyn.* 235, 1532–1542. doi: 10.1002/dvdy.20731

Meloty-Kapella, C. V., Degen, M., Chiquet-Ehrismann, R., and Tucker, R. P. (2008). Effects of tenascin-W on osteoblasts in vitro. *Cell Tissue Res.* 334, 445–455. doi: 10.1007/s00441-008-0715-4

Midwood, K. S., Chiquet, M., Tucker, R. P., and Orend, G. (2016). Tenascin-C at a glance. *J. Cell Sci.* 129, 4321–4327. doi: 10.1242/jcs.190546

Neidhardt, J., Fehr, S., Kutsche, M., Löhler, J., and Schachner, M. (2003). Tenascin-N: characterization of a novel member of the tenascin family that mediates neurite repulsion from hippocampal explants. *Mol. Cell. Neurosci.* 23, 193–209. doi: 10.1016/S1044-7431(03)00012-5

Orend, G., and Chiquet-Ehrismann, R. (2006). Tenascin-C induced signaling in cancer. *Cancer Lett.* 244, 143–163. doi: 10.1016/j.canlet.2006.02.017

Oskarsson, T., Acharyya, S., Zhang, X. H., Vanharanta, S., Tavazoie, S. F., Morris, P. G., et al. (2011). Breast cancer cells produce tenascin C as a metastatic niche component to colonize the lungs. *Nat. Med.* 17, 867–874. doi: 10.1038/nm.2379

Özbek, S., Balasubramanian, P. G., Chiquet-Ehrismann, R., Tucker, R. P., and Adams, J. C. (2010). The evolution of extracellular matrix. *Mol. Biol. Cell* 21, 4300–4305. doi: 10.1091/mbc.E10-03-0251

Scherberich, A., Tucker, R. P., Degen, M., Brown-Luedi, M., Andres, A. C., and Chiquet-Ehrismann, R. (2005). Tenascin-W is found in malignant mammary tumors, promotes alpha8 integrin-dependent motility and requires p38MAPK activity for BMP-2 and TNF-alpha induced expression in vitro. *Oncogene* 24, 1525–1532. doi: 10.1038/sj.onc.1208342

Scherberich, A., Tucker, R. P., Samandari, E., Brown-Luedi, M., Martin, D., and Chiquet-Ehrismann, R. (2004). Murine tenascin-W: a novel mammalian tenascin expressed in kidney and at sites of bone and smooth muscle development. *J. Cell Sci.* 117, 571–581. doi: 10.1242/jcs.00867

Schroeder, T. M., Nair, A. K., Staggs, R., Lamblin, A. F., and Westendorf, J. J. (2007). Gene profile analysis of osteoblast genes differentially regulated by histone deacetylase inhibitors. *BMC Genomics* 8:362. doi: 10.1186/1471-2164-8-362

Sieber-Blum, M., and Hu, Y. (2008). Mouse epidermal neural crest stem cell (EPI-NCSC) cultures. *J. Vis. Exp.* 15:772. doi: 10.3791/772

Sivasankaran, B., Degen, M., Ghaffari, A., Hegi, M. E., Hamou, M. F., Ionescu, M. C., et al. (2009). Tenascin-C is a novel RBPJkappa-induced target gene for Notch signaling in gliomas. *Cancer Res.* 69, 458–465. doi: 10.1158/0008-5472.CAN-08-2610

Sun, J. X., Horst, O. V., Bumgarner, R., Lakely, B., Somerman, M. J., and Zhang, H. (2012). Laser capture microdissection enables cellular and molecular studies of tooth root development. *Int. J. Oral Sci.* 4, 7–13. doi: 10.1038/ijos.2012.15

Swindle, C. S., Tran, K. T., Johnson, T. D., Banerjee, P., Mayes, A. M., Griffith, L., et al. (2001). Epidermal growth factor (EGF)-like repeats of human tenascin-C as ligands for EGF receptor. *J. Cell Biol.* 154, 459–468. doi: 10.1083/jcb.200103103

Tucker, R. P., and Chiquet-Ehrismann, R. (2009a). Evidence for the evolution of tenascin and fibronectin early in the chordate lineage. *Int. J. Biochem. Cell Biol.* 41, 424–434. doi: 10.1016/j.biocel.2008.08.003

Tucker, R. P., and Chiquet-Ehrismann, R. (2009b). The regulation of tenascin expression by tissue microenvironments. *Biochim. Biophys. Acta* 1793, 888–892. doi: 10.1016/j.bbamcr.2008.12.012

Tucker, R. P., Drabikowski, K., Hess, J. F., Ferralli, J., Chiquet-Ehrismann, R., and Adams, J. C. (2006). Phylogenetic analysis of the tenascin gene family: evidence of origin early in the chordate lineage. *BMC Evol. Biol.* 6:60. doi: 10.1186/1471-2148-6-60

Tucker, R. P., Ferralli, J., Schittny, J. C., and Chiquet-Ehrismann, R. (2013). Tenascin-C and tenascin-W in whisker follicle stem cell niches: possible roles in regulating stem cell proliferation and migration. *J. Cell Sci.* 126, 5111–5115. doi: 10.1242/jcs.134650

Tucker, R. P., Peterson, C. A., Hendaoui, I., Bichet, S., and Chiquet-Ehrismann, R. (2016). The expression of tenascin-C and tenascin-W in human ossicles. *J. Anat.* 229, 416–421. doi: 10.1111/joa.12496

Valcourt, U., Alcaraz, L. B., Exposito, J. Y., Lethias, C., and Bartholin, L. (2015). Tenascin-X: beyond the architectural function. *Cell Adh. Migr.* 9, 154–165. doi: 10.4161/19336918.2014.994893

Weber, P., Montag, D., Schachner, M., and Bernhardt, R. R. (1998). Zebrafish tenascin-W, a new member of the tenascin family. *J. Neurobiol.* 35, 1–16. doi: 10.1002/(SICI)1097-4695(199804)35:1<1::AID-NEU1>3.0.CO;2-9

Wyszko, E., Rolle, K., Nowak, S., Zukiel, R., Nowak, M., Piestrzeniewicz, R., et al. (2008). A multivariate analysis of patients with brain tumors treated with ATN-RNA. *Acta Pol. Pharm.* 65, 677–684.

Zuliani-Alvarez, L., Marzeda, A. M., Deligne, C., Schwenzer, A., McCann, F. E., Marsden, B. D., et al. (2017). Mapping tenascin-C interaction with toll-like receptor 4 reveals a new subset of endogenous inflammatory triggers. *Nat. Commun.* 8:1595. doi: 10.1038/s41467-017-01718-7

Conflict of Interest Statement: The authors declare that the research was conducted in the absence of any commercial or financial relationships that could be construed as a potential conflict of interest.

frontiers in Cell and Developmental Biology

REVIEW
published: 26 April 2019
doi: 10.3389/fcell.2019.00063

Acellular Extracellular Matrix Bioscaffolds for Cardiac Repair and Regeneration

*Simranjit S. Pattar, Ali Fatehi Hassanabad and Paul W. M. Fedak**

Section of Cardiac Surgery, Department of Cardiac Science, Cumming School of Medicine, Libin Cardiovascular Institute of Alberta, University of Calgary, Calgary, AB, Canada

Heart failure is a progressive deterioration of cardiac pump function over time and is often a manifestation of ischemic injury caused by myocardial infarction (MI). Post-MI, structural remodeling of the infarcted myocardium ensues. Dysregulation of extracellular matrix (ECM) homeostasis is a hallmark of structural cardiac remodeling and is largely driven by cardiac fibroblast activation. While initially adaptive, structural cardiac remodeling leads to irreversible heart failure due to the progressive loss of cardiac function. Loss of pump function is associated with myocardial fibrosis, wall thinning, and left ventricular (LV) dilatation. Surgical revascularization of the damaged myocardium via coronary artery bypass graft (CABG) surgery and/or percutaneous coronary intervention (PCI) can enhance myocardial perfusion and is beneficial. However, these interventions alone are unable to prevent progressive fibrotic remodeling and loss of heart function that leads to clinical end-stage heart failure. Acellular biologic ECM scaffolds can be surgically implanted onto injured myocardial regions during open-heart surgery as an adjunct therapy to surgical revascularization. This presents a novel therapeutic approach to alter maladaptive remodeling and promote functional recovery. Acellular ECM bioscaffolds have been shown to provide passive structural support to the damaged myocardium and also to act as a dynamic bioactive reservoir capable of promoting endogenous mechanisms of tissue repair, such as vasculogenesis. The composition and structure of xenogenic acellular ECM bioscaffolds are determined by the physiological requirements of the tissue from which they are derived. The capacity of different tissue-derived acellular bioscaffolds to attenuate cardiac remodeling and restore ECM homeostasis after injury may depend on such properties. Accordingly, the search and discovery of an optimal ECM bioscaffold for use in cardiac repair is warranted and may be facilitated by comparing bioscaffolds. This review will provide a summary of the acellular ECM bioscaffolds currently available for use in cardiac surgery with a focus on how they attenuate cardiac remodeling by providing the necessary environmental cues to promote endogenous mechanisms of tissue repair.

Keywords: extracellular matrix, myocardial infarction, heart failure, cardiac surgery, bio-scaffold, biomaterials, surgical revascularization, cardiac fibroblast

OPEN ACCESS

Edited by:
Charles D. Little, University of Kansas Medical Center, United States

Reviewed by:
Sigrid A. Langhans, Nemours/Alfred I. duPont Hospital for Children, United States
Namrata Gundiah, Indian Institute of Science (IISc), India

***Correspondence:**
Paul W. M. Fedak
paul.fedak@gmail.com

Specialty section:
This article was submitted to Cell Adhesion and Migration, a section of the journal Frontiers in Cell and Developmental Biology

Received: *16 November 2018*
Accepted: *08 April 2019*
Published: *26 April 2019*

Citation:
Pattar SS, Fatehi Hassanabad A and Fedak PWM (2019) Acellular Extracellular Matrix Bioscaffolds for Cardiac Repair and Regeneration. Front. Cell Dev. Biol. 7:63. doi: 10.3389/fcell.2019.00063

INTRODUCTION TO HEART FAILURE

According to the American Heart Association (AHA), the prevalence of congestive heart failure (CHF) is expected to increase by 46% from 2012 to 2030 with a staggering 960,000 new CHF cases reported annually (Benjamin et al., 2017). CHF is a progressive condition in which cardiac pump function deteriorates over time. Heart failure is often a manifestation of an ischemic injury to the heart caused by myocardial infarction (MI) (Velagaleti et al., 2008). Following an MI, structural remodeling of the infarcted myocardium ensues (Sutton and Sharpe, 2000; Fedak et al., 2005a,b). Initially, structural cardiac remodeling is adaptive, with the aim of preventing ventricular free wall rupture. However, prolonged structural cardiac remodeling leads to irreversible heart failure due to the progressive loss of cardiac function (Fedak et al., 2005a,b). Heart function deterioration results from myocardial fibrosis, wall thinning, and left ventricular (LV) dilatation (Fedak et al., 2005a,b; Fraccarollo et al., 2012; Xie et al., 2013).

HEART FAILURE MANAGEMENT AND BIOSCAFFOLDS

There are a plethora of pharmacological interventions, including antianginal medications such as beta blockers, which may be employed to improve the symptoms and prognosis of heart failure patients. However, pharmacotherapy alone is unable to elicit functional recovery of the infarcted myocardium (McDonald et al., 2017; Patel et al., 2017). Revascularization of the infarcted myocardium is currently achieved either through coronary artery bypass graft (CABG) surgery and/or percutaneous coronary intervention (PCI). While these approaches are indicated for improving morbidity and mortality, they are unable to prevent progressive cardiac fibrosis and structural remodeling which leads to end-stage heart failure (McDonald et al., 2017). CREDO-Kyoto (Coronary REvascularization Demonstrating Outcome Study in Kyoto) is a three-year outcome study of the PCI/CABG Registry Cohort. It revealed that of 392 patients undergoing CABG 12% were readmitted for heart failure and 4% required repeat revascularization. Similarly, of 672 patients undergoing PCI 22% were readmitted for heart failure and 19% required repeat revascularization (Marui et al., 2014).

In the past, the field of cardiovascular tissue engineering has focused on leveraging a stem cell-based or gene therapy-based approach as a solution to restoring cardiac function post-MI. However, the road to clinical translation of these approaches has largely been fraught with challenges, specifically uncertainty regarding clinical efficacy and feasibility (Balsam et al., 2004; Murry et al., 2004; Gyöngyösi et al., 2015; Kaiser, 2018; Reardon, 2018). Acellular extracellular matrix (ECM) bioscaffolds are a new and innovative solution being investigated as an adjunct therapy to the surgical revascularization of damaged myocardium (Mewhort et al., 2014, 2016b, 2017; Park et al., 2017; Svystonyuk et al., 2018). These acellular ECM bioscaffolds may hold the key to unlocking the potential of endogenous mechanisms of tissue repair and regeneration at the site of an MI. By providing the necessary environmental cues, the ultimate aim of acellular ECM bioscaffold therapy is to promote functional recovery of the damaged myocardium. In this review, we provide a summary of the acellular ECM bioscaffolds currently used and in development for use in cardiac surgery. Better understanding of this promising therapeutic strategy may facilitate its transition into clinical practice.

THE CENTRAL ROLE OF THE CARDIAC FIBROBLAST

Our research group is particularly interested in the central role that the cardiac fibroblast plays in maladaptive structural cardiac remodeling and the progression of cardiac fibrosis (Mewhort et al., 2014, 2016a,b, 2017; Svystonyuk et al., 2015, 2018; Teng et al., 2015; Park et al., 2017). As one of the predominant non-cardiomyocyte cell types that comprise the heart, cardiac fibroblasts contribute to the structural, mechanical, biochemical, and electrical properties of the heart (Camelliti et al., 2005; Souders et al., 2009). By responding to changes in the microenvironment, cardiac fibroblasts play a key role in maintaining ECM homeostasis via directly altering the synthesis and degradation of the cardiac ECM components (Fedak et al., 2005a,b; Krenning et al., 2010; Fan et al., 2012). The maintenance and regulation of the ECM is essential as it forms a structural network that supports and interconnects the cardiac cells. Further, the biochemical role of cardiac fibroblasts further impacts cardiac function as they secrete a diverse array of growth factors and ECM-regulatory proteins (Fedak et al., 2005a,b). For instance, angiogenesis is in part driven by a paracrine interaction amongst cardiac fibroblasts and neighboring endothelial cells which is mediated through fibroblast growth factor-2 (FGF-2) and vascular endothelial growth factor (VEGF) (Zhao and Eghbali-Webb, 2001). Finally, cardiac fibroblasts also play a role in establishing the normal electrophysiology of the heart. The electrical coupling of cardiac fibroblasts to cardiomyocytes via gap junction channel proteins connexin-43 and connexin-45 has been characterized *in-vitro* (Camelliti et al., 2004; Mahoney et al., 2016). In the event of ischemic injury and the resulting disruption of the local microenvironment of the infarcted myocardium, cardiac fibroblasts become activated to a myofibroblast state (Baum and Duffy, 2011; Dixon and Wigle, 2015; **Figure 1**). Myofibroblast activity drives maladaptive structural cardiac remodeling and fibrosis through dysregulation of ECM homeostasis and disruption of the local bioactive milieu, including growth factors and cytokines (Fedak et al., 2005a,b; Krenning et al., 2010; Dixon and Wigle, 2015).

MYOFIBROBLAST-MEDIATED EXTRACELLULAR MATRIX REMODELING

Specifically, the infarcted myocardium undergoes a three-stage wound healing process: (1) inflammatory stage, (2) proliferative

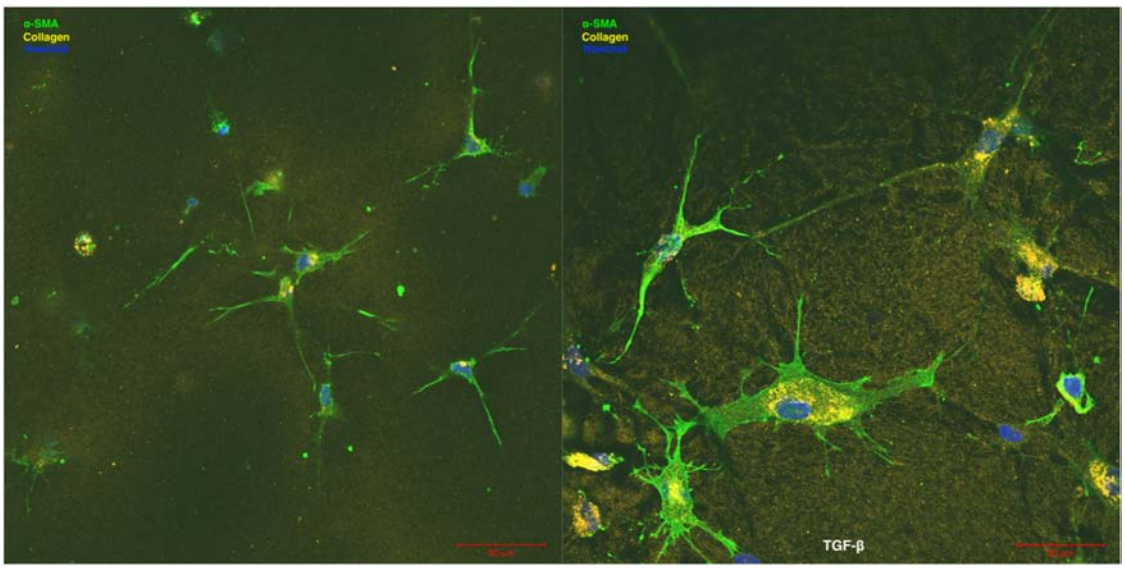

FIGURE 1 | Human cardiac fibroblast (left) compared to TGF-β activated human cardiac myofibroblasts (right). Myofibroblasts are larger in cell size, have an increased number of cell extensions, and increased cell extension length. Alpha smooth muscle actin (α-SMA) expression and collagen production and deposition (collagen, yellow) are both increased in human cardiac myofibroblasts compared to human cardiac fibroblasts. Hoechst staining is used to visualize cell nuclei (nuclei, blue). Images were provided courtesy of Dr. Guoqi Teng, University of Calgary.

stage, and (3) maturation stage (**Figure 2**). Initially, the inflammatory stage is characterized by cardiomyocyte and endothelial cell death, immune cell recruitment, and an increase in pro-inflammatory cytokines (Dobaczewski et al., 2010b; Shinde and Frangogiannis, 2014; Saxena and Frangogiannis, 2015). During this stage, cardiac fibroblasts assume a pro-inflammatory phenotype and contribute to inflammation via the production of various cytokines (IL-1α, IL-1β, IL-6, IL-8, and TNF-α) (Kawaguchi et al., 2011; Fan et al., 2012; Shinde and Frangogiannis, 2014). Next, the proliferative stage is marked by cardiac fibroblast differentiation to a myofibroblast phenotype and migration to the region of infarcted myocardium (Shinde and Frangogiannis, 2014; **Figure 2**). This shift may be driven by an upregulation in transforming growth factor beta (TGF-β), ED-A fibronectin, and mechanical stress (Serini et al., 1998; Lee et al., 1999; Vaughan et al., 2000; Tomasek et al., 2002; Zhao et al., 2007; Dobaczewski et al., 2010a; Shinde and Frangogiannis, 2014; **Figure 1**). Myofibroblasts are characterized by increased alpha-smooth muscle actin (α-SMA) expression (**Figure 1**), which corresponds with increased contractility and manipulation of the surrounding ECM environment (Leslie et al., 1991; Arora and McCulloch, 1994; Hinz et al., 2001). Myofibroblasts also display altered matrix metalloproteinase (MMP) and tissue inhibitors of matrix metalloproteinases (TIMPs) production (Fedak et al., 2005b). The altered expression of these ECM-regulatory proteins results in the net deposition of type I collagen, along with other ECM proteins (Brown et al., 2005; Heymans et al., 2005). Finally, the purpose of the maturation stage is scar tissue formation, wherein increased ECM deposition is necessary to form a collagenous scar and to prevent ventricular free wall rupture at the site of MI (Camelliti et al., 2005; Souders et al., 2009; **Figure 2**). It is in this reparative manner that myofibroblast activity and structural cardiac remodeling is initially adaptive.

However, persistent myofibroblast activation eventually leads to maladaptive scar thickening and expansion the result of which is mechanical stiffness, systolic and diastolic dysfunction, and progressive cardiac fibrosis (**Figure 2**). Regional and temporal changes in myocardial contractility following ischemic injury to the heart allow the local region of MI to be differentiated from the surrounding border zone and the remote unaffected myocardial tissue (Jackson et al., 2002; Park et al., 2006; Shimkunas et al., 2013; Arunachalam et al., 2018; Torres et al., 2018). In particular, the border zone is a normally perfused region of hypocontractility, where contractility has been shown to be reduced by 50% compared to that of the remoted unaffected zone *in-vivo,* and plays a central role in infarct expansion (Jackson et al., 2002; Blom et al., 2007; Shimkunas et al., 2011; Richardson and Holmes, 2015). Overall, the systolic and diastolic dysfunction that arises due to disrupted myocardial contractility contributes to poor cardiac pump function and may lead to clinical end-stage heart failure. Characterization of cardiac tissue obtained from patients undergoing heart transplantation as a result of clinical end-stage heart failure reveals a 36% reduction in the number of LV cardiomyocytes and a concomitant 28% increase in collagen content within this region (Beltrami et al., 1994). Furthermore, LV chamber volume is increased 4.6-fold, in conjunction with a 56% reduction in LV mass-to-chamber volume ratio (Beltrami et al., 1994).

While activation of the cardiac fibroblast to a myofibroblast state is central to the dysregulation of the cardiac ECM and the structural cardiac remodeling that ensues, it is important to note that these cells do not function in isolation. Cardiomyocytes,

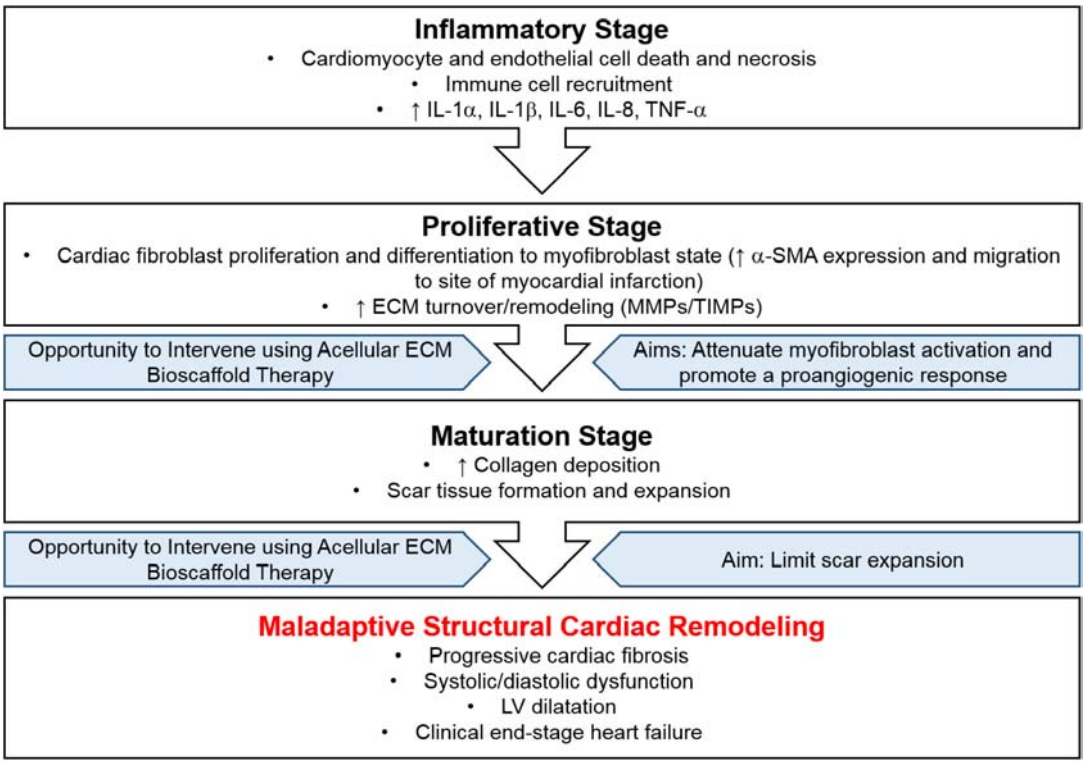

FIGURE 2 | Disease progression following myocardial infarction. The infarcted myocardium undergoes a three-stage wound healing process, (1) inflammatory stage, (2) proliferative stage, and (3) maturation stage, resulting in maladaptive structural cardiac remodeling. Intervention using acellular ECM bioscaffold therapy may be used to attenuate myofibroblast activation, promote a proangiogenic response, and limit scar expansion.

endothelial cells, and immune cells also play an important role in determining the structural, mechanical, biochemical, and electrical properties of the heart. However, as sentinel cells of the cardiac ECM, cardiac fibroblasts respond to a plethora of stimuli and modulate the function of the surrounding cardiac cells (Baudino et al., 2006; Souders et al., 2009; Saxena and Frangogiannis, 2015). Therefore, therapeutic solutions aimed at attenuating maladaptive structural cardiac remodeling should first focus on myofibroblast-mediated ECM remodeling.

ACELLULAR EXTRACELLULAR MATRIX BIOSCAFFOLDS AS A THERAPEUTIC SOLUTION

The ability to restore an optimal ECM microenvironment presents a therapeutic opportunity by which maladaptive structural cardiac remodeling may be influenced. Acellular ECM bioscaffolds can be leveraged to provide the necessary environmental cues to attenuate cardiac fibroblast activation, thereby preventing excessive infarct-derived scar expansion and thickening. These bioscaffolds may also promote endogenous mechanisms of repair and regeneration, such as angiogenesis or vasculogenesis, by way of their bioinductive properties (Mewhort et al., 2014, 2016b, 2017; Park et al., 2017; Svystonyuk et al., 2018). While an array of synthetic scaffold materials are also in development, this review will focus on acellular biologic ECM scaffolds used or in development for use in cardiac surgery post ischemic injury. The composition and structure of acellular ECM bioscaffolds are a function of the physiological requirements of the tissue from which they are derived. As the healthy cardiac ECM microenvironment is a complex milieu of ECM components, cardiac cells, growth factors, cytokines, and matricellular proteins, it stands to reason that a biologic ECM scaffold may provide additional benefits as it best approximates this complex and diverse ECM microenvironment.

Acellular ECM bioscaffolds may be differentiated by, (1) the tissue source from which they are derived, and (2) the fixation method, or lack thereof, implemented in processing the ECM bioscaffold (**Table 1**). Acellular porcine-derived small intestine submucosa (SIS) ECM and acellular bovine-derived pericardium (BP) ECM bioscaffolds have been the focal point of clinical investigations for use in cardiac surgery. Notably, while proprietary techniques of glutaraldehyde fixation are most commonly utilized for the fixation or cross-linking of most bioscaffolds, CorMatrix® is non-crosslinked (non-fixed) and PhotoFix™ is cross-linked using dye-mediated photo-oxidation (**Table 1**). Further, while the methods and intricacies regarding the decellularization of these bioscaffolds are beyond the scope of this review, many patented techniques exist to obtain an acellular ECM bioscaffold. The goal of decellularization is to achieve an acellular tissue-derived ECM bioscaffold from which

TABLE 1 | Partial list of commercially available ECM bioscaffolds for potential use in cardiac repair and regeneration.

Bioscaffold Product	Company	Donor Source	Tissue Source	Fixation Method
AltiPly®	Aziyo Biologics, Inc.	Human	Placental	Natural
CardioCel	Admedus Ltd.	Bovine	Pericardium	ADAPT®, glutaraldehyde-based
CorMatrix®	CorMatrix Cardiovascular, Inc.	Porcine	Small intestinal submucosa (SIS)	Natural
Edwards Pericardial Patch	Edwards Lifesciences Corp.	Bovine	Pericardium	XenoLogiX™, glutaraldehyde-based
Matrix Patch™	Auto Tissue Berlin GmbH	Equine	Pericardium	–
Miroderm®	Miromatrix Medical, Inc.	Porcine	Liver	Natural
No-React® Pericardial Patch	BioIntegral Surgical, Inc.	Bovine	Pericardium	No-React®, glutaraldehyde-based
NuShield®	Organogenesis, Inc.	Human	Placenta	–
Peri-Guard®	Synovis Life Technologies, Inc.	Bovine	Pericardium	Glutaraldehyde-based
PhotoFix™	Cryolife, Inc.	Bovine	Pericardium	Dye-mediated photo-oxidation
SJM™ Pericardial Patch	St. Jude Medical, Inc.	Bovine	Pericardium	EnCap™, glutaraldehyde-based
Tyke®	Aziyo Biologics, Inc.	Porcine	Small intestinal submucosa (SIS)	Natural
Vascutek Pericardial Patch	Vascutek Ltd.	Porcine	Pericardium	Glutaraldehyde-based
XenoSure®	LeMaitre® Vascular	Bovine	Pericardium	Glutaraldehyde-based

–, information not available.

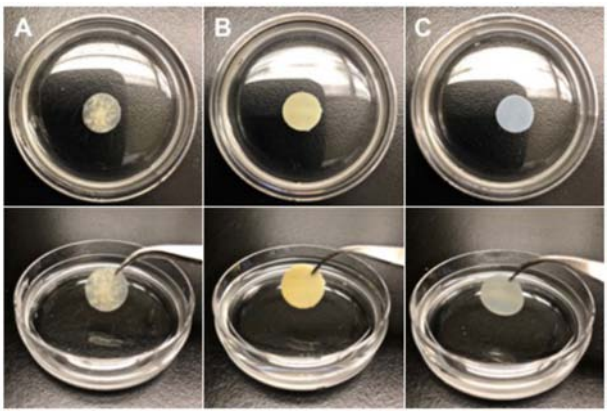

FIGURE 3 | Representative images of three acellular extracellular matrix bioscaffolds (1.2 × 1.2 cm cut-outs). **(A)** CorMatrix® (CorMatrix Cardiovascular, Inc., United States) porcine small intestine submucosa (SIS), natural, rehydrated in saline solution **(B)** Peri-Guard® (Synovis Life Technologies, Inc., United States) bovine pericardium, glutaraldehyde cross-linked, and **(C)** PhotoFix™ (Cryolife, Inc., United States) bovine pericardium, dye-mediated photo-oxidation cross-linked.

the antigenic epitopes associated with cell membranes and intracellular components have been removed; this minimizes the possibility of an adverse immunogenic response by recipients of the bioscaffold (Badylak et al., 2015).

ACELLULAR SMALL INTESTINE SUBMUCOSA DERIVED BIOSCAFFOLDS

Our research group has extensively characterized the therapeutic benefit of CorMatrix® - SIS-ECM (CorMatrix Cardiovascular, Inc., United States) for cardiac repair (**Figure 3A**). As the small intestine is a highly vascularized organ, it is unsurprising that SIS-ECM has been shown to contain essential proangiogenic growth factors, including FGF-2, VEGF, and HGF (Badylak, 2002; Mewhort et al., 2017). *In-vitro* characterization using human cardiac fibroblasts has demonstrated that CorMatrix® promotes an enhanced FGF-2 dependent cell-mediated proangiogenic response (Mewhort et al., 2017). Further, CorMatrix® enhances new blood vessel assembly both *in-vitro* using human umbilical vein endothelial cells (HUVEC) and *in-vivo* using a rat MI model (Mewhort et al., 2017). Using both a rat MI model and a pre-clinical porcine model of coronary ischemia-reperfusion, our research group has also shown that infarct repair using CorMatrix® attenuates myocardial infarct expansion and elicits functional recovery (Mewhort et al., 2016b, 2017). Specifically, surgical implantation of CorMatrix® sized to the area of infarcted myocardium displayed an improvement in ejection fraction and a trend toward improved LV compliance compared to sham, as measured by end-diastolic pressure-volume relationship (EDPVR) (Mewhort et al., 2017).

A recent systematic review of the initial preclinical and clinical findings of CorMatrix® highlights the therapeutic potential of CorMatrix®, but also underscores the need for further elucidation of its specific surgical indications (Mosala Nezhad et al., 2016). For instance, a prospective multicenter clinical study, including 103 patients that received CorMatrix® implants (38 – valve repair; 16 – septal reconstruction; 71 – arterial plasty; and 7 – other use), found no detectable calcification of the bioscaffold in patients at reoperation, follow-up imaging, or medium-term histological analysis after explanation (Padalino et al., 2015). As calcification is a primary drawback of glutaraldehyde fixed acellular ECM bioscaffolds, CorMatrix® shows significant promise in overcoming this translational hurdle. However, CorMatrix® has been shown to elicit an inflammatory response particularly in pediatric populations undergoing mitral or aortic valvuloplasties, which may be driven by the presence of the porcine α-gal epitope (Zaidi et al., 2014; Rosario-Quinones et al., 2015). It also remains unclear whether or not the bioscaffold itself is capable of remodeling and integrating into the native

cardiac environment (Zaidi et al., 2014; Padalino et al., 2015). Extracardiac applications or applications in low-mechanical force cardiac environments may be the most suitable surgical indication for CorMatrix® (Mosala Nezhad et al., 2016). There is value in further exploring the clinical potential of CorMatrix®, where more histopathological assessment of explanted bioscaffolds could be particularly beneficial. Our group is presently completing the first-in-man clinical feasibility pilot trial (NCT02887768) where acellular ECM bioscaffold therapy, CorMatrix®, is surgically implanted at the time of CABG surgery.

ACELLULAR PERICARDIUM DERIVED BIOSCAFFOLDS

Bovine-derived pericardium (BP) ECM bioscaffolds have a wide variety of uses in cardiac surgery, including but not limited to pericardial closure, valve repair and replacement, and septal reconstruction. Glutaraldehyde cross-linked BP-ECM bioscaffolds, such as Peri-Guard® (Synovis Life Technologies Inc., United States; **Figure 3B**) offer great utility in cardiac surgery due to their predictable and robust nature (Schmidt and Baier, 2000; Dunn, 2012). However, there are significant challenges associated with glutaraldehyde fixation, including calcification, the presence of an inflammatory reaction, and the cytotoxic nature of glutaraldehyde itself (Golomb et al., 1987; Dunn, 2012; van Steenberghe et al., 2017).

A variety of alternative strategies have emerged to neutralize or remove glutaraldehyde from cross-linked BP-ECM bioscaffolds, or to replace the use of glutaraldehyde entirely. PhotoFix™ (Cryolife Inc., United States; **Figure 3C**), is a BP-ECM bioscaffold that is cross-linked using a proprietary dye-mediated photo-oxidation technique as an alternative to glutaraldehyde cross-linking. PhotoFix™ has been shown to be non-immunogenic and non-calcific when compared to glutaraldehyde cross-linked counterparts *in-vivo,* using rat, rabbit, and sheep models (Bianco et al., 1996; Moore and Phillips, 1997; Moore et al., 1998). In addition, PhotoFix™ demonstrates an ability to integrate into the native cardiac environment by supporting cell adhesion and migration, as evidenced by partial endothelialization two-years post implantation (Bianco et al., 1996; Moore and Phillips, 1997; Moore et al., 1998; Schmidt and Baier, 2000). Recently, a retrospective study including 364 patients, median age 5.3 years (range, < 1 months to 56 years), who received PhotoFix™ implants (insertion site, 149 – right ventricular outflow tract; 168 – pulmonary artery; 21 – valve repair; 81 – septal reconstruction; 16 – superior vena cava reconstruction; 26 – aortic arch; and 29 – other), found that at follow-up 3.2 ± 1.6 years post-implantation there were no deaths related to PhotoFix™ bioscaffold failure (Baird et al., 2016). Moreover, histopathology of explanted PhotoFix™ bioscaffolds revealed in many cases absent or minimal inflammation and calcification (Baird et al., 2016). Currently, the clinical benefits of PhotoFix™ in vascular repair or reconstruction surgery are being explored in the ongoing post-market, prospective evaluation of PHOTO-oxidized Bovine Pericardium in Vascular Surgery (PHOTO-V) clinical trial (NCT03669042). While this study is powered to assess outcomes in patients undergoing vascular repair or reconstruction surgery, it may provide additional insight into the use of PhotoFix™ as an adjunct therapy to the surgical revascularization of infarcted myocardium post MI.

CardioCel® (Admedus Limited, Australia), is a BP-ECM bioscaffold that is cross-linked using a proprietary fixation technique known as ADAPT® (Pavy et al., 2017). Although this technique utilizes glutaraldehyde fixation, it employs a low concentration of glutaraldehyde (0.05%) compared to other clinical standards such as Peri-Guard (0.6%) (Neethling et al., 2018). Additionally, CardioCel® ADAPT® involves an additional detoxification step to remove any traces of glutaraldehyde (Pavy et al., 2017). Recently, *in-vivo* characterization of calcification compared CardioCel® to Peri-Guard®, PhotoFix™, and CorMatrix®, using a juvenile subcutaneous rat model. While a significant difference in calcification was not seen across groups, the extractable calcium level of CardioCel® was similar to that of PhotoFix™, 0.45 and 0.44 μg/mg tissue, respectively, and was lower than Peri-Guard®, 0.85 μg/mg tissue (Neethling et al., 2018). Variable outcomes have been shown *in-vivo;* CardioCel® displayed promising endothelialization and remodeling in the native cardiac ECM environment and resistance to calcification in a chronic juvenile sheep model of pulmonary valve and mitral valve reconstruction (Brizard et al., 2014). However, when used as an implant in the ascending aorta and/or pulmonary artery in a juvenile porcine model CardioCel® displayed poor integration or remodeling in the native ECM cardiac environment and significant calcification (Salameh et al., 2018). Similar trends have been observed in human pediatric patients where histopathological analysis of explanted CardioCel® reveals early graft failure due to calcification and intimal thickening in high pressure areas (aortic arch position) (Pavy et al., 2017). Notably, CardioCel® was well tolerated in lower pressure areas (septal, valvar, and pulmonary artery positions) (Pavy et al., 2017). Given its potential, these results clearly highlight the need for continued investigation of the optimal surgical indications of CardioCel®.

FUTURE DIRECTIONS FOR THE INVESTIGATION OF ACELLULAR EXTRACELLULAR MATRIX BIOSCAFFOLD THERAPY AS AN ADJUNCT TO CABG

As described above, the mechanical environment in which an acellular ECM bioscaffold is employed plays a role in determining its optimal surgical indication. The ideal mechanical properties, such as stiffness or elasticity (Young's modulus), of an acellular ECM bioscaffold for use as an adjunct to CABG remain unknown. For example, Peri-Guard® (mean Young's modulus, 95.67 MPa) exhibits greater stiffness or less elasticity compared to CorMatrix®, PhotoFix™, and CardioCel® (mean Young's modulus, 36.78, 33.50, and 50.21 MPa,

respectively) (Neethling et al., 2018). Further investigation is required to understand whether a more elastic acellular ECM bioscaffold, which may better approximate the native mechanical properties of the heart, is favorable to a less elastic acellular ECM bioscaffold that may provide greater structural support.

Additionally, the influence of acellular ECM bioscaffold therapy on the electrophysiology of the heart must also be considered. While the specific details are beyond the scope of this review, cardiac fibrosis is known to potentiate cardiac arrhythmia (Ten Tusscher and Panfilov, 2007; Pellman et al., 2016;Nguyen et al., 2017). By reducing cardiac fibrosis and improving microvascular perfusion of the infarcted myocardium, acellular ECM bioscaffold therapy may improve electrical conduction post-MI. In the case of CorMatrix®, our group has shown its bioinductive properties are responsible for stimulating endogenous mechanisms of vasculogenesis and functional recovery post-MI (Mewhort et al., 2014, 2016b, 2017). Further, FGF-2 enhanced-CorMatrix® has been shown to improve contractility and exhibit positive electrical conductivity in a porcine model of MI sixty-days after surgical implantation (Tanaka et al., 2015). Clearly, leveraging acellular ECM bioscaffold therapy to improve electrical conductivity in the infarcted myocardium is an important component in determining its utility as an adjunct to CABG.

Beyond those discussed above, there are many other acellular ECM bioscaffolds used or in development for use not only in cardiac surgery, but across a variety of other surgical applications (**Table 1**). In addition to porcine and bovine sources, acellular ECM bioscaffolds may be also be sourced from equine or human donors (**Table 1**). Further, these bioscaffolds may specifically be derived from a variety of other tissue sources including the dermis, liver, and placenta (**Table 1**). Perhaps, as it is a highly regenerative organ, acellular ECM bioscaffolds derived from the liver may retain the native structural and physiological properties necessary to drive pro-reparative mechanisms *in-situ*. Alternatively, as the placenta is a highly vascularized structure, it may be that an acellular ECM bioscaffold derived from placental tissue holds the necessary bioinductive cues to promote neovascularization and integration of the bioscaffold into the native cardiac ECM microenvironment itself. Overall, as the composition and structure of ECM bioscaffolds are a function of the physiological requirements of the tissue from which they are derived, future work should consider the therapeutic potential of these alternative tissue-sources in developing acellular ECM bioscaffolds for use in cardiac surgery.

Ultimately, our research group is interested in investigating the use of acellular ECM bioscaffolds to influence and direct the local cardiac ECM microenvironment at the site of MI. The goal is to leverage this innovative technology to drive endogenous mechanisms of repair, such as angiogenesis or vasculogenesis, and to attenuate the activation of cardiac myofibroblasts. In doing so, the maladaptive structural cardiac remodeling that ensues following ischemic injury to the heart may be better managed. There is a gap in knowledge regarding the application of currently available acellular ECM bioscaffolds as an adjunct at the time of CABG surgery. Similarly, little is known about the ability of these bioscaffolds to influence the dysregulated ECM microenvironment of the damaged myocardium, possibly by way of retained bioactive properties and/or mechanical support. Therefore, there is an opportunity to characterize the potential therapeutic benefits of acellular ECM bioscaffold-based infarct repair.

We describe the varied clinical outcomes of currently available acellular ECM bioscaffolds in various cardiac surgery applications. We believe that initial investigations of the utility of acellular ECM bioscaffolds for infarct repair should begin with rigorous *in-vitro* testing. These studies should be complemented with well-designed pre-clinical investigations, which can be used to assess specific indications of ECM bioscaffolds. Finally, there is a need for larger scale prospective clinical trials to evaluate the possible therapeutic benefits of ECM bioscaffolds.

CONCLUSION

A unique opportunity exists to leverage acellular ECM bioscaffolds for infarct repair. By implementing ECM bioscaffold therapy to modulate the local ECM microenvironment at the site of an MI, we could prevent maladaptive structural cardiac remodeling that often leads to irreversible heart failure. Future investigations should focus on the ability of these bioscaffolds to drive endogenous mechanisms of repair and to attenuate cardiac fibrosis. An ideal acellular ECM bioscaffold for infarct repair will be able to elicit functional recovery of the damaged myocardium. Acellular ECM bioscaffolds could have a significant clinical benefit and improve the prognosis of patients suffering from cardiac fibrosis and heart failure.

AUTHOR CONTRIBUTIONS

All authors designed, drafted, and revised the manuscript.

FUNDING

PF research group is funded by the Heart and Stroke Foundation of Canada.

ACKNOWLEDGMENTS

Images of human cardiac fibroblasts and human cardiac myofibroblasts were provided courtesy of Dr. Guoqi Teng, Research Associate, Campbell Family Cardiac Translational Laboratory, Libin Cardiovascular Institute of Alberta, University of Calgary, Calgary, AB, Canada.

REFERENCES

Arora, P. D., and McCulloch, C. A. G. (1994). Dependence of collagen remodelling on a-smooth muscle actin expression by fibroblasts. *J. Cell. Physiol.* 159, 161–175. doi: 10.1002/jcp.1041590120

Arunachalam, S. P., Arani, A., Baffour, F., Rysavy, J. A., Rossman, P. J., Glaser, K. J., et al. (2018). Regional assessment of in vivo myocardial stiffness using 3D magnetic resonance elastography in a porcine model of myocardial infarction. *Magn. Reson. Med.* 79, 361–369. doi: 10.1002/mrm.26695

Badylak, S. F. (2002). The extracellular matrix as a scaffold for tissue reconstruction. *Semin. Cell Dev. Biol.* 13, 377–383. doi: 10.1016/s1084952102000940

Badylak, S. F., Freytes, D. O., and Gilbert, T. W. (2015). Reprint of: extracellular matrix as a biological scaffold material: structure and function. *Acta Biomater.* 23(Suppl.), S17–S26. doi: 10.1016/j.actbio.2015.07.016

Baird, C. W., Myers, P. O., Piekarski, B., Borisuk, M., Majeed, A., Emani, S. M., et al. (2016). Photo-oxidized bovine pericardium in congenital cardiac surgery: single-centre experience. *Interact. Cardiovasc. Thorac. Surg.* 24:ivw315. doi: 10.1093/icvts/ivw315

Balsam, L. B., Wagers, A. J., Christensen, J. L., Kofidis, T., Weissman, I. L., and Robbins, R. C. (2004). Haematopoietic stem cells adopt mature haematopoietic fates in ischaemic myocardium. *Nature* 428, 668–673. doi: 10.1038/nature02460

Baudino, T. A., Carver, W., Giles, W., and Borg, T. K. (2006). Cardiac fibroblasts: friend or foe? *Am. J. Physiol. Circ. Physiol.* 291, H1015–H1026. doi: 10.1152/ajpheart.00023.2006

Baum, J., and Duffy, H. S. (2011). Fibroblasts and myofibroblasts: what are we talking about? *J. Cardiovasc. Pharmacol.* 57, 376–379. doi: 10.1097/FJC.0b013e3182116e39

Beltrami, C. A., Finato, N., Rocco, M., Feruglio, G. A., Puricelli, C., Cigola, E., et al. (1994). Structural basis of end-stage failure in ischemic cardiomyopathy in humans. *Circulation* 89, 151–163. doi: 10.1161/01.cir.89.1.151

Benjamin, E. J., Blaha, M. J., Chiuve, S. E., Cushman, M., Das, S. R., Deo, R., et al. (2017). Heart disease and stroke statistics—2017 update: a report from the American heart association. *Circulation* 135, e146–e603. doi: 10.1161/CIR.0000000000000485

Bianco, R. W., Phillips, R., Mrachek, J., and Witson, J. (1996). Feasibility evaluation of a new pericardial bioprosthesis with dye mediated photo-oxidized bovine pericardial tissue. *J. Heart Valve Dis.* 5, 317–322.

Blom, A. S., Pilla, J. J., Arkles, J., Dougherty, L., Ryan, L. P., Gorman, J. H., et al. (2007). Ventricular restraint prevents infarct expansion and improves borderzone function after myocardial infarction: a study using magnetic resonance imaging, three-dimensional surface modeling, and myocardial tagging. *Ann. Thorac. Surg.* 84, 2004–2010. doi: 10.1016/j.athoracsur.2007.06.062

Brizard, C. P., Brink, J., Horton, S. B., Edwards, G. A., Galati, J. C., and Neethling, W. M. L. (2014). New engineering treatment of bovine pericardium confers outstanding resistance to calcification in mitral and pulmonary implantations in a juvenile sheep model. *J. Thorac. Cardiovasc. Surg.* 148, 3194–3201. doi: 10.1016/J.JTCVS.2014.08.002

Brown, R. D., Ambler, S. K., Mitchell, M. D., and Long, C. S. (2005). THE CARDIAC FIBROBLAST: therapeutic target in myocardial remodeling and failure. *Annu. Rev. Pharmacol. Toxicol.* 45, 657–687. doi: 10.1146/annurev.pharmtox.45.120403.095802

Camelliti, P., Borg, T., and Kohl, P. (2005). Structural and functional characterisation of cardiac fibroblasts. *Cardiovasc. Res.* 65, 40–51. doi: 10.1016/j.cardiores.2004.08.020

Camelliti, P., Devlin, G. P., Matthews, K. G., Kohl, P., and Green, C. R. (2004). Spatially and temporally distinct expression of fibroblast connexins after sheep ventricular infarction. *Cardiovasc. Res.* 62, 415–425. doi: 10.1016/j.cardiores.2004.01.027

Dixon, I. M. C., and Wigle, J. (2015). *Cardiac Fibrosis and Heart Failure: Cause or Effect?* Berlin: Springer. doi: 10.1016/j.cardiores.2004.01.027

Dobaczewski, M., Bujak, M., Li, N., Gonzalez-Quesada, C., Mendoza, L. H., Wang, X.-F., et al. (2010a). Smad3 signaling critically regulates fibroblast phenotype and function in healing myocardial infarction. *Circ. Res.* 107, 418–428. doi: 10.1161/CIRCRESAHA.109.216101

Dobaczewski, M., Gonzalez-Quesada, C., and Frangogiannis, N. G. (2010b). The extracellular matrix as a modulator of the inflammatory and reparative response following myocardial infarction. *J. Mol. Cell. Cardiol.* 48, 504–511. doi: 10.1016/j.yjmcc.2009.07.015

Dunn, R. M. (2012). Cross-linking in biomaterials. *Plast. Reconstr. Surg.* 130, 18S–26S. doi: 10.1097/PRS.0b013e31825efea6

Fan, D., Takawale, A., Lee, J., and Kassiri, Z. (2012). Cardiac fibroblasts, fibrosis and extracellular matrix remodeling in heart disease. *Fibrogenesis Tissue Repair* 5:15. doi: 10.1186/1755-1536-5-15

Fedak, P. W. M., Verma, S., Weisel, R. D., and Li, R.-K. (2005a). Cardiac remodeling and failure: from molecules to man (Part I). *Cardiovasc. Pathol.* 14, 1–11. doi: 10.1016/j.carpath.2004.12.002

Fedak, P. W. M., Verma, S., Weisel, R. D., and Li, R.-K. (2005b). Cardiac remodeling and failure. *Cardiovasc. Pathol.* 14, 49–60. doi: 10.1016/j.carpath.2005.01.005

Fraccarollo, D., Galuppo, P., and Bauersachs, J. (2012). Novel therapeutic approaches to post-infarction remodelling. *Cardiovasc. Res.* 94, 293–303. doi: 10.1093/cvr/cvs109

Golomb, G., Schoen, F. J., Smith, M. S., Linden, J., Dixon, M., and Levy, R. J. (1987). The role of glutaraldehyde-induced cross-links in calcification of bovine pericardium used in cardiac valve bioprostheses. *Am. J. Pathol.* 127, 122–130.

Gyöngyösi, M., Wojakowski, W., Lemarchand, P., Lunde, K., Tendera, M., Bartunek, J., et al. (2015). Meta-analysis of cell-based CaRdiac stUdiEs (ACCRUE) in patients with acute myocardial infarction based on individual patient data. *Circ. Res.* 116, 1346–1360. doi: 10.1161/CIRCRESAHA.116.304346

Heymans, S., Schroen, B., Vermeersch, P., Milting, H., Gao, F., Kassner, A., et al. (2005). Increased cardiac expression of tissue inhibitor of metalloproteinase-1 and tissue inhibitor of metalloproteinase-2 is related to cardiac fibrosis and dysfunction in the chronic pressure-overloaded human heart. *Circulation* 112, 1136–1144. doi: 10.1161/CIRCULATIONAHA.104.516963

Hinz, B., Celetta, G., Tomasek, J. J., Gabbiani, G., and Chaponnier, C. (2001). Alpha-smooth muscle actin expression upregulates fibroblast contractile activity. *Mol. Biol. Cell* 12, 2730–2741. doi: 10.1091/mbc.12.9.2730

Jackson, B. M., Gorman, J. H., Moainie, S. L., Guy, T. S., Narula, N., Narula, J., et al. (2002). Extension of borderzone myocardium in postinfarction dilated cardiomyopathy. *J. Am. Coll. Cardiol.* 40, 1160–1167. doi: 10.1016/S0735-1097(02)02121-6

Kaiser, J. (2018). Suspect science leads to pause in stem cell trial. *Science* 362:513. doi: 10.1126/science.362.6414.513

Kawaguchi, M., Takahashi, M., Hata, T., Kashima, Y., Usui, F., Morimoto, H., et al. (2011). Inflammasome activation of cardiac fibroblasts is essential for myocardial ischemia/reperfusion injury. *Circulation* 123, 594–604. doi: 10.1161/CIRCULATIONAHA.110.982777

Krenning, G., Zeisberg, E. M., and Kalluri, R. (2010). The origin of fibroblasts and mechanism of cardiac fibrosis. *J. Cell. Physiol.* 225, 631–637. doi: 10.1002/jcp.22322

Lee, A. A., Delhaas, T., McCulloch, A. D., and Villarreal, F. J. (1999). Differential responses of adult cardiac fibroblasts to in vitro biaxial strain patterns. *J. Mol. Cell. Cardiol.* 31, 1833–1843. doi: 10.1006/JMCC.1999.1017

Leslie, K. O., Taatjes, D. J., Schwarz, J., Vonturkovich, M., and Lowt, R. B. (1991). Cardiac myofibroblasts express alpha smooth muscle actin during right ventricular pressure overload in the rabbit. *Am. J. Pathol.* 139, 207–216.

Mahoney, V. M., Mezzano, V., Mirams, G. R., Maass, K., Li, Z., Cerrone, M., et al. (2016). Connexin43 contributes to electrotonic conduction across scar tissue in the intact heart. *Sci. Rep.* 6:26744. doi: 10.1038/srep26744

Marui, A., Kimura, T., Nishiwaki, N., Komiya, T., Hanyu, M., Shiomi, H., et al. (2014). Three-year outcomes after percutaneous coronary intervention and coronary artery bypass grafting in patients with heart failure: from the CREDO-Kyoto percutaneous coronary intervention/coronary artery bypass graft registry cohort-2 The CREDO-Kyoto PCI/CAB. *Eur. J. Cardiothorac. Surg.* 47, 316–321. doi: 10.1093/ejcts/ezu131

McDonald, M. A., Ashley, E. A., Fedak, P. W. M., Hawkins, N., Januzzi, J. L., McMurray, J. J. V., et al. (2017). Mind the gap: current challenges and future state of heart failure care. *Can. J. Cardiol.* 33, 1434–1449. doi: 10.1016/j.cjca.2017.08.023

Mewhort, H. E. M., Lipon, B. D., Svystonyuk, D. A., Teng, G., Guzzardi, D. G., Silva, C., et al. (2016a). Monocytes increase human cardiac myofibroblast-mediated extracellular matrix remodeling through TGF-β 1. *Am. J. Physiol. Heart Circ. Physiol.* 310, H716–H724. doi: 10.1152/ajpheart.00309.2015

Mewhort, H. E. M., Turnbull, J. D., Satriano, A., Chow, K., Flewitt, J. A., Andrei, A. C., et al. (2016b). Epicardial infarct repair with bioinductive extracellular matrix promotes vasculogenesis and myocardial recovery. *J. Heart Lung Transplant.* 35, 661–670. doi: 10.1016/j.healun.2016.01.012

Mewhort, H. E. M., Svystonyuk, D. A., Turnbull, J. D., Teng, G., Belke, D. D., Guzzardi, D. G., et al. (2017). Bioactive extracellular matrix scaffold promotes adaptive cardiac remodeling and repair. *JACC Basic Transl. Sci.* 2, 450–464. doi: 10.1016/j.jacbts.2017.05.005

Mewhort, H. E. M., Turnbull, J. D., Meijndert, H. C., Ngu, J. M. C., and Fedak, P. W. M. (2014). Epicardial infarct repair with basic fibroblast growth factor–enhanced CorMatrix-ECM biomaterial attenuates postischemic cardiac remodeling. *J. Thorac. Cardiovasc. Surg.* 147, 1650–1659. doi: 10.1016/J.JTCVS.2013.08.005

Moore, M. A., and Phillips, R. E. (1997). Biocompatibility and immunologic properties of pericardial tissue stabilized by dye-mediated photooxidation. *J. Heart Valve Dis.* 6, 307–315.

Moore, M. A., Phillips, R. E., McIlroy, B. K., Walley, V. M., and Hendry, P. J. (1998). Evaluation of porcine valves prepared by dye-mediated photooxidation. *Ann. Thorac. Surg.* 66, S245–S248. doi: 10.1016/S0003-4975(98)01118-7

Mosala Nezhad, Z., Poncelet, A., de Kerchove, L., Gianello, P., Fervaille, C., and El Khoury, G. (2016). Small intestinal submucosa extracellular matrix (CorMatrix®) in cardiovascular surgery: a systematic review. *Interact. Cardiovasc. Thorac. Surg.* 22, 839–850. doi: 10.1093/icvts/ivw020

Murry, C. E., Soonpaa, M. H., Reinecke, H., Nakajima, H., Nakajima, H. O., Rubart, M., et al. (2004). Haematopoietic stem cells do not transdifferentiate into cardiac myocytes in myocardial infarcts. *Nature* 428, 664–668. doi: 10.1038/nature02446

Neethling, W. M. L., Puls, K., and Rea, A. (2018). Comparison of physical and biological properties of CardioCel® with commonly used bioscaffolds. *Interact. Cardiovasc. Thorac. Surg.* 26, 985–992. doi: 10.1093/icvts/ivx413

Nguyen, M.-N., Kiriazis, H., Gao, X.-M., and Du, X.-J. (2017). Cardiac fibrosis and arrhythmogenesis. *Compr. Physiol.* 7, 1009–1049. doi: 10.1002/cphy.c160046

Padalino, M. A., Quarti, A., Angeli, E., Frigo, A. C., Vida, V. L., Pozzi, M., et al. (2015). Early and mid-term clinical experience with extracellular matrix scaffold for congenital cardiac and vascular reconstructive surgery: a multicentric Italian study. *Interact. Cardiovasc. Thorac. Surg.* 21, 40–49. doi: 10.1093/icvts/ivv076

Park, D., Mewhort, H., Teng, G., Belke, D., Turnbull, J., Svystonyuk, D., et al. (2017). Heparin augmentation enhances bioactive properties of acellular extracellular matrix scaffold. *Tissue Eng. Part A* 24, 128–134. doi: 10.1089/ten.TEA.2017.0004

Park, T.-H., Nagueh, S. F., Khoury, D. S., Kopelen, H. A., Akrivakis, S., Nasser, K., et al. (2006). Impact of myocardial structure and function postinfarction on diastolic strain measurements: implications for assessment of myocardial viability. *Am. J. Physiol. Circ. Physiol.* 290, H724–H731. doi: 10.1152/ajpheart.00714.2005

Patel, M. R., Calhoon, J. H., Dehmer, G. J., Grantham, J. A., Maddox, T. M., Maron, D. J., et al. (2017). ACC/AATS/AHA/ASE/ASNC/SCAI/SCCT/STS 2017 appropriate use criteria for coronary revascularization in patients with stable ischemic heart disease. *J. Am. Coll. Cardiol.* 69, 2212–2241. doi: 10.1016/j.jacc.2017.02.001

Pavy, C., Michielon, G., Robertus, J. L., Lacour-Gayet, F., and Ghez, O. (2017). Initial 2-year results of CardioCel® patch implantation in children. *Interact. Cardiovasc. Thorac. Surg.* 26, 448–453. doi: 10.1093/icvts/ivx295

Pellman, J., Zhang, J., and Sheikh, F. (2016). Myocyte-fibroblast communication in cardiac fibrosis and arrhythmias: mechanisms and model systems. *J. Mol. Cell. Cardiol.* 94, 22–31. doi: 10.1016/j.yjmcc.2016.03.005

Reardon, S. (2018). US government halts heart stem-cell study. *Nature.* doi: 10.1038/d41586-018-07232-0

Richardson, W. J., and Holmes, J. W. (2015). Why is infarct expansion such an elusive therapeutic target? *J. Cardiovasc. Transl. Res.* 8, 421–430. doi: 10.1007/s12265-015-9652-2

Rosario-Quinones, F., Magid, M. S., Yau, J., Pawale, A., and Nguyen, K. (2015). Tissue reaction to porcine intestinal submucosa (CorMatrix) implants in pediatric cardiac patients: a single-center experience. *Ann. Thorac. Surg.* 99, 1373–1377. doi: 10.1016/J.ATHORACSUR.2014.11.064

Salameh, A., Greimann, W., Vondrys, D., and Kostelka, M. (2018). Calcification or not. This is the question. A 1-year study of bovine pericardial vascular patches (CardioCel) in minipigs. *Semin. Thorac. Cardiovasc. Surg.* 30, 54–59. doi: 10.1053/J.SEMTCVS.2017.09.013

Saxena, A., and Frangogiannis, N. G. (2015). "Fibroblast activation in the infarcted myocardium," in *Cardiac Fibrosis and Heart Failure: Cause or Effect?*, eds I. Dixon and J. T. Wigle (Cham: Springer International Publishing), 5–22. doi: 10.1007/978-3-319-17437-2_2

Schmidt, C. E., and Baier, J. M. (2000). Acellular vascular tissues: natural biomaterials for tissue repair and tissue engineering. *Biomaterials* 21, 2215–2231. doi: 10.1016/S0142-9612(00)00148-4

Serini, G., Bochaton-Piallat, M.-L., Ropraz, P., Geinoz, A., Borsi, L., Zardi, L., et al. (1998). The fibronectin domain ED-A is crucial for myofibroblastic phenotype induction by transforming growth factor-β1. *J. Cell Biol.* 142, 873–881. doi: 10.1083/JCB.142.3.873

Shimkunas, R., Wang, G.-Y., Zhang, Z., Guccione, J. M., Ratcliffe, M. B., and Baker, A. J. (2011). Myofilament dysfunction contributes to impaired myocardial contraction in the infarct border zone. *Am. J. Physiol. Heart Circ. Physiol.* 307, H1150–H1158. doi: 10.1016/j.bpj.2010.12.1823

Shimkunas, R., Zhang, Z., Wenk, J. F., Soleimani, M., Khazalpour, M., Acevedo-Bolton, G., et al. (2013). Left ventricular myocardial contractility is depressed in the borderzone after posterolateral myocardial infarction. *Ann. Thorac. Surg.* 95, 1619–1625. doi: 10.1016/j.athoracsur.2013.02.005

Shinde, A. V., and Frangogiannis, N. G. (2014). Fibroblasts in myocardial infarction: a role in inflammation and repair. *J. Mol. Cell. Cardiol.* 70, 74–82. doi: 10.1016/j.yjmcc.2013.11.015

Souders, C. A., Bowers, S. L. K., and Baudino, T. A. (2009). Cardiac fibroblast: the renaissance cell. *Circ. Res.* 105, 1164–1176. doi: 10.1161/CIRCRESAHA.109.209809

Sutton, M. G., and Sharpe, N. (2000). Left ventricular remodeling after myocardial infarction: pathophysiology and therapy. *Circulation* 101, 2981–2988. doi: 10.1161/01.cir.101.25.2981

Svystonyuk, D. A., Mewhort, H. E. M., and Fedak, P. W. M. (2018). Using acellular bioactive extracellular matrix scaffolds to enhance endogenous cardiac repair. *Front. Cardiovasc. Med.* 5:35. doi: 10.3389/fcvm.2018.00035

Svystonyuk, D. A., Ngu, J. M., Mewhort, H. E., Lipon, B. D., Teng, G., Guzzardi, D. G., et al. (2015). Fibroblast growth factor-2 regulates human cardiac myofibroblast-mediated extracellular matrix remodeling. *J. Transl. Med.* 13:147. doi: 10.1186/s12967-015-0510-4

Tanaka, A., Kawaji, K., Patel, A. R., Tabata, Y., Burke, M. C., Gupta, M. P., et al. (2015). In situ constructive myocardial remodeling of extracellular matrix patch enhanced with controlled growth factor release. *J. Thorac. Cardiovasc. Surg.* 150, 1280–1290.e2. doi: 10.1016/j.jtcvs.2015.07.073

Ten Tusscher, K. H., and Panfilov, A. V. (2007). Influence of diffuse fibrosis on wave propagation in human ventricular tissue. *Europace* 9, vi38–vi45. doi: 10.1093/europace/eum206

Teng, G., Svystonyuk, D., Mewhort, H. E. M., Turnbull, J. D., Belke, D. D., Duff, H. J., et al. (2015). Tetrandrine reverses human cardiac myofibroblast activation and myocardial fibrosis. *Am. J. Physiol. Heart Circ. Physiol.* 308, H1564–H1574. doi: 10.1152/ajpheart.00126.2015

Tomasek, J. J., Gabbiani, G., Hinz, B., Chaponnier, C., and Brown, R. A. (2002). Myofibroblasts and mechano-regulation of connective tissue remodelling. *Nat. Rev. Mol. Cell Biol.* 3, 349–363. doi: 10.1038/nrm809

Torres, W. M., Jacobs, J., Doviak, H., Barlow, S. C., Zile, M. R., Shazly, T., et al. (2018). Regional and temporal changes in left ventricular strain and stiffness in a porcine model of myocardial infarction. *Am. J. Physiol. Heart Circ. Physiol.* 315, 958–967. doi: 10.1152/ajpheart.00279.2018.-The

van Steenberghe, M., Schubert, T., Guiot, Y., Bouzin, C., Bollen, X., and Gianello, P. (2017). Enhanced vascular biocompatibility of decellularized xeno-/allogeneic matrices in a rodent model. *Cell Tissue Bank.* 18, 249–262. doi: 10.1007/s10561-017-9610-0

Vaughan, M. B., Howard, E. W., and Tomasek, J. J. (2000). Transforming growth factor-beta1 promotes the morphological and functional differentiation of the myofibroblast. *Exp. Cell Res.* 257, 180–189. doi: 10.1006/excr.2000.4869

Velagaleti, R. S., Pencina, M. J., Murabito, J. M., Wang, T. J., Parikh, N. I., D'Agostino, R. B., et al. (2008). Long-term trends in the incidence of heart

failure after myocardial infarction. *Circulation* 118, 2057–2062. doi: 10.1161/CIRCULATIONAHA.108.784215

Xie, M., Burchfield, J. S., and Hill, J. A. (2013). Pathological ventricular remodeling: mechanisms: part 1 of 2. *Circulation* 128, 388–400. doi: 10.1161/CIRCULATIONAHA.113.001878

Zaidi, A. H., Nathan, M., Emani, S., Baird, C., del Nido, P. J., Gauvreau, K., et al. (2014). Preliminary experience with porcine intestinal submucosa (CorMatrix) for valve reconstruction in congenital heart disease: histologic evaluation of explanted valves. *J. Thorac. Cardiovasc. Surg.* 148, 2216–2225.e1. doi: 10.1016/J.JTCVS.2014.02.081

Zhao, L., and Eghbali-Webb, M. (2001). Release of pro- and anti-angiogenic factors by human cardiac fibroblasts: effects on DNA synthesis and protection under hypoxia in human endothelial cells. *Biochim. Biophys. Acta* 1538, 273–282. doi: 10.1016/s0167-4889(01)00078-7

Zhao, X.-H., Laschinger, C., Arora, P., Szászi, K., Kapus, A., and McCulloch, C. A. (2007). Force activates smooth muscle alpha-actin promoter activity through the Rho signaling pathway. *J. Cell Sci.* 120, 1801–1809. doi: 10.1242/jcs.001586

Conflict of Interest Statement: The authors declare that the research was conducted in the absence of any commercial or financial relationships that could be construed as a potential conflict of interest.

frontiers in Cell and Developmental Biology

REVIEW
published: 13 December 2019
doi: 10.3389/fcell.2019.00340

Extracellular Matrix Composition and Remodeling: Current Perspectives on Secondary Palate Formation, Cleft Lip/Palate, and Palatal Reconstruction

Katiúcia Batista Silva Paiva[1], Clara Soeiro Maas[1], Pâmella Monique dos Santos[1], José Mauro Granjeiro[2,3] and Ariadne Letra[4,5,6]*

[1] Laboratory of Extracellular Matrix Biology and Cellular Interaction, Department of Anatomy, Institute of Biomedical Sciences, University of São Paulo, São Paulo, Brazil, [2] Clinical Research Laboratory in Dentistry, Federal Fluminense University, Niterói, Brazil, [3] Directory of Life Sciences Applied Metrology, National Institute of Metrology, Quality and Technology, Duque de Caxias, Brazil, [4] Center for Craniofacial Research, UTHealth School of Dentistry at Houston, Houston, TX, United States, [5] Pediatric Research Center, UTHealth McGovern Medical School, Houston, TX, United States, [6] Department of Diagnostic and Biomedical Sciences, UTHealth School of Dentistry at Houston, Houston, TX, United States

OPEN ACCESS

Edited by:
Charles D. Little, University of Kansas Medical Center, United States

Reviewed by:
Lidija Radenovic, University of Belgrade, Serbia
Zhizhan Gu, Dana-Farber Cancer Institute, United States

***Correspondence:**
Katiúcia Batista Silva Paiva
katipaiva@usp.br

Specialty section:
This article was submitted to Cell Adhesion and Migration, a section of the journal Frontiers in Cell and Developmental Biology

Received: *27 February 2019*
Accepted: *29 November 2019*
Published: *13 December 2019*

Citation:
Paiva KBS, Maas CS, Santos PM, Granjeiro JM and Letra A (2019) Extracellular Matrix Composition and Remodeling: Current Perspectives on Secondary Palate Formation, Cleft Lip/Palate, and Palatal Reconstruction. Front. Cell Dev. Biol. 7:340. doi: 10.3389/fcell.2019.00340

Craniofacial development comprises a complex process in humans in which failures or disturbances frequently lead to congenital anomalies. Cleft lip with/without palate (CL/P) is a common congenital anomaly that occurs due to variations in craniofacial development genes, and may occur as part of a syndrome, or more commonly in isolated forms (non-syndromic). The etiology of CL/P is multifactorial with genes, environmental factors, and their potential interactions contributing to the condition. Rehabilitation of CL/P patients requires a multidisciplinary team to perform the multiple surgical, dental, and psychological interventions required throughout the patient's life. Despite progress, lip/palatal reconstruction is still a major treatment challenge. Genetic mutations and polymorphisms in several genes, including extracellular matrix (ECM) genes, soluble factors, and enzymes responsible for ECM remodeling (e.g., metalloproteinases), have been suggested to play a role in the etiology of CL/P; hence, these may be considered likely targets for the development of new preventive and/or therapeutic strategies. In this context, investigations are being conducted on new therapeutic approaches based on tissue bioengineering, associating stem cells with biomaterials, signaling molecules, and innovative technologies. In this review, we discuss the role of genes involved in ECM composition and remodeling during secondary palate formation and pathogenesis and genetic etiology of CL/P. We also discuss potential therapeutic approaches using bioactive molecules and principles of tissue bioengineering for state-of-the-art CL/P repair and palatal reconstruction.

Keywords: palatogenesis, extracellular matrix, extracellular matrix remodeling, metalloproteinases, cleft lip/palate, palatal reconstruction, tissue bioengineering, biomaterials

INTRODUCTION

The first studies on palate development and cleft lip/palate (CL/P) date back to the beginning of the 20th century (Whitehead, 1902; Fawcett, 1906; Tweedie, 1910). These studies were fundamental to our understanding of the molecular and cellular aspects that drive palate formation, that when disrupted, may explain the occurrence of CL/P. CL/P is the most common craniofacial anomaly occurring in approximately 1 in 700 live births, and representing a substantial burden worldwide (Shaw, 2004; Massenburg et al., 2016). The treatment of this disorder is complex and demands a multiplicity of health professionals to perform numerous interventions throughout the patient's life (Kantar et al., 2019). Besides the high cost of treatment, CL/P imposes a significant impact on the quality of life of affected children and their families (Macho et al., 2017; Sundell et al., 2017). The primary treatment for CL/P repair is surgical correction, frequently including autologous bone grafts from the iliac crest to repair the palatal bone defect. This increases hospitalization time, pain, and donor site morbidity; hence, new strategies for the use of regenerative therapies and bone graft substitutes are needed to reduce the morbidity associated with the condition and improve treatment outcomes and patient's quality of life (Sharif et al., 2016). Further, the identification of key factors involved in the etiology of CL/P may provide the foundation for the development of bioactive molecules and precision therapy approaches for CL/P.

Extracellular matrix (ECM) genes, soluble factors, and enzymes responsible for ECM remodeling (e.g., metalloproteinases) are expressed during lip and palate development and suggested to play a role in the etiology of CL/P. However, a comprehensive evaluation of ECM dynamics during palatogenesis is still fragmented. Historically, the ECM was considered to be the scaffold that provided an adequate architecture for tissue structure. Subsequently, knowledge of the soluble factors secreted by the cells into the ECM and its function as storage site for the rapid bioavailability of several molecules demonstrated the role of ECM as a crucial component of the cellular microenvironment (Ricard-Blum and Vallet, 2016, 2019). An intricate balance between proteases that degrade the ECM components and their inhibitors maintain the ECM homeostasis. Abnormal ECM remodeling (excessive or inefficient) is often involved in the development and progression of several pathologies and conditions, including CL/P.

This review focuses on the role of genes involved in ECM composition and remodeling during secondary palate formation and with regard to the genetic etiology of CL/P. It also presents an overview of therapeutic approaches using bioactive molecules and principles of tissue bioengineering for state-of-the-art CL/P repair and palatal reconstruction.

CRANIOFACIAL DEVELOPMENT AND PALATOGENESIS

Embryonic development is a precise temporal and spatial multistep process that is coordinated by specific molecular patterns, cell–cell and reciprocal cell–ECM interactions from the totipotent stem cell up to a fully developed organism. The vertebrate craniofacial complex arises from three embryonic tissue layers (endoderm, mesoderm, and ectoderm) and multipotent migrating neural crest cells (NCCs), also known as the "fourth layer." NCCs are a population of epithelial cells within the neural tube, which migrate and then undergo epithelial–mesenchymal transition (EMT) prior to neural tube closure, delaminating from the neuroepithelium, and migrating toward the growing swellings. NCCs contribute to neural structures found in the whole vertebrate body and ectomesenchyme of the head and neck and originate the mesenchymal/stromal stem cells (MSCs)/progenitors that will differentiate into the dermis, skeletal, and connective tissues of the face and the neck, being the primary source of mesenchymal tissue in this region. They are also responsible for the bones and cartilage of the head and neck, while the trunk and appendicular members come from the mesoderm. Craniofacial development is one of the most complex processes in an organism and one-third of birth defects arise from errors in this process, causing significant infant mortality (Weston and Thiery, 2015; Francis-west and Crespo-Enriquez, 2016; Liu and Cheung, 2016; Dupin et al., 2018; Pla and Monsoro-Burq, 2018; Rothstein et al., 2018).

Lip and palate formation occurs in a series of coordinated steps, which take place between the fourth and 12th gestational week (GW) in humans and between the 11th and 15.5th embryonic day (ED) in mice. Facial development begins by frontonasal (central), maxillary, and mandibular (laterals) prominences growing around the primitive oral cavity, called the stomodeum, to give rise to the face. NCCs from distinct

Abbreviations: ABCA4, ATP-binding cassette, sub-family A (ABC1), member 4; ADAM, a disintegrin and metalloproteinase; ADAMST, a disintegrin and metalloproteinase with thrombospondin-like motifs; BMP, bone morphogenetic protein; BMSC, bone marrow stem cell; BTP, BMP-1/Tolloid-like proteases; CL/P, cleft and lip palate; CRISPLD2, cysteine-rich secretory protein LCCL domain-containing 2; CSPG, chondroitin sulfate proteoglycans; DFPSC, dental follicle progenitor stem cells; DMP-1, dentin matrix protein-1; DSPP, dentin sialophosphoprotein; DPP, dentin phosphoprotein; DPSC, dental pulp stem cell; ECM, extracellular matrix; ED, embryonic day; EGFR, epidermal growth factor receptor; EMT, epithelial-mesenchymal transition; EV, extracellular vesicles; FGF, fibrobast growth factor; FGFR, fibrobast growth factor receptor; FOXE1, forkhead box E1; GAG, glycosaminoglycans; GDF, growth differentiation factor; GH, growth hormone; GMP, good manufacturing practice; GMSC, gingival mesenchymal stem/progenitor cell; GPI, glycosyl-phosphatidyl-inositol; GW, gestational weeks; HA, hyaluronic acid; Has, hyaluronan synthase; Hh, hedgehog; IGFBPs, insulin-like growth factor binding proteins; IGF, insulin growth factor; IRF6, interferon regulatory factor 6; KO, knockout mice; LOX, lysyl oxidase; LOXL, lysyl oxidase-like; LTBPs, TGF-β binding proteins; MAFB, V-maf musculoaponeurotic fibrosarcoma oncogene homolog B; MEE, medial edge epithelia; MES, medial epithelial seam; MMP, matrix metalloproteinase; MSC, mesenchymal stem cell mTLD, tolloid; MTLL-1, tolloid-like 1; MSX1, Msh homeobox 1; MV, matrix vesicles; NCC, neural crest cells; NFkB, factor nuclear kappa B; NSCLP, nonsyndromic cleft and lip palate; OPG, osteoprotegerin; PAPP, pregnancy-associated plasma protein; PCPE, procollagen C-proteinase enhancer; PDGF, platelet-derived growth factor; PDLSC, periodontal ligament stem cell; PRF, platelet-rich fibrin; PRP, platelet-rich plasma; Rac1, Ras-related C3 botulinum toxin substrate 1; RANK, receptor activator of nuclear factor κB; RANKL, receptor activator of nuclear factor κB-ligand; SHED, stem cells from exfoliated deciduous teeth; SCAP, stem cells from apical papilla; SRLP, small rich-leucine proteoglycans; SIBLING, small integrin-binding ligand N-linked glycoprotein); TG, transglutaminase; TGF-α, transforming growth factor alpha; TGF-β, transforming growth factor beta; VAX1, ventral anterior homeobox 1; VEGF, vascular endothelial growth factor.

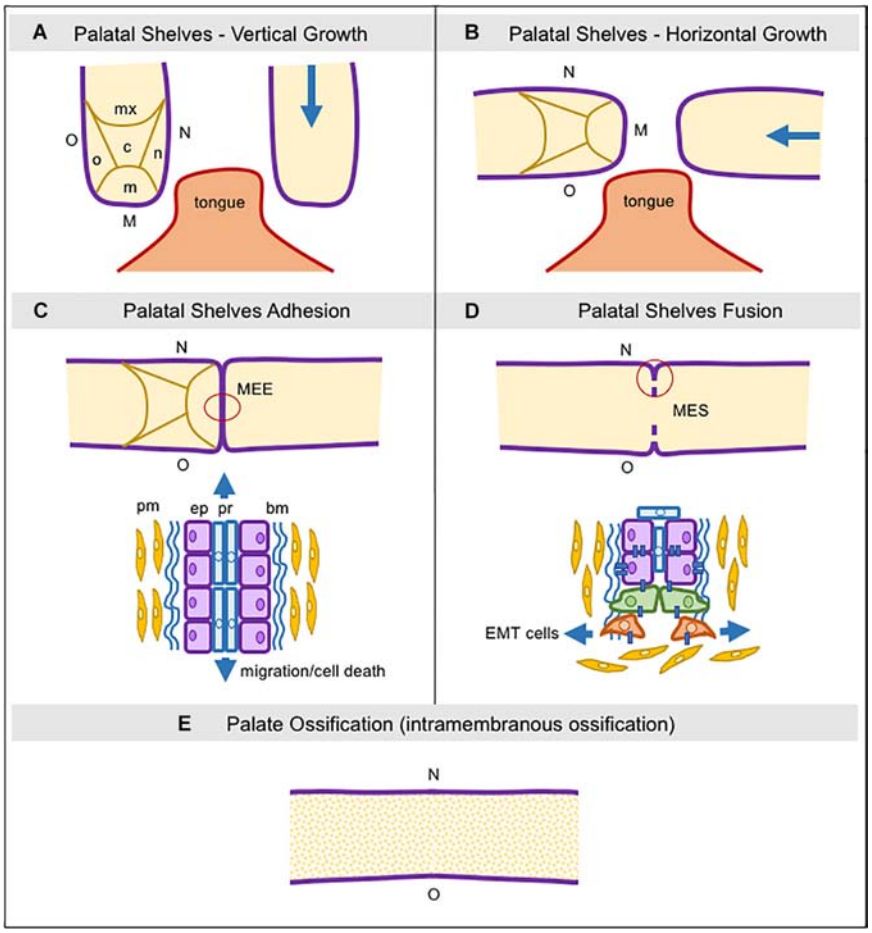

FIGURE 1 | Schematic representation of consecutive steps during secondary palatogenesis. **(A)** Initially, palatal shelves grow down, surrounding the tongue, and five regions in the palatal mesenchyme can be seen: nasal, medial, oral, central, and maxillary, as well as three regions in the palatal epithelium: nasal, medial, and oral. **(B)** Palatal shelve orientation switches from vertical to horizontal, toward each other and above the tongue. **(C)** The medial palatal epithelia from both shelves establish adhesion and it is now named the Media Edge Epithelia (MEE). In this area, we can see two different types of epithelial cells localized in two layers, the peridermal and the non-stratified cuboid epithelium. Peridermal cells start to migrate toward both nasal and oral epithelial sites. **(D)** The MEE starts the fragmentation since the epithelial layer begins the epithelial-to-mesenchymal transition and these cells then migrate into the palatal mesenchyme. **(E)** The MES completely disappears and the palatal mesenchymal cells start to differentiate into osteoblasts via intramembranous ossification. bm: basement membrane; c: central region; EMT: epithelial-to-mesenchymal transition; ep: epithelial cells; M: medial site; m: medial region; MEE: medial edge epithelia; MES: medial epithelial seam; mx: maxillary region; n: nasal region; N: nasal site; o: oral region; O: oral site; pm: palatal mesenchyme; pr: peridermal cells.

sites of the developing brain, such as the midbrain and forebrain cells (frontonasal), midbrain and hindbrain cells (maxillary), where the mix of the midbrain and hindbrain cells and mesenchyme from the first pharyngeal arch (mandibular) enrich these prominences (Jankowski and Márquez, 2016).

The frontonasal prominence is the most fundamental structure for external nose and the primary palate formation. Between the fifth–seventh GW and 10.0th–11.0th ED, it expands from two ectoderm nasal or olfactory placodes which each enlarge to divide into the nasomedial and nasolateral processes. The nasomedial processes grow downward and merge to originate the globular or intermaxillary process, which will form the philtrum of the upper lip and primary palate. Anatomically, the primary palate is anterior to the incisive foramen and contains the maxillary incisors (Jankowski and Márquez, 2016).

The maxillary prominences drive the formation of the upper part of the face, lip, upper jaw (maxillae), and the secondary palate. The mandibular prominences originate the lower part of the face, lip, and lower jaw (mandible). Briefly, the secondary palate develops from two mesenchymal projections (palatal shelves) derived from maxillary prominences extending inferiorly and bilaterally to the tongue (**Figure 1A**). With the progressive development of the mandible, these projections assume a horizontal position above the tongue (**Figure 1B**; Jankowski and Márquez, 2016). Subsequently, the adhesion of the epithelium from both palatal shelves forms a single line, called medial edge epithelia (MEE), which must disappear to allow for palatal tissue confluence and fusion (**Figure 1C**). Programmed cell death, EMT, and cell migration from the oral to the nasal epithelia, or a combination of these events have been suggested as

plausible mechanisms for MEE disintegration, albeit this remains a controversial issue (**Figure 1D**; Ray and Niswander, 2012; Hammond et al., 2017).

Once palatal fusion is complete, the anterior two-thirds mineralize by intramembranous ossification (hard palate) (**Figure 1E**), and the posterior third will give rise to a fibromuscular tissue (soft palate) under the signaling by numerous factors, particularly bone morphogenetic proteins (BMPs), fibroblast growth factors (FGFs), hedgehog (HH), vascular endothelial growth factor (VEGF), and Wnt/β-catenin signaling, which drive the palatal mesenchyme to undergo osteoblast differentiation for mineralization (Wu et al., 2008; Baek et al., 2011; Nelson et al., 2011; Pan et al., 2013; Smith et al., 2013; Hill et al., 2014, 2015; Nassif et al., 2014; Iyyanar and Nazarali, 2017; Zhang et al., 2017; Xu J. et al., 2018; Thompson et al., 2019).

Anatomically, the fusion of primary and secondary palates with the nasal septum originates the palate, a physical barrier that separates the fully developed nasal and oral cavities. Physiologically, it has a function in breathing, speech, and swallowing. The local regulation of palate development depends on a network of several factors, such as transcription factors, signaling molecules, soluble factors, ECM proteins, ECM remodeling enzymes, ECM cross-linkers, and cell adhesion molecules. Disturbance of this tightly controlled network may inhibit the fusion of the palatal shelves and, hence, result in a cleft palate (Funato, 2015).

ECM STRUCTURAL MOLECULES AND SOLUBLE FACTORS

Collectively, the secretome is the set of membrane proteins that are tethered on the cell surface and interact with the ECM, secreting molecules into ECM in soluble forms or inside of extracellular vesicles (EVs). Part of the secretome contains the matrisome, which encompasses all ECM-proteins and ECM-associated proteins. The core matrisome is composed mainly of structural proteins encoded by around 300 genes, whereas matrisome-associated proteins are those that modulate ECM functions and are encoded by about 700 genes, corresponding to 4% of the human or mouse genomes. The increasing knowledge regarding specific ECM tissue signatures contributes to the understanding of the role of the ECM in development, homeostasis, tissue repair, and disease (Hynes and Naba, 2012; **Figure 2**).

Fibrous proteins and proteoglycans are the two principal components of the core matrisome. Fibrous proteins are responsible for the matrisome's supportive function (collagen and elastin) and adhesive functions (fibronectin, laminin, nidogen, and vitronectin). These macromolecules interact with each other and can binding numerous growth factors (Raghunathan et al., 2019).

Proteoglycans are proteins conjugated to GAG chains and are crucial for conferring resistance to compression forces. Most GAGs are highly negatively-charged molecules that attract positively-charged sodium ions and, consequently, water, contributing to the viscosity and hydration within tissues. Among GAGs, chondroitin, dermatan, heparan, and keratan sulfate are the principal GAGs associated with proteoglycans in the connective tissues. High levels of hyaluronic acid or hyaluronan (HA), a non-sulfated GAG, are also found in the ECM (Garantziotis and Savani, 2019). Depending on the type of GAG associated with the proteoglycan, this will determine its location in the cytoplasm (the only member is serglycin), on the cell surface or within the ECM. Most of the heparan sulfate proteoglycans are anchored on the cell membrane via their transmembrane domains or glycosylphosphatidylinositol (GPI) anchors. Thus, proteoglycans can interact with many other molecules, including ECM remodeling enzymes and growth factors, thereby playing an important role in regulating ECM dynamics (Iozzo and Schaefer, 2015).

The provisional matrix is a transitory ECM found during the early stages of development, tissue repair, and disease which is later replaced by a tissue-specific ECM. It is formed by fibrin, fibrinogen, fibronectin, HA, and versican, a large chondroitin sulfate proteoglycan. HA provides a "glue" core to bind all other components and place it in the pericellular space, due to its interaction with a specific membrane receptor, CD44. Several growth factors can stimulate the expression of these macromolecules. The provisional matrix has a viscoelastic property that allows it to create spaces within the ECM, providing means for cell migration. For example, the migratory routes of NCCs during early embryonic development highly express high levels of versican (Barker and Engler, 2017; Chester and Brown, 2017; Wight, 2017) and tenascin (Riou et al., 1992). It is well known that collagens type I, III, IV, V, VI, fibronectin, HSPG, laminin, and tenascin are expressed during palatogenesis *in vivo* (Ferguson, 1988; Dixon et al., 1993a) and EGF or TGF-α can stimulate their expression on mouse embryonic palatal mesenchymal cells *in vitro* (Dixon et al., 1993b). The intrinsic "internal shelf force" for palatal elevation has been attributed to HA since it is the most abundant GAG in palatal ECM before shelf elevation (Ferguson, 1988). It is produced on the cell membrane surface by specific enzymes (HA synthases—Has 1-3) and these are differentially expressed in palatal mesenchyme and epithelium during palatogenesis (Galloway et al., 2013). In TGFβ-3 null mice, expression of all Has forms is decreased, leading to reduced amounts of HA and impaired shelf elevation (Galloway et al., 2013). Recently, Has2 has been described to be a crucial HA synthase in NCC-derived mesenchyme during craniofacial development and palatogenesis (Lan et al., 2019). Also, FGFs induce HA synthesis by mouse embryonic palatal mesenchymal cells *in vitro* (Sharpe et al., 1993). Fibronectin is found during embryonic development in areas characterized by cell migration (Schwarzbauer and DeSimone, 2011). It appears that fibronectin arrangement is vital for cell migration and palatal shelf elevation. In this case, Rac1 and cell density modulates fibronectin deposition in mid-palate (Tang et al., 2015). Moreover, Rac1 is downregulated by retinoic acid, leading to the cleft palate as a consequence of the disarrangement of fibronectin and cell migration as well (Tang et al., 2016).

Cellular communication is a well-known mechanism in which cells can communicate with each other and modify cell behavior

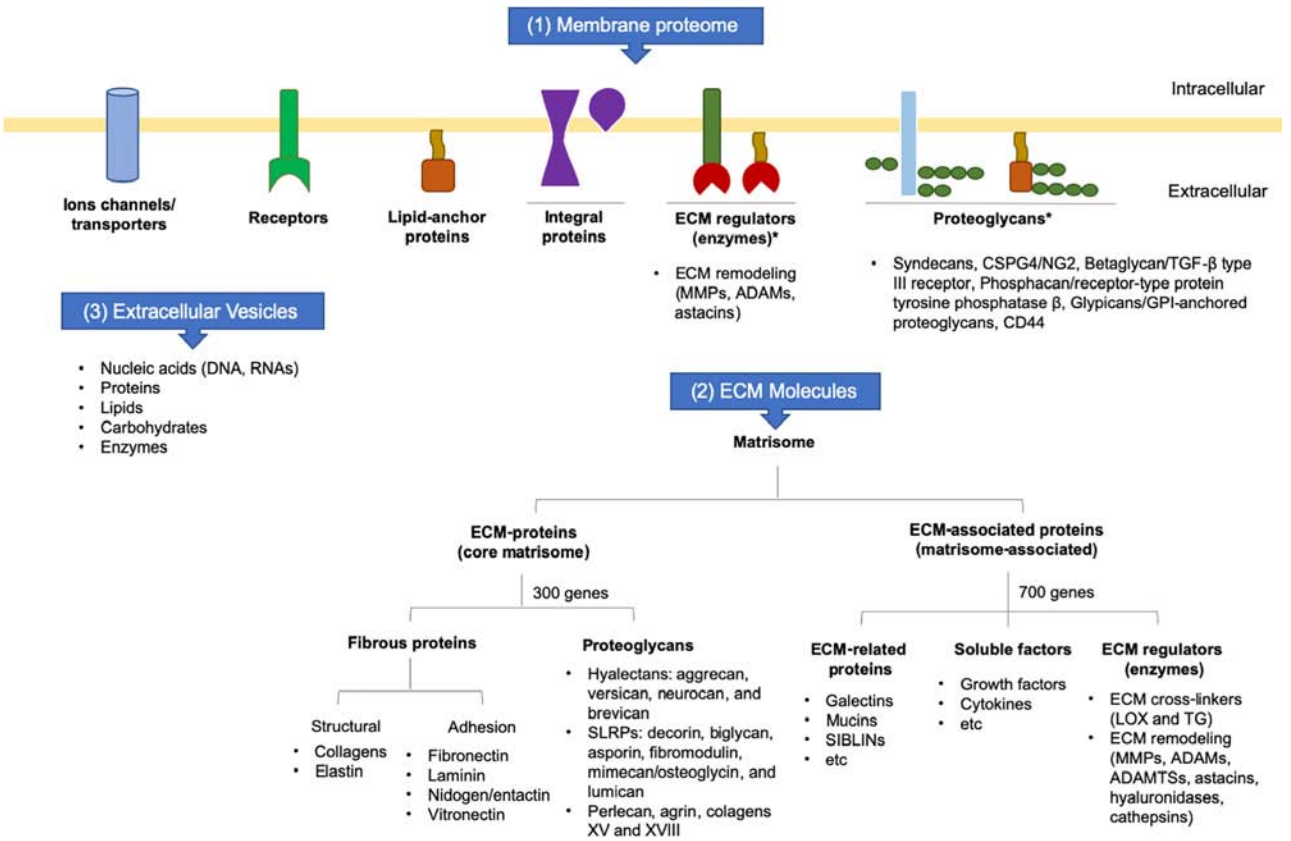

FIGURE 2 | Schematic representation of cell surface molecules and secretome. ADAM: adisintegrin and metalloproteinase; ADAMTS: adisintegrin and metalloproteinase with thrombospondin motifs; ECM: extracellular matrix; GPI: glycosylphosphatidylinositol; LOX: lysyl oxidase; MMP: matrix metalloproteinase; SIBLIN: small integrin-binding ligand *n*-linked glycoprotein; SLRP: small leucine-rich proteoglycans; TG: transglutaminase; TGF-: transforming growth factor beta.

through soluble factors. Intercellular communications occur via direct cellular interactions in which cell surface proteins act as mediators able, or not, to bind to the ECM (juxtacrine signaling). Alternatively, cells release local mediators into the ECM to create self-control signals (autocrine signaling) and send information to neighboring cells (paracrine signaling) or reach target cells in long distances via hormones (endocrine signaling) (Ansorge and Pompe, 2018). The local mediators are peptides or growth factors which control many cellular activities. During development, a combination of cell–cell interactions occurs, as well as the secretion of mediators named morphogens, which induce specific cell differentiation in a distinct spatial order and morphogen gradient-dependent manner (Inomata, 2017). The main morphogens are retinoic acid, HH, TGF-β, BMPs, and Wnt/β-catenin.

The actions of numerous morphogens in palatogenesis have been extensively studied, mainly secreted factors such as HH (Cobourne and Green, 2012; Dworkin et al., 2016; Xavier et al., 2016; Li et al., 2018), FGF (Jiang et al., 2006; Nie et al., 2006; Snyder-Warwick and Perlyn, 2012; Stanier and Pauws, 2012; Prochazkova et al., 2018; Weng et al., 2018), TGF-β (Nawshad et al., 2004; Iwata et al., 2011; Nakajima et al., 2018), BMP (Nie et al., 2006; Parada and Chai, 2012; Graf et al., 2016), and Wnt/β-catenin family proteins (He and Chen, 2012), which are responsible for guiding all steps of palate formation by reciprocal signaling between the embryonic oral epithelium and palatal mesenchyme, as well as transcription factor regulation (Greene and Pisano, 2010; Levi et al., 2011; Bush and Jiang, 2012; Li et al., 2017). Also, other morphogens and growth factors have emerged in palatogenesis, such as connective tissue growth factor (Tarr et al., 2018) and retinoic acid (Okano et al., 2014; Mammadova et al., 2016). Dysregulation of these pathways through genetic variations in individual genes has been suggested as strongly associated with CL/P (Pauws and Stanier, 2007; Krejci et al., 2009; Tang et al., 2013; Okano et al., 2014; Reynolds et al., 2019).

During the last decade, knowledge of new types of RNA with regulatory functions, located in non-coding regions of DNA, has improved our understanding of gene expression regulation (Scherrer, 2018). Many different microRNAs have been identified to temporally and spatially regulate morphogens and transcription factors during palatogenesis (Eberhart et al., 2008; Seelan et al., 2014; Ding et al., 2016; Reiss and Bhakdi, 2017; Schoen et al., 2017). Not surprisingly, microRNAs have been suggested as be new targets for investigating in CL/P studies (Li et al., 2010; Wang et al., 2013, 2017; Ma et al., 2014; Gao et al.,

2015; Li D. et al., 2016; Li J. et al., 2016; Schoen et al., 2017, 2018; Chen et al., 2018; Grassia et al., 2018; Pan et al., 2018; Suzuki et al., 2018; Wu N. et al., 2018; Xu M. et al., 2018).

ECM REMODELING

The extracellular microenvironment is dynamically modeled and remodeled by soluble or EV-associated proteases secreted into the ECM or membrane-anchored proteases, which are classified as cross-linkers and remodeling proteases (Sanderson et al., 2019). Of the ECM cross-linkers, lysyl oxidases (LOX) and transglutaminases (TGs) are the major families responsible for establishing cross-links between the central core matrisome proteins. Moreover, an intricate balance between proteases and their inhibitors maintains the ECM homeostasis; abnormal ECM remodeling (excessive or inefficient) is involved in the development and/or progression of several pathologies due to modifications in macromolecule composition (posttranscriptional control and posttranslational modifications), biophysical (architecture), and biomechanical properties (stiffness).

ECM Cross-Linkers

Post-translational modifications (cross-links) in collagen–collagen, collagen–ECM, and ECM–ECM interactions are relevant for the integrity, stiffness, and rigidity of the microenvironment. Once formed, cross-links formed are immature but become more stable due to multivalent cross-links that generate insoluble protein polymers that are resistant to proteolytic degradation, improving the biomechanical properties of the collagen network. Procollagen maturation takes place when both N- and C-termini are classically removed by ADAMTS and BMP-1/TLD (BTPs), respectively, but this cleavage may also be mediated by meprins, forming tropocollagen (**Figure 3A**). Subsequently, three main pathways promote the final fibrillogenesis: the LOX-mediated, TG-mediated, and sugar-mediated cross-linking pathways (**Figure 3B**). The latter pathway constitutes a non-enzymatic glycosylation reaction that occurs as the consequence of prolonged exposure to reducing sugars (e.g., ribose and glucose), producing advanced glycation end products (AGEs), which are associated with aging and diabetic complications (Benkovics et al., 2017; Cruz et al., 2018).

The LOX and LOX-like (1–4) proteins are a family of copper-dependent amine oxidase enzymes that catalyze the formation of unstable aldehydes by the oxidation of the ε-amino groups of lysine/hydroxylysine in collagens and lysine in elastin, forming covalent cross-linkages in collagen–collagen and collagen–elastin complexes, respectively. LOX is secreted as a proenzyme into the ECM, but is also found intracellularly, and is then processed by BMP-1, the same enzyme that cleaves fibrillar procollagens (**Figure 3**). As such, there is a direct relationship between the collagen process and its cross-linking, suggesting a major role for LOX in ECM orientation (Rodriguez-Pascual and Rosell-Garcia, 2018).

The TGs [formed of nine members, including tissue TG (tTG) or TG2, which is the most abundant in tissues] belong to a multi-functional family of calcium-dependent acyl-transferase enzymes that catalyze transamidation of glutamine and lysine to form covalent bonds both inside and outside of the cell. These cross-links form between collagen–collagen, collagen–ECM, or ECM–ECM and can involve fibronectin, mainly, and also nidogen/entactin, osteonectin, osteopontin, laminin, vitronectin, fibrinogen, and heparan sulfate proteoglycan. Initially, the TG catalyzes the formation of an isopeptide bond between γ-carboxamide groups of glutamine residue side chains and the ε-amino groups of lysine residue side chains with subsequent release of ammonia. Subsequently, glutamine and lysine residues are available to bind with peptides or proteins, and the intra- or inter-molecular ε-(γ-glutamyl)lysine cross-links take place. In the presence of water, TGs are also able to hydrolyze glutamine residues to glutamic acid by deamidation (**Figure 3B**). These cross-links exhibit high resistance to physical, chemical, and proteolytic degradation, mainly by matrix metalloproteinases (MMPs). Physiologically, TGs generate biological polymers that are indispensable for creating barriers and stable structures in several systems, while pathologically, they contribute to generating fibrotic matrices (Eckert et al., 2014; Savoca et al., 2018).

ECM Remodeling Enzymes: Metalloproteinases

Most of the ECM remodeling enzymes belong to the metzincin family (Stöcker et al., 1995), which share numerous similarities, including multiple domains, zinc-dependent endopeptidases, a typical structural profile and tertiary configurations of the catalytic domain (the secondary structure contains three histidines bound to zinc, at the catalytic site, and a methionine, or "Met-turn"). This family comprehends vertebrate matrixins (MMPs), adamalysins (ADAMs—a family of disintegrin and metalloproteinase, mainly sheddases; and ADAMTSs—a family of disintegrins and metalloproteinases with thrombospondin-like motifs, mainly formed of proteoglycanases and procollagen N-propeptidases), astacins (BMP-1/Tolloid-like protease 1 and Meprins, mainly formed of procollagen N- and C-propeptidases), and pappalysins (main bioavailability of IGFs) (Cerdà-Costa and Gomis-Rüth, 2014) and encodes around 200 genes, identified in humans and mice, comprising around ⅓ of proteases, the largest proteolytic enzyme group existent (López-Otín and Bond, 2008). Among them, MMPs are classically recognized to degrade all ECM components, but other metalloproteinases have been recognized to play essential roles in ECM maturation and to generate bioactive molecules. As a result of the extensive study of ECM remodeling enzymes over the last six decades, other biological functions have also been attributed to them, due to their broad spectrum of substrates, identified in both subcellular and extracellular compartments (Bond, 2019). Other enzymes, such as urokinase-type plasminogen activator, cathepsins, and heparanases, are also indispensable in these processes, and growth factor bioavailability within the ECM is protease-dependent. As a result of the extensive study of ECM remodeling enzymes over the last six decades, other biological functions have also

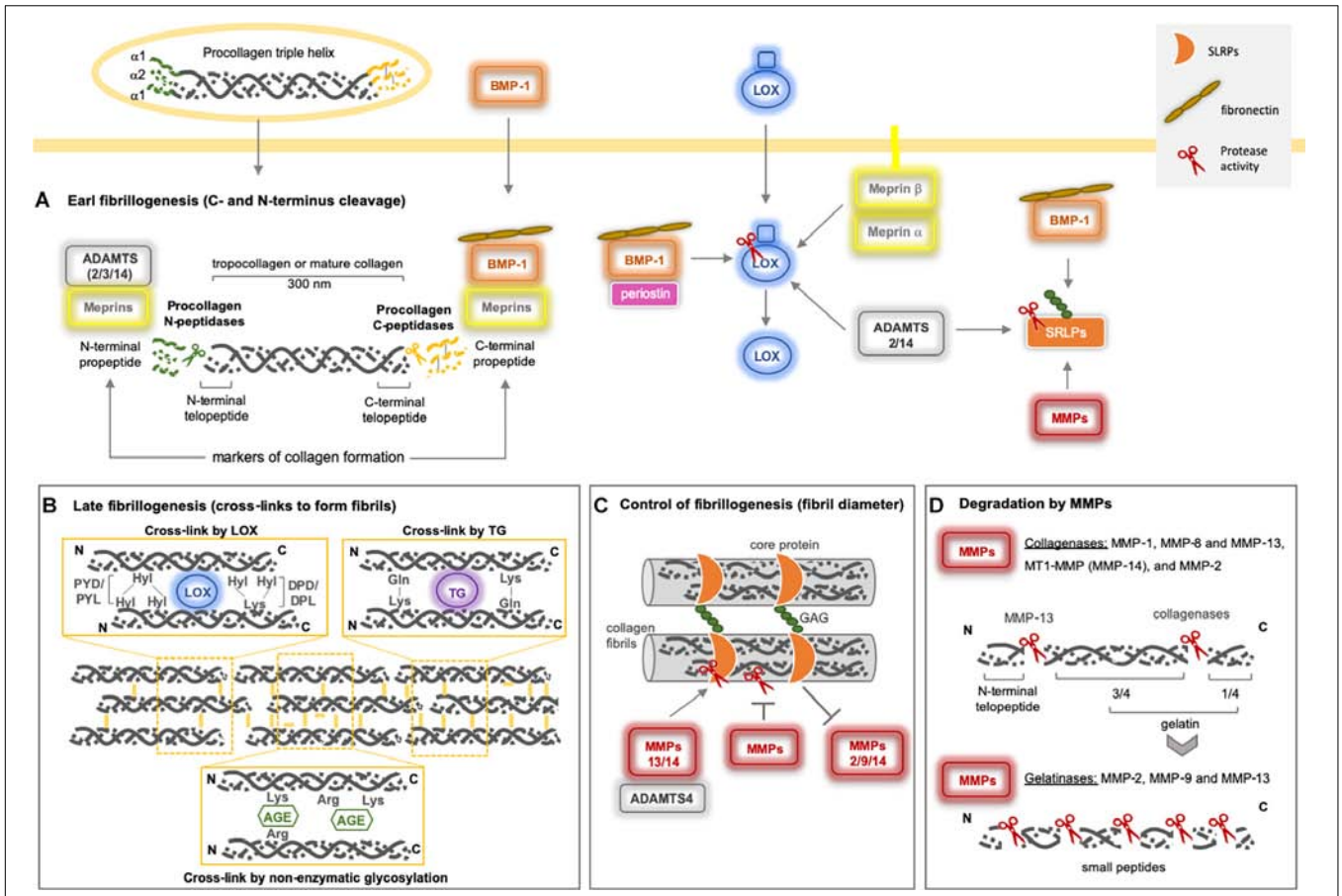

FIGURE 3 | Collagen type I assembly and degradation by metalloproteinases. **(A)** The early fibrillogenesis process on fibrillar procollagens starts by the excision of both the N- and C- termini by classical Procollagen N-peptidases (sub-group of the ADAMTS family) and Procollagen C-peptidases (BMP-1). They cleave procollagens I, II, III, and V (ADAMTS2/14 and BMP-1), where ADAMTS3 can cleave only procollagen II. Recently, both meprins have been reported to be able to remove both N- and C- terminus as well. **(B)** After N- and C- termini removal from procollagen, mature collagen is the target for ECM cross-linker enzymes (LOX and TG), which will form collagen fibrils. Under high glucose conditions, a non-enzymatic cross-link takes place, named AGE. **(C)** The level of collagen fibrillogenesisis controlled by proteoglycans (SRLPs), which can interact with collagen fibrils, resulting in the modification of the diameter of collagen fibers. Fibromodulin, decorin, and lumican prevent or delay the cleavage of collagen by MMP-1 and MMP-13. Lumican acts on MMP-14 enzymatic inhibition (Pietraszek et al., 2014) and gene expression (Niewiarowska et al., 2011; Malinowski et al., 2012). Decorin inhibits MMP-2 and MMP-9 gene expression and activity (Neill et al., 2012). MMP-14 can cleave human decorin (Mimura et al., 2009) and thelumican core (Li et al., 2004), MMP-13 and ADAMTS-4 also cleave decorin (Shu et al., 2019). **(D)** Among the metalloproteinases, only MMPs can cleave fibrillar collagens. The collagenases generate ¼ and ¾ fragments (gelatin) that are further cleaved by gelatinases (MMPs-2 and -9) and MMP-13. MMP-13 also removes the N-terminal telopeptide from collagen. Indirectly, metalloproteinases may modulate collagen fibrillogenesis by processing LOX and SRLPs. BMP-1 and ADAMTS2/14 activate proLOX in distinct sites and seem to be essential for LOX-collagen binding (Rosell-García et al., 2019). Periostin increases the proteolytic action of BMP-1 on proLOX (Maruhashi et al., 2010). BMP-1 promotes the maturation of SLRPs (von Marschall and Fisher, 2010), as well as the MMPs, after C-terminal excision. Fibronectin increases BMP-1 activity against biglycan and procollagen I (Huang et al., 2009). AGE: advanced glycation end products; ADAM: adisintegrin and metalloproteinase; ADAMTS: adisintegrin and metalloproteinase with thrombospondin motifs; LOX: lysyl oxidase; MMP: matrix metalloproteinase; SLRP: small leucine-rich proteoglycans; TG: transglutaminase.

been attributed to metalloproteinases, due to their broad spectrum of substrates, identified in both subcellular and extracellular compartments (Bond, 2019). We will focus only on metalloproteinases currently known to have a role in palatogenesis and CL/P.

Among metzincins, ADAMs, ADAMTSs, and MMPs are closely related in structure, regulation, and activation. However, they have different substrates and, therefore, distinct functions under physiological and pathological conditions. Structurally, the N-terminal ectodomain of most secreted MMPs is composed of pre-, pro-, and catalytic domains (metalloproteinase domain) and contains a furin region in all ADAM, ADAMTS, and membrane-anchorage MMPs. Complementary domains confer proteolytic specificity and localization. As such, MMPs are the most studied metalloproteinases and act in many cellular functions (e.g., proliferation, migration, differentiation, among others) due to their cleavage of substrates in the ECM, on the cell surface and intracellularly (cytoplasm and nucleus) to produce bioactive molecules. However, few studies have been conducted to understand the interrelationship between these metalloproteinases and how they work together to control cell behavior.

MMP Family

Over the years, the "degradative" activity of MMPs during physiological and pathological processes has led to their association with tissue destruction, due to their unique ability to cleave fibrillar collagens (Sprangers and Everts, 2019). However, "omic" studies and a better understanding of ECM dynamics support a broader role for MMPs in pathological and physiological events (Rodríguez et al., 2010). Several other core matrisome, ECM-associated proteins, and cell surface proteins, cleaved by MMPs, reveal hidden sequences and unblock the diverse cell functions (Butler and Overall, 2009; Deryugina and Quigley, 2010; Bauvois, 2012; Mannello and Medda, 2012).

Extensive reviews focus on MMPs regulation at both intra and extracellular levels and have been extensively reviewed. At the gene transcription level, signals from the ECM (cytokines, growth factors, EMMPRIN/ECM metalloproteinase inducer/CD147, integrins, ECM proteins, cellular stress, morphological changes, among others) significantly impact MMP expression. Mutations and polymorphisms in MMP genes (particularly in promoter regions), together with epigenetic modifications, have been shown to modulate MMP expression. Post-transcriptional regulation includes changes in mRNA stability through microRNAs, decoy RNAs, and degradation pathways. MMPs are targets of several PTMs that are crucial for correct cellular localization (via insertion of the GPI-anchor), intracellular activation of membrane-anchoring MMPs by furins, and insertion of carbohydrates (*N* and *O*-glycosylation) (Boyd, 2006; Reuben and Cheung, 2006; Vincenti, 2007; Clark et al., 2008).

In the ECM, soluble proenzymes are activated by other proteinases, mainly active MMPs, via the "cysteine switch mechanism." The catalytic activity may be inhibited by their endogenous inhibitors in the ECM (TIMPs) or on the cell membrane (RECK). Additionally, their proteolytic activity may be modulated by allosteric control in exosites outside of the catalytic site and also by interactions with proteoglycans and GAGs (Pietraszek-Gremplewicz et al., 2019). For example, MMP-2 interacts with syndecan-2 on the cell surface, which blocks the activation of proMMP-2. In some cases, proenzymes are associated with TIMP (low concentration) for correct activation; for example, the MMP-14/TIMP-2/proMMP-2 ternary complex. MMPs may be associated with other ECM components, such as proteoglycans and GAGs, leading to their specific localization in the cellular perimeter or at ECM sites distant from the cell secretion point (Van den Steen et al., 2001; Hernandez-Barrantes et al., 2002; Ra and Parks, 2007; Gabison et al., 2009; Hadler-Olsen et al., 2011; Piperi and Papavassiliou, 2012; Rietz and Spiers, 2012; Li et al., 2014; Arpino et al., 2015; Karamanos et al., 2019).

Due to their unique ability to cleave fibrillar collagens, collagenases MMP-1, -8, and -13 are the main enzymes for collagen turnover and generate gelatin (classical ¾ and ¼ fragments) (**Figure 3D**). MMP-2 and -9, along with membrane-anchored MMPs (MMP-14 and MMP-16), may also cleave fibrillar collagen with different affinities, as is the case of collagen I and III, which are preferentially cleaved by MMP-1, whereas collagen II is the preferred substrate for MMP-13. Additionally, stromelysins (MMP-3 and -10) can degrade just collagen III, but not collagen I or II (Sprangers and Everts, 2019). The interaction of the N-terminal site of specific SRLPs (decorin, fibromodulin, and lumican) with collagen fibrils forms a layer that can prevent or delay the collagen cleavage by MMPs (Geng et al., 2006). At the same time, different SRLPs are substrates or inhibitors of MMPs and ADAMTS (Shu et al., 2019; **Figure 3C**).

ADAMTS Family

N-glycosylation, O-fucosylation, and C-mannosylation are the most frequent post-translational modifications (located at the ancillary domains) to control ADAMTS activity. These modifications control secretion, localization, activation, and catalytic functions. Cleavage of the central thrombospondin type 1 sequence repeat (TSR—probably attached to the cell membrane) regulates both the proteinase activity and the localization of these enzymes. The proenzymes can be activated intracellularly, on the cell surface or within ECM by furin-like pro-protein convertases and then autocatalytic activation. Similarly to ADAMs, ADAMTSs are selectively inhibited by TIMPs, where TIMP-3 is the principal inhibitor (Bekhouche and Colige, 2015; Kelwick et al., 2015; Dancevic et al., 2016).

Although ADAMTS-like homologues lack protease domains, ancillary domains are present and may be involved in the regulation of ADAMTS due to competitive binding to substrates. Furthermore, they may have ADAMTS-independent functions in ECM, cell–EMC, or cell–cell interactions. Recently, an unexpected interaction between LOX-ADAMTSLs was reported, suggesting a role in microfibril assembly (Aviram et al., 2019). Mutations or deletions in ADAMTS have been implicated in many pathologies and syndromes, where they modulate tissue morphogenesis and remodeling, in cancer, inflammation, in the central nervous system, and in cartilage and vascular biology (Kintakas and McCulloch, 2011; Stanton et al., 2011; Lisi et al., 2014; Dubail and Apte, 2015; Hubmacher and Apte, 2015; Kelwick et al., 2015; Rodríguez-Manzaneque et al., 2015; Dancevic et al., 2016; Fu and Kong, 2017; Itoh, 2017; Lemarchant et al., 2017; Yang et al., 2017; Mead and Apte, 2018).

THE ROLES OF MMPS AND TIMPS IN PALATOGENESIS

The development of the facial primordia requires remodeling of the ECM, which is mediated in part by MMPs. During embryonic development, the process of morphogenesis involves MMP-mediated changes in the composition of the ECM that further allow for cell migration and differentiation, cell–cell interactions, and tissue resorption. MMPs act on ECM remodeling during palatal shelves orientation and during EMT events for palatal fusion (Brown et al., 2002).

Early studies in mice have provided biological evidence for the roles of MMPs and TIMPs in embryonic development (Gack et al., 1995; Iamaroon et al., 1996; Blavier and DeClerck, 1997). Several MMPs, TIMPs, and RECK mRNA and proteins are expressed, in association with enzymatic activity, throughout the stages of murine palate development. These expressions share the same specific spatial and temporal distribution patterns in areas in which their preferred substrates are also present

(Mansell et al., 2000; Morris-Wiman et al., 2000a,b; Blavier et al., 2001; Brown and Nazarali, 2010; de Oliveira Demarchi et al., 2010; Gkantidis et al., 2012).

The secretion of GAGs in the palatal mesenchyme is related to an increase in water content, and the specific accumulation of collagen I in the nasal side of the palatal mesenchyme may be necessary to generate internal forces required for shelf elevation. Furthermore, MMP expression increases in both the medial and oral epithelium before shelf elevation (Morris-Wiman et al., 2000a; de Oliveira Demarchi et al., 2010), as does MMP gelatinolytic activity in the basement membrane and beneath the mesenchyme of the nasopharyngeal epithelial folds that form during palatal shelf reorientation from vertical to horizontal position (Gkantidis et al., 2012; **Figure 4A**).

At ED13 and ED14, the secreted inhibitors, TIMP-1 and TIMP-2, display a similar spatial distribution to the MMPs and are widely expressed in the epithelial basement membrane. TIMP-3 is strongly expressed in the palatal epithelium although weakly expressed in the medial mesenchyme (Morris-Wiman et al., 2000a). Of the four TIMPs, TIMP-2 is the most abundant (Mansell et al., 2000), whereas TIMP-3 has different roles than the other TIMPs. Animals lacking the *Timp3* gene develop several pathologies associated with increased ECM degradation and loss of tissue integrity due to unregulated MMP, ADAM, and ADAMTS activity (Sahebjam et al., 2007). The anchored-membrane MMP inhibitor, RECK, is also expressed in the mesenchyme (de Oliveira Demarchi et al., 2010). RECK expression has been implicated in tissue integrity since its absence leads to extensive disarrangement of the connective tissue and embryos die *in utero* before craniofacial development (Oh et al., 2001). Expression of TIMP-3 and RECK in the different sites of the developing palatal epithelium suggests that they function in the maintenance of palatal tissue integrity by regulating epithelial–mesenchymal interactions (**Figure 4B**).

Matrix metalloproteinases are fundamental for the removal of the basement membrane and are expressed by epithelial cells in the EMT program to detach from MES and migrate to the adjacent mesenchyme to allow palatal fusion (Horejs, 2016). The participation of the membrane-anchored MMPs (MMPs -14, -16, and -25) appear to be crucial in this process (Shi et al., 2008; Brown and Nazarali, 2010). These observations are reinforced by the results of *in vitro* studies showing that addition of synthetic MMP inhibitors (Blavier et al., 2001), or the silencing of MMP genes (e.g., MMP-25) (Brown and Nazarali, 2010) in palatal cultures can prevent palatal fusion. Furthermore, *Tgf*β*-3*- and *Egfr*-knockout mice, which display a cleft palate phenotype, have decreased or absent MMP expression in the MEE or MES (Miettinen et al., 1999; Blavier et al., 2001). Heparanase has also been detected in the MEE and MES and co-localized with MMPs -2, -3, and -9 (Hirata et al., 2013). MMP-25 can cleave only collagen IV and, in terms of substrates, displays more similarities to MMP-3 than other MT-MMPs (English et al., 2001). High gelatinolytic activity and laminin expression have also been found in the MEE and MES (Gkantidis et al., 2012). Furthermore, MMP-3 cleaves E-cadherin (Lochter et al., 1997) and MMP-25 is co-localized with E-cadherin in cell–cell junctions (Radichev et al., 2010), a crucial step for epithelial EMT cells to acquire a mesenchymal phenotype. Taken together, the basement membrane and epithelial cell–cell junction degradation require the cooperative proteolytic actions of MMPs and other ECM degrading enzymes in the MEE and MES cells (**Figures 4C,D**).

TGFβ-3 is expressed explicity in the palatal epithelium, and is co-expressed with MMPs (Blavier et al., 2001; Brown and Nazarali, 2010). In *Tgf*β*-3* null mice, TIMP-2 and MMP-13 expression in the palatal epithelia were significantly decreased, whereas no changes in expression were noted for MMP-14 (Blavier et al., 2001). Similarly, the incubation of palatal culture with a TGFβ-3-neutralizing antibody decreases MMP-25 expression in the palatal epithelia (Brown and Nazarali, 2010). Collectively, these observations suggest that both MMP-13 and MMP-25 are downstream targets of TGFβ-3 (**Figure 4C**). MMP-13 is specifically expressed in sites of bone formation *in vivo* (Fuller and Chambers, 1995; Gack et al., 1995; Mattot et al., 1995; Stahle-Backdahl et al., 1997), and in physiological situations that require rapid and effective remodeling of collagenous ECM.

While MMP and TIMP expressions appear to be critical throughout all stages of palatal development, knockout mice for *Timp1, Timp2*, *Timp3, Timp4, Mmp2*, *Mmp9*, *Mmp13*, *Mmp14*, *Mmp16*, and *Mmp25* do not develop cleft palate (Paiva and Granjeiro, 2014; Soria-Valles et al., 2016). Interestingly, combined double knockout of *Mmp14* and *Mmp16* in mice leads to severe structural and craniofacial defects, including severe dysfunction in palatal shelf formation and cleft palate in 80% of the embryos (Shi et al., 2008). Among the membrane-anchored MMPs, MMP-16 is closely related to MMP-14 in terms of molecular structure and expression patterns in remodeling tissues (Szabova et al., 2005; Shi et al., 2008). While these findings suggest that potential compensatory mechanisms exist to overcome the loss of function of individual MMP genes, they also suggest that the loss of specific MMPs, in combination, may impair embryonic and palate development. Moreover, while individual MMP genes may not contribute a major gene effect to non-syndromic CL/P (NSCLP) susceptibility, they may act as modifiers on the background of other genes.

CLEFT LIP AND/OR PALATE

Orofacial clefts result from the failure of developing embryonic facial and palatal processes to ultimately merge or fuse. A multidisciplinary team including surgical, dental, speech, genetic, and nutrition experts are typically involved in patient care to mitigate the feeding, swallowing, breathing, speech, and hearing complications inherent to the condition. Orofacial clefts can be categorized as syndromic or non-syndromic (also termed isolated), based on the presence of additional structural abnormalities. Over 500 syndromes, including chromosomal abnormalities, have been reported in association with orofacial clefts, comprising 30% of all cleft cases. The remaining 70% of cases are all non-syndromic (i.e., isolated), and may segregate in families or appear in sporadic cases (Mossey et al., 2017).

Non-syndromic orofacial clefts are the most common of congenital craniofacial disabilities, affecting approximately 1 in

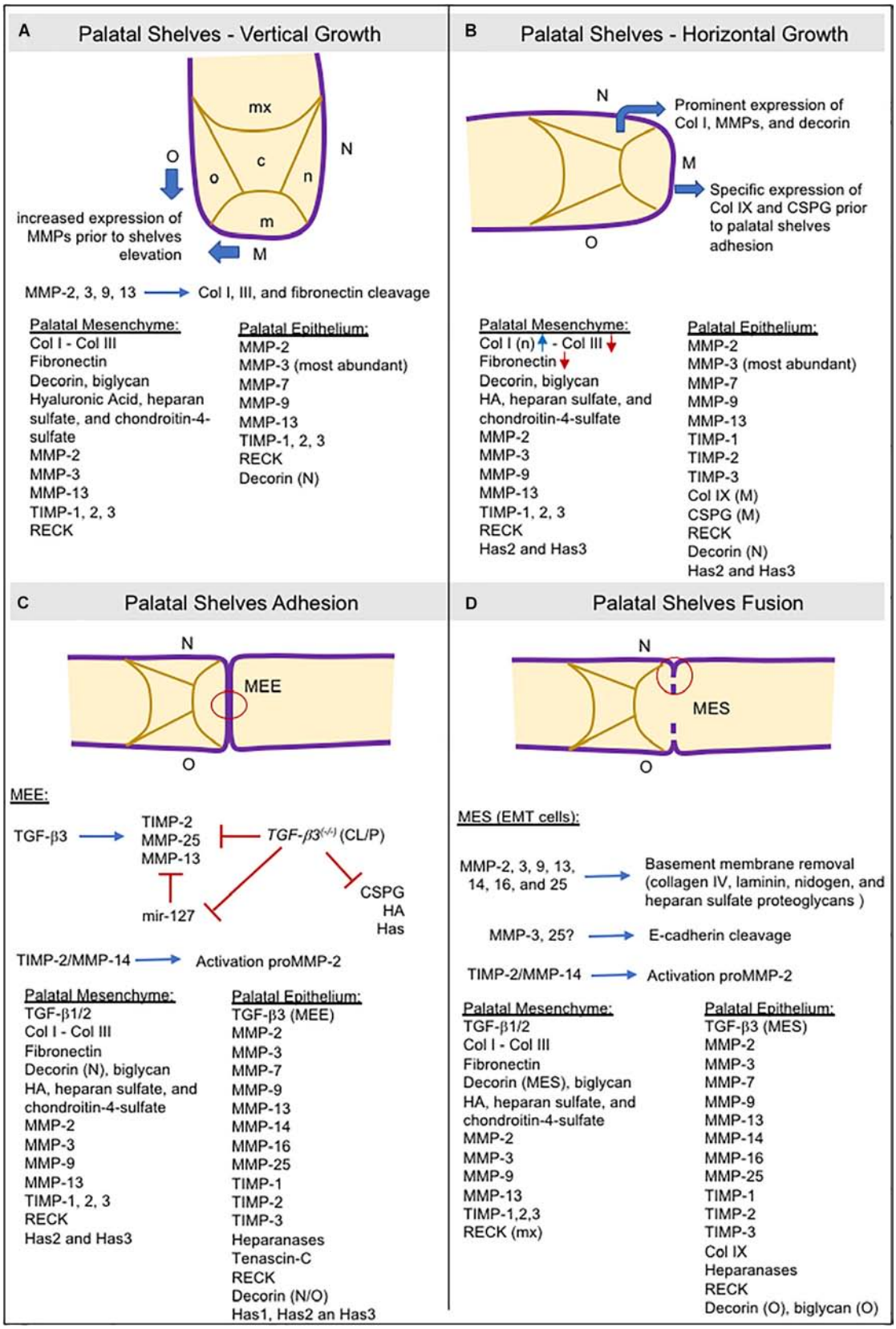

FIGURE 4 | Continued

FIGURE 4 | Schematic representation of consecutive steps during secondary palatogenesis and the molecules expressed in palatal mesenchyme ECM and palatal epithelium. Collagens type I and III, fibronectin, GAGs (hyaluronic acid, heparan sulfate, and chondroitin-4-sulfate), proteoglycans (biglycan, decorin), and TGF-β are the most abundant ECM molecules found in provisional ECM during palatogenesis. MMPs are the major protein responsible for ECM remodeling in both the ECM mesenchyme and basement membrane, but also expressing heparanases as well. Expression of TIMPs and RECK occurred, and they are crucial for ECM remodeling balance. **(A)** Most ECM components are widely present in palatal mesenchyme. MMP expression is high in the oral and medial epithelia before shelve elevation. **(B)** The increased expression of collagen I and decorin in the nasal region of the palatal mesenchyme may help with palatal elevation. Decorin can bind to collagen I and cause contraction of collagen *in vitro*. In the medial epithelium, the specific expression of collagen IX and CSPG is vital for adequate palatal shelve adhesion. **(C)** TGF-β3 modulates the expressions of TIMP-2, MMP-13, MMP-25, and CSPG in the MEE. TGF-β3 knockout mice downregulated these genes. mir-127 is upregulated, leading to repression of MMP-13 expression (Warner et al., 2015). **(D)** Other MMPs are required for MES disruption and are involved in basement membrane degradation by EMT cells. CSPG: chondroitin sulfate proteoglycans; EMT: epithelial-to-mesenchymal transition; HA: hyaluronic acid; Has: hyaluronan synthases; M: medial site; m: medial region; MEE: medial edge epithelia; MES: medial epithelial seam;mx: maxillary region; n: nasal region; N: nasal site; o: oral region; O: oral site; TGF-β: transforming growth factor beta.

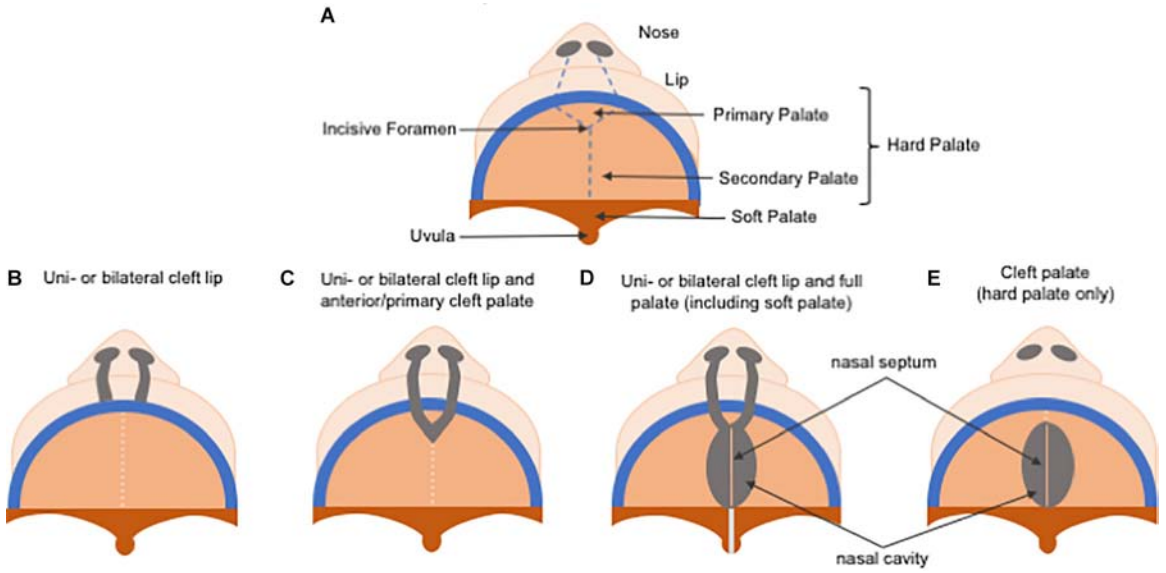

FIGURE 5 | Schematic representation of cleft lip and/or palate classification. **(A)** Normal palate. **(B)** In uni or bilateral cleft lip, only lip reconstruction is necessary. **(C)** In uni or bilateral cleft lip and anterior/primary cleft palate, repair of the alveolar bone repair in the primary hard palate (pre-maxilla) is also required. **(D)** In uni or bilateral complete cleft lip and palate, treatment is the most challenging due to the need to repair both primary and secondary palate, and the soft palate is affected as well. **(E)** A cleft palate, which only comprises the secondary palate.

700 live births worldwide each year, and have been divided historically into cleft lip, with or without cleft palate (CL/P), and cleft palate only (CP), due to the distinct developmental origins of the lip and the palate (**Figure 5**). While their reported prevalences vary considerably according to ancestral origin, Asians are the most frequently affected population, with birth prevalence rates as high as 1 in 500 live births, followed by Caucasians with a prevalence rate of about 1 in 1000 live births, and African populations showing the lowest prevalence rates at approximately 1 in 2500 live births (Kadir et al., 2017; Mossey et al., 2017; Ishorst et al., 2018). The presence of CL/P also differs by sex and laterality, with CL/P being more common in males than females at a 2:1 ratio, and CP being more common in females, meanwhile unilateral left CL/P is more common than unilateral right CL/P at a 2:1 ratio.

The etiology of non-syndromic orofacial clefts is complex, with both genetic and environmental factors contributing to the condition. While the identification of the genes involved in the syndromic forms of clefting has been mostly successful, much remains to be learned about the factors involved in non-syndromic cases. Genetic studies to date, using both family-based and case-control research approaches, have identified several genes and loci that may play a role in susceptibility to oral clefts (Vieira, 2008). Of these, the evidence is particularly strong for MSX1, IRF6, FOXE1, MAFB, WNT3, WNT9B, CRISPLD2, FGFR1, FGF8, BMP4, and the 8q24 chromosome region. Additional variants in numerous other genes (e.g., *TGF-β3*, *TGF-α*, *MMP3*, *VAX1*, *ABCA4*, *AXIN2*) have also been suggested as candidates for oral clefts with population-specific effects (Dixon et al., 2011; Beaty et al., 2016).

ECM REMODELING ENZYMES AS CANDIDATE GENES FOR OROFACIAL CLEFTS

Matrix metalloproteinases and TIMPs have been considered plausible candidate genes for CLP, based on their expression

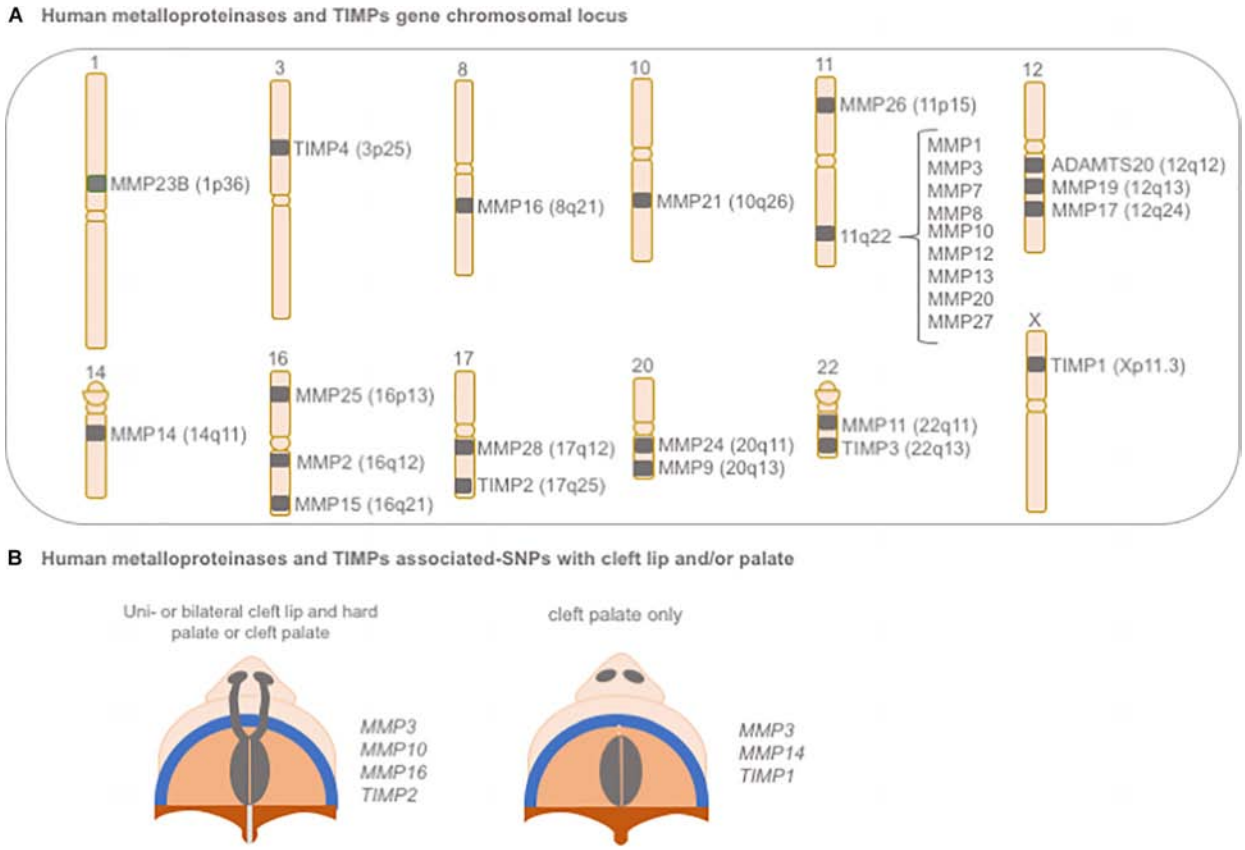

FIGURE 6 | Schematic representation of **(A)** gene chromosomal locus of human metalloproteinases and TIMPs and **(B)** their associated-SNPs with cleft lip and/or palate. SNP: single nucleotide polymorphism.

patterns in craniofacial tissues and their roles in tissue remodeling and morphogenesis during early embryogenesis; however, a functional role for any individual MMP or TIMP in palate development remains unknown (Brown et al., 2002; Verstappen and Von den Hoff, 2006).

In humans, significant associations between polymorphisms in MMP and TIMP genes with NSCLP have been reported (Blanton et al., 2004; Nikopensius et al., 2011; Letra et al., 2012; **Figure 6**). A large genome scan of multiplex NSCLP families first suggested evidence for linkage within a region on chromosome 16p13.3, in the same location for *MMP25* (Blanton et al., 2004). A later large and comprehensive study evaluated 45 polymorphisms spanning all biologically relevant MMP and TIMP genes for their association with NSCLP; significant associations ($P < 0.0004$) were noted for variants in *MMP3* (rs3025058, rs522616) and *TIMP2* (rs8179096), when considering CL/P, CP, and all cleft cases combined. Additional nominal associations were also found for variants in *MMP16* (rs7828497, $P = 0.01$) and *MMP10* (rs17293607, $P = 0.06$) in CL/P and all cleft cases. For CP, variants in *MMP3*, *MMP14*, and *TIMP1* also showed nominal associations ($P < 0.05$). Of note, certain allele combinations (i.e., haplotypes) involving these MMP and TIMP gene variants were also significantly associated with NSCLP (Letra et al., 2012).

Two polymorphisms, -1171 5A/6A (rs3025058) and -709 A/G (rs522616), located in the *MMP3* gene promoter were significantly associated with NSCLP and shown to have functional effects on gene transcription and protein function. The 5A/6A polymorphism consists of a common adenine insertion/deletion polymorphism (5A/6A) at position -1171 of the gene promoter and modulates transcription and local expression of the MMP-3 protein. The 6A allele showed an approximately twofold lower amount of gene product, compared with the 5A allele (Ye et al., 1996), and this difference in promoter activity was attributed to a likely differential binding of the transcriptional repressor to the 6A allele (Mercapide et al., 2003).

A positive regulatory element has also been described for *MMP3* -709 A/G, for which significantly higher (∼3.4-fold) promoter activity was found in the presence of allele A. This suggested that allele A can enhance promoter activity, possibly by augmenting transcription factor binding. Furthermore, this variant also appears to be modulated by the concomitant occurrence of the -1171 5A/6A variant. When analyzing the transcriptional effects of haplotypes containing both the -1171 5A/6A and -709 A/G variants, a 1.5-fold decrease in activity was observed for the combination of 5A_A alleles, in comparison with the 5A_G haplotype. Although speculative, this finding may represent a negative feedback loop effect, in an attempt to limit

transcription in the presence of the two "high transcription" alleles, 5A and A. In contrast, a fourfold increased activity was found with the 6A_G promoter. The 6A_A haplotype was the least active promoter, suggesting potential gene downregulation with this allelic combination (Letra et al., 2014). Taken together, these observations indicate that the -709 A/G variant may directly regulate *MMP3* promoter activity, although its function was shown to the driven by the 1171 5A/6A alleles in the background.

Polymorphisms in the *TIMP2* gene have also been associated with NSCLP in different populations. A promoter variant in *TIMP2* (-180C/T; rs8179096) was strongly associated with oral clefts in a Brazilian population, whereas additional variants of unknown significance (intronic) were associated with NSCLP in US and Northeastern European populations (Nikopensius et al., 2011; Letra et al., 2012). Furthermore, functional analysis suggests that this variant has distinct allele-dependent effects, with the T allele presenting a 2.5-fold increased promoter activity. Furthermore, both C and T alleles were found to be putative binding sites for NFκB, a key transcription factor involved in the innate immune system. While C and T alleles reduced binding capability when NFκB consensus binding oligo diverges from protein in the same reaction, introduction of a mutant NFκB immunized C and T alleles from binding abolition (Letra et al., 2014). Additional studies are still necessary to unveil the exact mechanisms by which MMPs and TIMPs might contribute to NSCLP; nonetheless, allelic polymorphisms in these genes and their interactions may partly explain the variance in individual susceptibility to oral clefts.

Few studies have described roles for other ECM remodeling or cross-link enzymes during palatogenesis and their potential association with CL/P. ADAMTS-9 and -20 have been shown to participate in versican remodeling during palatogenesis (Enomoto et al., 2010); furthermore, ADAMTS-9 null mice die *in utero* (Dubail and Apte, 2015). During physiological palate formation, ADAMTS9 expression in the palatal shelves was restricted to microvascular endothelial cells, derived from the mesoderm, whereas CNC-derived mesenchymal cells express ADAMTS20; in contrast, the expressions of ADAMTSs 4 and 5 were not detected during palatogenesis (Enomoto et al., 2010). More recently, a genome-wide association study in both dogs and humans independently identified *ADAMTS20* as a potential candidate gene for clefting. A region on chromosome 27 in dogs was found to segregate with a complex phenotype of cleft palate and syndactyly; follow-up whole genome sequencing studies then identified a frameshift mutation in the *ADAMTS20* gene as potentially etiologic. Furthermore, four novel risk variants in *ADAMTS20* were identified in Guatemalan cases with NSCLP (Wolf et al., 2015).

Additional genes with roles in collagen maturation and other ECM molecules have also been suggested to play a role in NSCLP. The *LOXL3* gene located on chromosome 2p13.1 and mutations in this gene have been reported in association with Stickler syndrome (MIM #108300), an autosomal recessive disorder characterized by ocular, auditory, skeletal, and orofacial abnormalities (Alzahrani et al., 2015). In mice, the deletion of *Loxl3* causes neonatal mortality due to impaired collagen assembly and cross-linking, as well as spine deformity and cleft palate (Zhang et al., 2015). Furthermore, its ortholog in zebrafish is required for adequate craniofacial morphogenesis, as its loss of function results in abnormal chondrogenesis with micrognathia or agnathia phenotype (van Boxtel et al., 2011). Recently, a missense mutation in *LOXL3* (rs17010021; p.Ile615Phe) was reported to contribute to an increased risk of NSCLP (10-fold) in a European population (Khan et al., 2018).

NEW APPROACHES TO STUDYING PALATOGENESIS AND CL/P *IN VITRO*

Studies of both palatogenesis and CL/P are usually carried out in animal models (mouse, chicken, zebrafish, and rat, respectively), especially mice, given the similarity of biological events in these animals to humans (Van Otterloo et al., 2016; Lough et al., 2017). *In vitro*, the most common method of study employs murine embryonic palatal cell culture and *ex vivo* palate organ culture (**Figure 7A**; Abbott, 2019).

Three-dimensional (3D) cell culture represents a promising approach to better elucidate cell behavior, ECM remodeling, tissue remodeling, and tissue fusion, and ultimately to investigate clinical applications for tissue engineering (Ong et al., 2017). 3D constructs are more similar to the tissue microenvironment than classical 2D cell cultures (plastic-based) as they demonstrate more realistic cell morphology and physiology; furthermore, observation of 3D cultures over time is considered to represent 4D systems (Bissell, 2017). Thus, over the last decade, numerous reviews have illustrated the switch from 2D to 3D cell cultures. Several methods to create 3D structures have been described, such as cell aggregates, spheroids or organoids (Alhaque et al., 2018), seeded onto decellularized matrices (Taylor et al., 2018), and cell sheets (Kim et al., 2019). Among these, cell spheroid is a technology in which cells are cultured in suspension to create a 3D structure using cell–cell interactions and "scaffold-free" strategy (**Figure 8B**). This technique yields detailed information regarding ECM remodeling through "omics" analysis since the generation, growth, and fusion of cells allow accurate monitoring (Fan et al., 2018; Schnellmann et al., 2018; Wong et al., 2018). Understanding the ECM and its soluble factors are essential to comprehend embryonic development and tissue repair and will contribute to the discovery of new therapeutic tools. Proteomics is an appropriate strategy to characterize ECM components under physiological and pathological conditions. A significant challenge for studying the ECM constitutes its solubilization and protein recovery. An optimized protocol developed by Naba et al. (2017) permitted the digestion of proteins into peptides that could be analyzed by mass spectroscopy; web tools were allowed the annotation and relative quantitation of the ECM proteins. These protocols allow a faster analysis of differentially expressed proteins in the ECM, eliciting the identification of biomarkers and therapeutic targets.

Stem cells from many tissue origins, especially MSCs, have been widely employed in 3D constructions due to their effortless isolation from various tissues of the body, potential for differentiation into mesenchymal and non-mesenchymal lineages, and therapeutic use (Han et al., 2019).

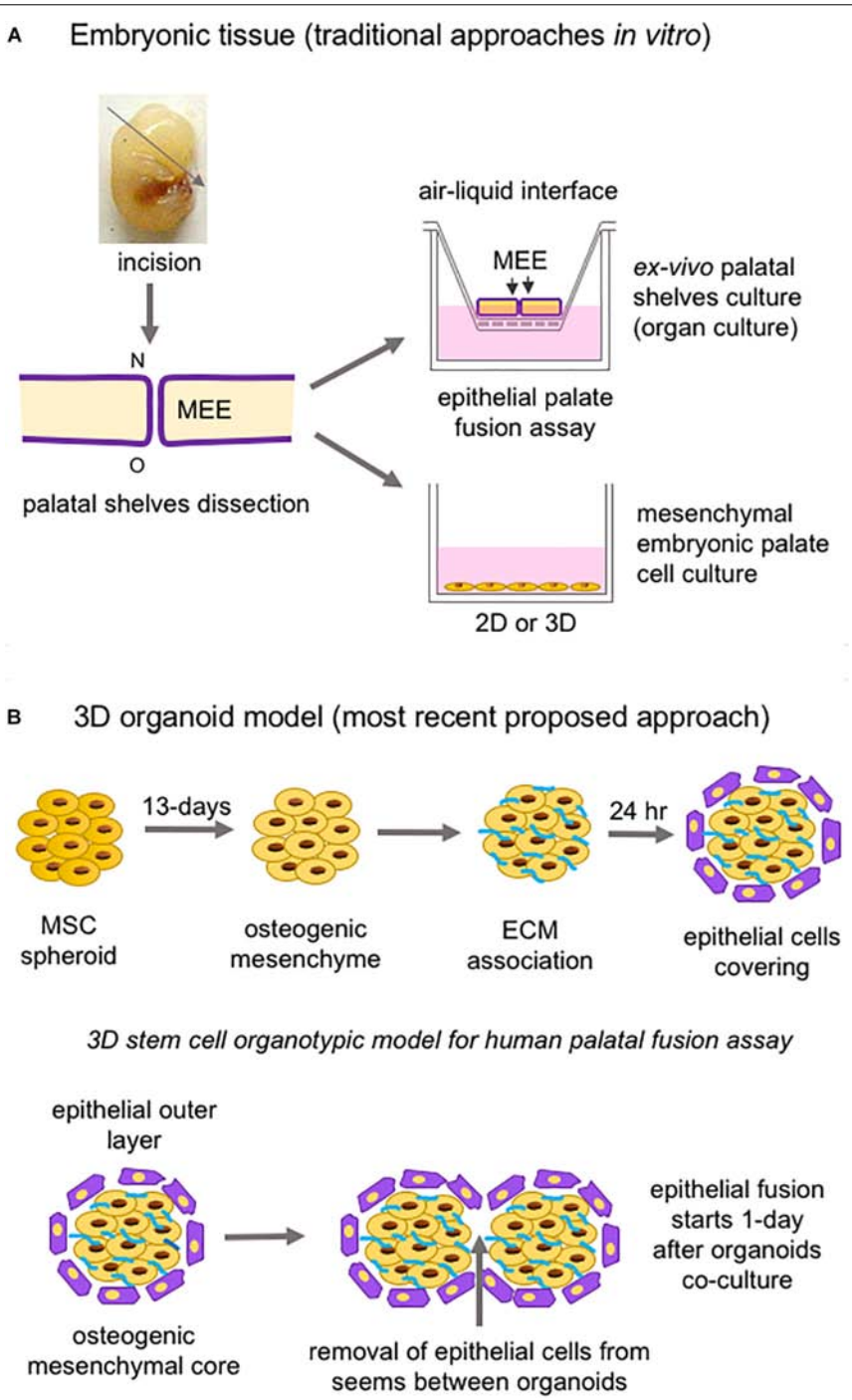

FIGURE 7 | Schematic representation of *in vitro* approaches to study palatogenesis. **(A)** The most traditional method is the mouse embryonic palate dissection before palatal shelves fusion; the dissected palate is placed on a membrane insert, and the top part is in an air-liquid interface (organ culture); also, mesenchymal embryonic palate cells are cultivated under adhesion and monolayer on or not embedded into a substrate. **(B)** The newest proposed 3D organoid model using mesenchymal stem cells and epithelial cells to form spheroids/organoids to mimetize the epithelial fusion. ECM: extracellular matrix; MEE: medial edge epithelia; MSC: mesenchymal stem cell; N: nasal site; o: oral region; O: oral site.

Cell spheroids to study epithelial palate fusion are available, and strategies employed consist of creating mesenchymal spheroids from human umbilical-derived MSCs undergoing osteogenic differentiation, covered with ECM to mimic basement membrane, which are then seeded with human progenitor epithelial keratinocytes. This 3D organotypic model of human

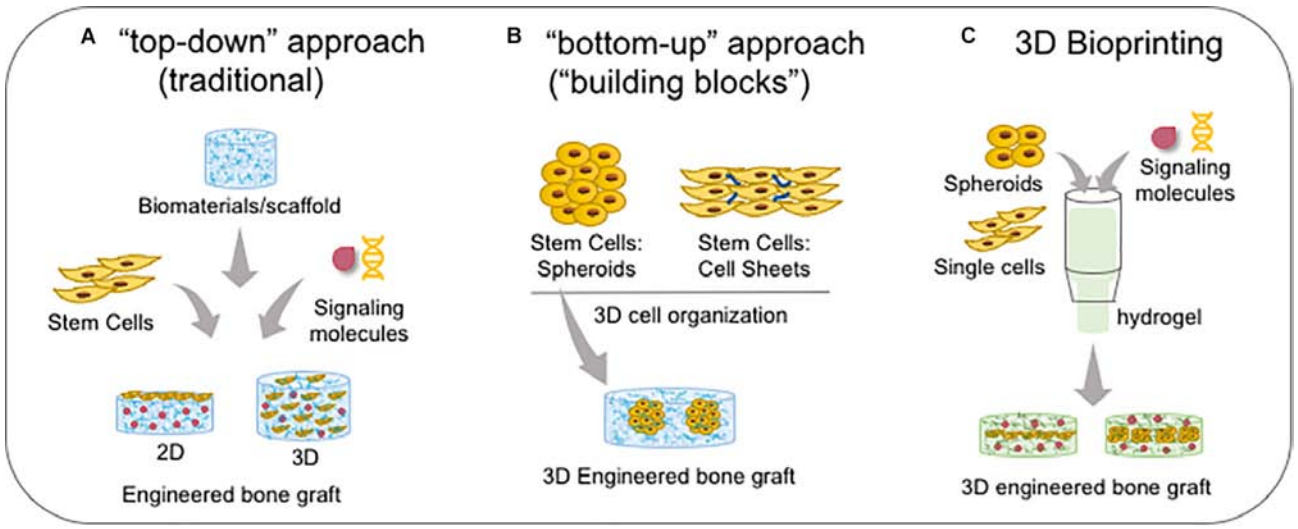

FIGURE 8 | Bone bioengineering based-techniques. **(A)** Traditional "top-down" approach which stem cells are associated with biomaterials and signalling molecules to create a 2D (when single cells are seeded onto the substrate/biomaterial) or 3D microenvironment (when single cells are seeded into the substrate/biomaterial). **(B)** The newest "bottom-up" approach which cells are self-assembled in a 3D conformation by cell-cell and cell-ECM interactions as spheroids or cell sheets, forming the functional "building blocks"; spheroids can be embedded into scaffolds/biomaterials. **(C)** Both sing cells and spheroids and/or signalling molecules are the components of bioink in association with a hydrogel, and then it is bioprinted in a specific 3D engineered bone graft.

palatal shelves can maintain cell viability for around 4 weeks, expresses alkaline phosphatase, and is responsive to EGF, leading to increased epithelial proliferation and the prevention of epithelial fusion between spheroids (**Figure 7B**; Wolf et al., 2018). A potential bias relies on the fact that the MSCs used in the spheroid generation do not have the same embryonic origin as the palatal mesenchyme or the epithelial cells.

STATE-OF-THE-ART OF CLEFT PALATE REPAIR AND PALATAL RECONSTRUCTION

Bone Regeneration

Bone repair is a mechanism in which bone development program is recapitulated to form new intramembranous or endochondral bone at injured sites. Intense ECM bone remodeling by MMPs is required (Paiva and Granjeiro, 2017) as well as the action of several growth factors (TGF-β, BMPs, FGFs, IGFs, PDGFs, and VEGFs), which are implicated in driving osteochondral differentiation, regulation of bone formation, and are responsible for triggering intracellular pathways, such as Wnt (Houschyar et al., 2019). Additionally, other metalloproteinases are important for collagen maturation and mineralization. PPAP-A increases osteoblast proliferation *in vitro* and bone formation *in vivo* by augmenting IGF bioavailability upon cleavage of IGFBP-4 (Qin et al., 2006). PPAP-B expression was associated with postnatal skeletal growth, bone mass, and structure due to cleavage of IGFBP-5, the most abundant IGF in bone (**Figure 9A**; Amiri and Christians, 2015; Christians et al., 2019).

In bone and dentin matrices, BTPs can cleave the acidic domain of SIBLINGs (small integrin-binding ligand, N-linked glycoproteins), specifically DMP-1 and DSPP (dentin sialophosphoprotein—generating DPP/dentin phosphoprotein), leading to an increase in the binding affinity of these proteins for calcium, which is necessary for mineralization and improving ECM stiffness (Steiglitz et al., 2004; von Marschall and Fisher, 2010; Tsuchiya et al., 2011). BMP-1 is highly expressed in both endochondral and intramembranous ossification sites during development and contributes to an increase in bone repair (Grgurevic et al., 2011). In addition, *BMP-1* expression is modulated by mutations in both alpha procollagen chains (Lindahl et al., 2011) and BMP-1-knockout mice develop an osteogenesis imperfecta-like phenotype due to inefficient procollagen processing and bone mineralization (**Figure 9B**; Muir et al., 2014). Although meprins also act on procollagen maturation and DSPP cleavage, meprin-β is inhibited in tissues with high concentrations of calcium and is, probably, not crucial in hard tissues since mice knocked out for meprins do not demonstrate alterations in bone and tooth development (Arnold et al., 2017).

Several ADAMs (8, 9, 10, 12, 15, 17, and 19) and ADAMTS (1, 4, and 5) are secreted by osteoblasts and bone tissue. Recently, ADAM17 has been reported to be a target of RUNX2 during osteoblastic differentiation, where ADAM17 is suppressed by RUNX2 (Araya et al., 2018). Human mutations in *ADAMTS10* and *17* are associated with related syndromes involved in alterations in skeletal development (Dagoneau et al., 2004; Morales et al., 2009). Recently, knockout mice for both *Adamts10* and *17* were shown to develop the recapitulate syndromic phenotype in human (**Figure 9C**; Mularczyk et al., 2018; Oichi et al., 2019). Reduced hypertrophic zone and increased deposition of fibrillin-2 alter the growth plates during endochondral ossification resulting in adults with short statures. Fibrillins

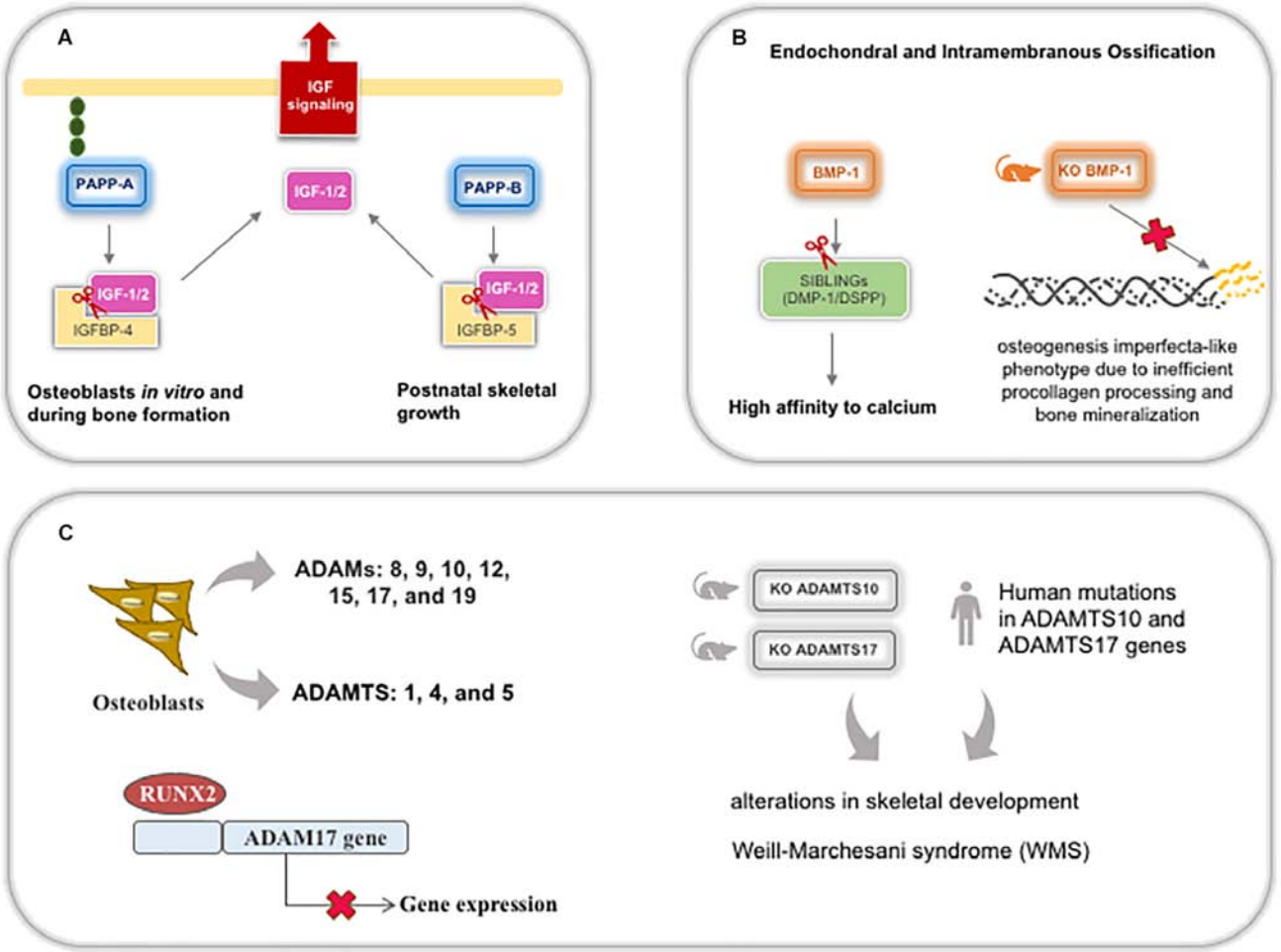

FIGURE 9 | Schematic representation of metalloproteinases (except MMPs) expression and roles during bone development and postnatal skeletal growth. **(A)** PPAPP-A and B cleavage the complex IGFBP/IGFs to bioavailable IGF for bone cells. **(B)** BMP-1 is important for SIBLINGs cleavage, specifically DMP-1 and DSPP, leading these glycoproteins to increase their affinity to calcium and contributing for mineralization. **(C)** Several ADAMs and ADAMTSs are expressed by osteoblasts, being ADAM17 downregulated by RUNX2 during osteoblastic differentiation. Both ADAMTS10 and 17 knockout mice and human mutations display the same bone phenotype recognized in Weill-Marchesani syndrome. ADAM: adisintegrin and metalloproteinase; ADAMTS: adisintegrin and metalloproteinase with thrombospondin motifs; DMP-1: dentin matrix acidic phosphoprotein; DSPP: dentin sialophosphoprotein; IGFBP: insulin-like growth factor binding protein; IGF: insulin-like growth factor; KO: knockout mice; PAPP: pregnancy-associated plasma protein.

are glycoproteins involved in microfibril formation and elastin deposition. Also, treatment with BMP-2 can rescue terminal chondrocyte differentiation, suggesting that ADAMTS17 is important for ossification through the modulation of BMP signaling (Oichi et al., 2019).

Extracellular matrix cross-linkers also contribute to bone formation and regeneration. In LOX knockout mice, general ECM architecture is profoundly affected in several tissues, and littermates die soon after birth. In bone, early and late osteoblastic differentiation and onset of mineralization are decreased in these mice as well as the gene expression of LOX isoforms (LOXL1-4) and osteoblastic markers (collagen type I, bone sialoprotein, and RUNX2) (Pischon et al., 2004).

The crosstalk between inflammatory cells, MSCs, chondrocytes, osteoblasts, osteoclasts, and osteocytes is necessary (Liu et al., 2018), and the success of bone regeneration results from the balance of the osteoprotegerin/RANK/RANKL axis. Most bone defects regenerate spontaneously; however, extensive bone loss due to trauma or aging-related fractures, metabolic bone disease, and congenital malformations do not regenerate *per se*, underscoring the search for better drug candidates. Biomaterials, biomolecules, and stem cells have been investigated to support bone repair, overcoming the limitations of autologous and allogeneic grafts (Collignon et al., 2017).

First Generation Palatal Reconstruction: Standard Surgical CL/P Management and Cleft Palate Repair

The treatment of CL/P patients is primarily surgical (plastic surgery for the lip and a bone graft for the palate) followed

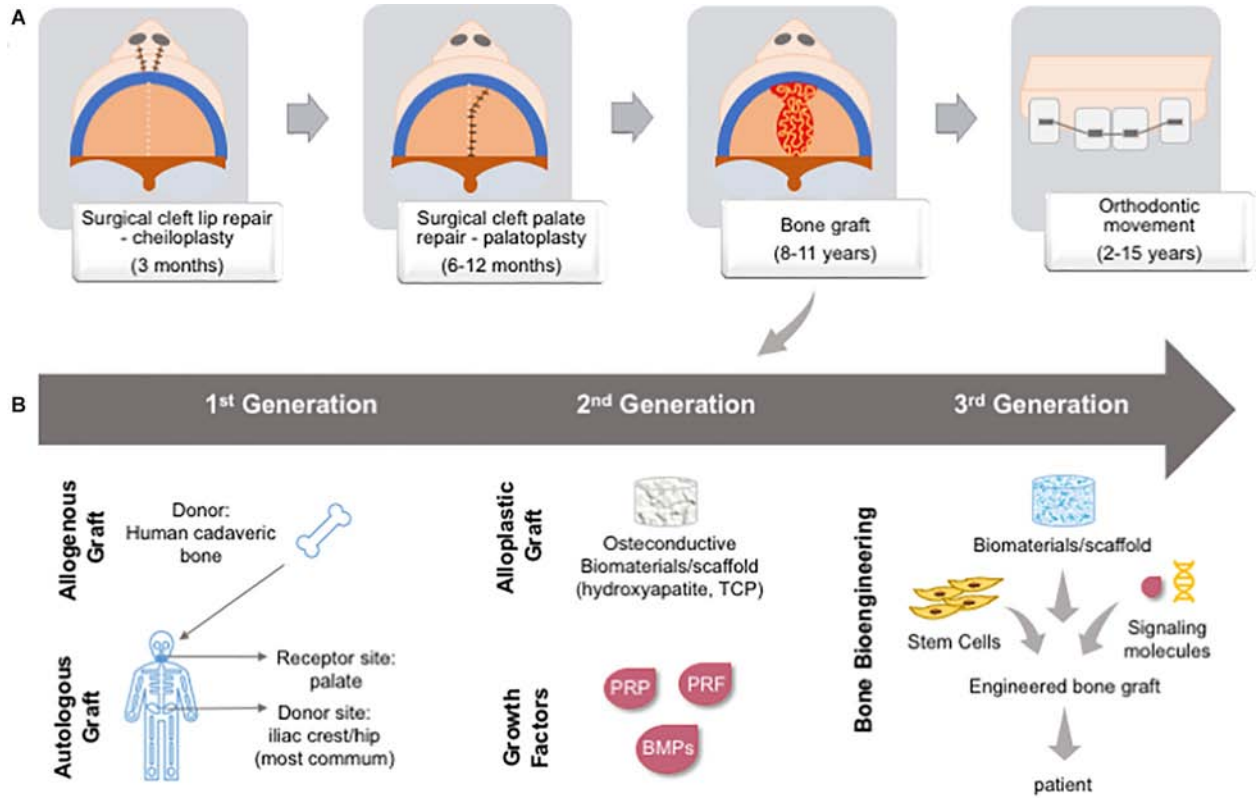

FIGURE 10 | Cleft lip and/or palate patient chronological management over time and types of bone graft. **(A)** First, patients are submitted to a lip reconstruction (around 3 months); followed by palate reconstruction (between 6–12 months); primary bone graft in the hard palate (between 8–11 years); and, then orthodontic movement (between 2–15 years). **(B)** Bone graft was developing from gold-standard autologous and allogenous graft (1st generation), the development of osteoconductive biomaterials and recombinant growth factors or natural adjuvants (2nd generation), and bone bioengineering is bringing a new possibility to associate stem cells from patient, biomaterials and signaling molecules to create an *in vitro* engineered bone graft to be implanted in the patient, being a personalized approach (3rd generation). BMP: bone morphogenetic protein; PRF: platelet-rich fibrin; PRP: platelet-rich plasma; TCP: tricalcium phosphate.

by orthodontic treatment in multiple stages over the years. The management is dependent on the cleft site, extension, and affected tissues (Farronato et al., 2014). The term "palatal reconstruction" is used to define any intervention able to restore the barrier between the oral and nasal cavities, and physiological functions. As such, several approaches, such as the lip and/or palate closure through plastic surgery, several types of bone graft, or a combination of these have been employed. More recently, the use of bioengineered bone has allowed palatal reconstruction (**Figure 10**). The decision with regard to the best treatment of choice depends on the type of CL/P and the extension of the tissue loss (Gupta et al., 2012).

Autogenous bone grafts are the gold standard for alveolar bone and cleft palate repairs. Throughout treatment stages, surgical procedures may require several grafts (e.g., primary, secondary, and tertiary graft). The most common bone donor sites are the anterior iliac crest, proximal tibia, mandibular symphysis, calvaria, and ribs. However, the bone amount and volume available from these sites are restricted, and a most advantageous site is still under debate. The use of autogenous bone graft has many drawbacks related to morbidity at the donor site, and patients may present chronic pain at the site, paresthesia of the thigh, and hypertrophic scar. The loss of the graft due to local inflammation, bone resorption, and the development of oronasal fistulas is also frequently associated with unsuccessful repair (Borba et al., 2014; Tavakolinejad et al., 2014; Shafi et al., 2015).

Second Generation of Palatal Reconstruction: Biomaterials and Growth Factors

Bone graft options available, such as allogeneic bone (Shirani et al., 2017), xenogeneic bone (Thuaksuban et al., 2010), and alloplastic graft (Kumar et al., 2013; Seifeldin, 2016; Sharif et al., 2016), still do not promote effective palatal reconstruction, stimulating the search for better alternatives. To overcome the limitations of autologous and allogeneic bone grafts, studies have investigated the use of the association, or not, of osteoconductive biomaterials, such as hydroxyapatite and tricalcium phosphate, with autologous bone graft or growth factors, such as BMP, which is known to stimulate bone formation and repair (Horch et al., 2006; Weijs et al., 2010; Lazarou et al., 2011; Benlidayi et al., 2012; De Ruiter et al., 2015; Takemaru et al., 2016;

Martín-Del-Campo et al., 2019). After the systematic review of 29 studies, just two were used for qualitative and quantitative analysis (Segura-Castillo et al., 2005; Dickinson et al., 2008). However, considering some aspects of randomization, allocation concealment, blinding, outcome data, and reporting, the authors concluded that the two selected articles presented a high risk of bias and that conclusions concerning the benefits of the interventions, compared to traditional iliac grafting, could not be made (Guo et al., 2011).

Growth factors such as BMPs (2, 4, and 7) and "natural adjuvant" platelet concentrates, denominated platelet-rich plasma (PRP) and platelet-rich fibrin (PRF), have been employed in palate reconstruction (Behnia et al., 2012; Seifeldin, 2016). Interestingly, PRF does not affect the expression of the RUNX2, BMP-2, or RANKL, but induces the expression of OPG, leading to the increase of OPG/RANKL, suggesting that PRF could boost osteoblastic differentiation (Sumida et al., 2019).

Clinical studies of alveolar bone repair in CL/P patients tested the association of BMPs or platelet concentrates with the gold standard of autologous bone graft. BMPs make relevant contributions to bone embryogenesis and repair (Salazar et al., 2016) and the inhibition of BMP receptors (Lai et al., 2016), mutations (Sahoo et al., 2011), and gene polymorphism (Savitha et al., 2015) are involved in cleft development. The association of bone graft with human recombinant BMP-2 (hrBMP-2) *in vitro* and *in vivo* demonstrated the production of mature bone (Shimakura et al., 2003). Furthermore, clinical studies corroborate that BMPs are, at least, just as efficient as autologous bone graft for the repair of alveolar/palate cleft (Chin et al., 2005; Canan et al., 2012; Ayoub et al., 2016; Hammoudeh et al., 2017). Very recently, 10 years of follow-up evidenced the safe use of BMP-7 for the reconstruction of the alveolar cleft (Ayoub and Gillgrass, 2019).

Evaluating the use of growth factors for the reconstruction of the alveolar cleft, Van Hout group accessed 291 studies using BMP-2, BMP-7, TGF-β, PDGF, IGF, FGF, VEGF, and PRP (van Hout et al., 2011). Only six articles met the authors' criteria for full analysis, who concluded that BMP-2 improved the quantity of bone formation during the reconstruction of the alveolar cleft, in association with reducing pain at the donor site, a reduction in surgery time, hospital stay, and overall cost. A recent study reported a similar effectiveness of autologous bone and rh-BMP2 during the maxillary reconstruction of cleft lip and palate patients (Scalzone et al., 2019).

A growing field of investigation aims to evaluate the use of cell-based therapies to treat alveolar and palate cleft (Gładysz and Hozyasz, 2015; Brozek et al., 2018) due to the ability of stem cells to differentiate into active osteoblasts that drive bone regeneration. Trabecular bone was enhanced after the treatment of 16 out of 17 alveolar clefts with MSCs together with hrBMP-2, but long-term follow-up studies are still needed (Fallucco and Carstens, 2009).

Two recent systematic reviews addressed the role of BMP2 (Scalzone et al., 2019) and tissue-engineered bone replacement materials (Kamal et al., 2018) in the efficient treatment of palate and alveolar cleft. Both studies concluded that there was no statistical difference between the autologous bone graft and the alternative materials. The meta-analysis comparing the bone repair with iliac crest bone graft (ICBG) versus BMP-2, acellular dermis matrix membrane, and cranium or rib grafts, indicated that ICBG is still the best choice for treatment (Wu C. et al., 2018). The association of BMP-2 with a collagen sponge provides similar results to those of ICBG, and PRP associated with ICBG increased bone retention for skeletally mature patients. However, better-designed controlled studies are required for long-term analysis of alveolar cleft reconstruction, with follow-ups of greater than 12 months (Seifeldin, 2016; Liang et al., 2018; Wu C. et al., 2018). Furthermore, the development of a consensus for standardized protocols, using multicenter studies, is still needed (de Ladeira and Alonso, 2012).

Third Generation of Palatal Reconstruction: Bone Bioengineering

Tissue bioengineering represents a new therapeutic alternative for palatal reconstruction, associating the use of stem cells, biomaterials/scaffolds, and signaling molecules. Two main approaches are dominant: the "top-down" approach, in which classically cells are seeded on or into biomaterials for recreating a new 3D tissue *in vitro*; and the "bottom-up" approach, which uses 3D construction techniques (described in the last section) to improve cell secretion of growth factors for tissue regeneration *in vivo* (**Figure 8**; Baptista et al., 2018). Furthermore, Good Manufacturing Practice (GMP) and animal-free supplements are crucial for clinical applications. The success of the bioengineered bone graft is directly related to the osteogenic potential of stem cells, biomaterial/scaffold specific properties, and adequate external signaling from growth factors.

Stem cells from different origins and potentialities represent the cutting-edge technology for palatal reconstruction (Zuk, 2008; Gładysz and Hozyasz, 2015). However, few studies of bone bioengineering approaches in animal models of palatal defects have been carried out. A large number of research articles have addressed bone bioengineering approaches for alveolar bone defects created in animal models to reproduce alveolar cleft or mid-palate cleft. However, here we consider only animal models of the mid-palate cleft and the use of human cells. Conejero et al. (2006) demonstrated that rat palatal critical-size defect filled with autogenous engineered graft (fat-derived stem cells previously differentiated into osteoblasts/osteocytes and seeded onto poly-L-lactic acid absorbable scaffolds) could regenerate bone at 6 or 12 weeks after surgery; bone defects filled only with the scaffold or scaffold plus undifferentiated cells had a fibrotic tissue with no bone. Another study used an autogenous multi-layered graft, which was simultaneously bioengineered for palate bone and oral mucosa in a rabbit palatal critical-size defect (Martín-Piedra et al., 2016). Initially, individual cell layers of adipose tissue-derived MSCs were seeded onto fibrin-agarose hydrogels and induced toward osteogenic differentiation; and with fibroblasts and keratinocytes seeded onto fibrin-agarose hydrogels, maintained in epithelial culture medium and under air–liquid conditions. Subsequently, the oral mucosa layer was placed on the top of the osteogenic layer and compressed to induce nanostructured fusion of the mucosal

stroma (fibroblasts) and the osteogenic layer. The 3D multi-layered graft was able to integrate with host tissue, and achieved partial bone differentiation; the authors suggested that complex multi-layer constructions could increase the maturation times compared to monolayers *in vivo*.

Bone-marrow stem cells (BMSCs) are the "gold standard" for several cell- and tissue-based clinical applications. These are, to date, the most studied stem cells and their properties are well known, but it is not clear whether the application of BMSCs or other MSCs in craniofacial bone regeneration requires handling *ex vivo* and/or pre-differentiation before clinical application (Shanbhag et al., 2019). For alveolar cleft repair in CL/P patients, scaffold-free BMSCs are safe, but this material is not suitable for extensive bone defect repair (Bajestan et al., 2017). The associations of BMSCs with commercial demineralized bone matrix (Osteoset DBM) (Behnia et al., 2009), tricalcium phosphate (Du et al., 2017), platelet-derived growth factor on biphasic hydroxyapatite/tricalcium phosphate (Behnia et al., 2012), or PRF membrane (Mossaad et al., 2019), have been shown to contribute to bone repair. However, the use of BMSC does not reduce the morbidity caused by iliac crest donor site handling even when using minimally invasive techniques. Thus, other sources of MSCs are necessary to eliminate this side effect.

The MSCs found in adult dental tissues display cranial NCC properties (Liu and Cheung, 2016; Niibe et al., 2017; Cui et al., 2018), as these embryonic cells are more similar to palate forming cells than BMSCs. In the oral cavity, human MSCs have been isolated and characterized from odontogenic and non-odontogenic origins, permitting the harvesting of healthy tissues during dental surgical procedures. Thus, a subset of cells displaying MSC properties and osteogenic properties have been described from gingival connective tissue [gingival mesenchymal stem/progenitor cells (GMSCs)] (Yang et al., 2013), oral periosteum of the palate (Caballero et al., 2010; Ceccarelli et al., 2016), the lower and upper vestibule (Ceccarelli et al., 2016), palatal connective tissue (Roman et al., 2013; Páll et al., 2015, Pall et al., 2017), and adipose stem cells from buccal fat pad (Farré-Guasch et al., 2010). Recently, palatal periosteum-derived MSCs cells, cultivated under serum- and xeno-free conditions, and cells were able to retain stem cell properties (Naung et al., 2019). One registered clinical trial was conducted using adipose stem cells from the buccal fat pad (Khojasteh et al., 2017), associated with ICBG, lateral ramus cortical bone plate, and bovine mineral graft, with all groups producing statistically similar results. However, these reports presented a limited source of tissue, and were assessed in specific situations, and therefore more effective cell sources are still required.

Five MSC populations are found in dental tissues: (I) in the dental follicle [dental follicle progenitor stem cells (DFPSCs)]; (II) in the apical papilla [stem cells from apical papilla (SCAPs)]; (III) in the ligament [periodontal ligament stem cells (PDLSCs)]; (IV) in the adult dental pulp [dental pulp stem cells (DPSCs)]; and (V) in the dental pulp of deciduous teeth [stem cells from exfoliated deciduous teeth (SHEDs)] (Baniebrahimi et al., 2018). Of these, SHEDs, which have exfoliative characteristics, are the most easily obtained odontogenic tissue, via a little or non-invasive procedure. The pulp tissue can be obtained during the period of the changing of the child's teeth, between 5 and 12 years of age, with insignificant ethical implications and provides a suitable alternative for pediatric regenerative medicine (Taguchi et al., 2019). SHEDs display high proliferative capacity, multi-lineage differentiation, secretion of immunomodulatory molecules. DPSCs, similarly to SHEDs, could be an alternative source of cells from teenagers or during adulthood during dental procedures being and are easily harvested from third molars routinely indicated to exodontia (Yamada et al., 2019). Both DPSCs and SHEDs allow cell sheets (Pedroni et al., 2018; Lee et al., 2019) and 3D spheroids cultures (Wang et al., 2010; Xiao et al., 2014). The high regenerative potential of SHEDs and DPSCs could be explained by its particular secretome content, including many types of paracrine soluble molecules and EVs, identified as immunogenic, pro-neurogenic, and pro-angiogenic (Kichenbrand et al., 2018; Marei and El Backly, 2018; Yusof et al., 2018). SHED secretome profile is also modulated during osteogenic differentiation leading to increase angiogenic potential (Mussano et al., 2018).

Concerning bone repair, SHEDs are better for forming new bone in a calvaria critical-size defect model, when compared to other dental MSCs and BMSCs. Recently, human SHEDs seeded onto dense collagen hydrogels, which were primed with FGF-2 and submitted to hypoxia conditions before implantation, improved intramembranous bone formation in an immunodeficient calvaria critical-size bone defect mouse model (Novais et al., 2019). Most of the 56 articles thoroughly analyzed in a systematic review reported good results and the relevance of human DPSCs for bone engineering in animal models or human clinical treatments (Leyendecker Junior et al., 2018). Similarly, a narrative review of 39 studies also concluded that DPSCs and SHEDs were of value for bone tissue regeneration (Cristaldi et al., 2018). Since 2005, many countries have started to collect and store healthy exfoliated teeth, creating biobanks, which are of low cost in comparison to umbilical cord banks (Campanella, 2018). Unfortunately, *ex vivo* manipulation of stem cells is still required, representing a challenge since this is a high cost and time-consuming procedure.

Little information is available regarding the use of MSCs harvested from CL/P patients. Bueno et al. (2011) isolated and characterized MSCs from *orbicularis oris* muscle (denominated by the authors as "cleft lip and palate muscle-derived stem cells"), usually discarded during the initial surgery repair (cheiloplasty) of CLP patients. These cells are able to express classical MSC cell surface proteins and differentiate into osteogenic, adipogenic, chondrogenic, and skeletal muscle cell lineages *in vitro*. The cells, when seeded onto collagen membranes, display the ability to repair bone in an immunocompromised rat critical-size cranial defect model. The analysis of DNA variants affecting the gene expression (cis-eQTLs) of cleft lip and palate muscle-derived stem cells allowed the discovery of a new susceptibility locus for NSCLP was discovered (rs1063588), coincident with the *MRPL53* gene (Masotti et al., 2017). Bueno et al. (2011) compared the gene expression profile of SHEDs from healthy donors and CL/P patients and verified that 87 genes presented differential expressions, with more than a half being glycoproteins related to the ECM (collagens, MMPs, integrins, and adhesion proteins).

This study showed that MSCs might be a powerful tool for genetic and "omic" studies of CL/P. Later, the same group showed that low power laser therapy could enhance the osteogenic potential of DPSCs from CL/P patients (Pinheiro et al., 2017). These results support the need for the study of MSCs from CL/P patients to better understand cell behavior, ECM secretion, and remodeling, and employ this knowledge to drive new strategies based on bone bioengineering for palatal reconstruction.

Another growing field related to regenerative medicine that could be applied to palate reconstruction is bioprinting. Spheroids are potential building blocks in 3D bioprinting, in a large-scale process for bone and cartilage tissue production. Growing evidence shows that 3D spheroids formed from MSC present increased angiogenic and chemotactic signaling (Costa et al., 2017). 3D bioprinted cryogels, formed from chitosan (CS)/gelatin-based scaffolds for personalized palate reconstruction, have been designed by CL/P computed tomography data (Hixon et al., 2017). A 3D bioprinted bioresorbable scaffold (polycaprolactone—approved by the Korean Ministry of Food and Drug Safety for clinical use) seeded with autologous BMSCs from the iliac crest in the operation room, was implanted in a 10-year-old Korean boy with a history of previously repaired unilateral CL/P presenting a cleft alveolus and an oronasal fistula. At 6 months after transplantation, the new bone formed reached around 45% of the total defect volume, suggesting that this new technology could be a promising alternative (Ahn et al., 2018).

Three-dimensional additive manufacture allows the production of biomaterials/scaffolds used successfully for bone bioengineering have to be biocompatible, specific porosity, chemical and topographical characteristics and surface properties for osteoconduction, biomechanical properties, biodegradability, and radiolucency, to induce osteogenesis (osteoinductivity) and vascular ingrowth. In a new vision, biomaterials may trigger immunological host responses to stimulate tissue regeneration (Franz et al., 2011). As we have previously seen, the provisional matrix is secreted by embryonic palatal cells to drive palatogenesis. Among biopolymers used as biomaterials/scaffolds for bone bioengineering, collagen type I, CS, and HA are the most commonly employed. CS is a polysaccharide chitin-derived present in invertebrate exoskeletons which displays many promising characteristics such as biocompatibility, antibacterial activity, biodegradability, porosity, immunomodulatory properties, promotes cell adhesion, proliferation, migration, and ultimately enhances bone regeneration due to stimulation of osteoblast differentiation and mineralization (Farhadihosseinabadi et al., 2019).

As we have seen previously, LOX and TGs are crucial enzymes for collagen–collagen cross-links. These enzymes have been employed to create cross-links in collagen-based biomaterials (Fortunati et al., 2014; Cai et al., 2017). This modern approach can replace the traditional chemical method employing aldehydes, isocyanates, and carbodiimides. Although this method creates strong stable cross-links, undesirable consequences such as cytotoxicity, calcification, and foreign body response are well known for these chemicals (Sorushanova et al., 2019). Specifically in bone tissue, TG induces the oligomerization of SIBLINSs, and calcium-binding proteins (osteopontin and bone sialoprotein), which may drive mineral nucleation or calcium crystal growth (Forsprecher et al., 2009).

CONCLUDING REMARKS

Although several MMPs and their inhibitors TIMPs are expressed during palatogenesis, the cell membrane-anchored MMPs appear to represent the principal pericellular collagenases (MMP-14 and MMP-16) and may be crucial for the development of CL/P. However, recent studies have demonstrated roles for other metalloproteinases, such as ADAMTS in this pathology. There seems to be a crucial compensatory effect between MMPs to ensure that the various stages of palate formation can occur. However, more studies should be carried out on other metalloproteinases to better understand the complexity of ECM remodeling, the generation of bioactive molecules, and the relationship between them.

Cleft therapy still is dependent on bone grafts, mainly of the ICBG, but new approaches have been under evaluation. Administration of BMP-2 and PDGF combined with bone graft is promising, but recent systematic reviews support the need for better-designed randomized controlled clinical trials with long-term follow-up (>12 months). The development of *in vitro* models using stem cells from CL/P patients may be an exciting approach for further studies of the biology of these cells as well as their potential use in new individualized therapeutic approaches for palatal reconstruction. 3D culture has been used to recapitulate the critical events of development, such as cell–cell interaction, differentiation, growth and cell fusion, which, coupled with "omics" analysis and computational biology, promote considerable advances in tissue remodeling and repair. Additionally, the emerging and exciting field of EVs may provide critical information via "omics" analyses to understand how this component of ECM contributes to the palatogenesis of CL/P.

The development of new biomaterials that simulate a provisional matrix during palatogenesis and provide the controlled release of growth factors may aid to improve new therapeutic approaches based on bone bioengineering. Emerging cell reprogramming or trans-differentiation technologies could provide other unusual sources of therapeutic cells. The former consists of differentiated adult cells, such as fibroblasts, that are forced to overexpress transcription factors that regulate pluripotency generating inducible pluripotent stem cells (iPSCs) displaying the same characteristics as embryonic stem cells (Spyrou et al., 2019). The second approach consists of the direct conversion of a fully differentiated cell type into another one; for example, the conversion of fibroblasts into osteoblasts (Cho and Ryoo, 2018). Furthermore, another possibility is to use EVs released by MSCs as potential cell-free tools for bone regeneration (Praveen Kumar et al., 2019). Finally, we now have a vast knowledge of craniofacial development, CL/P and CL/P treatment, associated with many advances in cell and material engineering technologies. So, multidisciplinary efforts must be made to achieve advances in the quality of life of CL/P patients.

AUTHOR CONTRIBUTIONS

KP contributed to the design, writing, and financial support of the manuscript. CM, PS, AL, and JG contributed to the design and writing of the manuscript.

FUNDING

We are grateful for financial support from the São Paulo Research Foundation (FAPESP KBSP fellowship 2017/26813-9).

REFERENCES

Abbott, B. D. (2019). Embryonic midfacial palatal organ culture methods in developmental toxicology BT - developmental toxicologys. *Methods Mol. Biol.* 1965, 93–105. doi: 10.1007/978-1-4939-9182-2_7

Ahn, G., Lee, J.-S., Yun, W.-S., Shim, J.-H., and Lee, U.-L. (2018). Cleft alveolus reconstruction using a three-dimensional printed bioresorbable scaffold with human bone marrow cells. *J. Craniofac. Surg.* 29, 1880–1883. doi: 10.1097/SCS.0000000000004747

Alhaque, S., Themis, M., and Rashidi, H. (2018). Three-dimensional cell culture: from evolution to revolution. *Philos. Trans. R. Soc. Lond. B. Biol. Sci.* 373:20170216. doi: 10.1098/rstb.2017.0216

Alzahrani, F., Al Hazzaa, S. A., Tayeb, H., and Alkuraya, F. S. (2015). LOXL3, encoding lysyl oxidase-like 3, is mutated in a family with autosomal recessive stickler syndrome. *Hum. Genet.* 134, 451–453. doi: 10.1007/s00439-015-1531-z

Amiri, N., and Christians, J. K. (2015). PAPP-A2 expression by osteoblasts is required for normal postnatal growth in mice. *Growth Horm. IGF Res.* 25, 274–280. doi: 10.1016/j.ghir.2015.09.003

Ansorge, M., and Pompe, T. (2018). Systems for localized release to mimic paracrine cell communication in vitro. *J. Control. Release* 278, 24–36. doi: 10.1016/j.jconrel.2018.03.028

Araya, H. F., Sepulveda, H., Lizama, C. O., Vega, O. A., Jerez, S., Briceño, P. F., et al. (2018). Expression of the ectodomain-releasing protease ADAM17 is directly regulated by the osteosarcoma and bone-related transcription factor RUNX2. *J. Cell. Biochem.* 119, 8204–8219. doi: 10.1002/jcb.26832

Arnold, P., Koopmann, L., Peters, F., Birkenfeld, F., Goff, S. V.-L., Damm, T., et al. (2017). Deficiency of the DSPP-cleaving enzymes meprin α and meprin β does not result in dentin malformation in mice. *Cell Tissue Res.* 367, 351–358. doi: 10.1007/s00441-016-2498-3

Arpino, V., Brock, M., and Gill, S. E. (2015). The role of TIMPs in regulation of extracellular matrix proteolysis. *Matrix Biol.* 4, 247–254. doi: 10.1016/j.matbio.2015.03.005

Aviram, R., Zaffryar-Eilot, S., Hubmacher, D., Grunwald, H., Mäki, J. M., Myllyharju, J., et al. (2019). Interactions between lysyl oxidases and ADAMTS proteins suggest a novel crosstalk between two extracellular matrix families. *Matrix Biol.* 7, 114–125. doi: 10.1016/j.matbio.2018.05.003

Ayoub, A., and Gillgrass, T. (2019). The clinical application of recombinant human bone morphogenetic protein 7 for reconstruction of alveolar cleft: 10 Years' Follow-Up. *J. Oral Maxillofac. Surg.* 77, 571–581. doi: 10.1016/j.joms.2018.08.031

Ayoub, A., Roshan, C. P., Gillgrass, T., Naudi, K., and Ray, A. (2016). The clinical application of rhBMP-7 for the reconstruction of alveolar cleft. *J. Plast. Reconstr. Aesthet. Surg.* 69, 101–107. doi: 10.1016/j.bjps.2015.09.004

Baek, J.-A., Lan, Y., Liu, H., Maltby, K. M., Mishina, Y., and Jiang, R. (2011). Bmpr1a signaling plays critical roles in palatal shelf growth and palatal bone formation. *Dev. Biol.* 350, 520–531. doi: 10.1016/j.ydbio.2010.12.028

Bajestan, M. N., Rajan, A., Edwards, S. P., Aronovich, S., Cevidanes, L. H. S., Polymeri, A., et al. (2017). Stem cell therapy for reconstruction of alveolar cleft and trauma defects in adults: a randomized controlled, clinical trial. *Clin. Implant Dent. Relat. Res.* 19, 793–801. doi: 10.1111/cid.12506

Baniebrahimi, G., Khanmohammadi, R., and Mir, F. (2018). Teeth-derived stem cells: a source for cell therapy. *J. Cell. Physiol.* 234, 2426–2435. doi: 10.1002/jcp.27270

Baptista, L. S., Kronemberger, G. S., Côrtes, I., Charelli, L. E., Matsui, R. A. M., Palhares, T. N., et al. (2018). Adult stem cells spheroids to optimize cell colonization in scaffolds for cartilage and bone tissue engineering. *Int. J. Mol. Sci.* 19:1285. doi: 10.3390/ijms19051285

Barker, T. H., and Engler, A. J. (2017). The provisional matrix: setting the stage for tissue repair outcomes. *Matrix Biol.* 6, 1–4. doi: 10.1016/j.matbio.2017.04.003

Bauvois, B. (2012). New facets of matrix metalloproteinases MMP-2 and MMP-9 as cell surface transducers: outside-in signaling and relationship to tumor progression. *Biochim. Biophys. Acta Rev. Cancer* 1825, 29–36. doi: 10.1016/j.bbcan.2011.10.001

Beaty, T. H., Marazita, M. L., and Leslie, E. J. (2016). Genetic factors influencing risk to orofacial clefts: today's challenges and tomorrow's opportunities. *F1000Research* 5:2800. doi: 10.12688/f1000research.9503.1

Behnia, H., Khojasteh, A., Soleimani, M., Tehranchi, A., and Atashi, A. (2012). Repair of alveolar cleft defect with mesenchymal stem cells and platelet derived growth factors: a preliminary report. *J. Cranio Maxillofac. Surg.* 40, 2–7. doi: 10.1016/j.jcms.2011.02.003

Behnia, H., Khojasteh, A., Soleimani, M., Tehranchi, A., Khoshzaban, A., Keshel, S. H., et al. (2009). Secondary repair of alveolar clefts using human mesenchymal stem cells. *Oral Surg. Oral Med. Oral Pathol. Oral Radiol. Endodontol.* 108, e1–e6. doi: 10.1016/j.tripleo.2009.03.040

Bekhouche, M., and Colige, A. (2015). The procollagen N-proteinases ADAMTS2, 3 and 14 in pathophysiology. *Matrix Biol.* 4, 46–53. doi: 10.1016/j.matbio.2015.04.001

Benkovics, A. H., Skopelitis, D. S., Benkovics, A. H., Husbands, A. Y., and Timmermans, M. C. P. (2017). Boundary formation through a direct threshold-based readout of mobile small RNA gradients. *Dev. Cell* 43, 265.e6–273.e6. doi: 10.1016/j.devcel.2017.10.003

Benlidayi, M. E., Tatli, U., Kurkcu, M., Uzel, A., and Oztunc, H. (2012). Comparison of bovine-derived hydroxyapatite and autogenous bone for secondary alveolar bone grafting in patients with alveolar clefts. *J. Oral Maxillofac. Surg.* 70, e95–e102. doi: 10.1016/j.joms.2011.08.041

Bissell, M. J. (2017). Goodbye flat biology – time for the 3rd and the 4th dimensions. *J. Cell Sci.* 130, 3–5. doi: 10.1242/jcs.200550

Blanton, S. H., Bertin, T., Serna, M. E., Stal, S., Mulliken, J. B., and Hecht, J. T. (2004). Association of chromosomal regions 3p21.2, 10p13, and 16p13.3 with nonsyndromic cleft lip and palate. *Am. J. Med. Genet.* 125A, 23–27. doi: 10.1002/ajmg.a.20426

Blavier, L., and DeClerck, Y. A. (1997). Tissue inhibitor of metalloproteinases-2 is expressed in the interstitial matrix in adult mouse organs and during embryonic development. *Mol. Biol. Cell* 8, 1513–1527. doi: 10.1091/mbc.8.8.1513

Blavier, L., Lazaryev, A., Groffen, J., Heisterkamp, N., DeClerck, Y. A., and Kaartinen, V. (2001). TGF-beta3-induced palatogenesis requires matrix metalloproteinases. *Mol. Biol. Cell* 12, 1457–1466. doi: 10.1091/mbc.12.5.1457

Bond, J. S. (2019). Proteases: history, discovery, and roles in health and disease. *J. Biol. Chem.* 294, 1643–1651. doi: 10.1074/jbc.TM118.004156

Borba, A. M., Borges, A. H., Da Silva, C. S. V., Brozoski, M. A., Naclério-Homem, M. D. G., and Miloro, M. (2014). Predictors of complication for alveolar cleft bone graft. *Br. J. Oral Maxillofac. Surg.* 52, 174–178. doi: 10.1016/j.bjoms.2013.11.001

Boyd, D. D. (2006). Regulation of matrix metalloproteinase gene. *Mol. Cell Biochem.* 253, 269–285. doi: 10.1002/JCP

Brown, G. D., and Nazarali, A. J. (2010). Matrix metalloproteinase-25 has a functional role in mouse secondary palate development and is a downstream target of TGF-3. *BMC Dev. Biol.* 10:93. doi: 10.1186/1471-213X-10-93

Brown, N. L., Yarram, S. J., Mansell, J. P., and Sandy, J. R. (2002). Matrix metalloproteinases have a role in palatogenesis. *J. Dent. Res.* 81, 826–830. doi: 10.1177/154405910208101206

Brozek, R., Kurpisz, M., and Koczorowski, R. (2018). Application of stem cells in dentistry for bone regeneration. *J. Physiol. Pharmacol.* 69, 23–33. doi: 10.26402/jpp.2018.1.03

Bueno, D. F., Sunaga, D. Y., Kobayashi, G. S., Aguena, M., Raposo-Amaral, C. E., Masotti, C., et al. (2011). Human stem cell cultures from cleft lip/palate patients show enrichment of transcripts involved in extracellular matrix modeling by comparison to controls. *Stem Cell Rev. Rep.* 7, 446–457. doi: 10.1007/s12015-010-9197-3

Bush, J. O., and Jiang, R. (2012). Palatogenesis: morphogenetic and molecular mechanisms of secondary palate development. *Development* 139, 231–243. doi: 10.1242/dev.067082

Butler, G. S., and Overall, C. M. (2009). Updated biological roles for matrix metalloproteinases and new "intracellular" substrates revealed by degradomics. *Biochemistry* 48, 10830–10845. doi: 10.1021/bi901656f

Caballero, M., Reed, C. R., Madan, G., and van Aalst, J. A. (2010). Osteoinduction in umbilical cord- and palate periosteum-derived mesenchymal stem cells. *Ann. Plast. Surg.* 64, 605–609. doi: 10.1097/SAP.0b013e3181ce3929

Cai, L., Xiong, X., Kong, X., and Xie, J. (2017). The role of the lysyl oxidases in tissue repair and remodeling: a concise review. *Tissue Eng. Regen. Med.* 14, 15–30. doi: 10.1007/s13770-016-0007-0

Campanella, V. (2018). Dental stem cells: current research and future applications. *Eur. J. Paediatr. Dent.* 19, 257–257. doi: 10.23804/ejpd.2018.19.04.1

Canan, L. W. J., da Silva Freitas, R., Alonso, N., Tanikawa, D. Y. S., Rocha, D. L., and Coelho, J. C. U. (2012). Human bone morphogenetic protein-2 use for maxillary reconstruction in cleft lip and palate patients. *J. Craniofac. Surg.* 23, 1627–1633. doi: 10.1097/SCS.0b013e31825c75ba

Ceccarelli, G., Graziano, A., Benedetti, L., Imbriani, M., Romano, F., Ferrarotti, F., et al. (2016). Osteogenic potential of human oral-periosteal cells (PCs) isolated from different oral origin: an in vitro study. *J. Cell. Physiol.* 231, 607–612. doi: 10.1002/jcp.25104

Cerdà-Costa, N., and Gomis-Rüth, F. X. (2014). Architecture and function of metallopeptidase catalytic domains. *Protein Sci.* 23, 123–144. doi: 10.1002/pro.2400

Chen, G., Li, M. X., Wang, H. X., Hong, J. W., Shen, J. Y., Wang, Q., et al. (2018). Identification of key genes in cleft lip with or without cleft palate regulated by miR-199a-5p. *Int. J. Pediatr. Otorhinolaryngol.* 111, 128–137. doi: 10.1016/j.ijporl.2018.06.005

Chester, D., and Brown, A. C. (2017). The role of biophysical properties of provisional matrix proteins in wound repair. *Matrix Biol.* 6, 124–140. doi: 10.1016/j.matbio.2016.08.004

Chin, M., Ng, T., Tom, W. K., and Carstens, M. (2005). Repair of alveolar clefts with recombinant human bone morphogenetic protein (rhBMP-2) in patients with clefts. *J. Craniofac. Surg.* 16, 778–789. doi: 10.1097/01.scs.0000166802.49021.01

Cho, Y., and Ryoo, H. (2018). Trans-differentiation via epigenetics: a new paradigm in the bone regeneration. *J. Bone Metab.* 25:9. doi: 10.11005/jbm.2018.25.1.9

Christians, J. K., Amiri, N., Schipilow, J. D., Zhang, S. W., and May-Rashke, K. I. (2019). Pappa2 deletion has sex- and age-specific effects on bone in mice. *Growth Horm. IGF Res.* 44, 6–10. doi: 10.1016/j.ghir.2018.10.006

Clark, I. M., Swingler, T. E., Sampieri, C. L., and Edwards, D. R. (2008). The regulation of matrix metalloproteinases and their inhibitors. *Int. J. Biochem. Cell Biol.* 40, 1362–1378. doi: 10.1016/j.biocel.2007.12.006

Cobourne, M. T., and Green, J. B. A. (2012). Hedgehog signalling in development of the secondary palate. *Front. Oral Biol.* 16, 52–59. doi: 10.1159/000337543

Collignon, A. M., Lesieur, J., Vacher, C., Chaussain, C., and Rochefort, G. Y. (2017). Strategies developed to induce, direct, and potentiate bone healing. *Front. Physiol.* 8:927. doi: 10.3389/fphys.2017.00927

Conejero, J. A., Lee, J. A., Parrett, B. M., Terry, M., Wear-Maggitti, K., Grant, R. T., et al. (2006). Repair of palatal bone defects using osteogenically differentiated fat-derived stem cells. *Plast. Reconstr. Surg.* 117, 857–863. doi: 10.1097/01.prs.0000204566.13979.c1

Costa, M. H. G., McDevitt, T. C., Cabral, J. M. S., da Silva, C. L., and Ferreira, F. C. (2017). Tridimensional configurations of human mesenchymal stem/stromal cells to enhance cell paracrine potential towards wound healing processes. *J. Biotechnol.* 262, 28–39. doi: 10.1016/j.jbiotec.2017.09.020

Cristaldi, M., Mauceri, R., Tomasello, L., Pizzo, G., Pizzolanti, G., Giordano, C., et al. (2018). Dental pulp stem cells for bone tissue engineering: a review of the current literature and a look to the future. *Regen. Med.* 13, 207–218. doi: 10.2217/rme-2017-0112

Cruz, L., Romero, J. A. A., Iglesia, R. P., and Lopes, M. H. (2018). Extracellular vesicles: decoding a new language for cellular communication in early embryonic development. *Front. Cell Dev. Biol.* 6:94. doi: 10.3389/fcell.2018.00094

Cui, D., Li, H., Wan, M., Peng, Y., Xu, X., Zhou, X., et al. (2018). The origin and identification of mesenchymal stem cells in teeth: from odontogenic to non-odontogenic. *Curr. Stem Cell Res. Ther.* 13, 39–45. doi: 10.2174/1574888X12666170913150403

Dagoneau, N., Benoist-Lasselin, C., Huber, C., Faivre, L., Mégarbané, A., Alswaid, A., et al. (2004). ADAMTS10 mutations in autosomal recessive weill-marchesani syndrome. *Am. J. Hum. Genet.* 75, 801–806. doi: 10.1086/425231

Dancevic, C. M., Mcculloch, D. R., and Ward, A. C. (2016). The ADAMTS hyalectanase family: biological insights from diverse species. *Biochem. J.* 473, 2011–2022. doi: 10.1042/BCJ20160148

de Ladeira, P. R. S., and Alonso, N. (2012). Protocols in cleft lip and palate treatment: systematic review. *Plast. Surg. Int.* 2012:562892. doi: 10.1155/2012/562892

de Oliveira Demarchi, A. C. C., Zambuzzi, W. F., Paiva, K. B. S., da Silva-Valenzuela, M. D., Nunes, F. D., de Cássia Sávio Figueira, R., et al. (2010). Development of secondary palate requires strict regulation of ECM remodeling: sequential distribution of RECK, MMP-2, MMP-3, and MMP-9. *Cell Tissue Res.* 340, 61–69. doi: 10.1007/s00441-010-0931-6

De Ruiter, A., Janssen, N., Van Es, R., Frank, M., Meijer, G., Koole, R., et al. (2015). Micro-structured beta-tricalcium phosphate for repair of the alveolar cleft in cleft lip and palate patients: a pilot study. *Cleft Palaten Craniofac. J.* 52, 336–340. doi: 10.1597/13-260

Deryugina, E. I., and Quigley, J. P. (2010). Pleiotropic roles of matrix metalloproteinases in tumor angiogenesis: contrasting, overlapping and compensatory functions2. *Biochim. Biophys. Acta* 1803, 103–120. doi: 10.1016/j.bbamcr.2009.09.017

Dickinson, B. P., Ashley, R. K., Wasson, K. L., O'Hara, C., Gabbay, J., Heller, J. B., et al. (2008). Reduced morbidity and improved healing with bone morphogenic protein-2 in older patients with alveolar cleft defects. *Plast. Reconstr. Surg.* 121, 209–217. doi: 10.1097/01.prs.0000293870.64781.12

Ding, H. L., Hooper, J. E., Batzel, P., Frank Eames, B., Postlethwait, J. H., Artinger, K. B., et al. (2016). MicroRNA profiling during craniofacial development: potential roles for mir23b and mir133b. *Front. Physiol.* 7:281. doi: 10.3389/fphys.2016.00281

Dixon, M. J., Carette, M. J. M., Moser, B. B., and Ferguson, M. W. J. (1993a). Differentiation of isolated murine embryonic palatal epithelium in culture: exogenous transforming growth factor alpha modulates matrix biosynthesis in defined experimental conditions. *Vitr. Cell. Dev. Biol.* 29A, 51–61. doi: 10.1007/bf02634371

Dixon, M. J., Foreman, D., Schor, S., William, M., and Ferguson, J. (1993b). Epidermal growth factor and transforming growth factor alpha regulate extracellular matrix production by embryonic mouse palatal mesenchymal cells cultured on a variety of substrata. *Roux Arch. Dev. Biol.* 203, 140–150. doi: 10.1007/BF00365053

Dixon, M. J., Marazita, M. L., Beaty, T. H., and Murray, J. C. (2011). Cleft lip and palate: understanding genetic and environmental influences. *Nat. Rev. Genet.* 12, 167–178. doi: 10.1038/nrg2933

Du, F., Wu, H., Li, H., Cai, L., Wang, Q., Liu, X., et al. (2017). Bone marrow mononuclear cells combined with beta-tricalcium phosphate granules for alveolar cleft repair: a 12-month clinical study. *Sci. Rep.* 7:13773. doi: 10.1038/s41598-017-12602-01

Dubail, J., and Apte, S. S. (2015). Insights on ADAMTS proteases and ADAMTS-like proteins from mammalian genetics. *Matrix Biol.* 4, 24–37. doi: 10.1016/j.matbio.2015.03.001

Dupin, E., Calloni, G. W., Coelho-Aguiar, J. M., and Le Douarin, N. M. (2018). The issue of the multipotency of the neural crest cells. *Dev. Biol.* 444, S47–S59. doi: 10.1016/j.ydbio.2018.03.024

Dworkin, S., Boglev, Y., Owens, H., and Goldie, S. J. (2016). The role of sonic hedgehog in craniofacial patterning, morphogenesis and cranial neural crest survival. *J. Dev. Biol.* 4:24. doi: 10.3390/jdb4030024

Eberhart, J. K., He, X., Swartz, M. E., Yan, Y. L., Song, H., Boling, T. C., et al. (2008). MicroRNA Mirn140 modulates Pdgf signaling during palatogenesis. *Nat. Genet.* 40, 290–298. doi: 10.1038/ng.82

Eckert, R. L., Kaartinen, M. T., Nurminskaya, M., Belkin, A. M., Colak, G., Johnson, G. V. W., et al. (2014). Transglutaminase regulation of cell function. *Physiol. Rev.* 94, 383–417. doi: 10.1152/physrev.00019.2013

English, W. R., Velasco, G., Stracke, J. O., Knauper, V., and Murphy, G. (2001). Catalytic activities of membrane-type 6 matrix metalloproteinase (MMP25)117. *FEBS Lett.* 491, 137–142. doi: 10.1016/s0014-5793(01)02150-0

Enomoto, H., Nelson, C. M., Somerville, R. P. T., Mielke, K., Dixon, L. J., Powell, K., et al. (2010). Cooperation of two ADAMTS metalloproteases in closure of the mouse palate identifies a requirement for versican proteolysis in regulating palatal mesenchyme proliferation. *Development* 137, 4029–4038. doi: 10.1242/dev.050591

Fallucco, M. A., and Carstens, M. H. (2009). Primary reconstruction of alveolar clefts using recombinant human bone morphogenic protein-2: clinical and radiographic outcomes. *J. Craniofac. Surg.* 20, 1759–1764. doi: 10.1097/SCS.0b013e3181b5d08e

Fan, S. M.-Y., Chen, P.-H., Tseng, Y.-T., Hong, J.-B., Chen, W., Tsai, T.-F., et al. (2018). Preclinical evaluation of melanocyte transplantation by chitosan-based melanocyte spheroid patch to skin prepared by controlled sunburn blistering. *J. Biomed. Mater. Res. B Appl. Biomater.* 106, 2535–2543. doi: 10.1002/jbm.b.34070

Farhadihosseinabadi, B., Zarebkohan, A., Eftekhary, M., and Heiat, M. (2019). Crosstalk between chitosan and cell signaling pathways. *Cell. Mol. Life Sci.* 76, 2697–2718. doi: 10.1007/s00018-019-03107-3103

Farré-Guasch, E., Martí-Pagès, C., Hernández-Alfaro, F., Klein-Nulend, J., and Casals, N. (2010). Buccal fat pad, an oral access source of human adipose stem cells with potential for osteochondral tissue engineering: an in vitro study. *Tissue Eng. C Methods* 16, 1083–1094. doi: 10.1089/ten.tec.2009.0487

Farronato, G., Kairyte, L., Giannini, L., Galbiati, G., and Maspero, C. (2014). How various surgical protocols of the unilateral cleft lip and palate influence the facial growth and possible orthodontic problems? Which is the best timing of lip, palate and alveolus repair? literature review. *Stomatologija* 16, 53–60.

Fawcett, E. (1906). On the development, ossification, and growth of the palate bone of man. *J. Anat. Physiol.* 40, 400–406.

Ferguson, M. W. (1988). Palate development. *Development* 103(Suppl.), 41–60.

Forsprecher, J., Wang, Z., Nelea, V., and Kaartinen, M. T. (2009). Enhanced osteoblast adhesion on transglutaminase 2-crosslinked fibronectin. *Amino Acids* 36, 747–753. doi: 10.1007/s00726-008-0125-7

Fortunati, D., Chau, D. Y. S., Wang, Z., Collighan, R. J., and Griffin, M. (2014). Cross-linking of collagen I by tissue transglutaminase provides a promising biomaterial for promoting bone healing. *Amino Acids* 46, 1751–1761. doi: 10.1007/s00726-014-1732-0

Francis-west, P., and Crespo-Enriquez, I. (2016). Vertebrate embryo: craniofacial development. *eLS* 1–15. doi: 10.1002/9780470015902.a0026602

Franz, S., Rammelt, S., Scharnweber, D., and Simon, J. C. (2011). Immune responses to implants - A review of the implications for the design of immunomodulatory biomaterials. *Biomaterials* 32, 6692–6709. doi: 10.1016/j.biomaterials.2011.05.078

Fu, Y., and Kong, W. (2017). Cartilage oligomeric matrix protein: matricellular and matricrine signaling in cardiovascular homeostasis and disease. *Curr. Vasc. Pharmacol.* 15, 186–196. doi: 10.2174/1570161115666170201121232

Fuller, K., and Chambers, T. J. (1995). Localisation of mRNA for collagenase in osteocytic, bone surface and chondrocytic cells but not osteoclasts. *J. Cell Sci.* 108, 2221–2230.

Funato, N. (2015). Molecular basis of cleft palates in mice. *World J. Biol. Chem.* 6, 121–138. doi: 10.4331/wjbc.v6.i3.121

Gabison, E. E., Huet, E., Baudouin, C., and Menashi, S. (2009). Direct epithelial-stromal interaction in corneal wound healing: role of EMMPRIN/CD147 in MMPs induction and beyond. *Prog. Retin. Eye Res.* 28, 19–33. doi: 10.1016/j.preteyeres.2008.11.001

Gack, S., Vallon, R., Schmidt, J., Grigoriadis, A., Tuckermann, J., Schenkel, J., et al. (1995). Expression of interstitial collagenase during skeletal development of the mouse is restricted to osteoblast-like cells and hypertrophic chondrocytes1. *Cell Growth Differ.* 6, 759–767.

Galloway, J. L., Jones, S. J., Mossey, P. A., and Ellis, I. R. (2013). The control and importance of hyaluronan synthase expression in palatogenesis. *Front. Physiol.* 4:10. doi: 10.3389/fphys.2013.00010

Gao, S., Moreno, M., Eliason, S., Cao, H., Li, X., Yu, W., et al. (2015). TBX1 protein interactions and microRNA-96-5p regulation controls cell proliferation during craniofacial and dental development: implications for 22q11.2 deletion syndrome. *Hum. Mol. Genet.* 24, 2330–2348. doi: 10.1093/hmg/ddu750

Garantziotis, S., and Savani, R. C. (2019). Hyaluronan biology: a complex balancing act of structure, function, location and context. *Matrix Biol.* 78-79, 1–10. doi: 10.1016/j.matbio.2019.02.002

Geng, Y., McQuillan, D., and Roughley, P. J. (2006). SLRP interaction can protect collagen fibrils from cleavage by collagenases. *Matrix Biol.* 25, 484–491. doi: 10.1016/j.matbio.2006.08.259

Gkantidis, N., Blumer, S., Katsaros, C., Graf, D., and Chiquet, M. (2012). Site-specific expression of gelatinolytic activity during morphogenesis of the secondary palate in the mouse embryo3. *PLoS One* 7:e47762. doi: 10.1371/journal.pone.0047762

Gładysz, D., and Hozyasz, K. K. (2015). Stem cell regenerative therapy in alveolar cleft reconstruction. *Arch. Oral Biol.* 60, 1517–1532. doi: 10.1016/j.archoralbio.2015.07.003

Graf, D., Malik, Z., Hayano, S., and Mishina, Y. (2016). Common mechanisms in development and disease: BMP signaling in craniofacial development. *Cytokine Growth Factor Rev.* 27, 129–139. doi: 10.1016/j.cytogfr.2015.11.004

Grassia, V., Lombardi, A., Kawasaki, H., Ferri, C., Perillo, L., Mosca, L., et al. (2018). Salivary microRNAs as new molecular markers in cleft lip and palate: a new frontier in molecular medicine. *Oncotarget* 9, 18929–18938. doi: 10.18632/oncotarget.24838

Greene, R. M., and Pisano, M. M. (2010). Palate morphogenesis: current understanding and future directions. *Birth Defects Res. C. Embryo Today* 90, 133–154. doi: 10.1002/bdrc.20180

Grgurevic, L., Macek, B., Mercep, M., Jelic, M., Smoljanovic, T., Erjavec, I., et al. (2011). Bone morphogenetic protein (BMP)1-3 enhances bone repair. *Biochem. Biophys. Res. Commun.* 408, 25–31. doi: 10.1016/j.bbrc.2011.03.109

Guo, J., Li, C., Zhang, Q., Wu, G., Deacon, S. A., Chen, J., et al. (2011). Secondary bone grafting for alveolar cleft in children with cleft lip or cleft lip and palate. *Cochrane Database Syst. Rev.* 6:CD008050. doi: 10.1002/14651858.CD008050.pub2

Gupta, V., Hospital, M. S., and Arshad, H. (2012). Palatal reconstruction. *Curr. Opin. Otolaryngol. Head Neck Surg.* 20, 225–230. doi: 10.1097/MOO.0b013e328355389f

Hadler-Olsen, E., Fadnes, B., Sylte, I., Uhlin-Hansen, L., and Winberg, J.-O. (2011). Regulation of matrix metalloproteinase activity in health and disease. *FEBS J.* 278, 28–45. doi: 10.1111/j.1742-4658.2010.07920.x

Hammond, N. L., Dixon, J., and Dixon, M. J. (2017). Periderm: life-cycle and function during orofacial and epidermal development. *Semin. Cell Dev. Biol.* 91, 75–83. doi: 10.1016/j.semcdb.2017.08.021

Hammoudeh, J. A., Fahradyan, A., Gould, D. J., Liang, F., Imahiyerobo, T., Urbinelli, L., et al. (2017). A comparative analysis of recombinant human bone morphogenetic protein-2 with a demineralized bone matrix versus iliac crest bone graft for secondary alveolar bone grafts in patients with cleft lip and palate: review of 501 cases. *Plast. Reconstr. Surg.* 140, 318e–325e. doi: 10.1097/PRS.0000000000003519

Han, H.-W., Asano, S., and Hsu, S. (2019). Cellular spheroids of mesenchymal stem cells and their perspectives in future healthcare. *Appl. Sci.* 9:627. doi: 10.3390/app9040627

He, F., and Chen, Y. (2012). Wnt signaling in lip and palate development. *Front. Oral Biol.* 16, 81–90. doi: 10.1159/000337619

Hernandez-Barrantes, S., Bernardo, M., Toth, M., and Fridman, R. (2002). Regulation of membrane type-matrix metalloproteinases. *Semin. Biol.* 12, 131–138. doi: 10.1006/scbi.2001.0421

Hill, C. R., Yuasa, M., Schoenecker, J., and Goudy, S. L. (2014). Jagged1 is essential for osteoblast development during maxillary ossification. *Bone* 62, 10–21. doi: 10.1016/j.bone.2014.01.019

Hill, C., Jacobs, B., Kennedy, L., Rohde, S., Zhou, B., Baldwin, S., et al. (2015). Cranial neural crest deletion of VEGFa causes cleft palate with aberrant vascular and bone development. *Cell Tissue Res.* 361, 711–722. doi: 10.1007/s00441-015-2150-7

Hirata, A., Katayama, K., Tsuji, T., Natsume, N., Sugahara, T., Koga, Y., et al. (2013). Heparanase localization during palatogenesis in mice. *Biomed Res. Int.* 2013:760236. doi: 10.1155/2013/760236

Hixon, K. R., Melvin, A. M., Lin, A. Y., Hall, A. F., and Sell, S. A. (2017). Cryogel scaffolds from patient-specific 3D-printed molds for personalized tissue-engineered bone regeneration in pediatric cleft-craniofacial defects. *J. Biomater. Appl.* 32, 598–611. doi: 10.1177/0885328217734824

Horch, H.-H., Sader, R., Pautke, C., Neff, A., Deppe, H., and Kolk, A. (2006). Synthetic, pure-phase beta-tricalcium phosphate ceramic granules (Cerasorb®) for bone regeneration in the reconstructive surgery of the jaws. *Int. J. Oral Maxillofac. Surg.* 35, 708–713. doi: 10.1016/j.ijom.2006.03.017

Horejs, C. M. (2016). Basement membrane fragments in the context of the epithelial-to-mesenchymal transition. *Eur. J. Cell Biol.* 95, 427–440. doi: 10.1016/j.ejcb.2016.06.002

Houschyar, K. S., Tapking, C., Borrelli, M. R., Popp, D., Duscher, D., Maan, Z. N., et al. (2019). Wnt pathway in bone repair and regeneration – what do we know so far. *Front. Cell Dev. Biol.* 6:170. doi: 10.3389/fcell.2018.00170

Huang, G., Zhang, Y., Kim, B., Ge, G., Annis, D. S., Mosher, D. F., et al. (2009). Fibronectin binds and enhances the activity of bone morphogenetic protein 1. *J. Biol. Chem.* 284, 25879–25888. doi: 10.1074/jbc.M109.024125

Hubmacher, D., and Apte, S. S. (2015). ADAMTS proteins as modulators of microfibril formation and function. *Matrix Biol.* 47, 34–43. doi: 10.1016/j.matbio.2015.05.004

Hynes, R. O., and Naba, A. (2012). Overview of the matrisome–an inventory of extracellular matrix constituents and functions. *Cold Spring Harb. Perspect. Biol.* 4:a004903. doi: 10.1101/cshperspect.a004903

Iamaroon, A., Wallon, U. M., Overall, C. M., and Diewert, V. M. (1996). Expression of 72-kDa gelatinase (matrix metailloproteinase-2) in the developing mouse craniofacial complex. *Arch. Oral Biol.* 41, 1109–1119. doi: 10.1016/S0003-9969(96)00097-0

Inomata, H. (2017). Scaling of pattern formations and morphogen gradients. *Dev. Growth Differ.* 59, 41–51. doi: 10.1111/dgd.12337

Iozzo, R. V., and Schaefer, L. (2015). Proteoglycan form and function: a comprehensive nomenclature of proteoglycans. *Matrix Biol.* 42, 11–55. doi: 10.1016/j.matbio.2015.02.003

Ishorst, N., Francheschelli, P., Böhmer, A. C., Khan, M. F. J., Heilmann-Heimbach, S., Fricker, N., et al. (2018). Nonsyndromic cleft palate: an association study at GWAS candidate loci in a multiethnic sample. *Birth Defects Res.* 110, 871–882. doi: 10.1002/bdr2.1213

Itoh, Y. (2017). Metalloproteinases in rheumatoid arthritis: potential therapeutic targets to improve current therapies. *Prog. Mol. Biol. Transl. Sci.* 148, 327–338. doi: 10.1016/bs.pmbts.2017.03.002

Iwata, J., Parada, C., and Chai, Y. (2011). The mechanism of TGF-β signaling during palate development. *Oral Dis.* 17, 733–744. doi: 10.1111/j.1601-0825.2011.01806.x

Iyyanar, P. P. R., and Nazarali, A. J. (2017). Hoxa2 inhibits bone morphogenetic protein signaling during osteogenic differentiation of the palatal mesenchyme. *Front. Physiol.* 8:929. doi: 10.3389/fphys.2017.00929

Jankowski, R., and Márquez, S. (2016). Embryology of the nose: the evo-devo concept. *World J. Otorhinolaryngol.* 6:33. doi: 10.5319/wjo.v6.i2.33

Jiang, R., Bush, J. O., and Lidral, A. C. (2006). Development of the upper lip: morphogenetic and molecular mechanisms. *Dev. Dyn.* 235, 1152–1166. doi: 10.1002/dvdy.20646

Kadir, A., Mossey, P. A., Orth, M., Blencowe, H., Sowmiya, M., Lawn, J. E., et al. (2017). Systematic review and meta-analysis of the birth prevalence of orofacial clefts in low- and middle-income countries. *Cleft Palate Craniofac. J.* 54, 571–581. doi: 10.1597/15-221

Kamal, M., Ziyab, A. H., Bartella, A., Mitchell, D., Al-Asfour, A., Hölzle, F., et al. (2018). Volumetric comparison of autogenous bone and tissue-engineered bone replacement materials in alveolar cleft repair: a systematic review and meta-analysis. *Br. J. Oral Maxillofac. Surg.* 56, 453–462. doi: 10.1016/j.bjoms.2018.05.007

Kantar, R. S., Cammarata, M. J., Rifkin, W. J., Diaz-Siso, J. R., Hamdan, U. S., and Flores, R. L. (2019). Foundation-based cleft care in developing countries. *Plast. Reconstr. Surg.* 143, 1165–1178. doi: 10.1097/PRS.0000000000005416

Karamanos, N. K., Theocharis, A. D., Neill, T., and Iozzo, R. V. (2019). Matrix modeling and remodeling: a biological interplay regulating tissue homeostasis and diseases. *Matrix Biol.* 7, 1–11. doi: 10.1016/j.matbio.2018.08.007

Kelwick, R., Desanlis, I., Wheeler, G. N., and Edwards, D. R. (2015). The ADAMTS (A Disintegrin and metalloproteinase with thrombospondin motifs) family. *Genome Biol.* 16:113. doi: 10.1186/s13059-015-0676-3

Khan, M. F. J., Little, J., Mossey, P. A., Steegers-Theunissen, R. P. M., Bonsi, M., Bassi Andreasi, R., et al. (2018). Association between a common missense variant in LOXL3 gene and the risk of non-syndromic cleft palate. *Congenit. Anom.* 58, 136–140. doi: 10.1111/cga.12288

Khojasteh, A., Kheiri, L., Behnia, H., Tehranchi, A., Nazeman, P., Nadjmi, N., et al. (2017). Lateral ramus cortical bone plate in alveolar cleft osteoplasty with concomitant use of buccal fat pad derived cells and autogenous bone: phase I clinical trial. *Biomed Res. Int.* 2017:6560234. doi: 10.1155/2017/6560234

Kichenbrand, C., Velot, E., Menu, P., and Moby, V. (2018). Dental pulp stem cell-derived conditioned medium: an attractive alternative for regenerative therapy. *Tissue Eng. B Rev.* 25, 78–88. doi: 10.1089/ten.teb.2018.0168

Kim, H., Kim, Y., Park, J., Hwang, N. S., Lee, Y. K., and Hwang, Y. (2019). Recent advances in engineered stem cell-derived cell sheets for tissue regeneration. *Polymers* 11:209. doi: 10.3390/polym11020209

Kintakas, C., and McCulloch, D. R. (2011). Emerging roles for ADAMTS5 during development and disease. *Matrix Biol.* 30, 311–317. doi: 10.1016/j.matbio.2011.05.004

Krejci, P., Prochazkova, J., Bryja, V., Kozubik, A., and Wilcox, W. R. (2009). Molecular pathology of the fibroblast growth factor family. *Hum. Mutat.* 30, 1245–1255. doi: 10.1002/humu.21067

Kumar, P., Vinitha, B., and Fathima, G. (2013). Bone grafts in dentistry. *J. Pharm. Bioallied Sci.* 5, S125–S127. doi: 10.4103/0975-7406.113312

Lai, Y., Xie, C., Zhang, S., Gan, G., Wu, D., and Chen, W. (2016). Bone morphogenetic protein type I receptor inhibition induces cleft palate associated with micrognathia and cleft lower lip in mice. *Birth Defects Res. A Clin. Mol. Teratol.* 106, 612–623. doi: 10.1002/bdra.23504

Lan, Y., Qin, C., and Jiang, R. (2019). Requirement of hyaluronan synthase-2 in craniofacial and palate development. *J. Dent. Res.* 98, 1367–1375. doi: 10.1177/0022034519872478

Lazarou, S. A., Contodimos, G. B., and Gkegkes, I. D. (2011). Correction of alveolar cleft with calcium-based bone substitutes. *J. Craniofac. Surg.* 22, 854–857. doi: 10.1097/SCS.0b013e31820f7f19

Lee, J.-M., Kim, H.-Y., Park, J.-S., Lee, D.-J., Zhang, S., Green, D. W., et al. (2019). Developing palatal bone using human mesenchymal stem cell and stem cells from exfoliated deciduous teeth cell sheets. *J. Tissue Eng. Regen. Med.* 13, 319–327. doi: 10.1002/term.2811

Lemarchant, S., Wojciechowski, S., Vivien, D., and Koistinaho, J. (2017). ADAMTS-4 in central nervous system pathologies. *J. Neurosci. Res.* 95, 1703–1711. doi: 10.1002/jnr.24021

Letra, A., Silva, R. M., Motta, L. G., Blanton, S. H., Hecht, J. T., Granjeirol, J. M., et al. (2012). Association of MMP3 and TIMP2 promoter polymorphisms with nonsyndromic oral clefts. *Birth Defects Res. A Clin. Mol. Teratol.* 94, 540–548. doi: 10.1002/bdra.23026

Letra, A., Zhao, M., Silva, R. M., Vieira, A. R., and Hecht, J. T. (2014). Functional significance of MMP3 and TIMP2 polymorphisms in cleft lip/palate. *J. Dent. Res.* 93, 651–656. doi: 10.1177/0022034514534444

Levi, B., Brugman, S., Wong, V. W., Grova, M., Longaker, T., Wan, D. C., et al. (2011). Palatogenesis Engineering, pathways and pathologies. *Organogenesis* 7, 242–254. doi: 10.4161/org.7.4.17926

Leyendecker Junior, A., Gomes Pinheiro, C. C., Lazzaretti Fernandes, T., and Franco Bueno, D. (2018). The use of human dental pulp stem cells for in vivo bone tissue engineering: a systematic review. *J. Tissue Eng.* 9:2041731417752766. doi: 10.1177/2041731417752766

Li, C., Lan, Y., and Jiang, R. (2017). Molecular and cellular mechanisms of palate development. *J. Dent. Res.* 96, 1184–1191. doi: 10.1177/0022034517703580

Li, D., Zhang, H., Ma, L., Han, Y., Xu, M., Wang, Z., et al. (2016). Associations between microRNA binding site SNPs in FGFs and FGFRs and the risk of non-syndromic orofacial cleft. *Sci. Rep.* 6, 1–8. doi: 10.1038/srep31054

Li, J., Zou, J., Li, Q., Chen, L., Gao, Y., Yan, H., et al. (2016). Assessment of differentially expressed plasma microRNAs in nonsyndromic cleft palate and nonsyndromic cleft lip with cleft palate. *Oncotarget* 7, 86266–86279. doi: 10.18632/oncotarget.13379

Li, L., Meng, T., Jia, Z., Zhu, G., and Shi, B. (2010). Single nucleotide polymorphism associated with nonsyndromic cleft palate influences the processing of miR-140. *Am. J. Med. Genet. A* 152, 856–862. doi: 10.1002/ajmg.a.33236

Li, N.-G., Tang, Y.-P., Duan, J.-A., and Shi, Z.-H. (2014). Matrix metalloproteinase inhibitors: a patent review (2011 – 2013). *Expert Opin. Ther. Pat.* 24, 1039–1052. doi: 10.1517/13543776.2014.937424

Li, R., Chen, Z., Yu, Q., Weng, M., and Chen, Z. (2018). The function and regulatory network of pax9 gene in palate development. *J. Dent. Res.* 98, 277–287. doi: 10.1177/0022034518811861

Li, Y., Aoki, T., Mori, Y., Ahmad, M., Miyamori, H., Takino, T., et al. (2004). Cleavage of lumican by membrane-type matrix metalloproteinase-1 abrogates this proteoglycan-mediated suppression of tumor cell colony formation in soft agar. *Cancer Res.* 64, 7058–7064. doi: 10.1158/0008-5472.CAN-04-1038

Liang, F., Leland, H., Jedrzejewski, B., Auslander, A., Maniskas, S., Swanson, J., et al. (2018). Alternatives to autologous bone graft in alveolar cleft reconstruction: the state of alveolar tissue engineering. *J. Craniofac. Surg.* 29, 584–593. doi: 10.1097/SCS.0000000000004300

Lindahl, K., Barnes, A. M., Fratzl-Zelman, N., Whyte, M. P., Hefferan, T. E., Makareeva, E., et al. (2011). COL1 C-propeptide cleavage site mutations cause high bone mass osteogenesis imperfecta. *Hum. Mutat.* 32, 598–609. doi: 10.1002/humu.21475

Lisi, S., D'Amore, M., and Sisto, M. (2014). ADAM17 at the interface between inflammation and autoimmunity. *Immunol. Lett.* 162, 159–169. doi: 10.1016/j.imlet.2014.08.008

Liu, H., Li, D., Zhang, Y., and Li, M. (2018). Inflammation, mesenchymal stem cells and bone regeneration. *Histochem. Cell Biol.* 149, 393–404. doi: 10.1007/s00418-018-1643-1643

Liu, J. A., and Cheung, M. (2016). Neural crest stem cells and their potential therapeutic applications. *Dev. Biol.* 419, 199–216. doi: 10.1016/j.ydbio.2016.09.006

Lochter, A., Galosy, S., Muschler, J., Freedman, N., Werb, Z., and Bissell, M. J. (1997). Matrix metalloproteinase stromelysin-1 triggers a cascade of molecular alterations that leads to stable epithelial-to-mesenchymal conversion and a premalignant phenotype in mammary epithelial cells. *J. Cell Biol.* 139, 1861–1872. doi: 10.1083/jcb.139.7.1861

López-Otín, C., and Bond, J. S. (2008). Proteases: multifunctional enzymes in life and disease. *J. Biol. Chem.* 283, 30433–30437. doi: 10.1074/jbc.R800035200

Lough, K. J., Byrd, K. M., Spitzer, D. C., and Williams, S. E. (2017). Closing the gap: mouse models to study adhesion in secondary palatogenesis. *J. Dent. Res.* 96, 1210–1220. doi: 10.1177/0022034517726284

Ma, L., Xu, M., Li, D., Han, Y., Wang, Z., Yuan, H., et al. (2014). A miRNA-binding-site SNP of MSX1 is associated with NSOC susceptibility. *J. Dent. Res.* 93, 559–564. doi: 10.1177/0022034514527617

Macho, P., Bohac, M., Fedeles, J. Jr., Fekiacova, D., and Fedeles, J. Sr. (2017). Impact of cleft lip and / or palate in children on family quality of life before and after reconstructive surgery. *Bratisl. Lek. Listy.* 118, 370–373. doi: 10.4149/BLL

Malinowski, M., Pietraszek, K., Perreau, C., Boguslawski, M., Decot, V., Stoltz, J. F., et al. (2012). Effect of lumican on the migration of human mesenchymal stem cells and endothelial progenitor cells: involvement of matrix metalloproteinase-14. *PLoS One* 7:e50709. doi: 10.1371/journal.pone.0050709

Mammadova, A., Zhou, H., Carels, C. E. L., and Von den Hoff, J. W. (2016). Retinoic acid signalling in the development of the epidermis, the limbs and the secondary palate. *Differentiation* 92, 326–335. doi: 10.1016/j.diff.2016.05.001

Mannello, F., and Medda, V. (2012). Nuclear localization of matrix metalloproteinases. *Prog. Histochem. Cytochem.* 47, 27–58. doi: 10.1016/j.proghi.2011.12.002

Mansell, J. P., Kerrigan, J., McGill, J., Bailey, J., TeKoppele, J., and Sandy, J. R. (2000). Temporal changes in collagen composition and metabolism during rodent palatogenesis. *Mech. Ageing Dev.* 119, 49–62. doi: 10.1016/s0047-6374(00)00168-8

Marei, M. K., and El Backly, R. M. (2018). Dental mesenchymal stem cell-based translational regenerative dentistry: from artificial to biological replacement. *Front. Bioeng. Biotechnol.* 6:49. doi: 10.3389/fbioe.2018.00049

Martín-Del-Campo, M., Rosales-Ibañez, R., and Rojo, L. (2019). Biomaterials for cleft lip and palate regeneration. *Int. J. Mol. Sci.* 20:E2176. doi: 10.3390/ijms20092176

Martín-Piedra, M. A., Alaminos, M., Fernández-Valadés-gámez, R., España-López, A., Liceras-Liceras, E., Sánchez-Montesinos, I., et al. (2016). Development of a multilayered palate substitute in rabbits: a histochemical ex vivo and in vivo analysis. *Histochem. Cell Biol.* 147, 377–388. doi: 10.1007/s00418-016-1489-5

Maruhashi, T., Kii, I., Saito, M., and Kudo, A. (2010). Interaction between periostin and BMP-1 promotes proteolytic activation of lysyl oxidase. *J. Biol. Chem.* 285, 13294–13303. doi: 10.1074/jbc.M109.088864

Masotti, C., Brito, L. A., Nica, A. C., Ludwig, K. U., Nunes, K., Savastano, C. P., et al. (2017). MRPL53, a new candidate gene for orofacial clefting, identified using an eqtl approach. *J. Dent. Res.* 97, 33–40. doi: 10.1177/0022034517735805

Massenburg, B. B., Jenny, H. E., Saluja, S., Meara, J. G., Shrime, M. G., and Alonso, N. (2016). Barriers to cleft lip and palate repair around the world. *J. Craniofac. Surg.* 27, 1741–1745.

Mattot, V., Raes, M. B., Henriet, P., Eeckhout, Y., Stehelin, D., Vandenbunder, B., et al. (1995). Expression of interstitial collagenase is restricted to skeletal tissue during mouse embryogenesis. *J. Cell Sci.* 108(Pt 2), 529–535.

Mead, T. J., and Apte, S. S. (2018). ADAMTS proteins in human disorders. *Matrix Biol.* 7, 225–239. doi: 10.1016/j.matbio.2018.06.002

Mercapide, J., Lopez De Cicco, R., Castresana, J. S., and Klein-Szanto, A. J. P. (2003). Stromelysin-1/matrix metalloproteinase-3 (MMP-3) expression accounts for invasive properties of human astrocytoma cell lines. *Int. J. Cancer* 106, 676–682. doi: 10.1002/ijc.11286

Miettinen, P. J., Chin, J. R., Shum, L., Slavkin, H. C., Shuler, C. F., Derynck, R., et al. (1999). Epidermal growth factor receptor function is necessary for normal craniofacial development and palate closure. *Nat. Genet.* 22, 69–73. doi: 10.1038/8773

Mimura, T., Han, K. Y., Onguchi, T., Chang, J. H., Kim, T. I., Kojima, T., et al. (2009). MT1-MMP-Mediated cleavage of decorin in corneal angiogenesis. *J. Vasc. Res.* 46, 541–550. doi: 10.1159/000226222

Morales, J., Al-Sharif, L., Khalil, D. S., Shinwari, J. M. A., Bavi, P., Al-Mahrouqi, R. A., et al. (2009). Homozygous mutations in ADAMTS10 and ADAMTS17 Cause lenticular myopia, ectopia lentis, glaucoma, spherophakia, and short stature. *Am. J. Hum. Genet.* 85, 558–568. doi: 10.1016/j.ajhg.2009.09.011

Morris-Wiman, J., Burch, H., and Basco, E. (2000a). Temporospatial distribution of matrix metalloproteinase and tissue inhibitors of matrix metalloproteinases during murine secondary palate morphogenesis. *Anat. Embryol.* 202, 129–141. doi: 10.1007/s004290000098

Morris-Wiman, J., Du, Y., and Brinkley, L. (2000b). Occurrence and temporal variation in matrix metalloproteinases and their inhibitors during murine secondary palatal morphogenesis. *J. Craniofac. Genet. Dev. Biol.* 19, 201–212.

Mossaad, A., Badry, T., El Abdelrahaman, M., Abdelazim, A., Ghanem, W., Hassan, S., et al. (2019). Alveolar cleft reconstruction using different grafting techniques. *Open Access Maced. J. Med. Sci.* 7, 1369–1373. doi: 10.3889/oamjms.2019.236

Mossey, P. A., Little, J., Steegers-Theunissen, R., Molloy, A., Peterlin, B., Shaw, W. C., et al. (2017). Genetic interactions in nonsyndromic orofacial clefts in Europe—EUROCRAN study. *Cleft Palate Craniofac. J.* 54, 623–630. doi: 10.1597/16-037

Muir, A. M., Ren, Y., Butz, D. H., Davis, N. A., Blank, R. D., Birk, D. E., et al. (2014). Induced ablation of Bmp1 and Tll1 produces osteogenesis imperfecta in mice. *Hum. Mol. Genet.* 23, 3085–3101. doi: 10.1093/hmg/ddu013

Mularczyk, E. J., Singh, M., Godwin, A. R. F., Galli, F., Humphreys, N., Adamson, A. D., et al. (2018). ADAMTS10-mediated tissue disruption in Weill–Marchesani syndrome. *Hum. Mol. Genet.* 27, 3675–3687. doi: 10.1093/hmg/ddy276

Mussano, F., Genova, T., Petrillo, S., Roato, I., Ferracini, R., and Munaron, L. (2018). Osteogenic differentiation modulates the cytokine, chemokine, and growth factor profile of ASCs and SHED. *Int. J. Mol. Sci.* 19:1454. doi: 10.3390/ijms19051454

Naba, A., Pearce, O. M. T., Del Rosario, A., Ma, D., Ding, H., Rajeeve, V., et al. (2017). Characterization of the extracellular matrix of normal and diseased tissues using proteomics. *J. Proteome Res.* 16, 3083–3091. doi: 10.1021/acs.jproteome.7b00191

Nakajima, A. F., Shuler, C., Gulka, A. O. D., and Hanai, J.-I. (2018). TGF-β signaling and the epithelial-mesenchymal transition during palatal fusion. *Int. J. Mol. Sci.* 19:E3638. doi: 10.3390/ijms19113638

Nassif, A., Senussi, I., Meary, F., Loiodice, S., Hotton, D., Robert, B., et al. (2014). Msx1 role in craniofacial bone morphogenesis. *Bone* 66, 96–104. doi: 10.1016/j.bone.2014.06.003

Naung, N. Y., Duncan, W., Silva, R., and Coates, D. (2019). Localization and characterization of human palatal periosteum stem cells in serum-free, xeno-free medium for clinical use. *Eur. J. Oral Sci.* 127, 99–111. doi: 10.1111/eos.12603

Nawshad, A., LaGamba, D., and Hay, E. D. (2004). Transforming growth factor β (TGFβ) signalling in palatal growth, apoptosis and epithelial mesenchymal

transformation (EMT). *Arch. Oral Biol.* 49, 675–689. doi: 10.1016/j.archoralbio.2004.05.007

Neill, T., Painter, H., Buraschi, S., Owens, R. T., Lisanti, M. P., Schaefer, L., et al. (2012). Decorin antagonizes the angiogenic network: concurrent inhibition of met, hypoxia inducible factor 1α, vascular endothelial growth factor A, and induction of thrombospondin-1 and tiMP3. *J. Biol. Chem.* 287, 5492–5506. doi: 10.1074/jbc.M111.283499

Nelson, E. R., Levi, B., Sorkin, M., James, A. W., Liu, K. J., Quarto, N., et al. (2011). Role of GSK-3β in the osteogenic differentiation of palatal mesenchyme. *PLoS One* 6:e25847. doi: 10.1371/journal.pone.0025847

Nie, X., Luukko, K., and Kettunen, P. (2006). FGF signalling in craniofacial development and developmental disorders. *Oral Dis.* 12, 102–111. doi: 10.1111/j.1601-0825.2005.01176.x

Niewiarowska, J., Brézillon, S., Sacewicz-Hofman, I., Bednarek, R., Maquart, F.-X., Malinowski, M., et al. (2011). Lumican inhibits angiogenesis by interfering with α2β1 receptor activity and downregulating MMP-14 expression. *Thromb. Res.* 128, 452–457. doi: 10.1016/j.thromres.2011.06.011

Niibe, K., Zhang, M., Nakazawa, K., Morikawa, S., Nakagawa, T., Matsuzaki, Y., et al. (2017). The potential of enriched mesenchymal stem cells with neural crest cell phenotypes as a cell source for regenerative dentistry. *Jpn. Dent. Sci. Rev.* 53, 25–33. doi: 10.1016/j.jdsr.2016.09.001

Nikopensius, T., Kempa, I., Ambrozaitytė, L., Jagomägi, T., Saag, M., Matuleviėienė, A., et al. (2011). Variation in FGF1, FOXE1, and TIMP2genes is associated with nonsyndromic cleft lip with or without cleft palate. *Birth Defects Res. A Clin. Mol. Teratol.* 91, 218–225. doi: 10.1002/bdra.20791

Novais, A., Lesieur, J., Sadoine, J., Slimani, L., Baroukh, B., Saubaméa, B., et al. (2019). Priming dental pulp stem cells from human exfoliated deciduous teeth with fibroblast growth factor-2 enhances mineralization within tissue-engineered constructs implanted in craniofacial bone defects. *Stem Cells Transl. Med.* 8, 844–857.

Oh, J., Takahashi, R., Kondo, S., Mizoguchi, A., Adachi, E., Sasahara, R. M., et al. (2001). The membrane-anchored MMP inhibitor RECK is a key regulator of extracellular matrix integrity and angiogenesis175. *Cell* 107, 789–800. doi: 10.1016/s0092-8674(01)00597-9

Oichi, T., Taniguchi, Y., Soma, K., Oshima, Y., Yano, F., Mori, Y., et al. (2019). Adamts17 is involved in skeletogenesis through modulation of BMP-Smad1/5/8 pathway. *Cell. Mol. Life Sci.* 76, 4795–4809. doi: 10.1007/s00018-019-03188-3180

Okano, J., Udagawa, J., and Shiota, K. (2014). Roles of retinoic acid signaling in normal and abnormal development of the palate and tongue. *Congenit. Anom.* 54, 69–76. doi: 10.1111/cga.12049

Ong, C. S., Yesantharao, P., Huang, C. Y., Mattson, G., Boktor, J., Fukunishi, T., et al. (2017). 3D bioprinting using stem cells. *Pediatr. Res.* 83:223. doi: 10.1038/pr.2017.252

Paiva, K. B. S., and Granjeiro, J. M. (2014). Bone tissue remodeling and development: focus on matrix metalloproteinase functions. *Arch. Biochem. Biophys.* 561, 74–87. doi: 10.1016/j.abb.2014.07.034

Paiva, K. B. S., and Granjeiro, J. M. (2017). Matrix metalloproteinases in bone resorption, remodeling, and repair. *Prog. Mol. Biol. Transl. Sci.* 148, 203–303. doi: 10.1016/bs.pmbts.2017.05.001

Pall, E., Cenariu, M., Kasaj, A., Florea, A., Soancă, A., Roman, A., et al. (2017). New insights into the cellular makeup and progenitor potential of palatal connective tissues. *Microsc. Res. Tech.* 80, 1270–1282. doi: 10.1002/jemt.22925

Páll, E., Florea, A., Soriţău, O., Cenariu, M., Petruţiu, A. S., and Roman, A. (2015). Comparative assessment of oral mesenchymal stem cells isolated from healthy and diseased tissues. *Microsc. Microanal.* 21, 1249–1263. doi: 10.1017/S1431927615014749

Pan, A., Chang, L., Nguyen, A., and James, A. (2013). A review of hedgehog signaling in cranial bone development. *Front. Physiol.* 4:61. doi: 10.3389/fphys.2013.00061

Pan, Y., Li, D., Lou, S., Zhang, C., Du, Y., Jiang, H., et al. (2018). A functional polymorphism in the pre-miR-146a gene is associated with the risk of nonsyndromic orofacial cleft. *Hum. Mutat.* 39, 742–750. doi: 10.1002/humu.23415

Parada, C., and Chai, Y. (2012). Roles of BMP signaling pathway in lip and palate development. *Front. Oral Biol.* 16, 60–70. doi: 10.1159/000337617

Pauws, E., and Stanier, P. (2007). FGF signalling and SUMO modification: new players in the aetiology of cleft lip and/or palate. *Trends Genet.* 23, 631–640. doi: 10.1016/j.tig.2007.09.002

Pedroni, A. C. F., Sarra, G., de Oliveira, N. K., Moreira, M. S., Deboni, M. C. Z., and Marques, M. M. (2018). Cell sheets of human dental pulp stem cells for future application in bone replacement. *Clin. Oral Investig.* 23, 2713–2721. doi: 10.1007/s00784-018-2630-8

Pietraszek, K., Chatron-Colliet, A., Brézillon, S., Perreau, C., Jakubiak-Augustyn, A., Krotkiewski, H., et al. (2014). Lumican: a new inhibitor of matrix metalloproteinase-14 activity. *FEBS Lett.* 588, 4319–4324. doi: 10.1016/j.febslet.2014.09.040

Pietraszek-Gremplewicz, K., Karamanou, K., Niang, A., Dauchez, M., Belloy, N., Maquart, F. X., et al. (2019). Small leucine-rich proteoglycans and matrix metalloproteinase-14: key partners? *Matrix Biol.* 7, 271–285. doi: 10.1016/j.matbio.2017.12.006

Pinheiro, C. C. G., de Pinho, M. C., Aranha, A. C., Fregnani, E., and Bueno, D. F. (2017). Low power laser therapy: a strategy to promote the osteogenic differentiation of deciduous dental pulp stem cells from cleft lip and palate patients. *Tissue Eng. Part A* 24, 569–575. doi: 10.1089/ten.tea.2017.0115

Piperi, C., and Papavassiliou, A. G. (2012). Molecular mechanisms regulating matrix metalloproteinases. *Curr. Top. Med. Chem.* 12, 1095–1112. doi: 10.2174/1568026611208011095

Pischon, N., Darbois, L. M., Palamakumbura, A. H., Kessler, E., and Trackman, P. C. (2004). Regulation of collagen deposition and lysyl oxidase by tumor necrosis factor-α in osteoblasts. *J. Biol. Chem.* 279, 30060–30065. doi: 10.1074/jbc.M404208200

Pla, P., and Monsoro-Burq, A. H. (2018). The neural border: induction, specification and maturation of the territory that generates neural crest cells. *Dev. Biol.* 444, S36–S46. doi: 10.1016/j.ydbio.2018.05.018

Praveen Kumar, L., Kandoi, S., Misra, R., Vijayalakshmi, S., and Verma, R. S. (2019). The mesenchymal stem cell secretome: a new paradigm towards cell-free therapeutic mode in regenerative medicine. *Cytokine Growth Factor Rev.* 46, 1–9. doi: 10.1016/j.cytogfr.2019.04.002

Prochazkova, M., Prochazka, J., Marangoni, P., and Klein, O. D. (2018). Bones, glands, ears and more: the multiple roles of FGF10 in craniofacial development. *Front. Genet.* 9:542. doi: 10.3389/fgene.2018.00542

Qin, X., Wergedal, J. E., Rehage, M., Tran, K., Newton, J., Lam, P., et al. (2006). Pregnancy-associated plasma protein-A increases osteoblast proliferation in vitro and bone formation in vivo. *Endocrinology* 147, 5653–5661. doi: 10.1210/en.2006-1055

Ra, H. J., and Parks, W. C. (2007). Control of matrix metalloproteinase catalytic activity. *Matrix Biol.* 26, 587–596. doi: 10.1016/j.matbio.2007.07.001

Radichev, I. A., Remacle, A. G., Shiryaev, S. A., Purves, A. N., Johnson, S. L., Pellecchia, M., et al. (2010). Biochemical characterization of the cellular glycosylphosphatidylinositol-linked membrane type-6 matrix metalloproteinase. *J. Biol. Chem.* 285, 16076–16086. doi: 10.1074/jbc.M110.107094

Raghunathan, R., Sethi, M. K., Klein, J. A., and Zaia, J. (2019). Proteomics, glycomics, and glycoproteomics of matrisome molecules. *Mol. Cell. Proteomics* 18, 2138–2148. doi: 10.1074/mcp.R119.001543

Ray, H. J., and Niswander, L. (2012). Mechanisms of tissue fusion during development. *Development* 139, 1701–1711. doi: 10.1242/dev.068338

Reiss, K., and Bhakdi, S. (2017). The plasma membrane: penultimate regulator of ADAM sheddase function. *Biochim. Biophys. Acta Mol. Cell Res.* 1864, 2082–2087. doi: 10.1016/j.bbamcr.2017.06.006

Reuben, P. M., and Cheung, H. S. (2006). Research service & geriatric research, education and clinical center, veterans administration Medical Center, Miami, Florida 33125, Department of Biomedical Engineering, University of Miami, Coral Gables, Florida 33146 and Department of Medicine, University of Miami School of Medicine, Miami, Florida 33101. *Front. Biosci.* 11, 1199–1215.

Reynolds, K., Kumari, P., Sepulveda Rincon, L., Gu, R., Ji, Y., Kumar, S., et al. (2019). Wnt signaling in orofacial clefts: crosstalk, pathogenesis and models. *Dis. Model. Mech.* 12:dmm037051. doi: 10.1242/dmm.037051

Ricard-Blum, S., and Vallet, S. D. (2016). Proteases decode the extracellular matrix cryptome. *Biochimie* 122, 300–313. doi: 10.1016/j.biochi.2015.09.016

Ricard-Blum, S., and Vallet, S. D. (2019). Fragments generated upon extracellular matrix remodeling: biological regulators and potential drugs. *Matrix Biol.* 7, 170–189. doi: 10.1016/j.matbio.2017.11.005

Rietz, A., and Spiers, J. (2012). The relationship between the MMP system, adrenoceptors and phosphoprotein phosphatases. *Br. J. Pharmacol.* 166, 1225–1243. doi: 10.1111/j.1476-5381.2012.01917.x

Riou, J.-F., Umbhauer, M., Shi, D. L., and Boucaut, J.-C. (1992). Tenascin: a potential modulator of cell-extracellular matrix interactions during vertebrate embryogenesis. *Biol. Cell* 75, 1–9. doi: 10.1016/0248-4900(92)90118-K

Rodríguez, D., Morrison, C. J., and Overall, C. M. (2010). Matrix metalloproteinases: what do they not do? New substrates and biological roles identified by murine models and proteomics. *Biochim. Biophys. Acta Mol. Cell Res.* 1803, 39–54. doi: 10.1016/j.bbamcr.2009.09.015

Rodríguez-Manzaneque, J. C., Fernández-Rodríguez, R., Rodríguez-Baena, F. J., and Iruela-Arispe, M. L. (2015). ADAMTS proteases in vascular biology. *Matrix Biol.* 4, 38–45. doi: 10.1016/j.matbio.2015.02.004

Rodriguez-Pascual, F., and Rosell-Garcia, T. (2018). Lysyl oxidases: functions and disorders. *J. Glaucoma* 27(Suppl. 1), S15–S19. doi: 10.1097/IJG.0000000000000910

Roman, A., Şoanca, A., Florea, A., and Páll, E. (2013). In vitro characterization of multipotent mesenchymal stromal cells isolated from palatal subepithelial tissue grafts. *Microsc. Microanal.* 19, 370–380. doi: 10.1017/S143192761201433X

Rosell-García, T., Paradela, A., Bravo, G., Dupont, L., Bekhouche, M., Colige, A., et al. (2019). Differential cleavage of lysyl oxidase by the metalloproteinases BMP1 and ADAMTS2/14 regulates collagen binding through a tyrosine sulfate domain. *J. Biol. Chem.* 294:11087. doi: 10.1074/jbc.RA119.007806

Rothstein, M., Bhattacharya, D., and Simoes-Costa, M. (2018). The molecular basis of neural crest axial identity. *Dev. Biol.* 444, S170–S180. doi: 10.1016/j.ydbio.2018.07.026

Sahebjam, S., Khokha, R., and Mort, J. S. (2007). Increased collagen and aggrecan degradation with age in the joints of Timp3-/- mice. *Arthritis Rheum.* 56, 905–909. doi: 10.1002/art.22427

Sahoo, T., Theisen, A., Sanchez-Lara, P. A., Marble, M., Schweitzer, D. N., Torchia, B. S., et al. (2011). Microdeletion 20p12.3 involving BMP2 contributes to syndromic forms of cleft palate. *Am. J. Med. Genet. A* 155A, 1646–1653. doi: 10.1002/ajmg.a.34063

Salazar, V. S., Ohte, S., Capelo, L. P., Gamer, L., and Rosen, V. (2016). Specification of osteoblast cell fate by canonical Wnt signaling requires Bmp2. *Development* 143, 4352–4367. doi: 10.1242/dev.136879

Sanderson, R. D., Bandari, S. K., and Vlodavsky, I. (2019). Proteases and glycosidases on the surface of exosomes: newly discovered mechanisms for extracellular remodeling. *Matrix Biol.* 7, 160–169. doi: 10.1016/j.matbio.2017.10.007

Savitha, S., Sharma, S. M., Veena, S., and Rekha, R. (2015). Single nucleotide polymorphism of bone morphogenetic protein 4 gene: a risk factor of non-syndromic cleft lip with or without palate. *Indian J. Plast. Surg.* 48, 159–164. doi: 10.4103/0970-0358.163053

Savoca, M. P., Tonoli, E., Atobatele, A. G., and Verderio, E. A. M. (2018). Biocatalysis by transglutaminases: a review of biotechnological applications. *Micromachines* 9, 9–11. doi: 10.3390/mi9110562

Scalzone, A., Flores-Mir, C., Carozza, D., d'Apuzzo, F., Grassia, V., and Perillo, L. (2019). Secondary alveolar bone grafting using autologous versus alloplastic material in the treatment of cleft lip and palate patients: systematic review and meta-analysis. *Prog. Orthod.* 20:6. doi: 10.1186/s40510-018-0252-y

Scherrer, K. (2018). Primary transcripts: from the discovery of RNA processing to current concepts of gene expression - Review. *Exp. Cell Res.* 373, 1–33. doi: 10.1016/j.yexcr.2018.09.011

Schnellmann, R., Sack, R., Hess, D., Annis, D. S., Mosher, D. F., Apte, S. S., et al. (2018). A selective extracellular matrix proteomics approach identifies fibronectin proteolysis by a disintegrin-like and metalloprotease domain with thrombospondin type 1 motifs (ADAMTS16) and its impact on spheroid morphogenesis. *Mol. Cell. Proteomics* 17, 1410–1425. doi: 10.1074/mcp.RA118.000676

Schoen, C., Aschrafi, A., Thonissen, M., Poelmans, G., Von den Hoff, J. W., and Carels, C. E. L. (2017). MicroRNAs in palatogenesis and cleft palate. *Front. Physiol.* 8:165. doi: 10.3389/fphys.2017.00165

Schoen, C., Glennon, J. C., Abghari, S., Bloemen, M., Aschrafi, A., Carels, C. E. L., et al. (2018). Differential microRNA expression in cultured palatal fibroblasts from infants with cleft palate and controls. *Eur. J. Orthod.* 40, 90–96. doi: 10.1093/ejo/cjx034

Schwarzbauer, J. E., and DeSimone, D. W. (2011). Fibronectins, their fibrillogenesis, and in vivo functions. *Cold Spring Harb. Perspect. Biol.* 3:a005041. doi: 10.1101/cshperspect.a005041

Seelan, R. S., Mukhopadhyay, P., Warner, D. R., Appana, S. N., Brock, G. N., Pisano, M. M., et al. (2014). Methylated MicroRNA genes of the developing murine palate. *MicroRNA* 3, 160–173. doi: 10.2174/2211536604666150131125805

Segura-Castillo, J. L., Aguirre-Camacho, H., González-Ojeda, A., and Michel-Perez, J. (2005). Reduction of bone resorption by the application of fibrin glue in the reconstruction of the alveolar cleft. *J. Craniofac. Surg.* 16, 105–112. doi: 10.1097/00001665-200501000-00020

Seifeldin, S. A. (2016). Is alveolar cleft reconstruction still controversial? (Review of literature). *Saudi Dent. J.* 28, 3–11. doi: 10.1016/j.sdentj.2015.01.006

Shafi, A., Ah-kee, E., and Khan, A. (2015). Cleft lip and palate and alveolar bone grafting in the united kingdom: a brief overview for non-specialists. *West Indian Med. J.* 65, 185–188. doi: 10.7727/wimj.2015.191

Shanbhag, S., Suliman, S., Pandis, N., Stavropoulos, A., Sanz, M., and Mustafa, K. (2019). Cell therapy for orofacial bone regeneration: a systematic review and meta-analysis. *J. Clin. Periodontol.* 46(Suppl. 21), 162–182. doi: 10.1111/jcpe.13049

Sharif, F., Ur Rehman, I., Muhammad, N., and MacNeil, S. (2016). Dental materials for cleft palate repair. *Mater. Sci. Eng. C Mater. Biol. Appl.* 61, 1018–1028. doi: 10.1016/j.msec.2015.12.019

Sharpe, P. M., Brunet, C. L., Foreman, D. M., and Ferguson, M. W. J. (1993). Localisation of acidic and basic fibroblast growth factors during mouse palate development and their effects on mouse palate mesenchyme cells in vitro. *Roux's Arch. Dev. Biol.* 202, 132–143. doi: 10.1007/BF00365303

Shaw, W. (2004). Global strategies to reduce the health care burden of craniofacial anomalies: report of who meetings on international collaborative research on craniofacial anomalies. *Cleft Palate Craniofac. J.* 41, 238–243. doi: 10.1597/03-214.1

Shi, J., Son, M.-Y., Yamada, S., Szabova, L., Kahan, S., Chrysovergis, K., et al. (2008). Membrane-type MMPs enable extracellular matrix permissiveness and mesenchymal cell proliferation during embryogenesis. *Dev. Biol.* 313, 196–209. doi: 10.1016/j.ydbio.2007.10.017

Shimakura, Y., Yamzaki, Y., and Uchinuma, E. (2003). Experimental study on bone formation potential of cryopreserved human bone marrow mesenchymal cell/hydroxyapatite complex in the presence of recombinant human bone morphogenetic protein-2. *J. Craniofac. Surg.* 14, 108–116. doi: 10.1097/00001665-200301000-00021

Shirani, G., Abbasi, A. J., Mohebbi, S. Z., and Moharrami, M. (2017). Comparison between autogenous iliac bone and freeze-dried bone allograft for repair of alveolar clefts in the presence of plasma rich in growth factors: a randomized clinical trial. *J. Cranio Maxillofac. Surg.* 45, 1698–1703. doi: 10.1016/j.jcms.2017.08.001

Shu, C. C., Flannery, C. R., Little, C. B., and Melrose, J. (2019). Catabolism of fibromodulin in developmental rudiment and pathologic articular cartilage demonstrates novel roles for MMP-13 and ADAMTS-4 in C-terminal processing of SLRPs. *Int. J. Mol. Sci.* 20:E579. doi: 10.3390/ijms20030579

Smith, T., Lozanoff, S., Iyyanar, P., and Nazarali, A. J. (2013). Molecular signaling along the anterior–posterior axis of early palate development. *Front. Physiol.* 3:488. doi: 10.3389/fphys.2012.00488

Snyder-Warwick, A. K., and Perlyn, C. A. (2012). Coordinated events: FGF signaling and other related pathways in palatogenesis. *J. Craniofac. Surg.* 23, 397–400. doi: 10.1097/SCS.0b013e318240fed7

Soria-Valles, C., Gutiérrez-Fernández, A., Osorio, F. G., Carrero, D., Ferrando, A. A., Colado, E., et al. (2016). MMP-25 metalloprotease regulates innate immune response through NF-κB signaling. *J. Immunol.* 197, 296–302. doi: 10.4049/jimmunol.1600094

Sorushanova, A., Delgado, L. M., Wu, Z., Shologu, N., Kshirsagar, A., Raghunath, R., et al. (2019). The collagen suprafamily: from biosynthesis to advanced biomaterial development. *Adv. Mater.* 31, 1–39. doi: 10.1002/adma.201801651

Sprangers, S., and Everts, V. (2019). Molecular pathways of cell-mediated degradation of fibrillar collagen. *Matrix Biol.* 7, 190–200. doi: 10.1016/j.matbio.2017.11.008

Spyrou, J., Gardner, D. K., and Harvey, A. J. (2019). Metabolism is a key regulator of induced pluripotent stem cell reprogramming. *Stem Cells Int.* 2019:7360121. doi: 10.1155/2019/7360121

Stahle-Backdahl, M., Sandstedt, B., Bruce, K., Lindahl, A., Jimenez, M. G., Vega, J. A., et al. (1997). Collagenase-3 (MMP-13) is expressed during human fetal ossification and re-expressed in postnatal bone remodeling and in rheumatoid arthritis. *Lab. Invest.* 76, 717–728.

Stanier, P., and Pauws, E. (2012). Development of the lip and palate: fgf signalling. *Front. Oral Biol.* 16, 71–80. doi: 10.1159/000337618

Stanton, H., Melrose, J., Little, C. B., and Fosang, A. J. (2011). Proteoglycan degradation by the ADAMTS family of proteinases. *Biochim. Biophys. Acta Mol. Basis Dis.* 1812, 1616–1629. doi: 10.1016/j.bbadis.2011.08.009

Steiglitz, B. M., Ayala, M., Narayanan, K., George, A., and Greenspan, D. S. (2004). Bone morphogenetic protein-1/tolloid-like proteinases process dentin matrix protein-1. *J. Biol. Chem.* 279, 980–986. doi: 10.1074/jbc.M310179200

Stöcker, W., Grams, F., Baumann, U., Reinemer, P., Gomis-Rüth, F. X., McKay, D. B., et al. (1995). The metzincins–topological and sequential relations between the astacins, adamalysins, serralysins, and matrixins (collagenases) define a superfamily of zinc-peptidases. *Protein Sci.* 4, 823–840. doi: 10.1002/pro.5560040502

Sumida, R., Maeda, T., Kawahara, I., Yusa, J., and Kato, Y. (2019). Platelet-rich fibrin increases the osteoprotegerin/receptor activator of nuclear factor-κB ligand ratio in osteoblasts. *Exp. Ther. Med.* 18, 358–365. doi: 10.3892/etm.2019.7560

Sundell, A. L., Törnhage, C.-J., and Marcusson, A. (2017). A comparison of health-related quality of life in 5- and 10-year-old Swedish children with and without cleft lip and/or palate. *Int. J. Paediatr. Dent.* 27, 238–246. doi: 10.1111/ipd.12253

Suzuki, A., Abdallah, N., Gajera, M., Jun, G., Jia, P., Zhao, Z., et al. (2018). Genes and microRNAs associated with mouse cleft palate: a systematic review and bioinformatics analysis. *Mech. Dev.* 150, 21–27. doi: 10.1016/j.mod.2018.02.003

Szabova, L., Yamada, S. S., Birkedal-Hansen, H., and Holmbeck, K. (2005). Expression pattern of four membrane-type matrix metalloproteinases in the normal and diseased mouse mammary gland. *J. Cell Physiol.* 205, 123–132. doi: 10.1002/jcp.20385

Taguchi, T., Yanagi, Y., Yoshimaru, K., Zhang, X.-Y., Matsuura, T., Nakayama, K., et al. (2019). Regenerative medicine using stem cells from human exfoliated deciduous teeth (SHED): a promising new treatment in pediatric surgery. *Surg. Today* 49, 316–322. doi: 10.1007/s00595-019-01783-z

Takemaru, M., Sakamoto, Y., Sakamoto, T., and Kishi, K. (2016). Assessment of bioabsorbable hydroxyapatite for secondary bone grafting in unilateral alveolar cleft. *J. Plast. Reconstr. Aesthet. Surg.* 69, 493–496. doi: 10.1016/j.bjps.2015.10.040

Tang, M., Wang, Y., Han, S., Guo, S., and Wang, D. (2013). Transforming growth factor-beta3 gene polymorphisms and nonsyndromic cleft lip and palate risk: a meta-analysis. *Genet. Test. Mol. Biomarkers* 17, 881–889. doi: 10.1089/gtmb.2013.0334

Tang, Q., Li, L., Jin, C., Lee, J.-M., and Jung, H.-S. (2015). Role of region-distinctive expression of Rac1 in regulating fibronectin arrangement during palatal shelf elevation. *Cell Tissue Res.* 361, 857–868. doi: 10.1007/s00441-015-2169-2169

Tang, Q., Li, L., Lee, M.-J., Ge, Q., Lee, J.-M., and Jung, H.-S. (2016). Novel insights into a retinoic-acid-induced cleft palate based on Rac1 regulation of the fibronectin arrangement. *Cell Tissue Res.* 363, 713–722. doi: 10.1007/s00441-015-2271-z

Tarr, J., Lambi, A., Bradley, J., Barbe, M., and Popoff, S. (2018). Development of normal and cleft palate: a central role for connective tissue growth factor (CTGF)/CCN2. *J. Dev. Biol.* 6:18. doi: 10.3390/jdb6030018

Tavakolinejad, S., Ebrahimzadeh Bidskan, A., Ashraf, H., and Hamidi Alamdari, D. (2014). A glance at methods for cleft palate repair. *Iran. Red Crescent Med. J.* 16:e15393. doi: 10.5812/ircmj.15393

Taylor, D. A., Sampaio, L. C., Ferdous, Z., Gobin, A. S., and Taite, L. J. (2018). Decellularized matrices in regenerative medicine. *Acta Biomater.* 74, 74–89. doi: 10.1016/j.actbio.2018.04.044

Thompson, J., Mendoza, F., Tan, E., Bertol, J. W., Gaggar, A. S., Jun, G., et al. (2019). A cleft lip and palate gene, Irf6, is involved in osteoblast differentiation of craniofacial bone. *Dev. Dyn.* 248, 221–232. doi: 10.1002/dvdy.13

Thuaksuban, N., Nuntanaranont, T., and Pripatnanont, P. (2010). A comparison of autogenous bone graft combined with deproteinized bovine bone and autogenous bone graft alone for treatment of alveolar cleft. *Int. J. Oral Maxillofac. Surg.* 39, 1175–1180. doi: 10.1016/j.ijom.2010.07.008

Tsuchiya, S., Simmer, J. P., Hu, J. C. C., Richardson, A. S., Yamakoshi, F., and Yamakoshi, Y. (2011). Astacin proteases cleave dentin sialophosphoprotein (Dspp) to generate dentin phosphoprotein (Dpp). *J. Bone Miner. Res.* 26, 220–228. doi: 10.1002/jbmr.202

Tweedie, A. R. (1910). Specimen of the face and mouth of a female infant, showing arrest of development of the right half of the tongue, combined with a cleft of the soft palate and a palatolingual fold. *Proc. R. Soc. Med.* 3, 99–102. doi: 10.1177/003591571000300673

van Boxtel, A. L., Gansner, J. M., Hakvoort, H. W. J., Snell, H., Legler, J., and Gitlin, J. D. (2011). Lysyl oxidase-like 3b is critical for cartilage maturation during zebrafish craniofacial development. *Matrix Biol.* 30, 178–187. doi: 10.1016/j.matbio.2010.12.002

Van den Steen, P. E., Opdenakker, G., Wormald, M. R., Dwek, R. A., and Rudd, P. M. (2001). Matrix remodelling enzymes, the protease cascade and glycosylation. *Biochim. Biophys. Acta* 1528, 61–73. doi: 10.1016/s0304-4165(01)00190-8

van Hout, W. M. M. T., Mink van der Molen, A. B., Breugem, C. C., Koole, R., and Van Cann, E. M. (2011). Reconstruction of the alveolar cleft: can growth factor-aided tissue engineering replace autologous bone grafting? a literature review and systematic review of results obtained with bone morphogenetic protein-2. *Clin. Oral Investig.* 15, 297–303. doi: 10.1007/s00784-011-0547-546

Van Otterloo, E., Williams, T., and Artinger, K. B. (2016). The old and new face of craniofacial research: how animal models inform human craniofacial genetic and clinical data. *Dev. Biol.* 415, 171–187. doi: 10.1016/j.ydbio.2016.01.017

Verstappen, J., and Von den Hoff, J. W. (2006). Tissue inhibitors of metalloproteinases (TIMPs): their biological functions and involvement in oral disease. *J. Dent Res.* 85, 1074–1084. doi: 10.1177/154405910608501202

Vieira, A. R. (2008). Unraveling human cleft lip and palate research. *J. Dent. Res.* 87, 119–125. doi: 10.1177/154405910808700202

Vincenti, M. P. (2007). Signal transduction and cell-type specific regulation of matrix metalloproteinase gene expression: can MMPs be good for you? *J. Cell Physiol.* 213, 355–364. doi: 10.1002/JCP

von Marschall, Z., and Fisher, L. W. (2010). Decorin is processed by three isoforms of bone morphogenetic protein-1 (BMP1). *Biochem. Biophys. Res. Commun.* 391, 1374–1378. doi: 10.1016/j.bbrc.2009.12.067

Wang, J., Bai, Y., Li, H., Greene, S. B., Klysik, E., Yu, W., et al. (2013). MicroRNA-17-92, a direct Ap-2α transcriptional target, modulates T-box factor activity in orofacial clefting. *PLoS Genet.* 9:e1003785. doi: 10.1371/journal.pgen.1003785

Wang, J., Wang, X., Sun, Z., Wang, X., Yang, H., Shi, S., et al. (2010). Stem cells from human-exfoliated deciduous teeth can differentiate into dopaminergic neuron-like cells. *Stem Cells Dev.* 19, 1375–1383. doi: 10.1089/scd.2009.0258

Wang, S., Sun, C., Meng, Y., Zhang, B., Wang, X., Su, Y., et al. (2017). A pilot study: screening target miRNAs in tissue of nonsyndromic cleft lip with or without cleft palate. *Exp. Ther. Med.* 13, 2570–2576. doi: 10.3892/etm.2017.4248

Warner, D., Ding, J., Mukhopadhyay, P., Brock, G., Smolenkova, I., Seelan, R., et al. (2015). Temporal expression of mirnas in laser capture microdissected palate medial edge epithelium from tgfβ3-/- mouse fetuses. *MicroRNA* 4, 64–71. doi: 10.2174/2211536604666150710125743

Weijs, W. L. J., Siebers, T. J. H., Kuijpers-Jagtman, A. M., Bergé, S. J., Meijer, G. J., and Borstlap, W. A. (2010). Early secondary closure of alveolar clefts with mandibular symphyseal bone grafts and β-tri calcium phosphate (β-TCP). *Int. J. Oral Maxillofac. Surg.* 39, 424–429. doi: 10.1016/j.ijom.2010.02.004

Weng, M., Chen, Z., Xiao, Q., Li, R., and Chen, Z. (2018). A review of FGF signaling in palate development. *Biomed. Pharmacother.* 103, 240–247. doi: 10.1016/j.biopha.2018.04.026

Weston, J. A., and Thiery, J. P. (2015). Pentimento: neural crest and the origin of mesectoderm. *Dev. Biol.* 401, 37–61. doi: 10.1016/j.ydbio.2014.12.035

Whitehead, A. L. (1902). The influence of nasal and nasopharyngeal obstruction upon the development of the teeth and palate. *Br. Med. J.* 1, 949–951. doi: 10.1136/bmj.1.2155.949

Wight, T. N. (2017). Provisional matrix: a role for versican and hyaluronan. *Matrix Biol.* 6, 38–56. doi: 10.1016/j.matbio.2016.12.001

Wolf, C. J., Belair, D. G., Becker, C. M., Das, K. P., Schmid, J. E., and Abbott, B. D. (2018). Development of an organotypic stem cell model for the study of human embryonic palatal fusion. *Birth Defects Res.* 110, 1322–1334. doi: 10.1002/bdr2.1394

Wolf, Z. T., Brand, H. A., Shaffer, J. R., Leslie, E. J., Arzi, B., Willet, C. E., et al. (2015). Genome-wide association studies in dogs and humans identify ADAMTS20 as a risk variant for cleft lip and palate. *PLoS Genet.* 11:e1005059. doi: 10.1371/journal.pgen.1005059

Wong, M. K., Shawky, S. A., Aryasomayajula, A., Green, M. A., Ewart, T., Selvaganapathy, P. R., et al. (2018). Extracellular matrix surface regulates self-assembly of three-dimensional placental trophoblast spheroids. *PLoS One* 13:e0199632. doi: 10.1371/journal.pone.0199632

Wu, C., Pan, W., Feng, C., Su, Z., Duan, Z., Zheng, Q., et al. (2018). Grafting materials for alveolar cleft reconstruction: a systematic review and best-evidence synthesis. *Int. J. Oral Maxillofac. Surg.* 47, 345–356. doi: 10.1016/j.ijom.2017.08.003

Wu, M., Li, J., Engleka, K. A., Zhou, B., Lu, M. M., Plotkin, J. B., et al. (2008). Persistent expression of Pax3 in the neural crest causes cleft palate and defective osteogenesis in mice. *J. Clin. Invest.* 118, 2076–2087. doi: 10.1172/JCI33715

Wu, N., Yan, J., Han, T., Zou, J., and Shen, W. (2018). Integrated assessment of differentially expressed plasma microRNAs in subtypes of nonsyndromic orofacial clefts. *Medicine* 97:e11224. doi: 10.1097/MD.0000000000011224

Xavier, G. M., Seppala, M., Barrell, W., Birjandi, A. A., Geoghegan, F., and Cobourne, M. T. (2016). Hedgehog receptor function during craniofacial development. *Dev. Biol.* 415, 198–215. doi: 10.1016/j.ydbio.2016.02.009

Xiao, L., Kumazawa, Y., and Okamura, H. (2014). Cell death, cavitation and spontaneous multi-differentiation of dental pulp stem cells-derived spheroids in vitro: a journey to survival and organogenesis. *Biol. Cell* 106, 405–419. doi: 10.1111/boc.201400024

Xu, J., Huang, Z., Wang, W., Tan, X., Li, H., Zhang, Y., et al. (2018). FGF8 signaling alters the osteogenic cell fate in the hard palate. *J. Dent. Res.* 97, 589–596. doi: 10.1177/0022034517750141

Xu, M., Ma, L., Lou, S., Du, Y., Yin, X., Zhang, C., et al. (2018). Genetic variants of microRNA processing genes and risk of non-syndromic orofacial clefts. *Oral Dis.* 24, 422–428. doi: 10.1111/odi.12741

Yamada, Y., Nakamura-Yamada, S., Kusano, K., and Baba, S. (2019). Clinical potential and current progress of dental pulp stem cells for various systemic diseases in regenerative medicine: a concise review. *Int. J. Mol. Sci.* 20:1132. doi: 10.3390/ijms20051132

Yang, C. Y., Chanalaris, A., and Troeberg, L. (2017). ADAMTS and ADAM metalloproteinases in osteoarthritis – looking beyond the 'usual suspects.'. *Osteoarthr. Cartil.* 25, 1000–1009. doi: 10.1016/j.joca.2017.02.791

Yang, H., Gao, L.-N., An, Y., Hu, C.-H., Jin, F., Zhou, J., et al. (2013). Comparison of mesenchymal stem cells derived from gingival tissue and periodontal ligament in different incubation conditions. *Biomaterials* 34, 7033–7047. doi: 10.1016/j.biomaterials.2013.05.025

Ye, S., Eriksson, P., Hamsten, A., Kurkinen, M., Humphries, S. E., and Henney, A. M. (1996). Progression of coronary atherosclerosis is associated with a common genetic variant of the human stromelysin-1 promoter which results in reduced gene expression. *J. Biol. Chem.* 271, 13055–13060. doi: 10.1074/jbc.271.22.13055

Yusof, M. F. H., Zahari, W., Hashim, S. N. M., Osman, Z. F., Chandra, H., Kannan, T. P., et al. (2018). Angiogenic and osteogenic potentials of dental stem cells in bone tissue engineering. *J. Oral Biol. Craniofac. Res.* 8, 48–53. doi: 10.1016/j.jobcr.2017.10.003

Zhang, J., Yang, R., Liu, Z., Hou, C., Zong, W., Zhang, A., et al. (2015). Loss of lysyl oxidase-like 3 causes cleft palate and spinal deformity in mice. *Hum. Mol. Genet.* 24, 6174–6185. doi: 10.1093/hmg/ddv333

Zhang, S., Wang, C., Xie, C., Lai, Y., Wu, D., Gan, G., et al. (2017). Disruption of hedgehog signaling by vismodegib leads to cleft palate and delayed osteogenesis in experimental design. *J. Craniofac. Surg.* 28, 1607–1614. doi: 10.1097/SCS.0000000000003790

Zuk, P. A. (2008). Tissue engineering craniofacial defects with adult stem cells? Are we ready yet? *Pediatr. Res.* 63, 478–486. doi: 10.1203/PDR.0b013e31816bdf36

Conflict of Interest: The authors declare that the research was conducted in the absence of any commercial or financial relationships that could be construed as a potential conflict of interest.

frontiers in Cell and Developmental Biology

REVIEW
published: 07 May 2019
doi: 10.3389/fcell.2019.00068

Unraveling the ECM-Immune Cell Crosstalk in Skin Diseases

Oindrila Bhattacharjee[1,2†], *Uttkarsh Ayyangar*[1,2†], *Ambika S. Kurbet*[1,2†], *Driti Ashok*[2] *and Srikala Raghavan*[2*]

[1] School of Chemical and Biotechnology, Sastra University, Thanjavur, India, [2] Institute for Stem Cell Biology and Regenerative Medicine, GKVK Campus, Bangalore, India

The extracellular matrix (ECM) is a complex network of proteins and proteoglycans secreted by keratinocytes, fibroblasts and immune cells. The function of the skin ECM has expanded from being a scaffold that provides structural integrity, to a more dynamic entity that is constantly remodeled to maintain tissue homeostasis. The ECM functions as ligands for cell surface receptors such as integrins, dystroglycans, and toll-like receptors (TLRs) and regulate cellular signaling and immune cell dynamics. The ECM also acts as a sink for growth factors and cytokines, providing critical cues during epithelial morphogenesis. Dysregulation in the organization and deposition of ECMs lead to a plethora of pathophysiological conditions that are exacerbated by aberrant ECM-immune cell interactions. In this review, we focus on the interplay between ECM and immune cells in the context of skin diseases and also discuss state of the art therapies that target the key molecular players involved.

Keywords: extracellular matrix, skin diseases, immune cells, crosstalk, therapeutics

OPEN ACCESS

Edited by:
Charles D. Little, University of Kansas Medical Center, United States

Reviewed by:
Lidija Radenovic, University of Belgrade, Serbia
Nagaraj Balasubramanian, Indian Institute of Science Education and Research, India

***Correspondence:**
Srikala Raghavan
srikala@instem.res.in

[†] These authors have contributed equally to this work and are co-first authors

Specialty section:
This article was submitted to Cell Adhesion and Migration, a section of the journal Frontiers in Cell and Developmental Biology

Received: *12 January 2019*
Accepted: *09 April 2019*
Published: *07 May 2019*

Citation:
Bhattacharjee O, Ayyangar U, Kurbet AS, Ashok D and Raghavan S (2019) Unraveling the ECM-Immune Cell Crosstalk in Skin Diseases. Front. Cell Dev. Biol. 7:68. doi: 10.3389/fcell.2019.00068

INTRODUCTION

Homeostasis in the skin, the largest organ of the body, is critical for maintaining its structural, protective and regulatory functions. Alterations in this homeostasis, as seen in major skin disorders such as Atopic Dermatitis (AD), Psoriasis, Epidermolysis Bullosa (EB), and skin cancer, lead to impaired skin hydration, thermoregulation, and increased susceptibility to infections (Mellerio, 2010; Romanovsky, 2014; Nyström and Bruckner-Tuderman, 2018). An important role in exacerbating the disease condition is played by dysregulated interactions between two important goal keepers of skin function, the immune cells and the extracellular matrix (ECM). Immune cells play a critical role in the breakdown, synthesis, and remodeling of ECM components that are important for physiological processes such as mammary gland remodeling, lung branching morphogenesis and wound healing (Allori et al., 2008; Rozario and DeSimone, 2010). ECM components such as laminin and collagens, on the other hand, act as ligands for immune cells and facilitate their adhesion and trafficking (Simon and Bromberg, 2017). Proteolytic enzymes secreted by the immune cells generate fragmented laminin and collagen peptides that can serve as chemotactic signals for the recruitment of immune cells (Bonnans et al., 2014). Moreover, ECM components and their physical properties can drive specific activation states of immune cells such as macrophages (McWhorter et al., 2015). In certain chronic disease conditions, excess ECM deposition results in fibrosis that can later develop into cancer (Bonnans et al., 2014). Therefore, maintaining a balance between remodeling by the immune system and ECM dynamics becomes critical to maintain homeostasis.

Skin diseases are largely incurable and therefore remain a major burden; globally posing an adverse socio-economic and psychological impact on the affected populations. The prevalence estimates of psoriasis can go as high as 1% in the U.S. to 8.5% in Norway (Parisi et al., 2013).

AD affects up to one-fifth of the population in developed countries (Weidinger and Novak, 2016). Skin cancers, especially non-melanoma skin cancer affects over 3 million Americans yearly with high mortality rates (Apalla et al., 2017). The prevalence of EB has risen to 11.07 per million live births globally and the numbers continue to rise (Fine, 2016). Commonly used treatment regimes for skin diseases include, the use of topical steroids and anti-inflammatory medications to control disease progression (Thomas et al., 2018; Yu et al., 2018). However, there is a paucity of curative therapies, which necessitates further understanding of the mechanisms that exacerbate the disease condition. Thus, focusing on the crosstalk between ECM and immune cells in skin diseases may help identify better targets for therapeutic interventions. In this review, we highlight the bidirectional interactions between ECM and immune cells in the major skin diseases and discuss the therapeutic strategies for dampening this "War of the Titans."

THE SKIN AND ITS ECM

Mammalian skin comprises of a stratified epithelium known as the epidermis and a connective tissue layer termed the dermis. The epidermis is made up of specialized cells containing keratin intermediate filaments known as keratinocytes and is stratified into different layers, namely, basal (stratum basale), suprabasal (stratum spinosum), granular (stratum granulosum), and cornified (stratum corneum) layers (**Figure 1**) (Fuchs and Raghavan, 2002; Breitkreutz et al., 2013). The basal keratinocytes comprise a pool of proliferating stem cells, which undergo terminal differentiation and eventually lose their nuclei to form the outermost cornified layer (Blanpain and Fuchs, 2006). Each of these epidermal layers is characterized by the expression of different structural proteins. The basal keratinocytes express keratin 5 and 14, which are replaced by keratin 1 and 10 as they differentiate into the spinous layer. The granular layer, as the name suggests, contains keratohyalin granules made up of lipids and precursors of proteins such as loricrin, filaggrin, and involucrin. These proteins and lipids are covalently crosslinked by transglutaminase to form the outermost layer, the stratum corneum that is 10–30 cell layers thick. The stratum corneum is composed of flattened, and enucleated cells embedded in matrix that is rich in proteins and insoluble lipids (Candi et al., 2005). Mutations in any of the above mentioned genes can lead to skin diseases, some of which are discussed later in the review (Chandran, 2013). The dermis is a highly vascularized tissue comprising of fibroblasts, adipocytes and various pools of innate and adaptive immune cells (Mueller et al., 2014). It is divided into a thin upper papillary dermis with loosely arranged collagen fibrils and a thick lower reticular dermis with dense collagen packing. Furthermore, the dermal and hypodermal compartments of the skin also comprise of triglyceride rich adipocyte depot called the dermal white adipose tissue (DWAT) and subcutaneous white adipose tissue (SWAT), respectively (Driskell et al., 2014).

ECM components in the skin are present in the basement membrane and interstitial matrix (Frantz et al., 2010). The BM is a non-cellular array of structural ECM components that separates epidermis from dermis. It is composed of different subtypes of laminins and collagens, primarily laminin 5 (laminin-332) and collagen IV, which are non-covalently connected through perlecan and nidogen (Breitkreutz et al., 2013). This forms a highly dynamic fibrous structure that also functions as a diffusion barrier and serves as a repository of growth factors (Jayadev and Sherwood, 2017). The interstitial matrix is localized to the interstitial spaces in the dermal compartments. These primarily comprise of other collagen subtypes that also impart structural stability to the tissue (Bonnans et al., 2014). Additionally, there are non-structural ECM components called matricellular proteins that are synthesized by the epidermal and dermal cells during development and under non-homeostatic conditions. Matricellular proteins are involved in modulating cell function by interacting with structural ECM proteins as well as with various receptors, hormones and proteases. These interactions are a function of local availability of growth factors and overall composition of the ECM. Tenascin-C (TNC), thrombospondin (TSP), a secreted protein, acidic and rich in cysteine (SPARC), osteopontin (OPN), decorin, periostin (POSTN), and cysteine-rich protein 61 (CCN-1) are some of the major matricellular proteins (Bornstein, 2009). While basement membrane components are relatively stable, matricellular proteins undergo rapid turnover (Bonnans et al., 2014).

Organization of the BM components is mediated through transmembrane heterodimeric cell surface receptors called integrins that are expressed by the basal keratinocytes (Hynes, 2002; Andriani et al., 2003). Integrins are composed of α and β subunits. There are 18 α and 8 β subunits that form 24 different combinations. In the skin epidermis, α2β1, α3β1, and α6β4 are the main integrin pairs that are expressed (Watt and Fujiwara, 2011). Integrin β4 and β1 are components of multi-protein cell-substratum junctional complexes known as hemidesmosomes and focal adhesions, respectively. These structures facilitate the adherence of basal keratinocytes to its underlying BM either via intermediate filaments (in hemidesmosomes) or via actin cytoskeleton network (in focal adhesions) (Tsuruta et al., 2011). ECM-integrin signaling at the BM is indispensable for several cellular processes such as cell proliferation, differentiation, adhesion, migration, and apoptosis (Hegde and Raghavan, 2013). Any disruptions in the ECM-integrin interactions lead to adhesion defects (Nelson and Larsen, 2015). Recent work from our laboratory uncovered the importance of ECM-integrin interaction in embryonic skin homeostasis. We showed that loss of integrin β1 in embryonic skin results in ECM degradation that is exacerbated through a sterile inflammatory response (Kurbet et al., 2016).

IMMUNOMODULATORY FUNCTIONS OF ECM

ECM molecules are potent regulators of immune cell function (**Table 1**). Alterations in the structure and composition of ECM in disease conditions provide immune cells with physical and biochemical cues that, in turn, affect their activation states. Several studies have shown that both enzymatically

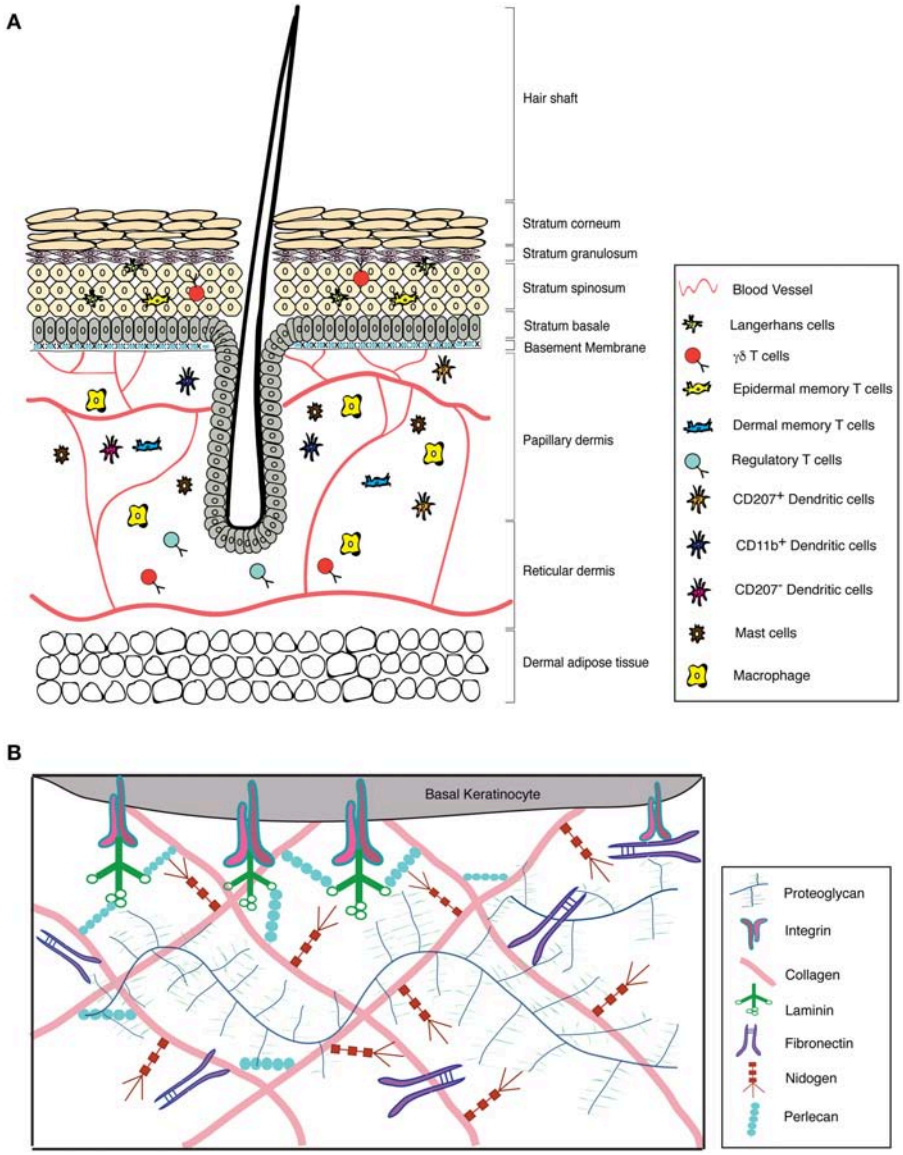

FIGURE 1 | Structure of the skin with its associated ECM and immune cell repertoire. **(A)** Structure of the skin and its immune components. **(B)** Graphical representation of the major components of the skin ECM.

digested ECM components as well as intact ECM proteins can modulate activation, fate determination, and chemotaxis of immune cells (Lu et al., 2011; Hallmann et al., 2015; Simon and Bromberg, 2017).

SKIN IMMUNE CELL REPERTOIRE AND ITS ROLE IN MAINTAINING ECM DYNAMICS

The skin contains a diverse population of immune cells that continuously surveil the organ to protect from assaults and maintain homeostasis. The epidermal and dermal compartments of the skin have distinct populations of immune cells that perform multiple functions including antigen cross-presentation to effector cells, tolerance induction, mediation of inflammation, promotion of growth and repair, regulation of stem cell quiescence, and maintenance of epidermal differentiation (Di Meglio et al., 2011). Langerhan cells and dendritic epidermal T cells are primarily located in the epidermis while, distinct populations of other dendritic cells and macrophages are present in the dermis (Heath and Carbone, 2013). Mast cells and T cell populations including αβ, γδT, Tregs, Th17, and memory T cells get recruited to both the epidermis and dermis depending on the homeostatic status of the skin (Matejuk, 2018). Details of the expression markers, location, and regulatory roles of immune cells in maintaining skin homeostasis are listed in **Table 2**.

TABLE 1 | Immune functions of ECM.

ECM component	Immune functions	ECM related skin diseases	References
STRUCTURAL COMPONENTS			
Laminin	• Laminin affects adhesion, migration, and proliferation of immune cells via integrin signaling. • Fragments or processed peptides of laminin chains act as DAMPs (damage associated molecular patterns), and can affect gene expression of cytokines and MMPs (Matrix metalloproteinases).	JEB and anti-laminin γ1 pemphigoid.	Adair-Kirk and Senior, 2008; Kamata et al., 2013; Senyürek et al., 2014; Simon and Bromberg, 2017
Collagen	• Collagen can bind to immune receptors thereby activating them that, in turn, can inhibit cytotoxic functions of natural killer and T cells. Collagen can affect proliferation of other immune cells. • Collagen can interact with other immune activating matricellular proteins such as cochlin to mount anti-pathogenic responses. • Collagen fragments can increase secretion of IL-1β by blood monocytes.	RDEB (Recessive dystrophic epidermolysis bullosa), EBA (Epidermolysis bullosa aquisita), Systemic lupus erythematosus and scleroderma.	Jimenez et al., 1996; Meyaard et al., 1997; Stultz et al., 2007; Rygiel et al., 2011; An and Brodsky, 2016; Nyström et al., 2018
Elastin	• Elastin peptides act as chemotactic agents for immune cells.	Cutis laxa, pseudoxanthonum elasticum	Uitto and Shamban, 1987; Fulop et al., 2012
ECM-1	• ECM-1 suppresses Th17 responses and can be secreted by Th2 immune cells in autoimmune diseases. • ECM-1 can interact with αv integrins and block TGF-β activation.	Lipoid proteinosis, lichen sclerosus	Oyama et al., 2003; Su et al., 2016
Fibronectin	• Fibronectin variants obtained by splicing and partial folding can activate TLR signaling and induce secretion of cytokines and chemokines by fibroblasts. • Fibronectin can be produced by Th1 cells and may be important in opsonizing intracellular pathogens.	Atopic dermatitis, psoriasis, perforating skin disorders.	Sandig et al., 2009; McFadden et al., 2011; Kelsh et al., 2014
MATRICELLULAR COMPONENTS			
Tenascin C	• Tenascin affects adhesion properties of monocytes, B and T cells. • Tenascin C binds to TLR-2 & TLR-4 and initiates a pro-inflammatory cascade.	Basal cell carcinoma, psoriasis, solar keratosis, Bowen's diseases	Rüegg et al., 1989; Schalkwijk et al., 1991; Zuliani-Alvarez et al., 2017
Osteopontin	• OPN promotes Th17 and Th1 while suppressing Th2 responses.	Systemic lupus erythematosus, psoriasis, contact dermatitis	Mori et al., 2008; Buback et al., 2009; Reduta et al., 2015
CCN	• CCN helps in macrophage adhesion via binding to cognate integrin receptors. • CCN activates NFκB mediated transcription followed by a pro-inflammatory cascade. • Promotes IL1β secretion by psoriatic keratinocytes.	Psoriasis, scleroderma	Bai et al., 2010; Sun et al., 2015; Henrot et al., 2018
Decorin	• Mounts pro-inflammatory responses by binding to TLR-2 and -4 or by suppressing TGF-β responses.	Delayed type hypersensitivity	Yamaguchi et al., 1990; Seidler et al., 2011; Bocian et al., 2013; Frey et al., 2013
TSP-1	• Promotes anti-tumor M1 macrophage recruitment via release of reactive oxygen species. • Facilitates adhesion of neutrophils and serves as chemotactic agent for monocytes and neutrophils. • Activates TGF-β	N/A	Bornstein, 2001; Martin-Manso et al., 2008
Periostin (POSTN)	• Activates keratinocytes by binding to αv integrins and stimulates them to secrete TSLP that can trigger a Th2 response.	Atopic dermatitis, dermal fibrosis	Liu et al., 2014; Yamaguchi, 2014

Immune cells are one of the most important regulators of ECM degradation, synthesis, assembly and remodeling. Mechanisms by which immune cells accomplish this include–(i) synthesis of enzymes that remodel ECM components, (ii) synthesis of cytokines and growth factors that induce ECM synthesis or degradation, and (iii) synthesis of ECM components.

(i) Synthesis of enzymes that remodel ECM components: Metalloproteinases are enzymes secreted by the immune cells that cleave ECM proteins leading to alterations in the physical and biochemical properties of the tissue. Degradation of ECM by metalloproteinases aids in the trafficking of immune cells, generates bioactive peptides, and releases the sequestered growth factors (Mott and Werb, 2004). Metalloproteinases include MMPs, (matrix metalloproteinases) adamlysins including ADAMS (a disintegrin and metalloproteinases), ADAMTs (ADAMs containing a thrombospondin motif), Meprins as well as serine proteases such as plasmins, granzymes, and cathepsins. These enzymes cleave collagens (MMP-1, -2, -3, -7, -8, -9, -10, -11, -12, -13, -14, -16, -19, -25, -26; ADAM-10, -12 and -15; Meprin a and b), elastins (MMP-2, -3, -7, -9, -10, -11, - 12), gelatins (MMP-2, -3, -7, -9, -12, -14, -15, -16, -17, -23A, - 23B, -24, -25; ADAM-9, -10, -12, -15), aggrecans (MMP-3, -13; ADAMTs), and laminins (MMP-3, -7, -11, -12, -14, -15, -19, Meprin α and β) (Bonnans et al., 2014). Several studies have highlighted the

TABLE 2 | Immune cell repertoire in skin.

Immune cell	Subsets	Marker expression		Localization	Functions in skin	References
		Human	Mouse			
Dendritic cells ($CD11c^+$, $MHC\text{-}II^+$)	Epidermal dendritic cells					
	Langerhans cells	$CD1a^+$ CD80, CD86, $HLA\text{-}DR^+$ CD83 DC-LAMP	$CD207^+$ (Langerin), $CD11b^+$, $CD103^-$, $CD86^+$, $EpCAM^+$, $SIRPa^+$	Epidermis, ORS of hair follicle	• Antigen cross-presentation. • Th17 cell differentiation. • CD4+ follicular helper T cell and Th2 cell proliferation. • IgE production during allergic conditions. • Tolerance induction. • Activation of skin resident regulatory cells. • Mediation of inflammation.	Hoeffel et al., 2012; Singh et al., 2016; Kaplan, 2017
	Dermal dendritic cells					
	1. Langerin+ DC	$CD141^{hi}$, $CD14^+$	$CD45^+$, $CD11b^{lo}$, CD11c, $MHC\text{-}II^+$, $CD103^+$, $XCR1^+$, $EpCam^-$, $Sirpa^-$	Dermis	• Phagocytosis of cell debris and infectious microorganism. • Activation of naïve T cells through antigen presentation. • Regulation of Th1 responses. • Promotion of cytotoxic and memory responses of CD8+ T cells.	Nagao et al., 2009; Henri et al., 2010; Chu et al., 2011; Flacher et al., 2014; Mildner and Jung, 2014
	2. $CD11B^+$ DC	$CD1a^+$, $CD1c^+$	$CD45^+$, $CD11b^{++}$, CD11c, MHC class II, $CD205^+$, CD103 -$EpCam^-$, $Sirpa^+$	Dermis	• Clearance of infection.	
	3. Langerin-$XCR1^-$ DC	ND	$CD207^-$, $CD11b^-$, $EpCAM^-$, $Sirpa^+$, $XCR1^-$, $CX3CD1^{++}$	Dermis	ND	
Macrophage		CD11b, F4/80, CD163, factor XIIIa, CD16, CD32 and CD64	$CD45^+$, $MHC\ II^+$, $MERTK^+$, CCR^{lo}, F4/80, $CD64^+$	Dermis	• Phagocytosis. • Modulation of tissue environment. • Promotion and suppression of inflammation. • Extravasation of neutrophils during inflammation. • Regulation of hair bulge stem cell populations.	Malissen et al., 2014; Yanez et al., 2017
T cells $CD3^+$	Dendritic epidermal T cells $CD8^+$, $V\gamma3V\delta1$ TCR			Epidermis and ORS of hair follicle	• Regulation of antimicrobial function. • Prevention of tumor formation. • Promotion of wound closure. • Maintenance of keratinocyte homeostasis through production of growth factors.	Macleod et al., 2013
	Memory T cells (Trm) ($CD8^+$, $CD103^+$)					
	1. Epidermal Trm	$CD45RO^+$, CLA^+, $CCR4^+$	$CD49^+$, CD49	Epidermis	• Antimicrobial defense.	Clark et al., 2006; Zaid et al., 2014; Cheuk et al., 2017
	2. Dermal Trm		$CD49^-$, $CD4^+$	Dermis	• Antimicrobial defense.	
	γδT cells (DETC)	$CD8^+$, γδ TCR^+	$CD8^+$, γδ TCR^+	Epidermis and dermis	• Promotion of Hair follicle regeneration. • Extravasation of neutrophils during inflammation. • Synthesis of keratinocytes and fibroblast growth factors.	Bos et al., 1990; Sumaria et al., 2011; Gay et al., 2013; Cruz et al., 2018

(Continued)

TABLE 2 | Continued

Immune cell	Subsets	Marker expression		Localization	Functions in skin	References
		Human	Mouse			
	αβT cells	$CD8^+/CD4^+$, αβ TCR $^+$	$CD8^+/CD4^+$, αβTCR $^+$	Epidermis and dermis	• Cytokine synthesis during tissue damage and infection. • Regulation of hair cycle. • Recruitment of other immune cells. • Promoting cell cytotoxicity.	
	Regulatory T cells (Tregs)	$FOXP3^+$, $CD45RO^+$, $CD4^+$, $CD25^+$, $CD127^-$	$FOXP3^+$, $CD25^+$	Around hair follicles	• Epithelial stem cell differentiation. • IL-17 secretion in inflammatory condition. • Maintenance of self-tolerance. • Suppression of inflammation.	Clark, 2010; Sakaguchi et al., 2010; Ali et al., 2017
	Th17 cells	$CD4^+$, $RORC^+$, $CD161^+$	$CD4^+$, $CD161^+$, $CCR6^+$, $IL17A^+$, $RORyt^+$	Epidermis and dermis	• Protection against pathogens by inducing synthesis of antimicrobial peptides. • Promotes synthesis of inflammatory cytokines and growth factors.	Koga et al., 2008; Maggi et al., 2010; Peck and Mellins, 2010
Mast cells		$FcyRI^-$, FcyRIIa, CD30	$CD117^+$, $CD25^+$	Epidermis and dermis	• Pathogens, production of antimicrobial peptides. • Regulation of allergic responses. • Maintenance of epidermal differentiation.	Sehra et al., 2016

important roles played by metalloproteinases, derived from immune cells, in remodeling the ECM thereby driving the pathophysiology and severity of various diseases. The T cell repertoire, particularly Th1 cells secrete gelatinases, MMP-2 and -9 that further stimulate the release of gelatinases from macrophages (Oviedo-Orta et al., 2008). In squamous cell carcinoma, mast cells, macrophages and neutrophils secrete MMP-9 that exacerbates the disease condition by increasing keratinocyte hyperproliferation and metastasis (Coussens et al., 2000). Dendritic and Langerhans cells in skin secrete MMP-2 and -9 to facilitate their trans-epithelial migration for antigen presentation (Ratzinger et al., 2002). Monocytes and lung resident macrophages are the primary source of MMP-8 that eventually contributes to fibrosis in idiopathic pulmonary fibrosis (Craig et al., 2014). Likewise, MMP-8 and -12 is synthesized by neutrophils and macrophages in cystic fibrosis accelerating disease progression (Wagner et al., 2016). Increased expression of MMP-9 by splenic and infiltrating T cells correlates with the growth in mammary tumors (Owen et al., 2003). Furthermore, in UVB irradiated skin, neutrophil elastase causes the degradation of ECM components by activating MMP-1, and MMP-2 (Takeuchi et al., 2010).

(ii) Synthesis of cytokines and growth factors that induce ECM synthesis or degradation: Cytokines (IL-4, IL-13, and IL-33) and growth factors (TGF-β) secreted by immune cells stimulate the synthesis of ECM components (Verrecchia et al., 2001; Fujitsu et al., 2003; Rankin et al., 2010). In mouse dermal fibroblasts, TGF-β signaling results in the activation of SMAD2/3, which, in turn, increases the expression of ECM, related genes such as *Col1a1* and *Col3a1* (Verrecchia et al., 2001; Li et al., 2003). IL-13 produced by innate lymphoid cells stimulates the differentiation of fibroblasts to myofibroblasts increasing collagen synthesis and its accumulation in fibrosis (Fichtner-Feigl et al., 2006). In bronchial asthma, Th2 cytokines IL-4 and IL-13 stimulate the synthesis of periostin from bronchial fibrocytes, leading to sub-epithelial fibrosis (Takayama et al., 2006; Aoudjehane et al., 2008). On the other hand, IL-6 and TNF-α produced by inflammatory immune cells can reduce the synthesis of MMP-2, which, in turn, protects liver hepatocytes from fibrosis (Bansal et al., 2005).

(iii) Synthesis of ECM components: Immune cells can themselves be a source for various ECM proteins. Macrophages and T cells present in tuberculosis associated granulomas produce OPN that aid in their chemotaxis, adhesion, and proliferation (O'regan et al., 1999). In a subset of patients with systemic stenosis, circulating $CD14^+$ monocytes overexpress versican, which is associated with the aggressive fibrosis (Masuda et al., 2013). TAMs (tumor associated åmacrophages) modify the architecture of the tumor matrix by synthesizing proteoglycans, fibronectin, OPN, SPARC and various collagen subtypes (Liguori et al., 2011).

Taken together, these studies point to a critical role played by immune cells in modulating ECM dynamics during normal development and in disease states.

SKIN DISEASES

Atopic Dermatitis

Atopic dermatitis (AD) is a chronic, relapsing and TH2 cell/IgE driven inflammatory skin disorder characterized by intense pruritus and eczematous lesions (Bieber, 2008). The onset of AD is caused by barrier dysfunction, due to heritable mutations in the filaggrin (*FLG*) gene, and environmental triggers culminating in loss of skin hydration, enhanced sensitization to allergens and susceptibility to pathogenic agents (Weidinger and Novak, 2016). Clinical manifestations of AD occur both in children (Childhood AD) and adults (Adult AD) with similar clinical symptoms but with discrete pathophysiologies. While childhood AD is characterized by additional Th17/Th22 driven cascades along with tight junction and lipid metabolism disorders, AD in adults is associated with a Th1 specific response with aberrations in the epidermal differentiation complex (Brunner et al., 2018). AD usually precedes other allergic disorders like food allergies, allergic rhinitis, and asthma, commonly referred to as the "Atopic March," the mechanism for which remains undefined (Dharmage et al., 2014).

Abnormalities in BM composition, suggesting ECM dysfunction, have been reported in AD. Affected skin in AD patients has decreased BM thickness, along with reduced expression of collagen-IV and integrin α6 in the BM zone (Kim et al., 2018). A report by Shin et al. (2015) also suggested that the loss of the regenerative capability of the skin correlated with lower expression of p63 protein, a putative stem cell marker, in AD affected skin (Shin et al., 2015). Several SNPs (single nucleotide polymorphisms) in *LAMA3* gene correlated with increased susceptibility to AD (Stemmler et al., 2014). In acute AD, an increase in the expression of hyaluronan (HA), an extracellular polysaccharide, and hyaluronan synthase 3 (HAS3), an epidermal specific enzyme responsible for the synthesis and extracellular transport of hyaluronan, is observed (Ohtani et al., 2009). Increased expression of HA has been associated with abnormal keratinocyte differentiation, a hallmark of AD (Malaisse et al., 2014).

IL-4 and IL-13 are important cytokines known to play a critical role in AD pathogenesis. *In situ* hybridization studies on skin biopsy samples show a greater number of IL-13 positive cells in asymptomatic, acute and chronically affected AD patients compared to unaffected individuals (Hamid et al., 1996). Optimum expression of IL-13 is critical to maintain epidermal barrier homeostasis since both excess and insufficient levels of IL-13 provoke epidermal barrier dysfunction (Strid et al., 2016). IL-4 and IL-13 downregulate the expression of filaggrin, involucrin, loricrin, and the production of antimicrobial peptides. This exacerbates the skin barrier dysfunction and predisposes AD-affected skin to infection by microbes (Howell et al., 2007; Kim et al., 2008; Kisich et al., 2008). IL-4 is also shown to repress the expression of fibronectin in immortalized human keratinocytes (Serezani et al., 2017). In a human skin equivalent model system, IL-13 expression leads to the loss of BM structure and regenerative capability of the skin, recapitulating the AD phenotype (Shin et al., 2015). Furthermore, IL-13 treated human keratinocytes attract $CD4^+$ $CCR4^+$ T cells *in vitro*, providing a mechanism for a feed-forward loop that recruits more Th2 cells to acute AD lesions (Purwar et al., 2006). A critical correlation exists between IL-13 and MMP-9 mediated BM protein remodeling in AD. IL-13 is co-expressed with MMP-9 in skin samples from atopic eczema patients and it also increases MMP-9 synthesis in cultured keratinocytes (Purwar et al., 2008). IL-4 and IL-13 treated keratinocytes show an overexpression of TNC aggravating the inflammatory response (Ogawa et al., 2005). While mast cells and $CD4^+$/$CD8^+$ T cells are well known sources of IL-13 in AD affected skin, other immune cells including macrophages and dendritic cells can also be potential sources, which warrants further investigation (Obara et al., 2002). Taken together, these studies highlight the critical role played by IL-4 and IL-13 in driving AD pathogenesis.

Immune cell mediated remodeling of ECM in AD has been widely reported. BM remodeling matrix metalloproteinases (MMPs) including MMP-1, -3, -7, -8, and -9 is involved in AD pathophysiology (Harper et al., 2010). AD patients have enhanced serum levels of MMP-8 and -9 (Devillers et al., 2007). An immediate early effect in increase of MMP-9 by langerhans cells is observed upon treatment of skin with hapten, a well-known model for contact hypersensitivity (Kobayashi, 1997). The hyperplasic epidermis in AD secretes thymic stromal lymphopoeitin (TSLP), an IL-2 family cytokine, that activate DCs. DCs, in turn, produce MMP-3 and -9 that aid in their migration to lymph nodes where they activate naïve T cells (Ratzinger et al., 2002). Additionally, degranulation product of epidermal mast cells in AD-affected skin is associated with increased expression of MMP-7 (Landriscina et al., 2015). These reports indicate an indirect immune cell mediated BM remodeling in the context of AD. However, focused studies addressing this crosstalk are limited.

Monocytes and macrophages also play an important role in AD pathogenesis. An insightful review on the role of macrophages in AD has been previously published (Kasraie and Werfel, 2013). In AD skin, the epidermis overexpresses monocyte chemoattractant protein 1 (MCP-1) and, this results in the recruitment of monocytes in a CCR-2 dependent manner (Vestergaard et al., 2004). Acute and chronically inflamed AD skin show enhanced infiltration of heterogeneous pools of macrophages (Kiekens et al., 2001). Immunohistochemistry and ELISA analysis of AD skin and peripheral blood show increased CD163 expressing macrophages. Their role in aggravating disease condition is suggested by *in vitro* studies where the macrophages show an impaired TLR-2 signaling and increased secretion of pro-inflammatory cytokines such as IL-1β, IL-8, and IL-6 (Niebuhr et al., 2009). Given the preponderance of evidence on ECM-macrophage crosstalk in diseases, it is tempting to speculate that these heterogeneous pools of macrophages may play an important role in ECM remodeling.

Interestingly, recent studies point to the importance of ECM driven cascades in AD pathogenesis. Mitamura et al., showed that IL-13 upregulates the synthesis of POSTN which, in turn, increases IL-24 expression in the epidermal keratinocytes. IL-24, in turn, downregulates the expression of filaggrin, that contributes to the barrier dysfunction seen in atopic dermatitis (Mitamura et al., 2018). Another study showed that, the binding

of TNF superfamily member 14 (TNFSF-14) to its receptor HVEM (herpes virus entry mediator) on keratinocytes resulted in the synthesis of POSTN and development of AD. Blocking this pathway by HVEM deletion and HVEM specific antibody resulted in suppression in AD symptoms (Herro et al., 2018). The importance of OPN in AD is highlighted in several studies. Its expression is elevated in the serum of patients with allergic contact dermatitis (Reduta et al., 2015). In disease conditions, immune cells such as T cells, NKT cells, and plasmacytoid dendritic cells synthesize OPN that acts as a bridging molecule between the innate and adaptive immune system (Clemente et al., 2016). OPN promotes a pro-inflammatory environment by enhancing production of IL-12 by macrophages and suppressing IL-27 production from conventional dendritic cells, thereby activating Th1 and Th17 cells (Clemente et al., 2016). OPN binds to CD44 receptors on mast cells leading to its recruitment and degranulation (Bulfone-Paus and Paus, 2008). Thus, studies on matricellular proteins POSTN and OPN have highlighted therapeutically targetable pathways that are the key drivers of AD symptoms.

Collectively, AD is characterized by a multitude of dysregulated immune responses, as well as close bidirectional interactions with matricellular and basement membrane components that exacerbate disease pathophysiology.

Psoriasis

Psoriasis is a skin disorder associated with pathological changes such as appearance of erythematous lesions, scaling of the epidermis, inflammation, and vascular abnormalities (Nestle et al., 2009). Lesions appear as red and scaly plaques in areas like the elbow, joints, lower back, and the scalp (Boehncke and Schön, 2015). It is classified into plaque, guttate, erythrodermic, and pustular types with plaque psoriasis (or psoriasis vulgaris) being the most common type associated with about 90% of the cases (Dubois Declercq and Pouliot, 2013). Based on the age of onset of the disease, psoriasis is classified as Type I (occurs in individuals below 40 years of age) and Type II (sets in after 40 years of age) (Langley et al., 2005). Type I is more common, runs in families and is associated with more severe phenotypes compared to Type II (Schmitt-Egenolf et al., 1991). The exact cause of this disease is still unknown. However, a combination of genetic and environmental factors such as infection, injury, and various administered drugs may be responsible for disease onset (Langley et al., 2005).

Cell death due to injury or trauma is thought to trigger the keratinocytes to produce antimicrobial peptides like LL-37 that activate plasmacytoid dendritic cells (pDCs) (Morizane and Gallo, 2012). The pDCs secrete IL-12 and IL-23 and mount a T cell mediated inflammatory response. The T cells, primarily Th1, Th17, and Th22, secrete the cytokines IFN-γ and TNF that promote inflammation in psoriatic skin. An increase in the infiltration of neutrophils, dendritic cells and T cells in the lesional skin of psoriatic patients evokes a crosstalk between the activated keratinocytes and immune cells (Baliwag et al., 2015; Albanesi et al., 2018). Although, T cells and dendritic cells primarily drive psoriasis, interesting roles for macrophages and neutrophils have recently emerged. Depletion of macrophages by clodronate treatment leads to alleviation of the psoriatic phenotypes in mice (Stratis et al., 2006). Neutrophil derived cytokines such as IL-1β, IL-6, IL-17, and IL-23 are associated with specific gene expression changes in keratinocytes that result in epidermal hyperproliferation and abnormal differentiation (Terui et al., 2000; Tecchio et al., 2014). In contrast, antibody mediated neutralization of neutrophils does not reduce inflammation. Interestingly, neutrophils in psoriatic skin form web-like extracellular traps, referred to as NET (Neutrophil extracellular trap) that is composed of chromatin and antimicrobial components such as LL-37, neutrophil elastase, and myeloperoxidase (Fuchs, 2007). The formation of NET is associated with NETosis, which involves killing of pathogens through the release of IL-17 and antimicrobial peptides (Hu et al., 2016).

Several studies have underscored the contribution of ECM proteins in the pathogenesis of psoriasis. A disorganized BM (laminin) in the psoriatic skin is associated with keratinocyte-derived plasminogen activating factor (McFadden et al., 2012). Laminin-332 and -511 are overexpressed in the BM of psoriatic skin lesions. Furthermore increased expression of laminin-511 in HaCat cells stimulated proliferation and inhibited apoptosis providing a mechanism for the observed epidermal hyperplasia (Natsumi et al., 2018). Additionally, alteration in laminin α1 chain along with overexpression of fibronectin in the papillary dermis and T cell lymphokines are correlated with abnormal cellular morphology (Vaccaro et al., 2002). While laminins are shown to facilitate neutrophil recruitment and enhance the phagocytic ability of dendritic cells, its role in immunomodulation in the context of psoriasis remains elusive (Wondimu et al., 2004; García-Nieto et al., 2010; Simon and Bromberg, 2017).

CCN-1, a matricellular protein is overexpressed in the lesional and non-lesional psoriatic epidermis in response to pro-inflammatory cytokines IL-17 and TNF-α. It binds to integrin α6β1 on keratinocytes and activates PI3K/Akt/NF-κB pathway and result in the upregulation of *ICAM, HLA-DR*, *and HLA-ABC* genes. These genes, in turn, increase the immune cell-keratinocyte interaction and mount an inflammatory response. Its role in promoting epidermal hyperplasia and inflammation was further demonstrated in IL-23 induced psoriatic skin lesions, where the knockdown of CCN-1 ameliorated the phenotypes (Sun et al., 2015). Other studies have shown that CCN-1 stimulates secretion of the cytokines IL-1β and IL-8 by psoriatic keratinocytes via the p38 MAPK and JNK/NF-κB signaling pathways, respectively underscoring its role in regulation of inflammation (Sun et al., 2017; Wu et al., 2017). Furthermore, CCN-1 promotes CCL-20 chemokine synthesis from hyperplasic epidermis of psoriatic skin that causes increased recruitment of immune cells (Li H. et al., 2017). Taken together, these studies highlight an important role played by CCN-1 in regulation inflammation in psoriatic skin.

OPN, expressed by epithelial cells, is shown to act as a potent pro-inflammatory stimulant and activates immune cells such as T-cells, dendritic cells, and macrophages/monocytes (Clemente et al., 2016). Interaction of OPN with integrin and CD44 leads to the promotion of Th1 response and suppression of Th2 response.

In psoriasis, OPN is highly expressed in the PBMCs (peripheral blood mononuclear cell), skin and plasma. Buommino et al showed that OPN secreted by PBMCs enhances the expression pro-inflammatory cytokines such as IL-1β, TNF-α, and IFN-γ. TNF-α upregulates OPN expression while anti-TNF-α antibody treatment abrogates its synthesis (Buommino et al., 2012).

Overall, these studies suggest that ECM components play a critical role in psoriatic skin by acting as co-stimulatory factors for keratinocytes and immune cell activation leading to chronic progression of the disease.

Epidermolysis Bullosa

Epidermolysis bullosa (EB) is a group of rare heritable diseases characterized by blistering and fragile skin. It is associated with anomalies such as palmar-plantar thickening, syndactyly, dysphagia, gingival hyperkeratosis, cardiomyopathy, and osteoporosis (Maldonado-Colin et al., 2017). The blistering results from mechanical stress that eventually gives rise to chronic wound conditions (Medeiros and Riet-Correa, 2015). EB is caused by mutations in hemidesmosomal and extracellular matrix genes and the mode of inheritance can be either dominant or recessive. EB has been broadly categorized into simplex (EBS), junctional (JEB), dystrophic (DEB) types, and kindler syndrome (Shinkuma, 2015; Barna et al., 2017). The severity of disease is a function of the location of the split and the genes affected. So far mutations in at least 19 genes are reported to cause different types of EBs (Vahidnezhad et al., 2018). The site of splitting associated with various mutations is illustrated in **Figure 2**.

EBS is caused by mutations in the genes coding for either keratin 5 (*KRT5*) or keratin 14 (*KRT14*) accounting for the four major subtypes. *KRT5/14* form a stable cytoskeletal network and are involved in maintaining tissue integrity (Coulombe and Lee, 2012). Mutations in *KRT5/14* result in rupture of basal keratinocytes leading to increased susceptibility to infection and dehydration. The least severe form of EBS is Weber-Cockayne type characterized by mild blistering restricted to feet and hands whereas the most severe form known as Dowling-Maera type is marked by extensive blistering, which however seems to get better with age. The other two subtypes are Koebner type and EBS with mottled pigmentation (Chung and Uitto, 2010a). Additionally, mutation in the plectin (*PLEC*) gene, a hemidesmosomal protein, is associated with a rare type of EBS known as Ogna type (Pfendner et al., 2005). The features common to all the subtypes are thickened palm and soles (palmoplantar keratoderma), non-scarring blisters, alopecia and dystrophic nails (Chung and Uitto, 2010a). EBS is the most prevalent and mildest type of EB, and exhibits an autosomal dominant inheritance pattern (Coulombe et al., 2009). Mouse knockouts for *Krt5* and *Krt14* serve as good models for studying EBS disease pathogenesis (Coulombe et al., 1991; Peters et al., 2001).

JEB is an autosomal recessive form of EB caused by mutations in the laminin-332 chains encoded by *LAMA3, LAMB3, LAMC2* genes, and *COL17A1* genes that code for collagen XVII/BP180 protein (Sawamura et al., 2010). Collagen-XVII is an important structural element of the hemidesmosomal complex that together with laminins in the BM, maintain the dermal-epidermal adhesion. JEB can be further classified into two subtypes; Herlitz and non-Herlitz based on its severity. Patients with the Non-Herlitz subtype display blisters primarily in the feet, elbows and knees, which are non-life threatening (Yancey and Hintner, 2010). The Herlitz subtype, on the other hand, causes severe disease, and is associated with widespread blistering of the lining of oral and digestive tracts, syndactyly and alopecia, and restricts life expectancy to 1 year after birth (Yuen et al., 2011).

Col17a1 knockout mice display the blistering pattern associated with the non-Herlitz subtype and show prolonged survival; whereas *Lama3* and *Lamc2* knockouts recapitulate the Herlitz type of EB, exhibiting severe skin blistering resulting in perinatal lethality (Bubier et al., 2010; Natsuga et al., 2010). Two other rare autosomal recessive forms of EB include EB with pyloric atresia (EB-PA) and EB with muscular dystrophy (EB-MD). EB-PA is caused by mutations in *ITGA6* and *ITGB4* genes whereas EB-MD is associated with mutations in the *PLEC* gene (Shimizu et al., 1999; Yancey and Hintner, 2010). *Itga6* and *Itgb4* knockout mouse models recapitulate the dermal-epidermal detachment leading to development of EB-PA (Georges-Labouesse et al., 1996; Mencía et al., 2016).

DEB is associated with mutations in *Col7a1* gene resulting in the loss of collagen-VII protein. Collagen-VII is an anchoring fibril protein crucial for dermal-epidermal integrity and is present in the BM on the side of papillary dermis (Chung and Uitto, 2010b). The two major subtypes of DEB based on mode of inheritance and severity include autosomal dominant (DDEB) and recessive (RDEB) types. Unlike EBS and JEB, DEB is associated with extensive scarring (Shinkuma, 2015). RDEB, the more severe subtype is characterized by pseudosyndactyly, alopecia with scarring, and esophageal stenosis that leads to dysphagia. This disease is further complicated by the development of aggressive squamous cell carcinoma in juvenile patients (Shinkuma, 2015). The conditional *Col7a1* KO mice recapitulate all of the phenotypes of RDEB and has proven to be an invaluable tool to understand disease progression as well as to test therapeutic interventions (Natsuga et al., 2010).

Kindler syndrome is the only skin disease known to be associated with actin cytoskeleton related abnormalities and is characterized by variable planes of cleavage in the skin (Medeiros and Riet-Correa, 2015). Keratinocytes express kindlin-1, a protein that regulates cellular processes such as proliferation, migration and cell-substratum adhesion (Rognoni et al., 2016). Mutations in the *FERMT1* gene, coding for the kindlin-1 protein, lead to this rare fragile skin blistering disorder with symptoms similar to other EB subtypes (Lai-Cheong et al., 2009). Kindlin-1 deficient mice display skin atrophy without blister formation (Ussar et al., 2008). The loss of kindlin-1 from keratinocytes results in dysregulated integrin signaling and focal adhesion turnover (Margadant et al., 2013).

Another form of EB called aquisita **(EBA)** is caused by the production of autoantibodies against collagen-VII protein. The two subtypes of EBA are classical and the inflammatory types. The classical form is characterized by trauma induced blistering in adults whereas the inflammatory form starts in childhood and show more widespread blistering that is not restricted to the injured sites (Kasperkiewicz et al., 2016).

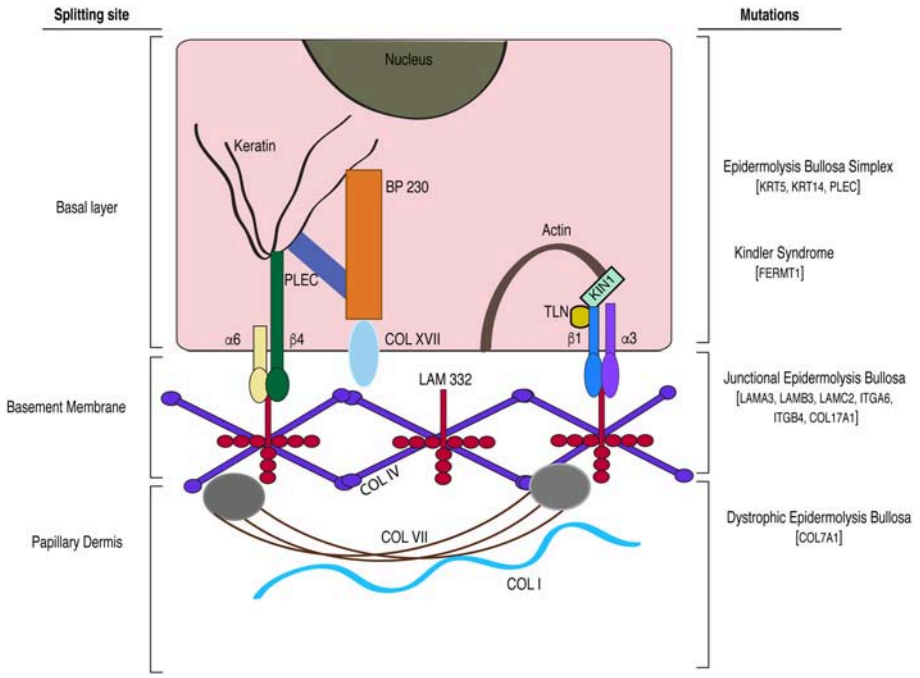

FIGURE 2 | A model depicting the gene mutations and the site of splitting associated with the different subtypes of epidermolysis bullosa. BP, bullous pemphigoid; TLN, Talin; α6, integrin alpha 6; β4, integrin beta 4; α3, integrin alpha 3; β1, integrin beta 1; LAM 332, laminin-332 protein; PLEC, plectin; COL, collagen; KIN1 (FERMT1), kindlin-1; KRT, keratin; ITG, integrin.

The null and conditional KO mouse models that have been discussed above recapitulate various aspects of disease progression of the EB class of skin disorders and are being used as platforms to develop therapeutic interventions for these devastating diseases (Georges-Labouesse et al., 1996; Cao et al., 2001; Peters et al., 2001; Bruckner-Tuderman et al., 2010).

Insights into the role of inflammation and immune cells in EB pathophysiology have come from the studies on *Krt*5, *Itgb4*, and *Col7a1* knockouts that cause EBS, EB-PA, and DEB, respectively. Increased expression of chemokines and cytokines such as CCL-2, CCL-19, CCL-20, IL-6, and IL-1β is reported in *Krt*5 knockout skin. The cytokine expression is associated with a 2-fold increase in the recruitment of Langerhans cells to the EB affected skin (Lu et al., 2007; Roth et al., 2009). Loss of *Itgb4* in mice leads to severe blistering associated with Th2 inflammatory response, which suggests involvement of immune cells in EB pathophysiology (Han et al., 2018). Knockout of *Col7a1* recapitulates RDEB and creates a chronic wound condition underscoring its role in maintenance of epidermal-dermal integrity. Collagen-VII deficient wounds display suprabasal expression of α6β4 that lead to a dysregulated α6β4-laminin-332-JNK-STAT3. This, in turn, delays wound re-epithelialization and prolongs the presence of inflammatory CD11b cells in skin (Nyström et al., 2013). Interestingly, depletion of collagen-VII from immunodeficient mice (NSG mice) results in a less severe disease phenotype. Taken together, these studies emphasize the critical role played by the immune cells in exacerbating the disease condition (Esposito et al., 2016).

Blisters in the bullous diseases are usually associated with increased infiltration of cytotoxic T cells, B cells, neutrophils and other immune cells as well as their secreted cytokines (Hussein et al., 2007). Previous work has suggested that there is a substantial increase in the levels of cytokines such as IL-1, IL-6, IL-15, and TNF-α, and chemokines such as CXCL-1, CXCL-2, CXCL-3, CCL-5, CCL-27 in the blister fluids of EB patients compared to healthy controls. Moreover, the cytokine and chemokine expression profile varies between EB subtypes such that early DEB and JEB blisters expressed lower levels of cytokines and chemokines compared to that of early EBS (Alexeev et al., 2017). In EBA, several groups have shown that autoantibody production against COL7A1 is mediated through a milieu of neutrophils, macrophages, B cells and T cells and these phenotypes are ameliorated by the depletion of neutrophils and T cells (Sitaru et al., 2010; Iwata et al., 2013; Bieber et al., 2016).

MMPs secreted by immune cells can also influence the recruitment pattern of other immune cells to the injured tissue. Studies have shown that the severity of RDEB is a function of the type of MMP synthesized, its expression level and the balance between MMPs and TIMPs (Bodemer et al., 2003). Interestingly, a SNP (single nucleotide polymorphism) in the *MMP1* gene has also been implicated in increasing disease severity by influencing the expression of collagen-VII (Titeux et al., 2008). Likewise the correlation between MMP-9 and blister formation was shown in a study where treatment with doxycycline derivative, an inhibitor of MMP-9, alleviated the phenotype (Lettner et al., 2013). Collectively MMPs can serve as effective therapeutic targets.

Since DEB is a disorder of the basement membrane zone (BMZ), it is not surprising that, in RDEB patients that lack collagen-VII, two major BM components collage-IV and laminin-332 display a disrupted distribution pattern and do not co-localize at the BMZ (Onetti Muda et al., 1996). The disruption precedes blister formation suggesting that it could be a direct consequence of the lack of collagen-VII. Dermal-epidermal splitting also leads to an increase in the expression of TNC at the site of the split, which could be in response to the cytokines secreted either by epidermis or the recruited immune cells (Schenk et al., 1995). These studies suggest that TNC can serve as a potential link between the immune and ECM components in DEB.

Interaction between collagen-VII and cochlin is required to mount an immune cell mediated antibacterial response. In RDEB patients, absence of this interaction leads to increased bacterial colonization that further exacerbates the disease condition (Nyström et al., 2018). Lack of collagen-VII in RDEB destabilize the BMZ and cause the release of TGF-β associated with ECM increasing its bioavailability. TGF-β mediated activation of dermal fibroblasts, in turn, cause excessive deposition of ECM components (Nyström and Bruckner-Tuderman, 2018). In a recent case study, monozygotic twins suffering from RDEB exhibited distinct phenotypes due to changes in the expression of TGF-β target genes, despite having similar loss of collagen-VII. The more affected individual displayed increased fibrosis, which was ameliorated by treatment with the anti-fibrotic the matricellular protein decorin (Odorisio et al., 2014). These data point to the complexity of managing and treating RDEB, a genetic disease that is associated with loss in ECM organization which is further exacerbated by TGF-β mediated alteration in ECM dynamics. The involvement of matricellular proteins in mounting an immune response in EB provides an additional avenue for therapeutic intervention. Taken together, while EBs remain one of the most challenging diseases to manage and treat, and future treatment paradigms will need to take into account the immune-ECM interactions.

Skin Cancers

Skin cancers are broadly classified as melanoma and non-melanoma types. Melanoma is an aggressive skin cancer that originates from melanocytes; the pigment producing cells in the skin (Villanueva and Herlyn, 2008). Non-melanoma skin cancers include Squamous cell carcinoma (SCC), Basal cell carcinoma (BCC), and Merkel cell carcinoma (MCC). SCCs originate from interfollicular stem or progenitor cell population in the epidermis and BCCs from the progenitor cells present in interfollicular epidermis and upper infundibulum (Donovan, 2009; Wang et al., 2011). MCCs, on the other hand, are the cancer of neuroendocrine (merkel) cells present in the basal layer of the epidermis (Munde et al., 2013). Other aggressive forms of skin cancer include cutaneous T and B lymphomas, a varied group of extranodal lymphoproliferative disorders associated with abnormal accumulation and proliferation of T and B lymphocytes in skin (Pandolfino et al., 2000; Siegel et al., 2012). Cutaneous T cell lymphomas are the most common with 65% incidence rate as compared to B cell lymphomas with a 25% incidence rate (Sokołowska-Wojdyło et al., 2015). All skin cancer types show a positive correlation with exposure to UV radiation as well as mutations in genes associated with tumor suppression, DNA repair, apoptosis and cell cycle regulation (D'Orazio et al., 2013; Kandoth et al., 2013).

Tumor resident and recruited immune cells play a dynamic role in regulating cancer progression. The tumor and its stroma recruit different populations of immune cells by releasing chemotactic factors and cytokines resulting in a chronic inflammatory condition (Binnewies et al., 2018). The immune cell repertoire, associated with the tumor microenvironment includes monocytes, macrophages, neutrophils, dendritic cells, natural killer cells, T and B cells (Cavallo et al., 2011). Factors such as CCL-2, CCL-5, CCL-17, CCL-22, CXCL-12, M-CSF, VEGF, and TGF-β synthesized by the tumor stroma aid in the recruitment of monocytes and subsets of T cells (Owen et al., 2003; Hiratsuka et al., 2006; Yang et al., 2008). In melanomas, the chemokines CCL-2, CCL-3, CCL-5, CXCL-9, and CXCL-10 recruit $CD8^+$ T cells (Harlin et al., 2009). In a recent study it was shown that, tumor derived factors such as colony stimulating factor-1 (CSF-1), CCL-2, IL-34, and VEGF recruit circulating macrophages to the melanomas (Pieniazek et al., 2018). In human melanomas, CCL-2, also known as MCP-1, is associated with an increased inflammatory response and recruitment of macrophages and T cells (Ilkovitch and Lopez, 2008). Similarly in BCCs, CXCL-9, CXCL-10, and CXCL-11 recruit CXCR-3 expressing effector and memory T cells (Lo et al., 2011). In BCCs, the chemokines, CCL-17, CCL-18, and CCL-22 that recruit Tregs are overexpressed in the tumor islands and peritumoral skin. The stromal cells in turn synthesize CCL-17, which suggests a mechanism for the Treg infiltration seen in the stroma surrounding the BCC nests (Omland et al., 2016). In MCC, a recent study has shown that over expression of CCL-17 and its receptor CCR-4, aid in recruitment of $CD4^+$ Tregs, Th2, and Th17 cells (Rasheed et al., 2018). Macrophage derived CCL-18 in cutaneous T cell lymphomas (CTCL) recruit T lymphocytes to the skin and is associated with enhanced invasion (Wu et al., 2014). Overall, the tumor and its stroma recruit a plethora of immune cells that contributes to tumor progression.

Dynamic crosstalk between the stroma and immune cells, change the tumor milieu from a tumor suppressive (or immunogenic) to tumorigenic (or immunosuppressive) state. Specifically, tumor associated macrophages (TAMs) switch from pro-inflammatory M1 macrophages, that are antigen presenting cells, to anti-inflammatory M2 macrophages, that are tissue remodeling and tumor growth promoting cells (Tariq et al., 2017). M1 macrophages phagocytose tumor cells, produce reactive oxygen (ROS) and nitrogen (RNS) species and secrete pro-inflammatory cytokines such as IL-6, IL-23, IL-12, and TNF-α that activate Th1 response (Komohara et al., 2014; Noy and Pollard, 2014). In contrast, M2 macrophages express anti-inflammatory cytokines like IL-10 and TGF-β that play a role in promoting tumor growth (Aras and Raza Zaidi, 2017). Depletion of M2 macrophages by treating with clodronate in CTCL xenograft mouse models, reduces angiogenesis and tumor growth (Wu et al., 2014). Human keratinocytes can inactivate T cell response by downregulating signaling pathways critical

for T cell recruitment and cytotoxicity (Bronte and Zanovello, 2005; Bluth et al., 2009). In SCCs and BCCs, immunosuppression is mediated by preventing the recruitment of T cells to the cancer site through the activation of EGFR-Ras-MAPK signaling pathway (Pivarcsi et al., 2007). Interestingly, Tregs are known to suppress immune response by producing IL-10 and TGF-β and compete for T-cells-activating pro-inflammatory cytokines (Jarnicki et al., 2006). They are critical for inducing tolerance to self-antigens and also inhibit the antigen presenting ability of DCs (Sakaguchi et al., 2009). The transcription factor FOXP3 is important in regulating Treg function. Increased *FOXP3* expressing Tregs correlates with poor disease outcome in SCCs, BCCs and melanomas (Moreira et al., 2010). In BCCs, recruited Tregs build an immunosuppressive niche by locally synthesizing TGF-β (Omland et al., 2016). In MCC, M2 macrophages and Tregs present in the tumor maintain an immunosuppressive state contributing to a pro-tumorigenic microenvironment (Gaiser et al., 2018). Interestingly, increased recruitment of $CD8^+$ T cells to the skin is associated with better prognosis in MCCs (Touzé et al., 2011).

Taken together, there is growing evidence that tumor microenvironment in cancers develop immune suppressive mechanisms to evade the T cell mediated cytotoxicity that can promote metastasis.

The ECM in cancer is highly remodeled and disorganized due to aberrant deposition by activated fibroblasts and enzymatic remodeling by the tumor and immune cells (Karagiannis et al., 2012). Changes in ECM dynamics promote tumor growth by regulating proliferation, survival, adhesion and migration (Pickup et al., 2014). The BM in melanomas has reduced thickness compared to healthy controls due to the absence of collagen-VII (Schmoeckel et al., 1989). A study of the BM in BCC affected skin showed aberrations in bullous pemphigoid antigens possibly due to its abnormal synthesis by the tumor associated cells (Stanley et al., 1982). Similarly, the BM structure in aggressive SCCs is irregular and discontinuous (Sakr et al., 1987). Matrix metalloproteinases such as MMP-1, -2, -3, -8, -9, -10, -13, -15, -16, and -26 can facilitate tumor growth, invasion, and angiogenesis in BCC, SCC and melanomas (Pittayapruek et al., 2016). In a recent study, expression profiling of BCCs showed an increase in ECM remodeling proteins including MMP-1, -3, -8, -9, and Cathepsin-K indicating the important role played by these enzymes in cancer progression (Ciazynska et al., 2018). In organ culture models of BCC the increased expression of MMP-2 and MMP-9 correlates with degradation of collagen-I and -IV at the tumor front (Goździalska et al., 2016). Likewise, the expression of ADAM-10, -12, and -17 was specifically observed in deep invasion area of BCC biopsies and correlated with the loss of collagen-XVII (Oh et al., 2009). The TAMs in BCCs induce COX-2 expression, which, in turn, results in a COX-2 dependent release of MMP-9, VEGF, and FGF that promotes tumor invasion (Tjiu et al., 2009). Interestingly, MMP-9 producing inflammatory macrophages and neutrophils are associated with BM degradation in BCC patients (Boyd et al., 2008).

Similarly, in SCCs the γ2 chain of laminin-332 is overexpressed in the invasive front (Hamasaki et al., 2011). In a DMBA (7,12-dimethylbenz-anthracene)-TPA (12-O-tetradecanoyl-phorbol-13-acetate) induced mouse model of SCCs, overexpression of collagen-XVII, integrin α6β4 and the γ2 chain of laminin, promoted tumorigenesis (Moilanen et al., 2017). Increased laminin-332 expression with high MMP-2 and MMP-14 activity is seen in invasive SCCs with poor prognosis (Marinkovich, 2007). Reduced expression of collagen-VII in SCCs enhances invasion, dysregulates epithelial differentiation and drives epithelial to mesenchymal transition (Martins et al., 2009). Loss of collagen-VII expression (in RDEB) results in an upregulation of TGF-β signaling and increased angiogenesis in SCCs underscoring the critical role played by collagen-VII in suppressing TGF-β signaling (Martins et al., 2016). Transgenic mice lacking MMP-9 reduced the tumor invasiveness in a mouse model of SCC whereas, transplanting MMP-9 producing bone marrow cells increased tumor invasiveness (Coussens et al., 2000). The cleaved oligosaccharides generated by heparinize digestion of heparin sulfate chains is shown to play an important role in tumor progression in BCCs and SCCs (Pinhal et al., 2016). The abundance and stiffness of collagen also play an important role in melanoma progression where it stimulates proliferation and differentiation in a YAP/PAX3/MITF dependent manner (Miskolczi et al., 2018). In melanoma and BCCs, cathepsin K expression is associated with a fibromucinous stroma around the tumor nests, indicative of ECM degradation (Ishida et al., 2013). Interestingly, the matricellular protein POSTN is associated with metastatic progression in melanoma by attenuating adhesion and promoting migration (Fukuda et al., 2015). Tumor fronts of aggressive BCCs and SCCs overexpress TNC (Schalkwijk et al., 1991; Dang et al., 2006). Likewise, CCN-1 and CCN-2 are overexpressed in keratinocytes of BCCs in a YAP dependent manner promoting cell proliferation and survival (Quan et al., 2014).

The crosstalk between immune cells and ECM is thought to be critical in driving skin cancer pathogenesis. In patient samples of SSCs, an increase in $CD163^+$ TAMs is associated with enhanced expression of MMP-9 and MMP-11, which promotes angiogenesis and tumor growth. The same study also reports the activation of IL-4 dependent STAT-6 signaling in TAMs that induces differentiation of Th2 cells, further maintaining an immune-suppressive environment (Pettersen et al., 2011). In a DMBA-TPA induced mouse model of SCC, $Gr1^+$ neutrophils produce remodeling enzymes including myeloperoxidase (MPO) and elastase, which are associated with poor disease outcome (Gasparoto et al., 2012). TNF-α and TGF-β secreted by macrophages synergistically increase melanoma migration in a NF-κB dependent manner through the release of MMP-1 and MT1-MMPs (Li R. et al., 2017). Hyaluronic and proteoglycan link protein (HAPLN-1) is an ECM protein highly expressed in young fibroblasts compared to aged fibroblasts and is important for maintaining stability of hyaluronan and collagen (Ecker et al., 2019). Since T cells use collagen fibrils to infiltrate tumors, downregulating HAPLN-1 expression in melanoma models results in decreased $CD3^+$ T cell infiltration associated with increased tumor cell extravasation. On the other hand treatment with recombinant HAPLN-1 increases the T cell recruitment and reduces the

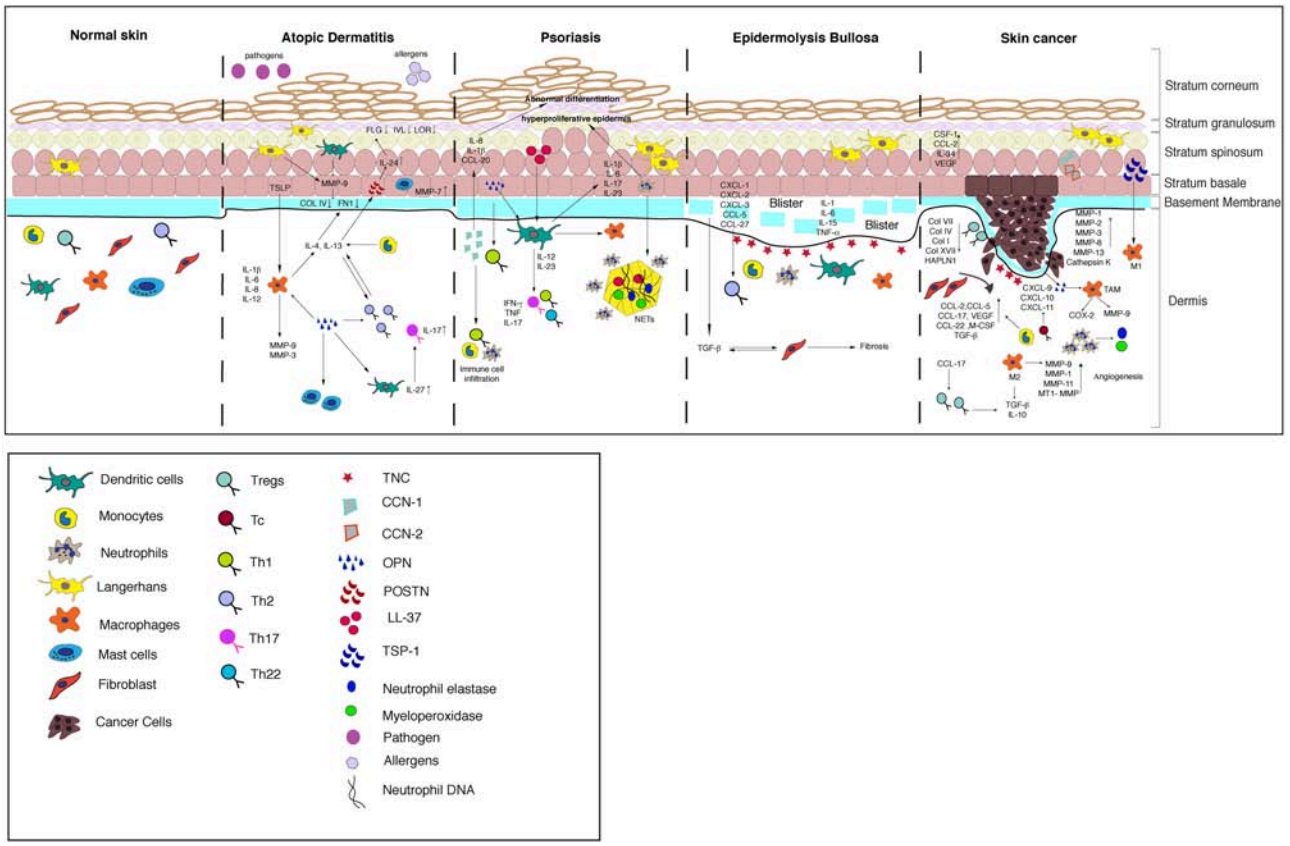

FIGURE 3 | A model summarizing the crosstalk between the ECM and immune cells in the skin diseases discussed in this review.

tumor growth. The association between collagen fiber stability and T cell migration has been suggested as one of the reasons for aggressive melanomas in aged individuals (Kaur et al., 2018). In CTCL, T lymphocytes localize toward the epidermis by expressing integrin α3β1 allowing them to bind with laminin-332 and migrate through the BM, which interestingly does not result in ECM disorganization (Wayner et al., 1993). Tumor derived OPN binds to macrophages through integrin α9β1 resulting in the overexpression of COX-2 and MMP-9 and promotes angiogenesis in melanomas (Kale et al., 2014). In melanoma models, IFN-γ induced by TSP-1 overexpression is critical for macrophage recruitment and polarization to the M1 state (Martin-Manso et al., 2008). This points to an important role played by TSP-1 in suppressing tumor growth.

The ECM-immune cell interactions have been well studied in the context of cancer since the ECM is highly remodeled by both the tumor and immune cells to facilitate the tumor growth. The tumor microenvironment can switch from being anti-tumorigenic to pro tumorigenic depending on dynamic interactions between the tumors; ECM and immune compartments and can result in aggressive cancer with poor prognosis. Understanding the signaling events regulating this process has led to the development of therapies targeting the immune system as evidenced by advent of immunotherapy in treating cancer. **Figure 3** summarizes the ECM-immune interactions in all of the skin diseases discussed in this review.

CURRENT STATE OF THE ART THERAPEUTIC INTERVENTIONS

Currently available treatment approaches for skin diseases involve treatment with anti-inflammatory drugs, analgesics, topical steroids, and anti-histamines (Grassberger et al., 2004; Abraham and Roga, 2014). Conventional therapies for the treatment of the diseases discussed in this review are listed in the **Table 3**. With the advent of techniques such as nanomedicine, gene therapy (genetic engineering), stem cell transplantation, and cell and protein replacement therapy, curative treatment of skin diseases seem achievable and have been discussed below.

Nanomedicine

Nanomedicine involves the use of particles within the nanometer range, for the detection and treatment of diseases. They are effective drug delivery agents for targeted therapy that enhance drug bioavailability and facilitate controlled drug release for long-term effect. Various nanoparticles as delivery agents for treatment of skin diseases include liposomes, solid lipid nanoparticles, polymeric micelles and nanospheres,

TABLE 3 | Conventional treatment strategies.

Skin Disease	Drugs	Mode of action	References
Atopic Dermatitis	Calcineurin inhibitors: tacrolimus and pimecrolimus	Prevent the activation of NFAT by inhibition of calcineurin phosphatase resulting in prevention of activation of T cells, mast cells, and cytokines like IL-4, -5, - 31, TNF-α.	Mayba and Gooderham, 2017; Papier and Strowd, 2018
	Phosphodiesterase inhibitors: crisaborole and Apremilast.	Prevent the conversion of cAMP to AMP that leads to accumulation of cAMP. This in turn causes suppression of NFAT, and NFKB pathways involved in inflammation.	
	Janus Associated Kinase-Signal Transducer and Activator of Transcription (JAK - STAT) inhibitors: Tofacitinib	Inhibit phosphorylation of JAK-1 and JAK-3 and prevent the activation of STATs. Reduce immune cell polarization and cytokine production.	
	Cytokine and cytokine signaling inhibitors: Dipulimab, Lebrikizumab, and Nemolizumab.	Dipulimab is an antibody that binds to the alpha subunit of the IL-4 receptor. This inhibits the pathways driven by IL-4 and IL-13 and reduces the expression level of genes involved in epidermal hyperplasia and immune cell activation. Lebrikizumab is an antibody that blocks IL-13 and the signaling pathways associated with it. Nemolizumab is an antibody against receptor A of IL-31. It blocks homing of CLA^+ T cells and decrease pruritus.	
	Systemic immunosuppressants: Ciclosporin A, Methotrexate, and Benvitimod	Inhibition of immune cell recruitment and production of pro-inflammatory cytokines.	
	Antihistamines: Hydroxyzine, Diphenhydramine, Chlorpheniramine	Inhibition of allergic responses and associated pruritis.	
Psoriasis	Vitamin D3 analogues: Calcitriol, Tacalcitol, and Calcipotriol.	Antiproliferative, pro-differentiation, suppression of T cell activation, increased production of Tregs, MHC-II suppression.	Duvic et al., 1997; Trémezaygues and Reichrath, 2011; Uva et al., 2012; Almutawa et al., 2013; Jacobi et al., 2015; Torsekar and Gautam, 2017
	Calcineurin inhibitors Pimecrolimus, and Tacrolimus.	Same as above.	
	Keratolytics - Salicyclic acid, and urea.	Increases shedding of corneocytes and reduction of pH.	
	Topical corticosteroids	Vasoconstrictive, antiproliferative, anti-inflammatory, and immunosuppressive.	
	Retinoids Tazarotene, and Acitercin	Binds to family of retinoic acid receptors - down-regulates keratinocyte differentiation, proliferation, and inflammation.	
	UV based therapy	Inhibition of inflammatory pathways, induction of apoptosis, downregulation of TH1/TH17 inflammatory axis, cell cycle arrest.	
	Phosphodiesterase inhibitor: Apremilast	Same as above	
	Systemic immunosuppressants: Ciclosporin, and Methotrexate.	Same as above	
	Cytokine and cytokine signaling inhibitors: Adalimumab, Etanercept, Infliximab, Secukinumab, and Ustekinumab.	Adalimumab, Etanercept, and infliximab are antibodies against TNF that result in inhibition of inflammation and immune cell recruitment. Secukinumab binds and neutralizes IL-17 that cause reduction in inflammation, immune cell recruitment and epidermal hyperproliferation. Ustekinumab binds to common receptor for cytokines IL-12 and IL-23 thereby reducing the activation and differentiation of Natural killer (NK) cells and $CD4^+$ T cells.	
	Anti-hyperproliferative Dithranol	Impedes DNA replication and reduces elevated cGMP levels.	
EB	Treatment involves draining blisters using sterile needles, surgeries for separating fused digits.		Nystrom et al., 2015
	A small-molecule angiotensin II type 1 receptor antagonist Losartan	Reduction in TGFβ expression slowing down fibrosis in RDEB.	
	NSAIDs, analgesics	Suppress inflammation.	Goldschneider et al., 2014

(Continued)

TABLE 3 | Continued

Skin Disease	Drugs	Mode of action	References
Squamous cell carcinoma	Single or in combinations—Surgery, thermal ablation, radiation		Ribero et al., 2017; Yanagi et al., 2018
	Epidermal growth factor receptor (EGFR) inhibitor: Cetuximab, Panitumumab, gefitinib, and erlotinib	Cetuximab and Panitumumab monoclonal antibody binds EGFR and inhibits EGF mediated signaling. Gefitinib and Erlotinib bind to tyrosine kinase domain of EGFR.	
	Tyrosine kinase inhibitors: imatinib	Imatinib binds close to ATP binding site of tyrosine kinases thereby preventing its activity.	
	26S proteasome inhibitor: Bortezomib	Bortezomib contains a boron atom which binds to active site of 26S proteasome and prevents degradation of ubiquitin tagged proteins thereby enhancing cell death.	
	Apoptosis inducer: Isotrenoin	Induces apoptosis in sebaceous gland cells and enhances neutrophil gelatinase-associated lipocalin (NGAL) production which induces sebocyte apoptosis.	
	Cytotoxic drugs: 5-Fluorouracil (5-FU), Doxorubicin, and Cisplatin	5-FU is an inhibitor of thymidylate synthase, which inhibits DNA replication. Doxorubicin inhibits topoisomerase II action. Cisplatin cross links DNA and prevents mitosis.	
	Immune checkpoint inhibitors: Anti-PD-1: Nivolumab and Pembrolizumab Anti-CTLA-4: Ipilimumab	Cytotoxic T cell mediated killing of tumor cells.	
Basal cell carcinoma	Surgical excision, cryotherapy, Laser therapy, Mohs micrographic surgery, photodynamic therapy and radiotherapy.		Lewin and Carucci, 2015; Migden et al., 2018
	Inhibitors of DNA replication: 5-FU.	Same as above.	
	Hedgehog pathway inhibitors: vismodegib and sonidegib	It is an antagonist of smoothened which in turn causes inactivation of GLI-1 and GLI-2 transcription factors.	
	Immune response modifier: imiquimod	Activates innate immune cells and incites an inflammatory response. This, in turn, activates adaptive immune cells.	
Melanoma	BRAF inhibitor: vemurafenib and dabrafenib	Inhibit the mutated kinase domain of BRAF involved in MAPK signaling.	Johnson and Sosman, 2015
	MEK inhibitor: Trametinib	Allosteric inhibitor of MEK1/2 that is constitutively activated.	
	Immunotherapy: Interleukin-2	Activates immune system to attack cancer cells. Also stimulate melanoma cells to secrete chemoattractants for immune cells.	
	Anti-PD-1: Nivolumab and Pembrolizumab	Same as above.	
	Anti-CTLA-4: Ipilimumab	Same as above	
Merkel cell carcinoma	Mohs micrographic surgery, lymph node dissection and radiation therapy. Sentinel lymph node biopsy		Tello et al., 2018
	Chemotherapy: Somatostatin analogs	Inhibition of endocrine tumor growth.	
	mTOR inhibitors	Blocking PI3K/Akt/mTOR pathway and inhibit cell proliferation and tumor growth.	
	Immune checkpoint inhibitors:		
	Anti-PD-1: Nivolumab and Pembrolizumab avelumab	Same as above.	
	Anti-CTLA-4: Ipilimumab	Same as above.	

(Continued)

TABLE 3 | Continued

Skin Disease	Drugs	Mode of action	References
Cutaneous lymphoma	Topical Corticosteroids		Wollina, 2012
	Phototherapy	Use of UVA on skin, which results in self destruction of T cells.	
	Topical chemotherapy: Mechlorethamine and carmustine.	Chemically modify DNA and prevent tumor growth.	
	Topical imiquimod	Aid in the release of IFN-γ and cytokines for suppressing tumor growth.	
	Cytokine therapy: TNF-α	Stimulate immune system to target tumor cells.	

dendrimers, nanotubes, quantum dots, gold particles etc. that has been reviewed previously (Dianzani et al., 2014). In mouse and rat models of AD and psoriasis, nanoparticle based delivery of drugs such as tacrolimus, corticosteroids, retinoids, methotrexate, and cyclosporine result in better outcomes (Palmer and DeLouise, 2016). Similarly, doxorubicin-loaded cationic solid lipid nanoparticles (DOX-SLN) have shown better drug penetration and inhibition of skin cancer tumor growth (Huber et al., 2015). In RDEB, localized delivery of gold nanoparticle coated with epigallocatechin-3-gallate (E3G) in SCC tumor site has been shown to abrogate the adverse effect of the drug in the liver (Manoukian et al., 2014). Additionally in EB, a novel nanocapsule based wound dressing technique has been developed. Upon infection, it releases antibiotics and undergoes a color change that indicates response to an active infection (Zhou et al., 2018). The promise of nanomedicine provides new therapeutic opportunities for treating skin disorders that have been refractory to treatment so far.

Gene and Stem Cell Therapy

Gene therapy involves the introduction of corrected copy of genes into cells for treating genetic disorders (Anguela and High, 2019). Likewise, stem cell therapy refers to stem cell transplantation, either from the same (autologous) or from a different (allogeneic) individual replacing affected cells. Alternatively, gene-corrected autologous stem cells can be engineered to generate skin substitutes followed by transplantation (Karantalis et al., 2015). Gene and stem cell therapy have proven highly beneficial for genetic skin disorders such as EB which continues to be a major health burden due to lack of effective treatment. The retroviral mediated transfer of COL7A1 into fibroblasts and keratinocytes have shown successful incorporation of collagen-VII at the dermal-epidermal junction of the engineered skin grafts (Ferrari et al., 2006; Piaceski et al., 2018). In a recent path-breaking paper, physicians were able to repair the skin of a 7-year old JEB patient who had lost 80% of his epidermis. The JEB was caused by a mutation in the *LAMB3* gene. Autologous non-lesional keratinocytes were used to introduce the corrected gene copy, and these cells were used to generate epidermal skin grafts. The patient showed complete recovery 2 years after the skin was grafted (Hirsch et al., 2017).

Under homeostatic conditions, bone marrow derived mesenchymal stem cells have been shown to regulate proliferation and maturation of T cells, NK cells, B cells, and dendritic cells. However, this regulation is perturbed in AD and psoriatic patients and bone marrow transplantation has been shown to result in remission of diseases (Li et al., 2015; Shin et al., 2017). Similarly, transplantation of bone marrow derived mesenchymal stromal cells into RDEB patients showed symptomatic improvement (Uitto, 2008).

Genetically engineered bone marrow cells have been designed to carry tumor antigens for targeting skin cancers. Autologous transplantation of lymphocytes that are genetically modified to express tumor antigen MAGE-A3 has been shown to mount effective tumor killing response in melanoma (Fontana et al., 2009). Furthermore, engineering T cells with NY-ESO-1, melanoma antigen resulted in tumor regression in clinical trials (Dummer et al., 2008). Adenovirus mediated transduction of T cells with IL-2 has also shown improved prognosis in clinical trials (Puzanov and Flaherty, 2010).

While at its infancy, stem cell therapies provide the promise of a "cure" particularly for devastating skin blistering disorders. The challenge will be to reduce the costs of such treatments to make it more accessible to patients.

Cell and Protein Replacement Therapy

Protein replacement therapy involves introduction of intact proteins for supplementing its loss from the patients and is primarily used in treatment of EB. Fibroblasts that can produce intact collagen-VII protein have been intradermally injected to RDEB patients and mouse models. The recipients, in turn, showed increased production of collagen-VII at the dermal-epidermal junction and enhanced wound healing (Nyström et al., 2013). Likewise, in mice that were grafted with skin from RDEB patients, topical application of recombinant collagen-VII protein to wounds resulted in collagen-VII incorporation in the wounded regions, and efficient repair (Uitto, 2008). More work will be required in the future to test the efficacy of this treatment in restoring normal skin function.

CONCLUSION, PERSPECTIVES AND FUTURE DIRECTIONS

In this review we have highlighted the signaling and regulatory cascades central to the interactions between ECM and immune cells in several skin diseases. Based on the extensive literature reviewed, it is conceivable that the pathways governing this crosstalk can serve in developing novel effective targets for therapeutic interventions. Therefore, an important area of future research would be to identify these cascades. While, in diseases like AD, Psoriasis, and cancer, the interaction is well understood, further investigation is required to discern the crosstalk in EB. Additionally, skin disease conditions are often accompanied by a systemic response thereby, necessitating the use of combinatorial therapies that target both the local and systemic responses. While available therapies primarily rely on mitigating inflammatory response, directly targeting of the ECM–immune cell pathways might contribute to better disease outcome. Additionally, with the emerging functions of matricellular proteins such as decorin, POSTN, OPN, and CCN-1 in driving the skin diseases, a thorough investigation of their roles could further aid in better understanding of disease pathophysiology. Ongoing state of art therapeutic interventions such as stem cell transplantation, immunotherapy, gene therapy, and nanomedicine hold the promise for treating the most intractable of these conditions.

AUTHOR CONTRIBUTIONS

All authors listed have made a substantial, direct and intellectual contribution to the work, and approved it for publication.

FUNDING

This paper has been funded by the DST Grant to SR and AK (EMR/2016/003199).

ACKNOWLEDGMENTS

We thank, Avinanda Banerjee, Sonakshi Mishra, and other members of the Raghavan lab for critical feedback on the manuscript. OB and UA are supported by DBT predoctoral fellowships.

REFERENCES

Abraham, A., and Roga, G. (2014). Topical steroid-damaged skin. *Indian J. Dermatol.* 59, 456–459. doi: 10.4103/0019-5154.139872

Adair-Kirk, T. L., and Senior, R. M. (2008). Fragments of extracellular matrix as mediators of inflammation. *Int. J. Biochem. Cell Biol.* 40, 1101–1110. doi: 10.1016/j.biocel.2007.12.005

Albanesi, C., Madonna, S., Gisondi, P., and Girolomoni, G. (2018). The interplay between keratinocytes and immune cells in the pathogenesis of psoriasis. Front. Immunol. 9:1549. doi: 10.3389/fimmu.2018.01549

Alexeev, V., Salas-Alanis, J. C., Palisson, F., Mukhtarzada, L., Fortuna, G., Uitto, J., et al. (2017). Pro-inflammatory chemokines and cytokines dominate the blister fluid molecular signature in patients with epidermolysis bullosa and affect leukocyte and stem cell migration. *J. Invest. Dermatol.* 137, 2298–2308. doi: 10.1016/j.jid.2017.07.002

Ali, N., Zirak, B., Rodriguez, R. S., Pauli, M. L., Truong, H. A., Lai, K., et al. (2017). Regulatory T cells in skin facilitate epithelial stem cell differentiation. *Cell* 169, 1119–1129. doi: 10.1016/j.cell.2017.05.002

Allori, A. C., Sailon, A. M., and Warren, S. M. (2008). Biological basis of bone formation, remodeling, and repair-part II: extracellular matrix. *Tissue Eng. Part B Rev.* 14, 275–283. doi: 10.1089/ten.teb.2008.0083

Almutawa, F., Alnomair, N., Wang, Y., Hamzavi, I., and Lim, H. W. (2013). Systematic review of UV-based therapy for psoriasis. *Am. J. Clin. Dermatol.* 14, 87–109. doi: 10.1007/s40257-013-0015-y

An, B., and Brodsky, B. (2016). Collagen binding to OSCAR: the odd couple. *Blood* 127, 521–522. doi: 10.1182/blood-2015-12-682476

Andriani, F., Margulis, A., Lin, N., Griffey, S., and Garlick, J. A. (2003). Analysis of microenvironmental factors contributing to basement membrane assembly and normalized epidermal phenotype. *J. Invest. Dermatol.* 120, 923–931. doi: 10.1046/j.1523-1747.2003.12235.x

Anguela, X. M., and High, K. A. (2019). Entering the modern era of gene therapy. *Annu. Rev. Med.* 70, 273–288. doi: 10.1146/annurev-med-012017-043332

Aoudjehane, L., Pissaia, A., Scatton, O., Podevin, P., Massault, P. P., Chouzenoux, S., et al. (2008). Interleukin-4 induces the activation and collagen production of cultured human intrahepatic fibroblasts via the STAT-6 pathway. *Lab. Investig.* 88, 973–985. doi: 10.1038/labinvest.2008.61

Apalla, Z., Lallas, A., Sotiriou, E., Lazaridou, E., and Ioannides, D. (2017). Epidemiological trends in skin cancer. *Dermatol. Pract. Concept.* 7, 1–6. doi: 10.5826/dpc.0702a01

Aras, S., and Raza Zaidi, M. (2017). TAMeless traitors: macrophages in cancer progression and metastasis. *Br. J. Cancer* 117, 1583–1591. doi: 10.1038/bjc.2017.356

Bai, T., Chen, C.-C., and Lau, L. F. (2010). Matricellular protein CCN1 activates a proinflammatory genetic program in murine macrophages. *J. Immunol.* 184, 3223–3232. doi: 10.4049/jimmunol.0902792

Baliwag, J., Barnes, D. H., and Johnston, A. (2015). Cytokines in psoriasis. *Cytokine.* 73, 342–350. doi: 10.1016/j.cyto.2014.12.014

Bansal, M. B., Kovalovich, K., Gupta, R., Li, W., Agarwal, A., Radbill, B., et al. (2005). Interleukin-6 protects hepatocytes from CCl4-mediated necrosis and apoptosis in mice by reducing MMP-2 expression. *J. Hepatol.* 42, 548–556. doi: 10.1016/j.jhep.2004.11.043

Barna, B. K., Eördegh, G., Iván, G., Piffkó, J., Silló, P., and Antal, M. (2017). Az epidermolysis bullosa szájüregi tünetei és annak ellátása. *Orv. Hetil.* 158, 1577–1583. doi: 10.1556/650.2017.30844

Bieber, K., Witte, M., Sun, S., Hundt, J. E., Kalies, K., Dräger, S., et al. (2016). T cells mediate autoantibody-induced cutaneous inflammation and blistering in epidermolysis bullosa acquisita. *Sci. Rep.* 6:38357. doi: 10.1038/srep38357

Bieber, T. (2008). Mechanism of disease atopic dermatitis. *N. Engl. J. Med.* 47, 193–218. doi: 10.1056/NEJMra074081

Binnewies, M., Roberts, E. W., Kersten, K., Chan, V., Fearon, D. F., Merad, M., et al. (2018). Understanding the tumor immune microenvironment (TIME) for effective therapy. *Nat. Med.* 24, 541–550. doi: 10.1038/s41591-018-0014-x

Blanpain, C., and Fuchs, E. (2006). Epidermal stem cells of the skin. *Annu. Rev. Cell Dev. Biol.* 22, 339–373. doi: 10.1146/annurev.cellbio.22.010305.104357

Bluth, M. J., Zaba, L. C., Moussai, D., Suárez-Farias, M., Kaporis, H., Fan, L., et al. (2009). Myeloid dendritic cells from human cutaneous squamous cell carcinoma are poor stimulators of T-cell proliferation. *J. Invest. Dermatol.* 129, 2451–2462. doi: 10.1038/jid.2009.96

Bocian, C., Urbanowitz, A. K., Owens, R. T., Iozzo, R. V., Gotte, M., and Seidler, D. G. (2013). Decorin potentiates interferon-γ activity in a model of allergic inflammation. *J. Biol. Chem.* 288, 12699–12711. doi: 10.1074/jbc.M112.419366

Bodemer, C., Tchen, S. I., Ghomrasseni, S., Séguier, S., Gaultier, F., Fraitag, S., et al. (2003). Skin expression of metalloproteinases and tissue inhibitor of metalloproteinases in sibling patients with recessive dystrophic epidermolysis and intrafamilial phenotypic variation. *J. Invest. Dermatol.* 121, 273–279. doi: 10.1046/j.1523-1747.2003.12325.x

Boehncke, W. H., and Schön, M. P. (2015). Psoriasis. *Lancet* 386, 983–994. doi: 10.1016/S0140-6736(14)61909-7

Bonnans, C., Chou, J., and Werb, Z. (2014). Remodelling the extracellular matrix in development and disease. *Nat. Rev. Mol. Cell Biol.* 15, 786–801. doi: 10.1038/nrm3904

Bornstein, P. (2001). Thrombospondins as matricellular modulators of cell function. *J. Clin. Invest*. 107, 929–934. doi: 10.1172/JCI12749

Bornstein, P. (2009). Matricellular proteins: an overview. *J. Cell Commun. Signal*. 3, 163–165. doi: 10.1007/s12079-009-0069-z

Bos, J. D., Teunissen, M. B. M., Cairo, I., Krieg, S. R., Kapsenberg, M. L., Das, P. K., et al. (1990). T-cell receptor γδ bearing cells in normal human skin. *J. Invest. Dermatol*. 94, 37–42. doi: 10.1111/1523-1747.ep12873333

Boyd, S., Tolvanen, K., Virolainen, S., Kuivanen, T., Kyllönen, L., and Saarialho-Kere, U. (2008). Differential expression of stromal MMP-1, MMP-9 and TIMP-1 in basal cell carcinomas of immunosuppressed patients and controls. *Virchows Arch*. 452, 83–90. doi: 10.1007/s00428-007-0526-0

Breitkreutz, D., Koxholt, I., Thiemann, K., and Nischt, R. (2013). Skin basement membrane: The foundation of epidermal integrity - BM functions and diverse roles of bridging molecules nidogen and perlecan. *Biomed Res. Int*. 2013:179784. doi: 10.1155/2013/179784

Bronte, V., and Zanovello, P. (2005). Regulation of immune responses by L-arginine metabolism. *Nat. Rev. Immunol*. 5, 641–654. doi: 10.1038/nri1668

Bruckner-Tuderman, L., McGrath, J. A., Robinson, E. C., and Uitto, J. (2010). Animal models of epidermolysis bullosa: update 2010. *J. Invest. Dermatol*. 130, 1485–1488. doi: 10.1038/jid.2010.75

Brunner, P. M., Israel, A., Zhang, N., Leonard, A., Wen, H. C., Huynh, T., et al. (2018). Early-onset pediatric atopic dermatitis is characterized by TH2/TH17/TH22-centered inflammation and lipid alterations. *J. Allergy Clin. Immunol*. 141, 2094–2106. doi: 10.1016/j.jaci.2018.02.040

Buback, F., Renkl, A. C., Schulz, G., and Weiss, J. M. (2009). Osteopontin and the skin: multiple emerging roles in cutaneous biology and pathology. *Exp. Dermatol*. 18, 750–759. doi: 10.1111/j.1600-0625.2009.00926.x

Bubier, J. A., Sproule, T. J., Alley, L. M., Webb, C. M., Fine, J. D., Roopenian, D. C., et al. (2010). A mouse model of generalized non-herlitz junctional epidermolysis bullosa. *J. Invest. Dermatol*. 130, 1819–1828. doi: 10.1038/jid.2010.46

Bulfone-Paus, S., and Paus, R. (2008). Osteopontin as a new player in mast cell biology. *Eur. J. Immunol*. 38, 338–341. doi: 10.1002/eji.200738131

Buommino, E., De Filippis, A., Gaudiello, F., Balato, A., Balato, N., Tufano, M. A., et al. (2012). Modification of osteopontin and MMP-9 levels in patients with psoriasis on anti-TNF-α therapy. *Arch. Dermatol. Res*. 304, 481–485. doi: 10.1007/s00403-012-1251-3

Candi, E., Schmidt, R., and Melino, G. (2005). The cornified envelope: a model of cell death in the skin. *Nat. Rev. Mol. Cell Biol*. 6, 328–340. doi: 10.1038/nrm1619

Cao, T., Longley, M. A., Wang, X. J., and Roop, D. R. (2001). An inducible mouse model for epidermolysis bullosa simplex: implications for gene therapy. *J. Cell Biol*. 152, 651–656. doi: 10.1083/jcb.152.3.651

Cavallo, F., De Giovanni, C., Nanni, P., Forni, G., and Lollini, P. L. (2011). 2011: The immune hallmarks of cancer. *Cancer Immunol. Immunother*. 60, 319–326. doi: 10.1007/s00262-010-0968-0

Chandran, V. (2013). The genetics of psoriasis and psoriatic arthritis. *Clin. Rev. Allergy Immunol*. 44, 149–156. doi: 10.1007/s12016-012-8303-5

Cheuk, S., Schlums, H., Gallais Sérézal, I., Martini, E., Chiang, S. C., Marquardt, N., et al. (2017). CD49a expression defines tissue-resident CD8+T cells poised for cytotoxic function in human skin. *Immunity* 46, 287–300. doi: 10.1016/j.immuni.2017.01.009

Chu, C.-C., Di Meglio, P., and Nestle, F. O. (2011). Harnessing dendritic cells in inflammatory skin diseases. *Semin. Immunol*. 23, 28–41. doi: 10.1016/j.smim.2011.01.006

Chung, H. J., and Uitto, J. (2010a). Epidermolysis bullosa with *Pyloric atresia*. *Dermatol. Clin*. 28, 43–54. doi: 10.1016/j.det.2009.10.005

Chung, H. J., and Uitto, J. (2010b). Type VII collagen: the anchoring fibril protein at fault in dystrophic epidermolysis bullosa. *Dermatol. Clin*. 28, 93–105. doi: 10.1016/j.det.2009.10.011

Ciazynska, M., Bednarski, I. A., Wódz, K., Kolano, P., Narbutt, J., Sobjanek, M., et al. (2018). Proteins involved in cutaneous basal cell carcinoma development. *Oncol. Lett*. 16, 4064–4072. doi: 10.3892/ol.2018.9126

Clark, R. A. (2010). Skin-resident T cells: the ups and downs of on site immunity. *J. Invest. Dermatol*. 130, 362–370. doi: 10.1038/jid.2009.247

Clark, R. A., Chong, B., Mirchandani, N., Brinster, N. K., Yamanaka, K.-I., Dowgiert, R. K., et al. (2006). The vast majority of CLA+ T cells are resident in normal skin. *J. Immunol*. 176, 4431–4439. doi: 10.4049/jimmunol.176.7.4431

Clemente, N., Raineri, D., Cappellano, G., Boggio, E., Favero, F., Soluri, M. F., et al. (2016). Osteopontin bridging innate and adaptive immunity in autoimmune diseases. *J. Immunol. Res*. 2016:7675437. doi: 10.1155/2016/7675437

Coulombe, P. A., Hutton, M. E., Vassar, R., and Fuchs, E. (1991). A function for keratins and a common thread among different types of epidermolysis bullosa simplex diseases. *J. Cell Biol*. 115, 1661–1674. doi: 10.1083/jcb.115.6.1661

Coulombe, P. A., Kerns, M. L., and Fuchs, E. (2009). Epidermolysis bullosa simplex: a paradigm for disorders of tissue fragility. *J. Clin. Invest*. 119, 1784–1793. doi: 10.1172/JCI38177

Coulombe, P. A., and Lee, C. H. (2012). Defining keratin protein function in skin epithelia: epidermolysis bullosa simplex and its aftermath. J. Invest. Dermatol. 132(3 Pt 2), 763–775. doi: 10.1038/jid.2011.450

Coussens, L. M., Tinkle, C. L., Hanahan, D., and Werb, Z. (2000). MMP-9 supplied by bone marrow-derived cells contributes to skin carcinogenesis. *Cell* 103, 481–490. doi: 10.1016/S0092-8674(00)00139-2

Craig, V. J., Polverino, F., Laucho-Contreras, M. E., Shi, Y., Liu, Y., Osorio, J. C., et al. (2014). Mononuclear phagocytes and airway epithelial cells: novel sources of matrix metalloproteinase-8 (MMP-8) in patients with idiopathic pulmonary fibrosis. *PLoS ONE* 9:e97485. doi: 10.1371/journal.pone.0097485

Cruz, M. S., Diamond, A., Russell, A., and Jameson, J. M. (2018). Human αβ and γδ T cells in skin immunity and disease. *Front. Immunol*. 9:1304. doi: 10.3389/fimmu.2018.01304

Dang, C., Gottschling, M., Roewert, J., Forschner, T., Stockfleth, E., and Nindl, I. (2006). Tenascin-C patterns and splice variants in actinic keratosis and cutaneous squamous cell carcinoma. *Br. J. Dermatol*. 155, 763–770. doi: 10.1111/j.1365-2133.2006.07401.x

Devillers, A. C., van Toorenenbergena, W., Klein Heerenbrink, G. J., Muldert, P. G. H., and Oranjea, P. (2007). Elevated levels of plasma matrix metalloproteinase-9 in patients with atopic dermatitis: a pilot study. *Clin. Exp. Dermatol*. 32, 311–313. doi: 10.1111/j.1365-2230.2007.02378.x

Dharmage, S. C., Lowe, A. J., Matheson, M. C., Burgess, J. A., Allen, K. J., and Abramson, M. J. (2014). Atopic dermatitis and the atopic march revisited. *Allergy Eur. J. Allergy Clin. Immunol*. 69, 17–27. doi: 10.1111/all.12268

Di Meglio, P., Perera, G. K., and Nestle, F. O. (2011). The multitasking organ: recent insights into skin immune function. *Immunity* 35, 857–869. doi: 10.1016/j.immuni.2011.12.003

Dianzani, C., Zara, G. P., Maina, G., Pettazzoni, P., Pizzimenti, S., Rossi, F., et al. (2014). Drug delivery nanoparticles in skin cancers. *Biomed Res. Int*. 2014:895986. doi: 10.1155/2014/895986

Donovan, J. (2009). Review of the hair follicle origin hypothesis for basal cell Carcinoma. *Dermatologic Surg*. 35, 1311–1323. doi: 10.1111/j.1524-4725.2009.01236.x

D'Orazio, J., Jarrett, S., Amaro-Ortiz, A., and Scott, T. (2013). UV radiation and the skin. *Int. J. Mol. Sci.* 14, 12222–12248. doi: 10.3390/ijms140612222

Driskell, R. R., Jahoda, C. A. B., Chuong, C. M., Watt, F. M., and Horsley, V. (2014). Defining dermal adipose tissue. *Exp. Dermatol*. 23, 629–631. doi: 10.1111/exd.12450

Dubois Declercq, S., and Pouliot, R. (2013). Promising new treatments for psoriasis. *Sci. World J*. 2013:980419. doi: 10.1155/2013/980419

Dummer, R., Rochlitz, C., Velu, T., Acres, B., Limacher, J. M., Bleuzen, P., et al. (2008). Intralesional adenovirus-mediated interleukin-2 gene transfer for advanced solid cancers and melanoma. *Mol. Ther*. 16, 985–994. doi: 10.1038/mt.2008.32

Duvic, M., Nagpal, S., Asano, A. T., and Chandraratna, R. A. S. (1997). Molecular mechanisms of tazarotene action in psoriasis. *J. Am. Acad. Dermatol*. 37, S18–S24. doi: 10.1016/S0190-9622(97)70412-2

Ecker, B. L., Kaur, A., Douglass, S. M., Webster, M. R., Almeida, F. V., Marino, G. E., et al. (2019). Age-related changes in HAPLN1 increase lymphatic permeability and affect routes of melanoma metastasis. *Cancer Discov*. 9, 82–95. doi: 10.1158/2159-8290.CD-18-0168

Esposito, S., Guez, S., Orenti, A., Tadini, G., Scuvera, G., Corti, L., et al. (2016). Autoimmunity and cytokine imbalance in inherited epidermolysis bullosa. *Int. J. Mol. Sci*. 17:1625. doi: 10.3390/ijms17101625

Ferrari, S., Pellegrini, G., Matsui, T., Mavilio, F., and De, L. M. (2006). Towards a gene therapy clinical trial for epidermolysis bullosa. *Rev.Recent Clin.Trials* 1, 155–162. doi: 10.2174/157488706776876472

Fichtner-Feigl, S., Strober, W., Kawakami, K., Puri, R. K., and Kitani, A. (2006). IL-13 signaling through the IL-13α2receptor is involved in induction of TGF-β1production and fibrosis. *Nat. Med*. 12, 99–106. doi: 10.1038/nm1332

Fine, J. D. (2016). Epidemiology of inherited epidermolysis bullosa based on incidence and prevalence estimates from the national epidermolysis Bullosa registry. *JAMA Dermatol.* 152, 1231–1238. doi: 10.1001/jamadermatol.2016.2473

Flacher, V., Tripp, C. H., Mairhofer, D. G., Steinman, R. M., Stoitzner, P., Idoyaga, J., et al. (2014). Murine Langerin+ dermal dendritic cells prime CD8+ T cells while Langerhans cells induce cross-tolerance. *EMBO Mol. Med*. 6, 1191–1204. doi: 10.15252/emmm.201404707

Fontana, R., Bregni, M., Cipponi, A., Raccosta, L., Rainelli, C., Maggioni, D., et al. (2009). Peripheral blood lymphocytes genetically modified to express the self/tumor antigen MAGE-A3 induce antitumor immune responses in cancer patients. *Blood* 113, 1651–1660. doi: 10.1182/blood-2008-07-168666

Frantz, C., Stewart, K. M., and Weaver, V. M. (2010). The extracellular matrix at a glance. J. Cell Sci. 123(Pt 24), 4195–4200. doi: 10.1242/jcs.023820

Frey, H., Schroeder, N., Manon-Jensen, T., Iozzo, R. V., and Schaefer, L. (2013). Biological interplay between proteoglycans and their innate immune receptors in inflammation. *FEBS J.* 280, 2165–2179. doi: 10.1111/febs.12145

Fuchs, E. (2007). Scratching the surface of skin development. *Nature* 445, 834–842. doi: 10.1038/nature05659

Fuchs, E., and Raghavan, S. (2002). Getting under the skin of epidermal morphogenesis. *Nat. Rev. Genet.* 3, 199–209. doi: 10.1038/nrg758

Fujitsu, Y., Fukuda, K., Kumagai, N., and Nishida, T. (2003). IL-4-induced cell proliferation and production of extracellular matrix proteins in human conjunctival fibroblasts. *Exp. Eye Res.* 76, 107–114. doi: 10.1016/S0014-4835(02)00248-8

Fukuda, K., Sugihara, E., Ohta, S., Izuhara, K., Funakoshi, T., Amagai, M., et al. (2015). Periostin is a key niche component for wound metastasis of melanoma. *PLoS ONE* 10:e0129704. doi: 10.1371/journal.pone.0129704

Fulop, T., Khalil, A., and Larbi, A. (2012). The role of elastin peptides in modulating the immune response in aging and age-related diseases. *Pathol. Biol.* 60, 28–33. doi: 10.1016/j.patbio.2011.10.006

Gaiser, M. R., Weis, C. A., Gaiser, T., Jiang, H., Buder-Bakhaya, K., Herpel, E., et al. (2018). Merkel cell carcinoma expresses the immunoregulatory ligand CD200 and induces immunosuppressive macrophages and regulatory T cells. *Oncoimmunology* 7:e1426517. doi: 10.1080/2162402X.2018.1426517

García-Nieto, S., Johal, R. K., Shakesheff, K. M., Emara, M., Pierre-Joseph, R., Chau, D. Y. S., et al. (2010). Laminin and fibronectin treatment leads to generation of dendritic cells with superior endocytic capacity. *PLoS ONE* 5:e10123. doi: 10.1371/journal.pone.0010123

Gasparoto, T. H., De Oliveira, C. E., De Freitas, L. T., Pinheiro, C. R., Ramos, R. N., Da Silva, A. L., et al. (2012). Inflammatory events during murine squamous cell carcinoma development. *J. Inflamm.* 9:46. doi: 10.1186/1476-9255-9-46

Gay, D., Kwon, O., Zhang, Z., Spata, M., Plikus, M. V., Holler, P. D., et al. (2013). Fgf9 from dermal γδ T cells induces hair follicle neogenesis after wounding. *Nat. Med.* 19, 916–923. doi: 10.1038/nm.3181

Georges-Labouesse, E., Messaddeq, N., Yehia, G., Cadalbert, L., Dierich, A., and Le Meur, M. (1996). Absence of integrin α6 leads to epidermolysis bullosa and neonatal death in mice. *Nat. Genet.* 13, 370–373. doi: 10.1038/ng0796-370

Goldschneider, K. R., Good, J., Harrop, E., Liossi, C., Lynch-Jordan, A., Martinez, A. E., et al. (2014). Pain care for patients with epidermolysis bullosa: best care practice guidelines. *BMC Med.* 12:178. doi: 10.1186/s12916-014-0178-2

Goździalska, A., Wojas-Pelc, A., Drag, J., Brzewski, P., Jaśkiewicz, J., and Pastuszczak, M. (2016). Expression of metalloproteinases (MMP-2 and MMP-9) in basal-cell carcinoma. *Mol. Biol. Rep.* 43, 1027–1033. doi: 10.1007/s11033-016-4040-9

Grassberger, M., Steinhoff, M., Schneider, D., and Luger, T. A. (2004). Pimecrolimus - an anti-inflammatory drug targeting the skin. *Exp. Dermatol.* 13, 721–730. doi: 10.1111/j.0906-6705.2004.00269.x

Hallmann, R., Zhang, X., Di Russo, J., Li, L., Song, J., Hannocks, M. J., et al. (2015). The regulation of immune cell trafficking by the extracellular matrix. *Curr. Opin. Cell Biol.* 36, 54–61. doi: 10.1016/j.ceb.2015.06.006

Hamasaki, H., Koga, K., Aoki, M., Hamasaki, M., Koshikawa, N., Seiki, M., et al. (2011). Expression of laminin 5-γ2 chain in cutaneous squamous cell carcinoma and its role in tumour invasion. *Br. J. Cancer.* 105, 824–832. doi: 10.1038/bjc.2011.283

Hamid, Q., Naseer, T., Minshall, E. M., Song, Y. L., Boguniewicz, M., and Leung, D. Y. M. (1996). *In vivo* expression of IL-12 and IL-13 in atopic dermatitis. *J. Allergy Clin. Immunol.* 98, 225–231. doi: 10.1016/S0091-6749(96)70246-4

Han, L., Wang, L., Tang, S., Yuan, L., Wu, S., Du, X., et al. (2018). ITGB4 deficiency in bronchial epithelial cells directs airway inflammation and bipolar disorder-related behavior. *J. Neuroinflammation* 15:246. doi: 10.1186/s12974-018-1283-5

Harlin, H., Meng, Y., Peterson, A. C., Zha, Y., Tretiakova, M., Slingluff, C., et al. (2009). Chemokine expression in melanoma metastases associated with CD8+ T-cell recruitment. *Cancer Res.* 69, 3077–3085. doi: 10.1158/0008-5472.CAN-08-2281

Harper, J. I., Godwin, H., Green, A., Wilkes, L. E., Holden, N. J., Moffatt, M., et al. (2010). A study of matrix metalloproteinase expression and activity in atopic dermatitis using a novel skin wash sampling assay for functional biomarker analysis. *Br. J. Dermatol.* 162, 397–403. doi: 10.1111/j.1365-2133.2009.09467.x

Heath, W. R., and Carbone, F. R. (2013). The skin-resident and migratory immune system in steady state and memory: innate lymphocytes, dendritic cells and T cells. *Nat. Immunol.* 14, 978–985. doi: 10.1038/ni.2680

Hegde, S., and Raghavan, S. (2013). A skin-depth analysis of integrins: role of the integrin network in health and disease. *Cell Commun. Adhes.* 20, 155–169. doi: 10.3109/15419061.2013.854334

Henri, S., Poulin, L. F., Tamoutounour, S., Ardouin, L., Guilliams, M., de Bovis, B., et al. (2010). CD207 + CD103 + dermal dendritic cells cross-present keratinocyte-derived antigens irrespective of the presence of Langerhans cells. *J. Exp. Med.* 207, 189–206. doi: 10.1084/jem.20091964

Henrot, P., Truchetet, M.-E., Fisher, G., Taïeb, A., and Cario, M. (2018). CCN proteins as potential actionable targets in scleroderma. *Exp. Dermatol.* 28, 11–18. doi: 10.1111/exd.13806

Herro, R., Shui, J. W., Zahner, S., Sidler, D., Kawakami, Y., Kawakami, T., et al. (2018). LIGHT - HVEM signaling in keratinocytes controls development of dermatitis. *J. Exp. Med.* 215, 415–422. doi: 10.1084/jem.20170536

Hiratsuka, S., Watanabe, A., Aburatani, H., and Maru, Y. (2006). Tumour-mediated upregulation of chemoattractants and recruitment of myeloid cells predetermines lung metastasis. *Nat. Cell Biol.* 8, 1369–1375. doi: 10.1038/ncb1507

Hirsch, T., Rothoeft, T., Teig, N., Bauer, J. W., Pellegrini, G., De Rosa, L., et al. (2017). Regeneration of the entire human epidermis using transgenic stem cells. *Nature* 551, 327–332. doi: 10.1038/nature24487

Hoeffel, G., Wang, Y., Greter, M., See, P., Teo, P., Malleret, B., et al. (2012). Adult Langerhans cells derive predominantly from embryonic fetal liver monocytes with a minor contribution of yolk sac-derived macrophages. *J. Exp. Med.* 209, 1167–1181. doi: 10.1084/jem.20120340

Howell, M. D., Kim, B. E., Gao, P., Grant, A. V., Boguniewicz, M., DeBenedetto, A., et al. (2007). Cytokine modulation of atopic dermatitis filaggrin skin expression. *J. Allergy Clin. Immunol.* 120, 150–155. doi: 10.1016/j.jaci.2007.04.031

Hu, S. C. S., Yu, H. S., Yen, F. L., Lin, C. L., Chen, G. S., and Lan, C. C. E. (2016). Neutrophil extracellular trap formation is increased in psoriasis and induces human β-defensin-2 production in epidermal keratinocytes. *Sci. Rep.* 6:31119. doi: 10.1038/srep31119

Huber, L. A., Pereira, T. A., Ramos, D. N., Rezende, L. C. D., Emery, F. S., Sobral, L. M., et al. (2015). Topical skin cancer therapy using doxorubicin-loaded cationic lipid nanoparticles and iontophoresis. *J. Biomed. Nanotechnol.* 11, 1975–1988. doi: 10.1166/jbn.2015.2139

Hussein, M. R., Ali, F. M. N., and Omar, A. E. M. M. (2007). Immunohistological analysis of immune cells in blistering skin lesions. *J. Clin. Pathol.* 60, 62–71. doi: 10.1136/jcp.2006.037010

Hynes, R. O. (2002). Integrins: bidirectional, allosteric signaling machines. *Cell* 110, 673–687. doi: 10.1016/S0092-8674(02)00971-6

Ilkovitch, D., and Lopez, D. M. (2008). Immune modulation by melanoma-derived factors. *Exp. Dermatol.* 17, 977–985. doi: 10.1111/j.1600-0625.2008.00779.x

Ishida, M., Kojima, F., and Okabe, H. (2013). Cathepsin K expression in basal cell carcinoma. *J. Eur. Acad. Dermatol. Venereol.* 27, 128–130. doi: 10.1111/j.1468-3083.2011.04436.x

Iwata, H., Bieber, K., Tiburzy, B., Chrobok, N., Kalies, K., Shimizu, A., et al. (2013). B cells, dendritic cells, and macrophages are required to induce an autoreactive

CD4 helper T cell response in experimental epidermolysis bullosa acquisita. *J. Immunol.* 191, 2978–2988. doi: 10.4049/jimmunol.1300310

Jacobi, A., Mayer, A., and Augustin, M. (2015). Keratolytics and emollients and their role in the therapy of psoriasis: a systematic review. *Dermatol. Ther.* 5, 1–18. doi: 10.1007/s13555-015-0068-3

Jarnicki, A. G., Lysaght, J., Todryk, S., and Mills, K. H. G. (2006). Suppression of antitumor immunity by IL-10 and TGF- -producing T cells infiltrating the growing tumor: influence of tumor environment on the induction of CD4+ and CD8+ regulatory T cells. *J. Immunol.* 177, 896–904. doi: 10.4049/jimmunol.177.2.896

Jayadev, R., and Sherwood, D. R. (2017). Basement membranes. *Curr. Biol.* 27, R207–R211. doi: 10.1016/j.cub.2017.02.006

Jimenez, S. A., Hitraya, E., and Varga, J. (1996). Pathogenesis of scleroderma. collagen. *Rheum. Dis. Clin. North Am.* 22, 647–674. doi: 10.1016/S0889-857X(05)70294-5

Johnson, D. B., and Sosman, J. A. (2015). Therapeutic advances and treatment options in metastatic melanoma. *JAMA Oncol.* 1, 380–386. doi: 10.1001/jamaoncol.2015.0565

Kale, S., Raja, R., Thorat, D., Soundararajan, G., Patil, T. V., and Kundu, G. C. (2014). Osteopontin signaling upregulates cyclooxygenase-2 expression in tumor-associated macrophages leading to enhanced angiogenesis and melanoma growth via α9β1 integrin. *Oncogene* 33, 2295–2306. doi: 10.1038/onc.2013.184

Kamata, M., Fujita, H., Hamanaka, T., Takahashi, K., Koga, H., Hashimoto, T., et al. (2013). Anti-laminin γ1 pemphigoid accompanied by autoantibodies to laminin α3 and γ2 subunits of laminin-332. *JAMA Dermatol.* 33, 2295–2306. doi: 10.1001/jamadermatol.2013.5358

Kandoth, C., McLellan, M. D., Vandin, F., Ye, K., Niu, B., Lu, C., et al. (2013). Mutational landscape and significance across 12 major cancer types. *Nature* 502, 333–339. doi: 10.1038/nature12634

Kaplan, D. H. (2017). Ontogeny and function of murine epidermal Langerhans cells. *Nat. Immunol.* 18, 1068–1075. doi: 10.1038/ni.3815

Karagiannis, G. S., Poutahidis, T., Erdman, S. E., Kirsch, R., Riddell, R. H., and Diamandis, E. P. (2012). Cancer-associated fibroblasts drive the progression of metastasis through both paracrine and mechanical pressure on cancer tissue. *Mol. Cancer Res.* 10, 1403–1418. doi: 10.1158/1541-7786.MCR-12-0307

Karantalis, V., Schulman, I. H., Balkan, W., and Hare, J. M. (2015). Allogeneic cell therapy: a new paradigm in therapeutics. *Circ. Res.* 116, 12–15. doi: 10.1161/CIRCRESAHA.114.305495

Kasperkiewicz, M., Sadik, C. D., Bieber, K., Ibrahim, S. M., Manz, R. A., Schmidt, E., et al. (2016). Epidermolysis bullosa acquisita: from pathophysiology to novel therapeutic options. *J. Invest. Dermatol.* 136, 24–33. doi: 10.1038/JID.2015.356

Kasraie, S., and Werfel, T. (2013). Role of macrophages in the pathogenesis of atopic dermatitis. *Mediators Inflamm.* 2013:942375. doi: 10.1155/2013/942375

Kaur, A., Ecker, B. L., Douglass, S. M., Kugel, C. H., Webster, M. R., Almeida, F. V., et al. (2018). Remodeling of the collagen matrix in aging skin promotes melanoma metastasis and affects immune cell motility. *Cancer Discov.* 9, 64–81. doi: 10.1158/2159-8290.CD-18-0193

Kelsh, R., You, R., Horzempa, C., Zheng, M., and McKeown-Longo, P. J. (2014). Regulation of the innate immune response by fibronectin: synergism between the III-1 and EDA domains. *PLoS ONE* 9:e102974. doi: 10.1371/journal.pone.0102974

Kiekens, R. C. M., Thepen, T., Oosting, A. J., Bihari, I. C., Van De Winkel, J. G. J., Bruijnzeel-Koomen, C. A. F. M., et al. (2001). Heterogeneity within tissue-specific macrophage and dendritic cell populations during cutaneous inflammation in atopic dermatitis. *Br. J. Dermatol.* 145, 957–965. doi: 10.1046/j.1365-2133.2001.04508.x

Kim, B. E., Leung, D. Y. M., Boguniewicz, M., and Howell, M. D. (2008). Loricrin and involucrin expression is down-regulated by Th2 cytokines through STAT-6. *Clin. Immunol.* 126, 332–337. doi: 10.1016/j.clim.2007.11.006

Kim, T. I., Park, H. J., Won, Y. Y., Choi, H., Jeong, K. H., Sung, J. Y., et al. (2018). Basement membrane status is intact in urticarial dermatitis vs. adult-onset atopic dermatitis. *Ann. Dermatol.* 30, 258–261. doi: 10.5021/ad.2018.30.2.258

Kisich, K. O., Carspecken, C. W., Fiéve, S., Boguniewicz, M., and Leung, D. Y. M. (2008). Defective killing of *Staphylococcus aureus* in atopic dermatitis is associated with reduced mobilization of human β-defensin-3. *J. Allergy Clin. Immunol.* 122, 62–68. doi: 10.1016/j.jaci.2008.04.022

Kobayashi, Y. (1997). Langerhan's cell produce type IV collagenase (MMP-9) following epicutaneous stimulation with haptens. *Immunology* 90, 496–501. doi: 10.1046/j.1365-2567.1997.00212.x

Koga, C., Kabashima, K., Shiraishi, N., Kobayashi, M., and Tokura, Y. (2008). Possible pathogenic role of Th17 cells for atopic dermatitis. *J. Invest. Dermatol.* 128, 2625–2630. doi: 10.1038/jid.2008.111

Komohara, Y., Jinushi, M., and Takeya, M. (2014). Clinical significance of macrophage heterogeneity in human malignant tumors. *Cancer Sci.* 105, 1–8. doi: 10.1111/cas.12314

Kurbet, A. S., Hegde, S., Bhattacharjee, O., Marepally, S., Vemula, P. K., and Raghavan, S. (2016). Sterile inflammation enhances ECM degradation in integrin β1 KO embryonic skin. *Cell Rep.* 16, 3334–3347. doi: 10.1016/j.celrep.2016.08.062

Lai-Cheong, J. E., Tanaka, A., Hawche, G., Emanuel, P., Maari, C., Taskesen, M., et al. (2009). Kindler syndrome: a focal adhesion genodermatosis. *Br. J. Dermatol.* 160, 233–242. doi: 10.1111/j.1365-2133.2008.08976.x

Landriscina, A., Rosen, J., Albanese, J., Amin, B., and Friedman, A. J. (2015). Identifying new biologic targets in atopic dermatitis (AD): A retrospective histologic analysis. *J. Am. Acad. Dermatol.* 73, 521–523. doi: 10.1016/j.jaad.2015.06.036

Langley, R. G. B., Krueger, G. G., and Griffiths, C. E. M. (2005). Psoriasis: epidemiology, clinical features, and quality of life. *Ann. Rheum. Dis.* 64(Suppl. 2): ii18–ii23. doi: 10.1136/ard.2004.033217

Lettner, T., Lang, R., Klausegger, A., Hainzl, S., Bauer, J. W., and Wally, V. (2013). MMP-9 and CXCL8/IL-8 are potential therapeutic targets in *Epidermolysis bullosa* simplex. *PLoS ONE* 8:e70123. doi: 10.1371/journal.pone.0070123

Lewin, J., and Carucci, J. (2015). Advances in the management of basal cell carcinoma. *F1000Prime Rep.* 7:53. doi: 10.12703/P7-53

Li, H., Li, H., Huo, R., Wu, P., Shen, Z., Xu, H., et al. (2017). Cyr61/CCN1 induces CCL20 production by keratinocyte via activating p38 and JNK/AP-1 pathway in psoriasis. *J. Dermatol. Sci.* 88, 46–56. doi: 10.1016/j.jdermsci.2017.05.018

Li, J. H., Huang, X. R., Zhu, H. J., Johnson, R., and Lan, H. Y. (2003). Role of TGF-β signaling in extracellular matrix production under high glucose conditions. *Kidney Int.* 63, 2010–2019. doi: 10.1046/j.1523-1755.2003.00016.x

Li, R., Hebert, J. D., Lee, T. A., Xing, H., Boussommier-Calleja, A., Hynes, R. O., et al. (2017). Macrophage-secreted TNFα and TGFβ1 influence migration speed and persistence of cancer cells in 3D tissue culture via independent pathways. *Cancer Res.* 77, 279–290. doi: 10.1158/0008-5472.CAN-16-0442

Li, X., Li, J., Wang, L., Niu, X., Hou, R., Liu, R., et al. (2015). Transmission of psoriasis by allogeneic bone marrow transplantation and blood transfusion. *Blood Cancer J.* 5:e288. doi: 10.1038/bcj.2015.15

Liguori, M., Solinas, G., Germano, G., Mantovani, A., and Allavena, P. (2011). Tumor-associated macrophages as incessant builders and destroyers of the cancer stroma. *Cancers* 3, 3740–3761. doi: 10.3390/cancers3043740

Liu, A. Y., Zheng, H., and Ouyang, G. (2014). Periostin, a multifunctional matricellular protein in inflammatory and tumor microenvironments. *Matrix Biol.* 37, 150–156. doi: 10.1016/j.matbio.2014.04.007

Lo, B. K. K., Jalili, R. B., Zloty, D., Ghahary, A., Cowan, B., Dutz, J. P., et al. (2011). CXCR3 ligands promote expression of functional indoleamine 2,3-dioxygenase in basal cell carcinoma keratinocytes. *Br. J. Dermatol.* 165, 1030–1036. doi: 10.1111/j.1365-2133.2011.10489.x

Lu, H., Chen, J., Planko, L., Zigrino, P., Klein-Hitpass, L., and Magin, T. M. (2007). Induction of inflammatory cytokines by a keratin mutation and their repression by a small molecule in a mouse model for EBS. *J. Invest. Dermatol.* 127, 2781–2789. doi: 10.1038/sj.jid.5700918

Lu, P., Takai, K., Weaver, V. M., and Werb, Z. (2011). Extracellular matrix degradation and remodeling in development and disease. *Cold Spring Harb. Perspect. Biol.* 3. doi: 10.1101/cshperspect.a005058

Macleod, A. S., Hemmers, S., Garijo, O., Chabod, M., Mowen, K., Witherden, D. A., et al. (2013). Dendritic epidermal T cells regulate skin antimicrobial barrier function. *J. Clin. Invest.* 123, 4364–4374. doi: 10.1172/JCI70064

Maggi, L., Santarlasci, V., Capone, M., Peired, A., Frosali, F., Crome, S. Q., et al. (2010). CD161 is a marker of all human IL-17-producing T-cell subsets and is induced by RORC. *Eur. J. Immunol.* 40, 2174–2181. doi: 10.1002/eji.200940257

Malaisse, J., Bourguignon, V., De Vuyst, E., Lambert De Rouvroit, C., Nikkels, A. F., Flamion, B., et al. (2014). Hyaluronan metabolism in human keratinocytes and atopic dermatitis skin is driven by a balance of hyaluronan synthases 1 and 3. *J. Invest. Dermatol.* 134, 2174–2182. doi: 10.1038/jid.2014.147

Maldonado-Colin, G., Hernández-Zepeda, C., Durán-McKinster, C., and García-Romero, M. (2017). Inherited epidermolysis bullosa: a multisystem disease of skin and mucosae fragility. *Indian J. Paediatr. Dermatol.* 88, 185–198. doi: 10.4103/ijpd.ijpd_16_17

Malissen, B., Tamoutounour, S., and Henri, S. (2014). The origins and functions of dendritic cells and macrophages in the skin. *Nat. Rev. Immunol.* 14, 417–428. doi: 10.1038/nri3683

Manoukian, M., Ott, S., Rajadas, J., and Inayathullah, M. (2014). Polymeric nanoparticles to combat squamous cell carcinomas in patients with dystrophic epidermolysis bullosa. *Recent Patents Nanomed.* 4, 15–24. doi: 10.2174/1877912304666140708184013

Margadant, C., Kreft, M., Zambruno, G., and Sonnenberg, A. (2013). Kindlin-1 regulates integrin dynamics and adhesion turnover. *PLoS ONE* 8:e65341. doi: 10.1371/journal.pone.0065341

Marinkovich, M. P. (2007). Tumour microenvironment: Laminin 332 in squamous-cell carcinoma. *Nat. Rev. Cancer.* 7, 370–380. doi: 10.1038/nrc2089

Martin-Manso, G., Galli, S., Ridnour, L. A., Tsokos, M., Wink, D. A., and Roberts, D. D. (2008). Thrombospondin 1 promotes tumor macrophage recruitment and enhances tumor cell cytotoxicity of differentiated U937 cells. *Cancer Res.* 68, 7090–7099. doi: 10.1158/0008-5472.CAN-08-0643

Martins, L., Caley, M. P., Moore, K., Szentpetery, Z., Marsh, S. T., Murrell, D. F., et al. (2016). Suppression of TGFβ and angiogenesis by Type VII collagen in cutaneous SCC. J. Natl. Cancer Inst. 108:djv293. doi: 10.1093/jnci/djv293

Martins, V. L., Vyas, J. J., Chen, M., Purdie, K., Mein, C. A., South, A. P., et al. (2009). Increased invasive behaviour in cutaneous squamous cell carcinoma with loss of basement-membrane type VII collagen. *J. Cell Sci.* 122, 1788–1799. doi: 10.1242/jcs.042895

Masuda, A., Yasuoka, H., Satoh, T., Okazaki, Y., Yamaguchi, Y., and Kuwana, M. (2013). Versican is upregulated in circulating monocytes in patients with systemic sclerosis and amplifies a CCL2-mediated pathogenic loop. *Arthritis Res. Ther.* 15:R74. doi: 10.1186/ar4251

Matejuk, A. (2018). Skin immunity. *Arch. Immunol. Ther. Exp.* 66, 45–54. doi: 10.1007/s00005-017-0477-3

Mayba, J. N., and Gooderham, M. J. (2017). Review of atopic dermatitis and topical therapies. *J. Cutan. Med. Surg.* 21, 227–236. doi: 10.1177/1203475416685077

McFadden, J., Fry, L., Powles, A. V., and Kimber, I. (2012). Concepts in psoriasis: psoriasis and the extracellular matrix. *Br. J. Dermatol.* 167, 980–986. doi: 10.1111/j.1365-2133.2012.11149.x

McFadden, J. P., Basketter, D. A., Dearman, R. J., and Kimber, I. R. (2011). Extra domain A-positive fibronectin-positive feedback loops and their association with cutaneous inflammatory disease. *Clin. Dermatol.* 29, 257–265. doi: 10.1016/j.clindermatol.2010.11.003

McWhorter, F. Y., Davis, C. T., and Liu, W. F. (2015). Physical and mechanical regulation of macrophage phenotype and function. *Cell. Mol. Life Sci.* 72, 1303–1316. doi: 10.1007/s00018-014-1796-8

Medeiros, G. X., and Riet-Correa, F. (2015). Epidermolysis bullosa in animals: a review. *Vet. Dermatol.* 26, 3–13. doi: 10.1111/vde.12176

Mellerio, J. E. (2010). Epidermolysis bullosa care in the United Kingdom. *Dermatol. Clin.* 28, 395–396. doi: 10.1016/j.det.2010.02.015

Mencía, Á., García, M., García, E., Llames, S., Charlesworth, A., de Lucas, R., et al. (2016). Identification of two rare and novel large deletions in ITGB4 gene causing epidermolysis bullosa with pyloric atresia. *Exp. Dermatol.* 25, 269–274. doi: 10.1111/exd.1293

Meyaard, L., Adema, G. J., Chang, C., Woollatt, E., Sutherland, G. R., Lanier, L. L., et al. (1997). LAIR-1, a novel inhibitory receptor expressed on human mononuclear leukocytes. *Immunity* 7, 283–290. doi: 10.1016/S1074-7613(00)80530-0

Migden, M. R., Chang, A. L. S., Dirix, L., Stratigos, A. J., and Lear, J. T. (2018). Emerging trends in the treatment of advanced basal cell carcinoma. *Cancer Treat. Rev.* 64, 1–10. doi: 10.1016/j.ctrv.2017.12.009

Mildner, A., and Jung, S. (2014). Development and function of dendritic cell subsets. *Immunity* 40, 642–656. doi: 10.1016/j.immuni.2014.04.016

Miskolczi, Z., Smith, M. P., Rowling, E. J., Ferguson, J., Barriuso, J., and Wellbrock, C. (2018). Collagen abundance controls melanoma phenotypes through lineage-specific microenvironment sensing. *Oncogene* 37, 3166–3182. doi: 10.1038/s41388-018-0209-0

Mitamura, Y., Nunomura, S., Nanri, Y., Ogawa, M., Yoshihara, T., Masuoka, M., et al. (2018). The IL-13/periostin/IL-24 pathway causes epidermal barrier dysfunction in allergic skin inflammation. *Allergy Eur. J. Allergy Clin. Immunol.* 73, 1881–1891. doi: 10.1111/all.13437

Moilanen, J. M., Löffek, S., Kokkonen, N., Salo, S., Väyrynen, J. P., Hurskainen, T., et al. (2017). Significant role of collagen XVII and integrin β4 in migration and invasion of the less aggressive squamous cell carcinoma cells. *Sci. Rep.* 7:45057. doi: 10.1038/srep45057

Moreira, G., Fulgêncio, L. B., de Mendonça, E. F., Leles, C. R., Batista, A. C., and da Silva, T. A. (2010). T regulatory cell markers in oral squamous cell carcinoma: relationship with survival and tumor aggressiveness. *Oncol. Lett.* 1, 127–132. doi: 10.3892/ol_00000023

Mori, R., Shaw, T. J., and Martin, P. (2008). Molecular mechanisms linking wound inflammation and fibrosis: knockdown of osteopontin leads to rapid repair and reduced scarring. *J. Exp. Med.* 205, 43–51. doi: 10.1084/jem.20071412

Morizane, S., and Gallo, R. L. (2012). Antimicrobial peptides in the pathogenesis of psoriasis. *J. Dermatol.* 39, 225–230. doi: 10.1111/j.1346-8138.2011.01483.x

Mott, J. D., and Werb, Z. (2004). Regulation of matrix biology by matrix metalloproteinases. *Curr. Opin. Cell Biol.* 16, 558–564. doi: 10.1016/j.ceb.2004.07.010

Mueller, S. N., Zaid, A., and Carbone, F. R. (2014). Tissue-resident T cells: dynamic players in skin immunity. Front. Immunol. 5:332. doi: 10.3389/fimmu.2014.00332

Munde, P., Khandekar, S., Dive, A., and Sharma, A. (2013). Pathophysiology of merkel cell. *J. Oral Maxillofac. Pathol.* 17, 408–412. doi: 10.4103/0973-029X.125208

Nagao, K., Ginhoux, F., Leitner, W. W., Motegi, S.-I., Bennett, C. L., Clausen, B. E., et al. (2009). Murine epidermal Langerhans cells and langerin-expressing dermal dendritic cells are unrelated and exhibit distinct functions. *Proc. Natl. Acad. Sci. U.S.A.* 106, 3312–3317. doi: 10.1073/pnas.0807126106

Natsuga, K., Shinkuma, S., Nishie, W., and Shimizu, H. (2010). Animal models of epidermolysis bullosa. *Dermatol. Clin.* 28, 137–142. doi: 10.1016/j.det.2009.10.016

Natsumi, A., Sugawara, K., Yasumizu, M., Mizukami, Y., Sano, S., Morita, A., et al. (2018). Re-investigating the basement membrane zone of psoriatic epidermal lesions: is Laminin-511 a new player in psoriasis pathogenesis? *J. Histochem. Cytochem.* 66, 847–862. doi: 10.1369/0022155418782693

Nelson, D. A., and Larsen, M. (2015). Heterotypic control of basement membrane dynamics during branching morphogenesis. *Dev. Biol.* 401, 103–109. doi: 10.1016/j.ydbio.2014.12.011

Nestle, F. O., Kaplan, D. H., and Barker, J. (2009). Mechanisms of disease psoriasis. *N. Engl. J. Med.* 361, 496–509. doi: 10.1056/NEJMra0804595

Niebuhr, M., Lutat, C., Sigel, S., and Werfel, T. (2009). Impaired TLR-2 expression and TLR-2-mediated cytokine secretion in macrophages from patients with atopic dermatitis. *Allergy Eur. J. Allergy Clin. Immunol.* 64, 1580–1587. doi: 10.1111/j.1398-9995.2009.02050.x

Noy, R., and Pollard, J. W. (2014). Tumor-associated macrophages: from mechanisms to therapy. *Immunity* 41, 49–61. doi: 10.1016/j.immuni.2014.09.021

Nyström, A., Bornert, O., Kühl, T., Gretzmeier, C., Thriene, K., Dengjel, J., et al. (2018). Impaired lymphoid extracellular matrix impedes antibacterial immunity in epidermolysis bullosa. *Proc. Natl. Acad. Sci. U.S.A.* 115, E705–E714. doi: 10.1073/pnas.1709111115

Nyström, A., and Bruckner-Tuderman, L. (2018). Injury- and inflammation-driven skin fibrosis: the paradigm of epidermolysis bullosa. *Matrix Biol.* 68–69, 547–560. doi: 10.1016/j.matbio.2018.01.016

Nystrom, A., Thriene, K., Mittapalli, V., Kern, J. S., Kiritsi, D., Dengjel, J., et al. (2015). Losartan ameliorates dystrophic epidermolysis bullosa and uncovers new disease mechanisms. *EMBO Mol. Med.* 7, 1211–1228. doi: 10.15252/emmm.201505061

Nyström, A., Velati, D., Mittapalli, V. R., Fritsch, A., Kern, J. S., and Bruckner-Tuderman, L. (2013). Collagen VII plays a dual role in wound healing. *J. Clin. Invest*. 123, 3498–3509. doi: 10.1172/JCI68127

Obara, W., Kawa, Y., Ra, C., Nishioka, K., Soma, Y., and Mizoguchi, M. (2002). T cells and mast cells as a major source of interleukin-13 in atopic dermatitis. *Dermatology* 205, 11–17. doi: 10.1159/000063145

Odorisio, T., di Salvio, M., Orecchia, A., di Zenzo, G., Piccinni, E., Cianfarani, F., et al. (2014). Monozygotic twins discordant for recessive dystrophic epidermolysis bullosa phenotype highlight the role of TGF-β signalling in modifying disease severity. *Hum. Mol. Genet*. 23, 3907–3922. doi: 10.1093/hmg/ddu102

Ogawa, K., Ito, M., Takeuchi, K., Nakada, A., Heishi, M., Suto, H., et al. (2005). Tenascin-C is upregulated in the skin lesions of patients with atopic dermatitis. *J. Dermatol. Sci*. 40, 35–41. doi: 10.1016/j.jdermsci.2005.06.001

Oh, S. T., Schramme, A., Stark, A., Tilgen, W., Gutwein, P., and Reichrath, J. (2009). The disintegrin-metalloproteinases ADAM 10, 12 and 17 are upregulated in invading peripheral tumor cells of basal cell carcinomas. *J. Cutan. Pathol*. 36, 395–401. doi: 10.1111/j.1600-0560.2008.01082.x

Ohtani, T., Memezawa, A., Okuyama, R., Sayo, T., Sugiyama, Y., Inoue, S., et al. (2009). Increased hyaluronan production and decreased E-cadherin expression by cytokine-stimulated keratinocytes lead to spongiosis formation. *J. Invest. Dermatol*. 129, 1412–1420. doi: 10.1038/jid.2008.394

Omland, S. H., Nielsen, P. S., Gjerdrum, L. M. R., and Gniadecki, R. (2016). Immunosuppressive environment in basal cell carcinoma: the role of regulatory T cells. *Acta Derm. Venereol*. 96, 917–921. doi: 10.2340/00015555-2440

Onetti Muda, A., Paradisi, M., Angelo, C., Puddu, P., and Faraggiana, T. (1996). Three-dimensional distribution of basement membrane components in dystrophic recessive epidermolysis bullosa. *J. Pathol.* 179, 427–431. doi: 10.1002/(SICI)1096-9896(199608)179:4<427::AID-PATH608>3.0.CO;2-T

O'regan, A. W., Chupp, G. L., Lowry, J. A., Goetschkes, M., Mulligan, N., and Berman, J. S. (1999). Osteopontin is associated with T cells in sarcoid granulomas and has T cell adhesive and cytokine-like properties *in vitro*. *J. Immunol.* 162, 1024–1031.

Oviedo-Orta, E., Bermudez-Fajardo, A., Karanam, S., Benbow, U., and Newby, A. C. (2008). Comparison of MMP-2 and MMP-9 secretion from T helper 0, 1 and 2 lymphocytes alone and in coculture with macrophages. *Immunology* 124, 42–50. doi: 10.1111/j.1365-2567.2007.02728.x

Owen, J. L., Iragavarapu-Charyulu, V., Gunja-Smith, Z., Herbert, L. M., Grosso, J. F., and Lopez, D. M. (2003). Up-regulation of matrix metalloproteinase-9 in T lymphocytes of mammary tumor bearers: role of vascular endothelial growth factor. *J. Immunol*. 171, 4340–4351. doi: 10.4049/jimmunol.171.8.4340

Oyama, N., Chan, I., Neill, S. M., Hamada, T., South, A. P., Wessagowit, V., et al. (2003). Autoantibodies to extracellular matrix protein 1 in lichen sclerosus. *Lancet* 362, 118–123. doi: 10.1016/S0140-6736(03)13863-9

Palmer, B. C., and DeLouise, L. A. (2016). Nanoparticle-enabled transdermal drug delivery systems for enhanced dose control and tissue targeting. *Molecules* 21:1719. doi: 10.3390/molecules21121719

Pandolfino, T. L., Siegel, R. S., Kuzel, T. M., Rosen, S. T., and Guitart, J. (2000). Primary cutaneous B-cell lymphoma: review and current concepts. *J. Clin. Oncol*. 18, 2152–2168. doi: 10.1200/JCO.2000.18.10.2152

Papier, A., and Strowd, L. C. (2018). Atopic dermatitis: a review of topical nonsteroid therapy. *Drugs Context* 7:212521. doi: 10.7573/dic.212521

Parisi, R., Symmons, D. P. M., Griffiths, C. E. M., and Ashcroft, D. M. (2013). Global epidemiology of psoriasis: a systematic review of incidence and prevalence. *J. Invest. Dermatol*. 133, 377–385. doi: 10.1038/jid.2012.339

Peck, A., and Mellins, E. D. (2010). Precarious balance: Th17 cells in host defense. *Infect. Immun*. 78, 32–38. doi: 10.1128/IAI.00929-09

Peters, B., Kirfel, J., Bü, H., Vidal, M., and Magin, T. M. (2001). Complete cytolysis and neonatal lethality in keratin 5 knockout mice reveal its fundamental role in skin integrity and in epidermolysis bullosa simplex. *Mol. Biol. Cell*. 12, 1775–1789. doi: 10.1091/mbc.12.6.1775

Pettersen, J. S., Fuentes-Duculan, J., Suárez-Farias, M., Pierson, K. C., Pitts-Kiefer, A., Fan, L., et al. (2011). Tumor-associated macrophages in the cutaneous SCC microenvironment are heterogeneously activated. *J. Invest. Dermatol*. 131, 1322–1330. doi: 10.1038/jid.2011.9

Pfendner, E. G., Sadowski, S. G., and Uitto, J. (2005). Epidermolysis bullosa simplex: recurrent and de novo mutations in the KRT5 and KRT14 genes, phenotype/genotype correlations, and implications for genetic counseling and prenatal diagnosis. *J. Invest. Dermatol*. 125, 239–243. doi: 10.1111/j.0022-202X.2005.23818.x

Piaceski, A. D., Larouche, D., Ghani, K., Bisson, F., Ghio, S. C., Larochelle, S., et al. (2018). Translating the combination of gene therapy and tissue engineering for treating recessive dystrophic epidermolysis bullosa. *Eur. Cells Mater*. 35, 73–86. doi: 10.22203/eCM.v035a06

Pickup, M. W., Mouw, J. K., and Weaver, V. M. (2014). The extracellular matrix modulates the hallmarks of cancer. *EMBO Rep*. 15, 1243–1253. doi: 10.15252/embr.201439246

Pieniazek, M., Matkowski, R., and Donizy, P. (2018). Macrophages in skin melanoma-the key element in melanomagenesis (Review). *Oncol. Lett*. 15, 5399–5404. doi: 10.3892/ol.2018.8021

Pinhal, M. A. S., Costa, A. S., Serrano, R. L., Almeida, M. C. L., Theodoro, T. R., and Machado Filho, C. D. S. (2016). Expression of heparanase in basal cell carcinoma and squamous cell carcinoma. *An. Bras. Dermatol*. 91, 595–600. doi: 10.1590/abd1806-4841.20164957

Pittayapruek, P., Meephansan, J., Prapapan, O., Komine, M., and Ohtsuki, M. (2016). Role of matrix metalloproteinases in photoaging and photocarcinogenesis. Int. J. Mol. Sci. 17:868. doi: 10.3390/ijms17060868

Pivarcsi, A., Müller, A., Hippe, A., Rieker, J., van Lierop, A., Steinhoff, M., et al. (2007). Tumor immune escape by the loss of homeostatic chemokine expression. *Proc. Natl. Acad. Sci. U.S.A*. 104, 19055–19060. doi: 10.1073/pnas.0705673104

Purwar, R., Kraus, M., Werfel, T., and Wittmann, M. (2008). Modulation of keratinocyte-derived MMP-9 by IL-13: a possible role for the pathogenesis of epidermal inflammation. *J. Invest. Dermatol.* 128, 59–66. doi: 10.1038/sj.jid.5700940

Purwar, R., Werfel, T., and Wittmann, M. (2006). IL-13-stimulated human keratinocytes preferentially attract CD4+CCR4+ T cells: possible role in atopic dermatitis. *J. Invest. Dermatol.* 126, 1043–1051. doi: 10.1038/sj.jid.5700085

Puzanov, I., and Flaherty, K. T. (2010). Targeted molecular therapy in melanoma. *Semin. Cutan. Med. Surg.* 29, 196–201. doi: 10.1016/j.sder.2010.06.005

Quan, T., Xu, Y., Qin, Z., Robichaud, P., Betcher, S., Calderone, K., et al. (2014). Elevated YAP and its downstream targets CCN1 and CCN2 in basal cell carcinoma: impact on keratinocyte proliferation and stromal cell activation. *Am. J. Pathol.* 184, 937–943. doi: 10.1016/j.ajpath.2013.12.017

Rankin, A. L., Mumm, J. B., Murphy, E., Turner, S., Yu, N., McClanahan, T. K., et al. (2010). IL-33 induces IL-13-dependent cutaneous fibrosis. *J. Immunol.* 184, 1526–1535. doi: 10.4049/jimmunol.0903306

Rasheed, K., Abdulsalam, I., Fismen, S., Grimstad, Ø., Sveinbjørnsson, B., Moens, U., et al. (2018). CCL17/TARC and CCR4 expression in Merkel cell carcinoma. *Oncotarget* 9, 31432–31447. doi: 10.18632/oncotarget.25836

Ratzinger, G., Stoitzner, P., Ebner, S., Lutz, M. B., Layton, G. T., Rainer, C., et al. (2002). Matrix metalloproteinases 9 and 2 are necessary for the migration of langerhans cells and dermal dendritic cells from human and murine skin. *J. Immunol.* 168, 4361–4371. doi: 10.4049/jimmunol.168.9.4361

Reduta, T., Niecinska, M., Pawłos, A., Sulkiewicz, A., and Sokołowska, M. (2015). Serum osteopontin levels in disseminated allergic contact dermatitis. *Adv. Med. Sci.* 60, 273–276. doi: 10.1016/j.advms.2015.05.001

Ribero, S., Stucci, L. S., Daniels, G. A., and Borradori, L. (2017). Drug therapy of advanced cutaneous squamous cell carcinoma: is there any evidence? *Curr. Opin. Oncol.* 29, 129–135. doi: 10.1097/CCO.0000000000000359

Rognoni, E., Ruppert, R., and Fässler, R. (2016). The kindlin family: functions, signaling properties and implications for human disease. *J. Cell Sci.* 129, 17–27. doi: 10.1242/jcs.161190

Romanovsky, A. A. (2014). Skin temperature: its role in thermoregulation. *Acta Physiol.* 210, 498–507. doi: 10.1111/apha.12231

Roth, W., Reuter, U., Wohlenberg, C., Bruckner-Tuderman, L., and Magin, T. M. (2009). Cytokines as genetic modifiers in K5-/- mice and in human epidermolysis bullosa simplex. *Hum. Mutat.* 30, 832–841. doi: 10.1002/humu.20981

Rozario, T., and DeSimone, D. W. (2010). The extracellular matrix in development and morphogenesis: a dynamic view. *Dev. Biol.* 341, 126–140. doi: 10.1016/j.ydbio.2009.10.026

Rüegg, C. R., Chiquet-Ehrismann, R., and Alkan, S. S. (1989). Tenascin, an extracellular matrix protein, exerts immunomodulatory activities. *Proc. Natl. Acad. Sci. U.S.A.* 86, 7437–7441.

Rygiel, T. P., Stolte, E. H., de Ruiter, T., van de Weijer, M. L., and Meyaard, L. (2011). Tumor-expressed collagens can modulate immune cell function through the inhibitory collagen receptor LAIR-1. *Mol. Immunol.* 49, 402–406. doi: 10.1016/j.molimm.2011.09.006

Sakaguchi, S., Miyara, M., Costantino, C. M., and Hafler, D. A. (2010). FOXP3 + regulatory T cells in the human immune system. *Nat. Rev. Immunol.* 10, 490–500. doi: 10.1038/nri2785

Sakaguchi, S., Wing, K., Onishi, Y., Prieto-Martin, P., and Yamaguchi, T. (2009). Regulatory T cells: How do they suppress immune responses? *Int. Immunol.* 21, 1105–1111. doi: 10.1093/intimm/dxp095

Sakr, W. A., Zarbo, R. J., Jacobs, J. R., and Crissman, J. D. (1987). Distribution of basement membrane in squamous cell carcinoma of the head and neck. *Hum. Pathol.* 18, 1043–1050. doi: 10.1016/S0046-8177(87)80221-6

Sandig, H., McDonald, J., Gilmour, J., Arno, M., Lee, T. H., and Cousins, D. J. (2009). Fibronectin is a TH1-specific molecule in human subjects. *J. Allergy Clin. Immunol.* 124, 528–535. doi: 10.1109/CSPA.2012.6194761

Sawamura, D., Nakano, H., and Matsuzaki, Y. (2010). Overview of epidermolysis bullosa. *J. Dermatol.* 37, 214–219. doi: 10.1111/j.1346-8138.2009.00800.x

Schalkwijk, J., Van Vlijmen, I., Oosterling, B., Perret, C., Koopman, R., Van den Born, J., et al. (1991). Tenascin expression in hyperproliferative skin diseases. *Br. J. Dermatol.* 124, 13–20. doi: 10.1111/j.1365-2133.1991.tb03276.x

Schenk, S., Bruckner-Tuderman, L., and Chiquet-Ehrismann, R. (1995). Dermo-epidermal separation is associated with induced tenascin expression in human skin. *Br. J. Dermatol.* 133, 13–22.

Schmitt-Egenolf, M., Boehncke, W. H., Christophers, E., Ständer, M., and Sterry, W. (1991). Type I and type II psoriasis show a similar usage of T-cell receptor variable regions. *J. Invest. Dermatol.* 97, 1053–1056. doi: 10.1111/1523-1747.ep12492569.

Schmoeckel, C., Stolz, W., Sakai, L. Y., Burgeson, R. E., Timpl, R., and Krieg, T. (1989). Structure of basement membranes in malignant melanoma and nevocytic nevi. *J. Invest. Dermatol.* 92, 663–668. doi: 10.1016/0022-202X(89)90179-6.

Sehra, S., Serezani, A. P. M., Ocaña, J. A., Travers, J. B., and Kaplan, M. H. (2016). Mast cells regulate epidermal barrier function and the development of allergic skin inflammation. *J. Invest. Dermatol.* 136, 1429–1437. doi: 10.1016/j.jid.2016.03.019.

Seidler, D. G., Mohamed, N. A., Bocian, C., Stadtmann, A., Hermann, S., Schafers, K., et al. (2011). The role for decorin in delayed-type hypersensitivity. *J. Immunol.* 187, 6108–6119. doi: 10.4049/jimmunol.1100373

Senyürek, I., Kempf, W. E., Klein, G., Maurer, A., Kalbacher, H., Schäfer, L., et al. (2014). Processing of laminin α chains generates peptides involved in wound healing and host defense. *J. Innate Immun.* 6, 467–484. doi: 10.1159/000357032

Serezani, A. P. M., Bozdogan, G., Sehra, S., Walsh, D., Krishnamurthy, P., Sierra Potchanant, E. A., et al. (2017). IL-4 impairs wound healing potential in the skin by repressing fibronectin expression. *J. Allergy Clin. Immunol.* 139, 142–151. doi: 10.1016/j.jaci.2016.07.012

Shimizu, H., Takizawa, Y., Pulkkinen, L., Murata, S., Kawai, M., Hachisuka, H., et al. (1999). Epidermolysis bullosa simplex associated with muscular dystrophy: phenotype-genotype correlations and review of the literature. *J. Am. Acad. Dermatol.* 41, 950–956. doi: 10.1016/S0190-9622(99)70252-5

Shin, J. W., Choi, Y. J., Choi, H. R., Na, J. I., Kim, K. H., Park, I. A., et al. (2015). Defective basement membrane in atopic dermatitis and possible role of IL-13. *J. Eur. Acad. Dermatol. Venereol.* 29, 2060–2062. doi: 10.1111/jdv.12596

Shin, T. H., Kim, H. S., Choi, S. W., and Kang, K. S. (2017). Mesenchymal stem cell therapy for inflammatory skin diseases: clinical potential and mode of action. Int. J. Mol. Sci. 18:244. doi: 10.3390/ijms18020244

Shinkuma, S. (2015). Dystrophic epidermolysis bullosa: a review. *Clin. Cosmet. Investig. Dermatol.* 8, 275–284. doi: 10.2147/CCID.S54681

Siegel, B. R. S., Pandolfino, T., Guitart, J., Rosen, S., and Kuzel, T. M. (2012). Primary cutaneous T-cell lymphoma : review and current concepts. *J. Clin. Oncol.* 18, 2908–2925. doi: 10.1200/JCO.2000.18.15.2908

Simon, T., and Bromberg, J. S. (2017). Regulation of the immune system by laminins. *Trends Immunol.* 38, 858–871. doi: 10.1016/j.it.2017.06.002

Singh, T. P., Zhang, H. H., Borek, I., Wolf, P., Hedrick, M. N., Singh, S. P., et al. (2016). Monocyte-derived inflammatory Langerhans cells and dermal dendritic cells mediate psoriasis-like inflammation. *Nat. Commun.* 7:13581. doi: 10.1038/ncomms13581

Sitaru, A. G., Sesarman, A., Mihai, S., Chiriac, M. T., Zillikens, D., Hultman, P., et al. (2010). T cells are required for the production of blister-inducing autoantibodies in experimental epidermolysis bullosa acquisita. *J. Immunol.* 184, 1596–1603. doi: 10.4049/jimmunol.0901412

Sokołowska-Wojdyło, M., Olek-Hrab, K., and Ruckemann-Dziurdzinska, K. (2015). Primary cutaneous lymphomas: diagnosis and treatment. *Postep. Dermatologii i Alergol.* 32, 368–383. doi: 10.5114/pdia.2015.54749

Stanley, J. R., Beckwith, J. B., Fuller, R. P., and Katz, S. I. (1982). A specific antigenic defect of the basement membrane is found in basal cell carcinoma but not in other epidermal tumors. *Cancer* 50, 1486–1490. doi: 10.1002/1097-0142(19821015)50:8<1486::AID-CNCR2820500807>3.0.CO;2-F

Stemmler, S., Parwez, Q., Petrasch-Parwez, E., Epplen, J. T., and Hoffjan, S. (2014). Association of variation in the LAMA3 gene, encoding the alpha-chain of laminin 5, with atopic dermatitis in a German case-control cohort. *BMC Dermatol.* 14:17. doi: 10.1186/1471-5945-14-17

Stratis, A., Pasparakis, M., Rupec, R. A., Markur, D., Hartmann, K., Scharffetter-Kochanek, K., et al. (2006). Pathogenic role for skin macrophages in a mouse model of keratinocyte-induced psoriasis-like skin inflammation. *J. Clin. Invest.* 116, 2094–2104. doi: 10.1172/JCI27179

Strid, J., McLean, W. H. I., and Irvine, A. D. (2016). Too much, too little or just enough: a goldilocks effect for IL-13 and skin barrier regulation? *J. Invest. Dermatol.* 136, 561–564. doi: 10.1016/j.jid.2015.12.025

Stultz, C. M., Thomas, A. H., and Edelman, E. R. (2007). Collagen fragments modulate innate immunity. *Exp. Biol. Med.* 232, 406–411. doi: 10.3181/00379727-232-2320406

Su, P., Chen, S., Zheng, Y. H., Zhou, H. Y., Yan, C. H., Yu, F., et al. (2016). Novel function of extracellular matrix protein 1 in suppressing Th17 cell development in experimental autoimmune encephalomyelitis. *J. Immunol.* 197, 1054–1064. doi: 10.4049/jimmunol.1502457.

Sumaria, N., Roediger, B., Ng, L. G., Qin, J., Pinto, R., Cavanagh, L. L., et al. (2011). Cutaneous immunosurveillance by self-renewing dermal γδ T cells. *J. Exp. Med.* 208, 505–518. doi: 10.1084/jem.20101824

Sun, Y., Zhang, J., Zhai, T., Li, H., Li, H., Huo, R., et al. (2017). CCN1 promotes IL-1β production in keratinocytes by activating p38 MAPK signaling in psoriasis. *Sci. Rep.* 7:43310. doi: 10.1038/srep43310

Sun, Y., Zhang, J., Zhou, Z., Wu, P., Huo, R., Wang, B., et al. (2015). CCN1, a pro-inflammatory factor, aggravates psoriasis skin lesions by promoting keratinocyte activation. *J. Invest. Dermatol.* 135, 2666–2675. doi: 10.1038/jid.2015.231

Takayama, G., Arima, K., Kanaji, T., Toda, S., Tanaka, H., Shoji, S., et al. (2006). Periostin: a novel component of subepithelial fibrosis of bronchial asthma downstream of IL-4 and IL-13 signals. *J. Allergy Clin. Immunol.* 118, 98–104. doi: 10.1016/j.jaci.2006.02.046

Takeuchi, H., Gomi, T., Shishido, M., Watanabe, H., and Suenobu, N. (2010). Neutrophil elastase contributes to extracellular matrix damage induced by chronic low-dose UV irradiation in a hairless mouse photoaging model. *J. Dermatol. Sci.* 60, 151–158. doi: 10.1016/j.jdermsci.2010.09.001

Tariq, M., Zhang, J., Liang, G., Ding, L., He, Q., and Yang, B. (2017). Macrophage polarization: anti-cancer strategies to target tumor-associated macrophage in breast cancer. *J. Cell. Biochem.* 118, 2484–2501. doi: 10.1002/jcb.25895

Tecchio, C., Micheletti, A., and Cassatella, M. A. (2014). Neutrophil-derived cytokines: facts beyond expression. *Front. Immunol.* 5:508. doi: 10.3389/fimmu.2014.00508

Tello, T. L., Coggshall, K., Yom, S. S., and Yu, S. S. (2018). Merkel cell carcinoma: an update and review: current and future therapy. *J. Am. Acad. Dermatol.* 78, 445–454. doi: 10.1016/j.jaad.2017.12.004

Terui, T., Ozawa, M., and Tagami, H. (2000). Role of neutrophils in induction of acute inflammation in T-cell-mediated immune dermatosis, psoriasis: a neutrophil-associated inflammation-boosting loop. *Exp. Dermatol.* 9, 1–10. doi: 10.1034/j.1600-0625.2000.009001001.x

Thomas, L. W., Elsensohn, A., Bergheim, T., Shiu, J., and Ganesan, A. (2018). Intramuscular steroids in the treatment of dermatologic disease: a systematic review. *J. Drugs Dermatol.* 17, 323–329.

Titeux, M., Pendaries, V., Tonasso, L., Décha, A., Bodemer, C., and Hovnanian, A. (2008). A frequent functional SNP in the MMP1 promoter is associated with higher disease severity in recessive dystrophic epidermolysis bullosa. *Hum. Mutat.* 29, 267–276. doi: 10.1002/humu.20647

Tjiu, J. W., Chen, J. S., Shun, C. T., Lin, S. J., Liao, Y. H., Chu, C. Y., et al. (2009). Tumor-associated macrophage-induced invasion and angiogenesis of human basal cell carcinoma cells by cyclooxygenase-2 induction. *J. Invest. Dermatol.* 129, 1016–1025. doi: 10.1038/jid.2008.310

Torsekar, R., and Gautam, M. (2017). Topical therapies in psoriasis. *Indian Dermatol. Online J.* 8, 235–245. doi: 10.4103/2229-5178.209622

Touzé, A., Le Bidre, E., Laude, H., Fleury, M. J. J., Cazal, R., Arnold, F., et al. (2011). High levels of antibodies against merkel cell polyomavirus identify a subset of patients with merkel cell carcinoma with better clinical outcome. *J. Clin. Oncol.* 29, 1612–1619. doi: 10.1200/JCO.2010.31.1704

Trémezaygues, L., and Reichrath, J. (2011). Vitamin D analogs in the treatment of psoriasis: where are we standing and where will we be going? *Dermatoendocrinology* 3, 180–186. doi: 10.4161/derm.17534

Tsuruta, D., Hashimoto, T., Hamill, K. J., and Jones, J. C. R. (2011). Hemidesmosomes and focal contact proteins: functions and cross-talk in keratinocytes, bullous diseases and wound healing. *J. Dermatol. Sci.* 62, 1–7. doi: 10.1016/j.jdermsci.2011.01.005

Uitto, J. (2008). Epidermolysis bullosa: prospects for cell-based therapies. *J. Invest. Dermatol.* 128, 2140–2142. doi: 10.1038/jid.2008.216

Uitto, J., and Shamban, A. (1987). Heritable skin diseases with molecular defects in collagen or elastin. *Dermatol. Clin.* 5, 63–84. doi: 10.1016/S0733-8635(18)30767-8

Ussar, S., Moser, M., Widmaier, M., Rognoni, E., Harrer, C., Genzel-Boroviczeny, O., et al. (2008). Loss of kindlin-1 causes skin atrophy and lethal neonatal intestinal epithelial dysfunction. *PLoS Genet.* 4:e1000289. doi: 10.1371/journal.pgen.1000289

Uva, L., Miguel, D., Pinheiro, C., Antunes, J., Cruz, D., Ferreira, J., et al. (2012). Mechanisms of action of topical corticosteroids in psoriasis. *Int. J. Endocrinol.* 2012:561018. doi: 10.1155/2012/561018

Vaccaro, M., Magaudda, L., Cutroneo, G., Trimarchi, F., Barbuzza, O., Guarneri, F., et al. (2002). Changes in the distribution of laminin α1 chain in psoriatic skin: immunohistochemical study using confocal laser scanning microscopy. *Br. J. Dermatol.* 146, 392–398. doi: 10.1046/j.1365-2133.2002.04637.x

Vahidnezhad, H., Youssefian, L., Saeidian, A. H., Touati, A., Sotoudeh, S., Jazayeri, A., et al. (2018). Next generation sequencing identifies double homozygous mutations in two distinct genes (EXPH5 and COL17A1) in a patient with concomitant simplex and junctional epidermolysis bullosa. *Hum. Mutat.* 39, 1349–1354. doi: 10.1002/humu.23592

Verrecchia, F., Chu, M. L., and Mauviel, A. (2001). Identification of novel TGF-β/Smad gene targets in dermal fibroblasts using a combined cDNA microarray/promoter transactivation approach. *J. Biol. Chem.* 276, 17058–17062. doi: 10.1074/jbc.M100754200

Vestergaard, C., Just, H., Baumgartner Nielsen, J., Thestrup-Pedersen, K., and Deleuran, M. (2004). Expression of CCR2 on monocytes and macrophages in chronically inflamed skin in atopic dermatitis and psoriasis. *Acta Derm. Venereol.* 84, 353–358. doi: 10.1080/00015550410034444

Villanueva, J., and Herlyn, M. (2008). Melanoma and the tumor microenvironment. *Curr. Oncol. Rep.* 10, 439–446. doi: 10.1007/s11912-008-0067-y

Wagner, C. J., Schultz, C., and Mall, M. A. (2016). Neutrophil elastase and matrix metalloproteinase 12 in cystic fibrosis lung disease. *Mol. Cell. Pediatr.* 3:25. doi: 10.1186/s40348-016-0053-7

Wang, G. Y., Wang, J., Mancianti, M.-L., and Epstein, E. H. Jr. (2011). Basal cell carcinomas arise from hair follicle stem cells in Ptch1(+/-) mice. *Cancer Cell.* 19, 114–124. doi: 10.1016/j.ccr.2010.11.007

Watt, F. M., and Fujiwara, H. (2011). Cell-extracellular matrix interactions in normal and diseased skin. *Cold Spring Harb. Perspect. Biol.* 3:a005124. doi: 10.1101/cshperspect.a005124

Wayner, E. A., Gil, S. G., Murphy, G. F., Wilke, M. S., and Carter, W. G. (1993). Epiligrin, a component of epithelial basement membranes, is an adhesive ligand for α3β1 positive T lymphocytes. *J. Cell Biol.* 121, 1141–1152. doi: 10.1083/jcb.121.5.1141

Weidinger, S., and Novak, N. (2016). Atopic dermatitis. *Lancet* 387, 1109–1122. doi: 10.1016/S0140-6736(15)00149-X

Wollina, U. (2012). Cutaneous Tcell lymphoma: update on treatment. *Int. J. Dermatol.* 51, 1019–1036. doi: 10.1111/j.1365-4632.2011.05337.x

Wondimu, Z., Geberhiwot, T., Ingerpuu, S., Juronen, E., Xie, X., Lindbom, L., et al. (2004). An endothelial laminin isoform, laminin 8 (α4β1γ1), is secreted by blood neutrophils, promotes neutrophil migration and extravasation, and protects neutrophils from apoptosis. *Blood* 104, 1859–1866. doi: 10.1182/blood-2004-01-0396

Wu, P., Ma, G., Zhu, X., Gu, T., Zhang, J., Sun, Y., et al. (2017). Cyr61/CCN1 is involved in the pathogenesis of psoriasis vulgaris via promoting IL-8 production by keratinocytes in a JNK/NF-κB pathway. *Clin. Immunol.* 174, 53–62. doi: 10.1016/j.clim.2016.11.003

Wu, X., Schulte, B. C., Zhou, Y., Haribhai, D., Mackinnon, A. C., Plaza, J. A., et al. (2014). Depletion of M2-like tumor-associated macrophages delays cutaneous T-cell lymphoma development *in vivo*. *J. Invest. Dermatol.* 134, 2814–2822. doi: 10.1038/jid.2014.206

Yamaguchi, Y. (2014). Periostin in skin tissue skin-related diseases. *Allergol. Int.* 63, 161–170. doi: 10.2332/allergolint.13-RAI-0685

Yamaguchi, Y., Mann, D. M., and Ruoslahti, E. (1990). Negative regulation of transforming growth factor-β by the proteoglycan decorin. *Nature* 346, 281–284. doi: 10.1038/346281a0

Yanagi, T., Kitamura, S., and Hata, H. (2018). Novel therapeutic targets in cutaneous squamous cell carcinoma. *Front. Oncol.* 8:79. doi: 10.3389/fonc.2018.00079

Yancey, K. B., and Hintner, H. (2010). Non-herlitz junctional epidermolysis bullosa. *Dermatol. Clin.* 28, 67–77. doi: 10.1016/j.det.2009.10.008

Yanez, D. A., Lacher, R. K., Vidyarthi, A., and Colegio, O. R. (2017). The role of macrophages in skin homeostasis. *Pflugers Arch. Eur. J. Physiol.* 469, 455–463. doi: 10.1007/s00424-017-1953-7

Yang, L., Huang, J., Ren, X., Gorska, A. E., Chytil, A., Aakre, M., et al. (2008). Abrogation of TGFβ signaling in mammary carcinomas recruits Gr-1+CD11b+ myeloid cells that promote metastasis. *Cancer Cell.* 13, 23–35. doi: 10.1016/j.ccr.2007.12.004

Yu, S. H., Drucker, A. M., Lebwohl, M., and Silverberg, J. I. (2018). A systematic review of the safety and efficacy of systemic corticosteroids in atopic dermatitis. *J. Am. Acad. Dermatol.* 78, 733–740.e11. doi: 10.1016/j.jaad.2017.09.074

Yuen, W. Y., Lemmink, H. H., Van Dijk-Bos, K. K., Sinke, R. J., and Jonkman, M. F. (2011). Herlitz junctional epidermolysis bullosa: diagnostic features, mutational profile, incidence and population carrier frequency in the Netherlands. *Br. J. Dermatol.* 165, 1314–1322. doi: 10.1111/j.1365-2133.2011.10553.x

Zaid, A., Mackay, L. K., Rahimpour, A., Braun, A., Veldhoen, M., Carbone, F. R., et al. (2014). Persistence of skin-resident memory T cells within an epidermal niche. *Proc. Natl. Acad. Sci. U.S.A.* 111, 5307–5312. doi: 10.1073/pnas.1322292111

Zhou, J., Yao, D., Qian, Z., Hou, S., Li, L., Jenkins, A. T. A., et al. (2018). Bacteria-responsive intelligent wound dressing: simultaneous *in situ* detection and inhibition of bacterial infection for accelerated wound healing. *Biomaterials* 161, 11–23. doi: 10.1016/j.biomaterials.2018.01.024

Zuliani-Alvarez, L., Marzeda, A. M., Deligne, C., Schwenzer, A., McCann, F. E., Marsden, B. D., et al. (2017). Mapping tenascin-C interaction with toll-like receptor 4 reveals a new subset of endogenous inflammatory triggers. *Nat. Commun.* 8:1595. doi: 10.1038/s41467-017-01718-7

Conflict of Interest Statement: The authors declare that the research was conducted in the absence of any commercial or financial relationships that could be construed as a potential conflict of interest.

Advantages of publishing in Frontiers

OPEN ACCESS
Articles are free to read for greatest visibility and readership

FAST PUBLICATION
Around 90 days from submission to decision

HIGH QUALITY PEER-REVIEW
Rigorous, collaborative, and constructive peer-review

TRANSPARENT PEER-REVIEW
Editors and reviewers acknowledged by name on published articles

Frontiers
Avenue du Tribunal-Fédéral 34
1005 Lausanne | Switzerland

Visit us: www.frontiersin.org
Contact us: info@frontiersin.org | +41 21 510 17 00

REPRODUCIBILITY OF RESEARCH
Support open data and methods to enhance research reproducibility

DIGITAL PUBLISHING
Articles designed for optimal readership across devices

FOLLOW US
@frontiersin

IMPACT METRICS
Advanced article metrics track visibility across digital media

EXTENSIVE PROMOTION
Marketing and promotion of impactful research

LOOP RESEARCH NETWORK
Our network increases your article's readership